NUEVAS ESTRATEGIAS METODOLÓGICAS Y DE ANÁLISIS DE DATOS DE CITOMETRÍA DE FLUJO APLICADAS AL DIAGNÓSTICO Y CLASIFICACIÓN DE LAS HEMOPATÍAS MALIGNAS

Juan Alejandro Flores Montero

Tesis doctoral

Director:

Dr. Alberto Orfao

Departamento de Medicina

Salamanca, 2016

VNiVERSiDAD D SALAMANCA
CAMPUS DE EXCELENCIA INTERNACIONAL

DEPARTAMENTO DE MEDICINA

D. Alberto Orfão de Matos Correia e Vale, Doctor en Medicina y Cirugía y Profesor Catedrático del Departamento de Medicina de la Universidad de Salamanca

C E R T I F I C A:

Que el trabajo doctoral realizado bajo mi dirección por Don. Juan Alejandro Flores Montero titulado: "NUEVAS ESTRATEGIAS METODOLÓGICAS Y DE ANÁLISIS DE DATOS DE CITOMETRÍA DE FLUJO APLICADAS AL DIAGNÓSTICO Y CLASIFICACIÓN DE LAS HEMOPATÍAS MALIGNAS", reúne las condiciones de originalidad requeridas para optar al grado de Doctor en Medicina por la Universidad de Salamanca.

Y para que así conste, firmo el presente certificado en Salamanca, a 7 de Enero del año 2016.

Fdo: Dr. Alberto Orfão de Matos

El trabajo recogido en esta tesis doctoral se presenta en la modalidad de *tesis por compendio de publicaciones*. Así, en esta memoria se incluyen dos trabajos (extensos) originales publicados en revistas científicas indexadas en el *Science Citation Reports*. Dichas publicaciones son el resultado del desarrollo de un proyecto multicéntrico financiado por la Unión Europea dentro de VI Programa Marco (EU-FP6, LSHB-CT-2006-018708), que contó con la participación de 8 centros de laboratorios de investigación clínica y diagnóstico, de centros académicos o asistenciales de un número idéntico de países europeos distintos y dos PYMES (empresas de tamaño pequeño/mediano) biotecnológicas del mismo ámbito. Aun cuando los resultados generados se han publicado de forma conjunta en dos artículos, cada uno de ellos esta a su vez conformado por un compendio de artículos, organizados en secciones, cada una de las cuales puede ser considerada por sí sola como una publicación individual debido a su contenido, fase experimental, resultados, impacto y la extensión que ocupa. A continuación se detallan estas secciones en las que el Doctorando ha tenido un papel central y muy destacado, por cada uno de los dos trabajos incluidos en la memoria:

1. **EuroFlow standardization of flow cytometer instrument settings and immunophenotyping protocols.**
   Kalina T[1], Flores-Montero J[2], van der Velden VHJ[3], Martin-Ayuso M[4], Böttcher S[5], Ritgen M[5], Almeida J[2], Lhermitte L[6], Asnafi V[6], Mendonça A[7], de Tute R[8], Cullen M[8], Sedek L[9], Vidriales MB[10], Pérez JJ[10], te Marvelde JG[3], Mejstrikova E[1], Hrusak O[1], Szczepanski T[9], van Dongen JJM[3], Orfao A[2] on behalf of the EuroFlow Consortium (EU-FP6, LSHB-CT-2006-018708).
   K.T. and F-M.J. have contributed equally to this work
   Leukemia (2012) 26, 1986–2010; doi:10.1038/leu.2012.122
   Se incluyen todas las secciones del artículo. En detalle:

2. **EuroFlow antibody panels for standardized n-dimensional flow cytometric immunophenotyping of normal, reactive and malignant leukocytes.**
   van Dongen JJM[3], Lhermitte L[6], Böttcher S[5], Almeida J[2], van der Velden VHJ[3], Flores-Montero J[2], Rawstron A[8], Asnafi V[6], Lécrevisse Q[2], Lucio P[7], Mejstrikova E[1], Szczepanski T[9], Kalina T[1], de Tute R[8], Brüggemann M[5], Sedek L[9], Cullen M[8], Langerak AW[3], Mendonça A[7], Macintyre E[6], Martin-Ayuso M[4], Hrusak O[1], Vidriales MB[10], Orfao A[2] on behalf of the EuroFlow Consortium (EU-FP6, LSHB-CT-2006-018708)
   Leukemia (2012) 26, 1908–1975; doi:10.1038/leu.2012.120

   Se incluyen las siguientes secciones:

Sección 2ª. Lymphoid screening tube (LST)

Flores-Montero J[2], Almeida J[2], Pérez JJ[10], Asnafi V[6], Lhermitte L[6], Vidriales MB[10], Böttcher S[5], Mendonça A[7], Lucio P[7], Tielemans D[3], Langerak AW[3], Lima M[11], Santos AH[11], de Tute R[8], Cullen M[8], Rawstron A[8], te Marvelde JG[3], Wind H[3], van der Velden VHJ[3], Sedek L[9], Szczepanski T[9], Kalina T[1], Lécrevisse Q[2], Hernández J[4], van Dongen JJM[3], Orfao A[2]

Sección 4ª. Plasma cell disorders (PCD) panel

Flores-Montero J[2], Almeida J[2], Pérez JJ[10], Mendonça A[7], Lucio P[7], de Tute R[8], Cullen M[8], Rawstron A[8], Mejstrikova E[1], Sedek L[9], Szczepanski L[9], Lhermitte L[6], van der Velden VHJ[3], Wind H[3], Böttcher S[5], Vidriales MB[10], Kalina T[1], San Miguel J[10], Orfao A[2]

Sección 9ª. Antibody panel for T-cell chronic lymphoproliferative diseases (T-CLPD)

Almeida J[2], Flores-Montero J[2], Pérez JJ[10], Vidriales MB[10], Lima M[11], Santos AH[12], Langerak AW[3], Tielemans D[3], Lhermitte D[6], Asnafi V[6], Macintyre E[6], Böttcher S[5], Mendonça A[7], Lucio P[7], de Tute R[8], Cullen M[8], Rawstron A[8], Sedek L[9], Szczepanski T[9], Kalina T[1], Martin-Ayuso M[4], van Dongen JJM[3], Orfao A[2]

Sección 10ª. Antibody panel for NK-cell chronic lymphoproliferative diseases (NK-CLPD)

Almeida J[2], Flores-Montero J[2], Lhermitte L[6], Asnafi V[6], de Tute R[8], Cullen M[8], Rawstron A[8], Tielemans D[3], Langerak AW[3], Pérez JJ[10], Lima[11], Santos AH[11], Mendonça A[7], Lucio P[7], Böttcher S[8], Sedek L[9], Szczepanski T[9], Kalina T[1], Muñoz M[4], van Dongen JJM[3], Orfao A[2]

---

[1]Department of Pediatric Hematology and Oncology, 2nd Faculty of Medicine, Charles University (DPH/O), Prague, Czech Republic; [2]Cancer Research Center (IBMCC-CSIC), Department of Medicine and Cytometry Service, University of Salamanca (USAL) and Institute of Biomedical Research of Salamanca (IBSAL), Salamanca, Spain; [3]Department of Immunology, Erasmus MC, University Medical Center Rotterdam, Rotterdam, The Netherlands; [4]Cytognos SL, Salamanca, Spain; [5]Second Department of Medicine, University Hospital of Schleswig Holstein, Campus Kiel (UNIKIEL), Kiel, Germany; [6]Department of Hematology, Hôpital Necker and UMR CNRS 8147, University of Paris Descartes (AP-HP), Paris, France; [7]Department of Hematology, Portuguese Institute of Oncology (IPOLFG), Lisbon, Portugal; [8]Haematological Malignancy Diagnostic Service (HMDS), University of Leeds (UNIVLEEDS), Leeds, UK; [9]Department of Pediatric Hematology and Oncology, Medical University of Silesia (SUM), Zabrze, Poland; [10]Department of Hematology, University Hospital Salamanca (HUS) and IBSAL, Salamanca; [11]Department of Hematology, Hospital de Santo António (HSA), Centro Hospitalar do Porto (CHP), Porto, Portugal

ÍNDICE GENERAL

GLOSARIO DE ABREVIATURAS

A

A: área
ACD: citrato ácido de dextrosa
AcMo: anticuerpo monoclonal
AF: alexa flúor
ALK: quinasa del linfoma anaplásico
AmCyan: proteína cianina fluorescente derivada del alga Anemonia Majano
APC: aloficocianina

B

β2M: β2 microglobulina
BC: Beckman Coulter
BD: Becton Dickinson Biosciences
BSA: albúmina bovina sérica
BV: fluorocromo violeta brillante

C

CD: "clúster" de diferenciación
CG: centro germinal
CMF: citometría de flujo
CP: célula plasmática
CPc: célula plasmática clonales
CV: coeficiente de variación
CVr: coeficiente de variación robusto
Cy5.5: cianina5.5
Cy7: cianina7
Cy: citoplasmático

D

DE: desviación estándar

E

EDTA: etilendiaminotetraacetato
ELPC-NK: enfermedad linfoproliferativa crónica de células NK

F

FCS: formato estándar de ficheros de datos de citometría de flujo
FITC: isotiocianato de fluoresceína
FRET: transferencia de energía entre fluorocromos
FSC: luz dispersada frontalmente

G

GMSI: gammapatía monoclonal de significado incierto

H

H: altura
H7: fluorocromo hilite7
HeNe: helio-neón
HEP: heparina de sodio
HV450: fluorocromo Horizon Violeta450

I

Ig: inmunoglobulina
IG: gen de las inmunoglobulinas
IMF: intensidad media de fluorescencia

K

KIR: receptores tipo Ig expresados por células “Killer”

L

LA-NK: leucemia agresiva de células NK
LB: linfoma de Burkitt
LCP: leucemia de células plasmáticas
LCR: líquido cefalorraquídeo
LF: linfoma folicular
LIR: receptores tipo Ig expresados por leucocitos
LLC-B: leucemia linfática crónica de células B
LLGG-T: leucemia de linfocitos grandes granulares T
LLTA: leucemia/linfoma de célula T del adulto
LPL-T: leucemia prolinfocítica T
LST: Tubo de rastreo diagnóstico de linfocitosis
LACG: linfoma anaplásico de célula grande
LTAI: linfoma T angioinmunoblástico

M

MALT: tejido linfoide asociado a mucosa
MLL: marcar, lisar, lavar
MLLF: marcar, lisar, lavar, fijar
MLNL: marcar, lisar, no lavar
MM: mieloma múltiple
MO: médula ósea
MPO: mieloperoxidasa

N

NCP: neoplasia de células plasmáticas

NH_4Cl: cloruro de amonio
NOS: no especificado

O
OMS: Organización Mundial de la Salud

P
PAAF: punción por aspiración con aguja fina
PacB: fluorocromo pacific blue
PacO: fluorocromo pacific orange
PBS: solución salina de tampón fosfato
PCD: panel EuroFlow para las neoplasias de células plasmáticas
PE: ficoeritrina
PerCP: proteína peridinina-clorofila
PFA: paraformaldehído
PMT: tubo foto multiplicador

R
RCN: receptores de citotoxicidad natural

S
SI: índice de tinción
SLPC: síndrome linfoproliferativo crónico
Sm: membrana de la superficie celular
SP: sangre periférica
SS: Síndrome de Sézary
SSC: luz dispersada lateralmente

T
TCL1: gen de leucemia/linfoma de célula T 1
TCR: receptor de célula T
TDS: Información técnica del fabricante
TdT: desoxinucleotidil-transferasa terminal
TL: tricoleucemia
TR: gen del receptor de célula T
TTSA: tubo teñido con un solo anticuerpo

V
VEB: virus de Epstein-Barr
VIH: virus de la inmunodeficiencia humana

W
W: anchura

I. INTRODUCCIÓN.

Hoy día, el diagnóstico y clasificación de las hemopatías malignas asienta sobre las características citomorfológicas e histopatológicas del tumor, el inmunofenotipo de las células tumorales y sus características genéticas y moleculares, consideradas en el contexto del comportamiento clínico de la enfermedad[1]. Aunque pueden emplearse diferentes técnicas inmunofenotípicas para la identificación y caracterización de las células patológicas, en los últimos años el inmunofenotipado por citometría de flujo ha adquirido especial relevancia, particularmente en el área de las hemopatías linfoides y las neoplasias de células plasmáticas[1-7]. Así, el inmunofenotipado por citometría de flujo multicolor constituye hoy una herramienta fundamental en el rastreo diagnóstico y la clasificación de los síndromes linfoproliferativos crónicos (SLPC) B, T y NK, así como en la identificación, caracterización y monitorización de las neoplasias de células plasmáticas (NCP)[2-4,8-10].

No obstante la utilidad clínica (diagnóstica) del inmunofenotipado, existe una gran disparidad respecto a los equipos de medida empleados, los reactivos y combinaciones de reactivos aplicados, las técnicas de preparación de muestras, las propias muestras y los anticoagulantes empleados, y sobre todo, las estrategias de análisis de los datos de citometría y los criterios aplicados a la hora de interpretar de los resultados[7,9,11-37]. Todo ello hace que en el momento de iniciar este trabajo, existiera una necesidad urgente de estandarización metodológica que indudablemente se vería beneficiada por la introducción simultánea de estandarización tecnológica e innovación.

En esta introducción, revisaremos en primer lugar los aspectos técnicos relacionados con la utilización de la citometría de flujo en el diagnóstico y clasificación inmunofenotípica de las hemopatías malignas, para centrarnos posteriormente en las estrategias empleadas actualmente para el análisis de la información generada, revisando finalmente de forma escueta, el estado actual de la aplicación de la citometría de flujo en el rastreo diagnóstico y clasificación de los SLPC B, T y NK, y de las NCP.

1. El citómetro de flujo y sus componentes

El citómetro de flujo es un instrumento capaz de identificar, cuantificar y caracterizar propiedades de partículas (e.g., células) que se encuentran en suspensión en un fluido en movimiento, haciendo incidir sobre ellas uno o varios haces de luz con longitudes de onda bien definidas (Figura 1)[38,39]. Aunque el paso de dichas partículas o células por delante de la(s) fuente(s) de luz se realiza de forma alineada y de una en una, dadas las características del equipo, es posible analizar un gran número de células/partículas (i.e., eventos) en un corto periodo de tiempo; esto permite recoger información estadísticamente robusta de las mediciones realizadas sobre (un gran número de) las partículas/células analizadas, que pueden además corresponder a uno o más grupos de eventos diferentes entre sí, por ejemplo, a distintas poblaciones celulares que coexisten de forma natural en la muestra analizada[38,40].

Figura 1. Representación esquemática de un citómetro de flujo y sus componentes principales (adaptado de Pedreira et al, 2013)[28]**.**

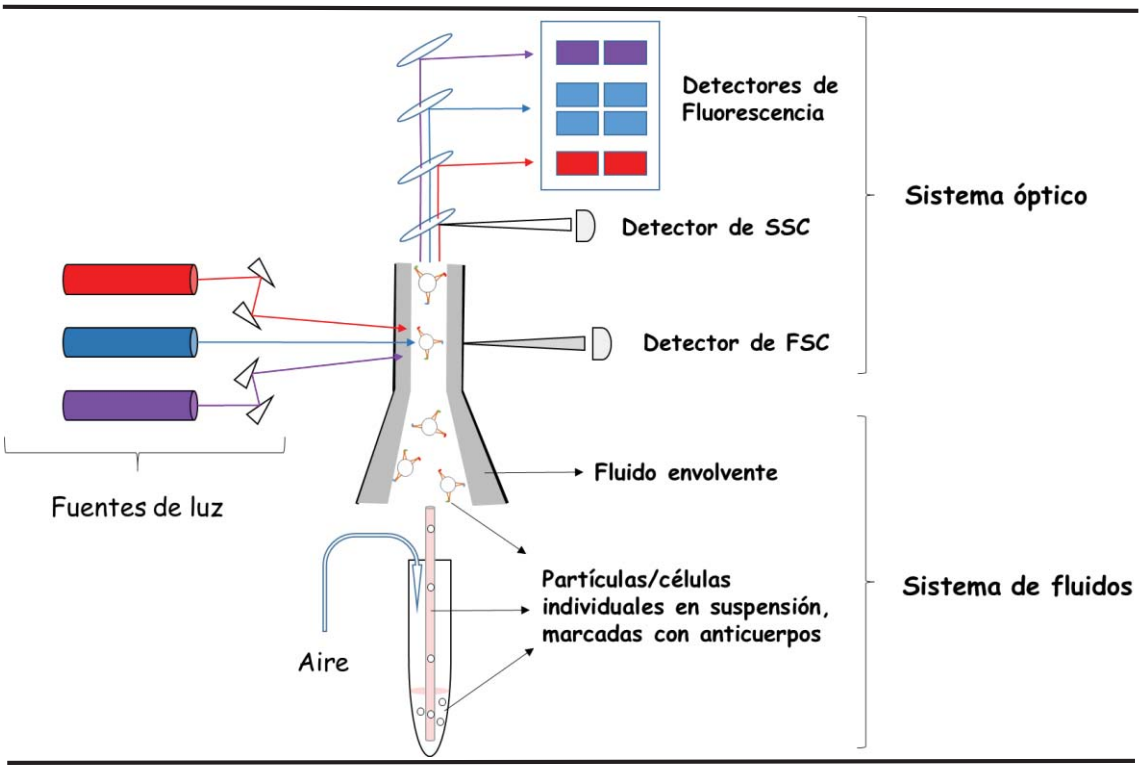

SSC, dispersión lateral de luz; FSC, dispersión frontal de luz

En términos generales, en un citómetro de flujo coinciden y se entremezclan de forma continua y desde hace décadas, los avances ocurridos en distintas áreas tecnológicas, incluida la tecnología láser, la producción de anticuerpos monoclonales, la química de los fluorocromos, la mecánica de fluidos, la óptica, la electrónica y la informática[12,14,28,38-54]. Por ello, es fácil entender que desde los primeros citómetros de flujo generados en la década de los 60, estos instrumentos hayan sufrido una evolución continua, incorporando los nuevos avances tecnológicos. Así, los citómetros analógicos han evolucionado a instrumentos digitales con una mayor capacidad analítica (e.g., velocidad de análisis), de los citómetros de una única fuente de luz se ha pasado a los equipos dotados de múltiples láseres y fibra óptica para la conducción de la luz asociado a su vez el análisis de un número progresivamente creciente de fluorocromos (i.e. hasta 28 fluorescencias distintas en sistemas con detectores tradicionales y 64 colores cuando se emplean detectores espectrales), y se han incorporado sistemas ópticos con recolección de luz optimizada sobre soportes octagonales para filtros y espejos (Figura 2)[49,55,56].

De este desarrollo tecnológico se han beneficiado de forma particular varias generaciones de citómetros de flujo enfocados al uso clínico. En este campo, la producción en 1986 del modelo de citómetro de flujo de 3 colores FACScan por la empresa Becton Dickinson Biosciences (BD; San José, CA, EEUU), supuso un hito clave para la citometría clínica multicolor[38]. Es precisamente en este año cuando adquiere especial relevancia la citometría clínica basada en el inmunofenotipado de leucocitos de sangre periférica (SP), teniendo especial desarrollo el recuento de linfocitos T $CD4^+$ en pacientes con infección por el virus de la inmunodeficiencia humana (VIH)[38]. Posteriormente, surgieron modelos de citómetros de flujo analógicos de uso clínico de 4, 5 y 6 colores, hasta los citómetros de flujo digitales de uso clínico actuales de entre 8 y 10 fluorescencias[39,47,54,57,58].

Pese a las grandes ventajas que el desarrollo tecnológico de la citometría de flujo (CMF) ha tenido en sus aplicaciones clínicas, dichos desarrollos han traído también una mayor

complejidad, que se refleja por ejemplo en: i) la mayor dificultad técnica a la hora de establecer una calibración adecuada y universal de los equipos, y de mantenerla estable a lo largo del

Figura 2. Representación esquemática del sistema óptico de un citometro de flujo en su configuración clásica (panel superior) y actual (panel inferior) para un láser azul de 488 nm (adaptado de Givan et al, 2001; McCoy et al, 2002[38,40] y; www.bdbiosciences.com)

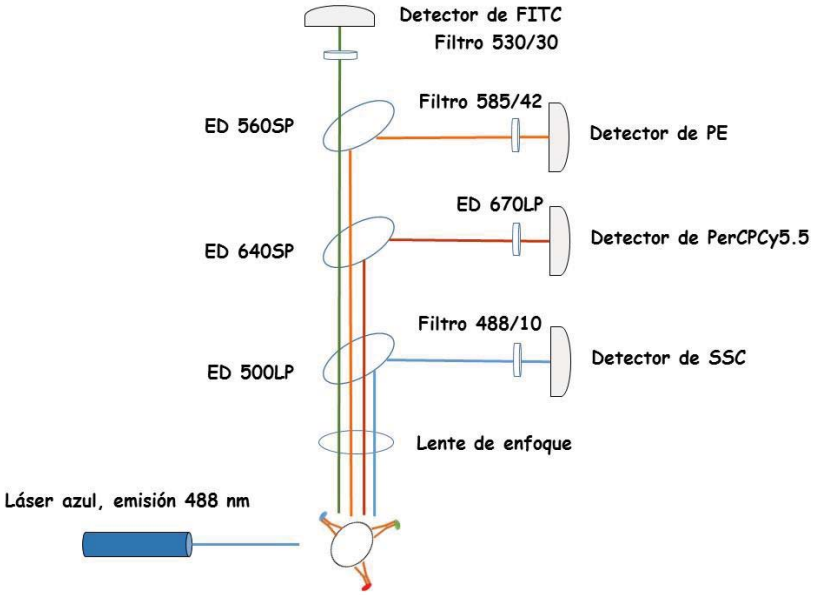

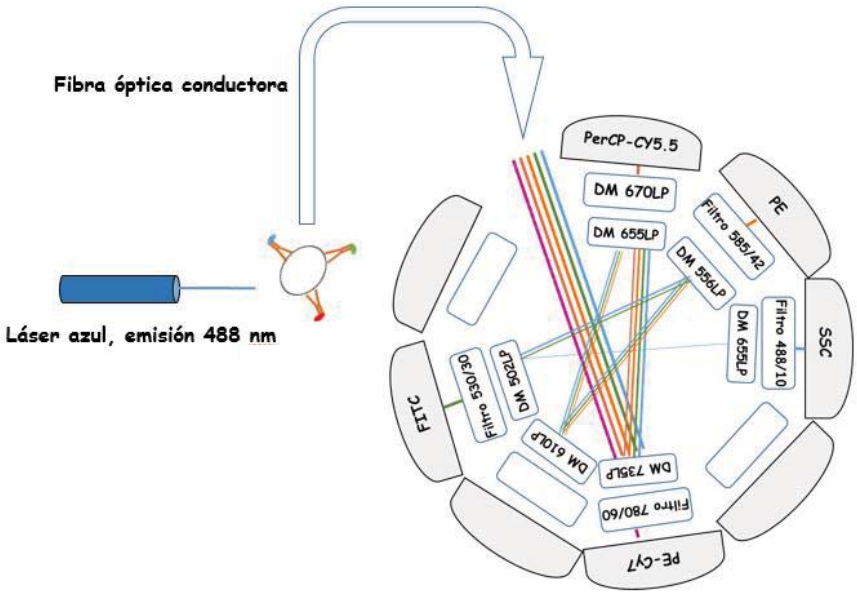

FITC, isotiocianato de fluoresceina; ED, espejo dicroico; SP, "short pass", identifica que el ED permite el paso de luz de longitud de onda inferior a la indicada; LP, "long pass", identifica que el ED permite el paso de luz de longitud de onda superior a la indicada; PE, ficoeritrina; PerCP-Cy.5., proteína peridinina-clorofila-cianina5.5; SSC, dispersión lateral de luz; PE-Cy7, ficoeritrina-cianina7.

tiempo; ii) un mayor número de posibilidades de combinaciones de fluorocromos, no siempre óptimas; iii) una complejidad creciente a la hora de diseñar paneles de reactivos (p. ej. combinaciones de anticuerpos conjugados con fluorocromos) y; iv) la imposibilidad de seguir empleando las estrategias de análisis de datos y de interpretación de los resultados (datos) generados, a no ser que este se realice a costa de una pérdida significativa de gran parte de la información generada[46].

En general, los componentes de un citómetro de flujo clínico estándar, incluyen 5 elementos básicos distintos: i) el sistema de fluidos, ii) las fuentes de luz, iii) el sistema óptico, iv) los componentes electrónicos y, v) el sistema informático.

1.1. Sistema de fluidos

El sistema de fluidos de un citómetro de flujo incluye aquellos componentes que permiten el transporte, enfoque y paso secuencial (y de una en una), de las partículas de la muestra a analizar por el punto (o puntos) en el que incide el haz (o haces) de luz (Figura 1). Con este fin, el líquido de la muestra ha de inyectarse en el interior de un fluido isotónico en movimiento, a una velocidad inferior a la de dicho fluido (i.e. el fluido envolvente). Con ello se origina un fluido global coaxial con características de flujo laminar, en el que ambos fluidos primarios se mantienen separados físicamente gracias a su diferente velocidad y localización (Figura 1). Mediante un juego de presiones entre ambos fluidos, podemos hacer variar el área del flujo correspondiente a la muestra y al líquido envolvente. Este ajuste de la presión diferencial entre ambos líquidos, permite alinear las partículas de la muestra, de modo que pasen centradas y de una en una por delante de la luz del (de los) láser(es) a menor o mayor velocidad (i.e. enfoque hidrodinámico) (Figura 1)[57]. Aunque existen otros sistemas para el alineamiento de la muestra (e.g. enfoque acústico)[59], la mayoría de los citómetros de flujo que se utilizan en los laboratorios

de diagnóstico clínico emplean el sistema de enfoque hidrodinámico con pocas variaciones respecto al principio descrito anteriormente.

1.2. Fuentes de luz

Actualmente, la mayoría de los citómetros de flujo empleados en los laboratorios clínicos utilizan dos o más fuentes de luz, generalmente láseres, que emiten a longitudes de ondas concretas y específicas. Como mínimo suelen estar dotados de un láser azul que emite a 488 nm y un láser rojo cuya emisión suele estar por encima de los 630 nm[38-40,53,54]. En caso de disponer de tres láseres, el tercer láser suele emitir a longitudes de onda correspondientes a luz violeta o ultravioleta[60-63]. En este punto merece destacar que, las distintas fuentes de luz suelen incidir sobre distintos puntos del flujo, aunque existen citómetros de flujo en los que los láseres pueden estar enfocados todos ellos en el mismo punto (p.ej., el SA3800 Spectral Analyzer, Sony Biotecnology Inc., Tokio, Japón).

Como veremos más adelante, la longitud de onda a la que emite cada láser y el perfil de excitación de los fluorocromos empleados para medir distintas características celulares, deben necesariamente coincidir. En consecuencia, la evolución de los láseres y el desarrollo de nuevos fluorocromos han estado relacionados y promovidos por la necesidad de definir con gran precisión, las distintas poblaciones celulares fenotípica y funcionalmente distintas que coexisten en diferentes proporciones en una muestra[49,64]. Aunque existen varios tipos de láseres, los más utilizados son los láseres de estado gaseoso como el láser de argón que emite a 488 nm, o el láser de helio-neón (HeNe) con emisión de luz a 633 nm; alternativamente, se emplean láseres de estado sólido como los láseres de diodo rojo que emiten a 635 nm o de diodo violeta con emisión a 407 nm[38,49].

1.3. Sistema óptico

El sistema óptico de un citómetro de flujo está integrado por todo el conjunto de lentes y prismas que permiten el enfoque del haz (haces) de luz, la fibra óptica que conduce la luz al punto preciso donde debe interceptar la muestra (i.e. punto de interrogación), y los filtros y espejos que dispuestos en una configuración óptima, seleccionan (y envían) luz con diferente longitud de onda (i.e. color) a distintos detectores (Figuras 1 y 2)[38,40,57]. Por un lado, los espejos dicroicos permiten seleccionar una o varias zonas del espectro de luz de forma específica, actuando a la vez como filtro y espejo, dirigiendo luz con distinto color (longitud de onda) a diferentes destinos o direcciones (Figuras 1 y 2)[40,65]. A su vez, los filtros delimitan aún más si cabe, el espectro de longitudes de onda seleccionado para llegar a cada detector, al permitir el paso hacia el mismo de bandas relativamente estrechas de luz. Como consecuencia de todo ello, a cada detector llega luz con una determinada longitud de onda (i.e. color), generada al interceptar la luz del láser a cada célula (Figura 1 y 2).

1.4. Sistema electrónico

El sistema electrónico del citómetro de flujo incluye aquellos componentes cuya misión es detectar y procesar la señal luminosa, transformándola en señal digital susceptible de ser almacenada y procesada mediante un sistema informático[38,40,65].

Los detectores son componentes del citómetro de flujo constituidos por placas recubiertas de compuestos fotosensibles como el silicio, capaces de recoger la luz que les llega y transformarla en corriente eléctrica y finalmente, en señal digital medible. En términos generales, en los citómetros de flujo se incluyen tres tipos principales de detectores: i) detectores de tipo fotodiodo, para intensidades relativamente elevadas de luz -p. ej. para la luz dispersada frontalmente (FSC, abreviado del inglés “forward scatter”)-, ii) tubos fotomultiplicadores (PMT; abreviado del inglés “photomultiplier tube”) para intensidades de luz mínimas y de una determinada longitud de onda -p. ej. detectores de luz dispersada

lateralmente (SSC, abreviado del inglés “sideward scatter”) y de fluorescencia, en citómetros convencionales- y, iii) detectores espectrales, empleados habitualmente para medir simultáneamente luz procedente de varios fluorocromos distintos con diferentes picos de emisión de luz. La cantidad total de luz recogida por el detector es directamente proporcional a la cantidad de moléculas de fluorocromo presentes en la partícula/célula analizada, así como a la cantidad de señal emitida por el detector[40]. Del número de detectores del que dispone el instrumento depende en gran medida, el número máximo de parámetros (colores) que pueden medirse simultáneamente; no obstante, dependiendo del tipo de detector (PMT o espectral) esto puede variar substancialmente[38,39,49,56]. Por ejemplo, con un solo detector de tipo espectral podemos medir simultáneamente las emisiones fluorescentes de más de 10 fluorocromos distintos; por el contrario, en el caso de los PMT se requieren más de 10 detectores para llevar a cabo un experimento de 10 colores[56].

A modo de resumen, del número y tipo de láseres que posee un citómetro de flujo, y de las características de sus detectores y sistema óptico, depende el número y tipo de parámetros que pueden ser evaluados simultáneamente.

1.5. Sistema informático

El sistema informático incluye un ordenador y uno o varios programas informáticos mediante los cuales, además de analizar los datos generados por las mediciones realizadas, se controlan los demás componentes del citómetro de flujo, incluyendo el diferencial de presiones entre la muestra y el líquido envolvente, el voltaje de los PMT o los umbrales establecidos para la adquisición, entre otras funciones[38].

2. Información generada en un citómetro de flujo

De lo anteriormente expuesto se entiende que un citómetro de flujo mide luz asociada a diferentes características de las partículas o células analizadas de forma individualizada; dicha

luz derivada de los cambios de dirección y color de la luz del láser (o láseres), que ocurren al pasar cada una de dichas partículas/células por delante del haz de luz. Así, por un lado, medimos la cantidad de luz del láser que al incidir sobre la célula se dispersa y, por otra parte, la cantidad de luz que es emitida por los diferentes fluorocromos que están presentes en la célula/partícula analizada, bien sea de forma natural o unidas a ella artificialmente[38]. En la gran mayoría de los citómetros de flujo de uso clínico, la luz dispersada es recogida en dos puntos distintos y que corresponden a ángulos cercanos a 180° con respecto a la fuente de luz (i.e., FSC) y a ángulos cercanos a 90° (i.e., SSC). Ambas medidas (FSC y SSC) reflejan características físicas de las partículas/células analizadas, siendo directamente proporcionales al tamaño (en el caso del FSC) y grado de "complejidad" o granularidad interna (en el caso del SSC). De manera similar, los diferentes fluorocromos presentes en la partícula/célula, y que son excitados por la luz del láser que incide sobre la misma, emiten luz con una longitud de onda inferior a la luz del láser incidente (es decir, de diferente color), comúnmente conocida como fluorescencia[38,40,65].

Las señales luminosas (i.e., fotones) del mismo o de distinto color respecto al de la fuente de luz, generadas por la interacción de las partículas/células con el haz de luz, son recogidas por los detectores. Estos detectores transforman y multiplican la señal luminosa (fotones) en electrones, generando corriente eléctrica. El número de electrones que se generan puede regularse mediante cambios en los diferenciales de voltaje que se aplican entre las distintas placas del detector (p. ej., del PMT) y que tienen un efecto directo sobre la sensibilidad del mismo a la luz (fotones) que le llega. Dicha corriente eléctrica alimenta un amplificador, encargado de transformarla en un pulso de un determinado voltaje, proporcional al número de electrones generados. Así, el voltaje de este pulso es proporcional al número de fotones que han llegado al detector, siempre y cuando se mantenga constante el voltaje del detector y la amplificación aplicada. Posteriormente, este pulso eléctrico se transforma en señal digital que puede visualizarse de forma directa en un sistema informático (e.g. pantalla de ordenador). En dicho sistema informático, la señal digital correspondiente al pulso eléctrico puede ser definida

en base a su altura (H, abreviado del inglés “height”), anchura (W, abreviado del inglés “width”) y área (A), valores que pueden almacenarse para ser utilizados posteriormente, a la hora de representar y visualizar la señal correspondiente a cada tipo de luz, y relacionada con distintas características de una partícula o célula. En los citómetros digitales actuales, la información (datos) generada es almacenada inmediatamente después de ser convertida en señal digital, sin ninguna modificación adicional y empleando una escala linear. Para la visualización de los resultados de forma gráfica, estos pueden transformarse empleando escalas lineares, logarítmicas o mixtas (“logical”). Así mismo, los ajustes requeridos para realizar la compensación de fluorescencias entre distintos fluorocromos (ver sección 5 de esta introducción sobre la compensación de fluorescencias) también pueden aplicarse de forma dinámica mediante herramientas informáticas, en el momento del análisis de los resultados, pudiendo así elegirse y modificarse estas a conveniencia[38,40,58,63,65].

Los datos resultantes de las mediciones realizadas para cada célula son almacenados en ficheros en forma de listado, de modo que todos los resultados generados para cada uno de los parámetros evaluados, asociados a cada célula/partícula medida, quedan registrados de forma consecutiva en una matriz que contiene toda la información generada para cada una de las células analizadas, siguiendo un formato FCS (abreviado del inglés “flow cytometry standards”) estándar creado para este tipo de datos y ficheros[57,66,67].

3. Reactivos para estudios de inmunofenotipado por citometría de flujo

Los estudios inmunofenotípicos, incluidos los realizados mediante CMF, hacen uso de anticuerpos y particularmente, de anticuerpos monoclonales (AcMo), para la identificación y caracterización de células[52]. En el caso concreto del inmunofenotipado por CMF, estos reactivos deben estar además, de preferencia conjugados directamente con fluorocromos[52].

3.1. Anticuerpos

La publicación de la técnica de producción de AcMo en 1975[41] ha sido uno de los factores claves para la expansión de la CMF desde los laboratorios de investigación básica a los laboratorios de diagnóstico clínico. Así, actualmente disponemos de miles de clones de AcMo distintos, agrupados muchos de ellos bajo la designación de "clústeres" de diferenciación (CD), según el antígeno frente al que van dirigidos[57,68,69]. En este sentido, hoy día disponemos de 401 grupos de anticuerpos distintos clasificados en 371 "clústeres" de diferenciación diferentes desde CD1 a CD371[69].

La disponibilidad de un abanico cada vez más amplio de AcMo con distintas especificidades, susceptibles de ser conjugados con fluorocromos, ha supuesto un importante avance en la estandarización de las técnicas de inmunofenotipado por CMF, al contribuir a incrementar de forma significativa la reproducibilidad de los estudios fenotípicos[47,54,57]. No obstante, desde hace décadas sabemos que los clones de AcMo incluidos dentro de un mismo código CD, aunque están dirigidos frente a un mismo antígeno, pueden unirse a epítopos diferentes a lo largo del mismo; esto condiciona el que puedan observarse patrones de marcaje celular potencialmente diferentes para distintos clones dentro de un mismo CD, dependiendo por ejemplo, de la "exposición" del epítopo en la configuración cuaternaria de la proteína, o de cambios en la misma resultantes de diferentes protocolos de procesamiento de la muestra, del estado de glicosilación de la proteína o del impedimento estérico generado como consecuencia de la realización de marcajes múltiples sobre una misma célula o molécula[11,13,70].

Así mismo, dependiendo del fluorocromo con el que está conjugado un anticuerpo, podemos observar también diferentes patrones de marcaje, al variar la intensidad de fluorescencia obtenida y/o la calidad del marcaje realizado[13]. Merece destacar que, estos factores y las correspondientes diferencias observadas en los patrones de expresión de una misma proteína, van a tener un efecto directo a la hora de identificar y caracterizar distintas poblaciones celulares que coexisten en una muestra, al poder afectar la discriminación entre

ellas y/o la correcta evaluación de sus características, parámetros en los que precisamente se apoya el análisis inmunofenotípico[11,71].

A pesar de las claras ventajas que ofrecen los anticuerpos monoclonales, en determinadas situaciones resultan más atractivos y útiles los anticuerpos policlonales. Un claro ejemplo de ello lo constituye la detección de cadenas ligeras de las inmunoglobulinas (Igs), donde la diversidad de unión a distintas cadenas pesadas y la existencia de diferentes regiones constantes de la cadena ligera lambda (identificadas por distintos anticuerpos monoclonales) hacen que su detección se beneficie del uso de este tipo de anticuerpos policlonales[72,73].

3.2. Fluorocromos

Un fluorocromo es un compuesto capaz de absorber luz de una determinada longitud de onda (i.e. espectro de excitación) y posteriormente, emitir luz con una longitud de onda inferior y específica (i.e. espectro de emisión), consumiéndose en este proceso energía y generándose calor[38,40,63]. La distancia entre los puntos máximos del espectro de excitación y de emisión de un fluorocromo se conoce como la "variación de Stoke"[38,57]. Para cada fuente de luz de la que esté dotado un citómetro de flujo, pueden habitualmente emplearse ≥ 1 fluorocromos simultáneamente, siempre y cuando estos puedan ser excitados por una misma longitud de onda (es decir, tengan un perfil de excitación similar/idéntico) y emitan, cada uno de ellos, en diferente longitud de onda, preferiblemente en longitudes de onda muy separadas entre sí.

La utilización simultánea de dos o más fluorocromos marcó el inicio de la CMF multicolor que conocemos en la actualidad[74]. Sin embargo, la cercanía entre el espectro de emisión de gran parte de las parejas de fluorocromos capaces de ser excitados con una misma fuente de luz, genera cierto grado de solapamiento de las fluorescencias emitidas por cada uno de ellos, obligando a emplear distintas estrategias para eliminar dicha interferencia, lo cual se conoce como "compensación de fluorescencias" (ver sección 5 de esta introducción sobre la compensación de fluorescencias)[38,65].

En términos generales, a la hora de seleccionar un determinado fluorocromo (o grupo de fluorocromos) óptimo(s) para un experimento, deben tomarse en consideración varias características del mismo. Entre ellas se incluyen: i) un perfil de excitación y emisión que sea compatible con la configuración óptica del equipo; ii) su intensidad de fluorescencia relativa; iii) el grado de solapamiento de su espectro de emisión con otros fluorocromos; iv) que pueda ser conjugados de forma fácil, estable y reproducible con anticuerpos monoclonales y; v) que sean biológicamente inactivo al no interaccionar de forma inespecífica con la célula[46,63]. Además, el fluorocromo no debe ver afectadas sus características de excitación y emisión por factores como el tipo de muestra, la localización a nivel celular del antígeno a detectar (i.e., en la superficie celular o intracitoplasmático), la población celular diana o los protocolos de preparación de la muestra y de marcaje a emplear, entre otros factores[44,63].

Globalmente, en la actualidad se dispone de un importante número y tipos de fluorocromos susceptibles de ser conjugados para ser utilizados en estudios de inmunofenotipado por CMF. De acuerdo con su origen, estos podrían agruparse en[44,49,50,63,75,76]: i) pequeñas moléculas orgánicas como el isotiocianato de fluoresceína (FITC), los fluorocromos de la familia Alexa Flúor (AF), y las cianinas que en general muestran una intensidad de fluorescencia relativamente baja; ii) grandes moléculas proteicas como la ficoeritrina (PE) o la aloficocianina (APC), la proteína peridinina-clorofila (PerCP); y la proteína de la familia de las cianinas derivada del alga *Anemonia Majano* (AmCyan); iii) nanocristales inorgánicos fluorescentes (i.e. quantum dots) que en su día aumentaron considerablemente el número de colores disponibles, pero cuya utilización se ve muy limitada por problemas de conjugación, solapamiento, y estabilidad, y; iv) polímeros orgánicos como los fluorocromos de la familia del violeta brillante 421 (BV421), que constituyen el grupo más reciente de fluorocromos, especialmente atractivos por su elevado grado de solubilidad, especificidad e intensidad de fluorescencia, respecto a otros fluorocromos empleados en CMF[44,49,50,75-78].

Además, algunos de estos fluorocromos, pueden conjugarse entre sí o con otras moléculas para generar parejas de fluorocromos conjugados químicamente y denominados tándems de fluorocromos como por ejemplo PerCP-cianinaCy5.5 (Cy5.5), APC-Cianina7 (Cy7), APC-hilite 7 (H7) o PE-Cy7[78]. En este sentido, los tándems de fluorocromos son compuestos formados por dos fluorocromos diferentes, en los que uno de ellos se comporta como fluorocromo "donante" de fluorescencia y el otro como fluorocromo "receptor"; de este modo, el fluorocromo resultante de esta combinación estaría compuesto por un fluorocromo cuyas propiedades de excitación y emisión coinciden con las del fluorocromo donante y receptor de fluorescencia que lo integran, respectivamente. De este modo, la luz del láser excita el fluorocromo donante del tándem, que emite fluorescencia capaz de ser absorbida por el fluorocromo receptor, que finalmente emitiría luz en su longitud de onda de emisión habitual. A este fenómeno se le conoce como transferencia de energía entre fluorocromos (FRET, abreviado del inglés "fluorescence resonance energy transfer"). Mediante el empleo de tándems de fluorocromos se ha logrado ampliar notablemente las opciones de fluorocromos disponibles para cada láser, al incrementar la variación de Stokes de los fluorocromos individuales y lograr espectros de emisión de luz previamente no disponibles en moléculas individuales para un determinado espectro de excitación[12,38,78]. En la Tabla 1 se recogen un listado de las diferentes familias de fluorocromos (incluidos los tándems de fluorocromos) y los representantes actuales más importantes de cada una de ellas.

En general, en el proceso de selección de reactivos para inmunofenotipado, no solo es relevante el clon a utilizar, sino que también son muy importantes las características concretas del fluorocromo con el que este esta conjugado, siendo muy difícil establecer combinaciones óptimas *a priori*, sin haberlas evaluado previamente[11,12]. Sin embargo, el conocimiento de los niveles de expresión de un antígeno en las poblaciones celulares de interés en las que se pretenda detectar su presencia, junto con el conocimiento de las características concretas del perfil y patrón de emisión de los fluorocromos con las que este está conjugado, y la combinación

de reactivos en la que finalmente quedará incluido, son un buen punto de partida. Aun así, a dicha selección teórica debe seguir una evaluación prospectiva de cada reactivo seleccionado, individualmente y en combinación, contando con la eventual necesidad de rediseñar y reevaluar dicha combinación de forma secuencial y repetida hasta alcanzar una elevada sensibilidad y una resolución óptima entre las poblaciones celulares relevantes[61]. Como regla general, en el diseño inicial de la combinación se recomienda emparejar fluorocromos y anticuerpos siguiendo una relación inversa entre la densidad de expresión del antígeno y la intensidad de fluorescencia proporcionada; es decir, emplear aquellos fluorocromos más sensibles para detectar antígenos celulares que muestren una baja expresión y los fluorocromos más tenues para moléculas altamente expresadas[63,71,79].

De la información generada en los experimentos de evaluación de un reactivo, resulta especialmente útil para evaluar la calidad del mismo, el índice de tinción (SI, abreviado del inglés "stain index")[43], que permite relacionar la intensidad de fluorescencia propia de una población celular de referencia específica, con el ruido de fondo presente en ese canal y con ese marcador en una población control que no expresa dicho marcador, al reflejar el valor de SI el poder de resolución del reactivo evaluado.

Finalmente, a la hora de diseñar un panel de combinaciones de anticuerpos o una combinación de anticuerpos, resulta también importante considerar la disponibilidad de los reactivos incluidos en el mismo.

4. Calibración del citómetro de flujo

Un requisito imprescindible a la hora de estandarizar las mediciones y obtener resultados altamente reproducibles y comparables, reside en la utilización de un instrumento de medida bien calibrado. El citómetro de flujo, como otros equipos de medición, permite cierto grado de flexibilidad en sus condiciones de medida; con ello se amplía el rango de detección y

Tabla 1. Fluorocromos: familias de fluorocromos y sus principales representantes[44,49,50,75-78*]

Tipo de fluorocromo	Familia	Representantes más comunes
Pequeñas moléculas orgánicas	Derivados de Xantinas	FITC; Texas Red[a]
	Alexa Flúor (AF)	AF488; AF647; AF700
	Cianinas	Cy3; Cy5; Cy5.5; Cy7
		Dylight405[a]; DyLight488[a]; DyLight594[a]; DyLight650[a]; DyLight755[a]
	Otros	Cascade Blue[a]; PacB; Cascade Yellow[b]; PacO; Krome Orange[c]; eFluor450[d]; eFluor660[d], HV450[e], HV500[e], VioBlue[f], VioGreen[f]
Grandes moléculas proteicas		PerCP; AmCyan[e]
	Filibicoproteinas	PE; APC
Nanocristales	Quatum dots (Qdot)	Qdot525[a]; Qdot545[a]; Qdot605[a]; Qdot705[a]
Polímeros orgánicos	Violeta brillante (BV)	BV421[e]; BV510[e]
Otros		OC515[g]
	Ultravioleta brillante (BUV)	BUV395[e]
	Azul brillante (BB)	BB515[e]
Tándems de fluorocromos	Tándem de PE	PE-Cy5; PE-Cy5.5; PE-Texas Red; PE-CF594[e]; PE-eFluor610[d]; PE-Cy7; PE-AF647; PE-Vio770[f] PE-AF750;
	Tándem de PercCP	PerCP-Cy5.5; PerCP-eFluor710[d]; PerCP-Vio700[f]
	Tándem de APC	APC-Cy7; APC-H7[e]; APC-R700[e]; APC-AF700; APC-AF750; APC-C750[g]; APC-Vio770[f]
	Tándem de polímeros orgánicos	BV605[e]; BV650[e]; BV711[e]; BV786[e]
	Otros	BUV496[e]; BUV661[e]; BUV737[e]; BUV805[e]

*complementada con información disponible de las empresas comercializadoras en sus páginas oficiales de internet
FITC, isotiocianato de fluoresceína; Cy3, cianina3; Cy5, cianina5; Cy7, cianina7; PacB, pacific blue; PacO, pacific orange; HV, Horizon Violet; PerCP, proteína peridinina-clorofila; AmCyan, proteína cianina fluorescente de *Anemonia Majano*; OC, orange Cytognos; Comercializador principal o exclusivo: [a], ThermoFisher Scientific (Waltham, MA, EEUU); [b], BioLegend (San Diego, CA, EEUU); [c], Beckman Coulter (Brea, CA, EEUU); [d], Affymetrix/eBiosciences (San Diego, CA, EEUU); [e], Becton Dickinson Biosciences (San Jose, CA, EEUU); [f], Miltenyi Biotech (Bergish Gladbach, Germany); [g], Cytognos SL (Salamanca, España)

cuantificación de diferentes señales y, en paralelo, el número de aplicaciones en las que puede emplearse el mismo equipo. Aunque esto impide el uso de una calibración en principio única que resulte óptima para las distintas aplicaciones posibles, no impide la utilización de

calibraciones distintas y óptimas cada una de ellas, para cada aplicación. Respecto a las aplicaciones de inmunofenotipado por CMF y las aplicaciones de CMF en hemato-oncología, hoy se conoce que es posible emplear una calibración prácticamente universal para todas ellas; dicha calibración ha de tener en cuenta de antemano, las características de las células y de los tipos de muestras habitualmente utilizadas para este fin[14,57,58].

En general, algunos aspectos claves en la calibración del equipo no son del dominio del usuario promedio y su ajuste no estaría a su alcance, siendo objeto de calibración y ajuste por parte del fabricante del equipo, especialmente en citómetros de uso clínico. En consecuencia, aspectos como la potencia de los láseres, su alineación con respecto al flujo de la muestra, la eficiencia y características de los fotodetectores y amplificadores, el ajuste fino de las presiones que gobiernan el sistema de fluidos y, el alineamiento y colocación de los prismas, son elementos cuya calibración depende directamente del servicio técnico del fabricante, siendo un prerrequisito para una calibración óptima del equipo que tendrá que completar realizar posteriormente el usuario en el laboratorio de diagnóstico clínico[14,80].

A su vez, el proceso de calibración del citómetro de flujo de forma específica para una aplicación como el inmunofenotipado de hemopatías malignas por CMF, y que debe completar el usuario, tiene como primer objetivo, establecer el punto óptimo en el que la sensibilidad de los detectores permita la medición exacta y eficiente de los diferentes tipos de señales asociados a las muestras que sean medidas posteriormente. Esto se logra mediante la regulación del voltaje que se aplica a cada detector y que determina su sensibilidad. La definición de este punto óptimo de detección se establece mediante la utilización de partículas de referencia cuyas características en cuanto a tamaño y/o fluorescencia son estables y conocidas de antemano (estándares). Habitualmente, estas partículas de referencia son partículas artificiales con forma de microesfera (i.e. esferas de calibración) o partículas biológicas (i.e. poblaciones celulares concretas) similares a las que serán evaluadas posteriormente. Las partículas de origen biológico son menos estables y su variabilidad (biológica) intrínseca condiciona el que en diferentes

momentos puedan obtenerse, calibraciones completamente reproducibles. Aun así, las partículas biológicas siguen utilizándose para establecer la calibración de algunos parámetros como los relacionados con medidas de dispersión de luz. Las microesferas artificiales son más estables y eficientes, cumpliendo con mayor precisión las características de un calibrador estándar. Además, pueden tener diferentes tamaños, densidades e intensidades de fluorescencia asociada, para los distintos detectores de los que está dotado un citómetro de flujo. Por todo ello, estas últimas son las partículas más utilizadas a la hora de establecer una calibración sensible y óptima en los equipos de citometría[14,57,58].

El rango y los límites alcanzados para cada medición vienen determinados por las características y sensibilidad de cada detector. Así, para poder evaluar la información generada, es necesario el ajuste individual de cada uno de los detectores de luz disipada y de fluorescencia, para que los valores de las mediciones a realizar se encuentren todos ellos dentro del "rango" de detección alcanzado y de la escala de visualización disponible para cada parámetro; a este rango se denomina habitualmente ventana de análisis o de la escala analítica[14,80]. Adicionalmente, estos límites teóricos de detección, deben quedar restringidos a la zona en la que el detector presenta mayor sensibilidad al voltaje administrado, con un comportamiento lineal de respuesta al mismo. Esta zona de linearidad puede calcularse mediante la evaluación simultanea de al menos dos partículas con tamaño y/o fluorescencias conocidas y diferentes, estableciendo cocientes entre ambas y confirmando, además, los límites del voltaje entre los cuales esa relación se mantiene estable e inalterada[14,80].

En el caso de mediciones de fluorescencia realizadas en el límite inferior de detección, el voltaje que define el punto de mayor eficiencia del detector se obtiene usando una partícula de referencia con fluorescencia débil, ligeramente superior a los niveles basales de fluorescencia (autofluorescencia) de las células hematopoyéticas a medir, siempre y cuando ésta esté claramente por encima de la zona de ruido[81]. La sensibilidad del detector y su capacidad de resolución en este punto, se calculan relacionando el coeficiente de variación (CV) resultante de

la medición de dichas partículas de referencia con el voltaje aplicado al detector. Para ello ha de determinarse el voltaje a partir del cual el CV obtenido al medir dicha partículas es el menor de los detectados y permanece inalterado, aun cuando se apliquen voltajes superiores; es decir, cuando ya no existe más contribución del ruido electrónico (luz que no proviene del propio sistema, sino luz externa que llega al detector) a la señal[82]. Con ello, la ventana de análisis estará ocupada en su límite inferior, por los eventos con la menor fluorescencia posible; en la práctica, con eventos que no presentan marcaje y cuya medición refleja únicamente el nivel de autofluorescencia propia de esas partículas/células, situado ligeramente por encima del nivel de ruido de fondo[80,82]. Este valor se considera como el punto óptimo de partida, aunque habitualmente cambiará con posterioridad, debido a los ajustes adicionales realizados para la calibración específica de cada tipo de medición a realizar. En esta última etapa, debe confirmarse por ejemplo, que al utilizar dicho valor (voltaje), las partículas de interés que presentan elevada fluorescencia siguen localizándose dentro del límite superior de la escala analítica, además de estar dentro del rango de linearidad del detector[82].

En el caso de los detectores especializados en la medición de la luz dispersada, la ventana de análisis tiene igualmente como límites los que vienen definidos por el funcionamiento de los propio detectores, debiendo calibrarse de tal manera que todos los eventos de interés se encentren igualmente dentro de los límites (rango) de detección y de linearidad del detector, excluyendo en la medida de lo posible, los detritos o restos celulares que carecen de relevancia mediante la colocación de un umbral en la región inferior del detector de medida de FSC[65,80]. En la práctica, la estandarización de los parámetros de medida de luz dispersada resulta mucho más sensible a la configuración de cada equipo de medida, ya que, por ejemplo, depende de los ángulos de medida de FSC y SSC, del ancho y ángulo de la barra de obscuración colocada delante del detector, o de su alineamiento con el haz de luz. Por todo ello, resultan medidas más difíciles de estandarizar entre equipos clínicos de diferente generación o de distintos fabricantes[14].

Una vez se han calibrado (y optimizado) los detectores de FSC, SSC y fluorescencia, se eligen referencias que posean una fluorescencia conocida y estable, pero asociadas a niveles elevados de detección de luz dispersada y de fluorescencia. Al realizar la medición de estos estándares, en cada detector se generan valores de referencia (valores "diana") que deben ser alcanzados y cumplidos a partir de entonces en cada medida realizada posteriormente de las mismas, en diferentes días y en distintos laboratorios. En este sentido, estas partículas de referencia y los criterios de calidad definidos en relación con los resultados que deben obtenerse tras su medición, cumplen tres objetivos principales: i) ser útiles para reproducir a lo largo del tiempo, con una misma calibración y en un mismo equipo, resultados de medidas distintas del mismo lote de partículas de referencia (estándares); ii) poder transferir las condiciones obtenidas en un instrumento de medida, a otros equipos equivalentes, y; iii) permitir una monitorización fácil y rápida de los equipos de medida, de modo a poder comprobar y demostrar un funcionamiento estable, dentro de los límites que aseguran una evaluación óptima y la reproducible de los resultados obtenidos[57].

Finalmente, merece destacar que, los diferentes aspectos abordados en esta sección se refieren de forma específica a los citómetros de flujo digitales, ya que son los equipos que actualmente más se utilizan en los laboratorios de diagnóstico clínico. No obstante, en general, todo lo expuesto es válido también para citómetros analógicos, aunque las recomendaciones específicas para la calibración de estos últimos, pueden diferir ligeramente en algunos aspectos[80,82].

5. Compensación de fluorescencias

La necesidad de compensar las fluorescencias se puso en evidencia tan pronto como se empezaron a utilizar marcajes simultáneos con dos o más fluorocromos en citómetros dotados en aquel momento de un único láser[74]. En este sentido, cuando se utilizan dos fluorocromos que se pretende sean excitados con una misma fuente de luz (un láser), es casi obligatorio que los

espectros de excitación de ambos sean similares, pero que cada uno muestre un espectro de emisión suficientemente separado del otro que permita discriminar entre la fluorescencia proveniente de cada fluorocromo con una interferencia mínima entre ambos. Dado que en la práctica, es difícil que dos fluorocromos que se excitan a la misma longitud de onda presenten espectros de emisión totalmente separados y sin solapamiento entre ellos, parte de la emisión de cada uno de los fluorocromos empleados suelen llegar al detector del otro fluorocromo. Como consecuencia de lo anteriormente expuesto, la señal obtenida mediante las mediciones realizadas en un detector a una determinada longitud de onda, está compuesta en principio, por la señal del fluorocromo asociado a esa posición; sin embargo, incluye también la posible luz contaminante proveniente de los demás fluorocromos empleados simultáneamente y cuyo espectro de emisión se solapa parcialmente con el del fluorocromo primario (Figura 3). Por todo ello, para la evaluación de la fluorescencia específica de cada fluorocromo empleado en una combinación multicolor, debemos asegurar que las interferencias entre los distintos fluorocromos son tenidas en cuenta y eliminadas. Ello permitirá además, una visualización e interpretación de los datos adecuada y (más) objetiva por parte del experto (Figura 3).

Figura 3. Imagen ilustrativa del solapamiento de fluorescencias entre 2 fluorocromos (FITC -fluorocromo primario- vs PE -fluorocromo secundario-) sin aplicar correcciones (panel A) y una vez calculado y aplicado el valor de compensación óptimo para estos fluorocromos (panel B).

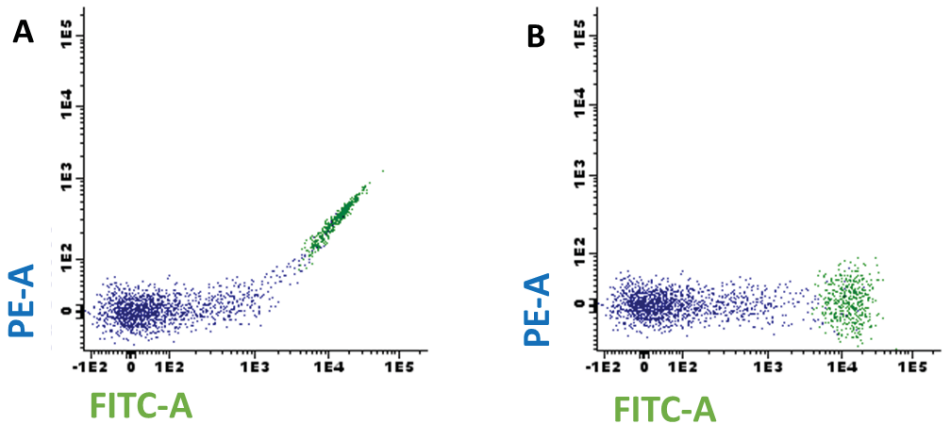

FITC, isotiocianato de fluoresceína, PE, ficoeritrina

Con el fin de evitar y minimizar los efectos adversos de la interferencia entre las señales de diferentes fluorocromos podemos, en primer lugar, seleccionar una combinación óptima de filtros y espejos que minimice la entrada a cada detector, de la luz de aquellos fluorocromos secundarios que no son específicos del mismo, sin afectar a la del fluorocromo primario asociado a ese detector. Aun así, resulta imposible evitar completamente dicha interferencia. Dado que la luz asociada a cada fluorocromo que contamina cada uno de los detectores es constante para un determinado fluorocromo concreto, siempre que la configuración óptica y la calibración de equipo sean estables, esta puede ser cuantificada y posteriormente eliminada mediante distintas fórmulas matemáticas, en un proceso que se denomina compensación de fluorescencias[49,82,83] (Figura 3). A modo de ejemplo, tanto el FITC como la PE son fluorocromos excitados de forma específica por luz azul (488 nm) con picos máximos de emisión suficientemente separados (i.e. 530 nm y 570 nm, respectivamente); esto permite que las fluorescencias del FITC y de la PE sean recogidas por detectores diferentes. Sin embargo, una cantidad relativamente pequeña de fluorescencia generada por el FITC contamina la luz recogida en el detector de la PE (Figura 3, panel A). Esta contaminación, no puede ser eliminada mediante filtros o espejos ya que coincide con la zona del espectro donde se recoge la señal emitida por la PE. De este modo, tiene que ser cuantificada la interferencia y posteriormente substraída del valor de fluorescencia obtenido en el detector de la PE. Esta corrección garantiza que la fluorescencia final cuantificada en el detector de PE, es equivalente en realidad a la fluorescencia, solo a la que se genera por el fluorocromo específico de ese detector y que se pretende recoger en el mismo; en este caso la fluorescencia de la PE (Figura 3, panel B).

Los diferentes protocolos de procesamiento de muestras, las condiciones en las que se almacenan los reactivos o en que se realizan las mediciones, o incluso las interacciones que pueden existir entre los fluorocromos y las células o elementos de las células marcadas, pueden potencialmente cambiar el perfil de fluorescencia emitido por un determinado fluorocromo,

debiendo tenerse en cuenta estas variables adicionales en el cálculo (y evaluación) de la compensación de fluorescencias[80,83]. En este sentido, merece destacar que en ocasiones, el deterioro del reactivo (e.g., del fluorocromo, como es el caso de los tándems de fluorocromos), puede hacer imposible mantener una compensación de fluorescencias adecuada para su medición[14,84].

Una limitación importante de la compensación de fluorescencias, consecuencia directa de la aplicación de la misma, es la reducción de la sensibilidad en aquellos detectores que reciben alta contaminación por parte de fluorocromos secundarios (i.e., fluorocromos asociados a otros detectores), debido al "ensanchamiento" de los datos en el eje en el que se cuantifica la fluorescencia asociada al fluorocromo donante, aun cuando están adecuadamente compensados; esto es en parte debido también, al efecto de la autofluorescencia de las células no marcadas, de errores introducidos por algunos amplificadores logarítmicos con un comportamiento subóptimo[83] y de errores en el recuento de los fotones que llegan al detector. Como consecuencia, además de una sensibilidad reducida del detector, este fenómeno interfiere con la aproximación clásica de análisis de datos de citometría empleando histogramas uni o biparamétricos para la visualización de los resultados y ventanas de análisis de tipo cuadrante, o la interpretación de los niveles de expresión de un marcador poco intenso vs los niveles basales de autofluorescencia (i.e. negatividad vs positividad)[78,82,83].

Actualmente, la necesidad de realizar una compensación de florescencias para experimentos de ≥ 8 colores se traduce en un procedimiento relativamente complejo, que involucra la valoración de todas las posibles combinaciones de dos en dos, de todos los fluorocromos empleados, siendo virtualmente imposible hacer un cálculo óptimo manualmente[71]. Además, el empleo de conjugados de fluorocromos de tipo tándem complica aún más si cabe el proceso, debido a diferencias entre lotes, y entre fluorocromos, e incluso con variaciones a lo largo del tiempo observados para un mismo lote de un reactivo[14,84,85].

En la práctica, para el cálculo de la compensación de fluorescencias se utilizan dos poblaciones de referencia para cada fluorocromo: una positiva y otra negativa[78,85]. Idealmente, entre sus niveles de fluorescencia debería existir la máxima diferencia posible, aunque siempre dentro del rango de medida del detector correspondiente. El proceso se completa, una vez se logre igualar la cantidad de fluorescencia obtenida para ambas poblaciones en cada uno de los detectores de fluorescencia secundaria y diferentes al detector primario empleado para medir la fluorescencia real del control (las partículas de referencia) positivo. En este sentido, resulta muy importante que ambos controles (positivo y negativo) tengan niveles basales de autofluorescencia similares[78].

En general, los perfiles de excitación y emisión obtenidos para la mayoría de los fluorocromos de molécula única, permanecen estables e invariables una vez conjugados con diferentes anticuerpos. Sin embargo, este no es el caso de los fluorocromos en tándem, que requieren casi de compensaciones específicas y de reactivos (e incluso lote de reactivo), debido a las características de producción de los mismos y los cambios posteriores que estos sufren una vez colocados en medio líquido[63,78,80]. De lo anteriormente expuesto se deduce, la necesidad de introducir un control de compensación específico para cada conjugado con fluorocromos de tipo tándem (y particularmente cada lote de dicho conjugado) incluido en un panel de dos o más combinaciones de anticuerpos en los que se utilicen dichos tándem de fluorocromos.

Como estándares para establecer la compensación de fluorescencias más adecuada, en la actualidad tenemos varias opciones. Pueden emplearse esferas de captura, capaces de captar una gran variedad de anticuerpos, siempre que estos se correspondan con el isotipo de inmunoglobulina para la(s) que las esferas está(n) diseñada(s). En general, las esferas de captura resultan ser estándares adecuados, que pueden emplearse para la compensación de fluorescencias entre fluorocromos y conjugados de fluorocromos que sean utilizados directamente en los paneles para los cuales se establece dicha compensación de fluorescencias. Sin embargo, como limitaciones más importantes, merece destacar que, no permiten unir todos

los tipos de anticuerpos, y proporcionan una intensidad de fluorescencia para la población positiva relativamente tenue, que puede llegar a ser insuficiente, es decir menor que la de las poblaciones celulares que se pretenden analizar posteriormente[78]. En este sentido, otro tipo de partículas estándar que puede utilizarse son esferas de espectro equivalente, es decir, esferas que están recubiertas de moléculas de los fluorocromos concretos para los cuales pretendemos calcular la matriz de compensación de fluorescencias, simplificando el procesamiento requerido y evitando la necesidad de unir los anticuerpos específicos a la esfera, paso requerido en el caso de las esferas de captura[86,87] (p. ej., BD FC Beads 8-color kit for BD ONEFLOW, BD). Sin embargo, las posibles diferencias en la estructura (y en consecuencia en los perfiles de excitación y emisión) de los fluorocromos de dichas esferas de referencia, respecto a la de los fluorocromos a emplear en los ensayos, unido a la posible baja intensidad de la población positiva y la imposibilidad de utilizar estas esferas de espectro equivalente como controles específicos para distintos lotes de reactivos que emplean tándems de fluorocromos, son aspectos que limitan también la utilidad de este segundo tipo de esferas de referencia[87]. Finalmente, cabe también la posibilidad de emplear células[14,78,85]. Esta opción, obliga a disponer de muestras biológicas que puedan ser utilizadas en el momento de establecer la compensación de fluorescencias, siendo además posible que el marcador a compensar no se encuentre expresado en la muestra de la que se dispone.

En resumen, en la actualidad no disponemos de estándares óptimos para establecer una adecuada compensación de fluorescencias en el día a día, empleándose habitualmente estrategias mixtas que incluyen dos o más tipos diferentes de estándares en un solo experimento de compensación de fluorescencias, en el que se asigna el estándar más apropiado para cada marcador específico a utilizar, sin que esto tenga un impacto negativo sobre los resultados que se obtienen posteriormente[61,78,79,82,88].

6. Procesamiento de muestras humanas para inmunofenotipado por citometría de flujo

Cualquier proceso de estandarización no estaría completo si no incluyera también la estandarización de aquellos aspectos relacionados con la muestra, y la preparación de la misma, para su adecuada lectura en el citómetro de flujo[14]. En el momento actual, existen diferentes protocolos estandarizados, y distintas recomendaciones de consenso, en relación con el procesamiento de muestras para inmunofenotipado por CMF, ya sea para la detección de antígenos de la membrana en la superficie celular (Sm, abreviado del inglés "surface membrane") o para marcajes que incluyan la detección simultanea de marcadores de membrana e intracitoplasmáticos (Cy, abreviado del inglés "cytoplasmic"); de igual manera, existen recomendaciones y protocolos de consenso adaptados de forma específica a la preparación y marcaje de distintos tipos de muestras (e.g. líquido cefalorraquídeo -LCR- vs SP)[13,15-22]. Sin embargo, en estos protocolos habitualmente no existe referencia a los resultados de la evaluación global de las variables implicadas, (por ejemplo en relación con el empleo de distintas soluciones de lisis de hematíes, de fijadores o de permeabilizantes de la membrana citoplasmática). Esto resulta especialmente relevante debido a que, cualquier modificación introducida en los pasos y en los reactivos empleados al procesar la muestra, tiene un impacto (mayor o menor) sobre los resultados obtenidos, incluyendo las características de dispersión de luz, el perfil de expresión antigénica o en el nivel de autofluorescencia de distintas subpoblaciones celulares, y su distribución en la muestra[13,20,23-25].

En condiciones óptimas, cualquier protocolo de preparación de muestras para inmunofenotipado por citometría de flujo, debería cumplir con las siguientes características: i) mantener una adecuada resolución entre de las poblaciones celulares mayoritarias de la muestra de acuerdo a sus parámetros de dispersión de luz; ii) minimizar la pérdida de células; iii) preservar al máximo la estabilidad de los epítopos antigénicos, de los fluorocromos y de la correspondiente intensidad de fluorescencia; iv) mantener bajos niveles de autofluorescencia y

de “debris”. En la elección final del protocolo más adecuado, debe tenerse en cuenta el equilibrio entre el poder alcanzar los objetivos del estudio y factores como el tiempo de procesamiento o el coste.

6.1. Variables pre-analíticas asociadas a la muestra

El tipo de tejido que debe someterse a análisis para el diagnóstico inmunofenotípico de hemopatías malignas varía, de acuerdo con las manifestaciones y el tipo de enfermedad subyacente. De todas las muestras analizadas, la SP y la médula ósea (MO) son las que más frecuentemente llegan al laboratorio de citometría de flujo[1,89]. Sin embargo, las biopsias de tejido sólido, punciones por aspiración con aguja fina (PAAF) o algunos líquidos corporales (e.g. LCR; humor vítreo o líquido sinovial, pleural o ascítico), son también referidos para estudio, con relativa frecuencia.

En muestras que contienen o puedan contener sangre, como las muestras de SP y/o MO, es importante ya de inicio, la selección del anticoagulante. En este sentido, los anticoagulantes más frecuentemente utilizados son el etilendiaminotetraacetato (EDTA), la heparina de sodio (HEP) y el citrato ácido de dextrosa (ACD)[16]. La elección inicial del anticoagulante con el que debe obtenerse la muestra, depende de varios factores entre los que se incluyen: el tipo de muestra, la necesidad o no de transporte o almacenamiento de la misma y/o el protocolo de procesamiento de la muestra que se empleará posteriormente. Así, en el caso de las muestras de SP que se emplean para realizar recuentos automáticos de células sanguíneas, se recomienda el uso de EDTA, mientras que en caso de que las muestras deba compartirse para estudios citogenéticos, la HEP sería el anticoagulante de elección. De estos anticoagulantes, la HEP permitir la conservación de la muestra en mejores condiciones por periodos de tiempo más prolongados, mientras que el EDTA requeriría un procesamiento inmediato[16]. Sin embargo, el tipo de anticoagulante también puede tener un impacto importante en la detección de antígenos celulares, siendo su efecto variable dependiendo del tipo de célula y antígeno que

pretendemos estudiar[90]. En el caso de biopsias de tejido, PAAF o LCR, el uso de anticoagulación aunque teóricamente no sería necesario, podría estar recomendado, ante la posibilidad de que exista contaminación sanguínea de la muestra. En cambio, en este tipo de muestras es obligatorio el uso de medio de cultivo o de preservantes artificiales, para mantener la viabilidad y/o la integridad celular[22,91].

Una vez extraída, la muestra debe procesarse y adquirirse de forma inmediata; si esto no es viable, debe intentarse hacerlo en el menor tiempo posible, habitualmente en las primeras 24 h tras la obtención de la muestra en el caso de SP y MO[16]. Una muestra envejecida puede resultar significativamente alterada, dificultando la identificación por ejemplo, de algunas poblaciones de células patológicas B, subestimando el grado de infiltración de la muestra por las mismas, especialmente en muestras con células que presentan una elevada tasa proliferativa (e.g., células del linfoma de Burkitt -LB-) o muestras en las que la viabilidad celular se ve comprometida por el propio tipo de muestra (e.g., LCR). Siempre que no sea posible el análisis de la muestra en el tiempo recomendado, debe documentarse el retraso y establecer criterios de tolerancia para que los resultados sean concluyentes, especialmente cuando no resulta posible (o viable) obtener una nueva muestra.

6.2. Protocolos de marcaje celular para inmunofenotipado por citometría de flujo

Habitualmente, para el marcaje de muestras celulares con anticuerpos para citometría de flujo se siguen un conjunto de pasos básicos comunes: i) incubación (marcaje) con los anticuerpos conjugados con fluorocromos; ii) exclusión (o lisis) de la población de células eritroides maduras; iii) lavado(s) de las células, y; iv) estabilización o fijación de los leucocitos (u otras células) de la muestra[13,20,23-25]. La utilización de protocolos que involucren marcajes indirectos con anticuerpos primarios no conjugados con fluorocromo[25], no son aplicados en general en la práctica diaria, en el laboratorio de citometría clínica.

Desde hace tiempo se conoce que existen diferencias en los resultados obtenidos, dependiendo de los reactivos concretos empleados, de los procedimientos de lavado y su número, del tiempo global de procesamiento de la muestra o de las soluciones de lisis y fijadoras empleadas, factores todos ellos que afectan directamente a las características físicas de las células, originando diferentes patrones de dispersión de luz, pérdidas (selectivas) de poblaciones celulares (sobre todo en los protocolos que involucran más lavados), reducción de la intensidad de fluorescencia específica de algunos anticuerpos, e incremento de los niveles de autofluorescencia y "debris". Merece destacar que, aunque en términos globales se observen tendencias, con frecuencia estos efectos varían según la población celular, el anticuerpo/antígenos en concreto a estudiar y el procedimiento de marcaje empleado[13,16,20,23-25].

6.3. Detección de marcadores intracelulares

Algunos de los marcadores más relevantes para el diagnóstico de las hemopatías malignas se encuentran en el interior de las células. En este sentido, muchas de las proteínas producidas por las células para ser expresadas posteriormente en la membrana citoplasmática o liberadas al medio, se acumulan inicialmente en el citoplasma (e.g., cadenas ligeras o pesadas de Ig y CD3); otras proteínas, aunque son altamente específicas de un tipo celular, se producen para llevar a cabo funciones a nivel intracelular, ya sea en el núcleo -e.g., desoxinucleotidil-transferasa terminal (TdT)- o a nivel citoplasmático -e.g., mieloperoxidasa (MPO), Lisozima, peroxidasa del eosinófilo-. Muchas de estas moléculas son de producción temprana y son altamente específicas de línea celular, por lo que su detección es de crucial importancia en el diagnóstico de las hemopatías malignas más inmaduras[13,92,93].

Respecto a las técnicas de fenotipado para antígenos de membrana, la detección de marcadores intracelulares involucra pasos adicionales de fijación y permeabilización celular. En este sentido, existen diferentes soluciones comerciales para permitir la detección de este tipo

de antígenos: BD Perm/Wash buffer (BD Biosciences, -BD- San José, CA, EEUU), Fix&Perm (AN DER GRUB Bio Research GmbH, Viena, Austria), IntraStain (Dako, Glostrup, Dinamarca) e IntraPrep (Beckman Coulet -BC-; Miami, FL, EEUU), entre otras[13,23,24]. De nuevo, cada una de ellas presenta efectos específicos bien conocidos sobre las características físicas de las células, los niveles de autofluorescencia y los patrones de expresión antigénica, dependiente estos últimos a su vez, de los clones, conjugados o fabricantes de los reactivos empleados[13,23,24,26].

6.4. Exclusión de glóbulos rojos

Los glóbulos rojos o hematíes son una población celular altamente representada en muestras de SP y MO. Su elevada concentración en este tipo de muestras (> 99 % de la celularidad global) puede interferir con el análisis. Clásicamente, se han eliminado los hematíes de muestras a estudiar por CMF mediante métodos de centrifugación en gradiente de densidad, capaces además de enriquecer la muestra en células mononucleadas al eliminar de forma selectiva también, los polinucleares neutrófilos. En la actualidad, debido a la gran pérdida de células observada con esta aproximación, la separación de células mononucleadas mediante gradiente de densidad se ha sustituido por métodos en los que los hematíes se eliminan, después del marcaje, mediante lisis osmótica[2,11,94]. Como principales ventajas, la lisis de los eritrocitos está asociada a una menor manipulación de la muestra, una mayor recuperación celular y a tiempos más cortos de procesamiento. Sin embargo, dependiendo de la solución de lisis utilizada para inducir la destrucción de los hematíes, se observan diferentes cambios en las características físicas de las demás células (marcadas) de la muestra y con frecuencia también, en los patrones de marcaje, al menos de algunos marcadores[19,20].

Entre otras soluciones hipotónicas, pueden emplearse: cloruro de amonio (NH_4Cl), FACS Lysing solution (BD), Quicklysis (Cytognos SL, Salamanca, España) o VersaLyse Lysing solution (BC). Estas últimas soluciones de lisis comerciales incluyen componentes como paraformaldehído (PFA), etilenglicol y metanol -i.e., FACS Lysing solution, nº de catálogo 349202,

información técnica del fabricante (TDS, abreviado del inglés "Technical Data Sheet")- o aminas que adquieren su capacidad lítica al entrar en contacto con la anhidrasa carbónica eritrocitaria (i.e., VersaLyse, nº de catálogo IM3648, TDS). De todas ellas, solo FACS Lysing solution contiene componentes que actúan como fijadores (i.e., PFA).

6.5. Titulación de anticuerpos

La intensidad de fluorescencia que potencialmente puede alcanzar una célula cuando se marca un determinado antígeno expresado en la misma, depende de los niveles de expresión del mismo, del número de células marcadas, la concentración del anticuerpo en el volumen final de marcaje, y del tiempo y condiciones del marcaje (p. ej. la temperatura). En este sentido, la intensidad de fluorescencia obtenida para un determinado marcador, solo sería la máxima posible cuando la cantidad y concentración de anticuerpo es suficiente para ocupar (i.e., saturar) todos los sitios disponibles del antígeno a detectar, en un tiempo aceptable de incubación en condiciones idóneas[70,95]. Solo en dichas condiciones podemos asegurar que la intensidad de fluorescencia alcanzada refleja fielmente la densidad de la molécula estudiada, permitiendo atribuir cualquier variación encontrada a otros factores como procesos normales de regulación de la expresión de dicha proteína (e.g., cambios madurativos), alteraciones genéticas y del micromedioambiente. Una baja concentración de anticuerpo se asociaría a niveles inferiores (y más heterogéneos) de expresión de la molécula diana del mismo, respecto a los esperados; por el contrario, un exceso del reactivo podría conllevar un aumento de uniones inespecíficas con incremento de la intensidad de fluorescencia en varias poblaciones celulares que no expresan ese marcador, además de las células diana del anticuerpo, dando lugar incluso a poblaciones celulares falsamente positivas[96]. En la mayoría de los casos, la cinética de unión antígeno-anticuerpo sigue una curva sigmoidea, siendo el punto óptimo de concentración del anticuerpo aquel donde la población de referencia con expresión del antígeno se encuentra en la zona plana de la curva, posterior a (y alejada de) la zona de crecimiento rápido o exponencial, mientras las

poblaciones de referencia negativas (que no expresan el antígeno y tienen baja susceptibilidad a uniones inespecíficas) se mantienen en el nivel más bajo posible de la escala[97]. El cálculo de este punto se realiza fácilmente mediante la medición de las intensidades de fluorescencia de las poblaciones de referencia positivas y negativas para concentraciones crecientes de anticuerpo, hasta detectar concentraciones que muestren un SI máximo (i.e. intensidad de fluorescencia máxima en la población positiva sin que existan apenas cambios en la negativa)[14,39,70]. Ni que decir tiene que, para poder establecer la concentración y el título apropiado de un anticuerpo, el protocolo de preparación de la muestra (en lo que se refiere a procedimiento, volúmenes y concentración de células) debe ser óptimo y mantenerse inalterado para todas las mediciones realizadas. El SI informa además, sobre el impacto de la dispersión de la población negativa en la separación de las poblaciones de referencia, como consecuencia de uniones inespecíficas o de la compensación de fluorescencias, al calcularse mediante la división entre la diferencia de las intensidades de fluorescencia de las poblaciones de referencia positiva(s) y negativa(s) y el doble de la desviación estándar (DE) de la población negativa de referencia[43]. Así, este indicador (i.e., SI) traduce el poder de resolución de un conjugado específico y puede utilizarse, tanto para determinar su concentración idónea, como para evaluar y comparar el funcionamiento global, individual y/o en combinación, de los anticuerpos.

7. Diseño de combinaciones y paneles de combinaciones de anticuerpos

Los tejidos linfoides y hematopoyéticos están constituidos todos ellos, por una mezcla de diversas poblaciones celulares pertenecientes a diferentes líneas, en distintos estadios madurativos y funcionales[6,27,64,98-100]. Así, la definición inmunofenotípica de una población celular concreta y la posibilidad de detectarla, identificarla (y discriminarla) del resto de poblaciones celulares que coexisten en la muestra, requiere de forma prácticamente sistemática, del marcaje con dos o más marcadores celulares característicos de la población celular de interés[28]; de igual modo, a medida que aumentamos el número de marcadores

empleados, se incrementa también el número de poblaciones celulares susceptibles de ser identificadas[46]. Con relativa frecuencia, para identificar una población celular normal o patológica, resulta necesario no solo emplear combinaciones de marcadores que permitan su identificación positiva, sino también el uso de otros marcadores complementarios que aumenten la especificidad, mediante la exclusión de posibles poblaciones celulares que pueden contaminar la región seleccionada. Dicho de otra manera, el incremento en el número de parámetros que pueden medirse simultáneamente se traduce a la vez, en una mayor especificidad a la hora de identificar una determinada población celular de interés y la posibilidad de realizar su detección específica, incluso cuando dicha población celular esté presente en baja frecuencia en la muestra (i.e. mayor sensibilidad). Todo ello se traduce en una mayor eficiencia[29], asociada al requerimiento de una menor cantidad de muestra (i.e., menos alícuotas o tubos para un mismo número de marcadores a estudiar) y de un menor número de tubos para el análisis[12,79]. Por todo lo anteriormente expuesto, la detección de un número progresivamente más elevado de parámetros se ha convertido en un requerimiento casi sistemático y permanente, especialmente si además de la identificación de las poblaciones celulares presentes en una muestra, tenemos como objetivo su caracterización con fines diagnósticos en enfermedades que pueden llegar a requerir de ≥ 30 parámetros fenotípicos distintos[7,27,28,30,31,33-35,37,101,102]. Esto contrasta con el hecho de que en la práctica clínica, la mayoría de los equipos disponibles actualmente para uso diagnóstico se limitan a la detección de entre 10 y 12 parámetros simultáneamente[103,104].

Con el fin de superar esta limitación se han establecido y ensayado desde hace años, varias estrategias. De todas ellas, las estrategia más extendida se fundamenta en la utilización de múltiples alícuotas de la misma muestra marcadas cada una de ellas con una combinación diferente de anticuerpos que en su conjunto incluyen algunos (uno o dos) anticuerpos en común, además del FSC y SSC; estos parámetros comunes permiten identificar de forma reproducible en cada alícuota(s), la(s) población(es) celular(es) de interés[30,31,105-107]. Así, cuando se emplea

esta estrategia, las diferentes combinaciones utilizadas para evaluar cada muestra, incluyen en general dos grupos de marcadores: i) marcadores dirigidos a identificar de forma sistemática la población (o poblaciones) celular(es) relevante(s) (i.e., marcadores de identificación), que se repiten en cada una de las combinaciones (e.g., alícuotas) empleadas, preferiblemente siempre en la misma posición, y; ii) marcadores de caracterización que varían en cada combinación (e.g., alícuota) y tienen como objeto definir el estadio madurativo y el estadio funcional de dichas subpoblaciones celulares, o la discriminación entre células normales y patológicas y la caracterización detallada de estas últimas[6,27,35,64,79,100,108,109]. Alternativamente, pueden utilizarse en una combinación de anticuerpos, dos o más marcadores diferentes conjugados con un mismo fluorocromo, siempre que dichos marcadores puedan ser evaluados de forma separada en la(s) población(es) celular(es) de interés, con la ayuda de los demás parámetros incluidos en dicha combinación y que han de permitir discriminar las poblaciones relevantes que expresan de forma diferencial los marcadores conjugados con un mismo fluorocromo[99].

La selección de los marcadores concretos que han de ser evaluados en una combinación es un aspecto relevante, que depende prácticamente de forma exclusiva de la biología y fisiopatología de cada tipo diferente de enfermedad. En este sentido, diferentes grupos de trabajo han propuesto listas de marcadores que se considera proporcionan información clínicamente relevante en el campo de los estudios inmunofenotípicos de hemopatías malignas[5,7,30,35,77,110-117].

Dentro de los marcadores propuestos, a veces se incluyen diferentes niveles de recomendación dependiendo de lo que se considera es la utilidad real de cada marcador, incluyendo marcadores obligatorios, recomendados o potencialmente informativos[5,7,30,35,110-114,117,118]. En la práctica, estos consensos no incluyen recomendaciones acerca de los clones concretos, de los fluorocromos específicos con los que deben estar conjugados dichos anticuerpo o de su posición en una combinación multicolor. Todo ello dificulta enormemente la disponibilidad de recomendaciones sobre combinaciones concretas para el estudio de

diferentes hemopatías malignas, ya que la construcción de un panel de combinaciones de anticuerpos no solo depende de la lista de los marcadores a incluir en el mismo, sino que varía también según el reactivo concreto, la posición que ocupa y la combinación final de reactivos empleada para la identificación y caracterización de las poblaciones celulares de interés presentes en una muestra, variables que *a posteriori* terminan también por comprometer la reproducibilidad de los resultados[46].

De acuerdo con lo anteriormente expuesto, en la construcción de un panel de combinaciones de anticuerpo, debe: i) seleccionarse los marcadores informativos que deben ser incluidos en la misma, ya sea para la caracterización de una o varias poblaciones de células normales y/o patológicas presentes en la muestra a evaluar, ii) evaluar individualmente cada uno de los reactivos (clones y/o conjugados con diferentes fluorocromos) disponibles para cada marcador (ver sección 3, sobre "reactivos para estudios de inmunofenotipado por citometría de flujo"); iii) diseñar prototipos de las combinaciones potencialmente más informativas; iv) evaluar prospectivamente dichas combinaciones prototipo, y; v) optimizar la combinación mediante ciclos secuenciales de evaluación, modificación/optimización y re-evaluación, repitiendo dicho ciclo tantas veces cuanto sea necesario, hasta alcanzar una combinación óptima para los fines deseados[46,49,61].

En el proceso de validación de una combinación o de un panel de combinaciones de anticuerpos es esencial además, que se evalúen muestras reales, en las que se empleen los protocolos de preparación de muestras y el tipo de muestras que se usarán posteriormente en la rutina del laboratorio de diagnóstico clínico. Finalmente, debe seleccionarse también la estrategia a emplear. Clásicamente para el inmunofenotipado de hemopatías malignas se han empleado dos estrategias generales diferentes. Así, mientras que algunos laboratorios grandes han optado por la aplicación de un único panel (muy) amplio de reactivos, independientemente de la indicación médica que llevó a la solicitud del estudio, en la gran mayoría de los laboratorios se ha optado por una estrategia diferente, en dos etapas consecutivas: en la primera etapa, se

realiza un rastreo diagnóstico con un número limitado de marcadores y dirigido de acuerdo a un grupo de indicaciones médicas; en caso de que existan hallazgos compatibles con la presencia de una hemopatía, en la segunda fase se lleva a cabo su caracterización fenotípica detallada. A diferencia de la primera, esta segunda estrategia se asocia con un menor consumo de reactivos y de muestra, a costa de un tiempo (teóricamente) alargado hasta la obtención de los resultados finales[60,79]. Sin embargo, la realización de un rastreo diagnóstico previo al estudio detallado, hace que para muchas muestras el tiempo se acorte, especialmente cuando se concluye que no existen indicios de infiltración tumoral en la muestra analizada.

En conjunto, lo anteriormente expuesto indica que la construcción de paneles de anticuerpos para inmunofenotipado por citometría de flujo es un proceso largo y costoso, que requiere del establecimiento inicial de decisiones de consenso, seguidas de una evaluación prospectiva que involucra, tanto aspectos técnicos cómo biológicos e incluso clínicos, relacionados entre sí. Por todo ello, no es de extrañar que la mayoría de los usuarios, ante la imposibilidad real de realizar este proceso en su laboratorio, se apoyen en recomendaciones de otros grupos, validadas o no prospectivamente[79].

8. Análisis de datos

Según lo reflejado anteriormente en esta introducción, los avances tecnológicos ocurridos tanto en el campo de los reactivos para inmunofenotipado como en los equipos de medida de citometría, han facilitado la detección de un número cada vez mayor de parámetros en un número progresivamente más elevado de células. Como consecuencia, se ha incrementado de forma exponencial la complejidad de los datos generados, convirtiéndose el análisis de los mismos en uno de los procesos asociados al inmunofenotipado por citometría de flujo que demandan mayor grado de experiencia, conocimiento, dedicación y tiempo[12]. En este sentido, cabe señalar que las estrategias clásicas de análisis de datos de citometría, se han convertido en

aproximaciones ineficientes en las que se elimina (no se considera) la mayor parte de la información generada sobre una muestra[12].

Inicialmente, las aproximaciones empleadas para el análisis de datos de citometría en la caracterización fenotípica de leucemias y linfomas estaban basadas en estrategias simples asociadas a marcajes de hasta un máximo de 4 colores/fluorocromos. Habitualmente consistían en un primer paso de selección de las células de interés y en una segunda etapa de caracterización de las mismas empleando representaciones uni- o bi-dimensionales, y umbrales arbitrarios para definir la positividad para cada marcador[12,38,57,119]. Por otra parte, la selección de poblaciones de interés se centraba habitualmente en una única población celular para la que se emplean una o dos regiones para su definición ("gate"), y entre 2 y 4 marcadores adicionales para su caracterización por alícuota de la muestra (o por combinación de anticuerpos)[38,79,108].

La ampliación del número de marcadores utilizados para la caracterización fenotípica de las células tumorales, unido a la relevancia asignada a la estimación de los niveles de expresión de cada marcador, incrementaron la cantidad de información generada y su complejidad, asociando la caracterización inmunofenotípica de hemopatías a un proceso basado en la interpretación de los niveles de expresión de cada marcador en las células tumorales en un conjunto cada vez mayor de imágenes bi-dimensionales o "dot-plots", requiriéndose para dicha interpretación de un experto con un conocimiento cada vez más profundo y detallado de los patrones fenotípicos de las células normales y tumorales[2,14,40,49,79,95]. En cualquier caso, los resultados con esta estrategia se expresan en forma de un listado de los marcadores analizados para "la" población celular de interés, con la descripción del patrón de expresión observado para cada molécula individualmente, haciendo referencia o no al patrón observado en su contrapartida normal en lo que a línea celular, estadio madurativo y funcional se refiere[35,120].

La información descriptiva sobre las características de las poblaciones celulares patológicas evaluadas con este tipo de estrategias, basándose en la interpretación de imágenes por un experto, puede obtenerse también directamente con los programas informáticos de análisis de

datos fenotípicos convencionales, que permiten obtener información estadística descriptiva de cada una de las poblaciones celulares identificadas con cada combinación de marcadores empleadas (i.e., distribución relativa de la población, intensidad de los marcadores expresados y grado de uniformidad/heterogeneidad de esa expresión)[38]. No obstante, con los paneles de 3 o 4 colores, esto resulta en un proceso tedioso ya que la información acerca de las distintas poblaciones celulares presentes en la muestra debe obtenerse de forma separada para cada combinación y ésta varía de forma sistemática con cada combinación de anticuerpos empleada.

Más recientemente, el incremento en el número de parámetros que pueden evaluarse simultáneamente (≥ 8 parámetros fluorescentes) para cada célula analizada, permite definir con mayor precisión (y en una sola combinación) la mayoría de las poblaciones celulares presentes en la muestra[12,49,121]. No obstante, su identificación con las herramientas y estrategias informáticas convencionales sigue siendo un proceso complejo, tedioso, subjetivo y demasiado demorado. Así, con ≥8 marcadores podemos llegar a identificar más de 50 poblaciones celulares normales en una muestra de sangre periférica[45,49,121]. Si por cada subpoblación celular, requerimos del establecimiento de (en media) tres regiones distintas, esto significa la elaboración de cerca de 150 regiones/tubo, para la identificación de cada subpoblación celular. En paralelo, para la caracterización de algunas hemopatías malignas puede ser necesario el estudio de > 25 marcadores distintos, lo que implica la elaboración de varias combinaciones (4 o 5) de anticuerpos monoclonales para ser incluidos en un mismo panel, y por lo tanto, el análisis de forma separada de la información generada en cada alícuota con los inconvenientes antes mencionados[27,28,30,31,33,34,37,101,102].

En este sentido, cabe señalar que al menos desde el punto de vista teórico, sería posible establecer algoritmos matemáticos basados en principios como el del (los) vecino(s) más próximo(s)[122] podrían ser utilizados para generar ficheros de datos con un número ilimitado de parámetros (medidos o calculados) para cada célula individual analizada en cada tubo[109,123,124]. Para ello es imprescindible que cada fichero que obtengamos tras la medición de una alícuota

de una misma muestra, contenga información sobre un número mínimo de parámetros comunes a todos los ficheros y que con ellos, sea factible identificar en cada fichero y de forma idéntica, la(s) población(es) celular(es) de interés (e.g. las células tumorales). Al fusionar la información derivada de todos los ficheros correspondientes al panel completo aplicada a una misma muestra, podemos entonces obtener información completa del fenotipo detallado y para cada marcador, de las células de interés[109]. Con esta estrategia innovadora se abre la posibilidad de valorar un número casi ilimitado de parámetros simultáneamente, para una población celular determinada. No obstante, ello requiere también de nuevas estrategias para la visualización de los datos que faciliten la interpretación de los resultados, ya que los histogramas convencionales de 1, 2 o 3 dimensiones resultan insuficientes y muy limitadas [79].

El número de posibles representaciones uni- o bi-paramétricas que pueden generarse, está exponencialmente relacionado con el número de parámetros evaluados, resultando progresivamente más difícil para un experto memorizar imágenes de referencia e interpretar la información mostrada en todas y cada una de las posibles representaciones (p. ej., bidimensionales) tanto de células normales como de poblaciones patológicas, al incrementarse al número de parámetros evaluados simultáneamente[12,99]. Bastaría con mencionar que, para una combinación de 10 parámetros pueden generarse hasta 45 representaciones bidimensionales diferentes para poder visualizar los datos, lo cual hace difícil o casi imposible, su interpretación correcta y reproducible. Todo ello apunta a la necesidad de emplear nuevas formas de representación de los datos de citometría derivadas de análisis multivariantes (y a ser posible en tiempo real) de esos mismos datos, como el análisis de componentes principales o el análisis canónico, entre otras aproximaciones[125-127]. Se trata pues de conseguir mediante análisis multivariantes[127] una representación bidimensional que contiene la información más relevante de combinaciones de “n” parámetros evaluados simultáneamente y que permite optimizar la resolución (separación) existente entre el mayor número posible de poblaciones celulares que

coexisten en una muestra, preservando a la vez, a ser posible, la proporcionalidad de la información en el espacio multidimensional original[36,126].

La estrategia referida, basada en la fusión de ficheros de datos de diferentes alícuotas de una misma muestra de un mismo paciente, puede ser aplicada también para la fusión de ficheros (que a su vez pueden estar previamente fusionados) de diferentes muestras de sujetos normales o con diferentes subtipos de enfermedades, con la intención de generar ficheros de referencia que contengan información sobre poblaciones celulares normales y grupos representativos de poblaciones celulares tumorales de enfermedades (o grupos de enfermedades concretas) para un determinado panel de marcadores[28,109]. Con ello podemos generar perfiles fenotípicos de referencia de células normales y patológicas, frente a los que comparar de forma prospectiva los perfiles obtenidos en muestras problemas del mismo tipo (p. ej., SP, MO, ganglio linfático), marcadas con el mismo panel de combinación de anticuerpos y adquiridos bajo idénticas condiciones de calibración del equipo y procesamiento de muestra. Esta comparación contribuiría en definitiva a un diagnóstico y una clasificación inmunofenotípica más objetiva de las hemopatías malignas[126].

9. Estandarización del inmunofenotipado de leucemias y linfomas

La necesidad de obtener datos objetivos y reproducibles en los que apoyar la toma de decisiones diagnósticas, es un requisito obligatorio de cualquier test y proceso diagnóstico, incluida la citometría de flujo[79]. Por ello resulta imprescindible la estandarización completa de todo el proceso de inmunofenotipado, desde la muestra y los reactivos empleados hasta el análisis de datos, pasando por los equipos de medida[14,88]. Aunque desde hace tiempo se reconoce esta necesidad de estandarización en citometría clínica[2,12,14,26,117,128,129], y en especial en el diagnóstico inmunofenotípico de leucemias y linfomas, esta está lejos de alcanzarse, al no haber sido abordada de una forma integral. Especial hincapié merece en este punto, la

estandarización de los instrumentos de medida a través de un protocolo estandarizado de calibración y monitorización de los equipos de destinados a este fin.

En este sentido, si bien es verdad que hoy disponemos de citómetros de flujo en los que muchas variables están estandarizadas y controladas (p. ej., la potencia de emisión de los láseres o su alineamiento), otras siguen requiriendo de especial atención, especialmente en lo que se refiere a la puesta a punto de los detectores y la compensación de fluorescencias, o su monitorización diaria mediante estándares y controles internos, o a la participación en programas de control de calidad externos que incluyan todos los pasos del proceso (pre-analíticos, analíticos y post-analíticos)[38,79]. Por todo ello, resulta imprescindible definir y establecer protocolos estandarizados no sólo de calibración de los equipos, sino también de manejo y preparación de muestras, que reduzcan al máximo la variabilidad actual de los análisis de citometría de flujo realizados. Solo con la estandarización global de todo el proceso aseguraremos la posibilidad de obtener resultados reproducibles que faciliten la comparación directa y prospectiva de los datos obtenidos frente a patrones de referencia utilizando tanto estrategias clásicas de análisis, como las estrategias y herramientas innovadoras más recientes descritas de forma parcial en el capítulo anterior de esta introducción. En este proceso de estandarización, es clave también la definición de los anticuerpos y conjugados de referencia, el control estricto de los diferentes lotes de reactivos y su estabilidad, y la adopción de protocolos de preparación de muestras y de análisis de datos estandarizados.

10. La citometría de flujo en el estudio inmunofenotípico de las hemopatías malignas

Las neoplasias hematológicas representan un grupo muy heterogéneo de enfermedades, integrado por cerca de un centenar de entidades distintas, para cuyo diagnóstico y clasificación se requiere de criterios específicos. En conjunto, los tumores hematológicos representan entre

7% y 8% de los cánceres humanos, con una incidencia en la Unión Europea de 120.000 casos nuevos al año[1,130,131].

En la clasificación actual de la Organización Mundial de la Salud (OMS), el diagnóstico y clasificación de las hemopatías malignas se apoya en los resultados derivados de técnicas de laboratorio como la citología y la histología, el inmunofenotipo y los estudios genéticos y moleculares[1]. Según la línea celular involucrada las neoplasias hematológicas se clasifican en tres grandes grupos: i) neoplasias de origen mieloide, ii) neoplásicas de origen linfoide, y iii) neoplasias de histiocitos/células dendríticas[1,130]. De estos tres grupos, las neoplasias de origen linfoide son de lejos las más prevalente (aproximadamente 75% de todas las hemopatías malignas)[1]. En un segundo nivel, las neoplasias linfoides se subclasifican según el grado de madurez de la célula tumoral, en neoplasias de células precursoras o inmaduras (e.g., las leucemias agudas y los linfomas linfoblásticos) y neoplasias de células maduras (e.g., neoplasias de células linfoides periféricas/maduras)[1]. En un nivel siguiente, tanto las neoplasias de células precursoras como las de células maduras se subdividen de nuevo de acuerdo a la contrapartida normal de la célula tumoral (estadio madurativo) y/o la presencia de alteraciones genéticas típicas o características de cada entidad (Tablas 2, 3 y 4).

Desde hace más de tres décadas que se reconoce la importancia de los estudios inmunofenotípicos por CMF para el diagnóstico y clasificación de las hemopatías malignas, área en la que ha alcanzado gran relevancia en los últimos años[2,3]. Así, hoy día, el análisis inmunofenotípico es uno de los pilares en los que se apoya el diagnóstico, clasificación y seguimiento de pacientes con hemopatías malignas, convirtiéndose en el método de elección más importante para la evaluación de las características inmunofenotípicas de las diferentes poblaciones celulares normales/reactivas y/o patológicas presentes en diferentes tipos de muestras empleadas para el diagnóstico de estas enfermedades[1,2,5-8,22,130,132-140]. Todo ello ha ido asociado a los avances tecnológicos que han ocurrido en el campo de la citometría y en especial, en la citometría multiparamétrica. En concreto, el inmunofenotipo se utiliza para: i) el

diagnóstico de enfermedad (vs situaciones normales o procesos reactivos) incluyendo la orientación respecto al posible tipo de neoplasia hematológica subyacente; ii) su (sub)clasificación en entidades con pronóstico o tratamiento potencialmente diferentes; iii) su estadiaje; iv) la identificación de posibles dianas terapéuticas, y; v) la monitorización de la respuesta al tratamiento (i.e., detección de enfermedad mínima residual) asociada habitualmente a diferente riesgo de recaída y/o tratamiento.

No obstante la gran utilidad del fenotipo y los avances tecnológicos incorporados en las últimas décadas, la cantidad y complejidad de la información generada mediante inmunofenotipado por citometría de flujo se ha incrementado de forma exponencial, lo cual ha tenido también impacto negativo sobre la reproducibilidad de los resultados debido a la gran variabilidad y subjetividad introducidas, especialmente en la interpretación de los mismos, y a la falta de estandarización de las técnicas, los paneles de combinaciones de anticuerpos, los procedimientos de preparación de muestras o las estrategias de análisis de los resultados. De hecho, los elevados niveles de variabilidad asociados a todo el proceso -i.e. desde las etapas pre analíticas (e.g. selección de instrumentos y reactivos de procesamiento de la muestra, calibración del equipo y adquisición), hasta el análisis e interpretación de los resultados- han tenido un impacto negativo sobre la percepción que de la verdadera utilidad clínica de la CMF tienen muchos hematólogos clínicos y patólogos. La necesidad imperiosa de un experto, con un conocimiento amplio de los aspectos técnicos asociados al método y de los aspectos biológicos y clínicos relacionados con la enfermedad, han hecho aún más difícil la interpretación global de esta técnica diagnóstica, a la vez que ha introducido un importante grado de subjetividad en la misma[11,12]. Todo ello ha contribuido sin duda, a que con frecuencia se observen importantes diferencias en por ejemplo, la frecuencia de expresión de antígenos concretos en enfermedades específicas (i.e. la expresión de CD117 en pacientes con mieloma múltiple (MM) varía según las series entre 18% y 37%)[141-145] o la controversia suscitada en relación al impacto pronóstico de marcadores fenotípicos como ha ocurrido con la expresión de marcadores linfoides en LMA y

marcadores mieloides en LLA, donde pueden encontrarse resultados que apoyan o descartan completamente su utilidad [146].

Tabla 2. Clasificación actual de la OMS de los neoplasias de células B maduras[a] (Adaptado de Swerdlow et al, 2008 y Campo et al, 2011)[1,130]

Leucemia linfática crónica B / Linfoma linfocítico de célula B pequeña
Leucemia prolinfocítica de célula B
Linfoma esplénico de zona marginal
Tricoleucemia
Linfoma/leucemia esplénico, inclasificable*
Linfoma difuso esplénico de células B de la pulpa roja*
Tricoleucemia variante*
Linfoma linfoplasmocítico
Macroglobulinemia de Waldenström
Linfoma de zona marginal extranodal de tejido linfoide asociado a mucosas
Linfoma de zona marginal nodal
Linfoma pediátrico de zona marginal nodal*
Linfoma folicular
Linfoma folicular pediátrico*
Linfoma cutáneo primario centrofolicular
Linfoma de células del manto
Linfoma B difuso de célula grandes (LBDCG), no especificado
LBDCG rico en células T/histiocitos
LBDCG primario del Sistema Nervioso Central
LBDCG primario cutáneo, tipo miembro inferior
LBDCG con virus de Epstein-Barr-positivo del anciano*
LBDCG asociado a inflamación crónica
Granulomatosis linfomatoide
Linfoma B de célula grande primario de mediastino (tímico)
Linfoma B de célula grande intravascular
Linfoma B de célula grande ALK-positivo
Linfoma plasmablástico
Linfoma B de célula grande en enfermedad de Castleman multicéntrica asociada a HHV8
Linfoma primario de cavidades
Linfoma de Burkitt (LB)
Linfoma B, inclasificable, de características intermedias entre LBDCG y LB
Linfoma B, inclasificable, con características intermedias entre LBDCG y linfoma de Hodgkin clásico

OMS, Organización Mundial de la Salud; ALK, quinasa del linfoma anaplásico; HHV8, Virus herpes humano tipo 8
[a], No incluye las neoplasias de células plasmáticas
*Entidades histológicas provisionales con evidencia actual insuficiente para reconocerlos como entidades definitivas

Una de las estrategias utilizadas (con más frecuencia que éxito) con la intención de disminuir los niveles de variabilidad referidos, se ha centrado en establecer consensos y recomendaciones acerca de cómo llevar a cabo dichos estudios, especialmente en lo que se refiere a los marcadores a emplear. Aunque estos esfuerzos han sido beneficiosos, se han quedado a medio camino en lo que a la resolución del problema de fondo se refiere[22,30,35,89,95,110,112-

[118,120,128,134,135,138,140,147-151]. Básicamente, esto es debido a que dichas recomendaciones se obtienen por consenso entre un grupo de expertos con experiencia, pero sin llegar en ningún caso a evaluar de forma prospectiva y demostrar la posible utilidad y mejoría introducidos por la adopción de las recomendaciones propuestas.

Pese a todo lo anterior, y al grado de estandarización relativamente limitado de la técnica, el inmunofenotipado por CMF es una de las técnicas más atractivas y prometedoras en el campo del diagnóstico y seguimiento de las hemopatías malignas. Ello se debe a que es una técnica capaz de identificar de forma precisa y específica células tumorales, distinguiéndolas de su contrapartida normal y de células reactivas, aun cuando las primeras están presentes en una muestra en baja frecuencia[2,3,9,152-159], además, proporciona información sobre las células acompañantes y la calidad de la muestra analizada[95,160-162].

Clásicamente se reconoce que, en la gran mayoría de las neoplasias hematológicas, las células tumorales expresan fenotipos aberrantes, conocidos también como fenotipos asociados a leucemia/linfoma, ausentes en células normales, que permiten su discriminación de estas últimas de forma específica y sensible. Dichos fenotipos aberrantes incluyen: i) asincronismos madurativos; ii) expresión anormalmente elevada o baja de un antígeno; iii) alteraciones del tamaño y/o la complejidad celular; iv) presencia de fenotipos ectópicos (en localizaciones no habituales), y; v) expresión de antígenos asociados a otras líneas hematopoyéticas[3-5,7,9,11,31,33,34,79,107,117,140,153,155,158,163-175].

10.1. Utilidad de la citometría de flujo en el diagnóstico y clasificación de los síndromes linfoproliferativos crónicos (SLPC)

Los SLPC constituyen un grupo heterogéneo de enfermedades caracterizadas por la expansión y acumulación (mono)clonal de células de estirpe linfoide de aspecto maduro y que pueden reflejar (al menos parcialmente) las características de distintas poblaciones de células linfoides normales bloqueadas en diferentes estadios madurativos. En general, los SLPC se clasifican de

acuerdo a la población linfoide comprometida en SLPC de línea B, T y NK; no obstante, en la clasificación actual de la OMS, los SLPC-T y -NK se consideran de forma conjunta, debido a que algunos subtipos presentan características clínicas, morfológicas y/o una historia natural de la enfermedad similares, o con un importante grado de solapamiento, con independencia de la naturaleza T vs NK de la célula tumoral/clonal[1].

Tabla 3 Clasificación actual de la OMS de los neoplasias de células T y NK maduras agrupadas según la localización típica de cada entidad. (Adaptado de Swerdlow et al, 2008 y Campo et al, 2011)[1,130]

Neoplasias diseminadas (leucémicas)
Leucemia prolinfocítica T
Leucemia de linfocitos grandes granulares T
Enfermedad linfoproliferativa crónica de células NK*
Leucemia agresiva de células NK
Enfermedad linfoproliferativa sistémica de células T VEB positivas de la infancia
Leucemia/linfoma T del adulto
Neoplasias extranodales
Linfoma T/NK extranodal, tipo nasal
Linfoma T asociado a enteropatía
Linfoma T hepatoesplénico
Neoplasias cutáneas
Micosis fungoide / Síndrome de Sézary
Síndromes linfoproliferativos T CD30+ primariamente cutáneos
Linfoma anaplásico de célula grande primariamente cutáneo
Linfoma T tipo paniculitis subcutánea
Linfoma T gamma delta primariamente cutáneo
Linfoma T cutáneo citotóxico epidermotrópico agresivo $CD8^+$ primariamente cutáneo*
Linfoma T de célula pequeña/media $CD4^+$ primariamente cutáneo*
Linfoma tipo “Hydroa vaccinifome”
Neoplasias ganglionares
Linfoma T periférico no especificado
Linfoma T angioinmunoblástico
Linfoma anaplásico de célula grande ALK positivo
Linfoma anaplásico de célula grande ALK negativo*

** Entidades provisionales;* OMS, organización mundial de la salud; VEB, virus de Epstein-Barr

Por definición, los diferentes SLPC B y T en su conjunto derivan de células linfoides maduras que han finalizado el proceso de reordenamiento de los genes de inmunoglobulinas (IG) o del receptor de célula T (TR, abreviado del inglés “T-cell receptor”) y que tienen como contrapartida normal los linfocitos de SP y órganos linfoides secundarios -i.e., ganglio linfático, bazo, MO y tejido linfoide asociado a mucosas (MALT; abreviado del inglés “mucosa-associated lymphoid tissue”). Estas células, representan diferentes clones (millones de millones de clones) que

expresan un solo tipo de receptor de célula T (TCR; abreviado del inglés "T-cell receptor") en el caso de los linfocitos T o de cadena ligera (κ o λ) y pesada (IgG_1, IgG_2, IgG_3, IgG_4, IgA_1, IgA_2,IgM, IgD o IgE) de las Igs en los linfocitos B, la única excepción la constituirían los linfocitos B *naïve* y las células B de memoria que no han realizado el cambio de isotipo de Ig y coexpresan cadenas IgM e IgD simultáneamente . De todos los SLPC, los que afectan a la línea linfoide B son los más frecuentes involucrando entre 90-95% de todos los casos[176].

Así como ocurre con los SLPC T/NK, los SLPC-B incluyen un número relativamente elevado de entidades clínico-biológicas diferentes (Tablas 2 y 3)[1,140,176,177]. En términos madurativos, incluyen neoplasias de irían los linfocitos inmaduros/transicionales, linfocitos B vírgenes (o *naïve*) y de memoria (Tabla 2) y de las células plasmáticas productoras de anticuerpos (Tabla 4).

Tabla 4.- Clasificación actual de la OMS de las neoplasias de células plasmáticas (Adaptado de Swerdlow et al, 2008 y Campo et al, 2011)[1,130]

Gammapatía monoclonal de significado incierto (GMSI)
Mieloma múltiple (MM)
MM asintomático
Leucemia de células plasmáticas
Plasmocitoma
Plasmocitoma solitario de hueso
Plasmocitoma extraóseo
Síndrome de POEMS
Enfermedades por depósito de Igs
Amiloidosis primaria
Enfermedades sistémicas por depósitos de cadenas ligeras o de cadenas pesadas de Ig

POEMS, polineuropatía, visceromegalia(s), endocrinopatía, gammapatía monoclonal y alteraciones dérmicas; Ig, inmunoglobulinas.

El primer linfocito B normal que sale de MO, se caracteriza por presentar aun marcadores de inmadurez (CD38 y CD10) junto a SmIgM, CD5 y expresión parcial de CD23[64], i.e., linfocito B inmaduro. En su paso a célula B *naïve*, el linfocito inmaduro pierde expresión de CD10, CD38 y CD5, coexpresa SmIgM y SmIgD y mantiene la expresión de CD20 y CD19[178]. Posteriormente, el linfocito B *naïve* migra desde la SP a los órganos linfoides secundarios donde, caso reconozca antígeno y con la cooperación de las células T, inicia la respuesta inmune pasando por una

segunda etapa de diferenciación B dependiente de antígeno[179]. Así, fenotípicamente el linfocito B activado por el antígeno adquiere de nuevo CD10 y CD38, y expresa CD27[179]. Dependiendo de su vía de diferenciación, posteriormente incrementa la expresión de CD38, adquiere expresión de CyIgs, pierde progresivamente la expresión de SmIg y adquiere CD138 en su diferenciación a célula plasmática (CP)[27,64]. Por el contrario, en la transición a linfocito B de memoria, la célula B del centro germinal (CG) pierde la expresión de CD38 y CD10, mantiene la positividad para SmIg en ausencia de CyIg y otros marcadores específicos de CP[180]. Merece destacar que, una proporción importante de los linfocitos B de memoria, y de CP, al reconocer el antígeno llevan a cabo el cambio de isotipo de Ig de SmIgM/D a sobre todo IgA o IgG; las restantes células B de memoria siguen expresando SmIgM y SmIgD simultáneamente[64,181], mientras que las CP expresan solo IgM y en menor medida también solo IgD[27].

Aunque es posible encontrar las distintas subpoblaciones maduras de células B en SP, MO y/o ganglio linfático, su distribución y fenotipo pueden variar de forma muy significativa. Así por ejemplo, mientras que en SP predominan las células B *naïve* y de memoria, siendo la población de CP (con fenotipo inmaduro) minoritaria, las células B del CG se localizan de forma prácticamente exclusiva en los órganos linfoides secundarios, y las CP maduras predominan en MO donde coexisten con linfocitos B y precursores B en todos los estadios madurativos.

A diferencia de los linfocitos B, la maduración de los precursores T ocurre de forma específica en el timo[182]; desde allí salen a la SP linfocitos T maduros TCR$\gamma\delta^+$, TCR$\alpha\beta^+$ $CD4^+$ $CD8^-$, y TCR$\alpha\beta^+$ $CD4^-$ $CD8^+$ con fenotipo *naïve*, y células T reguladoras de tipo II (TCR$\alpha\beta^+$ $CD4^+$ $CD25^+$ $FoxP3^+$). Los linfocitos T vírgenes ($CD45RA^+$, $CCR7^+$, $CD28^+$, $CD62L^+$, $CD27^+$, $CD45RO^-$) circulan entre SP y los órganos linfoides secundarios donde, al encontrar su antígeno, pueden activarse mostrando a partir de ese momento disminución de la expresión de CD7, aumento de la expresión de CD2 y CD11a (y CD11c en la células T $CD8^+$) junto con CD69, CD25, HLADR, CD38, CD57 y CD45RO[165,183], posteriormente, estos linfocitos T se diferencian a linfocitos T de memoria

central (CCR7^{+} CD45RA^{-} CD45RO^{+} CD27^{+}) y periférica (CCR7^{-} CD45RA^{-} CD45RO^{+} CD27^{+}) y/o a linfocitos T efectores (CD45RA^{+}, CCR7^{-}, CD28^{-}, CD62L^{-}, CD45RO$^{-/+}$)[184,185].

A diferencia de lo que ocurre con la linfopoyesis T y B, la maduración de las células NK, es un proceso que sigue siendo en gran medida desconocido[186,187]. No obstante, un número progresivamente mayor de evidencias indican que las células NK pueden compartir un origen común con las células T en MO, pudiendo llevar a cabo su diferenciación en diferentes tejidos, especialmente en los órganos linfoides secundarios (vs timo), donde se identifica una población de células NK con expresión fuerte de CD56 y que supera en número a las células NK maduras CD56$^{+débil}$, que predominan en MO y SP[186-190]. Así, las células NK circulantes presentan en su mayoría un fenotipo caracterizado por la expresión de CD56$^{+débil}$ y/o CD16^{+}, CD3^{-}, CD7^{+}, CD161^{+}, Cygranzima^{+}, Cyperforina^{+}, CD11b^{+} y CD122^{+}, asociado a expresión heterogénea de CD2, CD94, CD11c y CD57[163,190-192]. Al igual que ocurre con las células T, las células NK al activarse, muestras cambios fenotípicos asociados a un aumento de la expresión de CD2, CD94 y CD11c, expresión transitoria de HLADR, CD57 y CD45RO, y disminución de la positividad para CD7, CD38 y CD11b[163,165,193-195].

10.1.1. Rastreo diagnóstico de clonalidad T, B y NK en SLPC

Los SLPC representan habitualmente una expansión clonal de linfocitos maduros fenotípicamente aberrantes[1]. En términos generales, esta expansión es consecuencia de una ventaja proliferativa y/o una mayor supervivencia y resistencia a la apoptosis de las células clonales respecto a su contrapartida normal[196,197]. La expansión progresiva de las células B clonales deriva en los hallazgos de laboratorio (e.g. leucocitosis con linfocitosis en SP y/o presencia de componente monoclonal en suero) y clínicos (e.g. organomegalias) que desencadenan el proceso diagnóstico[89,175].

Ante la sospecha de un proceso linfoproliferativo, clásicamente, la citomorfología ha constituido la primera aproximación metodológica al rastreo diagnóstico y caracterización de los

SLPC. En un primer periodo, los estudios inmunofenotípicos quedaban relegados a un segundo plano, contribuyendo solo a la confirmación y caracterización del proceso una vez identificado mediante microscopía convencional[139,198]. Con el tiempo, el inmunofenotipado por CMF ha ido adquiriendo mayor relevancia como herramienta de primera línea en el diagnóstico de los SLPC al ser un método más rápido, sensible y específico para el rastreo diagnóstico de clonalidad linfoide en SP, MO, tejidos linfoides o fluidos corporales (p. ej., LCR, líquido ascítico y/o derrame pleural)[1,91,99,140,158,175].

En términos generales, una alteración en la distribución relativa de las diferentes poblaciones celulares linfoides (o su concentración en términos absolutos en SP), constituyen uno de los signos más habituales y característico de la posible existencia de infiltración por un SLPC[199]. Sin embargo, la simple expansión numérica con frecuencia resulta un criterio poco específico y debe asociarse con la identificación de un perfil inmunofenotípico alterado que permitan la discriminación de forma (más) específica y sensible entre los linfocitos clonales/tumorales y las células normales o reactivas, incluso cuando las primeras están presentes en bajo número[31,33,34,79,140,164,166,169,175].

10.1.1.1. Rastreo diagnóstico de clonalidad en SLPC-B

Tradicionalmente el rastreo diagnóstico de clonalidad B se ha basado en la comprobación de la existencia de un desequilibrio importante entre el número de células B Igκ^+ e Igλ^+ [175,199-202]. Aunque se han propuesto diferentes puntos de corte para el cociente de células B Igκ^+/Igλ^+, hoy se considera que valores superiores a 3/1 o inferiores 1/2 se asocian con elevada probabilidad, a la presencia de células B clonales[175,199-202]. No obstante, se trata de un criterio que además de no ser específico, puede resultar además poco sensible, especialmente cuando se observan infiltración por pequeñas poblaciones de células B clonales[156]. Por ello, en la actualidad se considera conveniente, siempre que sea posible, asegurar la naturaleza clonal de las células B presentes en una muestra, mediante la demostración de fenotipos aberrantes, esta estrategia,

además de proporcionar especificidad, incrementa notablemente la sensibilidad del método[31,79,89,99]. Por ello, hoy se considera importante evaluar, junto con la expresión de las cadenas ligeras κ y λ, la presencia o ausencia de expresión de otros marcadores cuyos niveles están frecuentemente alterados en SLPC-B; tal es el caso de los niveles de expresión de CD20, CD38, y/o CD5 que contribuyen a distinguir entre células patológicas y normales en base a la expresión de perfiles fenotípicos aberrantes, incluso cuando las células patológicas están presentes a muy baja frecuencia[99]. En este sentido, estudios previos han demostrado que incluso en ausencia de "exceso clonal", la presencia de linfocitos B aberrantes es habitualmente suficiente para establecer un diagnóstico de certeza de clonalidad[31]. Dichos fenotipos aberrantes proporcionan además, información útil a la hora de clasificar la enfermedad, ya que existen perfiles característicos de distintas categorías diagnósticas de SLPC-B [1,2,8,9,31,156,158,168]. A modo de ejemplo, la presencia de células B maduras con expresión débil de CD20 y positivad para CD5, se asocia de forma estrecha a la leucemia linfática crónica de células B (LLC-B) o la linfocitosis monoclonal B de tipo LLC dependiendo del número (>5.000/μL o <5.000/μl) de linfocitos B clonales presentes en SP[203]; de forma similar una expresión disminuida o ausente de CD19 en células B de pequeño tamaño, se ha asociado al linfoma folicular (LF)[31,158,204], mientras que la sobrexpresión de CD20 y CD19 en células de tamaño heterogéneo (de pequeño a grande) es típica de la tricoleucemia (TL). Con esta estrategia, se ha descrito la presencia de dos o más clones diferentes de células B no relacionados, en hasta el 5% de los SLPC-B incluso cuando se observa un cociente normal entre células B Igκ$^+$ y células B Igλ^{+}[156].

10.1.1.2. Rastreo diagnóstico de clonalidad en SLPC-T

En el caso de los SLPC-T, el rastreo diagnóstico de clonalidad T requiere de una estrategia un poco más compleja debido fundamentalmente a la existencia de un mayor número de poblaciones de linfocitos T distintas y asociado a un repertorio mucho más amplio de los receptores TCRαβ y TCRγδ[169,205,206]. Así habitualmente, se emplea inicialmente una estrategia

basada en criterios numéricos, asociados a un desequilibrio entre las poblaciones mayoritarias de células T o al aumento significativo de poblaciones minoritarias, especialmente cuando asociados a la detección de fenotipos T aberrantes o poco habituales relacionados con los asociados a SLPC-T[166,169,207,208]. Dentro de los fenotipos aberrantes resultan especialmente útiles los cambios de expresión (ausencia o pérdida de expresión, y en menor medida la sobreexpresión) observados en SLPC-T en marcadores pan-T como CD7 o CD5, la presencia de asincronismos madurativos o la presencia de una población celular que exprese o carezca simultáneamente (doble positiva o doble negativa) de CD4 y CD8. Sin embargo, estos criterios alcanzan una eficacia relativamente limitada, respecto a los descritos para SLPC-B, al estar presentes únicamente en 60-70% de los pacientes con SLPC-T[32,166,209,210]. Como consecuencia, el método de referencia para el diagnóstico de clonalidad T, sigue estando basado con relativa frecuencia en técnicas moleculares dirigidas a la detección de reordenamientos clonales de los genes que codifican para las diferentes cadenas del TCR, especialmente de los genes *TCRB* y *TCRG*[211]. Alternativamente, en los últimos 15 años se ha demostrado que la utilización de un amplio panel de AcMo específicos de distintas versiones de las cadenas TCRVβ, TCRVδ y TCRVγ, pueden contribuir de forma variable a un rastreo diagnóstico rápido de clonalidad en SLPC-T[205,206]. No obstante, se ha demostrado que en ausencia de un fenotipo aberrante, con frecuencia se requiere con esta estrategia de una expansión relativamente significativa de las células T clonales dentro del compartimento global de linfocitos T (>60%), que expresen una misma familia TCRVβ o TCRVγ y TCRVδ[79,183,205,206], para poder afirmar con elevado grado de certeza que se trata de una expansión clonal T[212-221]. En este sentido, resulta más interesante la combinación del estudio del repertorio TCR con el análisis simultáneo de marcadores expresados de forma aberrante en las células T. Sin embargo, debido al gran número de anticuerpos anti-TCRVβ, Vα, Vγ y Vδ requeridos, esta estrategia suele quedar relegada a una segunda etapa en el rastreo diagnóstico de clonalidad T, después de analizar la distribución global de las poblaciones T mayoritarias y minoritarias.

10.1.1.3. Rastreo diagnóstico de clonalidad en SLPC-NK

En el caso de las células NK, el rastreo de clonalidad resulta aún más complejo al quedar limitada la posibilidad de confirmar la naturaleza clonal de las expansiones de esta población celular a un grupo relativamente reducido de pacientes portadores de alteraciones citogenéticas, secuencias genómicas de origen vírico de naturaleza clonal integradas en el genoma y/o un patrón clonal de inactivación del cromosoma X en mujeres[33,222-227]. Aunque se han descrito patrones fenotípicos que podría resultar útiles a la hora de detectar clonalidad NK, en la actualidad, con esta estrategia no se logran niveles de sensibilidad y especificidad similares a los referidos actualmente para las células B y T, lo que impide (o al menos limita) su utilización de manera sistemática en el rastreo diagnóstico de clonalidad NK[224,225,228-230].

Pese a todo lo anterior, estudios recientes sugieren que las células NK clonales de SLPC NK podían expresar un patrón restringido de i) receptores tipo Ig expresados por células "Killer"(KIR; abreviado del inglés "killer-cell Ig-like receptor) en especial de CD158a y CD158b, ii) receptores tipo Ig expresados por leucocitos (LIR; abreviado del inglés "leukocyte Ig-like receptors"), y iii) receptores tipo-lectina de tipo C, cuyo estudio podría resultar ser de utilidad para la detección de clonalidad NK[224,225,229,230]. Sin embargo, se requiere de estudios en series más amplias de pacientes y de paneles muy amplios de anticuerpos para identificar clonalidad NK mediante este tipo de aproximaciones.

Por todo ello, la identificación de clonalidad NK en el rastreo diagnóstico de SLPC suele estar basada en una primera fase, en criterios puramente numéricos como la expansión de las células NK maduras, definidas como linfocitos $CD45^+$ que no expresan marcadores asociados a célula T (CD3) o B (p. ej., CD19), y son positivos para CD56, CD16, CD7 y/o CD2, con un patrón alterado o poco habitual de expresión de estos marcadores[33].

10.1.2. Características inmunofenotípicas de los SLPC-T

Los SLPC T, son neoplasias relativamente poco frecuentes (entre 10-15% de todos los linfomas no-Hodgkin) que derivan de células T periféricas o maduras (post-tímica)[1,177,231,232]. Debido en parte a su baja frecuencia, además de la ausencia de marcadores genéticos típicos de la mayoría de los distintos grupos diagnósticos de SLPC-T, este grupo de neoplasias no esta tan bien caracterizada como ocurre con los SLPC-B, estando constituido por una gran variedad de entidades que pueden presentar también gran heterogeneidad dentro de cada uno de ellos (Tabla 3)[1,130,233,234].

Pese a lo anteriormente expuesto, en la última década se ha avanzado de forma importante en el conocimiento de los SLPC-T. Así, hoy sabemos que el linfocito T-colaborador de tipo folicular constituye la contrapartida normal del linfocito T tumoral del linfoma T angioinmunoblástico (LTAI); de forma similar, hoy conocemos que la leucemia/linfoma T del adulto (LLTA) está constituida por la expansión tumoral de células T reguladoras $CD4^{+}$ $CD25^{++}$ $CyFoxp3^{+}$ [1,233,235-237]. Por otra parte, se han identificado alteraciones genéticas características (incluso específicas) de algunos subgrupos diagnósticos de SLPC-T, como es el caso de las translocaciones que implican el gen de la quinasa del linfoma anaplásico (gen *ALK*) que permite subclasificar los linfomas anaplásicos de célula grande (LACG) en dos entidades distintas según esté presente o no esta alteración, o de las translocaciones que implican el gen *TCL1* (leucemia/linfoma de célula T 1) que se ha visto constituyen una lesión genética característica de la leucemia prolinfocítica T (LPL-T)[238-240], teniendo ambas alteraciones genéticas como consecuencia, la sobreexpresión de las proteínas implicadas (ALK y TCL1, respectivamente).

A continuación revisaremos de forma específica las características fenotípicas de aquellos subtipos de SLPC-T en los que los estudios inmunofenotípicos resultan especialmente útiles para su diagnóstico y clasificación:

Leucemia prolinfocítica T (LPL-T): La célula tumoral de la LPL-T habitualmente muestra un fenotipo de célula T TCR$\alpha\beta^+$ $CD4^+$ madura *naïve* ($CD45RA^+$, $CCR7^+$, $CD27^+$, $CD45RO^-$, $CD28^+$ y $CD26^+$) con expresión elevada de CD7 y CD5, asociada en la mayoría de los casos (≈80%) a expresión de CyTCL1. Con menor frecuencia, se han descrito también casos de LPL-T con fenotipo $CD4^+$ $CD8^+$ o $CD4^-$ $CD8^+$ (cerca de 25% y 10% de los casos, respectivamente)[231,240].

Leucemia de linfocitos grandes granulares T (LLGG-T): Estos pacientes muestran en su mayoría una expansión de células T clonales TCR$\alpha\beta^+$ $CD8^+$, aunque también se han descrito casos con fenotipo $CD4^+$ o $CD4^-$ $CD8^{-/+débil}$ TCR$\gamma\delta^+$ [166]. En cualquier caso, la célula T tumoral invariablemente muestra un fenotipo de célula efectora de tipo citotóxico, asociado a expresión de Cygranzima B, Cyperforina, CD16, CD56, CD57, CD11c y/o CD94, y positividad intensa para CD45RA, en ausencia de CD27, CCR7(CD197) y CD28. Tanto CD45RO, como los marcadores pan T CD5, CD7 y CD2, pueden mostrar una expresión variable en la célula tumoral de estos pacientes[238,241-244].

Leucemia/linfoma T del adulto (LLTA): El fenotipo de la célula tumoral de pacientes con LLTA recuerda al del linfocito T regulador $CD4^+$ $CD25^{++}$ $CyFoxp3^+$, con características de célula de memoria asociada a expresión débil (o ausente) de CD7 y, en menor medida también de CD3 y TCR$\alpha\beta$[1,37,231,245].

Linfoma T asociado a enteropatía: El linfocito T en el que tiene su origen este tumor, es una célula T intraepitelial de fenotipo citotóxico (granzima B^+), habitualmente TCR$\alpha\beta^+$, en ausencia de CD4 y con expresión débil o ausente de CD8; con menor frecuencia puede tratarse de un linfocito T, TCR$\gamma\delta^+$. De la misma manera, las células T tumorales de este linfoma, pueden presentar expresión de CD103 y CD30, en ausencia de CD5[246-248]. En esta enfermedad, se distinguen 2 grupos, según se asocie (Tipo I) o no (Tipo II) a enfermedad celíaca, que muestran algunas diferencias inmunofenotípicas; así, en el Tipo II es habitual la expresión de CD56 y CD8, en ausencia de CD30[249].

Linfoma T hepatoesplénico: La contrapartida normal de este SLPC-T parece ser el linfocito T periférico TCR$\gamma\delta^+$ con fenotipo citotóxico de memoria. Así, las células clonales son habitualmente TCD$\gamma\delta^+$, y suelen mostrar un fenotipo $CD4^-$ $CD8^{-/+débil}$ $CD5^-$, asociado a expresión débil o ausente de CD56 y positividad para granzima B y perforina[1,250].

Síndrome de Sézary y micosis fungoide: En este subtipo de SLPC-T, el linfocito T clonal habitualmente presenta un fenotipo de célula T $CD4^+$ colaboradora con tropismo por la piel[210,231,251,252]. Fenotípicamente, esta célula suele mostrar una expresión anormalmente disminuida de CD7, CD3, TCR$\alpha\beta$ y CD2, lo que constituye un fenotípico característico aunque no es completamente específico de la enfermedad. Desde el punto de vista madurativo, la célula de Sézary presenta un fenotipo de célula de memoria central con expresión de CD28, CD45RO, CCR7(CD197) y $CD5^+$ [241].

Linfoma anaplásico de célula grande (LACG): En la actualidad sigue sin identificarse la contrapartida normal del LACG aunque posiblemente se trata de un linfocito T activado. En la mayoría de los casos, la célula tumoral presenta un fenotipo TCR$\alpha\beta^+$ y $CD4^+$, asociado a expresión intensa de CD30 y un FSC (tamaño) anormalmente elevado[1,37,253]. Como hemos referido anteriormente, dentro de este tumor se han definido grupos de pacientes con diferente pronóstico, dependiendo de si presentan o no alteración del gen *ALK*, asociada a sobreexpresión del producto del mismo.

Linfoma T tipo paniculitis subcutánea: El linfoma T tipo paniculitis subcutánea se caracteriza por presentar infiltración del tejido subcutáneo en ausencia de diseminación periférica, mostrando habitualmente la población T clonal un fenotipo TCR$\alpha\beta^+$ $CD8^+$, con expresión de marcadores de célula T citotóxica, en ausencia de CD56[1].

Linfoma T angioinmunoblástico (LTAI): hoy se conoce que el LTAI tiene su origen en una célula con fenotipo de célula T colaboradora de tipo folicular; de forma característica esta célula muestra expresión de CD4, CD10, CD28 y CD279, junto con expresión variable (habitualmente disminuida) de CD3[1,233,235,237].

Linfoma T periférico NOS (abreviado del inglés "not otherwise specified"): Este subtipo de linfomas T constituye uno de los grupos más frecuentes, si no el más frecuente, de SLPC-T. Está integrado por un grupo de neoplasias T post-tímicas que no presentan características fenotípicas claramente distintivas o específicas[1,254,255]. Esto es debido a que incluye todos aquellos linfomas T que con frecuencia muestran expresión periférica, y que no cumplen los criterios diagnósticos de ningún otro SLPC-T[1,254,255] (i.e., diagnóstico de exclusión). La mayoría de los SLPC T periféricos NOS, muestra expresión de CD4 (65%); y solo una pequeña proporción de los mismos son $CD8^+$, $CD4^-$ $CD8^-$ o $CD4^+$ $CD8^+$ (15%, 10% y 10% de los casos, respectivamente).

10.1.3. Características inmunofenotípicas de los SLPC-NK

Los SLPC-NK son, en conjunto, los SLPC menos frecuentes (<1% de todos los linfomas y SLPC en el mundo occidental)[256]. Al igual que los SLPC-T, son un grupo heterogéneo de entidades raras y relativamente poco conocidas. La clasificación actual de la OMS considera 3 grupos principales de neoplasias NK: la leucemia agresiva de célula NK (LA-NK); el linfoma T/NK extranodal, tipo nasal, y; la enfermedad linfoproliferativa crónica de célula NK (ELPC-NK) (Tabla 3). Mientras que los 2 primeros grupos suelen mostrar un curso clínico agresivo, la ELPC-NK (que constituye el subgrupo más frecuente de neoplasias NK), presenta habitualmente un curso más indolente[1]. En la actualidad la ELPC-NK, constituye una entidad provisional dentro de la clasificación OMS de SLPC T/NK, que incluye aquellos casos conocidos anteriormente como linfocitosis NK, leucemias de linfocitos grandes granulares NK y linfocitosis de células grandes granulares NK[1,257].

Fenotípicamente, aunque con frecuencia se observan alteraciones en los perfiles de expresión de marcadores asociados a célula NK citotóxica como cambios de expresión de CD2, CD7, HLADR y CD94[1,33,34,165,258,259], el fenotipo de la célula NK expandida suele presentar un elevado grado de solapamiento con el fenotipo de las células NK normales/reactivas, con características típicas de cada entidad diagnóstica.

Leucemia agresiva de células NK: De los 3 subgrupos diagnósticos de neoplasias NK, la LA-NK es la menos frecuente, pero a la vez, la más agresiva[254]. Generalmente está asociada a infección por el VEB. Fenotípicamente, muestra un perfil de expresión proteica fenotipo variable y característico de células NK, siendo habitual la expresión de CD95 en ausencia de CD57 [260]; no obstante, en ocasiones resulta difícil confirmar el origen NK de la célula tumoral, por la ausencia de expresión de marcadores típicos de célula NK más habituales (p. ej., CD56 y CD16).

Enfermedad linfoproliferativa crónica de células NK: Al igual que en el linfoma extranodal de tipo nasal, la célula expandida en la ELPC-NK suele mostrar un fenotipo característico de célula NK madura[1]. No obstante, con relativa frecuencia presenta expresión débil (o incluso ausente), de marcadores NK como CD56 y CD2[33], asociado de forma casi sistemática a sobreexpresión de CD94 y HLADR[261]

Linfoma (T)/NK extranodal, de tipo nasal: Esta entidad muestra también una asociación evidente con la infección por el virus de Epstein-Barr (VEB)[227], mostrando las células tumorales un fenotipo NK típico; no obstante, una minoría de casos se observa expresión de CD3 en la superficie celular (fenotipo de célula T citotóxica)[37].

10.2. Neoplasias de células plasmáticas

Las CPs son células productoras de anticuerpos que representan el último estadio de maduración de linfocitos B activados tras el reconocimiento antigénico en los órganos linfoides secundarios. Es precisamente en los órganos linfoides secundarios, donde se generan las CPs y desde donde estas emigran a través de la SP hacia la MO y/u otros tejidos periféricos dónde anidan, alcanzan la diferenciación final y producen anticuerpos[27,262]. Desde el punto de vista fenotípico la CP de MO normal se caracterizan por la pérdida parcial o completa de expresión de la mayoría de antígenos asociados a linfocito B (p. ej. CD20, CD22, CD24, CD79b, SmIg); por el contrario muestran positividad intensa para CyIgs, CD38 y CD138[64,263,264]. Tanto la expresión intensa de CD38 como la positividad para CD138, son considerados marcadores específicos de

CPs[27,265]. No obstante, el perfil inmunofenotípico de las CPs normales es heterogéneo, pudiendo definirse varias subpoblaciones asociadas a menor o mayor grado de diferenciación. Así, por ello, el fenotipo global de las CPs normales suele definirse como el de una célula de tamaño y granularidad intermedios, que muestra expresión intensa de CD38 y es $CD138^{+}$, $CD27^{+}$, $CyIg\kappa^{+}$ o $CyIg\lambda^{+}$; por el contrario, es $CD19^{-/+}$, $CD56^{-/+débil}$, $CD45^{-/+débil}$, $CD81^{-/+}$ y $CD28^{-/+}$, con una fracción variable de células positivas para cada marcador (Tabla 5)[4,157,168].

Las NCPs se caracterizan por mostrar una proliferación y/o expansión clonal de CPs tumorales que se acumulan en cantidades anormalmente altas en MO y/o otros tejidos. En la mayoría de los casos, la CP tumoral mantiene la capacidad de producir y secretar Igs que al ser de naturaleza (mono)clonal, originan la aparición en suero y orina de un "componente Monoclonal"[1,266].

Tabla 5. Marcadores fenotípicos reconocidos como relevantes para el estudio fenotípico de las neoplasias de células plasmáticas y su perfil de expresión en células plasmáticas normales y tumorales[4,5,143,152,154,157,168,264,267-279]

Marcador	Patrón fenotípico en CPs normales de MO	Patrón fenotípico aberrante en GM	% de casos con fenotipos aberrantes
CD19	-/+ (% $CD19^{+}$: ≈ 64%)	-	96%
CD20	- (% $CD20^{+}$: ≈ 4%)	+débil	17-30%
CD27	+ (% $CD27^{débil}$, ND)	- o +débil	40-68%
CD28	- (% $CD28^{+}$: ≈ 15%)	+	15-45%
CD33	- (% $CD33^{débil}$: ≈ 6%)	+	18%
CD38	++	+débil	80%
CD45	-/+ (% $CD45^{+}$: ≈ 6%)	-	73%
CD54	+	+débil	60-80%
CD56	-/+ (% $CD56^{débil}$: ≈ 10%)	++	60-75%
CD81	+	- o +débil	55%
CD117	-	+	30-32%
CD138	+	NR	
CD200	-/+ (% $CD200^{+}$: ≈ 49%)	+/++	≥70%
CD229	+	NR	
CD307	+	++	NA
CD319	+	+débil	
SmIg	-	+	<5%

GM, gammapatía monoclonal; CP, célula plasmática; MO, médula ósea; Sm, expresión en la superficie de la membrana celular.

Al igual que ocurre con los SLPC, las NCPs incluyen también un grupo heterogéneo de enfermedades entre las que se incluyen, entre otras, la gammapatía monoclonal de significado incierto (GMSI), el MM, el plasmocitoma solitario, y algunas variantes de las mismas (Tabla 4)[1,266]. De todas ellas, la GMSI es de lejos la entidad más prevalente (≈5% de todos los adultos mayores de 70 años)[5]. En la actualidad, el diagnóstico diferencial y la clasificación de estas entidades se basa en gran medida en: i) la detección y localización de infiltración tisular por CPs; ii) la presencia, subtipo y concentración del componente monoclonal, y; iii) la evidencia de daño/lesión con afectación funcional de distintos a órganos, atribuible a la enfermedad[1,266]. Pese a la existencia de criterios diagnósticos bien definidos para cada entidad, sigue observándose un cierto grado de solapamiento entre ellas con un riesgo variable de transformación a formas más avanzadas como MM o leucemia de células plasmáticas (LCP)[280-283].

En este sentido merece destacar que, el inmunofenotipo ha tenido un papel relativamente marginal en el diagnóstico y clasificación de las NCPs[4,79]. No obstante lo anterior, fenotípicamente resulta factible diferenciar claramente entre CPs clonales y CPs normales y reactivas, debido a que las primeras, además de estar aumentadas de forma significativa en número en los tejidos infiltrados de la mayoría de los pacientes, muestran de forma sistemática fenotipos aberrantes asociados a la detección de expresión restringida de cadenas ligeras κ o λ a nivel citoplasmático. En la actualidad existe un consenso generalizado respecto a que para la identificación y recuento preciso de las CPs mediante inmunofenotipo, son necesarios al menos dos marcadores específicos de CPs (CD38 y CD138); estos marcadores, junto con las características de dispersión de luz y CD45 permiten definir de forma inequívoca y en diferentes tipos de muestras, las CPs presentes en la misma, excluyendo otras poblaciones celulares[4,5,264]. El análisis de marcadores adicionales permite además, identificar perfiles inmunofenotípicos aberrantes en la práctica totalidad de los pacientes que presentan NCPs. Así, hoy se reconoce que las CPs tumorales con frecuencia muestran una expresión anormalmente disminuida de los niveles de CD19, CD45, CD38, CD27 y/o CD81, junto con sobrexpresión de CD56, CD28 y/o CD33,

y expresión asíncrona de CD20, CD117 y/o SmIgs (Tabla 5)[4,5,143,152,154,157,168,264,267-279]. No obstante cabe señalar que, pese a la frecuencia con la que se detectan fenotipos aberrantes en las CPs de pacientes con NCPs y la diversidad y variabilidad de dichos fenotipos, hasta la fecha no se han podido definir patrones fenotípicos que permitan diferenciar claramente entre diferentes entidades diagnósticas[1,266]. Aun así, en la actualidad se reconoce el papel de los estudios inmunofenotípicos por CMF en el diagnóstico, clasificación, evaluación pronóstica y/o monitorización de enfermedad mínima residual en estos pacientes, siendo especialmente útil desde el punto de vista pronóstico, la determinación de la proporción existente en MO entre CP normales y patológicas[4,5]. Así, la existencia de una mayor proporción de CPs patológicas en MO (>95% de las CPs totales) se asocia a MM (vs MGUS) y dentro de los pacientes con MGUS y MM indolente, a una mayor tasa de progresión a MM sintomático y a un peor pronóstico[281].

En paralelo, la expresión de algunos marcadores individuales o de perfiles inmunofenotípicos concretos, se ha asociado también en pacientes con MM, con el pronóstico de la enfermedad. En este sentido, el patrón de expresión conjunta de CD28 y CD117 se ha demostrado, define tres grupos de paciente con diferente pronóstico, asociándose la expresión de CD28 en ausencia de CD117 con un peor pronóstico, y el fenotipo inverso con una supervivencia más alargada[275]. De forma similar, la expresión de CD81 en las CPs mielomatososas confiere también un peor pronóstico a pacientes con MM sintomático[279].

II. HIPÓTESIS DE TRABAJO Y OBJETIVOS.

Los estudios inmunofenotípicos mediante CMF se han convertido en uno de los pilares del diagnóstico y clasificación de las hemopatías malignas. Sin embargo, existe una importante heterogeneidad en las técnicas, paneles y estrategias empleadas en distintos laboratorios para el inmunofenotipado de leucemias y linfomas, asociado a un importante grado de subjetividad en el análisis e interpretación de los resultados. La falta de estandarización, junto con el componente interpretativo subjetivo, hacen que existan importantes niveles de variabilidad en los resultados obtenidos en diferentes centros e incluso en diferentes momentos, en un mismo centro. Todo ello, unido a los importantes desarrollos tecnológicos ocurridos en las últimas décadas que ha incrementado de forma significativa la cantidad de información disponible sobre cada muestra tanto en lo que se refiere al número de parámetros analizados en cada combinación de anticuerpos o panel de combinaciones de anticuerpos, como al número de células analizadas han incrementado aún más la complejidad de todo el proceso. Por otra parte, el número de fluorocromos con los que podemos conjugar cada anticuerpo, ha crecido también de forma muy significativa, generando un número casi ilimitado de posibilidades de combinaciones de estos con los marcadores reconocidos como útiles para el diagnóstico y clasificación de las hemopatías malignas.

Como consecuencia de todo lo anteriormente expuesto, actualmente en prácticamente cada laboratorio de diagnóstico se utiliza un panel de anticuerpos distinto, con niveles variables de conocimiento de los perfiles fenotípicos normales de referencia para cada panel, además de la variabilidad asociada a la muestra, las técnicas empleadas para y su procesamiento y el tipo de equipo empleado para realizar las mediciones.

Esta mayor complejidad y variabilidad han incrementado notablemente a su vez, la necesidad de formación de expertos con un elevado nivel de conocimientos sobre las características clínicas de la enfermedad, la biología de las células tumorales y su contrapartida normal, además de los aspectos técnicos y metodológicos relacionados con el

inmunofenotipado por citometría de flujo. Este problema se agrava aún más si cabe, si tenemos en cuenta que, pese al incremento exponencial de la cantidad de información generada, en paralelo no se han desarrollado las herramientas informáticas necesarias para un análisis e interpretación completa, rápida, sencilla y adecuada de los datos generados.

La única forma de atajar el problema de manera eficiente y disminuir de modo significativo los niveles de variabilidad existentes en los resultados obtenidos en este campo, reside en encontrar soluciones innovadoras a los problemas y retos planteados y la definición (y evaluación) de estrategias, paneles de reactivos y protocolos optimizados o estandarizados; en dos palabras, la solución estaría en introducir innovación y estandarización en el inmunofenotipado de las hemopatías malignas mediante CMF para disminuir la variabilidad y subjetividad de todo el proceso, desde las etapas pre-analíticas al informe de los resultados. De hecho, este ha sido en los últimos 10 años, el objetivo del trabajo realizado por el grupo EuroFlow, contexto en el que se encuadra la presente tesis doctoral al asumir el doctorando la responsabilidad de los desarrollos a realizar en aspectos de estandarización técnica en general, y en el rastreo diagnóstico de SLPC (incluidas las NCPs) y la clasificación de los SLPC T y NK, en particular.

Por ello, planteamos como **objetivo general** de este trabajo doctoral desarrollar, evaluar e implementar nuevas estrategias y herramientas para la estandarización de las técnicas de inmunofenotipo de hemopatías malignas por citometría de flujo, enfocadas de forma específica al rastreo diagnóstico de SLPC y NCPs y la clasificación de los SLPC T y NK. Para lograr este objetivo, planteamos cuatro **objetivos específicos:**

1. Desarrollar un procedimiento estandarizado y validado para la calibración y monitorización de citómetros de flujo digitales de uso habitual en los laboratorios de diagnóstico

hematológico, que permitan de forma optimizada, obtener mediciones reproducibles tanto dentro de cada laboratorio, como entre diferentes laboratorios.

2. Establecer y validar un procedimiento estandarizado para el procesamiento de los diferentes tipos de muestras hematológicas empleadas para estudios de inmunofenotipado por CMF, que minimice el impacto del procesamiento de muestras en la variabilidad de los resultados finales.

3. Desarrollar, evaluar e implementar nuevas aproximaciones metodológicas y herramientas informáticas para el análisis objetivo y automatizado de datos de CMF, que contribuyan a simplificar y estandarizar los análisis multidimensionales dirigidos al reconocimiento de los perfiles inmunofenotípicos de células tumorales frente a los de células normales, presentes en muestras biológicas con sospecha diagnóstica de infiltración por una hemopatía maligna.

4. Diseñar, evaluar y estandarizar paneles basados en combinaciones de ≥ 8 anticuerpos para el rastreo diagnóstico de SLPC y NCPs y la clasificación de SLPC T y NK.

III. MATERIAL, MÉTODOS Y RESULTADOS.

A continuación, en esta sección se detallan los materiales y métodos empleados, así como los resultados obtenidos, mediante la inclusión de los artículos originales publicados como resultado del trabajo de doctorado. Con el fin de facilitar una rápida comprensión del trabajo desarrollado y de los resultados obtenidos, y de su significado, se incluye además un breve resumen en castellano de cada uno de las secciones de los artículos.

1. Artículo 1: Estandarización de protocolos los para la calibración de citómetros de flujo e inmunofenotipado según la estrategia EuroFlow.

1.1. Introducción general:

El inmunofenotipo constituye en la actualidad uno de los pilares básicos del diagnóstico y clasificación de las hemopatías malignas. Esto es debido en gran medida, a los avances que han ocurrido en los últimos años, avances que sin embargo, han estado asociados también a una mayor complejidad, tanto en lo que se refiere a los aspectos técnicos como a la interpretación de los datos, con una consiguiente mayor variabilidad en los resultados obtenidos. Con el fin de alcanzar mayor reproducibilidad en los resultados, a lo largo de las últimas décadas se han realizado diferentes propuestas de consenso que sin embargo, solo han sido parcialmente exitosas. Con el objetivo de disminuir la variabilidad referida y alcanzar altos niveles de reproducibilidad deseada, el grupo EuroFlow se propuso desarrollar protocolos estandarizados y validados para el inmunofenotipo de leucemias y linfomas que incluyeran: i) una selección optimizada de las combinaciones de fluorocromos más adecuados para paneles de 8 colores; ii) la definición de protocolos estándar para la calibración del citómetro de flujo; iii) la compensación de fluorescencias, y; iv) el procesamiento y marcaje de muestras biológicas para inmunofenotipado de leucemias y linfomas, sentando además las bases para; v) el desarrollo de nuevas estrategias de análisis de datos e interpretación de los resultados basadas en la utilización de ficheros de referencia para, finalmente, vi) demostrar la elevada reproducibilidad

de los resultados alcanzados a nivel multicéntrico con la aplicación de los protocolos desarrollados, aspectos que constituyen las diferentes secciones del presente trabajo.

1.2. Sección 1ª: Selección de fluorocromos para paneles de inmunofenotipado con 8 fluorocromos distintos

Introducción. La selección de una combinación de fluorocromos es un paso clave en el diseño de paneles de inmunofenotipaje. Aunque la selección de fluorocromos depende de las características propias de cada fluorocromo, en la misma intervienen también la configuración óptica del equipo y/o los láseres y, la disponibilidad de los mismos. Considerando que las combinaciones de anticuerpos para inmunofenotipado de leucemias y linfomas pueden llegar a requerir de hasta cuatro marcadores comunes para la identificación de las poblaciones celulares de interés, y para que puedan emplearse al menos cuatro marcadores adicionales para la caracterización fenotípica de dichas poblaciones, estratégicamente planteamos la construcción de combinaciones de 8 fluorocromos distintos.

Objetivo. Seleccionar citómetros de flujo clínicos capaces de medir ≥8 fluorescencias simultáneamente y establecer en base a la configuración óptica de los mismos, la combinación óptima de 8 fluorocromos a utilizar en la construcción de los paneles EuroFlow para diagnóstico y clasificación de hemopatías malignas.

Material y métodos. La selección de los citómetros de flujo se centró en los equipos de tres láseres disponibles en el momento de iniciar este trabajo, con capacidad para medir ≥8 colores y que pudieran ser utilizados en laboratorios de diagnóstico clínico. La evaluación de los fluorocromos se realizó en 2 pasos consecutivos. En primer lugar se seleccionó un grupo de fluorocromos que de acuerdo a la experiencia previa eran óptimos. En una segunda etapa y para las demás posiciones, se compararon los fluorocromos candidatos empleando conjugados de un mismo clon y/o de clones dirigidos frente a un mismo antígeno diana. La evaluación de cada

fluorocromo se basó en la comparación de la intensidad media de fluorescencia (IMF) obtenida con el mismo, su SI y grado de solapamiento con otros canales de fluorescencia. Así, para la primera posición del láser violeta se evaluaron seis AcMo distintos (CD2, CD3, CD4, CD20, CD45 y HLADR) conjugados con los fluorocromos "pacific blue" (PacB) y "Horizon Violeta450" (HV450). A su vez, para la segunda posición del láser violeta se evaluaron tres conjugados de AcMo CD45 con AmCyan, "pacific orange" (PacO) y "Horizon V500" (HV500). Finalmente, para la segunda posición del láser rojo, se compararon tres conjugados del anticuerpo anti-CD4 con los fluorocromos APC-Cy7, APC-H7 y AF700. Para cada comparación se marcaron 5 muestras de SP de donantes sanos, procesadas en los 8 laboratorios del grupo EuroFlow, siguiendo los protocolos de calibración de equipos y de procesamiento de muestras, descritos más adelante en las secciones 2ª y 4ª del presente trabajo, respectivamente. Con el fin de determinar el posible significado estadístico de las diferencias observadas entre los AcMo conjugados con los distintos fluorocromos se emplearon los test de la U de Mann-Whitney o de la T de Student.

Resultados. En el momento de iniciar este trabajo existían cuatro modelos diferentes de citómetros de flujo de dos fabricantes distintos con una configuración compatible con los requerimientos planteados. Estos 4 modelos (FACSCantoII, FACSAria y LSR II de BD, y CyAn ADP de Dako/BC) poseían una configuración muy similar en cuanto a las fuentes de luz (3 láseres: azul, rojo y violeta, con emisiones a 488 nm, 633/635 nm y, 405/407 nm, respectivamente) y sistema óptico, permitiendo la detección de al menos 4 fluorescencias diferentes asociadas al láser azul, dos al rojo y dos al láser violeta.

Dentro del primer grupo de fluorocromos se seleccionaron el FITC, la PE, el tándem PerCP-Cy5.5 y el tándem PE-Cy7 para los 4 detectores de láser azul, además de la APC para el primer detector del láser rojo. Respecto a las demás posiciones, los diferentes conjugados de PacB y HV450 mostraron un perfil de fluorescencia muy similar -diferencias menores (<10%) en cuanto a la IMF y SI en comparaciones realizadas en paralelo de conjugados del mismo clon y fabricante ($p>0.05$)-, sin que se observaran tampoco diferencias significativas en los requerimientos de

compensación con otros canales entre ambos fluorocromos. No obstante, las diferencias alcanzaron significación estadística ($p<0.05$), al comparar AcMo que aunque estaban dirigidos frente al mismo antígeno eran de diferentes clones y/o fabricantes. De acuerdo con estos resultados, se seleccionó PacB sobre HV450 en base a una mayor disponibilidad comercial de conjugados con este fluorocromo. Por el contrario, al comparar los fluorocromos AmCyan, PacO y HV500 se observaron diferencias significativas ($p<0.01$) en la IMF que era progresivamente menor para AmCyan, HV500 y PacO; de forma similar, los requerimientos de compensación de estos fluorocromos fueron también distintos, siendo progresivamente menores para AmCyan vs HV500 vs PacO. Sin embargo, los 3 fluorocromos mostraron SI similares (4.8 vs 3.8 vs 3.8, para AmCyan, HV500 y PacO, respectivamente). Como resultado, se seleccionó PacO para esta posición, a pesar de su intensidad relativamente baja, al proporcionar un poder de resolución (i.e., SI) similar al de los otros candidatos con un menor solapamiento de fluorescencias con los otros canales de fluorescencia. Finalmente, la comparación entre los AcMo conjugados con APC-Cy7, AF700 y APC-H7, mostró una intensidad de fluorescencia superior para los reactivos conjugados con APC-Cy7, asociada a un elevado solapamiento con el canal de fluorescencia reservado para APC, como consecuencia de la inestabilidad del tándem de fluorocromos. AF700 mostró menos interferencia en el canal de APC, pero también una menor IMF, requiriendo su utilización una modificación de la configuración óptica del equipo. A su vez, los conjugados de APC-H7, mostraban menor solapamiento en el canal de fluorescencia para la detección de APC que APC-Cy7, unido a una IMF intermedia entre los otros dos fluorocromos evaluados, sin que hubiera necesidad de modificar la configuración óptica original del citómetro de flujo para este fluorocromo; por todo ello, este fluorocromo (APC-H7) fue el seleccionado para la última posición del láser rojo.

Conclusión. En un primer paso, se seleccionaron para este trabajo los 4 modelos de citómetros de flujo existentes con configuración óptica compatible con ≥ 8 colores: FACSCantoII, FACSAria, LSR II y, CyAn ADP. De acuerdo con la experiencia previa en cada uno de los 8 centros EuroFlow,

y la evaluación realizada, se seleccionaron como fluorocromos de referencia para los paneles EuroFlow de 8 colores, PacB, PacO, FITC, PE, PerCPCy5.5, PECy7, APC y APC-H7, siendo factible sustituir algunos de estos fluorocromos como por ejemplo PacB por HV450 o PacO por HV500, aunque para ello habría que comparar prospectivamente y de forma específica cada uno de los AcMo que se pretenda reemplazar.

1.3. Sección 2ª: Procedimiento estándar para la puesta a punto y calibración del citómetro de flujo.

Introducción. Para realizar una medición óptima de las características de dispersión de luz y fluorescencia de las diferentes poblaciones celulares que coexisten en una muestra, el citómetro de flujo debe estar calibrado de forma óptima y específica para las mediciones a realizar. Si además pretendemos obtener datos comparables, derivados de mediciones realizadas a lo largo del tiempo en un mismo citómetro de flujo o en citómetros diferentes y en distintos centros, debemos disponer de un procedimiento de calibración estandarizado que garantice la obtención de resultados reproducibles.

Objetivo. Definir un procedimiento estándar para la puesta a punto y calibración de citómetros de flujo destinados a evaluar los paneles EuroFlow para diagnóstico y clasificación de hemopatías malignas.

Material y métodos. En este apartado, para la definición y evaluación del protocolo estándar para la puesta a punto y calibración de equipos, se emplearon siete citómetros de flujo del modelo FACSCanto II en siete centros diferentes y un citómetro de flujo LSR II y otro Cyan ADP disponible en el octavo centro, según las especificaciones descritas en la primera sección de este trabajo. Para la puesta a punto, calibración y monitorización de los parámetros de dispersión de luz, se utilizaron linfocitos maduros de SP de controles sanos, siguiendo el protocolo de procesamiento de muestras descrito en la Sección 4ª del presente trabajo. A su vez, para la

puesta a punto, calibración y monitorización de los detectores de fluorescencia, se empleó un mismo lote de esferas de calibración (Eight peaks Rainbow calibration particles, Spherotech, Lake Forest, IL, EEUU). Para la caracterización de cada detector de fluorescencia, empleamos como referencia uno de los 9 citómetros de flujo. Con este fin se registraron los valores del coeficiente de variación robusto (CVr) correspondiente al segundo pico menos fluorescente de las esferas de calibración, para variaciones de 50 mV en 50 mV (desde 300 mV a 999 mV), en cada detector. Se definió como voltaje óptimo para cada PMT, aquel voltaje a partir del cual la contribución del ruido electrónico de fondo del detector tenía un impacto mínimo sobre el CVr. El valor óptimo de dicho voltaje se calculó mediante la relación existente entre los valores del CVr obtenido y el valor del voltaje aplicado para cada medición, como el valor de voltaje que se sitúa al comienzo de la parte plana de la curva obtenida. Con ese voltaje se cuantificó y se estableció como referencia el valor de la IMF correspondiente al pico más brillante de fluorescencia de las esferas (8º pico), denominándose la IMF obtenida para dicho pico como el "canal diana". Posteriormente, se evaluó la estrategia establecida en cada uno de los nueve citómetros de flujo, confirmándose que en todos ellos el 2º pico fluorescente menos intenso se encontraba también por encima del nivel basal del ruido electrónico de fondo, mientras que los marcadores más intensamente positivos (todos los seleccionados para evaluación en los diferentes paneles EuroFlow), permanecían dentro de la ventana de análisis establecida en cada equipo. Con ello se definió el valor final de los canales diana para cada detector como la media de los canales diana obtenidos en los distintos citómetros de flujo. Estos mismos canales diana (y las correspondientes desviación estándar) fueron utilizados también para la monitorización de los equipos y la definición de los criterios de aceptación vs no-aceptación de los resultados obtenidos con la monitorización diaria de los mismos.

Resultados. Los valores de referencia para los parámetros de dispersión de luz establecidos para linfocitos de sangre periférica normal fueron de 13.000 (± 2.000) y de 55.000 (± 5.000) canales para FSC y SSC, respectivamente. De forma similar, los canales diana de referencia obtenidos

para el 8º pico de las esferas fluorescentes del lote de referencia en cada detector de fluorescencia fueron de: 195.572 y 231.265, para los detectores de PacB y PacO, respectivamente; 59.574, 101.900, 216.064, 27.462, para los detectores de FITC, PE, PerCP-Cy5.5 y PE-Cy7, respectivamente, y; 176.780 y 56.437 para los detectores de APC y APC-H7, respectivamente. El control diario de los equipos, permitió la detección temprana de desviaciones fuera de los límites establecidos (diferencias mayores a ± 15% con respecto al canal diana original y/o un CV superior a 4% para los canales de fluorescencia correspondientes a los láseres violeta y azul, o superior a 6% para los canales de fluorescencia del láser rojo). La observación de dichas desviaciones justificaba la intervención por parte del usuario (i.e., realización de una nueva calibración) o del servicio técnico, hasta obtener de nuevo resultados dentro de los niveles establecidos como aceptables. El nivel de estandarización entre diferentes citómetros de flujo se confirmó en dos momentos diferentes, observándose en ambas ocasiones un elevado grado de reproducibilidad, con diferencias entre los canales diana propuestos y los alcanzados una vez calibrado cada equipo, sistemáticamente menores a 5,5%.

Conclusión: El protocolo estandarizado EuroFlow para la calibración y monitorización de equipos, basado en el uso diario de partículas (i.e., estándares) de referencia para establecer o calcular el valor del canal diana para cada detector, asegura un elevado grado de reproducibilidad entre los resultados obtenidos en diferentes equipos, en distintos laboratorios y en distintos momentos. Además, la monitorización diaria del estado de la calibración del equipo, permite la detección precoz de desviaciones que indican la necesidad de realizar una nueva calibración del equipo que garantice la calidad y reproducibilidad de los resultados obtenidos.

1.4. Sección 3ª: Diseño y validación de procedimientos estándar para la compensación de fluorescencias.

Introducción. La mayoría de los fluorocromos tienen un espectro de emisión relativamente amplio, por lo que la detección de su florescencia en un citómetro de flujo convencional no queda restringida a un solo detector (i.e., el detector primario configurado para recogerla), sino que parte ella es detectable también en los detectores configurados para medir otros fluorocromos (i.e., detectores secundarios). Este solapamiento de fluorescencias genera señales (falsamente) positivas en los canales de fluorescencia secundarios. Aunque la proporción de la fluorescencia que se solapa en los detectores secundarios depende de la configuración óptica del equipo, para una determinada configuración estable y constante para un mismo fluorocromo, es posible calcular y sustraer matemáticamente, el porcentaje de fluorescencia global que entra en cada detector secundario que es atribuible a dicho fluorocromo o; a este proceso se denomina compensación de fluorescencias. Los controles o estándares utilizados para establecer la compensación de fluorescencias idónea deben mostrar características espectrales idénticas a las de los fluorocromos a utilizar posteriormente, conteniendo simultáneamente una población negativa de referencia con niveles de autofluorescencia basal similares a los de las células a medir, y una población positiva que al menos resulte tan fluorescente como el marcador más intenso de los que vayan a medirse en cada detector concreto. La compensación de fluorescencias solo debe realizarse una vez se haya establecido una calibración adecuada del citómetro, debido al impacto que tiene esta última en la intensidad de fluorescencia de la población positiva de referencia.

Objetivo. Definir un procedimiento estandarizado y validado para el cálculo de los requerimientos de compensación entre los diferentes fluorocromos (y conjugados de estos) que forman parte de los paneles EuroFlow de 8 colores.

Material y métodos. Se utilizaron como estándares para el establecimiento de los requerimientos de compensación entre los diferentes fluorocromos, subpoblaciones específicas de leucocitos de SP teñidas marcados con un solo anticuerpo en tubos separados (TTSA), buscando de preferencia que el marcador empleado se expresara de forma variable (desde negativo a positivo fuerte) en las células empleadas. Para aquellos tándem de fluorocromos conjugados con anticuerpos dirigidos frente a marcadores no expresados de forma intensa en ninguna población de leucocitos de SP (p. ej. CD117-PE-Cy7 o CD10-APC-H7), empleamos esferas de captura recubiertas de anticuerpos anti-Ig de ratón (CompBeads, BD). Los diferentes TTSA se adquirieron haciendo uso de la rutina de compensación incluida en los programas informáticos de adquisición de datos de los citómetros de flujo empleados (FACSDiva o Summit, para citómetros de BD o de Dako, respectivamente) y que permiten generar una matriz de compensación para su aplicación de forma automatizada a las mediciones realizadas posteriormente con los paneles de combinaciones de anticuerpos EuroFlow de 8 colores para diagnóstico y clasificación de leucemias y linfomas. Para la validación de las matrices de compensación generadas, se emplearon muestras normales y patológicas marcadas con mezclas de anticuerpos de 8-colores que contenían marcadores distintos a los de los paneles EuroFlow. Las matrices de compensación generadas en dos momentos diferentes en cada centro, fueron finalmente comparadas (14 matrices generadas en 7 centros distintos).

Resultados. Un análisis detallado de las matrices de compensación de fluorescencias obtenidas en los diferentes centros, demostró que podían utilizarse compensaciones genéricas para todos los anticuerpos conjugados con los fluorocromos PacB, PacO, FITC, PE, APC y PerCP-Cy5.5. Por el contrario, para los demás tándem de fluorocromos (PE-Cy7 y APC-H7) se requerían valores de compensación diferentes para cada anticuerpo conjugado con estos fluorocromos. Asimismo, la comparación entre las 14 matrices de compensación distintas generadas en los 7 centros participantes mostró que en conjunto estas eran muy similares, siendo las diferencias obtenidas entre centros, de similar magnitud a las diferencias obtenidas al comparar las compensaciones

calculadas dentro de un mismo laboratorio y para un mismo equipo en tiempos distintos (p>0,05). En general, la compensación requerida era alta para las fluorescencias PacB vs PacO, y para PE vs PerCP-Cy5.5; a su vez, el solapamiento entre las fluorescencias PerCP-Cy5.5 y PE-Cy7, FITC y PE, PE-Cy7 y APC-H7, y APC y APC-H7 requería de valores intermedios de compensación, mientras que estos eran nulos o muy bajos para las demás combinaciones de fluorocromos.

Conclusión. Es posible establecer un procedimiento genérico de compensación de fluorescencias óptimo y estandarizado para la utilización de los paneles EuroFlow de 8-colores para diagnóstico y clasificación de hemopatías malignas, siendo la matriz de compensación obtenida estable a lo largo del tiempo (al menos 1 mes). Sin embargo, la complejidad del procedimiento es superior a la deseada debido a la necesidad de establecer compensaciones específicas para cada uno de los reactivos conjugados con PE-Cy7 y APC-H7 e incluidos en las combinaciones de dichos paneles.

1.5. Sección 4ª. Preparación y marcaje de muestras.

Introducción. En la actualidad existe gran variabilidad en lo que se refiere a los protocolos empleados para el procesamiento y marcaje de muestras para citometría de flujo, estando la mayoría de ellos adaptados principalmente para el marcaje de antígenos de membrana en SP y MO. En general, la mayoría de estos protocolos, incluyen un paso inicial de marcaje de la muestra con AcMo, seguido de uno o más lavados y de la eliminación de los hematíes. El procesamiento de otros tipos de muestra (p. ej. LCR, biopsias de ganglio linfático, derrame pleural o humor vítreo), así como la detección de antígenos intracelulares, habitualmente requieren de protocolos que incluyan pasos adicionales y/o distintos de los empleados para el marcaje de antígenos de membrana en muestras de SP y/o MO.

Objetivo. Definir protocolos estandarizados y validados para el procesamiento y marcaje de muestras para inmunofenotipado por citometría de flujo que permitan obtener una separación

óptima de las poblaciones leucocitarias mayoritarias según sus parámetros de dispersión de luz y/o los niveles de expresión de marcadores característicos de las mismas, en ausencia de perdidas celulares significativas, de un descenso de la fluorescencia específica de cada fluorocromo o tándem de fluorocromos, o de un incremento de la autofluorescencia basal de las poblaciones celulares estudiadas. Los protocolos establecidos deberían además reducir los niveles de variabilidad entre laboratorios y, mantener una adecuada relación coste/beneficio.

Material y métodos. En esta sección, se marcaron 30 muestras de SP de adultos sanos, provenientes de los 8 laboratorios que participaban en el estudio. Cada una de las muestras se marcó con 3 combinaciones diferentes de anticuerpos: combinación 1) CD4-PacB CD8-AmCyan CD45-FITC CD19-PE CD14-APC; combinación 2) CD4-PerCP-Cy5.5 CD19-PE-Cy7 CD8-APC-H7; y combinación 3) CD19-PE-Cy7. Para cada combinación se evaluaron un total de cuatro soluciones de lisis de hematíes diferentes: 1) solución de NH_4Cl (preparada localmente en cada laboratorio), 2) FACS Lysing Solution (BD), 3) QuickLysis (Cytognos SL), y 4) VersaLyse (BC). En cada uno de los tubos marcados se usaron 50 μL de muestra a los que se añadieron posteriormente los AcMo, manteniéndose un volumen final de incubación (15 min) de 100 μL. Posteriormente, a las muestras marcadas se añadió la solución de lisis siguiendo las recomendaciones de cada fabricante. Una vez finalizada la lisis de hematíes, se centrifugaron las muestras realizándose dos lavados a 540 g (5 min); la muestra fue finalmente resuspendida en un volumen final de 250 μL usando una solución salina de tampón fosfato (PBS, abreviado del inglés “phosphate buffer saline”) con 0,5% de albúmina bovina sérica (BSA, del inglés “bovine serum albumin”). Para la cuantificación del número absoluto de células de cada población, a la combinación 1 de anticuerpos se añadieron 50 μL de esferas PerfectCount (Cytognos SL) de forma previa a la adquisición en el citómetro de flujo. La adquisición de información para cada tubo se realizó en cuatro momentos distintos (0 h, 1 h, 3 h y 24 h), conservándose la muestra marcada, entre las adquisiciones a 4 °C. La comparación entre los distintos métodos se basó en la separación observada con la combinación 1 entre las poblaciones mayoritarias de leucocitos (i.e.,

eosinófilos, neutrófilos, monocitos y linfocitos totales) de acuerdo al canal medio y CV obtenido para FSC y SSC, el número absoluto de eosinófilos, neutrófilos, monocitos, linfocitos B $CD19^{+}$, linfocitos T $CD4^{+}$ y linfocitos T $CD8^{hi}$, y la IMF y CV obtenido para CD45 en cada una de las poblaciones celulares anteriores, además de la IMF y CV obtenidos para CD19, CD4, CD8 y CD14 en los linfocitos B $CD19^{+}$, los linfocitos T $CD4^{+}$, los linfocitos T $CD8^{hi}$ y los monocitos, respectivamente. Además, con las combinaciones 2 y 3, se valoró la IMF y CV de la población positiva y de su contrapartida negativa para cada marcador, registrándose para los marcadores conjugados con tándems de fluorocromos, además de la IMF de la población positiva, los valores de IMF en cada uno de los demás canales de fluorescencia secundarios. Adicionalmente, cada uno de estos parámetros y condiciones se evaluó siguiendo tres protocolos de marcaje diferentes: 1) marcar, lisar, lavar (MLL); 2) marcar, lisar, lavar, fijar (MLLF); y 3) marcar, lisar, no lavar (MLNL). A diferencia del protocolo 1, los protocolos 2 y 3 implicaban el uso de PFA al 0,5% añadido al tampón (i.e., PBS) utilizado para resuspender la muestra de forma previa a su adquisición en el citómetro de flujo (protocolo 2) y la omisión de todos los pasos posteriores a la incubación con los anticuerpos (protocolo 3), respectivamente.

Resultados. La mejor discriminación que se obtuvo para las poblaciones celulares mayoritarias de SP en base a FSC y SSC, se alcanzó con la lisis con FACS Lysing solution y NH_4Cl, independientemente del protocolo de marcaje utilizado. Así mismo, el protocolo MLNL fue el que se asoció con CV más bajos para todas las poblaciones celulares con todas las soluciones de lisis, a excepción de FACS Lysing que mostró CVs más bajos con el protocolo de MLL. De forma similar, el protocolo MLNL, fue el que mostró menor pérdida celular, observándose con los otros dos protocolos pérdidas específicas de linfocitos y sus subpoblaciones, siendo dichas pérdidas significativamente menores cuando se usaba FACS Lysing vs otras soluciones de lisis. Respecto a la IMF de las poblaciones de referencia, cabe señalar que los protocolos que incluían lavados y/o fijación final con PFA se asociaban a una menor intensidad de fluorescencia. En general, el uso de FACS Lysing se asoció en los distintos protocolos con valores de IMF más altos, mientras

que las diferentes soluciones de lisis evaluadas no mostraron ningún efecto específico sobre el requerimiento de compensación de fluorescencias. Finalmente, la adquisición de muestras en diferentes momentos evidenció una tendencia de todos los marcadores a reducir su IMF con el tiempo, siendo este descenso más marcado cuando la solución de lisis no contenía fijador.

En resumen, los resultados más estables se obtuvieron cuando se empleó FACS Lysing solution siguiendo los protocolos MLL y MLNL, mientras que la variabilidad era máxima para las adquisiciones realizadas a partir de las 3h después de preparadas las muestras. Una vez definido este como el protocolo de referencia para el procesamiento de muestra y marcaje de antígenos de membrana, se realizaron recomendaciones para el marcaje de otros tipos de muestras (p. ej., LCR), Ig de superficie y antígenos intracelulares, de acuerdo con los resultados de estudios previos referidos en la bibliografía. Además, se empleó el protocolo de referencia para marcaje de antígenos de membrana para realizar la titulación de todos y cada uno de los anticuerpos incluidos en los paneles EuroFlow.

Conclusión. En base a los resultados obtenidos, se seleccionó el protocolo MLL de preparación de muestras con FACS Lysing solution, como el mejor procedimiento para el marcaje de antígenos presentes en la membrana celular, debiendo realizarse la adquisición de las muestras en el citómetro de flujo durante la primera hora tras la finalización de la preparación y marcaje de la muestra. Para la detección de Igs de superficie y de marcadores intracelulares, así como para el procesamiento de muestras de SP o MO con escasa celularidad o de otros tipos de muestras (p. ej., LCR), deben realizarse modificaciones específicas al referido protocolo estándar para marcadores de membrana.

1.6. Sección 5ª. Nuevas herramientas y estrategias EuroFlow para el análisis de datos de citometría de flujo.

Introducción. En las últimas dos décadas, la citometría de flujo ha sufrido importantes cambios derivados de la incorporación de los avances tecnológicos ocurridos en ese periodo. Con estos avances se ha incrementado considerablemente la cantidad y complejidad de la información generada. Esto contrasta con los avances relativamente limitados que han ocurrido en el mismo periodo en las herramientas y estrategias empleadas para el análisis e interpretación de los datos de citometría; todo ello ha contribuido a mantener un elevado grado de complejidad y subjetividad en el proceso de análisis e interpretación de los resultados de los estudios de inmunofenotipado de leucemias y linfomas por CMF.

Objetivo. Definir y construir nuevas herramientas y estrategias para el análisis e interpretación de datos de citometría, para su aplicación al diagnóstico y clasificación de las hemopatías malignas.

Material y métodos. En esta sección del presente trabajo se elaboraron nuevas herramientas informáticas para la manipulación, visualización, análisis e interpretación de datos de citometría empleando en ocasiones el programa Matlab (MathWorks, Natick, MA, EEUU) como plataforma de validación de las herramientas de visualización. Dichas herramientas se han integrado en un paquete informático disponible comercialmente, el programa Infinicyt (Cytognos SL), utilizando para su construcción lenguaje Java (ORACLE, Redwood Shores, CA, EEUU).

Resultados. Para la manipulación de ficheros de datos de citometría se elaboró una herramienta informática que permite la fusión de ficheros de citometría en base a los parámetros comunes a dichos ficheros; esta herramienta permite unificar en un solo fichero de datos, la información obtenida sobre cada una de la alícuotas de una muestra marcada con diferentes combinaciones de anticuerpos, recogiéndose así en dicho fichero de datos toda la información fenotípica generada para una misma muestra. Una segunda herramienta desarrollada y relacionada con la

anterior, es la función de estimación que permite relacionar cada célula de una población de interés que esté presente en uno de los tubos marcados con una combinación específica de anticuerpos, con sus células equivalentes presentes en otras alícuotas de la misma muestra, utilizando la estrategia del "vecino más próximo" en el espacio multidimensional generado por los parámetros comunes a las diferentes alícuotas de esa misma muestra, para finalmente asignar informáticamente la información derivada de una alícuota de la muestra a todos los eventos equivalentes presentes en las demás alícuotas, aun cuando esta información no haya sido medida realmente en cada una de estas últimas. Un requisito imprescindible para que las herramientas informáticas de fusión y estimación de datos funcionen de forma idónea reside en que los parámetros comunes permitan identificar de forma precisa la población celular de interés y mostrar además su posible heterogeneidad. Para el funcionamiento adecuado de la función de estimación, se desarrolló una tercera herramienta informática que permite la armonización de las diferencias potencialmente existentes en los parámetros comunes entre diferentes alícuotas de una misma muestra, como consecuencia por ejemplo, de la aplicación de distintos protocolos de marcaje (e.g., diferencias en los valores de FSC y SSC en alícuotas procesadas para el marcaje exclusivo de antígenos de membrana, o de antígenos de membrana e intracitoplasmáticos).

Las herramientas informáticas descritas anteriormente permiten además generar ficheros de muestras de referencia mediante la fusión de dos o más ficheros que contienen cada uno de ellos, toda la información fenotípica (real y/o estimada) sobre una población celular concreta (i.e., los blastos leucémicos) presentes en diferentes muestras. Estos ficheros de referencia, pueden contener información sobre poblaciones de células normales o patológicas que sirvan como poblaciones celulares de referencia frente a las que podemos comparar "casos nuevos" marcados con el mismo panel de anticuerpos y protocolos de preparación de muestras y adquiridos bajo las mismas condiciones. Estas bases de datos/casos de referencia sirven también para evaluar la utilidad de distintos anticuerpos en los paneles empleados en el rastreo

diagnóstico y clasificación de hemopatías malignas. Para ello, ha sido clave la introducción de algoritmos de análisis (multivariante) de datos como el análisis de componentes principales que, una vez se combinan con las correspondientes herramientas de representación gráfica, permiten visualizar en dos o tres dimensiones (por ejemplo, representaciones del componente principal 1 vs 2, o del componente principal 1 vs 2 vs 3) la posición de cada grupo de células/poblaciones celulares de referencia en el espacio n-dimensional definido por (todos) los parámetros inmunofenotípicos evaluados; estos análisis proporcionan a la vez información objetiva sobre la utilidad de cada parámetro individualmente.

Conclusión. Las nuevas herramientas informáticas desarrolladas y que incluyen el uso secuencial de la fusión de ficheros, la estimación de parámetros y la creación de ficheros de referencia representativos de situaciones de normalidad o de grupos concretos de enfermedades, proporcionan la base para una nueva estrategia para el rastreo diagnóstico y clasificación inmunofenotípica de hemopatías malignas y la evaluación de la utilidad de los paneles de marcadores empleados, a través de la comparación de poblaciones celulares individuales o de grupos de poblaciones celulares. Con esta estrategia se simplifica el análisis e interpretación de datos de citometría de flujo, disminuyendo además la subjetividad asociada a todo el proceso. No obstante, cabe señalar que esta nueva estrategia solo es aplicable cuando se apoya en procedimientos y paneles estandarizados según lo definido anteriormente en este trabajo.

1.7. Sección 6ª. Validación multicéntrica de los protocolos EuroFlow

Introducción. La última fase del presente trabajo ha tenido como objetivo realizar una evaluación más profunda de los protocolos estandarizados desarrollados, mediante su implementación a nivel multicéntrico. Solo de esta forma podríamos generar evidencia experimental del grado de estandarización alcanzado a nivel global, y de su posible impacto en los resultados obtenidos.

Objetivo. Determinar si con los protocolos técnicos desarrollados y descritos anteriormente en este trabajo, se reduce la variabilidad técnica a niveles insignificantes, respecto a las diferencias biológicas existentes entre distintas poblaciones celulares y que permiten una discriminación inequívoca entre ellas, a nivel multicéntrico.

Material y métodos. En esta sección se distribuyó una muestra de SP de un donante sano estabilizada con TransFix (Cytomark, Buckingham, Reino Unido) y dividida en alícuotas de 1 mL, a cada uno de los 8 centros participantes. Adicionalmente, en cada centro se obtuvieron (localmente) entre 3 y 4 muestras de SP de diferentes donantes sanos. Cada una de las muestras se marcó con una versión modificada del panel EuroFlow para la evaluación de muestras con escasa celularidad (SST, abreviado del inglés "small sample tube") y que específicamente incluía los siguientes AcMo: CD20-PacB, CD45-PacO, CD8-FITC, CD27-PE, CD4-PerCP-Cy5.5, CD19-PE-Cy7, CD14-APC y CD3-APC-H7. Para cada muestra, localmente se identificaron las siguientes poblaciones celulares: linfocitos totales (SSC^{bajo} $CD45^{+}$), monocitos ($CD45^{+}$ $CD14^{+}$), linfocitos B ($CD20^{hi}$ $CD19^{+}$) y linfocitos T de memoria ($CD3^{+}$/$CD27^{+}$) dentro de las subpoblaciones T $CD4^{+}$ y $CD8^{+}$. Para cada una de las subpoblaciones celulares referidas se registró la IMF obtenida para los marcadores que resultaron positivos en las mismas. Posteriormente, se enviaron los resultados obtenidos junto con los ficheros de datos originales para su análisis centralizado. En dicho envío se incluyó también la información sobre los valores obtenidos localmente para el pico de referencia de las esferas de calibración, el día en que se realizó el experimento. A nivel central se calcularon los CVs para los valores de IMF obtenidos para cada población celular y canal de fluorescencia, para todas las muestras. Para la visualización de las diferencias/similitudes, se fusionaron los ficheros de datos y se identificaron con distinto color cada una de las poblaciones celulares de referencia. En todos los centros, la calibración del equipo, la compensación de fluorescencias y el marcaje de las muestras se realizó siguiendo los protocolos estandarizados descritos en las secciones anteriores.

Resultados. La comparación de los valores de IMF del pico de referencia de las esferas de calibración, mostró un CV entre los diferentes citómetros empleados en cada centro de < 5,5%. Las mediciones locales de la muestra de la sangre estabilizada y distribuida a cada centro mostró CVs para las IMF de cada población celular sistemáticamente <44%. Este valor fue similar al valor máximo (44%) obtenido en las muestras de sangre periférica obtenidas, procesadas y analizadas localmente en cada centro y que correspondía con la variación observada en la expresión del marcador CD3-APC-H7. Merece destacar que para 4 de los 8 marcadores analizados se obtuvieron CVs inferiores a 17% para en las distintas poblaciones celulares analizadas. La fusión de los ficheros de datos generados en cada centro, seguida de la identificación de las diferentes subpoblaciones de linfocitos y monocitos presentes en las mismas, mostró como estas formaban grupos de eventos claramente diferentes y que se correspondían con cada una de las diferentes poblaciones celulares identificadas manualmente, demostrando que las diferencias biológicas no se veían afectadas por la posible variabilidad técnica.

Conclusión. Los resultados derivados de la validación a nivel multicéntrico de los protocolos estandarizados para la calibración del citómetro de flujo, la compensación de fluorescencias, el marcaje para antígenos de membrana y el análisis de datos, demuestran que con ellos se obtienen datos con un nivel de variabilidad técnica despreciable, respecto a la variabilidad biológica existente entre diferentes poblaciones celulares humanas de sangre periférica.

Leukemia (2012) **26**, 1986–2010

www.nature.com/leu

Open

SPECIAL REPORT

EuroFlow standardization of flow cytometer instrument settings and immunophenotyping protocols

T Kalina[1,11], J Flores-Montero[2,11], VHJ van der Velden[3], M Martin-Ayuso[4], S Böttcher[5], M Ritgen[5], J Almeida[2], L Lhermitte[6], V Asnafi[6], A Mendonça[7], R de Tute[8], M Cullen[8], L Sedek[9], MB Vidriales[10], JJ Pérez[10], JG te Marvelde[3], E Mejstrikova[1], O Hrusak[1], T Szczepański[9], JJM van Dongen[3] and A Orfao[2] on behalf of the EuroFlow Consortium (EU-FP6, LSHB-CT-2006-018708)

The EU-supported EuroFlow Consortium aimed at innovation and standardization of immunophenotyping for diagnosis and classification of hematological malignancies by introducing 8-color flow cytometry with fully standardized laboratory procedures and antibody panels in order to achieve maximally comparable results among different laboratories. This required the selection of optimal combinations of compatible fluorochromes and the design and evaluation of adequate standard operating procedures (SOPs) for instrument setup, fluorescence compensation and sample preparation. Additionally, we developed software tools for the evaluation of individual antibody reagents and antibody panels. Each section describes what has been evaluated experimentally versus adopted based on existing data and experience. Multicentric evaluation demonstrated high levels of reproducibility based on strict implementation of the EuroFlow SOPs and antibody panels. Overall, the 6 years of extensive collaborative experiments and the analysis of hundreds of cell samples of patients and healthy controls in the EuroFlow centers have provided for the first time laboratory protocols and software tools for fully standardized 8-color flow cytometric immunophenotyping of normal and malignant leukocytes in bone marrow and blood; this has yielded highly comparable data sets, which can be integrated in a single database.

Leukemia (2012) **26,** 1986–2010; doi:10.1038/leu.2012.122

Keywords: flow cytometry; standardization; compensation; software; fluorochromes; immunophenotyping

INTRODUCTION

Immunophenotyping is currently one of the fundamental pillars for the diagnosis and classification of leukemia and lymphoma.[1] In the last two decades multiparameter flow cytometry has become the preferred method to assess the immunophenotypic features of cells present in peripheral blood (PB), bone marrow (BM), lymph node (LN) biopsy specimens, cerebrospinal fluid (CSF) and other types of samples suspected of containing neoplastic hematopoietic cells.[1,2] During the first part of this period, the list of clinically useful antibodies (Abs) has progressively increased,[3–5] leading to the definition of complex immunophenotypic profiles. In parallel, the number of antigens that can be assessed in a single measurement has increased dramatically owing to the availability of new multicolor digital instruments and a greater number of compatible fluorochromes.[6,7] This has facilitated more precise identification and phenotypic characterization of specific populations of tumor cells in samples over the background of the coexisting residual normal leukocyte subsets.[8] However, the higher complexity of the immunophenotypic approaches and panels of reagents involved in such characterization demanded increasing expertise for correct interpretation of the data obtained. As a consequence, disturbing levels of subjectivity have been introduced, depending on the experience and knowledge of individual experts and the variable panels of reagents applied in different clinical diagnostic laboratories.

In order to decrease such variability and subjectivity, consensus recommendations and guidelines have been produced by several expert groups.[3,5,9–14] These documents have had a wide impact and they have been followed by many centers around the world, but they have been only partially successful for several reasons. First, they focus on lists of markers without specific recommendations about reagent clones, fluorochrome conjugates or optimally designed antibody combinations in the panel. Second, they fail to provide robust protocols for the selection of the most appropriate (i) combinations of fluorochromes and fluorochrome-conjugated reagents in a panel, (ii) sample preparation techniques, (iii) standard operating procedures (SOPs) to establish instrument settings prior to the measurements and (iv) the most adequate strategies for data analysis. Most importantly, the so far proposed sets of markers have never been prospectively evaluated.

In 2006 the EU-supported EuroFlow Consortium (EU-FP6, LSHB-CT-2006-018708) started a project aimed at the prospective design and evaluation of panels of antibodies for the diagnosis

[1]Department of Pediatric Hematology and Oncology, 2nd Faculty of Medicine, Charles University (DPH/O), Prague, Czech Republic; [2]Cancer Research Center (IBMCC-CSIC), Department of Medicine and Cytometry Service, University of Salamanca (USAL) and Institute of Biomedical Research of Salamanca (IBSAL), Salamanca, Spain; [3]Department of Immunology, Erasmus MC, University Medical Center Rotterdam, Rotterdam, The Netherlands; [4]Cytognos SL, Salamanca, Spain; [5]Second Department of Medicine, University Hospital of Schleswig Holstein, Campus Kiel (UNIKIEL), Kiel, Germany; [6]Department of Hematology, Hôpital Necker and UMR CNRS 8147, University of Paris Descartes (AP-HP), Paris, France; [7]Department of Hematology, Portuguese Institute of Oncology (IPOLFG), Lisbon, Portugal; [8]Haematological Malignancy Diagnostic Service (HMDS), University of Leeds (UNIVLEEDS), Leeds, UK; [9]Department of Pediatric Hematology and Oncology, Medical University of Silesia (SUM), Zabrze, Poland and [10]Department of Hematology, University Hospital Salamanca (HUS) and IBSAL, Salamanca, Spain. Correspondence: Professor JJM van Dongen, Department of Immunology, Erasmus MC, University Medical Center Rotterdam, Dr Molewaterplein 50, 3015 GE Rotterdam, The Netherlands.
E-mail: j.j.m.vandongen@erasmusmc.nl or b.vanbodegom@erasmusmc.nl
[11]Shared first authorship, because TK and JFM have equally contributed to this manuscript.
Received 12 January 2012; accepted 14 February 2012

and classification of the most frequent subtypes of leukemias and lymphomas in which immunophenotyping has proven to be relevant. The major objectives were (i) to provide comprehensive multicolor combinations of fluorochrome-conjugated antibodies aimed at answering those medical questions for which multicolor flow cytometry immunophenotyping is indicated, (ii) to prospectively evaluate their performance in multiple diagnostic laboratories and (iii) to optimize the reagent panel whenever required. For this purpose, proven reproducibility in multiple diagnostic laboratories was mandatory. Therefore, the definition of optimal antibody panels also required an effort in the selection of the most appropriate combination of compatible fluorochromes, the design and evaluation of adequate SOPs for instrument setup, fluorescence compensation and sample preparation and elaboration of adequate software tools for the overall evaluation of the phenotypic profiles obtained.

In the first five sections of this paper, we provide detailed information about the selection of the most appropriate combination of fluorochromes for 8-color panels, the protocols recommended for instrument settings, fluorochrome compensation and sample preparation, together with the data analysis strategies adopted to evaluate the tested antibody reagents and panels. In the last section, results of multicentric evaluation of the level of reproducibility that can be achieved by implementation of all standardization efforts are provided. In each of the sections, we indicate what has been specifically evaluated versus adopted based on existing data.

SECTION 1. FLUOROCHROME SELECTION FOR 8-COLOR PANELS

J Flores-Montero[1], T Kalina[2], JJ Pérez[3], S Böttcher[4], VHJ van der Velden[5], J Almeida[1], L Lhermitte[6], A Mendonça[7], R de Tute[8], M Cullen[8], L Sedek[9], E Mejstrikova[2], JJM van Dongen[5] and A Orfao[1]

[1]USAL, Salamanca, Spain; [2]DPH/O, Prague, Czech Republic; [3]HUS, Salamanca, Spain; [4]UNIKIEL, Kiel, Germany; [5]Erasmus MC, Rotterdam, The Netherlands; [6]AP-HP, Paris, France; [7]IPOLFG, Lisbon, Portugal; [8]UNIVLEEDS, Leeds, UK and [9]SUM, Zabrze, Poland

BACKGROUND

Selection of the most appropriate combination of fluorochromes is a key step in designing a multicolor immunophenotypic panel.[15] Usage of the new digital flow cytometers capable of simultaneously measuring multiple (for example, $\geqslant 6$) different fluorescence emissions has only recently become possible in diagnostic laboratories because of the increasing availability of compatible fluorochromes.[16–21] However, the varying spectral overlap of such fluorochromes has also led to a higher complexity of fluorescence compensation matrices.[6,22,23]

Fluorochrome selection largely depends on the intrinsic characteristics of each individual fluorescent compound, particularly its excitation and emission profile, its relative brightness, the spillover into other fluorescence detectors and its stability.[24] The selection of the most adequate fluorochrome combination also depends on the specific optical configuration of the flow cytometer, that is, the number and type of laser lines it contains, the number of detectors available for each laser and the specific set of filters for each individual laser.[7] Furthermore, the aim of an antibody panel, the type of samples to be stained (that is, PB, BM versus small cell samples) and the cells contained in it also contribute to the decision on the minimum number of reagents to be simultaneously assessed in individual tubes.[25,26] Finally, the availability of optimal clones of fluorochrome-conjugated antibodies also determines the selection of specific combinations of reagents in a panel.[27,28]

On the basis of the innovative immunophenotyping strategy designed by the EuroFlow group in which new data merge and calculation tools are combined for improved diagnosis and classification of hematological malignancies, a minimum requirement of 8-color panels for cost-effective immunophenotyping was foreseen. Such panels should allow simultaneous usage of (i) backbone markers aimed at specific identification of the cell populations of interest and (ii) additional antibody markers devoted to a more detailed characterization of the said cell populations.[29]

In this section we review the selection of flow cytometer instruments, their optical configuration and the set of compatible fluorochromes, as performed during the construction and evaluation of the EuroFlow 8-color panels.

Selection of flow cytometry instruments and their optical configurations

At the time the EuroFlow project started in March 2006, four $\geqslant$8-color flow cytometry instruments from two different manufacturers were available, with flexible and compatible optical configurations (Table 1), which could potentially be used in diagnostic laboratories. The four instruments were taken into consideration in selecting the combinations of fluorochromes to be used in the EuroFlow panels. All four instruments have a three laser-line configuration, with blue (488 nm), red (633 or 635 nm) and violet (405 or 407 nm) lasers.

Selection of fluorochromes

A two-step approach was used by the EuroFlow group for selection of fluorochromes: (i) some fluorochromes were predefined without further specific testing based on previous experience, whereas (ii) others were evaluated prior to their selection. Accordingly, the first two positions for the blue laser line (emission at 488 nm) were pre-selected as fluorescein isothiocyanate (FITC) and phycoerythrin (PE) because of the extensive experience available with both fluorochromes, the large number of high-quality commercially available reagents and their compatibility with the optical configuration of all the four $\geqslant$8-color instruments listed in Table 1. The same selection criteria were applied for Allophycocyanin (APC) as the first fluorochrome for the red laser line (emission at 633/635 nm). Similarly, either peridinin–chlorophyll–protein complex (PerCP) or PerCP–Cyanin5.5 (PerCPCy5.5) and PE–Cyanin7 (PECy7) were left as the most suitable fluorochrome choices for the third and fourth detectors of the blue laser line, respectively. In contrast, APC-Cyanin7 (APCCy7), Alexa Fluor 700 (AF700) and APC-Hilite7 (APCH7) were compared for the second detector of the red laser line, and Pacific Blue (PacB) versus Horizon V450 (HV450) and Pacific Orange (PacO) versus *Anemonia Majano* cyan fluorescent protein (AmCyan)[17] versus Horizon V500 (HV500) were evaluated for the first and second detector of the violet laser line (emission at 405/407 nm), respectively.

For these evaluations several fluorochrome-conjugated antibody reagents were compared: PacB-conjugated CD2(TS1/8), CD3(UCHT1), CD4(RPA-T4), CD20(2H7), CD45(T29/33) and HLADR(L243) versus HV450-conjugated CD2(S5.2), CD3(UCHT1), CD4(RPA-T4), CD20(L27), CD45(HI30) and HLADR(L243); AmCyan-conjugated CD45(2D1) versus PacO-conjugated CD45(HI30) versus HV500-conjugated CD45(HI30); and APCCy7-conjugated CD4(RPA-T4) versus AF700-conjugated CD4(RPA-T4) versus APCH7-conjugated CD4(RPA-T4) antibody(clone) reagents. Antigen expression was evaluated as both mean fluorescence intensity (MFI) and stain index (SI; defined as the difference between the MFI of positive and negative cells divided by 2 s.d.'s of the MFI observed for the negative cell population).[24] In all cases, staining of $\geqslant$5 PB samples was used to evaluate the staining patterns of each pair/group of reagents to be compared. Sample preparation and instrument

Table 1. Typical default optical configuration and most common fluorochromes available for each detector of three lasers, ⩾8-color flow cytometry instruments available in March 2006

Channel	*FACSCanto II (BD Biosciences)*			*FACSAria (BD Biosciences)*			*LSR II (BD Biosciences)*			*CyAn ADP (Dako/Beckman Coulter)*			*Most commonly available fluorochromes*
	Laser	*DM*	*EF*	*Laser*	*DM*	*EF*	*Laser*	*DM*	*EF*	*Laser*	*DM*	*EF*	
1	30 mW Violet (405 nm)		450/50	10 mW Violet (407 nm)		450/50	25 mW Violet (405 nm)		450/50	100 mW Violet (405 nm)		450/50	PacB/HV450
2	30 mW Violet (405 nm)	502	510/50	10 mW Violet (407 nm)	502	530/30	25 mW Violet (405 nm)	502	525/50	100 mW Violet (405 nm)	502	530/40	AmCyan/PacO/HV500
3	20 mW Blue (488 nm)	502	530/30	13 mW Blue (488 nm)	502	530/30	20 mW Blue (488 nm)	502	530/30	25 mW Blue (488 nm)	502	530/40	FITC/AF488
4	20 mW Blue (488 nm)	556	585/42	13 mW Blue (488 nm)	556	585/42	20 mW Blue (488 nm)	556	575/26	25 mW Blue (488 nm)	556	585/42	PE
5				13 mW Blue (488 nm)	610	616/23				25 mW Blue (488 nm)		613/20	PE-TR
6	20 mW Blue (488 nm)	655	670LP	13 mW Blue (488 nm)	655	695/40	20 mW Blue (488 nm)	655	695/40	25 mW Blue (488 nm)	655	680/30	PerCP/PerCPCy5.5
7	20 mW Blue (488 nm)	735	780/60	13 mW Blue (488 nm)	735	780/60	20 mW Blue (488 nm)	735	780/60	25 mW Blue (488 nm)	735	750LP	PECy7
8	17 mW Red (633 nm)		660/20	11 mW Red (633 nm)		660/20	35 mW Red (633 nm)		660/20	60 mW Red (635 nm)		665/20	APC/AF647
9	17 mW Red (633 nm)	735	780/60	11 mW Red (633 nm)	735	780/60	35 mW Red (633 nm)	735	780/60	60 mW Red (635 nm)	735	750LP	APCCy7/APCH7/AF700[a]

Abbreviations: AF, alexa fluor; AmCyan, *Anemonia Majano* cyan fluorescent protein; APC, allophycocyanin; Cy5.5, cyanin5.5; Cy7, cyanin7; DM, dichroic mirror; EF, emission filter; FITC, fluorescein isothiocyanate; H7, hilite7; HV450, Horizon V450; HV500, Horizon V500; LP, long pass; PacB, pacific blue; PacO, pacific orange; PE, phycoerythrin; PerCP, peridinin–chlorophyll–protein; TR, Texas Red. [a]AF700 requires a 710/50 emission filter.

settings were performed in the eight different EuroFlow laboratories as described in Section 2 and Section 4 of this manuscript.

Comparison between the Pacific Blue (PacB) and Horizon V450 (HV450) fluorochromes

The PacB and HV450 fluorochromes showed very similar fluorescence profiles that adequately fit with the optical configuration of the first detector for the violet laser of the four flow cytometry instruments. Detailed comparison of the needs for compensation for the spillover into other detectors of the fluorescence emissions of these two fluorochromes showed that these were slightly higher ($P>0.05$; Mann–Whitney *U* test) for PacB versus HV450; nonetheless, both fluorochromes showed no spillover into any detector except for the second detector of the violet laser (Table 2).

Regarding MFI and SI values, similar results with $<10\%$ differences were found when the same clone and manufacturer were compared. Conversely, when either the clones or the manufacturers were not the same, differences between reagents were higher (Table 3). We have chosen PacB for the EuroFlow panels, based on broader availability of PacB conjugates at the time of testing.

Comparison among the *Anemonia Majano* cyan fluorescent protein (AmCyan), Pacific Orange (PacO) and Horizon V500 (HV500) fluorochromes

Specific comparisons for the second detector of the violet laser line were made for the AmCyan, PacO and HV500 fluorochrome dyes. These fluorochromes showed clearly different fluorescence profiles. Accordingly, in terms of needs for fluorescence compensation, a higher spillover into other channels was observed for AmCyan, particularly in the first detector of the violet laser line ($P<0.01$ versus both PacO and HV500; paired Student's *T*-test) and in the first detector of the blue laser ($P<0.01$ versus both PacO and HV500; paired Student's *T*-test), where either PacB or HV450, and FITC, respectively, are typically measured. Table 2 summarizes the compensation matrix values obtained for these three dyes. In general, the MFI obtained for monoclonal Ab reagents conjugated with these fluorochromes directed against the same antigen was also higher for AmCyan, although different clones were compared and fluorescence differences may not be solely related to the fluorochrome (Table 3). AmCyan showed a higher resolution power, but the higher fluorescence intensity represented a disadvantage when a strong AmCyan signal for a marker was combined with a dim signal of FITC-conjugated reagents in the same cell populations, because of its relatively higher overlap with the first detector of the blue laser (data not shown). In turn, PacO showed low spillover into other channels (Table 2), together with clearly dimmer MFI values (Table 3); nonetheless, its resolution power, as reflected by the observed SI, was comparable to that of AmCyan (Table 3). HV500 showed an intermediate profile between AmCyan and PacO in terms of both needs for compensation and fluorescence intensity of positive cells (higher than PacO but lower than AmCyan), associated with a comparable resolution power (SI) between different cell populations (Table 3).

Comparisons among the Allophycocyanin–Cyanin7 (APCCy7), Alexa Fluor 700 (AF700) and Allophycocyanin–Hilite7 (APCH7) fluorochromes

Comparison of APCCy7, AF700 and APCH7 was performed in sequential steps. First, the performance of each individual fluorochrome was assessed. Accordingly, APCCy7 showed a relatively high intensity (Table 3), while its main disadvantage was the over-time instability, especially in the presence of formaldehyde-based fixatives. This instability resulted in a relatively high and variable degradation-associated 'spillover' into the first channel of the red laser and the appearance in this

Table 2. Mean values of compensation matrices ($n = 5$) obtained at different time points in up to five different EuroFlow flow cytometer instruments for fluorochromes compared for the same fluorescence channel

Laser channel	*Compensation requirements in other fluorescence channels*							
	PacB	*HV450*	*PacO*	*AmCyan*	*HV500*	*APCCy7*	*AF700*	*APCH7*
Violet-1	NA	NA	2.2 ± 0.3*	11.5 ± 1.5	7.5 ± 1.6	0.2 ± 0.3	0.1 ± 0.1	0.1 ± 0.3
Violet-2	27.9 ± 2.8	23.8 ± 2.3	NA	NA	NA	0.3 ± 0.4	0.1 ± 0.1	NR
Blue-1	0.1 ± 0.1	0.1 ± 0.1	0.8 ± 0.4	17.1 ± 2.6	2.8 ± 1.2	0.4 ± 0.4	0.2 ± 0.1	0.2 ± 0.4
Blue-2	NR	0.1 ± 0.1	0.4 ± 0.2	1.4 ± 0.2	0.5 ± 0.2	0.2 ± 0.2	NR	0.1 ± 0.2
Blue-3	0.1 ± 0.1	0.1 ± 0.1	0.5 ± 0.2	0.4 ± 0.1	0.3 ± 0.2	1.2 ± 1.0	3.6 ± 0.7	0.6 ± 1.2
Blue-4	NR	NR	0.1 ± 0.1	NR	NR	3.3 ± 1.9	1.3 ± 0.3	1.7 ± 0.8
Red-1	NR	NR	0.3 ± 0.4	NR	NR	4.8 ± 2.5	0.8 ± 0.2	2.0 ± 1.1
Red-2	0.1 ± 0.1	NR	0.1 ± 0.2	NR	NR	NA	NA	NA

Abbreviations: AF700, alexa fluor 700; AmCyan, *Anemonia Majano* cyan fluorescent protein; APC, allophycocyanin; Cy7, cyanin7; H7, hilite7; HV450, Horizon V450; HV500, Horizon V500; NA, not applicable; NR, not required; PacB, pacific blue; PacO, pacific orange. Results are expressed as percentage values ± s.d. *$P < 0.01$ versus both AmCyan and HV500 (paired Student's *T*-test).

Table 3. Mean fluorescence intensity (MFI) and stain index (SI) values obtained for different sets of reagents evaluated in normal PB samples ($n = 5$)

Marker		*PacB*	*HV450*	P-*value*[a]				
CD2	Clone (manufacturer)	TS1/8 (BioLegend)	S5.2 (BD B)					
	MFI ± s.d. of $CD2^+$ T and NK-cells	5741 ± 755.7	8259 ± 1792.8	0.02				
	SI[c]	37.0	41.4					
CD3	Clone (manufacturer)	UCHT1 (BD Ph)	UCHT1 (BD B)					
	MFI ± s.d. of T-cells	15 774 ± 1503.7	17 246 ± 814.2	0.08	*APCCy7*	*AF700*	*APCH7*	P-*value*[b]
	SI[d]	117.2	130.5					
CD4	Clone (manufacturer)	RPA-T4 (BD Ph)	RPA-T4 (BD B)		RPA-T4 (BD B)	RPA-T4 (BD B)	RPA-T4 (BD B)	
	MFI ± s.d. of $CD4^+$ T-cells	9474 ± 710.2	9195 ± 408.2	0.46	13 596 ± 686.5	4307 ± 174.1	9910 ± 414.3	< 0.001
	SI[e]	61.8	66.6		42.6	41.4	35.0	
CD20	Clone (manufacturer)	2H7 (eBiosciences)	L27 (BD B)					
	MFI ± s.d. of B-cells	30 073 ± 3783.5	38 152 ± 2857.4	0.005	*PacO*	*AmCyan*	*HV500*	P-*value*[b]
	SI[f]	219.61	222.8					
CD45	Clone (manufacturer)	T29/33 (Dako)	HI30 (BD B)		HI30 (Invitrogen)	2D1 (BD B)	HI30 (BD B)	
	MFI ± s.d. of lymphocytes	30 742 ± 824.8	53 709 ± 2062.2	< 0.001	5521 ± 150.6	30 681 ± 2838.3	19 157 ± 686.3	< 0.001
	SI[g]	3.9	5.2		3.8	4.8	3.8	
HLADR	Clone (manufacturer)	L243 (BioLegend)	L243 (BD B)					
	MFI ± s.d. of monocytes	11 509 ± 1721.4	16 874 ± 1934.3	0.002				
	SI[h]	47.7	64.8					

Abbreviations: AF700, alexa fluor 700; AmCyan, *Anemonia Majano* cyan fluorescent protein; APCCy7, allophycocyanin–cyanin7; APCH7, allophycocyanin–hilite7; BD Ph, BD Pharmingen; BD B, BD Biosciences; HV450, Horizon V450; HV500, Horizon V500; PacB, pacific blue; PacO, pacific orange. [a]Paired Student's *T*-test. [b]$P < 0.001$ for the following comparisons: APCH7 versus AF700, AF700 versus APCCy7, APCCy7 versus APCH7, PacO versus AmCyan, PacO versus HV500 and AmCyan versus HV500 (paired Student's *T*-test). [c]Positive reference population (PRP): $CD2^+$ T- and NK-cells and negative reference population (NRP), $CD2^-$ lymphocytes. [d]PRP, T-cells; NRP, B- and NK-cells. [e]PRP, $CD4^+$ T-cells; NRP, $CD4^-$ T-cells. [f]PRP, B-cells; NRP, T- and NK-cells. [g]PRP, lymphocytes; NRP, neutrophils. [h]PRP, monocytes; NRP, lymphocytes.

channel of false-positive events (data not shown), in line with previous observations.[24] More recently, such instability has also been related to a cell-dependent degradation phenomenon.[30] In addition, APCCy7 showed great lot-to-lot differences in brightness and compensation needs (data not shown). AF700 showed little spillover into this latter channel (Table 2), but this dye required the use of a different mirror and filter –680 nm long pass (LP) and 710/50 nm band pass (BP), respectively– than those available by default in all four flow cytometers evaluated. In addition, the fluorescence intensity of AF700 translated into suboptimal discrimination of some antigens expressed at relatively low levels, particularly when they were expressed on cells that had a bright APC signal (decreased SI due to compensation-induced data spread; data not shown). Finally, the APCH7 dye, a more stable APC-based tandem dye with a long Stoke's shift, was tested. It showed a lower SI and MFI than its equivalent APCCy7-antibody

conjugates (Table 3), but the major advantages of APCH7 conjugates included (i) improved stability and (ii) better compensation profile, while (iii) keeping the default optical configuration of the instrument unchanged. These results are illustrated by direct comparison of APCCy7, APCH7 and AF700 conjugates of the same CD4 monoclonal Ab clone from the same manufacturer after staining of normal PB samples ($n = 5$) (Table 3).

CONCLUSION

Selection of appropriate fluorochromes to be combined was a key and pre-requisite step in developing the 8-color EuroFlow panels. On the basis of existing knowledge, experience and proven quality of evaluated reagents, several fluorochromes were pre-selected. For other fluorochrome positions, extensive comparisons were required. Finally, we selected the combination of PacB (or HV450), PacO (or HV500), FITC, PE, PerCPCy5.5, PECy7, APC and APCH7. However, it should be noted that some of these fluorochromes performed at the desirable conditions, but others (for example, APCH7) still leave room for improvement. Substitution of PacO by HV500 and PacB by HV450 might be feasible, provided that identical clones are used, that the new reagents are extensively compared to the reference reagents, and that new compensation matrices are applied, which are adequate for the selected fluorochromes.

SECTION 2. EUROFLOW STANDARD OPERATING PROCEDURE (SOP) TO ESTABLISH STANDARDIZED INSTRUMENT SETTINGS AT MULTIPLE SITES

T Kalina[1], JG te Marvelde[2], VHJ van der Velden[2], J Flores-Montero[3], D Thűrner[1], S Böttcher[4], M Cullen[5], L Lhermitte[6], AS Bedin[6], L Sedek[7], A Mendonça[8], O Hrusak[1], JJM van Dongen[2] and A Orfao[3]

[1]DPH/O, Prague, Czech Republic; [2]Erasmus MC, Rotterdam, The Netherlands; [3]IBMCC-CSIC-USAL, USAL, Salamanca, Spain; [4]UNIKIEL, Kiel, Germany; [5]UNIVLEEDS, Leeds, UK; [6]AP-HP, Paris, France; [7]SUM, Zabrze, Poland and [8]IPOLFG, Lisbon, Portugal

BACKGROUND

Flow cytometers are relatively flexible instruments that allow simultaneous measurement of the light scatter properties of different types of cells and the fluorescence emissions of distinct fluorophores attached to them.[31] Because of their flexibility, adequate setting of instrument conditions, including fine tuning of the light scatter and fluorescence detectors, is required prior to a specific measurement, in order to establish the optimal window of analysis. An additional goal within the EuroFlow project was to define SOPs to establish standardized instrument settings that would allow reproducible (identical or at least highly comparable) measurements at different times in the same instrument or in different instruments at the same or at distinct sites through the application of predefined scatter and MFI values for specific reference particles. In general, with such SOPs, all particles that will be measured should fall in the previously defined window of analysis for the light scatter and each fluorescence detector.

The EuroFlow light scatter settings aim at reaching two goals: (i) all populations of interest (from small erythroblasts to eosinophils and plasma cells) fall centered within the scale limits and (ii) adequate scatter resolution between individual cell populations is obtained, for both cell surface and intracellular staining procedures. Lymphocytes were chosen as an internal biological reference population to control for adequate placement of instrument light scatter settings.

The EuroFlow setting of photomultiplier tube (PMT) voltages for a fluorescence detector is established at a voltage above the electronic noise in such a way that the least autofluorescent cell type to be measured is placed at the left side of the scale, as 'negative' events clearly distinguishable from debris in the multidimensional space generated, dim fluorescent events can be discriminated from the negative, and no cell- or bead-associated fluorescence measurement reaches the upper limit of the scale.[32] Each PMT is characterized by a response of accuracy to PMT voltage measured, as the robust coefficient of variation (rCV) of a dim particle. Optimal PMT voltage is set at the beginning of the plateau of a rCV versus PMT voltage curve.[32] In this way, the electronic noise contribution to the signal is minimal whereas maximal dynamic range is left for the measurement of fluorescence. At the time of writing, Cytometer Setup and Tracking (CS&T) beads (BD Biosciences, San Jose, CA, USA) and Cyto-Cal Multifluor Plus Violet Intensity Calibrator (Thermo Scientific, Freemont, CA, USA) are being evaluated by EuroFlow as potentially suitable additional calibrators for long-term, multi-center studies.

In this section we summarize the most critical and relevant steps included in the EuroFlow SOPs developed for optimal placement of instrument settings.

Instruments and reagents

FACSCanto II (BD Biosciences) flow cytometers were used in seven centers and both an LSR II (BD Biosciences) and a CyAn ADP (Dako, Glostrup, Denmark/Beckman Coulter, Brea, CA, USA) were used in another center. All cytometers were equipped with three lasers emitting at 405/407, 488 and 633/635 nm. Optical filter configurations were identical, with the exceptions described in Table 1. Eight-peak Rainbow bead calibration particles (Spherotech, Lake Forest, IL, USA) were used throughout the study for initial PMT characterization and for setting target MFI values, as well as for daily checks; the same master lot of beads (RCP-30-5A master lot X02) was used throughout the study.

Placement of PMT voltages for fluorescence measurements

To place PMT voltages, the following sequential steps were used: the Rainbow 8-peak bead population showing the second dimmest fluorescence was gated and the rCV of that peak was calculated in each fluorescence channel for PMT voltages ranging from 300 to 999 mV at increments of 50 mV.[33] The optimal voltage for each channel was first determined on one instrument (LSR II) and set at the beginning of the plateau phase of the curve generated. Using the PMT value obtained in this way, the brightest peak was gated and its fluorescence intensity recorded in all channels and then used as preliminary 'Target MFIs' for all other instruments. Subsequently, verification of PMT settings was performed on each individual EuroFlow instrument. For verification of the lower boundary, PMT settings were checked on the rCV versus PMT voltage curve, as described above for the reference instrument. For the 'Target MFI' to be accepted, PMT voltage on each instrument had to be at the plateau of the curve for all nine instruments. Additionally, all bright markers from the EuroFlow antibody panels[29] were tested in the corresponding channels of all instruments; if the target MFI setting resulted in suboptimal PMT setting on any instrument, the target MFI values were adjusted accordingly till consensus target MFI values assuring optimal PMT settings for each instrument were reached.

Placement of instrument settings for light scatter measurements

Fine tuning of scatter settings was based on usage of normal human PB lymphocytes. For this purpose, 50 μl of PB samples obtained from healthy donors (after informed consent was given) and measured within the first 24 h after venipuncture were used at each site. Prior to measurement, non-nucleated red cells were lysed (10 min) using 2 ml of 10X FACS Lysing Solution (BD Biosciences) and diluted 1/10 (vol/vol) in distilled water (dH_2O),

according to the recommendations of the manufacturer. Then, the sample was centrifuged (5 min at 540 *g*), the cell pellet was washed with 2 ml of phosphate buffer saline (PBS; pH = 7.4) containing 0.5% (w/v) bovine serum albumin (BSA; SIGMA-ALDRICH, St Louis, MO, USA) and 0.09% of sodium azide (NaN_3; SIGMA-ALDRICH), centrifuged again under the same conditions and finally resuspended in 250 µl of PBS with 0.5% BSA + 0.09% NaN_3, and measured in the flow cytometer at a 'low' flow rate mode within the first hour after sample preparation. PMT voltages were adjusted so that forward scatter (FSC)/sideward scatter (SSC)-gated lymphocyte singlets reached mean SSC and FSC values of 55 000 ± 5000 and 13 000 ± 2000, respectively.

EuroFlow instrument settings

Final PMT voltages for each fluorescence channel were set for each instrument to reach target MFI values using the brightest peak of Rainbow 8-peak beads of the same lot. Subsequent rainbow bead lots were assigned new target MFI values by cross-calibration using the previous lot for an instrument in a single laboratory (DPH/O, Prague, Czech Republic) (Table 4, see also www.euroflow.org for the updated target MFI of other Rainbow bead lots). In turn, light scatter settings were placed as described above. Inclusion of the FSC-H parameter will allow discrimination of doublets in a FSC-Area (FSC-A) versus FSC-Height (FSC-H) bivariate plot, contributing further to the accuracy of the results.[34] The final instrument settings for both light scatter and fluorescence-associated PMT voltages are further referred as EuroFlow settings. The detailed EuroFlow SOP for instrument setup is available at the EuroFlow website (www.euroflow.org).

Monitoring of instrument performance

Monitoring of instrument performance was done daily (at each cold start) after laser stabilization was allowed for 30 min. Rainbow 8-peak beads were acquired under EuroFlow settings (under 'disabled compensation' conditions) and the MFI of the brightest peak in each fluorescence channel was compared with the corresponding target MFI value. The following criteria had to be reached for the instrument to pass the check: (i) MFI values within the target MFI ± 15%, and (ii) coefficient of variation (CV) of the brightest peak <4% for the blue and violet laser channels, but <6% for the red laser channels and the PECy7 channel. Whenever instrument performance failed, measures such as thorough cleaning, de-gassing flow cell and laser delay verification were taken. When the performance was not restored to pass the monitoring criteria, a service visit was requested. After a service visit, PMT settings were adjusted as described above and a new compensation experiment was performed as described in Section 3 of this manuscript.

MFI values of the brightest Rainbow bead peak were daily reported for each individual flow cytometer. As the scaling of axes is different on FACSCanto II and LSR II (262 144 channels) as compared to CyAn ADP (4096 channels), the Rainbow beads

Table 4. Target mean fluorescence intensity (MFI) values obtained after optimal PMT adjustments for each fluorescence channel for the brightest peak of Rainbow 8-peak calibration beads in the LSR II instrument

Fluorochrome channel	*MFI values Rainbow lot no.*		
	X02, Y02	*Z02*	*EAB01*
PacB	195 572	194 818	215 352
PacO	231 265	216 293	217 908
FITC	59 574	58 372	65 283
PE	101 900	98 520	84 847
PerCPCy5.5	216 064	223 940	228 818
PECy7	27 462	27 185	29 865
APC	176 780	226 435	252 000
APCH7	56 437	81 371	102 099

Abbreviations: APC, allophycocyanin; Cy7, cyanin7; FITC, fluorescein isothiocyanate; H7, hilite7; PacB, pacific blue; PacO, pacific orange; PE, phycoerythrin; PerCPCy5.5, peridinin–chlorophyll–protein–cyanin5.5.

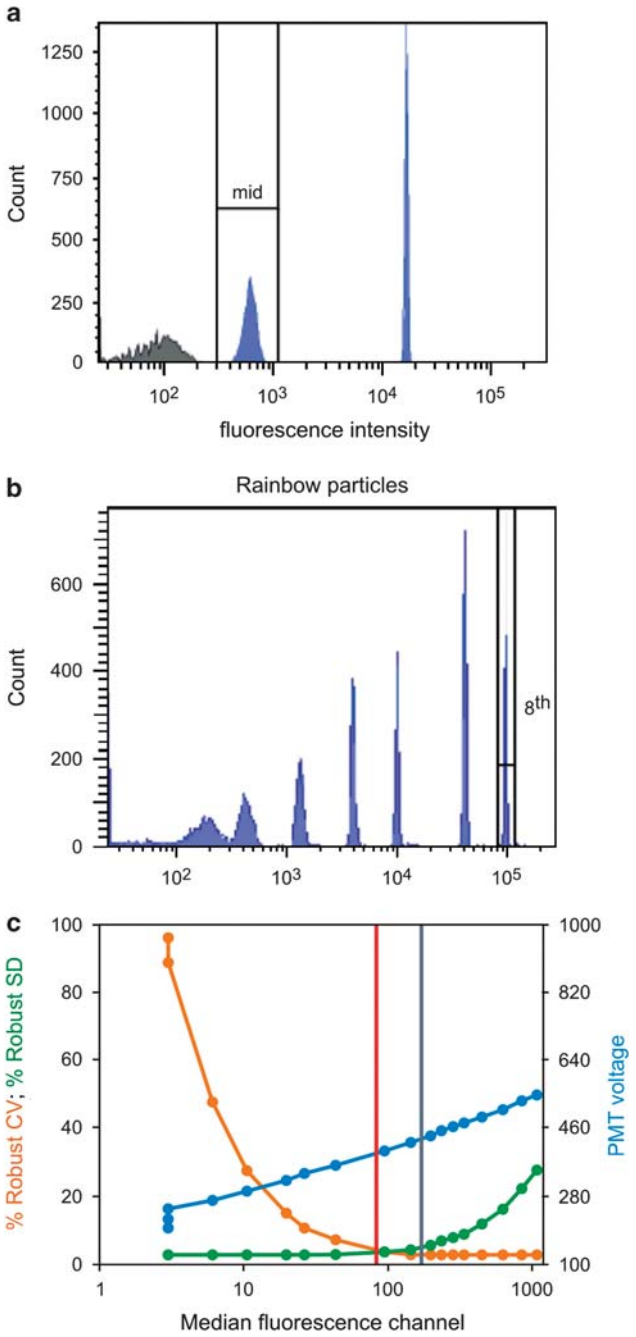

Figure 1. Comparison of cytometer setting & tracking (CS&T) module and EuroFlow baseline settings obtained for the fluorescein isothiocyanate (FITC) channel (blue laser line) in one representative instrument. CS&T (mid-fluorescence peak in **a**) and EuroFlow (Rainbow beads brightest, eighth peak in **b**) baseline settings are compared in **c** (gray and red vertical lines, respectively) for the robust coefficient of variation (CV) and robust electronic noise (SD_{EN}). Note that although EuroFlow settings used lower PMT voltages, the robust CV values (orange line) and robust SD_{EN} values (green line) are still in their plateau phases.

Table 5. Variation of mean fluorescence intensity (MFI) values obtained for the brightest bead population of the Rainbow 8-peak beads in individual instruments placed in eight different EuroFlow centers (seven FACSCanto II and one LSR II flow cytometers)

Fluorochrome-associated PMT detector	*Target MFI*	*Mean MFI[a] of individual measurements (n = 12)*	*CV*
PMT 1—PacB	195 572	193 109	5.40%
PMT 2—PacO	231 265	225 152	4.63%
PMT 3—FITC	59 574	59 003	2.08%
PMT 4—PE	101 900	100 763	2.38%
PMT 5—PerCPCy5.5	216 064	215 596	2.11%
PMT 6—PECy7	27 462	27 639	3.13%
PMT 7—APC	176 780	176 190	1.68%
PMT 8—APCH7	56 437	56 610	2.16%

Abbreviations: APC, allophycocyanin; CV, coefficient of variation; Cy7, cyanin7; FITC, fluorescein isothiocyanate; H7, hilite7; PacB, pacific blue; PacO, pacific orange; PE, phycoerythrin; PerCPCy5.5, peridinin–chlorophyll–protein–cyanin5.5; PMT, photomultiplier tube. [a]Results are expressed as arbitrary MFI channel values scaled from 0 to 262 144.

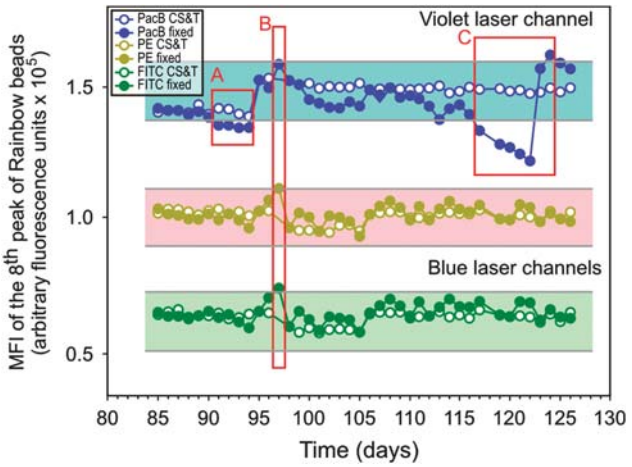

Figure 2. Overtime stability of Rainbow 8-peak bead mean fluorescence intensity (MFI) profile, illustrating the results obtained for three fluorescence channels: pacific blue (PacB) channel of the violet laser (blue dots); phycoerythrin (PE) channel of the red laser (yellow dots); and fluorescein isothiocyanate (FITC) channel of the green laser (green dots), for the same flow cytometer instrument upon long-term monitoring of MFI measurements for the brightest peak of the Rainbow 8-peak beads. As shown, faulty violet laser was recognized as a source for the decreased MFI values falling below 15% of the target MFI (boxes A and C). Acceptable ± 15% range for each channel are depicted by gray lines and a colored background. After a service visit and laser alignment, MFI values above 15% of the target MFI were detected (box B); thus, photomultiplier tube (PMT) voltages were adjusted at this time point manually (closed circles). Please note that by placement of instrument settings as per the cytometer setting & tracking (CS&T) module the PMT could be adjusted to correct for the violet laser failure (open circles) until the laser failed completely and was replaced.

data file was first converted to FCS 2.0 format and then read with the CyAn ADP's Summit software (Dako) to calculate the corresponding numerical values with the same distribution over the scale.

Automated baseline settings and instrument monitoring

When FACSDiVa V6.0 software with the CS&T module and BD CS&T beads (BD Biosciences) were introduced in 2008, baseline PMT settings were placed according to the manufacturers' instructions for the FACSCanto II and the LSR II instruments. Subsequently, PMT voltage settings were adjusted manually in the CS&T module, to create EuroFlow baseline settings. Electronic noise (SD_{EN}) and rCV of the dimmest CS&T bead values obtained with the two baseline settings were compared for eight instruments (data of one representative instrument is shown in Figure 1).

Instrument monitoring with the CS&T module was performed in parallel to the EuroFlow instrument performance-monitoring SOP on three different instruments (two FACSCanto II and one LSR II), for a 3-month period. To evaluate instrument performance, we calculated the CV of MFI values obtained for the brightest peak of 8-peak Rainbow particles.

Reproducibility of fluorescence intensity measurements with EuroFlow settings

The level of standardization of the EuroFlow settings was evaluated at two different time points, before standardization evaluation experiments were performed as described in Section 6. Results of such evaluation showed nearly identical MFI values for individual PMTs when their voltage was set to match the target MFI fluorescence channels listed in Table 4. In all eight instruments, the CV for the MFI values obtained for the brightest peak of Rainbow beads was systematically lower than 5.5% (Table 5).

Long-term evaluation of the MFI signal fluctuation with fixed PMT voltages revealed that in each of the eight instruments evaluated, changes of up to ± 15% of the mean target MFI might transiently occur, whereas significant maintenance or hardware issues were highlighted by not meeting the above-described monitoring criteria, with deviations in these values (Figure 2).

Electronic noise level with EuroFlow settings

The SD_{EN} level obtained with individual flow cytometers using EuroFlow settings was highly comparable to that obtained through the CS&T module (Figure 1), except for the PerCPCy5.5 channel (Table 6). Thus, it could be concluded that the EuroFlow approach for PMT settings yields high-quality data with no impairment of the quality of the results obtained, due to higher electronic noise over individual CS&T module baseline. On average, the EuroFlow approach set PMT voltages at lower levels (Table 6), which allows for slightly larger dynamic ranges for measurements on the detectors. Of note, the significantly higher SD_{EN} value obtained

Table 6. PMT voltages and electronic noise (SD_{EN}) obtained with the EuroFlow settings versus the CS&T module

Fluorochrome-associated PMT detector	*PMT voltage*		*SD_{EN}*		P-*value*[a]
	CS&T module settings	*EuroFlow settings*	*CS&T module settings*	*EuroFlow settings*	
PMT 1—PacB	431 (357–490)	412 (360–460)	24.1 (20–29.8)	24 (20.6–29.1)	0.92
PMT 2—PacO	509 (414–633)	466 (395–581)	25.2 (21.3–28.1)	24.5 (20.2–27.3)	0.08
PMT 3—FITC	483 (399–555)	438 (375–518)	28.2 (25.4–31.2)	28.9 (26.2–29.7)	0.98
PMT 4—PE	462 (411–501)	395 (370–445)	30.9 (18.1–33.6)	31.1 (18.3–32.4)	0.46
PMT 5—PerCPCy5.5	543 (456–610)	522 (440–591)	28.1 (18.1–31.3)	29.1 (18.2–32.9)	0.03
PMT 6—PECy7	624 (589–757)	552 (539–707)	29 (22.1–32.6)	29.5 (20.7–31.8)	0.49
PMT 7—APC	614 (543–687)	576 (501–629)	26 (16.8–28.9)	25.9 (12.8–28.9)	0.95
PMT 8—APCH7	489 (435–662)	524 (481–687)	25.1 (17.5–36)	26 (14.1–36.6)	0.50

Abbreviations: APC, allophycocyanin; CS&T, Cytometer Setting & Tracking; Cy7, cyanin7; FITC, fluorescein isothiocyanate; H7, hilite7; PacB, pacific blue; PacO, pacific orange; PE, phycoerythrin; PerCPCy5.5, peridinin–chlorophyll–protein–cyanin5.5; PMT, photomultiplier tube. [a]Two-tailed Student's *T*-test. Results are expressed as mean (min–max) values.

for the PerCPCy5.5 channel was still well-fitted in the plateau phase of the voltage versus SD_{EN} curve.

CONCLUSION

The EuroFlow SOP was designed to establish and daily monitor standard instrument settings for a common bright signal placed at the same level in different flow cytometer instruments. Overall, our results show optimal performance at different sites and instruments (even from different manufacturers), with early alarms for changes in hardware components that may impact the results. At the same time, the EuroFlow SOP avoids performing full calibration of the instrument (including compensation) on a daily basis.

SECTION 3. DESIGN AND EVALUATION OF EUROFLOW STANDARD OPERATING PROCEDURE FOR ESTABLISHING OPTIMAL COMPENSATION SETTINGS

T Kalina[1], JG te Marvelde[2], VHJ van der Velden[2], J Flores-Montero[3], D Thűrner[1], S Böttcher[4], M Cullen[5], L Lhermitte[6], L Sedek[7], A Mendonça[8], O Hrusak[1], JJM van Dongen[2] and A Orfao[3]

[1]DPH/O, Prague, Czech Republic; [2]Erasmus MC, Rotterdam, The Netherlands; [3]USAL, Salamanca, Spain; [4]UNIKIEL, Kiel, Germany; [5]UNIVLEEDS, Leeds, UK; [6]AP-HP, Paris, France; [7]SUM, Zabrze, Poland and [8]IPOLFG, Lisbon, Portugal

BACKGROUND

Most fluorochromes used in multicolor flow cytometry have relatively broad fluorescence emission spectra.[7,35] Therefore, measurement of their fluorescence emissions is typically not restricted to a single fluorescence channel but the emissions are also measured in detectors other than the primary channel for a particular fluorochrome (secondary fluorescence channels).[7] Spectral overlap of light into secondary channels might lead to false-positive signals. However, the proportion of light spillover from the total fluorescence emission is constant for each fluorochrome, implying that this spillover can be mathematically calculated and subtracted.[7] The term 'fluorescence compensation' is typically used to describe this calculation and subtraction process. In general, the specific compensation values required depend on the spectral characteristics of the dyes, the optical bandpass filters and dichroic mirrors mounted in the flow cytometer, the intensity of the measured signal and the specific voltage used for the PMT where it is detected.[7] In digital flow cytometers, fluorescence compensation is applied after data acquisition.[36] Accurate calculation of the compensation values for a set of fluorochromes across multiple detectors is provided by the compensation tools available in conventional flow cytometry software once applied to data derived from the flow cytometric measurement of one or more sets of single fluorochrome-stained standards/controls.[36] A full compensation matrix is calculated by the software based on each standard/control, and then it is applied to the measured data. A prerequisite to establish appropriate compensation settings is that the spectral characteristics of light emissions collected in individual channels for the standards/controls exactly match those of the dye(s) used in the experiment. Despite this, special attention should be paid to the fact that several currently used dyes are compound tandem dyes, where one fluorochrome serves as an acceptor of laser light energy and transfers this energy to the second dye of the tandem by fluorescence resonance energy transfer (FRET).[7] Tandem dyes greatly enhance the Stoke's shift of the compound fluorochrome, but their manufacturing process may lead to non-uniform spectral characteristics of the tandems.[7] Thus, tandem dyes (that is, PECy7, APCH7) present with variable spillover light to the donor dye channel depending on the proximity and amount of FRET acceptor dyes used;[7] this frequently translates into the need for specific compensation controls/standards and settings for individual 8-color combinations containing different reagents conjugated to the same tandem dye.[7] A second prerequisite for optimal compensation settings is that standards/controls must contain bright signals, so that the distance between the positive

Table 7. List of fluorochrome-conjugated antibodies used to set up fluorescence compensation matrices at individual centers

Generic fluorochromes and tandem fluorochromes					
Generic fluorochromes		*Tandem fluorochromes*			
Generic targets	*Positive target (bead or cell) population*[a]	*PECy7 targets*	*Positive target (bead or cell) population*[a]	*APCH7 targets*	*Positive target (bead or cell) population*[a]
CD20-PacB	B-cells	CD2-PECy7	$CD2^+$ T/NK-cells	CD3-APCH7	T-cells
CD45-PacO	Lymphocytes	CD8-PECy7	$CD8^{hi}$ T-cells	CD4-APCH7	$CD4^+$ T-cells
CD8-FITC	$CD8^{hi}$ T-cells	CD10-PECy7[b]	CompBead	CD8-APCH7	$CD8^{hi}$ T-cells
CD8-PE[c]	$CD8^{hi}$ T-cells	CD16-PECy7	NK-cells	CD9-APCH7[b]	CompBead
CD5-PerCPCy5.5[d]	$CD5^+$ T-cells	CD19-PECy7	B-cells	CD10-APCH7[b]	CompBead
CD8-APC[c]	$CD8^{hi}$ T-cells	CD45RA-PECy7	$CD45RA^+$ T-cells	CD14-APCH7[e]	Monocytes
		CD45RO-PECy7	$CD45RO^+$ T-cells	CD19-APCH7	B-cells
		CD56-PECy7	NK- and $CD56^+$ T-cells	CD24-APCH7	B-cells
		CD117-PECy7[b]	CompBead	CD38-APCH7	$CD38^{hi}$ Lymphocytes
		HLADR-PECy7	B- and $HLADR^{hi}$ T-cells	CD43-APCH7	T-cells
				CD49d-APCH7	T-cells
				CD71-APCH7[b]	CompBead
				CD81-APCH7	B-cells
				anti-λ – APCH7[b]	CompBead

Abbreviations: APC, allophycocyanin; Cy7, cyanin7; FITC, fluorescein isothiocyanate; H7, hilite7; PacB, pacific blue; PacO, pacific orange; PE, phycoerythrin; PerCPCy5.5, peridinin–chlorophyll–protein–cyanin5.5. [a]Unless otherwise indicated, the negative reference population used for each reagent was the lymphocytes from the 'unstained' control tube. For more information about the specific clones used, please see van Dongen *et al.*[29] [b]'Negative' CompBead used as negative reference population. [c]The CD8-PE and CD8-APC antibodies are not part of the EuroFlow antibody panels and might be used from any reliable source. [d]This tandem dye requires generic compensation; [e]Artificially $CD14^-$ monocyte population created by 'appending' 5000 events from the unstained tube to this single antibody-stained tubes (SAbST) acquisition.

and negative subsets of events used to calculate fluorescence compensation values is as high as the maximum distance in the experimental samples to be measured. In practice, single reagent-stained cells or mouse immunoglobulin (Ig)-capture beads are used as compensation standards.[37] It should be noted that compensation settings must be defined only after the PMT voltage is set for the experiment, because of its impact on fluorescence intensity and spillover into secondary channels.[37]

In this section we describe the procedures used to design and evaluate the compensation matrix required for routine use of the EuroFlow panels proposed for the different 8-color combinations of fluorochrome-conjugated antibodies, defined in the EuroFlow 8-color panels.[29]

Fluorescence compensation standards and controls

Specific subsets of PB leukocytes stained with fluorochrome-conjugated antibody reagents in single antibody-stained tubes (SAbST) were used as standards (Table 7) to establish the fluorescence compensation matrices to be applied to flow cytometric data measured using the 8-color EuroFlow panels for the diagnosis and classification of leukemias and lymphomas. SAbST were prepared as described in Section 4 for multiple single-stained aliquots of a normal PB sample showing negative to very bright expression of the stained reagents. In addition, reagent-specific SAbSTs for molecules not present on normal PB cells (for example, CD117 PECy7) were created using Ig-capture beads (CompBead, BD Biosciences) as specific standards for these specific reagents in the panel. Furthermore, normal and patient samples stained with the preliminary and final versions of the EuroFlow panels were used to confirm the utility of the calculated compensation matrices. The specific set of reagents used for fluorescence compensation purposes varied depending on the selected fluorochrome-conjugated antibodies at each round of evaluation of the EuroFlow panels, as described in van Dongen *et al.*[29] Table 7 displays the set of markers used for the final version of the EuroFlow panels.[29]

Fluorescence compensation setup

Compensation standards and controls were acquired with FACSDiVa software or Summit software using the software compensation tools. The setup containing the PMT voltage for each fluorescence channel and the compensation matrix calculated by the software was saved as 'EuroFlow' Setup into the FACSDiVa Setup Catalog, or as 'EuroFlow Protocol' in Summit. Templates were prepared for experiments and tubes labeled with the reagents' names beforehand, linked to the EuroFlow settings. Thus, reagent-specific compensation was applied accurately to the matching reagent labels, even when the compensation matrix was recalculated. In every center, compensation setup experiments were performed by default once a month. Whenever instrument monitoring failed and PMT voltages were reset to match target MFI values, the compensation setup experiment was repeated.

Comparison of fluorescence compensation matrices obtained at different days and at distinct centers

Compensation setup experiments showed that generic compensation matrices could be used for all antibody reagents in the EuroFlow panels conjugated with the PacB, PacO, FITC, PE and APC fluorochromes, as well as for the PerCPCy5.5 tandem fluorochrome (data not shown). In contrast, different values were required for both the PECy7 and APCH7 tandem fluorochromes, depending on the specific reagent conjugates used (Supplementary Table 1).

To evaluate and compare the fluorescence compensation settings established at different times in each center, compensation matrices were evaluated from 14 listmode data files in FCS 3.0 format, measured in seven centers (two per center); each of the

Table 8. Fluorescence compensation matrix values obtained from listmode data files ($n = 14$) generated in 7 centers at two different time points for a total of 7 different flow cytometry instruments[a]

			Secondary fluorescence channel							
			PacB	*PacO*	*FITC*	*PE*	*PerCPCy5.5*	*PECy7*	*APC*	*APCH7*
Primary fluorescence channel	PacB	MIN		24.3	0.0		0.0	0.0		
		MEDIAN	**NA**	**27.7**	**0.0**	**NR**	**0.0**	**0.0**	**NR**	**NR**
		MAX		31.0	0.2		0.6	0.1		
	PacO	MIN	1.9		0.2	0.0	0.0	0.0	0.0	0.0
		MEDIAN	**2.4**	**NA**	**0.4**	**0.2**	**0.3**	**0.0**	**0.0**	**0.0**
		MAX	2.9		0.5	0.3	0.5	0.1	0.3	0.5
	FITC	MIN	0.0	4.8		10.0	3.0	0.2	0.0	0.0
		MEDIAN	**0.0**	**5.6**	**NA**	**12.0**	**3.5**	**0.3**	**0.0**	**0.0**
		MAX	0.1	6.4		16.0	4.0	0.5	0.2	0.2
	PE	MIN	0.0	0.0	0.2		30.1	2.2	0.0	
		MEDIAN	**0.0**	**0.1**	**1.3**	**NA**	**32.9**	**2.5**	**0.1**	**NR**
		MAX	0.1	0.3	1.7		38.9	2.8	0.1	
	PerCPCy5.5	MIN	0.0	0.0	0.0	0.0		12.5	1.6	1.0
		MEDIAN	**0.0**	**0.0**	**0.0**	**0.0**	**NA**	**16.5**	**2.4**	**5.5**
		MAX	0.9	0.9	0.2	0.1		18.8	3.7	8.0
	PECy7	MIN	0.0	0.0	0.0	0.2	0.6		0.0	3.2
		MEDIAN	**0.0**	**0.0**	**0.1**	**0.7**	**2.9**	**NA**	**0.0**	**6.8**
		MAX	0.4	0.6	0.5	13.1	5.7		0.9	9.1
	APC	MIN					1.0	0.1		8.5
		MEDIAN	**NR**	**NR**	**NR**	**NR**	**1.2**	**0.1**	**NA**	**9.6**
		MAX					1.4	0.2		11.6
	APCH7	MIN	0.0	0.0	0.0	0.0	0.0	1.3	1.3	
		MEDIAN	**0.0**	**0.0**	**0.0**	**0.0**	**0.0**	**1.5**	**1.8**	**NA**
		MAX	0.2	0.1	0.2	0.1	0.2	2.0	3.9	

Abbreviations: APC, allophycocyanin; Cy7, cyanin7; FITC, fluorescein isothiocyanate; H7, hilite7; NA, not applicable; NR, compensation was never required; PacB, pacific blue; PacO, pacific orange, PE, phycoerythrin; PerCPCy5.5, peridinin–chlorophyll–protein–cyanin5.5. [a]Results are expressed as median percentage values and range. Median values are highlighted in bold.

two compensation matrices used per center had been established after a new compensation experiment (Table 8).

Overall, compensation matrices were shown to be similar in all seven instruments evaluated (Table 8) and their variability among instruments was similar to that observed with time within each of the laboratories for individual instruments ($P > 0.05$, paired Student's *T*-test). Although compensation requirements depend on the specific PMT voltage settings, overall, high spillover was detected for the PacB into the PacO channel and for PE into the PerCPCy5.5 channel. Furthermore, intermediate spillover was found between PerCPCy5.5 and PECy7, between FITC and PE, PECy7 and APCH7, and between APC and APCH7 detectors (Table 8). Compensation experiments performed 1 month apart yielded very similar compensation values ($P > 0.05$; paired Student's *T*-test).

CONCLUSION

Fluorescence compensation setup procedures were designed to establish fluorescence compensation matrices for every individual 8-color combination of fluorochrome-conjugated reagents in the 8-color EuroFlow panels.[29] The complexity of the procedure was higher than desired due to the need for different compensation values for reagents conjugated with the PECy7 and APCH7 fluorochrome tandems. Fortunately, the frequency of compensation could be set to a time interval of 1 month, during which only minor deviations from target MFI values were recorded on well-performing instruments, as assessed by routine (daily) monitoring of the standard instrument settings (see Section 2). Notably, highly stable compensation matrices were obtained at different times among all different EuroFlow laboratories with the proposed fluorescence compensation setup SOP. This suggests that in the future, software solutions for automated establishment of compensation matrices to experiments performed with adjusted PMT voltages to target MFI values may potentially be developed and implemented.

SECTION 4. SAMPLE PREPARATION AND STAINING

VHJ van der Velden[1], J Flores-Montero[2], JG te Marvelde[1], S Böttcher[3], L Lhermitte[4], AS Bedin[4], J Almeida[2], JJ Pérez[5], M Cullen[6], P Lucio[7], E Mejstrikova[8], T Szczepański[9], T Kalina[8], A Orfao[2] and JJM van Dongen[1]

[1]Erasmus MC, Rotterdam, The Netherlands; [2]USAL, Salamanca, Spain; [3]UNIKIEL, Kiel, Germany; [4]AP-HP, Paris, France; [5]HUS, Salamanca, Spain; [6]UNIVLEEDS, Leeds, UK; [7]IPOLFG, Lisbon, Portugal; [8]DPH/O, Prague, Czech Republic and [9]SUM, Zabrze, Poland

BACKGROUND

At present multiple protocols and reagents are available for staining leukocytes.[5,26,38–42] Most protocols include a staining

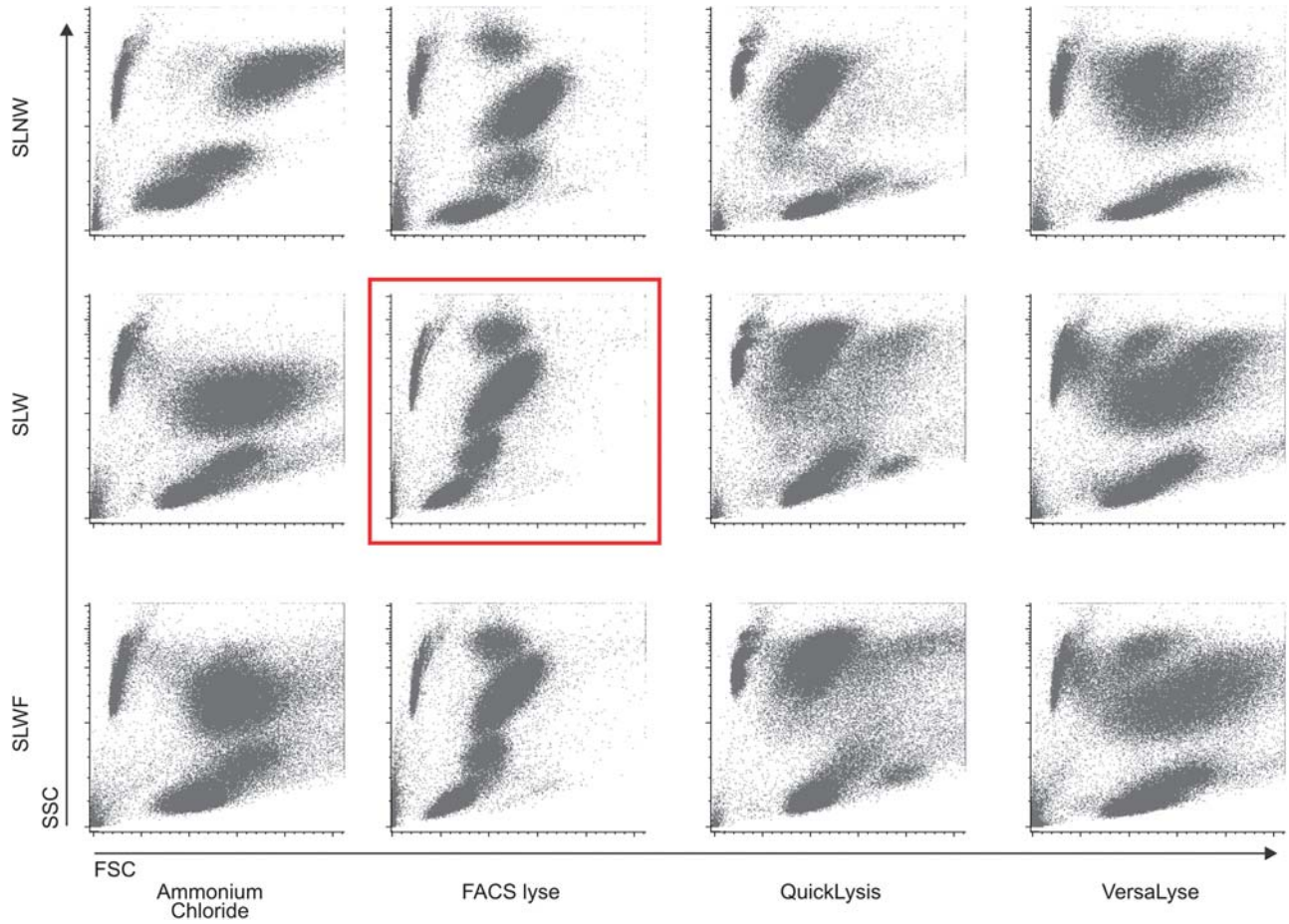

Figure 3. Illustrating example of the differences in the light scatter characteristics of the major subsets of peripheral blood leukocytes observed for the distinct lysing solutions and staining protocols. Please note the significant reduction in the light scatter CV for the different leukocyte populations observed with FACS Lysing Solution and a SLW protocol (red square). Events shown in the upper-left corner of each dot plot correspond to PerfectCOUNT beads (Cytognos SL) introduced for the evaluation of cell loss. SLW, stain-lyse-wash; SLWF, stain-lyse-wash-fix; SLNW, stain-lyse-no wash.

step, one or more washing steps and an erythrocyte lysing step (whenever non-nucleated red cells are present in the sample), but for enumeration of leukocytes the washing step is frequently omitted.[5] Erythrocytes can be lysed using ammonium chloride or other commercially available reagents, for example, FACS Lysing Solution, QuickLysis (Cytognos SL, Salamanca, Spain) and VersaLyse (Beckman Coulter).[5] For staining of intracellular proteins (for example, cytoplasmic (Cy)CD3, CyMPO, nuclear (Nu)TdT) the leukocytes need to be fixed and permeabilized as well.[38,42] For this purpose, several reagents, such as BD Perm/Wash buffer (BD Biosciences), Fix&Perm (AN DER GRUB Bio Research GmbH, Vienna, Austria), IntraStain (Dako) and IntraPrep (Beckman Coulter), are commercially available. Cell samples other than BM and PB, such as LN biopsies, CSF, pleural effusion fluid and vitreous humor, may need extra steps prior to the staining procedure.[43] For example, CSF samples need to be collected in tubes with special medium in order to prevent substantial cell loss[26] and LN biopsies need to be cut into small pieces and homogenized.[41]

The choice of procedure and reagents applied to stain leukocytes depends on the aim of the experiment, but generally the best procedure should fulfill the following criteria: (a) low CVs on FSC and SSC; (b) large differences in mean channel values for FSC and SSC between major leukocyte populations; (c) minimal cell loss; (d) preservation of fluorochrome brightness; (e) no impact on the stability of tandem fluorochromes; (f) low background staining; (g) minimal inter-laboratory variation; and (h) easy and fast performance. Taking this into account, the EuroFlow Consortium has evaluated several procedures for the staining of samples suspected of containing neoplastic hematopoietic cells.

Cell samples

The EuroFlow antibody panels[29] are designed for diagnosis and classification of all major hematological malignancies. Although most EuroFlow antibody panels are primarily designed for evaluation of BM and/or PB samples, other samples, for example, pleural effusions and fine-needle aspirates, can be used as well. The preferred patient materials for these panels are discussed elsewhere.[29]

Erythrocyte lysing and staining procedures evaluated

Overall, four different erythrocyte lysing solutions (ammonium chloride, FACS Lysing Solution, QuickLysis and VersaLyse) were evaluated to assess which best fulfilled the above-listed criteria. Reagents were evaluated in all eight EuroFlow centers on PB samples obtained from 30 healthy donors, who gave their informed consent to participate in the study. Three different tubes were stained for each lysing solution: (1) CD4-PacB, CD8-AmCyan, CD45-FITC, CD19-PE and CD14-APC (all from BD Biosciences); (2) CD4-PerCPCy5.5, CD19-PECy7 and CD8-APCH7 (all from BD Biosciences) and (3) CD19-PECy7 (from Beckman Coulter). Briefly, 50 μl of PB was incubated (15 min in darkness) with the antibodies in a final volume of 100 μl. Subsequently, the lysing solution was added to the tube according to the instructions of the manufacturers and incubated for 10 min at room temperature in darkness. After centrifugation (5 min at 540 *g*), the supernatant was discarded and the cell pellet resuspended in 2 ml PBS + 0.5% BSA. After another centrifugation step (5 min at 540 *g*), the supernatant was discarded and the cell pellet resuspended in 250 μl PBS + 0.5% BSA. For tube 1, 50 μl of PerfectCOUNT beads (Cytognos SL) was added immediately prior to the acquisition in

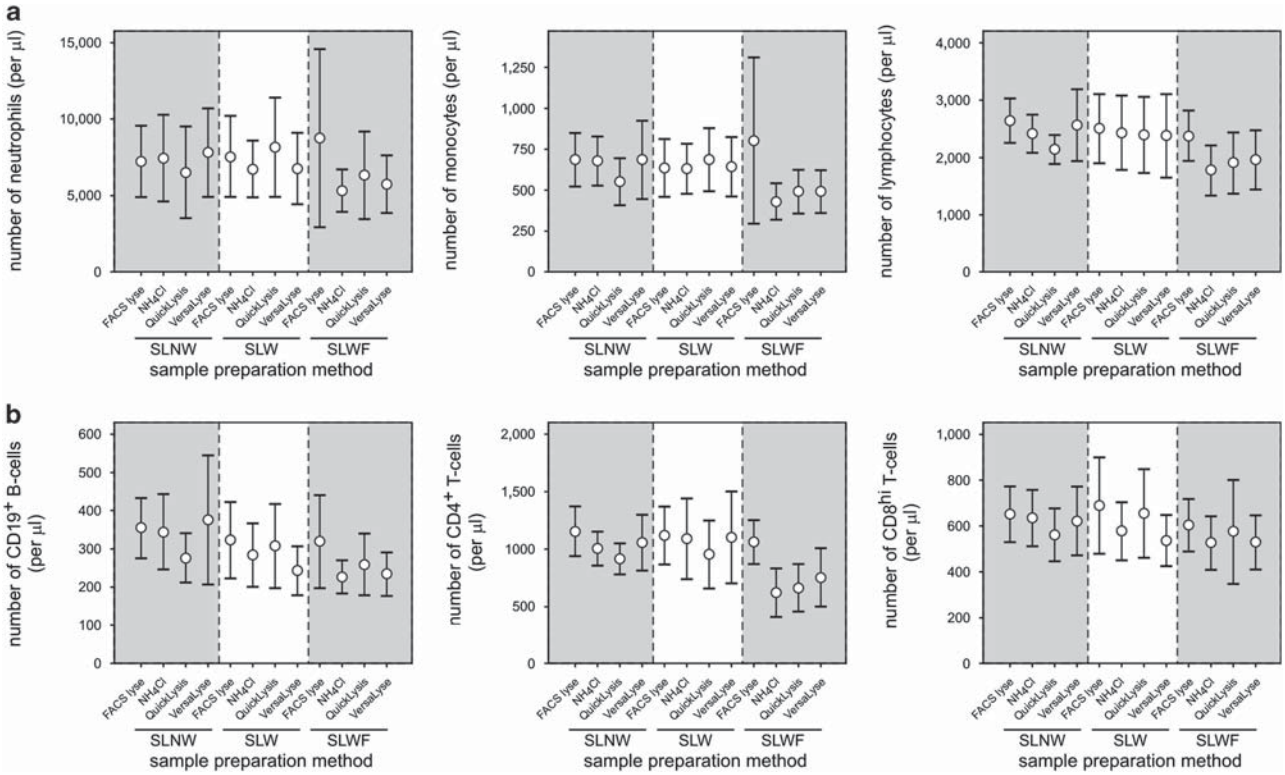

Figure 4. Comparison of the absolute cell counts of major leukocyte populations (**a**) and lymphocyte subsets (**b**) obtained with the four different lysing solutions (FACS Lysing Solution, Ammonium Chloride, QuickLysis and VersaLyse Lysing Solution) evaluated in combination with the three different staining procedures (SLNW, SLW, SLWF) tested. Results are shown as mean values (open circles) and 95% confidence intervals (vertical lines). FACS Lyse, FACS Lysing Solution; NH_4Cl, ammonium chloride; VersaLyse, VersaLyse Lysing Solution. SLW, stain-lyse-wash; SLWF, stain-lyse-wash-fix; SLNW, stain-lyse-no wash.

the flow cytometer. All samples were acquired in a flow cytometer at four different time points (0, 1, 3 and 24 h after staining) and data about 100 000 events per tube were recorded and stored. Stained samples were stored at 4 °C till acquisition at the 1-, 3- and 24-h time points.

Data recorded for tube 1 included: (a) qualitative comparison of the separation obtained among major leukocyte populations; (b) mean FSC and SSC channel and CVs detected for eosinophils, neutrophils, monocytes and total lymphocytes; (c) absolute number of eosinophils, neutrophils, monocytes, $CD19^+$ B-cells, $CD4^+$ T-cells and $CD8^{hi}$ T-cells; (d) MFI and CV values observed for CD45 (for each cell population) and for CD19, CD4, CD8 and CD14 for $CD19^+$ B-cells, $CD4^+$ T-cells, $CD8^{hi}$ T-cells and $CD14^{hi}$ monocytes, respectively. Data recorded for the other two monoclonal Ab combinations (tubes 2 and 3) included MFI and CVs of positive cells in the specific channel, MFI and CVs of negative cells in the same channel, and, for the tandem fluorochromes, the fluorescence signals (MFI values) in all other channels than the primary fluorochrome-specific one.

Overall, three different staining procedures were evaluated: stain-lyse-wash (SLW), stain-lyse-wash-fix (SLWF) and stain-lyse-no wash (SLNW). The SLW procedure is described above; for the SLWF procedure the final cell pellet was resuspended in PBS containing 0.5% paraformaldehyde instead of PBS + 0.5% BSA. For the SLNW procedure, sample preparation ended after incubation (10 min) with the lysing solution without any further washing step.

Qualitative comparison of the scatter characteristics of the major PB cell populations for the four erythrocyte lysing solutions evaluated showed that FACS Lysing Solution and ammonium chloride yielded the best discrimination among them, independently of the staining procedure used. Furthermore, comparison between the three staining procedures tested showed that CVs for both FSC and SSC were lower and more homogeneous with the SLNW method, except when the FACS Lysing Solution was used, which improved the FSC and SSC CVs with the washing step (Figure 3).

In general, the SLNW resulted in the highest cell numbers, whereas specific loss of lymphocytes (Figure 4a) and lymphocyte subsets (Figure 4b) was observed with the SLW and SLWF procedures. However, cell loss was significantly lower when FACS Lysing Solution was used (versus all other lysing reagents) (Figure 4).

Subsequently, we evaluated the effect of the different lysing solutions and staining procedures on the fluorescence intensities. Both the washing step and the final fixation step induced some decrease in the MFI of all antibodies evaluated. Overall, FACS Lysing Solution generally resulted in the highest MFI values (Figure 5). There were no clear differences in MFI values or spillover of fluorescence emissions into secondary channels (MFI of 'non-specific' channels) between the four different lysing solutions tested.

Based on the data derived from the performance of the four different lysing reagents and the different sample preparation protocols, it was decided to use a stain-lyse-wash procedure with FACS Lysing Solution for all cell surface membrane (Sm) labelings. The detailed protocols recommended are shown in Table 9. As displayed there, due to the presence of Igs in plasma, membrane stainings for Ig chains (for example, Igκ, Igλ and Igμ) required washing steps prior to antibody incubation. Based on experience, practical feasibility and additional testing (data not shown), it was agreed to include NaN_3 (at a concentration of 0.09%) in all washing solutions and to ensure that all immunostainings including SmIgs were preceded by two washing steps with 10 ml PBS + 0.5% BSA (Table 9). The latter procedure resulted in maximal SmIg staining intensities (data not shown).

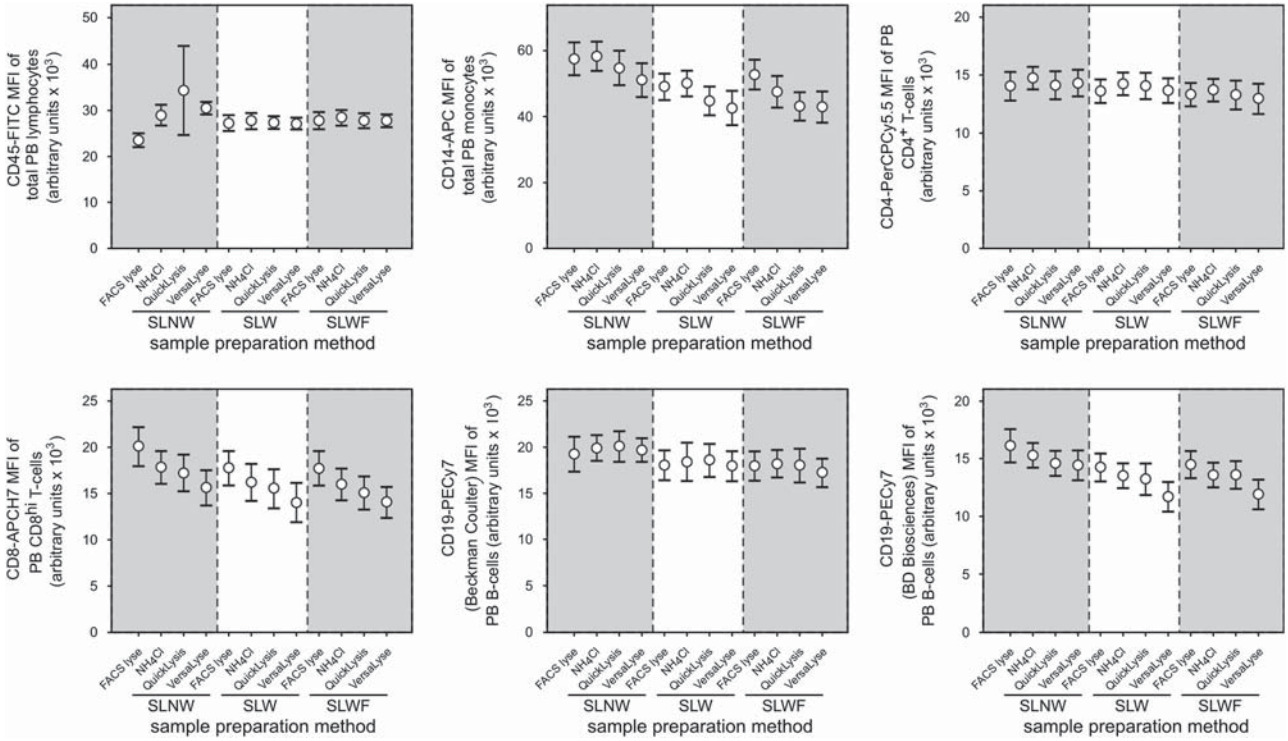

Figure 5. Comparison of the mean fluorescence intensity (MFI) values of six fluorochrome-conjugated antibodies obtained with the four different lysing solutions evaluated in combination with the three different staining procedures (SLNW, SLW, SLWF) tested. CD45-fluorescein isothiocyanate (FITC) was evaluated on total peripheral blood (PB) lymphocytes, CD14-allophycocyanin (APC) was evaluated on PB monocytes, CD4-peridinin chlorophyll protein cyanin5.5 (PerCPCy5.5) was evaluated on PB $CD4^+$ T-lymphocytes, CD8-APC hilite7 (H7) on PB $CD8^{hi}$ T-lymphocytes and the two CD19-phycoerythrin cyanin 7 (PECy7) reagents were both evaluated on PB $CD19^+$ B-lymphocytes. Results are shown as mean values (open circles) and 95% confidence intervals (vertical lines). FACS Lyse, FACS Lysing Solution; NH_4Cl, ammonium chloride; VersaLyse, VersaLyse Lysing Solution. SLW, stain-lyse-wash; SLWF, stain-lyse-wash-fix; SLNW, stain-lyse-no wash.

Table 9. Detailed EuroFlow Standard Operating Procedures (SOPs) for sample preparation and staining

A. Common initial procedure when the EuroFlow antibody panel includes SmIg staining

If the EuroFlow antibody panel is going to be applied to a sample that includes SmIg staining, follow these initial steps; otherwise go directly to the backbone, surface or intracellular staining protocols (sections B, C, D, respectively):

1. Pipette 300 μl of sample into a 10-ml tube (see Note 1). *Note 1:* For small samples (i.e. CSF, vitreous aspirates) spin down the total volume (5 min at 540 *g*), discard the supernatant (see point 5) and resuspend in 300 μl of PBS + 0.5% of bovine serum albumin (BSA) + 0.09% sodium azide (NaN_3).
2. Add 10 ml filtered PBS + 0.5% BSA + 0.09% NaN_3
3. Mix well
4. Centrifuge for 5 min at 540 *g*
5. Discard the supernatant using a Pasteur pipette or vacuum system without disturbing the cell pellet
6. Add 10 ml PBS + 0.5% of BSA + 0.09% NaN_3 to the cell pellet
7. Mix well
8. Centrifuge for 5 min at 540 *g*
9. Discard the supernatant using a Pasteur pipette or vacuum system without disturbing the cell pellet
10. Resuspend the cell pellet in 200 μl of PBS + 0.5% BSA + 0.09% NaN_3
11. Continue with conventional EuroFlow SOPs for staining of cell surface or cell surface plus intracellular markers as described below in procedures B, C and D, respectively

B. Staining of backbone markers

1. Calculate the total volume of surface membrane backbone antibodies based on the number of tubes in the panel (see Note 2).
   Note 2: Intracellular backbone markers should not be added here.
2. Pipette these antibodies in one tube (backbone tube)
3. Calculate the total volume of sample to be stained, also based on the number of tubes in the panel and a volume of 50 μl per tube
4. Pipette this sample volume into the backbone tube
5. Mix well
6. Pipette equal amounts of the sample/backbone mix into the various tubes included in the applied EuroFlow panel (see Note 3).
   Note 3: Both the volume pipetted into each tube and the overall number of tubes depends on the specific EuroFlow panel that is applied.
7. Continue with the steps described below in procedure C

C. Staining of surface markers only (see Note 4):

Note 4: PCD tube 2 is processed identically to PCD tube 1 as described in section D if CD138-PacO is used.

1. Add the appropriate volume of antibodies directed against cell surface markers (except for the backbone markers), as recommended for each specific EuroFlow panel
2. If necessary, use PBS + 0.5% BSA + 0.09% NaN_3 to reach a final volume of 100 μl per tube (see information on the EuroFlow panels)
3. Mix well
4. Incubate for 15 min at room temperature (RT) protected from light
5. Add 2 ml of 1x FACS Lysing Solution (10x FACS Lysing Solution diluted 1/10 vol/vol in distilled water (dH_2O))
6. Mix well
7. Incubate for 10 min at RT protected from light
8. Centrifuge for 5 min at 540 *g*
9. Discard the supernatant using a Pasteur pipette or vacuum system without disturbing the cell pellet, leaving approximately 50 μl residual volume in each tube
10. Add 2 ml of PBS + 0.5% BSA + 0.09% NaN_3 to the cell pellet
11. Mix well
12. Centrifuge for 5 min at 540 *g*
13. Discard the supernatant using a Pasteur pipette or vacuum system without disturbing the cell pellet, leaving approximately 50 μl residual volume in each tube
14. Resuspend the cell pellet in 200 μl PBS + 0.5% BSA + 0.09% NaN_3
15. Acquire the cells after staining or (if not immediately acquired) store at 4 °C maximally for 3 h until measured in the flow cytometer

D. Combined staining of intracellular and surface membrane markers (see Note 5):

Note 5: Tube 4 of the AML/MDS panel should be stained/processed further as described in Procedure E

1. Add the appropriate volumes of antibodies for cell surface markers, as recommended for each specific EuroFlow panel
2. If necessary, use PBS + 0.5% BSA + 0.09% NaN_3 to reach a volume of 100 μl per tube (see information on the EuroFlow panels)
3. Mix well
4. Incubate for 15 min at RT protected from light
5. Add 2 ml of PBS + 0.5% BSA + 0.09% NaN_3 to the cell pellet
6. Mix well
7. Centrifuge for 5 min at 540 *g*
8. Discard the supernatant using a Pasteur pipette or vacuum system without disturbing the cell pellet, leaving approximately 50 μl residual volume in each tube
9. Resuspend the cell pellet by mixing gently
10. Add 100 μl of Reagent A (fixative; Fix&Perm, An der Grub, Vienna, Austria)
11. Incubate for 15 min at RT protected from light
12. Add 2 ml of PBS + 0.5% BSA + 0.09% NaN_3 to the cell pellet
13. Mix well
14. Centrifuge for 5 min at 540 *g*
15. Discard the supernatant using a Pasteur pipette or vacuum system without disturbing the cell pellet, leaving approximately 50 μl residual volume in each tube
16. Resuspend the cell pellet by mixing gently
17. Add 100 μl of Reagent B (permeabilizing solution; Fix&Perm)
18. Mix well
19. Add the appropriate volume of the intracellular antibodies (see EuroFlow panels)

Table 9. (Continued)

20. Mix well
21. Incubate for 15 min at RT protected from light
22. Add 2 ml of PBS + 0.5% BSA + 0.09% NaN_3 to the cell pellet
23. Mix well
24. Centrifuge for 5 min at 540 *g*
25. Discard the supernatant using a Pasteur pipette or vacuum system without disturbing the cell pellet, leaving approximately 50 μl residual volume in each tube
26. Resuspend the cell pellet in 200 μl PBS + 0.5% BSA + 0.09% NaN_3
27. Acquire the cells after staining or (if not immediately acquired) store at 4 °C maximally for 3 h until measured in the flow cytometer.

E. Nuclear (Nu)TdT staining (Tube 4 AML/MDS EuroFlow panel):
1. Continued from procedure C step 13
2. Add the appropriate amount of the TdT antibody to the cell pellet
3. Mix well
4. Incubate for 15 min at RT protected from light
5. Add 2 ml of PBS + BSA 0.5% + 0.09% NaN_3 to the cell pellet
6. Mix well
7. Centrifuge for 5 min at 540 *g*
8. Resuspend the cell pellet in 200 μl PBS + BSA 0.5% + 0.09% NaN_3
9. Acquire the cells after staining or (if not immediately acquired) store at 4 °C maximally for 3 h until measured in the flow cytometer.

Overview of protocol Sections for the various EuroFlow antibody panels and corresponding tubes.

Antibody panel	*Tube(s)*	*Protocol procedure*				
		A	*B*	*C*	*D*	*E*
ALOT	1				X	
BCP-ALL	1,4	X	X	X		
	2,3	X	X		X	
T-ALL	1–4		X		X	
AML/MDS	1–3, 5–7		X	X		
	4		X	X		X
LST	1	X		X		
SST	1	X		X		
PCD	1–2		X		X	
B-CLPD	1–4	X	X	X		
T-CLPD	1,2,4,6		X	X		
	3,5		X		X	
NK-CLPD	1,2		X	X		
	3		X		X	

Abbreviations: ALOT, acute leukemia orientation tube; AML/MDS, acute myeloid leukemia and myelodysplastic syndrome; BCP-ALL, B-cell precursor acute lymphoblastic leukemia; CLPD, chronic lymphoproliferative disorder; LST, lymphoid screening tube; PCD, plasma cell disorders; SST, small sample tube; T-ALL, T-cell acute lymphoblastic leukemia.

Intracellular stainings

For the staining of intracellular antigens, special procedures are needed to permeabilize and fix the cells.[38,42] On the basis of the extensive experience of the EuroFlow laboratories, the Fix&Perm reagents were selected for this purpose; no additional comparison with other commercially available reagents was performed. The detailed protocols are shown in Table 9.

Although the Fix&Perm reagents work well for NuTdT staining, it was decided that within the acute myeloid leukemia (AML)/myelodysplastic syndrome (MDS) protocol, staining of NuTdT will be done using FACS Lysing Solution, based on the performance previously reported,[38] because all tubes can then be treated in a similar way and additional effects on the light scatter characteristics of leukocytes (which could potentially hamper their use as common parameters to every stained aliquot) are avoided. This was not applied to staining of NuTdT in the BCP-ALL and T-ALL panels,[29] because in such cases additional stainings for other intracellular markers were required (that is, CyIgμ, CyTCRβ and CyCD3), for which Fix&Perm reagents already was shown to be of utility.[38,42]

To ensure similar staining intensities of the backbone markers in all tubes (for both membrane and intracellular stainings), all antibodies were titrated for a total volume (antibodies and sample) of 100 μl in every tube. If this volume was not reached, PBS + 0.5% BSA + 0.09% NaN_3 was added to increase the volume to 100 μl. In some EuroFlow tubes, the total volume exceeded 100 μl. This was accepted as long as the total volume remained below 115 μl, as such minor deviations had no impact on the staining intensities of the backbone markers (data not shown).

Processing of cell samples with low nucleated cell counts

As described above, the sample preparation protocols and the different lysing solutions tested here were evaluated for the staining of whole BM and PB samples. However, in some patients the cell count may be rather low. This occurs, for example, in a substantial number of pediatric MDS patients and certainly will occur in samples obtained during therapy. We therefore evaluated whether it was possible to perform bulk lysis of erythrocytes with ammonium chloride prior to the EuroFlow protocol, to increase considerably the concentration of nucleated cells in the sample. Initially, within the AML/MDS panel,[29] slight differences were observed for CD16, CD11b and CD15, but after titration of antibodies, fluorescence emissions were highly comparable

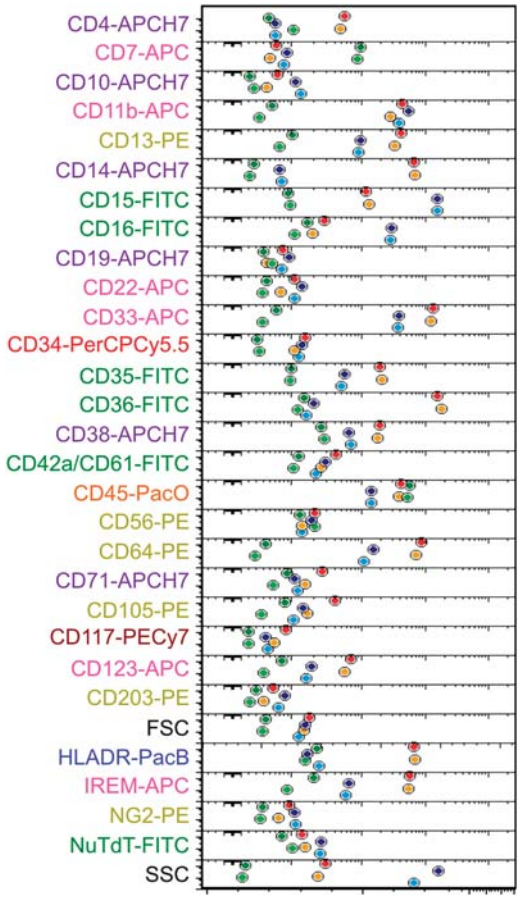

Figure 6. Parameter band plot of all individual parameters evaluated in a bone marrow sample from an MDS patient treated according to the EuroFlow protocol with (light colors) or without (dark colors) prior bulk lysis. Colored circles represent median scatter and fluorescence intensity (MFI) values obtained for the lymphocytes (dark green/light green), monocytes (red/orange) and neutrophils (dark blue/light blue).

between both procedures (Figure 6). Therefore, bulk lysis may be used prior to antibody staining when nucleated cell concentration needs to be increased, such as for the AML/MDS EuroFlow panel.[29] As low cell counts less likely occur in other hematological diseases at diagnosis, prior bulk lysis was not specifically tested for these protocols.

Sample acquisition in the flow cytometer

As the time between staining of the samples and data acquisition in the flow cytometer may have an impact on the MFI of individual markers (particularly of those detected by reagents containing tandem fluorochromes), we acquired the samples immediately after staining, as well as 1, 3 and 24 h after sample preparation was completed. Our results show that MFI generally decreased over time, particularly when lysing solutions that did not contain fixative (that is, ammonium chloride) were used (Figure 7a). The most stable results were obtained with FACS Lysing Solution combined with either the SLNW or the SLW procedures (Figure 7b). Data became somewhat more variable when acquired 3 h and particularly 24 h after staining (Figures 7a and b).

On the basis of the results reported above, it was agreed that all samples should preferably be acquired within 1 h after completing the staining procedure. If not measured immediately, they should be stored at 4 °C in the darkness. Samples should be acquired on flow cytometers that have been set up according to the EuroFlow SOPs as described in Sections 2 and 3. For the EuroFlow screening and orientation tubes (acute leukemia orientation tube (ALOT), lymphoid screening tube (LST), small sample tube (SST) and plasma cell dyscrasia (PCD)),[29] a minimum of 50 000 cells (typically 100 000) should be acquired in order to reach sufficient sensitivity for recognition of abnormal populations.

CONCLUSION

The EuroFlow protocols for sample preparation and staining were designed based on previous experience and experimental data available in the literature together with the results of specific experiments performed by the EuroFlow Consortium. Based on the combined results, the EuroFlow Consortium favors the use of a SLW procedure with FACS Lysing Solution for cell surface antigens, where measurements are performed shortly (<1 h) after sample preparation is completed. Special situations were envisaged for the staining of SmIgs, intracellular markers and samples with low nucleated cell counts, where introduction of additional washing steps, a fixation/permeabilization step and bulk lysis prior to staining, respectively, are recommended. The EuroFlow sample preparation and staining protocols described here are designed to be used together with EuroFlow SOPs for instrument setup (Section 2) and fluorescence compensation (Section 3) for the selected fluorochromes (Section 1). The proposed sample preparation and staining protocols perfectly fit with the EuroFlow antibody panels designed for the diagnosis and classification of hematological malignancies[29] when using the most common types of samples, such as PB and BM. Specific issues related to other types of samples that have peculiar features and require unique sample preparation protocols (for example, CSF) are addressed in the EuroFlow antibody panel report.[29]

SECTION 5. EUROFLOW STRATEGIES AND TOOLS FOR DATA ANALYSIS

M Martín-Ayuso[1], ES Costa[2], CE Pedreira[3], Q Lécrevisse[4], J Hernández[1], L Lhermitte[5], S Böttcher[6], JJM van Dongen[7] and A Orfao[4]

[1]Cytognos SL, Salamanca, Spain; [2]Universidade Federal do Rio de Janeiro (UFRJ), Rio de Janeiro, Brazil; [3]Engineering Graduate Program, Electrical Engineering Program (COPPE PEE) and Faculty of Medicine (FM), Universidade Federal do Rio de Janeiro (UFRJ), Rio de Janeiro, Brazil; [4]USAL, Salamanca, Spain; [5]AP-HP, Paris, France; [6]UNIKIEL, Kiel, Germany and [7]Erasmus MC, Rotterdam, The Netherlands

BACKGROUND

Even though we have seen considerable improvements of clinical flow cytometry over the last years, the multicolor capabilities of currently available flow cytometers are still far behind the requested needs in routine clinical diagnostic laboratories. For example, the current immunophenotypic diagnosis of distinct WHO categories of hematological malignancies frequently requires the assessment of $\sim$30 different markers on neoplastic cells, which cannot be routinely studied on the same cell, owing to technical limitations.[44–47] In order to overcome these technical limitations, multiple aliquots of a sample are stained with different combinations of markers.[47] In this approach, a few markers aim at the reproducible definition of the cell population(s) of interest; the so-called backbone markers are repeatedly used in every aliquot of the same sample and combined with other sets of markers, which together aim at the detailed immunophenotypic characterization of the cell population(s) of interest.[47]

Despite their clear benefits, these advances in multiparameter flow cytometry have led to a significantly increased complexity of data analysis and data interpretation because of the higher

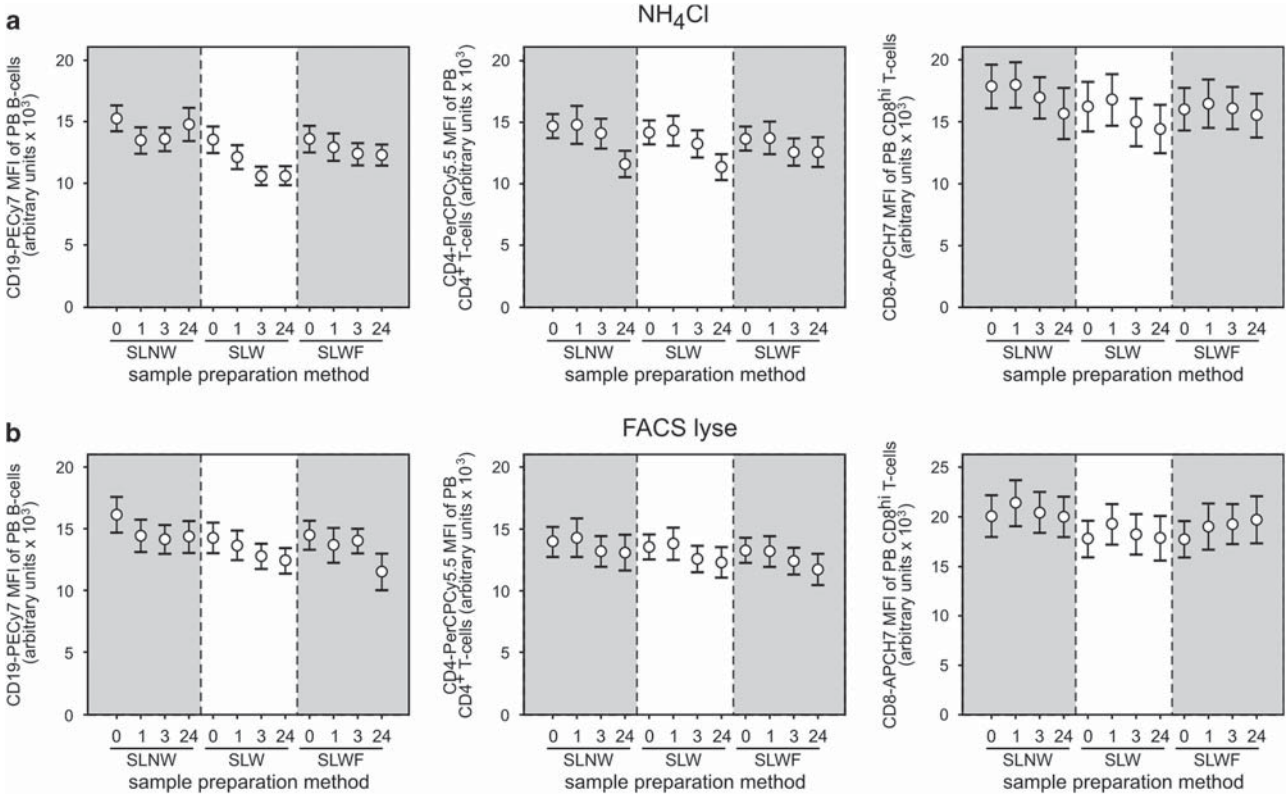

Figure 7. Effect of time between completion of staining and data acquisition in the flow cytometer (0 h, 1 h, 3 h and 24 h) and the sample preparation protocol on the mean fluorescence intensity (MFI) of CD19-phycoerythrin cyanin 7 (PECy7), CD4-peridinin chlorophyll protein cyanin5.5 (PerCPCy5.5) and CD8-allophycocyanin hilite7 (APCH7) on peripheral blood (PB) B-cells, $CD4^+$ T-cells and $CD8^{hi}$ T-cells, using ammonium chloride (**a**) or FACS Lysing Solution (**b**) as lysing reagents. Three different sample preparation protocols were evaluated: SLNW; SLW and SLWF. Results are shown as mean values (open circles) and 95% confidence intervals (vertical lines). FACS Lyse, FACS Lysing Solution; NH_4Cl, ammonium chloride. SLW, stain-lyse-wash; SLWF, stain-lyse-wash-fix; SLNW, stain-lyse-no wash.

number of parameters simultaneously assessed in greater numbers of individual cells, and the expanded number of variables that might have an impact on the quality of the results.[44–47] Moreover, these technical improvements have not been paralleled (or followed) by innovations of data analysis and interpretation tools in the software packages routinely used in hematology laboratories. This lack of innovation has further contributed to the increased complexity of immunophenotyping of hematological malignancies.[44,45] In recent years, the EuroFlow Consortium has proposed several new data analysis tools[48–50] aimed at decreasing such complexity through the development of new and more objective data analysis and interpretation strategies.[48–51] These novel tools have been progressively incorporated into the Infinicyt software (Cytognos SL) developed by the EuroFlow Consortium.

In this section we describe the new data analysis strategy proposed by the EuroFlow Consortium to be used in combination with the EuroFlow antibody panels and the EuroFlow SOPs for multiparameter immunophenotypic diagnosis and classification of hematological disorders.

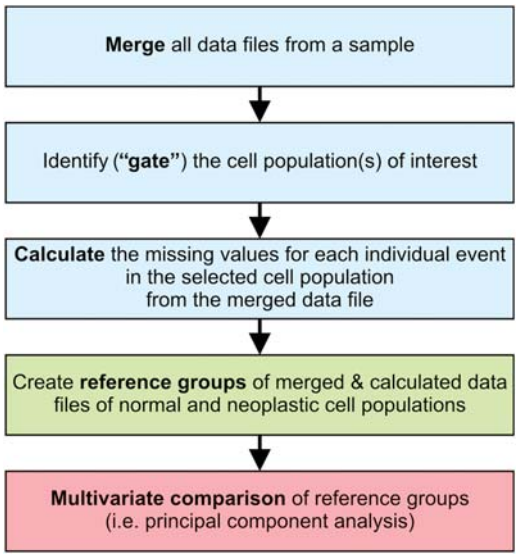

Figure 8. Flow chart diagram illustrating the sequential steps used during data analysis for the evaluation of the performance of the EuroFlow antibody panels.

Merge of flow cytometry data files and calculation of 'missing values'

The EuroFlow antibody panels are composed of multiple 8-color combinations of antibodies that contain three or four fluorochrome-conjugated antibodies as common backbone markers, essential for gating the cells of interest in every aliquot of a sample stained with a specific EuroFlow antibody panel.[29] The Merge function (first step in Figure 8) was used to fuse different data files corresponding to distinct aliquots of the same sample, each stained with a unique combination of reagents from the EuroFlow antibody panels. This results in a new single merged data file that contains all information measured in the same sample.[52,53] Such data file consists of a data matrix (Figure 9) in which the information (the measured parameters) for each different cellular event evaluated is aligned in one column per

	Tube number				
Parameters evaluated	1	2	3	4	5
FSC	C	C	C	C	C
SSC	C	C	C	C	C
CD20-PacB	C	C	C	C	C
CD45-PacO	C	C	C	C	C
SmIgλ-FITC	R				
SmIgκ-PE	R				
CD5-PerCPCy5.5	R				
CD19-PECy7	C	C	C	C	C
SmCD3-APC	R				
CD38-APCH7	R				
CD23-FITC		R			
CD10-PE		R			
CD79b-PerCPCy5.5		R			
CD200-APC		R			
CD43-APCH7		R			
CD31-FITC			R		
LAIR1-PE			R		
CD11c-PerCPCy5.5			R		
SmIgμ-APC			R		
CD81-APCH7			R		
CD103-FITC				R	
CD95-PE				R	
CD22-PerCPCy5.5				R	
CXCR5-APC				R	
CD49d-APCH7				R	
CD62L-FITC					R
CD39-PE					R
HLADR-PerCPCy5.5					R
CD27-APC					R

Figure 9. Data matrix obtained from the EuroFlow B-CLPD (B-cell chronic lymphoproliferative disorders) antibody panel, showing merging of five original data files into a single data file containing data about 29 parameters (2 scatter parameters and 27 markers). Columns correspond to the different B-CLPD tubes (sample aliquots) measured and rows correspond to the different parameters evaluated. 'C' means 'common' marker defined as measured in all aliquots; 'R' means 'real' data measured in any of the tubes. Blank spaces represent the parameter information that was not measured on an individual aliquot of the sample.

tube, which includes light scatter- and fluorescence emission-associated parameters, placed in different rows of the data matrix. The data matrix contains filled and unfilled boxes, corresponding to parameters that were directly measured and parameters not evaluated directly (missing values) for an individual event in a given aliquot of the sample, respectively[48] (Figure 9).

A calculation function was used to fill in the 'missing values' in the above-mentioned data matrix corresponding to the merged data file. For this purpose, the common backbone parameters were used for identification of the neoplastic and/or normal cell populations of interest present in each of all tubes coming from a single sample (second step in Figure 8). Afterwards, a new data file was created, which only contained information about those parameters measured for individual events contained in the gated cell population.[48] Then, the 'missing values' in the data matrix corresponding to the gated cell population were calculated (third step in Figure 8). For this latter purpose, for each event to be calculated inside the selected population, the software searches for the 'nearest neighbor'[54,55] event in each of the other aliquots of the sample, based only on its unique position in the multidimensional space created by all common backbone parameters (Figure 10). Therefore, the 'nearest neighbor' of each event to be calculated in a merged data file measured in one sample aliquot will be the event showing the shortest distance from it in the *n*-dimensional space generated by the same common parameters in another sample aliquot from the merged data file. Finally, the software applies the values obtained for the 'nearest neighbor' for all those parameters measured for the event in the latter sample aliquot but not measured in the former sample aliquot. This calculation process is done for each individual event in the merged data file till the data set is completed. At the end of the calculation process, the new data file contains both the data that were actually measured in the flow cytometer for each event and the calculated data for those parameters not measured in the same group of events in the other aliquots.[48] The calculation process requires optimal definition with maximum biological heterogeneity within the cell population to become apparent with the common parameters (for example, backbone parameters) for the cell population to be calculated; thus, backbone marker selection is crucial. In order to obtain a high accuracy of the calculation process, each event in the cell population of interest is required for its definition in the EuroFlow antibody panels, based on five or six backbone parameters (two scatter parameters and three to four fluorescence markers).

As previously described in this paper (see Section 4), EuroFlow antibody panels include both surface and intracellular stainings. Therefore, variations in the FSC/SSC values or in the fluorescence levels of the backbone markers may occur because of the different sample preparation procedures (Table 9). In order to allow the calculation process when cells are treated with different staining protocols, a harmonization procedure was developed[56] and applied to those cell populations of interest, for all parameters measured in common in the different sample aliquots, which are prepared differently (Figure 11). Such harmonization process consists of the translation of a data matrix defined in a tube by a given set of parameters for a given cell population into a data matrix defined by the same parameters for the same cell population measured in another tube under different conditions (for example, surface versus surface plus intracellular stainings). Of note, this harmonization tool did not affect the calculation process, as similar results were obtained when we compared the calculated values in files that contained information about a sample for which some aliquots/tubes were submitted to intracellular staining procedures and others were treated for Sm staining only.

As an end result of the calculation procedure, all individual events from each of the original data files corresponding to different aliquots of the same sample contain information about each reagent/parameter included in the whole antibody panel. The overall number of parameters for which values can be assigned to each individual cellular event included in the new data file are virtually unlimited, and equals that of the number of parameters measured in the whole set of merged data files for a given number of stained aliquots of a sample. This allows visualization of previously 'impossible' bivariate dot plots for individual events (for example, staining patterns for two reagents conjugated with the same fluorochrome) [48] (Figure 10).

Generation of reference data files

A reference data file is a data file constructed by merging two or more data files, each corresponding to a cell population measured in different samples with the same panel of reagents (fourth step in Figure 8). Hereby, the reference data file contains information about all parameters (measured or calculated) for each individual event of the targeted cell population.[50] Reference data files may contain information about normal or neoplastic cell populations, which may be homogeneous or heterogeneous with regard to different parameters evaluated. The generation of the reference data files aims at building libraries of reference cases to be compared between each other or with a new case that has been stained with the same panel of reagents (fifth step in Figure 8). On the basis of the existence of different patterns of protein expression in normal versus neoplastic cells, as well as among different WHO disease entities, a library can be built, which contains all normal and aberrant patterns that represent each of the different normal and pathological cell populations studied with the different EuroFlow

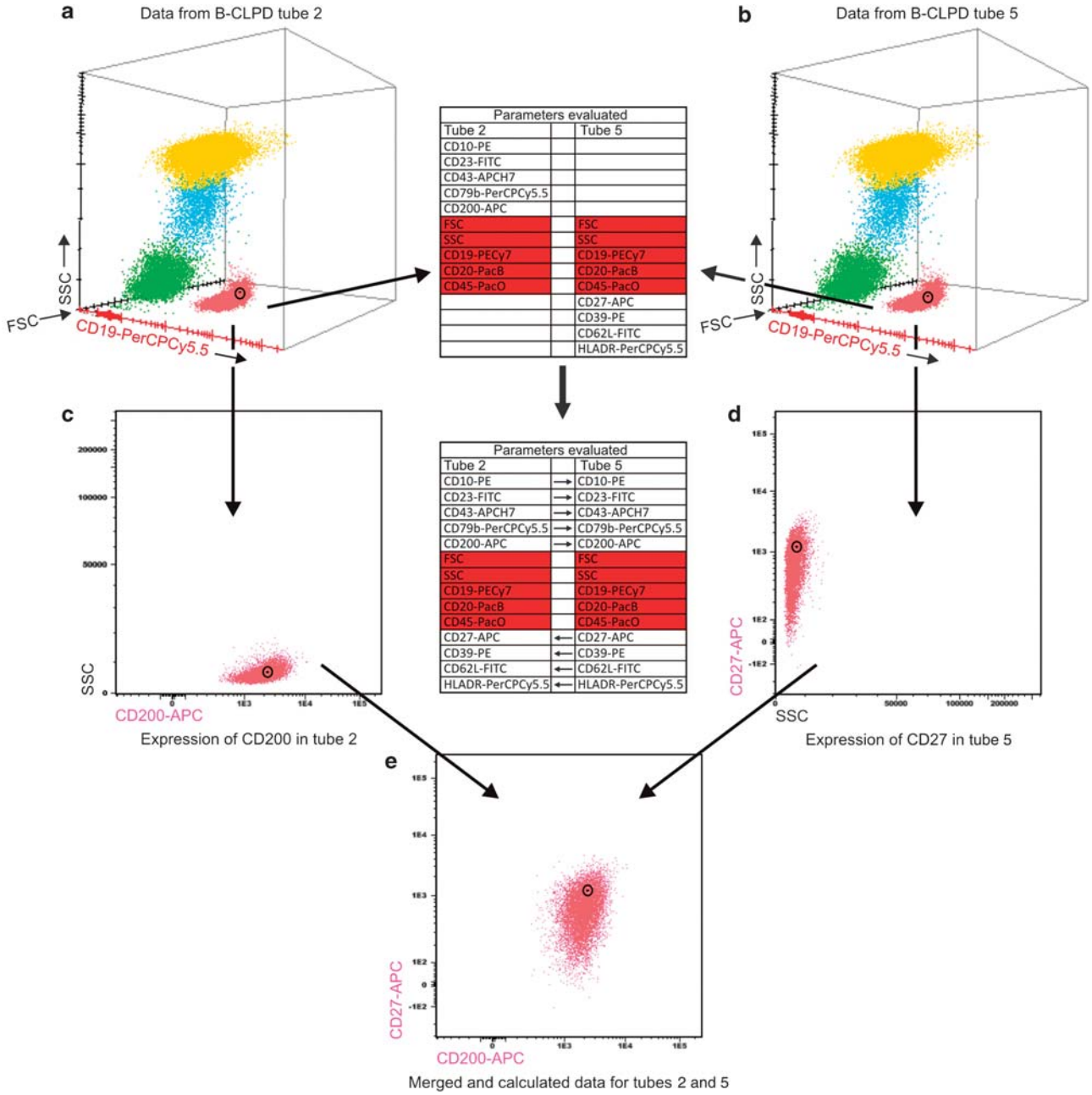

Figure 10. Schematic representation of the data calculation process with the Infinicyt software based on the 'nearest neighbor' principle. First, one event from a cell population (B-cells highlighted in red) in **a** is identified in a first data file (tube 2 of B-cell chronic lymphoproliferative disorders (B-CLPD) panel) based on the backbone markers; then the event corresponding to the nearest neighbor of this event is identified in the second data file (right; tube 5 of B-CLPD panel) as that event occupying the same (closest) position in a multidimensional space formed by the same backbone parameters (**b**). Third, through the data calculation process the values for those parameters that were only measured for the later event in the second data file (**d**) but not for the former event in the first data file are assigned to the said event in the first data file and *vice versa* (**c**). Finally, the calculation process is completed for all other events in the cell population of interest (red events). Through this approach, all events in the merged and calculated data file have information about each of the parameters measured in both tubes (**e**).

antibody panels. Such a library can be used for (1) further evaluation of the utility and performance of antibody panels and (2) pattern-guided prospective classification of new cases diagnosed in different individual laboratories, which use the same EuroFlow antibody panels and laboratory procedures.[50]

Evaluation of the EuroFlow antibody panels based on comparisons of groups of reference data files

The EuroFlow 8-color antibody panels for the diagnosis and classification of hematological malignancies are designed to answer specific clinical questions, which can be grouped into two general categories: (1) Is a given hematopoietic cell population normal or reactive/regenerating or abnormal/neoplastic? (2) When an abnormal/neoplastic cell population is identified, which WHO disease category does it belong to? In order to evaluate the utility and performance of the EuroFlow antibody panels, different groups of reference files that had been stained with the same antibody panels have been constructed. To answer the first question, reference data files from a normal/reactive cell population were compared with their neoplastic counterpart from

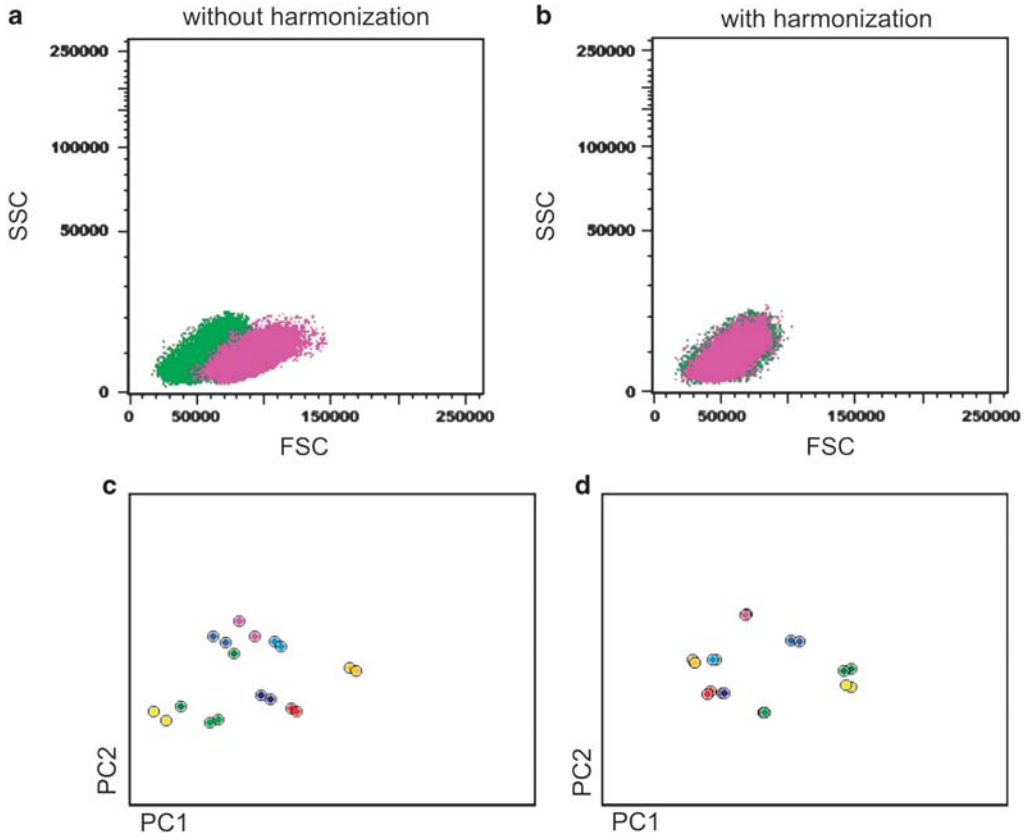

Figure 11. Illustrating example of the impact of different sample preparation protocols on the immunophenotypic and light scatter features of lymphocytes from a normal peripheral blood (PB) sample (**a**) and blast cells from B-cell precursor acute lymphoblastic leukemia (BCP-ALL) ($n = 9$; **c**) and how the harmonization process reduces such impact (**b** and **d**, respectively). In **a** and **b**, FSC versus SSC representation of duplicates of a sample stained with two different protocols (permeabilized versus non-permeabilized lymphocytes) is shown without (**a**) and with (**b**) data harmonization applied, respectively; in both **a** and **b**, green and violet populations correspond to non-permeabilized and permeabilized aliquots, respectively. In **c** and **d**, different BCP-ALL blast cell populations from nine different BCP-ALL patients each stained in five different aliquots with the BCP-ALL EuroFlow panel are displayed. Each population is represented as median values in a principal component (PC) 1 versus PC2 analysis diagram (automatic population separator (APS)1 view based on the discrimination obtained for the following parameters: FSC, SSC, CD19, CD34 and CD45), where paired duplicated samples are colored identically. In **c** samples contain both permeabilized and non-permeabilized aliquots within the panel and the harmonization process was applied for five patient samples (duplicates colored dark yellow, light green, dark violet, red and cyan) for which duplicates show a very close position in the APS1 view; conversely for the other pairs of duplicates (light yellow, dark green, violet, dark blue show greater differences between paired samples). In **d**, one group of duplicates was processed by permeabilizing all aliquots within the panel, while in the other group each sample contained permeabilized and non-permeabilized sample aliquots, with data harmonization being applied to the latter group; note that now all pairs of sample duplicates overlap, confirming that with data harmonization blast cell populations processed differently (permeabilized versus non-permeabilized) are highly comparable to those who underwent a uniform sample preparation protocol.

one or multiple WHO disease entities in a multivariate 1×1 set of comparisons approach. To answer the second question, reference data files corresponding to the neoplastic cell population from multiple cases of a single WHO disease entity were compared against single or multiple reference data files corresponding to one or more WHO disease entities.

For such comparisons, multiple approaches such as principal component analysis (PCA) can be used with the corresponding multiple-dimensions (that is, bi- or tridimensional) graphical representations of, for example, Principal Component (PC) X versus PC Y, and PC X versus PC Y versus PC Z, respectively, using the Automatic Population Separator (APS) graphical representation of the Infinicyt software (Figure 12).

On the basis of this APS representation, information about the separation between the two groups of reference data files is obtained through definition of median and/or mean $\pm$ s.d. borders (Figure 12) together with information about the most informative (versus redundant) parameters.[57] It also allows re-evaluation of a panel after excluding one or multiple markers to objectively evaluate the contribution of each marker. A similar approach can then be used to prospectively compare one new case against two different groups of reference data files. Through such comparison, information is obtained about whether new cases belong to one of the reference groups or whether they differ from the reference groups, for those markers which are relevant in such comparison.

Through such comparisons one can also easily and objectively identify the phenotypic differences and similarities between the cell populations compared in the different reference groups and the markers that account for them. In fact, it allows direct (multivariate) comparisons of one or more cell populations from a given sample with other (for example, reference) cell populations from a pool of $\geqslant 2$ different samples (Figure 12). In a certain way, this mimics what an expert follows in his mind when he compares the immunophenotypic profiles obtained with a given antibody panel in a sample with the profiles obtained for the same combinations of antibodies in another sample (or group of samples) composed of normal, reactive, activated, aberrant or malignant cells. For example, the APS comparison of normal with malignant B-cell precursors allows identification of the best combination of markers to distinguish between them and thereby define the most common aberrant

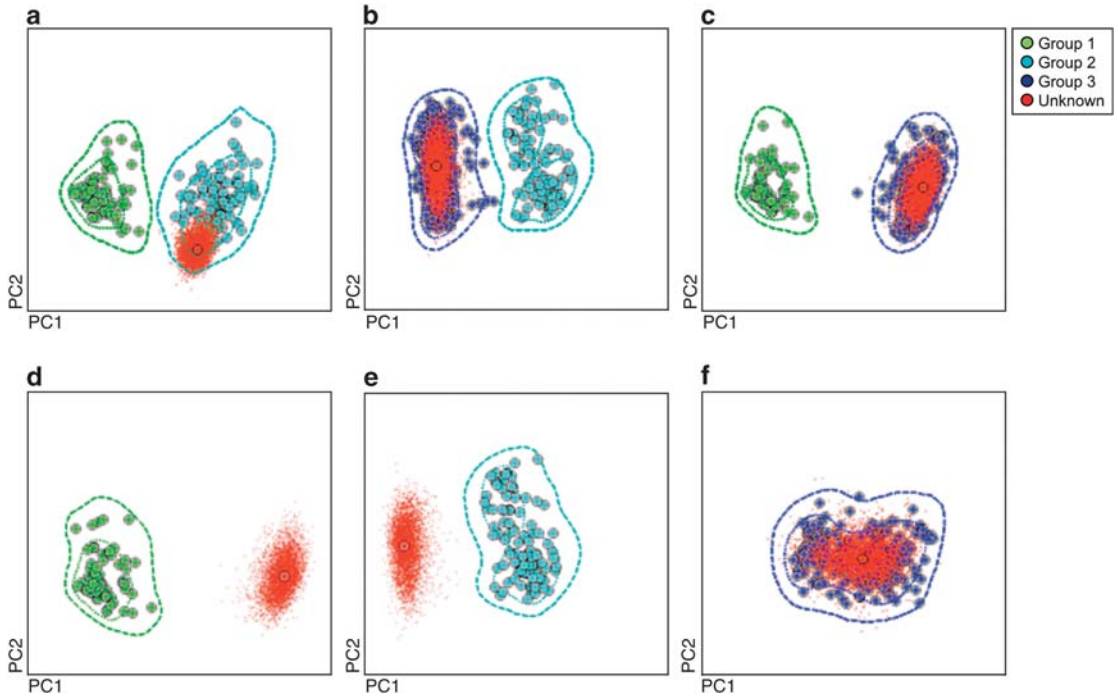

Figure 12. Example of principal component (PC1 versus PC2) analysis (PCA; automatic population separator (APS)1 views) for comparison of a new sample—red circles (median values) and dots—with a library of cases (median values/case represented as circles) from three different reference groups, each being colored differently (green, cyan and violet circles). In the upper panels the unknown case is compared to each pair of reference groups and it only overlaps systematically with the dark blue cases (**a**–**c**). In the lower panels (**d**–**f**), the new sample is separately compared with each individual reference group, showing again a high degree of overlap with the dark blue reference cases (**f**). Contour lines in each panel correspond to one (inner line) and two (outer line) s.d.'s of the mean value of the corresponding group of reference cases.

phenotypes. In addition, APS comparison between malignant B-cells from patients with different B-cell chronic lymphoproliferative disorders (B-CLPD) defined according to the WHO 2008 classification[1] allows identification of the most informative parameters for their differential diagnosis. Noteworthily, fully objective information is obtained through this approach about the specific contribution of each marker in the panel.[49]

CONCLUSION

During the last 6 years, the EuroFlow Consortium has built new approaches for data analysis, which provide a new objective strategy for evaluation of the performance and utility of individual markers and antibody panels. The newly proposed strategy for data analysis of samples stained with the EuroFlow antibody panels includes a set of sequential steps (Figure 8): merge of data files corresponding to individual samples stained with the EuroFlow antibody panels, calculation of missing values for the cell populations of interest, merge of data files for the reference groups and evaluation of antibody panels through multiple comparisons between different sets of reference cases stained with the same panel of reagents. This new analytical strategy also provides a pattern-guided approach for the immunophenotypic classification of normal and malignant cell populations.[49,50] The tools required to use the new analytical approach have been implemented into the Infinicyt software by the EuroFlow Consortium, which allows their usage in routine practice by any other group around the world. Herewith a full set of flow cytometry data analysis tools is provided to the flow cytometry field to help expert-based interpretation of highly complex multiparameter data sets. In combination with the reference data files generated, the new software tools also provide a robust and reliable method for data comparison between different diagnostic laboratories on a sample-by-sample basis. The robustness and reliability of this approach is also based on the use of antibody panels with sufficient and adequate backbone markers that have been selected for careful identification of the subset of cells of interest, which is essential for accurate calculation of missing data and their graphical representation. Accordingly, use of the EuroFlow antibody panels and the EuroFlow SOPs for sample preparation allows for (1) building databases with reference groups of well-defined WHO categories; (2) classification of a new case; (3) assuring internal and external quality control by any other user if the same tools and reference groups are used. Therefore, the new software tools contribute significantly to the standardization of flow cytometry data analysis.

SECTION 6. RESULTS OF MULTICENTER MEASUREMENTS

T Kalina[1], J Flores-Montero[2], VHJ van der Velden[3], S Böttcher[4], M Cullen[5], L Lhermitte[6], L Sedek[7], A Mendonça[8], HK Wind[3], JG te Marvelde[3], E Mejstrikova[1], O Hrusak[1], JJM van Dongen[3] and A Orfao[2]

[1]DPH/O, Prague, Czech Republic; [2]USAL, Salamanca, Spain; [3]Erasmus MC, Rotterdam, The Netherlands; [4]UNIKIEL, Kiel, Germany; [5]UNIVLEEDS, Leeds, UK; [6]AP-HP, Paris, France; [7]SUM, Zabrze, Poland and [8]IPOLFG, Lisbon, Portugal

BACKGROUND

In order to design and apply the EuroFlow antibody panels for the immunophenotypic diagnosis and classification of leukemias and lymphomas, SOPs were developed and evaluated as described in the previous sections. However, multicentric implementation of such antibody panels[29] and SOPs would require further evaluation of the protocols at the multicentric level. For this purpose two different series of experiments could be envisaged: (1) staining of comparable samples with the same SOPs and antibody panels at

Table 10. Overall results of synchronized experiments expressed in terms of variability obtained in the 8 EuroFlow laboratories for the measurement of antigen expression profiles in normal PB monocytes and lymphocytes ($n = 30$ different samples), stained, prepared and measured in all 8 centers in parallel *versus* a stabilized sample obtained in a single center, distributed and then stained, prepared and measured locally at each center

Channel	*PacB*	*PacO*	*FITC*	*PE*	*PerCPCy5.5*	*PECy7*	*APC*	*APCH7*
Target MFI (Rainbow beads)	195 572	231 265	59 574	101 900	216 064	27 462	176 780	56 437
Mean actual MFI (Rainbow beads)	193 109	225 152	59 003	100 763	215 596	27 639	176 190	56 610
CV of Rainbow MFI	5.4%	4.6%	2.1%	2.4%	2.1%	3.1%	1.7%	2.2%
Antibody conjugate evaluated	CD20	CD45	CD8	CD27	CD4	CD19	CD14	CD3
Gating parameters and cell subset	$CD20^{hi}$/ $CD19^{+}$ B-cells	$CD45^{hi}$ total lymphocytes	$CD3^{+}$/ $CD8^{hi}$ T-cells	$CD3^{+}$/ $CD27^{+}$ memory T-cells	$CD3^{+}$/ $CD4^{+}$ T-cells	$CD20^{hi}$/ $CD19^{+}$ B-cells	$CD45^{hi}$/ $CD14^{+}$ monocytes	$CD3^{+}$ T-cells
MFI CV for the cell subset ($n = 8$ for 1 stabilized sample)	15.2%	13.9%	11.4%	32.9%	24.7%	11.1%	43.8%	38.7%
MFI CV of the cell subset ($n = 30$ samples)	16.9%	15.5%	16.9%	28.0%	28.4%	15.4%	22.7%	48.4%

Abbreviations: APC, allophycocyanin; Cy7, cyanin7; CV, coefficient of variation; FITC, fluorescein isothiocyanate; MFI, mean fluorescence; H7, hilite7; PacB, pacific blue; PacO, pacific orange; PB, peripheral blood; PE, phycoerythrin; PerCPCy5.5, peridinin–chlorophyll–protein–cyanin5.5.

multiple sites, and (2) staining of the same sample at different sites with the EuroFlow antibody panels and SOPs.

Results of the multi-step procedure to standardize EuroFlow setup of all instruments were evaluated on a set of PB samples following the two approaches. The variation observed in multi-center experiments may be caused by multiple factors. Among them, the most relevant ones include (1) the pattern of expression of the molecule investigated (that is, tight peaks for CD4 expression versus non-homogeneous expression of CD27 in T-cells); (2) stability of the fluorochrome and its emission spectra (that is, stable FITC emitting in green versus relatively less stable APCH7 and PECy7 tandem fluorochromes with emission in far red resulting in variation due to photon-counting statistics); and (3) affinity and thus titration profile of antibodies (that is, for some antibody clones pipetting errors may lead to changes in staining levels).

The present experiment was chosen to allow analysis of distinct populations defined by positive markers in every fluorescence channel and it was designed to mimic the performance of the antibody panels for the EuroFlow 'small sample tube'.[29] A complex, 8-color tube was chosen as testing tube to include correct compensation in the end-point of the test. All measurements were subjected to the previously described EuroFlow SOPs, including analysis of merged data files using the Infinicyt software. The main question of the presented experiment was whether biological differences between distinct cell subsets will be resolved well when all setup procedures described so far are used in eight different EuroFlow laboratories and when the merged data are analyzed by the same software tools.

Standardized instrument settings and SOP evaluation experiments

The PB of one donor was stabilized using TransFix reagent (Cytomark, Buckingham, UK) and distributed in 1-ml aliquots to the eight EuroFlow centers; in addition, PB samples were obtained (after informed consent) from 30 different healthy volunteers—that is, one PB sample distributed to all eight centers and 30 different PB samples analyzed at eight centers (three to four samples per center). Instrument setup, compensation and sample preparation were performed exactly as described in Sections 2, 3 and 4, respectively. Reagents used for staining were modified from one of the 8-color EuroFlow panels (that is, SST)[29] as follows: CD20-PacB (eBiosciences, San Diego, CA, USA), CD45-PacO (Invitrogen, Carlsbad, CA, USA), CD8-FITC, CD27-PE (ExBio, Prague, Czech Republic), CD4-PerCPCy5.5, CD14-APC and CD3-APCH7 (all from BD Biosciences) and CD19-PECy7 (Beckman Coulter). After acquisition in the flow cytometers, data were exported as FCS 3.0 data files. At each center, the following cell subsets were gated: $SSC^{lo}/CD45^{hi}$ total lymphocytes, $CD14^{+}/CD45^{hi}$ monocytes, $CD20^{hi}/CD19^{+}$ B-lymphocytes, and $CD3^{+}/CD27^{+}$ memory T-lymphocytes with both $CD3^{+}/CD4^{+}$ T-cells and $CD3^{+}/CD8^{hi}$ T-cells. Then the MFI values obtained for individual markers were calculated and reported (Table 10 and Figure 13a). Subsequently, both MFI values and the original listmode data files were sent to one center (DPH/O, Prague, Czech Republic) for central analysis. Then, the CV of the MFI values obtained for each subset in each channel was calculated. In addition, listmode data files were merged with Infinicyt software (version 1.3), monocytes were gated as $CD45^{hi}/CD14^{+}$ cellular events and total lymphocytes were gated as $FSC^{lo}/SSC^{lo}/CD45^{hi}$ events and their subsets further defined as listed in Table 10. Next, the merged file was displayed in an APS view (PC1 versus PC2), where each subset was color-coded, and the median of each subset was depicted as a color-coded circle as illustrated in Figures 13b and c.

Comparison of data obtained at each of the centers showed that instrument-related differences caused a CV of target MFI values of $<5.5\%$ (see Section 2 and Table 10). When a stabilized PB sample obtained at one center was stained, measured and analyzed manually at each of the eight centers, CVs for the MFI values of each cell population evaluated were systematically $<44\%$. Similarly, a maximal CV of 44% for CD3-APCH7 on T-cells was observed for normal PB samples obtained, stained, measured and analyzed at each individual center. Notably, CVs below 17% were obtained for 4/8 fluorochrome-conjugated markers assessed in specific cell subsets. Merging all listmode data files, followed by gating on the different subsets of lymphocytes and monocytes showed that we were able to clearly distinguish clusters of PB events corresponding to the same cell subsets from samples drawn from different donors, stained at different centers and measured on different instruments (Figures 13a and b). This illustrates that biological differences are not hidden or affected by the technical variability. To test the feasibility of merged data analysis across flow cytometry platforms, we acquired the same tube (except for CD14-APC) on LSR II and CyAn ADP instruments. Both the conventional analysis of dot plots (Supplementary Figure 1A) and graphical analysis of the APS view (Supplementary Figure 1B) showed separation of major lymphocyte subsets.

CONCLUSION

Our collective experiments showed that standardized instrument settings, compensation procedures, staining protocols and data analysis in multi-institutional collaboration programs are feasible. Data variation resulting from hardware differences (optical

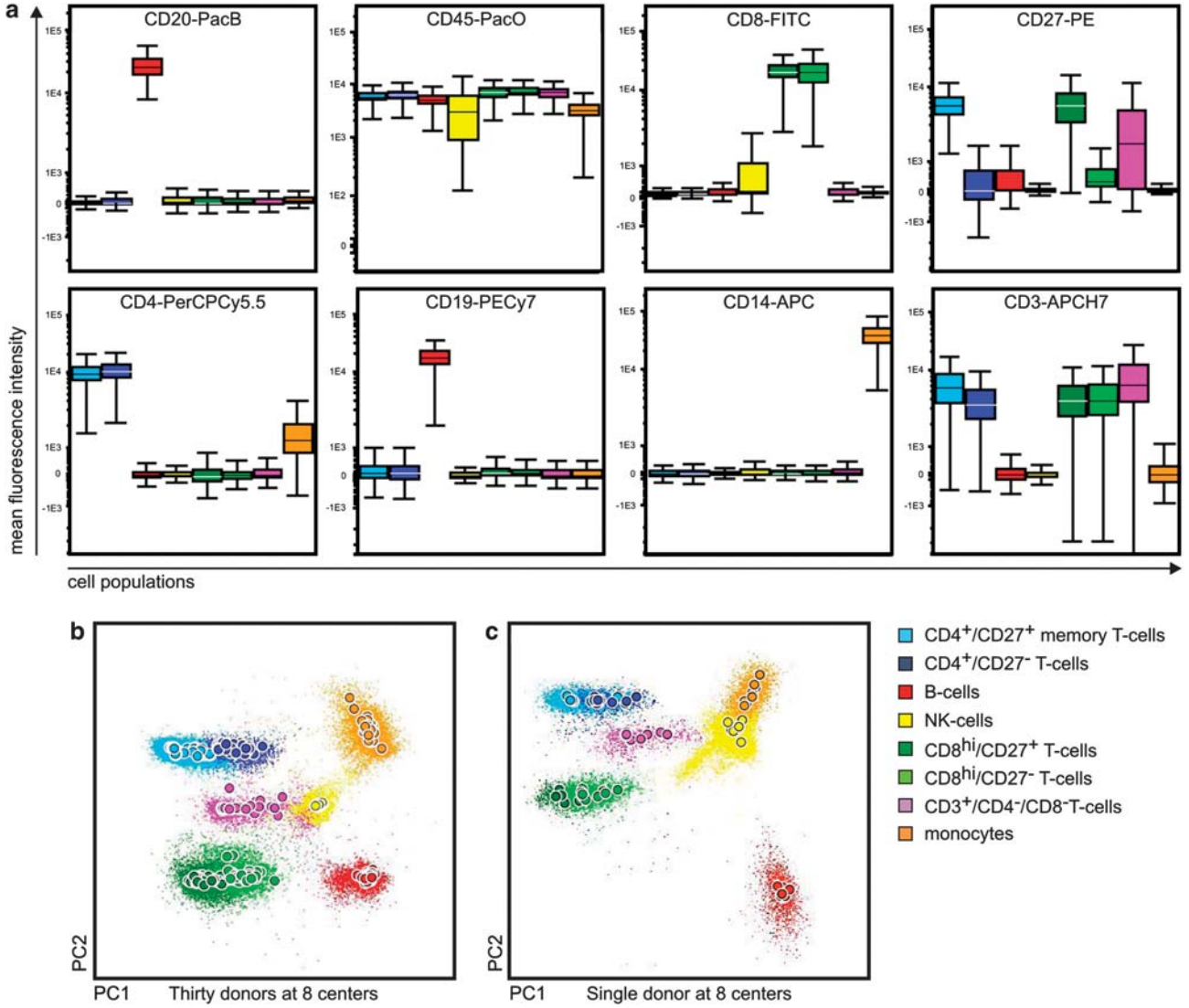

Figure 13. Results of synchronized EuroFlow experiments performed on different centers and instruments. (**a**) Box plot representations of mean fluorescence intensity (MFI) values observed for all antigens evaluated in the eight gated subsets of peripheral blood (PB) monocytes and lymphocytes from 30 healthy donor PB samples. Results corresponding to a total of 30 merged data files are displayed. (**b**) Principal component (PC)1 versus PC2 view (automatic population separator (APS) 1 view) of individual cellular events of the cell populations depicted in **a**; the median values of each gated subset (circles) are color-coded as follows: B-cells, red; $CD4^+/CD27^+$ memory T-cells, light blue; $CD4^+/CD27^-$ T-cells, dark blue; $CD8^{hi}/CD27^+$ memory T-cells, dark green; $CD8^{hi}/CD27^-$ T-cells, light green; $CD3^+/CD4^-$ and $CD8^-$ T-cells, violet; NK-cells, yellow and monocytes, orange. (**c**) APS1 view of a single stabilized peripheral blood sample measured in 8 different EuroFlow laboratories for illustration of intra-donor variability (color coding is the same as in **b**). In **a**, results are displayed as box plots, where the line in the middle represents median values, the upper and lower limits of the box represent the 75th and 25th percentiles, respectively, and the upper and lower ends of vertical lines represent the 95% confidence interval. In **b**, each population is represented as a circle surrounded by dots corresponding to median values of median expression for all immunophenotypic parameters measured and to individual cells, respectively.

elements might have different quality; in some channels different filters are used on LSR II and FACSCanto II instruments) or variation from other sources is negligible when compared to biological differences between cell types. However, initial training of local operators in the applied SOPs is strongly recommended.

DISCUSSION

In constructing the EuroFlow antibody panels for the diagnosis and classification of leukemias and lymphomas using $\geqslant$8-color flow cytometry, among all technical issues, selection of the most adequate and feasible combination of fluorochromes to be used in the available multicolor flow cytometers was a pre-requisite. Usage of an increasingly high number of fluorochromes is associated with an exponential increase in the amount of information obtained from a single combination of fluorochrome-conjugated antibodies. However, such multicolor/multi-marker approaches are associated with an increasing complexity and the need to select the most appropriate/optimal combinations of individual reagents, including compatible fluorochromes for which the required high-quality antibodies are commercially available. As stated above, several fluorochromes were pre-selected because of the extensive experience and proven utility of a high number of good-quality antibody conjugates and their match with the

default optical configuration of the available instruments. In contrast, for other fluorochrome positions, extensive experimental comparisons among different fluorochrome conjugates were required. Finally, the combination of PacB, PacO, FITC, PE, PerCPCy5.5, PECy7, APC and APCH7 was selected. However, while the majority of these fluorochromes performed satisfactorily well, others still require improvement (for example, APCH7). Preliminary testing of several new alternative fluorochromes (e.g., HV450, HV500 and brilliant violet fluorochromes) show promising results, implying that they might be suited as replacements. However, for some fluorochrome positions, alternative fluorochromes are not available (or became available very recently) or they are just conjugated with a restricted number of CD markers, which limits their current applicability but also points to the need for further improvements.

The technical EuroFlow approach was designed to establish and monitor standard instrument settings to a common bright signal placed at the same level in different flow cytometer instruments. This implies the possibility that some variation might occur in the measurement of dim/negative signals owing to small differences between individual instruments. However, it assures that individual flow cytometers work above their detector's background noise. Slight differences in laser power output, sharpness of the optical filters' edges and other hardware-associated variables might account for such small deviations.[32,33] In fact, we detected higher MFI for unstained cells in the violet laser fluorescence channels at one occasion in one instrument. The violet laser of this instrument had to be replaced by the manufacturer owing to a low laser power delivered to the flow cell. In 2008 the CS&T module was introduced in the 6.0 version of the FACSDiVa software.[58] Please note that this module is made for automated instrument characterization and automated calculation of optimal voltage settings for single instruments and does not deal with standardized multicenter setting approaches. With the CS&T module, PMT voltages are set at a value that is 10 times the standard deviation of electronic noise. Small differences were found between CS&T and EuroFlow settings owing to the different criteria for optimal setting of PMT voltages. Whereas CS&T favors higher sensitivity for dim signals, the EuroFlow settings are tailored to measure both dim signals and signals generated by molecules with very high levels of expression (for example, CD38 expression on normal plasma cells). In practice, both methods (the EuroFlow settings and the CS&T module) were associated with optimal PMT settings and allow for an early detection of instrument failure (for example, laser failure). Unfortunately, automated adjustments at daily monitoring by the CS&T module systematically require a full new compensation experiment, even if the variation obtained for the new adjustment is as low as ± 1 mV with no real impact on the compensation matrix. Daily performance of a full compensation experiment is expensive, time-consuming and consequently inefficient in diagnostic laboratories. In addition, it is not supported by the minor changes observed in the compensation matrix. An additional advantage of the EuroFlow approach is its flexibility and its applicability for 8-color flow cytometers from different manufacturers. Based on the long-term stability of MFI measurements, once-fixed PMT voltages were used. We adopted acceptance criteria for deviations of up to 15% from the target MFI values, for instrument settings to pass during daily monitoring. A user-friendly software tool and graphics were built into the Infinicyt software for a quick color-code assessment of any deviation from the accepted criteria for optimal instrument settings. The stringency of such criteria should be driven by the purpose of standardization. In immunophenotyping of hematological malignancies, the biological intra- and inter-sample differences are quite high and they are not hidden or affected by changes in fluorescence intensity values of up to 30% (EuroFlow data; not shown). As described in Section 5 with new automated software-driven analytical approaches that simultaneously take into account all markers and their intensities at the same time, the relative relevance of small MFI changes in individual markers is significantly diminished. In addition, we also show that these criteria can be easily met by different instruments at different sites.

Usage of an optimal fluorescence compensation matrix is currently considered as a requirement for optimal identification of single- versus double-positive cells in multicolor flow cytometry immunophenotyping.[37] The complexity of the procedure designed to set up the optimal fluorescence compensation matrix depends on the specific multicolor antibody panels. As could be predicted, single compound dyes were represented by one 'generic' SAbST (one representative marker stained in a specific cell population), while tandem fluorochromes were represented by one tube for each specific fluorochrome conjugate antibody. The only exception to this rule was the PerCPCy5.5 tandem fluorochrome. However, it should be noted that, in contrast to PECy7 and APCH7, PerCPCy5.5 is a tandem fluorochrome where both compounds of the tandem show maximum emission into the same bandpass filter; this could explain why no fluorochrome-specific compensation is needed. The similar spillover values for different PerCPCy5.5 reagents were confirmed in a small-scale experiment (data not shown).

Fluorescence compensation experiments consisting of a full set of compensation controls ($n = 30$ tubes) represent a challenge for time-stressed laboratories as well as a burden for laboratory budget. Thus, the frequency of compensation could be set to a time interval of 1 month, during which only minor deviations from target MFI were recorded on well-performing instruments. However, gradual 405-nm laser power failures often resulted in significant signal shifts that required new instrument setup and compensation experiments, more frequently than initially planned. Careful selection of reagents with sufficient life-span, especially with regard to tandem fluorochromes, and protection of light-sensitive reagents is crucial for acquisition of high-quality data in the once-per-month compensation scheme. Based on the comparison of the fluorescence compensation matrices obtained over time for the same instrument, we concluded that it is not necessary to repeat the compensation experiment whenever both the reagents and the signal collection on the instrument are stable. However, the stability of tandem fluorochromes is not reliably constant for all manufacturers and it depends on the storage and handling conditions. Our 1-month compensation approach was feasible as judged by evaluation of $\geqslant 2000$ merged PB, BM, LN, CSF and vitreous humor samples of multiple disease categories acquired over the past 6 years (data not shown). In turn, a software solution that would allow automated and rapid establishment of fluorescence compensation settings to experiments, after PMT voltages had been adjusted to 'Target MFI', could be of great help for clinical flow cytometry laboratories. Interestingly, our multicenter results indicate that such an approach is apparently feasible, owing to the highly stable compensation settings observed in our study at both the inter- and intra-laboratory level.

The EuroFlow SOPs for sample preparation was developed because of its ability to provide robust and reliable data that meet all the criteria indicated above. In combination with the standardized EuroFlow SOPs to define instrument settings and fluorescence compensation, it allows generation of highly comparable and reproducible data for a single instrument and between different instruments within the same laboratory and between different laboratories. Such highly reproducible data are required not only for the comparison of data obtained within the different EuroFlow laboratories, but also for the construction of a database with immunophenotypic data from large numbers of patients suffering from the various subtypes of relevant

hematological malignancies, which can be potentially used as a reference by any laboratory worldwide.

Until now, standardization of flow cytometry in hematological diagnostic processes remains a challenge and it is rarely achieved in a multi-institutional setting. There have been some attempts to standardize the analysis of minimal residual disease in multiple study groups[9,59–61] that restricted the standardization on the analytical stage by exchanging the listmode data files. Kraan *et al.*[62] have presented general rules for cytometer setup in clinical settings using analog flow-cytometric systems with up to four colors, whereas Shankey *et al.*[63] presented complete standardization of 4-color ZAP-70 investigation in three institutions. Our present study goes further beyond the so-far-reported multi-center studies and aims at standardization of the data to the level at which listmode files measured in all centers can be meta-analyzed by software tools specifically designed for this purpose. The whole process of cytometer settings, compensation settings, fluorochrome selection and antibody panel selection was re-evaluated and fully controlled. The need for such extensive standardization arises from the possibilities that are brought by three-laser $\geqslant$8-color digital flow cytometers to measure increasingly detailed subsets in complex cellular samples. Cell definitions using >4 colors are thought to enhance the accuracy of rare cell detection such as used for minimal residual disease studies. Analysis of surface/cytoplasmic expression patterns on large cohorts of samples by computational tools is possible only when the input data are supplied in a fully standardized format. Sharing of knowledge and diagnosing rare diseases will be made possible by manual or computer-assisted analysis of data files acquired in multi-institutional cooperation. Here again, appropriate interpretation of the data is possible only when standardized instrument settings and controls are used, the quality of the data is ensured, and the performance of the antibody panels is evaluated and taken into account during analysis.

We conclude that the 6 years of extensive collaborative experiments and the analysis of hundreds of patients' samples in the EuroFlow centers have indeed provided innovative protocols, software tools and antibody panels for fully standardized diagnosis and classification of hematological malignancies.

CONFLICT OF INTEREST

The EuroFlow Consortium is an independent scientific consortium which aims at innovation and standardization of diagnostic flow cytometry. All acquired knowledge and experience will be shared with the scientific and diagnostic community after protection of the relevant Intellectual Property, for example by filing of patents. The involved patents are collectively owned by the EuroFlow Consortium and the revenues of the patents are exclusively used for EuroFlow Consortium activities, such as for covering (in part) the costs of the Consortium meetings, the EuroFlow Educational Workshops and the purchase of custom-made reagents for collective experiments. Cytognos is for-profit company developing the Infinicyt software.

ACKNOWLEDGEMENTS

We are grateful to Dr Jean-Luc Sanne of the European Commission for his support and monitoring of the EuroFlow project. We thank Marieke Comans-Bitter for graphic design of the figures and for her continuous support in the management of the EuroFlow Consortium, and Bibi van Bodegom, Caroline Linker, and Monique van Rossum for their secretarial support of the consortium activities. We are grateful to Ria Bloemberg and Gellof van Steenis for support in the financial management of the project funds. The research activities of the EuroFlow Consortium were supported by the European Commission (grant STREP EU-FP6, LSHB-CT-2006-018708, entitled 'Flow cytometry for fast and sensitive diagnosis and follow-up of hematological malignancies') and the following national grants: Spanish Network of Cancer Research Centers (ISCIII RTICC-RD06/0020/0035-FEDER), FIS 08/90881 from the 'Fondo de Investigación Sanitaria', Ministerio de Ciencia e Innovación (Madrid, Spain), SA016-A-09 from the Consejería de Educación, Junta de Castilla y León, Valladolid, Spain, and PIB2010BZ-00565 from the Dirección General de Cooperación Internacional y Relaciones Institucionales, Secretaría de Estado de Investigación, Ministerio de Ciencia e Innovación (Madrid, Spain). T Kalina, E Mejstrikova and O Hrusak were supported by the Czech Ministry of Education Grant No. MSM0021620813, Czech Ministry of Health grant NT/12425-4 and TK is supported as an ISAC Scholar by The International Society for Advancement of Cytometry.

REFERENCES

1 Swerdlow SH, Campo E, Harris NL, Jaffe ES, Pileri SA, Stein H *et al. WHO Classification of Tumours of Haematopoietic and Lymphoid Tissues*. 4th edn. International Agency for Research on Cancer: Lyon, 2008, 439 pp.
2 Davis BH, Holden JT, Bene MC, Borowitz MJ, Braylan RC, Cornfield D *et al.* Bethesda International Consensus recommendations on the flow cytometric immunophenotypic analysis of hematolymphoid neoplasia: medical indications. *Cytometry B Clin Cytom* 2007; **72**(Suppl 1): S5–S13.
3 Wood BL, Arroz M, Barnett D, DiGiuseppe J, Greig B, Kussick SJ *et al.* Bethesda International Consensus recommendations on the immunophenotypic analysis of hematolymphoid neoplasia by flow cytometry: optimal reagents and reporting for the flow cytometric diagnosis of hematopoietic neoplasia. *Cytometry B Clin Cytom* 2007; **72**(Suppl 1): S14–S22.
4 Stewart CC, Behm FG, Carey JL, Cornbleet J, Duque RE, Hudnall SD *et al.* U.S.-Canadian Consensus recommendations on the immunophenotypic analysis of hematologic neoplasia by flow cytometry: selection of antibody combinations. *Cytometry* 1997; **30**: 231–235.
5 Stetler-Stevenson M, Ahmad E, Barnett D, Braylan R, DiGiuseppe J, Marti G *et al. Clinical Flow Cytometric Analysis of Neoplastic Hematolymphoid Cells*. Approved guideline. 2nd edn. CLSI document H43-A2 ed. Clinical and Laboratory Standards Institute: Wayne, PA, 2007.
6 Perfetto SP, Chattopadhyay PK, Roederer M. Seventeen-colour flow cytometry: unravelling the immune system. *Nat Rev Immunol* 2004; **4**: 648–655.
7 Baumgarth N, Roederer M. A practical approach to multicolor flow cytometry for immunophenotyping. *J Immunol Methods* 2000; **243**: 77–97.
8 Craig FE, Foon KA. Flow cytometric immunophenotyping for hematologic neoplasms. *Blood* 2008; **111**: 3941–3967.
9 van de Loosdrecht AA, Alhan C, Bene MC, Della Porta MG, Drager AM, Feuillard J *et al.* Standardization of flow cytometry in myelodysplastic syndromes: report from the first European LeukemiaNet working conference on flow cytometry in myelodysplastic syndromes. *Haematologica* 2009; **94**: 1124–1134.
10 Rawstron AC, Orfao A, Beksac M, Bezdickova L, Brooimans RA, Bumbea H *et al.* Report of the European Myeloma Network on multiparametric flow cytometry in multiple myeloma and related disorders. *Haematologica* 2008; **93**: 431–438.
11 Ruiz-Arguelles A, Rivadeneyra-Espinoza L, Duque RE, Orfao A. Report on the second Latin American consensus conference for flow cytometric immunophenotyping of hematological malignancies. *Cytometry B Clin Cytom* 2006; **70**: 39–44.
12 Owens MA, Vall HG, Hurley AA, Wormsley SB. Validation and quality control of immunophenotyping in clinical flow cytometry. *J Immunol Methods* 2000; **243**: 33–50.
13 Davis BH, Foucar K, Szczarkowski W, Ball E, Witzig T, Foon KA *et al.* U.S.-Canadian Consensus recommendations on the immunophenotypic analysis of hematologic neoplasia by flow cytometry: medical indications. *Cytometry* 1997; **30**: 249–263.
14 Bene MC, Nebe T, Bettelheim P, Buldini B, Bumbea H, Kern W *et al.* Immunophenotyping of acute leukemia and lymphoproliferative disorders: a consensus proposal of the European LeukemiaNet Work Package 10. *Leukemia* 2011; **25**: 567–574.
15 Mahnke YD, Roederer M. Optimizing a multicolor immunophenotyping assay. *Clin Lab Med* 2007; **27**: 469–485.
16 Roederer M, Kantor AB, Parks DR, Herzenbergzzz LA. Cy7PE and Cy7APC: bright new probes for immunofluorescence. *Cytometry* 1996; **24**: 191–197.
17 Matz MV, Fradkov AF, Labas YA, Savitsky AP, Zaraisky AG, Markelov ML *et al.* Fluorescent proteins from nonbioluminescent Anthozoa species. *Nat Biotechnol* 1999; **17**: 969–973.
18 Berlier JE, Rothe A, Buller G, Bradford J, Gray DR, Filanoski BJ *et al.* Quantitative comparison of long-wavelength Alexa Fluor dyes to Cy dyes: fluorescence of the dyes and their bioconjugates. *J Histochem Cytochem* 2003; **51**: 1699–1712.
19 Telford W, Kapoor V, Jackson J, Burgess W, Buller G, Hawley T *et al.* Violet laser diodes in flow cytometry: an update. *Cytometry A* 2006; **69**: 1153–1160.
20 Abrams B, Diwu Z, Guryev O, Aleshkov S, Hingorani R, Edinger M *et al.* 3-Carboxy-6-chloro-7-hydroxycoumarin: a highly fluorescent, water-soluble violet-excitable dye for cell analysis. *Anal Biochem* 2009; **386**: 262–269.
21 Maecker H, Trotter J. *Selecting Reagents for Multicolor Flow Cytometry*. Application Note. BD Biosciences: San Jose, CA, 2009.
22 Stewart CC, Stewart SJ. Four color compensation. *Cytometry* 1999; **38**: 161–175.
23 Roederer M. Spectral compensation for flow cytometry: visualization artifacts, limitations, and caveats. *Cytometry* 2001; **45**: 194–205.
24 Maecker HT, Frey T, Nomura LE, Trotter J. Selecting fluorochrome conjugates for maximum sensitivity. *Cytometry A* 2004; **62**: 169–173.
25 Wood B. 9-color and 10-color flow cytometry in the clinical laboratory. *Arch Pathol Lab Med* 2006; **130**: 680–690.

26 Kraan J, Gratama JW, Haioun C, Orfao A, Plonquet A, Porwit A *et al.* Flow cytometric immunophenotyping of cerebrospinal fluid. *Curr Protoc Cytom* 2008; Chapter 6: Unit 6 25.
27 Basso G, Buldini B, De Zen L, Orfao A. New methodologic approaches for immunophenotyping acute leukemias. *Haematologica* 2001; **86**: 675–692.
28 McLaughlin BE, Baumgarth N, Bigos M, Roederer M, De Rosa SC, Altman JD *et al.* Nine-color flow cytometry for accurate measurement of T cell subsets and cytokine responses. Part I: Panel design by an empiric approach. *Cytometry A* 2008; **73**: 400–410.
29 van Dongen JJM, Lhermitte L, Böttcher S, Almeida J, van der Velden VHJ, Flores-Montero J *et al.* EuroFlow antibody panels for standardized n-dimensional flow cytometric immunophenotyping of normal, reactive and malignant leukocytes. *Leukemia* 2012; doi:10.1038/leu.2012.120.
30 Le Roy C, Varin-Blank N, Ajchenbaum-Cymbalista F, Letestu R. Flow cytometry APC-tandem dyes are degraded through a cell-dependent mechanism. *Cytometry A* 2009; **75**: 882–890.
31 Hulett HR, Bonner WA, Sweet RG, Herzenberg LA. Development and application of a rapid cell sorter. *Clin Chem* 1973; **19**: 813–816.
32 Maecker HT, Trotter J. Flow cytometry controls, instrument setup, and the determination of positivity. *Cytometry A* 2006; **69**: 1037–1042.
33 Perfetto SP, Ambrozak D, Nguyen R, Chattopadhyay P, Roederer M. Quality assurance for polychromatic flow cytometry. *Nat Protoc* 2006; **1**: 1522–1530.
34 Hughes OR, Stewart R, Dimmick I, Jones EA. A critical appraisal of factors affecting the accuracy of results obtained when using flow cytometry in stem cell investigations: where do you put your gates? *Cytometry A* 2009; **75**: 803–810.
35 Shapiro HM. Excitation and emission spectra of common dyes. *Curr Protoc Cytom* 2004; Chapter 1: Unit 1 19.
36 Tung JW, Parks DR, Moore WA, Herzenberg LA. New approaches to fluorescence compensation and visualization of FACS data. *Clin Immunol* 2004; **110**: 277–283.
37 Roederer M. Compensation in flow cytometry. *Curr Protoc Cytom* 2002; **1**: 1 Chapter 1: Unit 1 14.
38 Groeneveld K, te Marvelde JG, van den Beemd MW, Hooijkaas H, van Dongen JJ. Flow cytometric detection of intracellular antigens for immunophenotyping of normal and malignant leukocytes. *Leukemia* 1996; **10**: 1383–1389.
39 Macey MG, McCarthy DA, Milne T, Cavenagh JD, Newland AC. Comparative study of five commercial reagents for preparing normal and leukaemic lymphocytes for immunophenotypic analysis by flow cytometry. *Cytometry* 1999; **38**: 153–160.
40 Stewart CC, Stewart SJ. Immunophenotyping. *Curr Protoc Cytom* 2001; Chapter 6: Unit 6 2.
41 Holmes K, Lantz LM, Fowlkes BJ, Schmid I, Giorgi JV. Preparation of cells and reagents for flow cytometry. *Curr Protoc Immunol* 2001; Chapter 5: Unit 5 3.
42 Kappelmayer J, Gratama JW, Karaszi E, Menendez P, Ciudad J, Rivas R *et al.* Flow cytometric detection of intracellular myeloperoxidase, CD3 and CD79a. Interaction between monoclonal antibody clones, fluorochromes and sample preparation protocols. *J Immunol Methods* 2000; **242**: 53–65.
43 Quijano S, Lopez A, Sancho JM, Panizo C, Deben G, Castilla C *et al.* Identification of leptomeningeal disease in aggressive B-cell non-Hodgkin's lymphoma: improved sensitivity of flow cytometry. *J Clin Oncol* 2009; **27**: 1462–1469.
44 Owens MA, Loken MR. *Flow Cytometry Principles for Clinical Laboratory Practice: Quality Assurance for Quantitative Immunophenotyping*. Wiley-Liss: New York; Chichester, 1995, xiii, 224 pp.
45 Caraux A, Klein B, Paiva B, Bret C, Schmitz A, Fuhler GM *et al.* Circulating human B and plasma cells. Age-associated changes in counts and detailed characterization of circulating normal CD138- and CD138+ plasma cells. *Haematologica* 2010; **95**: 1016–1020.
46 Braylan RC, Orfao A, Borowitz MJ, Davis BH. Optimal number of reagents required to evaluate hematolymphoid neoplasias: results of an international consensus meeting. *Cytometry* 2001; **46**: 23–27.
47 Sanchez ML, Almeida J, Vidriales B, Lopez-Berges MC, Garcia-Marcos MA, Moro MJ *et al.* Incidence of phenotypic aberrations in a series of 467 patients with B chronic lymphoproliferative disorders: basis for the design of specific four-color stainings to be used for minimal residual disease investigation. *Leukemia* 2002; **16**: 1460–1469.
48 Pedreira CE, Costa ES, Barrena S, Lecrevisse Q, Almeida J, van Dongen JJ *et al.* Generation of flow cytometry data files with a potentially infinite number of dimensions. *Cytometry A* 2008; **73**: 834–846.
49 Pedreira CE, Costa ES, Almeida J, Fernandez C, Quijano S, Flores J *et al.* A probabilistic approach for the evaluation of minimal residual disease by multiparameter flow cytometry in leukemic B-cell chronic lymphoproliferative disorders. *Cytometry A* 2008; **73A**: 1141–1150.
50 Costa ES, Pedreira CE, Barrena S, Lecrevisse Q, Flores J, Quijano S *et al.* Automated pattern-guided principal component analysis vs expert-based immunophenotypic classification of B-cell chronic lymphoproliferative disorders: a step forward in the standardization of clinical immunophenotyping. *Leukemia* 2010; **24**: 1927–1933.
51 Costa ES, Arroyo ME, Pedreira CE, Garcia-Marcos MA, Tabernero MD, Almeida J *et al.* A new automated flow cytometry data analysis approach for the diagnostic screening of neoplastic B-cell disorders in peripheral blood samples with absolute lymphocytosis. *Leukemia* 2006; **20**: 1221–1230.
52 Robinson JP, Durack G, Kelley S. An innovation in flow cytometry data collection and analysis producing a correlated multiple sample analysis in a single file. *Cytometry* 1991; **12**: 82–90.
53 Robinson JP, Ragheb K, Lawler G, Kelley S, Durack G. Rapid multivariate analysis and display of cross-reacting antibodies on human leukocytes. *Cytometry* 1992; **13**: 75–82.
54 Cover TM, Hart PE. Nearest neighbour pattern clasification. *IEEE Trans Inf Theory* 1967; **IT-13**: 21–27.
55 Duda RO, Hart PE, Stork DG, RO Duda. PC, scene a. In: Duda RO, Hart PE, Stork DG (eds) *Pattern Classification*. 2nd edn Wiley: New York; Chichester, 2001; 654 pp.
56 Costa ES, Peres RT, Almeida J, Lecrevisse Q, Arroyo ME, Teodosio C *et al.* Harmonization of light scatter and fluorescence flow cytometry profiles obtained after staining peripheral blood leucocytes for cell surface-only versus intracellular antigens with the Fix & Perm reagent. *Cytometry B Clin Cytom* 2010; **78**: 11–20.
57 Lugli E, Roederer M, Cossarizza A. Data analysis in flow cytometry: the future just started. *Cytometry A* 2010; **77**: 705–713.
58 Stall A. *Qr and Br in BD FACSDiva v6 Software: Parameters for Characterizing Detector Performance*. Application Note 23-10516-00. BD Biosciences: San Diego, CA, 2008.
59 Bjorklund E, Matinlauri I, Tierens A, Axelsson S, Forestier E, Jacobsson S *et al.* Quality control of flow cytometry data analysis for evaluation of minimal residual disease in bone marrow from acute leukemia patients during treatment. *J Pediatr Hematol Oncol* 2009; **31**: 406–415.
60 Dworzak MN, Gaipa G, Ratei R, Veltroni M, Schumich A, Maglia O *et al.* Standardization of flow cytometric minimal residual disease evaluation in acute lymphoblastic leukemia: multicentric assessment is feasible. *Cytometry B Clin Cytom* 2008; **74**: 331–340.
61 Irving J, Jesson J, Virgo P, Case M, Minto L, Eyre L *et al.* Establishment and validation of a standard protocol for the detection of minimal residual disease in B lineage childhood acute lymphoblastic leukemia by flow cytometry in a multicenter setting. *Haematologica* 2009; **94**: 870–874.
62 Kraan J, Gratama JW, Keeney M, D'Hautcourt JL. Setting up and calibration of a flow cytometer for multicolor immunophenotyping. *J Biol Regul Homeost Agents* 2003; **17**: 223–233.
63 Shankey TV, Forman M, Scibelli P, Cobb J, Smith CM, Mills R *et al.* An optimized whole blood method for flow cytometric measurement of ZAP-70 protein expression in chronic lymphocytic leukemia. *Cytometry B Clin Cytom* 2006; **70**: 259–269.

Supplementary Information accompanies the paper on the Leukemia website (http://www.nature.com/leu)

2. Artículo 2: Paneles de combinaciones de anticuerpos EuroFlow para el inmunofenotipado estandarizado en n-dimensiones de leucocitos normales, reactivos y tumorales.

2.1. Introducción general.

En las últimas décadas el inmunofenotipado se ha afianzado como una de las herramientas básicas para el diagnóstico, clasificación y monitorización de hemopatías malignas. En términos generales, el análisis inmunofenotípico de las células presentes en una muestra y que se sospecha puedan ser patológicas, se basa en la comparación de sus características con las de las células hematopoyéticas normales presentes habitualmente en ese tipo de muestra; esta comparación permite establecer la línea celular y el estadio madurativo de dichas células en base al parecido existente entre su perfil fenotípico y el de las células normales, y asegurar el carácter maligno vs normal/reactivo, en el caso de que presenten fenotipos aberrantes. Para ello se requiere de una cuidadosa selección de aquella(s) combinación(es) de marcadores que mejor reflejen estas características (i.e., línea celular, estadio madurativo y fenotipos aberrantes) entendiendo por marcador no solo el antígeno diana sino también el clon y conjugado fluorescente más adecuado a su identificación y caracterización. En este sentido, merece destacar que aunque la evaluación inicial del funcionamiento de cada clon/conjugado fluorescente es fundamental para el proceso de selección del mejor reactivo, con relativa frecuencia el patrón resultante se ve afectado por interacciones que ocurren una vez este se haya incluido dentro de una combinación de marcadores. Por ello, en una segunda etapa, cada reactivo debe ser valorado en el contexto de la combinación en la que será utilizado.

Cada combinación de anticuerpos que se incluye en un panel debe dar respuesta a una o más indicaciones médicas que hayan desencadenado el proceso diagnóstico. Así, mientras que en algunas ocasiones se desconoce de entrada el tipo de población celular concreta que pudiera ser representativo de la enfermedad que se sospecha, en otras existe cierto grado de certeza

respecto a la presencia y tipo de enfermedad y célula patológica que infiltra la muestra obtenida para su estudio. Como consecuencia, deben definirse diferentes estrategias para cada uno de estos dos grupos de situaciones. Así, mientras que en el primer caso debe buscarse una estrategia de rastreo inicial rápido basado preferentemente en una sola combinación (i.e. tubo) de un número (a ser posible) limitado de anticuerpos que permitan la identificación de todas las células relevantes, en el segundo caso, es recomendable una caracterización más exhaustiva de las células patológicas mediante la identificación inequívoca de las mismas y su caracterización detallada con una o más combinaciones de anticuerpos. A la hora de aplicar ambas estrategias, estas deben estar coordinadas y ser empleadas de forma secuencial, aplicando primero los tubos de rastreo diagnóstico, con el objetivo de establecer la naturaleza normal o reactiva vs clonal/patológica de las células de la muestra y, posteriormente, los paneles más amplios de caracterización fenotípica para la clasificación de dichas células y de la enfermedad concreta a la que presumiblemente representan. La elección del tubo (o tubos) concretos de rastreo diagnóstico, así como de los paneles de caracterización fenotípica debe orientarse de acuerdo con la información clínica disponible en el momento de iniciar el estudio (p. ej., el/los diagnósticos de sospecha).

En las siguientes secciones de este resumen se describen de forma breve el proceso empleado para el de diseño y validación de los paneles y combinaciones de anticuerpos EuroFlow para el diagnóstico y clasificación de leucemias y linfomas, de los que hemos sido responsables dentro de este trabajo doctoral: 1) tubo EuroFlow para el rastreo diagnóstico de linfocitosis maduras (sección 2ª), 2) paneles EuroFlow para el rastreo diagnóstico y clasificación de neoplasias de células plasmáticas (sección 4ª), 3) panel EuroFlow para la clasificación diagnóstica de síndromes linfoproliferativos crónicos T (sección 9ª) y, 4) panel EuroFlow para la caracterización diagnóstica de síndromes linfoproliferativos crónicos de células NK (sección 10ª).

En términos generales para cada panel se seleccionaron inicialmente aquellos marcadores que, de acuerdo con la literatura y la experiencia previa de los grupos EuroFlow, se había

demostrado son útiles (o podrían potencialmente serlo) para, posteriormente, evaluar su verdadera utilidad en rondas secuenciales de evaluación, optimización y re-evaluación de las combinaciones seleccionadas, empleando los protocolos estandarizados y las herramientas informáticas desarrolladas según lo descrito anteriormente en este trabajo doctoral.

2.2. Sección 2ª. Tubo EuroFlow para el rastreo diagnóstico de linfocitos maduros (LST, abreviado del inglés "lymphoid screening tube")

Introducción. Los SLPC son un grupo heterogéneo de enfermedades caracterizadas por la expansión y acumulación de una o más poblaciones de linfocitos maduros B, T y/o NK bloqueados en distintos estadio madurativos y portadores de diferentes alteraciones fenotípicas y genotípicas. El acúmulo de linfocitos patológicos puede generar linfocitosis cuando ocurre en SP, infiltrados linfoides en MO y/o organomegalias (e.g. adenomegalias, esplenomegalias, entre otras) al tener lugar en ganglios linfáticos, bazo u otros tejidos del organismo; estos hallazgos, entre otros, que a su vez ponen en marcha la realización del estudio fenotípico dirigido a establecer la naturaleza clonal/patológica vs normal o reactiva de las células expandidas. En la actualidad, la identificación de linfocitos clonales/patológicos se basa tanto en la constatación de un desequilibrio numérico en la distribución de las distintas subpoblaciones de linfocitos B, T y NK, como en la presencia de perfiles inmunofenotípicos aberrantes que permiten discriminar claramente entre células patológicas y linfocitos normales/reactivos. Dichos hallazgos deben orientar además, sobre el posible subtipo diagnóstico de SLPC subyacente.

Objetivos. Diseñar y validar una combinación de marcadores en 8 colores, para el rastreo diagnóstico de SLPC de forma rápida y sencilla, en muestras de SP, MO y tejido linfoide, que permita establecer la(s) línea(s) linfoide(s) comprometida(s) (e.g., linfocitos B, T y/o NK) y orientar sobre la estrategia diagnóstica a seguir una vez definida la naturaleza clonal/patológica vs normal/reactiva de dichas células.

Material y métodos. En conjunto, en esta sección se evaluaron un total de 463 muestras (292 muestras de SP, 13 muestras de células mononucleadas de SP obtenidas mediante separación por gradiente de densidad, 127 MO, 20 biopsias de ganglio linfático -GL-, 8 PAAF y 3 muestras de otro tipo). En términos generales, el proceso incluyó el diseño y evaluación de 7 versiones consecutivas de la combinación LST. En la combinación inicial de anticuerpos seleccionados (i.e., versión 1 de LST), se incluyeron marcadores dirigidos a identificar linfocitos maduros y discriminar entre sus subpoblaciones mayoritarias, como CD45 para linfocitos en general, CD3 para linfocitos T, CD19 y CD20 para linfocitos B, y CD56 que, junto a positividad intensa para $CD45^{+}$ en ausencia de expresión de SmCD3 y CD19, identifica células NK; además, a estos marcadores se añadieron SmIgκ y SmIgλ para el estudio de clonalidad B y, CD4, CD8 y CD56, para la identificación de las poblaciones mayoritarias de linfocitos T y NK. Esta versión y cada una de las siguientes (hasta alcanzar la versión 7 definitiva), se evaluaron en paralelo en un número variable de muestras con el método diagnóstico empleado en cada centro: 9, 29, 97, 26, 19, 12 y 271 muestras para las versiones 1 a 7 del LST.

En algunas posiciones (i.e., fluorocromos del tubo LST) se combinaron dos marcadores, siendo esto posible siempre y cuando cada marcador usado en la misma fluorescencia estuviese restringido a una población específica que pudiera ser identificada positivamente mediante otro(s) marcador(es) presentes en otras posiciones de la combinación de marcadores. Para el análisis de los datos, incluida la identificación de cada una de las subpoblaciones linfocitarias presentes en las muestras normales y patológicas evaluadas con cada versión de la combinación LST, se empleó el programa informático Infinicyt, que incluía las herramientas de fusión de ficheros, estimación de datos y análisis de componentes principales desarrolladas y descritas previamente en esta memoria.

Resultados. La evaluación de la versión inicial y de las versiones siguientes del LST mostró importantes limitaciones; para solventarlas se introdujeron cambios hasta alcanzar la versión 7 definitiva. De forma breve, los cambios incorporados durante el proceso de re-diseño y re-

evaluación de la combinación LST desde la versión 1 a la 7 incluyeron: i) añadir CD38, anti-TCRγδ y CD5 para una caracterización más precisa de las poblaciones linfoides B, T y NK, asociada a un incremento en el número de subpoblaciones identificables, para obtener una mejor orientación sobre los paneles a aplicar posteriormente, en caso de identificar células patológicas y; ii) redistribuir los marcadores dentro de la combinación, como consecuencia de la necesidad de seleccionar clones de anticuerpos y conjugados de fluorocromos más adecuados y óptimos, y mantener una estructura compatible con el panel EuroFlow para clasificación diagnóstica de SLPC-B en cuanto a marcadores comunes se refiere. La versión final (i.e., versión 7) que incluía CD4 & CD20-PacB/CD45-PacO/CD8 & SmIgλ-FITC/CD56 & SmIgκ-PE/CD5-PerCP-Cy5.5/CD19 & TCRγδ-PE-Cy7/CD3-APC/CD38-APC-H7 se evaluó en un amplio número (n=271) de muestras. En 84% (228/271) de las muestras evaluadas con la versión 7 se detectó la presencia de al menos una población linfoide aberrante que representaba en media 31% (rango: 0,04-98%) de la celularidad global de la muestra, siendo la concordancia observada del 100% respecto al método de rutina usado en cada laboratorio en paralelo, y alcanzando una sensibilidad de 0,1% (10^{-3}). En términos globales, esta última versión de LST permitía evaluar de forma bastante completa y detallada el compartimiento linfoide de los diferentes tipos de muestras analizadas, facilitando además la selección del panel de caracterización fenotípica más adecuado para completar el estudio (paneles EuroFlow de clasificación diagnóstica de SLPC B, T y/o NK). Además, la información proporcionada podía ser integrada de forma completa con la del panel EuroFlow para la clasificación diagnóstica de SLPC-B. Finalmente, el análisis de muestras normales (n=22) permitió establecer los fenotipos normales de referencia para cada subpoblación de células linfoides estudiada con la combinación de anticuerpos seleccionada, agrupándose cada una de ellas en "clústeres" diferentes, al emplear los análisis multivariantes (p. ej., análisis de componentes principales) incluidos en el programa informático Infinicyt sobre el espacio de 10 dimensiones generado por los parámetros de dispersión de luz y fluorescencia recogidos. Así mismo, la comparación del perfil fenotípico de cada población celular patológica (n=249) vs su

correspondiente población de células normales de referencia empleando análisis de componentes principales, demostró la presencia de poblaciones aberrantes de linfocitos B en 149/150 (99,4%) SLPC B estudiados, de poblaciones aberrantes de linfocitos T en 61/65 (94%) SLPC-T analizados -poblaciones T $CD4^{+}/CD8^{-/+débil}$ en 33/36 (91%), poblaciones T $CD8^{hi}/CD4^{-}$ en 13/14 (93%) y en la totalidad de los SLPC con fenotipo T $CD4^{-}/CD8^{-/+débil}/TCR\gamma\delta^{-}$ (n=3), $CD4^{-}/CD8^{-/+débil}/TCR\gamma\delta^{+}$ (n=11), y $CD4^{+}/CD8^{+}$ (n=1)- y de poblaciones anormales o expandidas de células NK en 17/18 (94,4%) SLPC NK estudiados. Cabe señalar que en aquellos SLPC en los que no se detectó ninguna población celular linfoide claramente aberrante y completamente distinta de las células linfoides normales existía, en todos ellos, un fenotipo parcialmente aberrante y/o una desviación en la distribución numérica (relativa o absoluta) de la población patológica.

Conclusión. En su configuración final, el tubo LST de 12-parametros/8-colores propuesto y resultante de 7 rondas de diseño, evaluación, optimización y re-evaluación, mostró una concordancia del 100% con las combinaciones de anticuerpos y estrategias empleadas hasta ese momento en cada centro; además, este tubo demostró una gran utilidad a la hora de discriminar linfocitos normales/reactivos vs clonales/patológicos al permitir detectar fenotipos aberrantes en la práctica totalidad de los SLPC de linfocitos B (>99%) y la gran mayoría (≥94%) de los SLPC T y NK analizados (eficiencia global del 97,4%) con una sensibilidad de 0,1% (10^{-3}). Por todo ello, el tubo LST puede considerarse como una combinación óptima de anticuerpos de referencia para el rastreo diagnóstico de SLPC B, T y NK.

2.3. Sección 4ª. Panel EuroFlow para el rastreo diagnóstico y clasificación de neoplasias de células plasmáticas (PCD, abreviado del inglés "plasma cell disorders")

Introducción. Las neoplasias de células plasmáticas (NCP) integran un grupo de enfermedades caracterizadas por la presencia de CP clonales (CPc) en MO u otros tejidos. Habitualmente, estas CPc son capaces de secretar una Ig clonal (i.e., componente monoclonal -M-) detectable en

suero y/u orina. Además de la información clínica y laboratorial convencional, en los últimos años se ha demostrado que la CMF proporciona información relevante para el diagnóstico y clasificación de este grupo de enfermedades, contribuyendo además a la discriminación de diferentes grupos de riesgo con distinto pronóstico. Desde el punto de vista práctico, la información más importante que proporciona el inmunofenotipado por citometría de flujo, se relaciona con la identificación de la presencia de CPc y su distribución relativa dentro del conjunto de CPs de MO; así, niveles más elevados de CPc se asocian dentro de este grupo de enfermedades a formas malignas y a progresión a formas más avanzadas de esta patología. Por otra parte, algunos perfiles inmunofenotípicos concretos como el patrón de expresión de CD28, CD117 y β2 microglobulina (β2M) se han asociado también a alteraciones genéticas concretas y/o a subgrupos de pacientes con MM con diferente pronóstico. En el momento de iniciar este trabajo, se consideraba ya que la mejor combinación de marcadores inmunofenotípicos para la identificación y cuantificación de CPs incluiría los antígenos CD38, CD138 y CD45, junto con las características de dispersión de luz; a su vez, se considera que los marcadores CD19, CD56, CD117, CD20, CD28, CD27 y CD81 y la evaluación de la expresión de las cadenas ligeras de Igs a nivel intracitoplasmático, entre otros, permitirían discriminar de forma específica entre CP normales y CPc en base a sus características fenotípicas, con la correspondiente utilidad diagnóstica.

Objetivo. Diseñar y validar una combinación de marcadores para el rastreo diagnóstico y la clasificación de NCP de forma rápida y sencilla, a través de la identificación, recuento y caracterización de CPc vs CP normales.

Material y métodos. En conjunto, evaluamos un total de 214 muestras (212 muestras de MO y 2 de SP) que incluían muestras de 10 donantes (adultos) sanos y de 204 pacientes con diferentes enfermedades: 173 muestras de pacientes con NCP analizadas al diagnóstico, en recaída o durante seguimiento; 3 muestras de pacientes con SLPC B sin evidencia de afectación del compartimiento de CPs, y 28 muestras de pacientes con enfermedades no relacionadas con NCP.

Una parte de las muestras (n=114) se emplearon para evaluar las diferentes versiones iniciales (versiones 1 a 5) del panel, mientras que las 100 restantes, correspondientes a 31 muestras de CP normales y reactivas de referencia (provenientes de 10 pacientes con enfermedades no relacionadas con NCP al diagnóstico, 13 MO en regeneración post-quimioterapia por enfermedades no relacionadas con NCP y 8 MO de donantes sanos) y 63 muestras de CPc de pacientes con NCP -38 MM, 23 GMSI, 2 LCP- y, 6 muestras de MO de pacientes con sospecha de NCP en los que no se demostró presencia de CPc, formaron parte de la serie empleada para la evaluación de la versión final (versión 6) del mismo panel. Estratégicamente, para la versión 1 se seleccionaron 4 marcadores como marcadores comunes a todos los tubos del panel (i.e., CD38, CD138, CD45 y CD19) y dirigidos a identificar las CP totales y a discriminar dentro de ellas entre CP normales y clonales, en base a los fenotipos aberrantes más frecuentes. La primera versión del panel, incluía además un segundo grupo de 8 marcadores (CD56, CD27, CD28, CD81, CD117, β2M, y CyIgλ y CyIgκ) para una caracterización inmunofenotípica completa de ambas poblaciones de células plasmáticas y la confirmación de la naturaleza clonal de las CP aberrantes, respectivamente. Por todo ello, la versión inicial de este panel se configuró en 2 tubos de 8 colores. En total se realizaron 6 rondas de diseño, evaluación, optimización y, re-evaluación del panel, hasta alcanzar la configuración final (Versión 6) evaluada en paralelo con los protocolos y paneles empleados en cada centro. Para la identificación de las poblaciones de células plasmáticas de las muestras normales/reactivas y de las muestras de pacientes, se empleó el programa informático Infinicyt, incluyendo las herramientas de fusión de ficheros, estimación de datos y análisis de componentes principales desarrollados y descritos previamente en esta memoria.

Resultados. El panel definitivo fue el resultado de 6 rondas de diseño, evaluación, optimización y re-evaluación. Los cambios introducidos en cada versión del panel involucraron principalmente la redistribución de los marcadores en diferentes canales de fluorescencia en cada uno de los tubos hasta que se alcanzó una configuración óptima de clones y conjugados de fluorocromos

en la versión final (versión 6). Así, el panel para rastreo diagnóstico y clasificación de NCP mantuvo la configuración de 2 tubos (i.e., combinaciones de anticuerpos) de 8 colores que incluían 4 marcadores comunes a ambos (CD45-PacB, CD138-PacO, CD38-FITC y CD19-PECy7), y 4 marcadores adicionales distintos en cada combinación (CD56-PE/β2M-PerCP-Cy5.5/CyIgκ-APC/CyIgλ-APC-H7 en el tubo 1 y CD28-PE/CD27-PerCP-Cy5.5/CD117-APC/CD81-APC-H7 en el tubo 2). La evaluación de la versión final demostró que este panel permitía la correcta identificación y caracterización de las CP clonales/aberrantes vs su contrapartida normal/reactiva en el 100% de las muestras (n=100) que correspondían a muestras que contenían poblaciones de CPc (63/63 casos) y/o normales (88/88), según los resultados obtenidos con los protocolos de rutina y aplicados en paralelo en cada centro. En los 49 casos en los que coexistían poblaciones de CPc y CP normales/reactivas, el tubo 1 fue suficiente para detectar ambas poblaciones en base a su distinto perfil inmunofenotípico y la restricción de la expresión de cadenas ligeras de Igs a nivel intracitoplasmático. Así mismo, mediante análisis multivariante de componentes principales empleando el programa Infinicyt, comprobamos que las CP normales del grupo de referencia (n= 31) formaban un "clúster" relativamente homogéneo con un elevado grado de solapamiento entre el perfil inmunofenotípico de las CP normales y reactivas de MO. Por el contrario, al comparar las poblaciones de CPc de cada una de las muestras patológicas de pacientes con NCP con el grupo de referencia de CP normales/reactivas, observamos como las primeras formaban sistemáticamente, un grupo claramente diferente y separado del grupo de CP normales/reactivas de referencia, siendo esta separación suficiente para distinguir ambas poblaciones de CPs con la combinación de marcadores del tubo 1 en todos los casos analizados (n=63); los marcadores adicionales del tubo 2 contribuían a incrementar aún más dicha separación entre ambos grupos de células plasmáticas.

Conclusión. El panel para rastreo diagnóstico y clasificación de NCP compuesto por 2 combinaciones de anticuerpos de 8 colores, demostró ser una herramienta eficiente para la

identificación, cuantificación y caracterización de CP normales y la discriminación entre CP normales/reactivas y CPc en pacientes con NCP, siendo la combinación de reactivos del tubo 1, suficiente para alcanzar estos objetivos. En este sentido, el tubo 1 de este panel podría emplearse inicialmente como tubo único para el rastreo diagnóstico de NCP, en una aproximación en dos pasos, en la que el tubo 2 completaría la caracterización fenotípica de la población de CP patológicas en aquellos casos en los que estuviese indicada dicha caracterización fenotípica complementaria.

2.4. Sección 9ª. Panel EuroFlow para la clasificación de síndromes linfoproliferativos crónicos T (SLPC-T)

Introducción. Los SLPC-T son un grupo heterogéneo de neoplasias malignas de linfocitos T maduros T (post tímicos) relativamente poco frecuentes. Incluyen un grupo amplio de entidades diferentes y relativamente menos conocidas que los SLPC B, debido a su baja frecuencia, heterogeneidad y a la ausencia, en la mayoría de los casos, de marcadores genéticos/moleculares recurrentes. En los últimos años, se ha avanzado de forma importante en la comprensión de la patogénesis de algunos SLPC-T como consecuencia de la identificación de la posible contrapartida normal de algunas de estas enfermedades (e.g., las células T colaboradoras foliculares en el LTAI o las células T reguladoras $CD4^{+}/CD25^{++}/CyFoxp3^{+}$ en el caso de LLTA). Además, se han identificado también marcadores genéticos que definen subgrupos específicos de SLPC-T, como por ejemplo los reordenamientos de los genes *TCL1* y *ALK* asociados a sobreexpresión de ambas proteínas, característicos de la LPL-T y del LACG, respectivamente.

Objetivo. Diseñar y validar un panel de combinaciones de anticuerpos para la confirmación de la naturaleza clonal de poblaciones de linfocitos T aberrantes y/o expandidas, detectadas mediante el tubo LST, y la subclasificación diagnóstica de los SLPC-T.

Material y métodos. En conjunto, para la construcción del panel de SLPC-T se realizaron cuatro rondas de diseño, evaluación, optimización y re-evaluación, hasta alcanzar la configuración final del panel. En total, en este apartado del trabajo doctoral se analizaron 109 muestras que incluían 23 muestras de SP para la evaluación y selección de la configuración final de marcadores comunes a todas las combinaciones del panel, y 86 muestras (78 SP, 7 MO, y 1 líquido ascítico, correspondientes a 37 expansiones clonales de linfocitos T $CD4^+$, 18 SLPC de linfocitos T $CD8^+$ y 11 SLPC de células T $CD4^-/CD8^{-/+débil}$) para la evaluación de las 2 versiones completas del panel: 19 muestras para la evaluación de la versión 1 y 67 para la versión 2. De los 67 casos empleados en la evaluación de la versión 2, 34 presentaban un fenotipo T $CD4^+$ (9 casos de SS, 5 de LPL-T, 4 LLTA, 4 LLGG-T, 2 LTAI y 10 casos de linfomas T periféricos NOS), 11 tenían fenotipo $CD8^+$ (10 muestras de pacientes con LLGG-T y 1 linfoma T periférico NOS) y 11 casos correspondían a SLPC-T con fenotipo $CD4^-/CD8^{-/+débil}$ (9 casos de LLGG-T $TCR\gamma\delta^+$, 1 Linfoma T hepatoesplénico $TCR\gamma\delta^+$ y 1 SLPC-T $TCR\alpha\beta^+$), además de 11 muestras de donantes sanos. La selección de los marcadores a evaluar se basó en la experiencia existente entre los miembros de los distintos grupos EuroFlow y en la valoración prospectiva de los mismos; así partimos de una larga lista de marcadores candidatos, entre los que se incluían marcadores clásicos pan-T que con relativa frecuencia se expresan de manera aberrante en los SLPC-T, marcadores de maduración, moléculas co-estimuladoras, marcadores de activación, proteínas relacionadas con citotoxicidad y marcadores con expresión restringida y/o característica de subtipos diagnósticos específicos de SLPC-T. Para el análisis de datos se empleó el programa informático Infinicyt que incluía las herramientas de fusión de ficheros, estimación de datos y análisis de componentes principales desarrollados y descritos en apartados anteriores de este trabajo doctoral. En 30/56 muestras que contenían poblaciones T expandidas o aberrantes, se confirmó la naturaleza clonal de las mismas mediante métodos moleculares.

Resultados. El diseño y la construcción del panel para la clasificación diagnóstica de SLPC-T se realizó en 4 etapas en las que se emplearon dos versiones reducidas y 2 versiones extendidas

del panel. Los cambios introducidos en las diferentes versiones de este panel incluyeron la redistribución de las posiciones de los marcadores incluidos en la combinación, la eliminación de marcadores redundantes y la incorporación de marcadores adicionales con el fin de incrementar la definición del LTAI. En su configuración final, el panel EuroFlow para SLPC-T quedó compuesto por 6 tubos de ≤8-colores que conservan la estructura general de otros paneles con la presencia de 4 marcadores comunes (i.e., SmCD3-PerCP-Cy5.5, CD45-PacO, CD4-PacB, y CD8-APC-H7) para la identificación inequívoca de las células T maduras ($CD45^+/SmCD3^+$) y de sus principales subpoblaciones (i.e., linfocitos T $CD4^+/CD8^-$, $CD4^+/CD8^+$, $CD4^-/CD8^{-/+débil}$ y $CD4^-/CD8^{hi}$) y hasta 4 marcadores variables/tubo completando un total de 20 marcadores adicionales para la caracterización fenotípica detallada de la población T patológica (FITC, PE, PE-Cy7 y APC): 1) CD7, CD26, CD2, CD28 en el tubo 1; 2) CD27, CD197, CD45RO, CD45RA en el tubo 2; 3) CD5, CD25, HLADR, CyTCL1 en el tubo 3; 4) CD57, CD30, (--), CD11c, en el tubo 4 y; 5) Cyperforina, Cygranzima B, CD16, CD94, en el tubo 5; el tubo 6 contenía solo CD279-PE, además de los 4 marcadores comunes. En términos globales, con la versión final del panel EuroFlow para la clasificación de SLPC-T se identificaron las poblaciones aberrantes/expandidas de células T presentes en los mismos en 100% de los casos, según las aproximaciones convencionales empleadas en cada centro. Además, el análisis multivariante de componentes principales mostró que dentro de los SLPC-T, los casos analizados que correspondían a SS (n=9), LPL-T (n=5), LLTA (n=4), LLGG-T $CD4^+$ (n=4) y LTAI (n=2), formaban grupos completamente separados entre sí y distintos fenotípicamente de las células T $CD4^+$ normales de referencia de SP de adultos sanos; la única excepción la constituían los linfomas T periféricos NOS (n=10), debido a su conocida heterogeneidad. No obstante, al comparar individualmente las células T patológicas de cada linfomas T periférico $CD4^+$ NOS, con los linfocitos T $CD4^+$ de referencia de otras entidades, encontramos un solapamiento parcial en entre sus fenotipos en 4/10 casos cuando comparamos con el grupo de pacientes con SS, sin que se observase solapamiento con el fenotipo de las células T $CD4^+$ normales de referencia. A su vez, en todos los pacientes con

SLPC-T en los que la población T expandida y/o aberrante presentaba un fenotipo $CD8^{hi}$ (n=11) o $CD4^{-}/CD8^{-/+débil}$ (n=11), se observó también una separación clara entre las células tumorales y su contrapartida normal de referencia, con la excepción de dos casos (1 caso con fenotipo de LLGG-T $CD8^{+}$ y 1 caso LLGG-T $CD4^{-}$ $CD8^{-/+débil}$). Por el contrario, no se observaron diferencias en los perfiles inmunofenotípicos globales de las células T neoplásicas de pacientes con LLGG-T $TCR\alpha\beta^{+}$ vs linfomas T periféricos NOS, ni entre los LLGG-$TCR\gamma\delta^{+}$ vs linfoma T hepatoesplénico, tanto para las poblaciones T patológicas $CD8^{hi}$ como para los $CD4^{-}/CD8^{-/+débil}$, respectivamente.

Conclusiones. El panel EuroFlow de 8-colores para la clasificación diagnóstica de SLPC-T, permite diferenciar entre células T normales y linfocitos T aberrantes/clonales en la gran mayoría de los casos (54/56; 96,4%), a la vez que aporta información relevante para la subclasificación de la enfermedad en entidades específicas según la clasificación OMS del año 2008. En este sentido, aunque este panel permite la distinción clara entre células T neoplásicas de los distintos subtipos diagnósticos de SLPC T $CD4^{+}$, el poder de discriminación entre diferentes categorías OMS parece ser más limitado cuando se trata de SLPC-T $CD8^{+}$.

2.5. Sección 10ª. Panel EuroFlow para la caracterización diagnóstica de síndromes linfoproliferativos crónicos de células NK (SLPC-NK)

Introducción. Los SLPC de células NK son entidades relativamente raras que involucran tanto proliferaciones reactivas como clónales de células NK, difíciles de diferenciar entre sí, debido fundamentalmente a la ausencia de marcadores universales de clonalidad NK. Así, este grupo de SLPC comprende un conjunto heterogéneo de entidades, entre las que se incluyen: la leucemia agresiva de células NK (LA-NK), el linfoma T/NK extranodal de tipo nasal y, la enfermedad linfoproliferativa crónica de células NK (ELPC-NK); de ellas, la enfermedad linfoproliferativa crónica de células NK constituye una categoría provisional que incluye pacientes con distintos subtipos de expansiones NK que se solapan parcialmente entre ellas.

Aunque se ha demostrado la existencia de aberraciones fenotípicas asociadas a clonalidad NK, en la actualidad seguimos sin disponer de una lista de marcadores fenotípicos que permita distinguir de forma inequívoca entre células NK reactivas y clonales y, dentro de estas últimas, entre los diferentes subtipos diagnósticos de SLPC-NK.

Objetivos. Diseñar y validar un panel de combinaciones de anticuerpos para la caracterización diagnóstica de las expansiones de células NK que permita, por un lado, establecer su naturaleza clonal vs reactiva y por otra parte, servir de herramienta eficiente de apoyo al diagnóstico y clasificación de los SLPC NK.

Material y métodos. En términos globales, en esta sección se incluyeron un total de 64 muestras de SP, de las cuales 26 se emplearon para la selección de los marcadores comunes a cada combinación de anticuerpos, y las 38 restantes (10 donantes sanos y 28 expansiones de células NK; 13 varones y 15 mujeres) para la validación de la versión final del panel de combinaciones de anticuerpos. Los marcadores candidatos a integrar las distintas combinaciones de anticuerpos se seleccionaron en base al conocimiento existente y la evaluación prospectiva realizada en cada ciclo de diseño, evaluación y optimización. Inicialmente, los marcadores propuestos incluían moléculas características de células NK, marcadores relacionados con la activación celular, los receptores de interleucina 2, proteínas citotóxicas, enzimas intracitoplasmáticas, receptores KIR, receptores LIR, receptores de tipo lectina (e.g. NKG2A/D, CD94 y CD161) y receptores de citotoxicidad natural (RCN), entre otros. Los criterios de selección se basaron en su capacidad para discriminar entre subpoblaciones de células NK normales, reactivas y clonales y/o para definir un fenotipo efector de tipo citotóxico. Para el análisis de los datos generados con las distintas versiones del panel de SLPC-NK se empleó el programa informático Infinicyt y las herramientas de fusión de ficheros, estimación de datos y análisis de componentes principales desarrolladas según lo descrito anteriormente en esta memoria. En 11 de las 15 muestras de mujeres con expansiones NK se investigó la posible naturaleza clonal vs reactiva de células NK purificadas mediante HUMARA, resultando dichas células clonales en 6/11

casos. En dos de las pacientes que presentaban expansiones clonales de células NK mediante HUMARA, y con fenotipo $CD56^{-/+débil}$, se excluyó además clonalidad T mediante métodos moleculares.

Resultados. En el diseño y construcción del panel de combinaciones de marcadores para diagnóstico y caracterización de SLPC-NK, conservamos una estructura similar a la de otros paneles descritos anteriormente. Así, este panel incluía 4 marcadores comunes a todas las combinaciones (i.e., CD45-PacO, SmCD3-PerCPCy5.5, CD56-PE-Cy7, y CD19-APC-H7) para la identificación inequívoca de las células NK en base a su fenotipo habitual (CD45+, CD56-/+, SmCD3-, CD19-) y 12 marcadores adicionales para la caracterización fenotípica de la población patológica. La configuración final del panel se alcanzó tras tres rondas de diseño, evaluación, optimización y re-evaluación, en las que esta se modificó mediante la redistribución y selecciones de clones y conjugados de fluorocromos óptimos para los marcadores comunes. La versión final del panel para diagnóstico y caracterización de SLPC-NK, se configuró en 3 tubos de 8-clores que, además de los marcadores comunes, contenían los siguientes marcadores (PacB, FITC, PE y APC): 1) CD2, CD7, CD26 y CD5 en el tubo 1; 2) CD16, CD57, CD25 y CD11c en el tubo 2, y; 3) HLADR, Cyperfonina, Cygranzima B y CD94 en el tubo 3. Los 6 casos en que se demostró la naturaleza clonal de la expansión NK (dos con fenotipo $CD56^{+}$ y 4 con fenotipo $CD56^{-/+débil}$), mostraron todos ellos a título individual un perfil inmunofenotípico diferente, tanto de la población de células NK normales de referencia, como de las células NK de sujetos que presentaban expansiones reactivas (i.e. no clonales). Utilizando esta misma estrategia, de aquellos 17 casos restantes en los que no se pudo confirmar la naturaleza clonal de la expansión de células NK, 9 mostraron un perfil inmunofenotípico claramente aberrante y distinto de las poblaciones de células NK normales y/o reactivas, 3 mostraron un solapamiento fenotípico importante con las células NK normales de SP y 2 con el fenotipo de células NK reactivas. En los 3 casos restantes no pudo establecerse de forma clara su pertenencia a ninguno de los grupos de referencia, solapándose simultáneamente, con al menos 2 de los 3 grupos de células NK.

Conclusión. Nuestros resultados muestran que, pese al número relativamente limitado de casos analizados, el panel EuroFlow para diagnóstico y caracterización de SLPC NK contribuye a una mayor precisión diagnóstica en este grupo de enfermedades, mediante la identificación de perfiles inmunofenotípicos que permiten distinguir entre expansiones de células NK normales/reactivas y clonales.

Leukemia (2012) **26**, 1908–1975

www.nature.com/leu

Open

ORIGINAL ARTICLE

EuroFlow antibody panels for standardized *n*-dimensional flow cytometric immunophenotyping of normal, reactive and malignant leukocytes

JJM van Dongen[1], L Lhermitte[2], S Böttcher[3], J Almeida[4], VHJ van der Velden[1], J Flores-Montero[4], A Rawstron[5], V Asnafi[2], Q Lécrevisse[4], P Lucio[6], E Mejstrikova[7], T Szczepański[8], T Kalina[7], R de Tute[5], M Brüggemann[3], L Sedek[8], M Cullen[5], AW Langerak[1], A Mendonça[6], E Macintyre[2], M Martin-Ayuso[9], O Hrusak[7], MB Vidriales[10] and A Orfao[4] on behalf of the EuroFlow Consortium (EU-FP6, LSHB-CT-2006-018708)

Most consensus leukemia & lymphoma antibody panels consist of lists of markers based on expert opinions, but they have not been validated. Here we present the validated EuroFlow 8-color antibody panels for immunophenotyping of hematological malignancies. The single-tube screening panels and multi-tube classification panels fit into the EuroFlow diagnostic algorithm with entries defined by clinical and laboratory parameters. The panels were constructed in 2–7 sequential design–evaluation–redesign rounds, using novel Infinicyt software tools for multivariate data analysis. Two groups of markers are combined in each 8-color tube: (i) backbone markers to identify distinct cell populations in a sample, and (ii) markers for characterization of specific cell populations. In multi-tube panels, the backbone markers were optimally placed at the same fluorochrome position in every tube, to provide identical multidimensional localization of the target cell population(s). The characterization markers were positioned according to the diagnostic utility of the combined markers. Each proposed antibody combination was tested against reference databases of normal and malignant cells from healthy subjects and WHO-based disease entities, respectively. The EuroFlow studies resulted in validated and flexible 8-color antibody panels for multidimensional identification and characterization of normal and aberrant cells, optimally suited for immunophenotypic screening and classification of hematological malignancies.

Leukemia (2012) **26**, 1908–1975; doi:10.1038/leu.2012.120

Keywords: EuroFlow; antibody panel; lymphoma; flow cytometry; 8-color immunostaining; standardization; hematological malignancies

INTRODUCTION

For more than two decades, immunophenotyping has been providing relevant information for the diagnosis, classification and monitoring of hematological malignancies.[1,2] Together with cyto/histomorphology and molecular (cyto)genetics, immunophenotyping is crucial for the identification, enumeration and characterization of leukemia and lymphoma cells. Consequently, it has acquired a prominent position in the current World Health Organization (WHO) classification of hematological malignancies.[3] Preferably, the immunophenotypic profiles of suspected cells should be compared with those of normal hematopoietic cells. Immunophenotypic similarities between the suspected cells and their potential normal counterparts allow the assignment of such cells to a given hematopoietic cell lineage and maturational stage, as well as the identification of aberrant phenotypes, such as leukemia-associated immunophenotypes.[4–14] Such immunophenotyping requires careful selection of unique combinations of individual markers based on their degree of specificity for the identification of a given cell lineage, maturation stage and aberrant phenotype, as well as the selection of appropriate antibody clones and fluorochrome conjugates to be used in multicolor combinations; the performance of these marker combinations is even more relevant than that of the individual markers. Consequently, such careful selection of reagents is essential for the design of standardized multicolor antibody combinations that provide unique staining patterns for each normal or aberrant cell population in a given sample.[6,15,16]

Each marker combination should be designed to answer one or multiple relevant clinical questions, through the identification, enumeration and characterization of the relevant cell populations in a sample. As the target cell population may not be known in advance or might have been defined previously, a different strategy is required in each situation. In the former situation, a rapid screening step based on a limited number of antibodies (preferably in a single tube) directed at differential identification of all relevant cell subsets in the sample is generally most

[1]Department of Immunology, Erasmus MC, University Medical Center Rotterdam (Erasmus MC), Rotterdam, The Netherlands; [2]Department of Hematology, Hôpital Necker-Enfants-Malades (AP-HP) and UMR CNRS 8147, University of Paris Descartes, Paris, France; [3]Second Department of Medicine, University Hospital of Schleswig Holstein, Campus Kiel (UNIKIEL), Kiel, Germany; [4]Cancer Research Center (IBMCC-CSIC), Department of Medicine and Cytometry Service, University of Salamanca (USAL) and Institute of Biomedical Research of Salamanca (IBSAL), Salamanca, Spain; [5]Haematological Malignancy Diagnostic Service (HMDS), University of Leeds (UNIVLEEDS), Leeds, UK; [6]Department of Hematology, Portuguese Institute of Oncology (IPOLFG), Lisbon, Portugal; [7]Department of Pediatric Hematology and Oncology, 2nd Faculty of Medicine, Charles University (DPH/O), Prague, Czech Republic; [8]Department of Pediatric Hematology and Oncology, Medical University of Silesia (SUM), Zabrze, Poland; [9]Cytognos SL, Salamanca, Spain and [10]Department of Hematology, University Hospital Salamanca (HUS) and IBSAL, Salamanca, Spain. Correspondence: Professor JJM van Dongen, Department of Immunology, Erasmus MC, University Medical Center Rotterdam, Dr Molewaterplein 50, 3015 GE Rotterdam, The Netherlands.
E-mail: j.j.m.vandongen@erasmusmc.nl
Received 21 March 2011; revised 14 February 2012; accepted 19 April 2012; accepted article preview online 3 May 2012

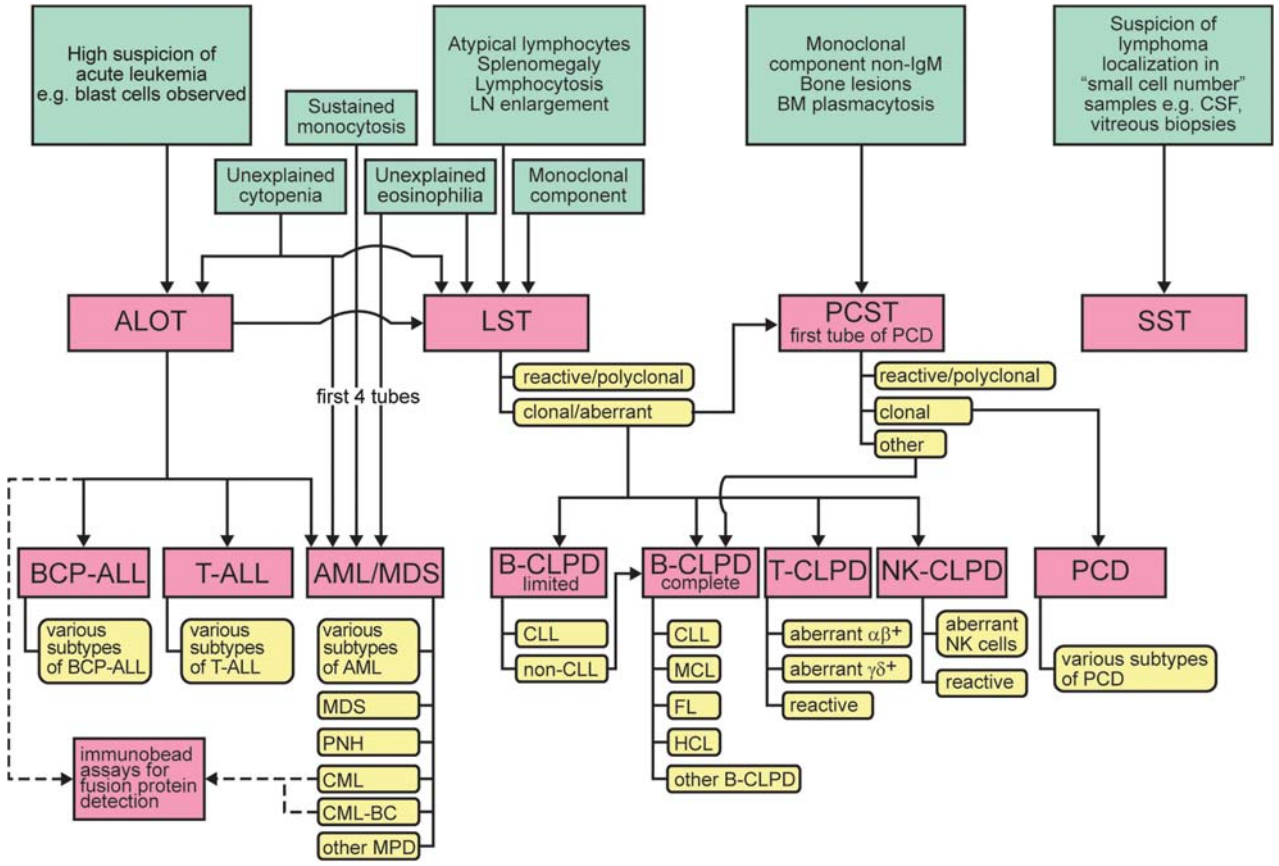

Figure 1. Flowchart diagram of the EuroFlow strategy for immunophenotypic characterization of hematological malignancies. On the basis of several entries of clinical and laboratory parameters, hematological malignancies are screened using a limited screening panel (i.e., typically one single tube) prior to appropriate and comprehensive characterization using extended antibody combinations. Abbreviations: ALOT, acute leukemia orientation tube; AML, acute myeloid leukemia; BC, blast crisis; BCP, B-cell precursor; BM, bone marrow; CLL, chronic lymphocytic leukemia; CLPD, chronic lymphoproliferative disorders; CML, chronic myeloid leukemia; CSF, cerebrospinal fluid; FL, follicular lymphoma; HCL, hairy cell leukemia; LN, lymph node; LST, lymphoid screening tube; MCL, mantle cell lymphoma; MDS, myelodysplastic syndrome; MPD, myeloproliferative disorders; PCD, plasma cell disorders; PCST, plasma cell screening tube; PNH, paroxysmal nocturnal hemoglobinuria; SST, small sample tube.

efficient[7,17–20] (Figure 1). In the latter situation, usage of a full antibody panel is recommended for the characterization and diagnostic classification of the suspected cells, using several (common) backbone markers for reliable and reproducible identification of the target cells in each multicolor combination of the antibody panel[13,14,20–24] (Figure 1). Preferably, the single-tube screening antibody panels and the multi-tube disease-classification antibody panels fit in a diagnostic algorithm with entries defined by clinical and laboratory parameters. Such a diagnostic algorithm is proposed here by the EuroFlow Consortium (Figure 1) as a critical prerequisite in the design of optimal antibody panels for diagnostic immunophenotyping.[25,26]

Multiple consensus panels have been proposed in the last two decades,[12–14,21–23,26–29] but they typically included largely overlapping lists of cluster of differentiation (CD) markers per disease category. Virtually all consensus proposals lack information about reference antibody clones for the proposed CD markers and they only provide limited information on the most appropriate combinations of relevant markers in multicolor antibody panels for immunophenotypic diagnosis and classification of hematological malignancies.[12–14,21–23,26–29] Given the number of CD antigens, the broad range of antibody clones and the variety of fluorochrome-conjugated reagents currently available for each individual CD marker, selection of optimal panels of reagents cannot be based exclusively on experience and expert opinions. In contrast, this requires extensive prospective testing in multicentric studies. The evaluation of the performance of a given antibody conjugate may be based on absolute measures (for example, fluorescence intensity and stain index (SI) obtained for a given control cell population),[30] but these criteria may not apply once the marker is combined with other reagents in a single-tube combination or a multi-tube antibody panel. Therefore, each reagent needs to be evaluated for its unique staining pattern obtained for the distinct cell populations in a multidimensional space defined by all parameters of the newly designed multicolor tube. Consequently, evaluation of the immunophenotypic profiles of leukemia cell populations should preferably be based on a detailed comparison of the phenotypes of individual cells for all markers together, rather than on subjective interpretation of arbitrary mean fluorescence levels (for example: negative versus positive, dim versus strong, homogeneous versus heterogeneous patterns) of a list of single markers. Visualization of such multidimensional spaces and selection of the most relevant parameters for optimal discrimination between the relevant cell populations require new software tools. Such tools were developed by the EuroFlow group and they proved to be essential for the critical evaluation and (re)design of the antibody combinations.[31–33] Among the new tools, reference data files of normal and distinct disease entities were built and the panels evaluated through paired multidimensional statistical comparisons of such normal versus disease-specific data files, as well as of data files corresponding to different well-characterized leukemia/lymphoma entities (Figure 2). In this way we could

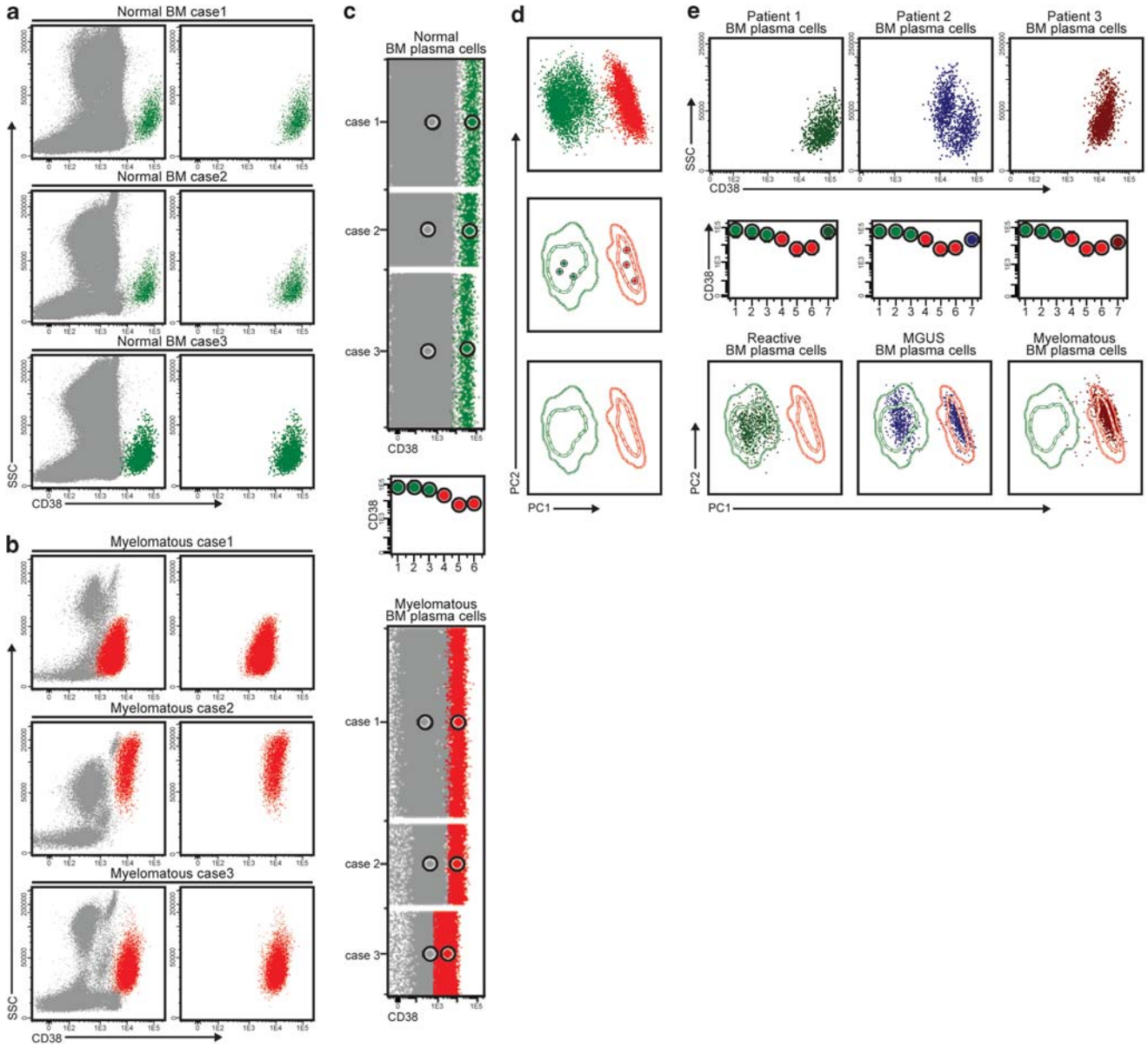

Figure 2. Schematic illustration of how reference data files of normal and leukemia/lymphoma cells were built and used for evaluation of antibody panels and software-guided comparison of individual cell populations from a new interrogated sample. In panels **a** and **b** it is shown how normal (green events in **a**) and tumoral plasma cells (red events in **b**) derived from six different normal ($n = 3$) and myelomatous ($n = 3$) bone marrow samples stained with the plasma cell disorders (PCD) EuroFlow panel (12 different immunophenotypic markers grouped in two 8-color tube combinations) were selected and merged to create a new reference data file (**c**). In (**d** and **e**), it is shown how the PCD panel allows clear discrimination between both types of plasma cells using principal component analysis (**d**) and prospective comparison and classification of plasma cells from new independent bone marrow samples corresponding to a reactive plasmocytosis (green dots in the left column of (**e**) clustered in the normal green plasma cell area in the lower plots), a multiple myeloma (MM) patient (brown dots in the right column of (**e**) clustered in the aberrant plasma cell area in the lower plots) and an MGUS (monoclonal gammopathy of undetermined significance) patient (blue dots in the middle column of panel **e** clustered into two distinct populations localized in the lower plots in the normal and aberrant reference plasma cell areas, respectively). Each individual large and small circle represents median values for single immunophenotypic parameters of the plasma cell populations shown in dot plot diagrams and the median fluorescence expression value for all immunophenotypic parameters measured in the principal component (PC)1 versus PC2 plots for individual samples, respectively; contour lines in these plots represent s.d. curves (dotted and continuous lines represent 1s.d. and 2s.d., respectively).

objectively evaluate the overall performance of the proposed panels for answering the specific clinical questions.

Here we describe the EuroFlow antibody panels developed for comprehensive immunophenotypic diagnosis and classification of hematological malignancies. The proposed panels were initially designed based on the experience and knowledge accumulated in the literature as well as in the individual EuroFlow laboratories. Subsequently, they were optimized in multiple successive evaluation rounds using large numbers of patient samples in the participating laboratories, taking advantage of the reference data files of normal and leukemia and lymphoma samples and the new software tools. The panels are designed in a flexible way to fit the needs of distinct diagnostic laboratories and they can be applied in one or multiple sequential steps. For each

antibody panel, detailed information is provided about the design procedure and about the utility, based on results derived from prospective evaluation of large series of well-defined patient samples.

MATERIALS AND METHODS

Patient and control samples

Multiple types of biological samples were collected from healthy volunteers and patients with suspicion or diagnosis of different types of hematological malignancies and other non-clonal hematological and non-hematological disorders, as specified later in each section of this paper. The collected samples concerned peripheral blood (PB), bone marrow (BM), fine needle aspirates (FNA), biopsies from lymphoid and non-lymphoid tissues, cerebrospinal fluid (CSF) and vitreous samples. For all patients with a hematological malignancy, the diagnosis was established according to the WHO criteria.[3]

Informed consent procedures and forms were proposed and approved at the first EuroFlow meeting (see the Editorial in this *Leukemia* issue). Informed consent was given by donors or their guardians (for example, parents) in case of children according to the guidelines of the local Medical Ethics Committees and in line with the Declaration of Helsinki Protocol. All participants obtained approval or no-objection from the local Medical Ethics Committees for secondary use of remaining diagnostic material for the EuroFlow studies, which also allows the inclusion of anonymized flow cytometric results into a central (public) database to define reference values for normal, reactive, regenerating and malignant cell samples.

Immunophenotypic studies

For immunophenotypic studies, all samples were systematically processed in parallel with the EuroFlow protocol versus the local routine procedures. Accordingly, the EuroFlow standard operating procedures (SOP) for instrument setup, instrument calibration, sample preparation, immunostaining and data acquisition[16] were used at individual centers in parallel to the corresponding local protocols and techniques used for routine diagnosis and classification of hematological malignancies according to the WHO criteria. For data analysis, the Infinicyt software (Cytognos SL, Salamanca, Spain) was used in parallel to the local data analysis software programs and procedures.

For multivariate analysis of samples measured with the EuroFlow SOP and antibody panels, the Infinicyt software was used. For this purpose, the merge and calculation functions were applied for multi-tube panels prior to the analysis, as described elsewhere.[31,32] Briefly, prior to multivariate analyses, the populations of interest were selected and stored each in a distinct data file. Data files corresponding to the same cell population from an individual sample but stained with a different antibody tube of a multi-tube panel were merged into a single data file containing all information measured for that specific cell population. In a second step, 'missing' data in one tube about markers only stained in the other tubes were calculated using previously described algorithms and tools implemented in the Infinicyt software.[32] Consequently, the generated final data file contained data about each parameter measured in the multi-tube panel for each of the events composing the cell population in that data file (Figure 2). This data file was further merged with the data files of other samples either to create a reference pool of a population of normal, reactive or malignant cells or to compare it with one or more of such reference pool data files, through multivariate analysis, for example, principal component analysis (PCA).[31]

SECTION 1. ACUTE LEUKEMIA ORIENTATION TUBE (ALOT)

L Lhermitte[1], V Asnafi[1], J Flores-Montero[2], Q Lécrevisse[2], L Sędek[3], T Szczepański[3], S Böttcher[4], M Brüggemann[4], E Mejstrikova[5], T Kalina[5], A Mendonça[6], P Lucio[6], M Cullen[7], S Richards[7], JG te Marvelde[8], H Wind[8], VHJ van der Velden[8], AJ van der Sluijs-Gelling[9], MB Vidriales[10], J Hernández[11], ES Costa[12], AS Bedin[1], E Macintyre[1], JJM van Dongen[8] and A Orfao[2]

[1]AP-HP, Paris, France; [2]USAL, Salamanca, Spain; [3]SUM, Zabrze, Poland; [4]UNIKIEL, Kiel, Germany; [5]DPH/O, Prague, Czech Republic; [6]IPOLFG, Lisbon, Portugal; [7]UNIVLEEDS, Leeds, UK; [8]Erasmus MC, Rotterdam, The Netherlands; [9]Dutch Childhood Oncology Group (DCOG), The Hague, The Netherlands; [10]HUS, Salamanca, Spain; [11]Cytognos, Salamanca, Spain and [12]Federal University of Rio de Janeiro (UFRJ), Rio de Janeiro, Brazil

BACKGROUND

Acute leukemias comprise a heterogeneous group of malignant diseases characterized by clonal expansion of immature hematopoietic precursor cells. Current international classifications that are used for therapeutic stratification categorize acute leukemias mainly on the basis of the lineage of the blast cells and the type of additional cytogenetic/molecular lesions and, to a lesser extent, detailed immunophenotype.[3] Two major categories of acute leukemias are recognized: (i) lymphoid precursor neoplasms, which are subdivided into B- and T-cell precursor acute lymphoblastic leukemia/lymphoma (BCP-ALL and T-ALL, respectively),[34,35] and (ii) acute myeloid leukemia (AML) and related precursor neoplasms.[3] A small number of cases do not fit into these two major groups because they either show no clear evidence of differentiation along a single lineage or express differentiation antigens highly specific of more than one lineage, making assignment to a single lineage difficult.[36] These cases represent less than 5% of all acute leukemia cases[36–38] and they are categorized separately in the current WHO classification as acute leukemias of ambiguous lineage, including both acute undifferentiated leukemia (AUL) and mixed phenotype acute leukemia (MPAL).[36]

Flow cytometry has an essential role in the diagnosis and classification of acute leukemias.[24,35,39] Together with cytomorphology and cytochemistry, immunophenotyping is crucial for the detection and lineage assignment of blast cells in suspected samples, including the definition of acute leukemias of ambiguous lineage.[37,38,40] Comparison of the immunophenotypic features of blasts cells versus normal hematopoietic precursors and immature cells contributes to the definition of the stage of maturation arrest of the blast population within the B- and T-lymphoid lineages as well as the neutrophilic, monocytic, megakaryocytic or erythroid lineages. In addition, specific immunophenotypic profiles have been associated with prognosis and/or unique cytogenetic and molecular abnormalities.[41–46] Finally, flow cytometric immunophenotyping has also proven to be of great utility for sensitive detection of low levels of residual blast cells and their distinction from normal regenerating immature cells in the BM of acute leukemia patients during treatment.[47]

During the past 5 years, the EuroFlow group has designed and evaluated a set of 8-color antibody panels for the diagnosis and classification of acute leukemias, which can be used in combination with novel software tools in order to optimize flow cytometric *n*-dimensional immunophenotypic characterization of blast cells. As for most EuroFlow protocols, the acute leukemia panels were designed in such a way that they can be applied in two consecutive steps (Figure 1). Depending on the precise clinical question associated with a sample suspected of containing blast cells, the first step includes a single 8-color tube, the ALOT, complemented by a multi-tube panel designed for full characterization of the malignancy. The choice of the second panel depends on the results obtained with the ALOT, that is, the antibody panel for confirmation and classification of BCP-ALL, T-ALL, or the antibody panel for non-lymphoid acute leukemia, the so-called AML/myelodysplastic syndrome (MDS) panel. Rare cases of ambiguous lineage leukemias are identified with the ALOT as requiring the use of more than one complementary panel (for example, the BCP-ALL and AML/MDS panels). This section focuses on the design and evaluation of the ALOT, whereas the subsequent characterization panels are described below in other sections: BCP-ALL (Section 5), T-ALL (Section 6) and AML/MDS (Section 7).

General principle for the design of the ALOT as an 'orientation' tube for blast cells

The ALOT was designed for initial assessment of the nature of immature populations of hematopoietic cells in acute leukemia samples (B- or T-lymphoid versus non-lymphoid lineage or mixed phenotype) in order to allow appropriate orientation towards the complementary BCP-ALL, T-ALL and AML/MDS antibody panels.

More specifically, ALOT was designed for rapid and efficient analysis of a sample, known to contain blasts according to cytomorphology or when the clinical and/or laboratory data are indicative for infiltration of the sample, for example, high white blood cell (WBC) count in PB co-existing with one or multiple cytopenias. However, screening for minimal numbers of blast cells reflecting disseminated disease or exclusion of a hematological malignancy in a systematic way is not possible with the ALOT screening tube alone.

Selection of antibodies

The criteria for antibody selection of the ALOT in order to optimally orientate the acute leukemia sample depend on lineage-associated specificity and sensitivity of the recognized antigens. An ideal orientation marker is constantly expressed by all cells of a single lineage and shows no cross-lineage reactivity. With the potential exception of cytoplasmic (Cy)CD3 in T-ALL patients,[48] if we exclude the exceptional cases of natural killer (NK)-cell acute leukemia,[49] such a marker has not been identified. Because of the inclusion of this antigen (CyCD3), the consequent need for intracytoplasmic staining within the ALOT was assumed to be essential. Very few membrane-bound target antigens are lineage specific; for example, CD7 and CD19 are T- and B-lineage associated markers, respectively, which are expressed in a significant number of AML cases.[50–55] Conversely, myeloid antigens such as CD13 and CD33 can be frequently found in BCP-ALL or T-ALL.[45,56–58] The very few membrane-bound antigens that are *stricto sensu* lineage-specific (for example, antigen receptors in lymphoid lineage) often appear late at the cell surface membrane during physiological ontogeny and, as such, they are expressed in only a minor subset of acute leukemia cases, thus lacking sensitivity. Most lineage-specific markers expressed at early stages of maturation are intracellular markers (for example, CyMPO, CyLysozyme, CyCD3). We therefore opted for a limited selection of intracellular and membrane-bound markers to fit into a single 8-color tube.

Based on previous reports[27] and on our knowledge and experience, all potentially valuable markers were considered. These included, among others, CD7, CD5, CD10, CD13, CD19, CD33, CD117, nuclear (Nu)TdT, HLADR, CyCD3, CyCD79a, CyMPO, CyLysozyme and potentially also mixtures of markers (for example, CD13 + 33). Noteworthily, virtually none of these markers perfectly matched the aforementioned criteria. As lineage commitment has to be assessed by flow cytometry on well-identified immature cells, markers that could contribute to the definition of immaturity and the identification of blast cells were considered independently (for example, CD34, CD45, CD117 and NuTdT). We then designed a list of markers that would be comparatively evaluated following the criteria and rationale described below.

Differentiation of hematopoietic cells comes with a specific pattern of $CD45^{lo}$ intensity correlated with both lineage and maturation stage. Thus, CD45 was a major marker for (i)

Table 1. Design of ALOT in five consecutive rounds with inclusion of backbone markers in common with the acute leukemia panels[a]

Version (no. of cases[b]*)*	*Fluorochromes and markers*							
	PacB	*AmCyan*	*FITC*	*PE*	*PerCPCy5.5*	*PECy7*	*APC*	*AF700*
1 ($n = 35$)	SmCD3	CD45	CyMPO	CyCD79a	CD34	CD19	CD7	CyCD3
2 ($n = 55$)	SmCD3	CD45	CyMPO	CyCD79a	CD34	CD19	CyCD3	CD7
	PacB	*PacO*	*FITC*	*PE*	*PerCPCy5.5*	*PECy7*	*APC*	*APCH7*
3 ($n = 102$)	SmCD3	CD45	CyMPO	CyCD79a	CD34	CD19	CD7	CyCD3
4 ($n = 35$)	SmCD3	CD45	CyCD79a	CyMPO	CD34	CD19	CD7	CyCD3
5 (Final)[c] ($n = 158$)	$CyCD3^{T}$	$CD45^{B,T,M}$	CyMPO	CyCD79a	$CD34^{B,M}$	$CD19^{B}$	CD7	$SmCD3^{T}$

Abbreviations: AF700, alexa fluor 700; ALL, acute lymphoblastic leukemia; ALOT, acute leukemia orientation tube; AmCyan, *Anemonia Majano* cyan fluorescent protein; AML, acute myeloblastic leukemia; APC, allophycocyanin; AUL, acute undifferentiated leukemia; BCP, B-cell precursor; Cy, cytoplasmic; Cy5.5, cyanin5.5; Cy7, cyanin7; FITC, fluorescein isothiocyanate; H7, hilite7; MPAL, mixed phenotype acute leukemia; PacB, pacific blue; PacO, pacific orange; PE, phycoerythrin; PerCP, peridinin–chlorophyll–protein; Sm, surface membrane. [a]Further information about markers and hybridomas is provided in the Appendix. [b]A total of 385 acute leukemia cases were evaluated: 190 BCP-ALL, 57 T-ALL, 132 AML, 6 AUL/MPAL. [c]T = backbone markers in common with T-ALL antibody panel; B = backbone markers in common with BCP-ALL antibody panel; M = markers in common with AML/MDS antibody panel. Highlighted boxes: changes as compared to previous version.

Table 2. Utility of ALOT markers

Target antigen	*Maturation markers*	*Lineage markers*		*Shared backbone markers*
		1st level	*2nd level*	
CyCD3		T		T-ALL
CD45	Immature			BCP-ALL/T-ALL/AML-MDS
CyMPO		My		
CyCD79a			B[a]	
CD34	Immature			BCP-ALL/AML-MDS
CD19		B[b]		BCP-ALL
CD7			T[b]	
SmCD3	Mature[c]			T-ALL

Abbreviations: ALL, acute lymphoblastic leukemia; ALOT, acute leukemia orientation tube; AML, acute myeloblastic leukemia; B, B lineage; BCP, B-cell precursor; Cy, cytoplasmic; MDS, myelodysplastic syndrome; My, myeloid lineage; Sm, surface membrane; T, T lineage. [a]Also present in some T-ALL. [b]Also present in some AML. [c]SmCD3 is used as a maturity marker for T-lineage, as identification of suspected immature T-cells relies on detection of $CyCD3^{+/lo}$ $SmCD3^{-}$ $CD34^{+/-}$ blasts.

identification of the suspected cell population on the basis of its dim expression and, (ii) exclusion of normal residual cells.[59–61] To refine the blast cell gating and further confirm the immature nature of the pathological population, CD34 was selected, as it is expressed by a significant number of acute leukemias from any lineage. Lineage-associated markers were then added for final blast cell gating and assessment of blast cell lineage. CyMPO was selected as a highly specific myeloid marker. CyCD3 was included as a specific T-lineage marker, which should be interpreted in combination with surface membrane (Sm)CD3 in order to identify a CyCD3^{+}/SmCD3$^{-/lo}$ pattern, the most frequent phenotype of T-ALL. CD19 was selected as a very sensitive B-lineage marker, which is expressed during the early stages of B-cell commitment as well as in virtually all BCP-ALL cases. However, CD19 lacks specificity as it is also expressed in a subset of AML cases, albeit at lower and more heterogeneous levels. Consequently, CyCD79a was added to improve B-lineage assignment, even though it is also expressed in t(8;21)$^{+}$ AML cases[50,51,54,55] and at low levels in a significant number of T-ALL cases, particularly the immature and T-cell receptor (TCR)$\gamma\delta^{+}$ T-ALL subgroups.[62–64] Of note, CyCD79a was preferred to CyCD22 because CD22 is not lineage specific as it is also expressed at high levels in normal basophils, mast cells and some dendritic cells.[65–67] Finally, CD7 was selected because it is positive in virtually all cases of T-ALL and in a subset of, usually CyMPO-negative, AML. The other markers listed above were discarded because they were felt to be not specific enough or they have been found to be redundant with other markers. The choice between NuTdT and CD34 was discussed extensively. For this purpose, 34 cases were analyzed using TdT/CD34 in parallel, including 17 BCP-ALL, 11 AML and 6 T-ALL; the value of each marker was individually appreciated for gating of blast cells for all cases. NuTdT and CD34 were found to be positive and informative in 88 and 82% of BCP-ALL, 83 and 33% of T-ALL, and 18 and 55% of AML cases, respectively. The utility of each marker was overall strictly similar in this series (65% of CD34 or NuTdT positivity over the different disease categories), supporting no evidence in favor of one marker or the other. However, the contribution of each marker did not affect the same cases as the expression of TdT and CD34 was not systematically correlated (15% of cases CD34^{+}/NuTdT^{-}, 15% CD34^{-}/NuTdT^{+}). This highlighted a certain complementarity of CD34 and TdT in this perspective. Owing to constraints of 8-color cytometry, it was chosen to include only one additional immaturity marker. CD34 had the advantage of identifying immature cells of all lineages and was finally selected in order to leave free the fluorescein isothiocyanate (FITC) channel in favor of MPO staining in the ALOT, and to serve as a valuable backbone marker in the BCP-ALL panel, avoiding intracellular staining.

Design of the configuration of the ALOT antibody combination

Once the eight individual markers had been selected, the labeling of antibodies and the specific fluorochrome configuration of the ALOT had to be set. The final configuration of the ALOT (Table 1) was designed to meet two criteria: (i) optimal detection of antigen expression, which may be fluorochrome dependent, and (ii) choice of backbone markers compatible with the different subsequent acute leukemia characterization panels so that information from the ALOT could be integrated with them in a final multiparameter analysis of the whole blast cell phenotype. This meant that the ALOT had to be developed in close synergy with the design of the backbones of the three independent acute leukemia characterization panels (BCP-ALL, T-ALL and AML/MDS panels), and had to be re-tested following each modification proposed for the characterization panels. Consequently, the CD45, CD34 and CD19 markers of the ALOT also serve as backbone markers when information regarding the ALOT is combined (using the merge and calculation functions of the Infinicyt software) with the BCP-ALL panel (see Section 5), whereas the CyCD3, CD45 and SmCD3 markers serve as backbone markers when information regarding the ALOT is combined with the T-ALL panel (see Section 6). CD45 and CD34 are also used as part of the backbone marker set in the AML/MDS panel (see Section 7) (Table 1). The final combination designed with selected target antigens is given in Table 1, whereas the utility of the included markers is summarized in Table 2. Details of the antibody clones are given in the Appendix.

Evaluation of the ALOT antibody combination

The final ALOT antibody combination is the result of multiple evaluation rounds performed to optimize the choice of target antigens, antibody clones, fluorochrome conjugates and combinations of antibody reagents. In total, the ALOT underwent five rounds of evaluation and redesigning with repeated testing on both control and patient samples, including the full spectrum of acute leukemias (Table 1). After analysis of a total of 385 acute

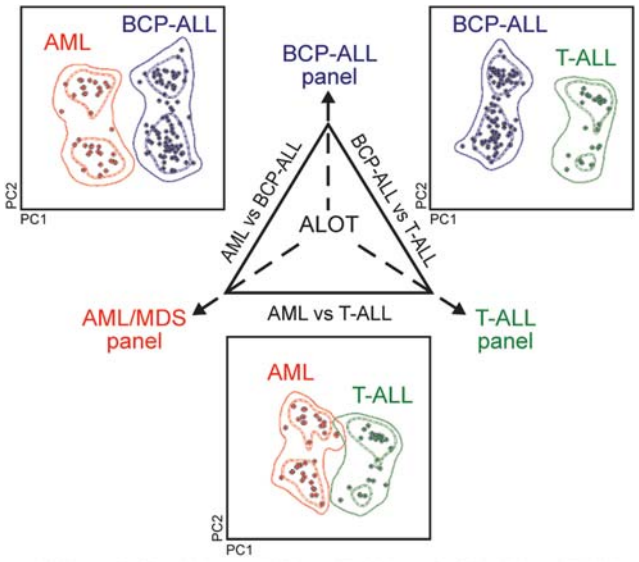

AML vs BCP-ALL	
CD19	32%
CyMPO	27%
CyCD79a	20%
CD45	8%
CyCD3	6%

AML vs T-ALL	
CyMPO	26%
CD7	26%
CyCD3	26%
CD34	15%
SmCD3	6%

BCP-ALL vs T-ALL	
CD19	23%
CyCD3	22%
CD7	22%
CyCD79a	14%
CD34	9%

Figure 3. Results of the preliminary study aimed at classification of 158 acute leukemia samples—89 B-cell precursor (BCP)–acute lymphoblastic leukemia (ALL), 27 T-ALL, 37 acute myeloid leukemia (AML) and 5 acute undifferentiated leukemia (AUL)/mixed phenotype acute leukemia (MPAL)—stained with the final acute leukemia orientation tube (ALOT) combination, using principal component (PC) analysis implemented in the automated population separator (APS) software tool. Comparison of well-defined entities (BCP-ALL, blue circles; T-ALL, green circles; AML, orange circles) shows proper classification based on the expression of the eight antigens, evaluated in the ALOT. Light scatter characteristics were excluded from APS analysis, despite their utility, because standardization had not been achieved at the time those samples were analyzed. Each individual circle represents a single case expressed as median fluorescence expression for all immunophenotypic parameters measured in the PC1 versus PC2 plot, and contour lines represent s.d. curves (dotted and continuous lines represent 1s.d. and 2s.d., respectively). The five most informative markers contributing to the best discrimination between each diagnostic entity are displayed at the bottom in a decreasing order of percentage contribution to the discrimination.

leukemia samples, this tube was considered to be in its 'final' configuration. In every evaluation round, variants of the final combination were tested in a multi-centric setting in parallel to in-house procedures. Briefly, initial testing ($n = 35$) included CD45 – *Anemonia Majano* cyan fluorescent protein (AmCyan) and CD3-Alexa Fluor 700 (AF700) fluorochrome-conjugated antibodies (version 1 of the ALOT) (Table 1). A CD7-AF700 antibody was tested ($n = 55$) in order to leave the bright Allophycocyanin (APC) fluorochrome position for the CyCD3 reagent (version 2 of the ALOT), but the obtained results were not satisfactory (Table 1). We then compared the performance of CD45 – Pacific Orange (PacO)/CD3 – APC Hilite7 (APCH7) (version 3 of the ALOT) with that of CD45 – AmCyan/CD3 – AF700 reference conjugates and validated the switch of fluorochromes to these new conjugates ($n = 102$ samples) to get rid of spectral overlap and to improve the brightness of the stainings. Additional evaluations were performed to evaluate alternative clones and antibody labeling, such as the CD79a and MPO FITC and phycoerythrin (PE) conjugates ($n = 35$) (version 4 of the ALOT) (Table 1). Given that CD3 antibodies are conjugated to almost all new fluorochromes, we also checked which fluorochrome was optimal for CyCD3 detection and whether the fluorochrome-conjugated CD3 antibodies were affected by fixation and permeabilization reagents (for example, Fix&Perm, An der Grub, Vienna, Austria). To address this issue, 26 acute leukemia samples (including 3 T-ALL) were analyzed with both SmCD3-APCH7/CyCD3-PacB and CyCD3-APCH7/SmCD3-PacB combinations in parallel. The average SI of residual T-cells measured was 14.9/19.9 with the SmCD3-APCH7/CyCD3-PacB combination, and 8.7/45.6 for the CyCD3-APCH7/SmCD3-PacB combination. In addition, the mean SI of blast cells from T-ALL samples was improved with CyCD3-PacB staining as compared to CyCD3-APCH7 (27.2 versus 9.1 for CyCD3-PacB and CyCD3-APCH7, respectively). We concluded that the results were in favor of a CyCD3-PacB/ SmCD3-APCH7 combination for optimal detection of immature T-cells. This allowed us to fix the final configuration, which was validated on 158 acute leukemia samples (version 5 of the ALOT): CyCD3 – PacB/CD45 – PacO/CyMPO – FITC/CyCD79a – PE/CD34 – peridinin chlorophyll protein complex-Cyanin5.5 (PerCPCy5.5)/CD19 – PECyanin7 (Cy7)/CD7 – APC/SmCD3 – APCH7 (Table 1). Overall, data obtained with the final ALOT version performed similarly to local immunostaining protocols and the stainings were of good quality, with low background signal when fresh and well-preserved samples (within 48 h of sample collection) were analyzed. Deviation from this criterion was notably associated with increasing background for CyCD3 and CD45, and with unspecific SmCD3 staining that could generally be solved by discarding dead cells.

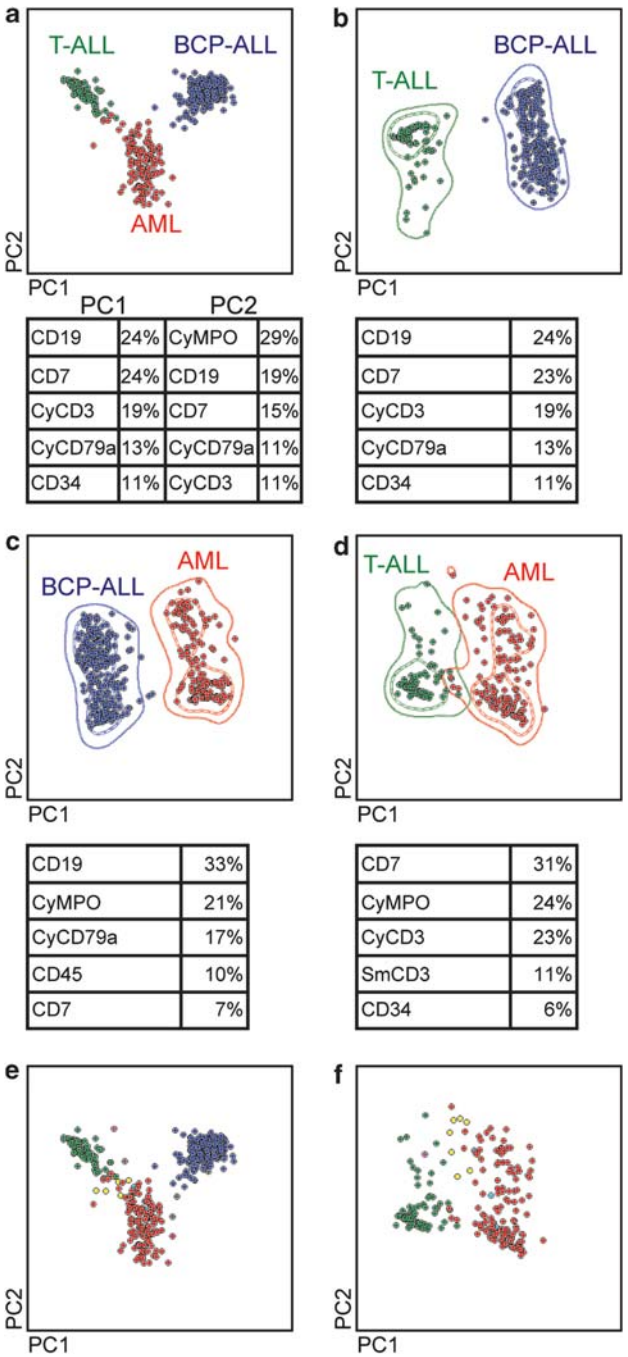

PC1		PC2	
CD19	24%	CyMPO	29%
CD7	24%	CD19	19%
CyCD3	19%	CD7	15%
CyCD79a	13%	CyCD79a	11%
CD34	11%	CyCD3	11%

CD19	24%
CD7	23%
CyCD3	19%
CyCD79a	13%
CD34	11%

CD19	33%
CyMPO	21%
CyCD79a	17%
CD45	10%
CD7	7%

CD7	31%
CyMPO	24%
CyCD3	23%
SmCD3	11%
CD34	6%

Conventional and multivariate analysis of acute leukemia samples

The ALOT configuration was fixed based on conventional analysis of an initial series of 158 acute leukemia samples (89 BCP-ALL,

Figure 4. Automated population separator (APS) results of the multicentric evaluation of the acute leukemia orientation tube (ALOT) in its final configuration ($n = 466$ acute leukemia patients). The orientation tube was applied routinely to any fresh acute leukemia sample in all eight EuroFlow laboratories. Results are shown as APS plots of the eight fluorescence parameters with exclusion of light scatter parameters—B-cell precursor (BCP)–acute lymphoblastic leukemia (ALL), blue circles; T-ALL, green circles; acute myeloid leukemia (AML), *orange circles*. (**a**) APS classification of the three well-defined entities; the principal component (PC)1-axis (horizontal) displays B- versus T-discrimination, while the PC2-axis (vertical) highlights lymphoid versus myeloid separation. (**b**–**d**) Pairwise APS analyses of the same well-defined acute leukemia samples. The PC1 axis (horizontal) highlights intergroup differences, while PC2 axis (vertical) displays intragroup heterogeneity. Classification is optimal between BCP-ALL and T-ALL and between BCP-ALL and AML, whereas some overlap is seen between T-ALL and AML, mainly reflecting the intrinsic biological proximity of certain cases ($n = 8/466$; 1.7%) of these diseases. (**e**, **f**) Overlay of unusual acute leukemia samples on the previously defined classification APS plots. Noteworthily, most of these mixed phenotype acute leukemia (MPAL), T + Myeloid (My), My + B and T + B cases map in between the two groups they belong to phenotypically, while acute undifferentiated leukemia (AUL) cases fall together with the non-lymphoid AML cluster. MPAL T + My, yellow; MPAL B + My, grey; MPAL B + T, brown; AUL, blue. Each individual circle represents a single case expressed as median fluorescence expression for all immunophenotypic parameters measured in the PC1 versus PC2 plot, and contour lines represent s.d. curves (dotted and continuous lines represent 1s.d. and 2s.d., respectively). The five most informative markers contributing to the best discrimination between each diagnostic group are displayed at the bottom of the corresponding APS plot, in a decreasing order of percentage contribution to the discrimination.

27 T-ALL, 37 AML and 5 AUL/MPAL). Testing of these 158 cases demonstrated a good correlation between the information provided by the ALOT and both in-house procedures and the final WHO diagnosis of the disease. Further confirmation of the ALOT efficiency was obtained when processing the data using PCA (Infinicyt software). For this purpose, each ALOT data file was computed to specifically extract the information relative to the blast cell population. All blast populations derived from the different patients were merged into a single data file and plotted together on an automated population separator (APS) view for automated separation by PCA.[16] Pairwise analysis of well-defined acute leukemia subgroups (BCP-ALL versus T-ALL versus AML) demonstrated excellent discrimination of each disease category, thus validating the approach (Figure 3). The dispersion observed within each reference group resulted mainly from the wide spectrum of CD34 expression in all acute leukemia subgroups.

The approved ALOT antibody combination was then prospectively applied to an independent cohort of 483 freshly collected acute leukemia cell samples (see Supplementary Table 1), mainly PB ($n=89$) and BM ($n=387$), but also some pleural effusions ($n=5$) and other body fluids ($n=2$) obtained from well-characterized patients at diagnosis: 259 BCP-ALL, 131 AML, 76 T-ALL and 17 AUL/MPAL patients. An additional set of 41 samples were analyzed, consisting of other hematological malignancies ($n=21$), such as diffuse large B-cell lymphoma (DLBCL), Burkitt lymphoma (BL), chronic mature B-cell lymphoproliferative disorders (B-CLPD) and MDS as well as reactive BM samples ($n=20$). Each ALOT data file contained information on 6000 blast cells per patient and was analyzed with the Infinicyt software, through direct PCA comparison with each pair of acute leukemia groups (BCP versus T-ALL, T-ALL versus AML and BCP-ALL versus AML), as described above.

Analysis of the 466 well-characterized BCP-ALL, T-ALL and AML cases, excluding AUL/MPAL samples ($n=17$), highlighted excellent discrimination of BCP-ALL from both AML and T-ALL (Figure 4). Conversely, T-ALL and AML groups showed a slight overlap. Of note, overlapping cases (8 out of 466; 1.7%) mostly corresponded to immature T-ALL that fit the criteria for the recently described Early T-cell Progenitor T-ALL[68–71] with unusually dim CyCD3 expression and immature CD34$^+$/CyMPO$^-$/CD7$^+$ AML (Figure 5). This overlap may be the consequence of both the biological nature of immature blast cells in some malignancies arrested at a stage of early T/Myeloid (My) development, and the high phenotypic heterogeneity of non-lymphoid acute leukemia cases. Consequently, the few cases falling into this area should optimally benefit from further evaluation with both the T-ALL and AML antibody panels for complete characterization. Acute leukemia of ambiguous lineage (17 out of 483; 3.5%) represented a heterogeneous category, which comprised AUL ($n=4$; 0.8%), MPAL with populations from two distinct lineages ($n=2$; 0.4%) and MPAL with mixed lineage cell populations, either T + My or B + My ($n=11$; 2.3%) (Figure 4). When analyzed in the multidimensional PCA view with supervision based on well-defined entities, MPAL from T + My lineages and also B + T cases clustered as expected in between T-ALL and AML and in between BCP and T-ALL clusters (Figure 4). By contrast, MPAL from B + My lineages appeared more heterogeneous, as two out of five patients clustered in between AML and BCP-ALL, whereas two other clustered together with BCP-ALLs, and one was close to T-ALL, owing to strong expression of CD7. Noteworthily, three out of four AUL cases fall together with non-lymphoid acute leukemia reference cases (Figure 4). These preliminary data suggest that multicenter collection of a large number of ambiguous lineage cases combined with multivariate comparison of harmonized results will be useful to significantly increase the number of these rare cases in order to delineate relevant individual clusters within the AUL/MPAL category that will pinpoint cases that require specific characterization. Until such an extensive database becomes available, cases with suggestive phenotypic criteria of belonging to AUL/MPAL groups according to the WHO classification should be analyzed with appropriate combinations of characterization panels (for example, T-ALL and AML/MDS antibody panels).

In order to further appreciate the value of each individual marker included in the ALOT the analyses were repeated leaving out each marker one by one. Results showed that most of the seven-antibody combinations led to decreased discrimination of the well-defined entities (Figure 6). For instance, exclusion of CD19 significantly impaired separation of BCP-ALL and AML

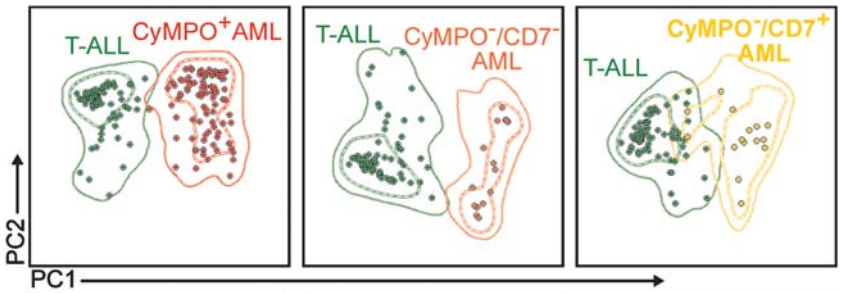

CD7	30%	CD7	35%	CD34	34%
CyMPO	26%	CyCD3	26%	CyCD3	27%
CyCD3	22%	CD34	20%	CD7	19%
CD34	10%	CyMPO	8%	SmCD3	8%
SmCD3	6%	SmCD3	7%	CyMPO	7%

Figure 5. Pairwise analysis of the T-acute lymphoblastic leukemia (ALL) and acute myeloid leukemia (AML) cases after AML subsetting based on CD7 and CyMPO expression. AML are known to harbor major phenotypic heterogeneity. Pairwise analysis of AML phenotypic subsets demonstrates that the overlap is mainly observed with CyMPO$^-$ CD7$^+$ AML cases and immature forms of T-ALL (T-ALL, green; CyMPO$^+$ AML, red; CyMPO$^-$/CD7$^-$ AML, orange; CyMPO$^-$/CD7$^+$ AML, yellow). Each individual circle represents a single case expressed as median fluorescence expression for all immunophenotypic parameters measured in the principal component (PC)1 versus PC2 plot, and contour lines represent s.d. curves (dotted and continuous lines represent 1s.d. and 2s.d., respectively). The five most informative markers contributing to the best discrimination between each entity group are displayed at the bottom of the corresponding automated population separator (APS) plot, in a decreasing order of percentage contribution to the discrimination.

entities, as expected, while not much affecting discrimination between the T-ALL and BCP-ALL groups. Comparable results were obtained for all markers left out, except for CD45 and SmCD3, whose exclusion had less impact on the quality of the separation of all the well-characterized acute leukemias. These markers contributed less to disease category discrimination but were not excluded from the combination and replaced by alternative markers because they were considered as essential for blast cell identification and gating, as well as for exclusion of residual non-malignant cells.

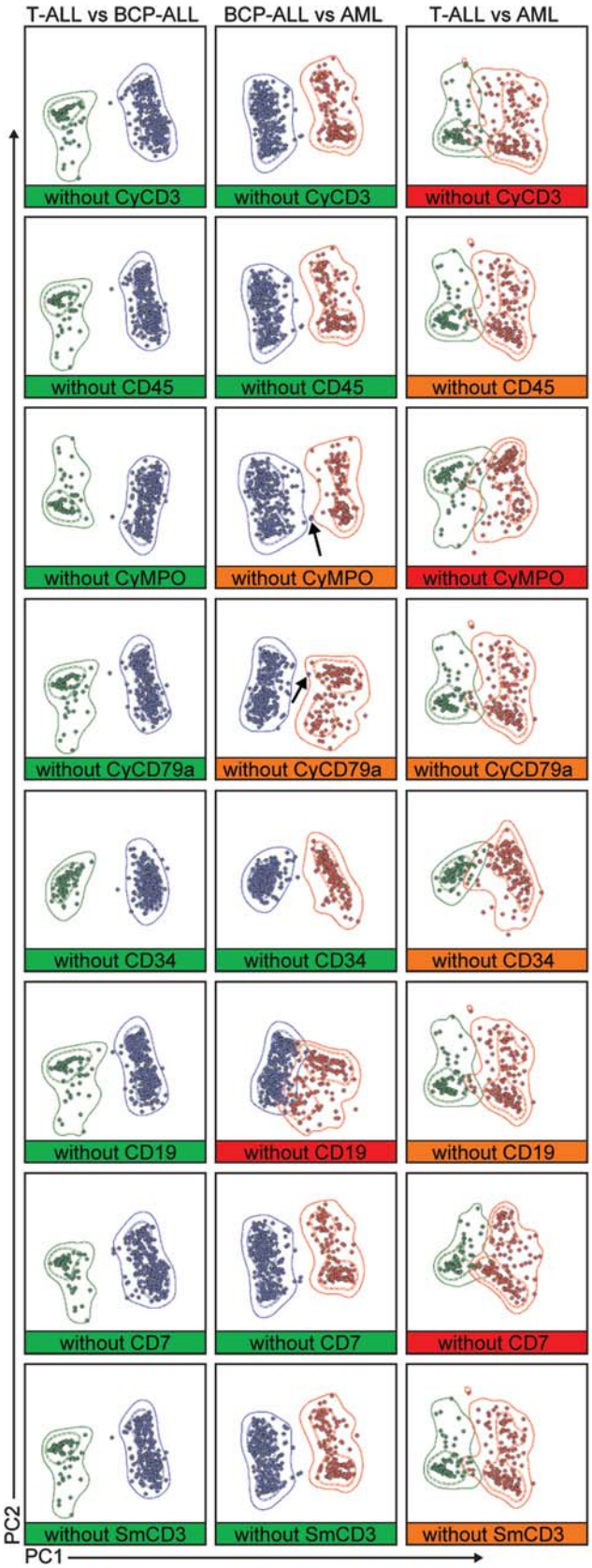

Finally, the non-acute leukemia samples ($n = 41$) were directed with the ALOT towards the expected panels for further investigation. For example, mature B cell disorders were assigned to a BCP-ALL panel, which allowed exclusion of BCP-ALL and orientation towards the appropriate B-CLPD panel. It should be noted that the ALOT alone using conventional or multivariate analyses did not allow direct re-orientation towards the mature B-CLPD panel as the $CD45^+/CyCD79a^+/CD19^+/CD34^-$ phenotype may correspond to both $CD34^-$ BCP-ALL or a mature B-cell malignancy, regardless of the level of CD45 expression.[72,73] The BCP-ALL panel, however, contains sufficient markers for re-orientation towards the mature B-CLPD panel, such as surface immunoglobulin (Ig) light and heavy chains as well as numerous maturation markers. As expected, non-AML myeloid neoplasias (for example, MDS) clustered with the AML group and were consequently oriented to be further analyzed with the AML/MDS panel.

CONCLUSION

Here we propose an extensively tested single tube with an 8-color combination of antibodies for fast and efficient orientation of acute leukemias towards a full BCP-ALL, T-ALL and/or AML characterization panel. An unprecedented orientation efficiency of 98.3% for non-ambiguous lineage cases was shown for the ALOT combination with a series of 483 newly diagnosed acute leukemia cases, tested prospectively at different centers. In addition, the combination of ALOT and the PCA-based data analysis facilitates standardized orientation to subsequent BCP-ALL, T-ALL and/or AML panel testing. However, the classification efficiency using APS remains to be assessed with an independent validation cohort. Interestingly, in a small fraction of cases an early T/My precursor acute leukemia phenotype is likely to be identified using multivariate analysis, which requires evaluation by more than one of the three acute leukemia multitube antibody panels. Phenotypic clustering of unusual MPAL/AUL cases will require collection of a vast number of acute leukemia cases in order to achieve relevant characterization. Altogether, the ALOT tube with an integrated analysis of only eight markers appeared to be an unprecedentedly strong tool for acute leukemia diagnosis.

Figure 6. Utility of each individual marker of the acute leukemia orientation tube (ALOT) for acute leukemia classification. Classification results using all possible seven-parameter combinations show the importance of the contribution of the eighth marker for disease category discrimination. The quality of separation between classical entities is demonstrated using a traffic-light code: optimal separation (>2s.d.), green; minimal overlap (1–2s.d.), orange; major overlap (<1s.d.), red. Automated population separator (APS) plots illustrate the corresponding pairwise comparisons (B cell precursor (BCP)–acute lymphoblastic leukemia (ALL) cases are plotted as blue circles; T-ALL as green circles; and acute myeloid leukemia (AML) as orange circles). Each individual circle represents a single case expressed as median fluorescence expression for all immunophenotypic parameters measured in the principal component (PC)1 versus PC2 plot, and contour lines represent s.d. curves (dotted and continuous lines represent 1s.d. and 2s.d., respectively).

SECTION 2. LYMPHOID SCREENING TUBE (LST)

J Flores-Montero[1], J Almeida[1], JJ Pérez[2], V Asnafi[3], L Lhermitte[3], MB Vidriales[2], S Böttcher[4], A Mendonça[5], P Lucio[5], D Tielemans[6], AW Langerak[6], M Lima[7], AH Santos[7], R de Tute[8], M Cullen[8], A Rawstron[8], JG te Marvelde[6], H Wind[6], VHJ van der Velden[6], L Sedek[9], T Szczepański[9], T Kalina[10], Q Lécrevisse[1], J Hernández[11], JJM van Dongen[6] and A Orfao[1]

[1]USAL, Salamanca, Spain; [2]HUS, Salamanca, Spain; [3]AP-HP, Paris, France; [4]UNIKIEL, Kiel, Germany; [5]IPOLFG, Lisbon, Portugal; [6]Erasmus MC, Rotterdam, The Netherlands; [7]Department of Hematology, Hospital de Santo António (HSA), Centro Hospitalar do Porto (CHP), Porto, Portugal; [8]UNIVLEEDS, Leeds, UK; [9]SUM, Zabrze, Poland; [10]DPH/O, Prague, Czech Republic and [11]Cytognos SL, Salamanca, Spain

BACKGROUND

Detection of phenotypically aberrant and clonal mature lymphocytes is the diagnostic hallmark of CLPD. Clonogenic events lead to the expansion and accumulation of mature-appearing lymphocytes, which carry a proliferative and/or survival advantage over their normal counterparts.[3,74,75] This translates into progressive accumulation of clonal cells and their products causing PB lymphocytosis, BM lymphoid infiltrates, enlargement of one or multiple other tissues (for example, lymphadenopathy, splenomegaly or other organomegalies), or emergence of a serum monoclonal component. Clinical manifestations and laboratory findings related to the increased number of lymphocytes initiate the diagnostic process (Figure 1).[18,25] In addition, functional impairment of tissues involved may also lead to other diagnostic information such as cytopenias, unexplained neurological symptoms or serous effusions. Such findings demand for assessment of the potentially clonal or neoplastic nature of the mature lymphoid cells in the various types of samples.[25,76] Identification of the abnormal lymphocytes and their discrimination from normal and reactive cells are key steps in establishing a final diagnosis. For decades now, flow cytometric immunophenotyping is an essential tool for the diagnostic screening of CLPD and for the specific identification and characterization of the expanded aberrant lymphocytes.[6] Over the years, refined approaches have been developed and technical improvements implemented, which have progressively increased the efficiency of the diagnostic screening of CLPD in clinical and laboratory settings.[17,20]

Identification of aberrant lymphocytes currently not only relies on their absolute or relative numerical distribution among all lymphocytes (or their subpopulations) present in the sample, but also mainly searches for more specific 'abnormal' immunophenotypic profiles. These aberrant phenotypes can clearly be distinguished from normal and reactive patterns in the multidimensional space generated by unique combinations of fluorochrome-conjugated antibodies.[17,18,77–81]

At present, different screening protocols, antibody panels and immunophenotypic strategies are used in individual laboratories for the diagnostic screening of CLPD. Overall, it is well established that in a diagnostic screening step the informative markers have to be combined whenever possible in a single antibody combination that can easily and rapidly be evaluated. The EuroFlow group has designed and evaluated an 8-color, 12-marker combination of antibodies aiming at the detection of phenotypically aberrant populations of mature B-, T- and NK-cells in PB, BM, lymph nodes (LN) and other types of body tissues and fluids, which can be used in the diagnostic screening of CLPD. The use of multiple markers conjugated with the same fluorochrome has previously been shown to be highly efficient in this regard.[17] The antibody combination in this so-called lymphoid screening tube (LST) can guide the need for further immunophenotyping with appropriate antibody panel(s) for accurate diagnosis and classification of lymphoid malignancies, through the EuroFlow panels for B-CLPD (Section 8), T-CLPD (Section 9), and NK-CLPD (Section 10).

Selection of antibodies for the LST

The selection of antibodies for the LST aimed at dissecting lymphoid cells into their major subsets with a set of reagents that can simultaneously define aberrant and clonal phenotypes. Initially CD45 was selected for the definition of the compartments of mature versus immature lymphocytes, CD3 for the identification of T-cells, and both CD19 and CD20 for the selection of B-cells; these two later markers combined with CD45 would allow subsetting of B-cells into mature B-lymphocytes ($CD19^+$, $CD20^{hi}$ and $CD45^{hi}$) and B-cell precursors ($CD19^+$, $CD20^{-/lo}$, $CD45^{lo}$). NK-cells should fulfill the criteria for mature lymphocytes ($CD45^{hi}$, SSC^{lo}) in the absence of CD19 and SmCD3 expression and they would typically show reactivity for CD56. Additional markers selected for further subsetting of B, T and NK-cells included (i) SmIgκ and SmIgλ, (ii) CD4, CD8 and CD56 and (iii) CD56 and CD8, respectively. These antibody reagents were arranged into a first version of an 8-color LST (Table 3). Additional markers were incorporated later in the LST, as described below.

Design and construction of the LST

The proposed LST resulted from a seven-round process of design–evaluation–redesign of successive LST versions (Table 3). Each LST version was evaluated in a large but variable number of normal, reactive and neoplastic patient samples obtained at diagnosis, as well as at other disease time-points (for example follow-up or relapse) in parallel to the routine approaches applied for the same purpose in each participating center (6 EuroFlow centers).

Version 1 of the LST (Table 3) proved to be a robust combination that allowed identification of the major populations of normal B-, T- and NK lymphocytes and their dissection into up to 13 normal lymphoid subsets: (1) $SmIg\kappa^+$ and $SmIg\lambda^+$ mature B-cells, plus B-cell precursors; (2) $CD4^+$, $CD8^{hi}$, $CD4^+/CD8^{lo}$ and $CD4^-/CD8^{-/lo}$ T-lymphocytes (further divided according to CD56 expression into (i) $CD4^+/CD56^-$ and $CD4^+/CD56^+$; (ii) $CD8^{hi}/CD56^-$ and $CD8^{hi}/CD56^+$; (iii) $CD4^+/CD8^{lo}/CD56^-$ and $CD4^+/CD8^{lo}/CD56^+$; and (iv) $CD4^-/CD8^{-/lo}/CD56^-$ and $CD4^-/CD8^{-/lo}/CD56^+$ T-cells, respectively) and both $CD56^+/CD8^{-/lo}$ and $CD56^{hi}/CD8^{-/lo}$ NK-cells.

Preliminary evaluation of version 1 of the LST showed comparable results with the local approaches for the identification of the aberrant or clonal populations of mature lymphocytes ($n = 9/9$). However, this LST version also showed some unwanted features. First, some antibody conjugates performed below the expectations, for example, CD19-AmCyan and CD3-APC Cyanin7 (Cy7) showed suboptimal performance (low resolution) for positive identification of the B- and T-cell populations (data not shown). Second, the relatively high degree of overlap observed between the PE and PerCPCy5.5 fluorochrome conjugates pointed out the need for a more careful selection of the markers included at these two fluorochrome positions. Finally, inclusion of CD38 was proposed to provide complementary information about the normal versus abnormal populations of lymphocytes, to increase the accuracy in discriminating B-cell precursors, particularly in BM samples, and to evaluate additional subsets of B-cells (for example, plasma cells).

The reagents selected to solve these issues were included in version 2 of the LST, evaluated in 29 samples (Table 3). New CD19 and CD20 conjugates were selected and subsequently incorporated in the LST owing to poor resolution of CD19 – PerCPCy5.5 and CD20 – APC, which were replaced in version 3 by CD19 – PECy7 and CD20 – PacB. In version 4, CD38 – AF700 was replaced by a custom-made CD38 – APCH7 conjugate (Table 3). These fluorochrome replacements resulted in a better discrimination between the different populations of normal lymphoid cells. With this version only CD45 – AmCyan showed suboptimal performance owing to relatively high fluorescence spillover into the FITC channel. Additionally, inclusion of an anti-TCRγδ antibody was proposed for version 5 of the LST (Table 3). This 'matured' LST

Table 3. Design of LST in seven consecutive rounds[a]

Version (no. of cases)[b]	*Fluorochromes and markers*							
	PacB	*AmCyan*	*FITC*	*PE*	*PerCPCy5.5*	*PECy7*	*APC*	*APCCy7*
1 ($n=9$)	CD45	CD19	SmIgλ	SmIgκ	CD8	CD56	CD4 and CD20	SmCD3
	PacB	*AmCyan*	*FITC*	*PE*	*PerCPCy5.5*	*PECy7*	*APC*	*AF700*
2 ($n=29$)	SmCD3	CD45	CD8 and SmIgλ	CD56 and SmIgκ	CD19	CD4	CD20	CD38
3 ($n=97$)	CD20	CD45	CD8 and SmIgλ	CD56 and SmIgκ	CD4	CD19	SmCD3	CD38
	PacB	*AmCyan*	*FITC*	*PE*	*PerCPCy5.5*	*PECy7*	*APC*	*APCH7*
4 ($n=26$)	CD20	CD45	CD8 and SmIgλ	CD56 and SmIgκ	CD4	CD19	SmCD3	CD38
5 ($n=19$)	CD20	CD45	CD8 and SmIgλ	CD56 and SmIgκ	CD4	CD19 and TCRγδ	SmCD3	CD38
	PacB	*PacO*	*FITC*	*PE*	*PerCPCy5.5*	*PECy7*	*APC*	*APCH7*
6[c,d] ($n=12$)	CD4 and CD20	CD45	CD8 and SmIgλ	CD56 and SmIgκ	CD5	CD19 and TCRγδ	CD10	SmCD3
7 (Final) ($n=271$)	CD4 and CD20	CD45	CD8 and SmIgλ	CD56 and SmIgκ	CD5	CD19 and TCRγδ	SmCD3	CD38

Abbreviations: AF700, alexa fluor 700; AmCyan, *Anemonia Majano* cyan fluorescent protein; APC, allophycocyanin; BM, bone marrow; Cy7, cyanin7; FITC, fluorescein isothiocyanate; FNA, fine needle aspirate; H7, hilite7; LNB, lymph node biopsy; PacB, pacific blue; PacO, pacific orange; PB, peripheral blood; PB-MNC, PB mononuclear cells; PE, phycoerythrin; PerCPCy5.5, peridinin–chlorophyll–protein–cyanin5.5; Sm, surface membrane. [a]Further information about markers and hybridomas is provided in the Appendix. [b]A total of 463 samples (292 PB, 13 PB-MNC, 127 BM, 20 LNB, 8 FNA, 3 other types of samples) was evaluated. Among them, 384 abnormal lymphoid populations were detected: 266 B (1 showed an immature B-cell phenotype), 95 T, 23 NK. No abnormal lymphoid population could be detected in 90 cases (healthy donors and non-infiltrated samples). [c]Samples included for evaluation of this version were stained in parallel with version 5. [d]One center tested this combination in an additional group of 1285 cases. Results were always concordant with local routine diagnostics. Single cases might include more than one abnormal population. One sample showed abnormal lymphoplasmocytoid cells and four cases displayed abnormal plasma cell populations. Highlighted boxes: changes as compared to previous version.

combination (version 5; Table 3) was further fine-tuned by replacing CD45 − AmCyan by CD45 − PacO and including CD5 as a consequence of the direct comparison performed between versions 5 and 6 of the LST. As a result, a final configuration (Table 3) was proposed with two options where either CD10 (version 6) or CD38 (version 7) were alternatively used. Addition of CD10 was proposed for achieving a more B-cell-oriented approach in laboratories in which B-CLPD represent the major fraction of the screened samples.

In summary, major modifications introduced after the evaluation of each version of the LST (versions 1–7) aimed at (i) inclusion of markers that could improve the characterization of the lymphoid cell populations (for example, CD38), (ii) increasing the number of lymphocyte populations and subsets that could be identified (for example, positive discrimination of plasma cells with CD38 or discrimination of TCRγδ$^+$ from other CD8$^{-/lo}$ T-cells with the anti-TCRγδ antibody) and/or (iii) providing a more sensitive and/or robust orientation on subsequent analyses, when lymphocyte populations with aberrant or clonal phenotypes had been detected (for example, CD5 and CD38 in B- and/or T-cell CLPD). Further description of the utility of each marker included in the final version is shown in Table 4. In addition, redistribution of informative markers into other fluorescence channels and substitution of specific fluorochromes showed improved performance.[16] These fluorochrome changes also aimed at keeping compatibility with other EuroFlow panels designed in parallel, for example, markers and conjugates used as backbone markers for the B-CLPD panel were kept in the LST at the same fluorochrome positions (see Section 8).

As already mentioned above, in some fluorescence channels two different markers were placed to overcome the limited number of fluorescence detectors with respect to the number of antibody reagents required. Of note, each pair of markers placed in the same fluorescence channel was arranged in such a way that their expression is typically restricted to different (normal or abnormal) cell populations that could be positively identified and selected using other markers present in the LST. Based on this strategy, any potential misinterpretation of their differential reactivity in normal and neoplastic lymphoid cells can be avoided, if all major and minor phenotypes of normal lymphocytes are identified (for example, CD20^{lo} cytotoxic T-cells). [82]

Evaluation of the LST, version 6

Version 6 of the LST was designed to address the potential need for a more B-cell-oriented approach in some laboratories by including slight modifications with respect to version 5. These modifications aimed at increasing the sensitivity of the combination using relevant markers for B-cell subsetting in combination with SmIgκ and SmIgλ. Inclusion of CD5 and CD10 in version 6 (versus version 5) was considered appropriate because of the kinetics of expression of the two markers during normal maturation and their association with specific B-CLPD entities;[74] CD38 was taken out to leave room for these markers. Version 6 of the LST was extensively evaluated for the screening of abnormal lymphoid cells at one center in a total of 1285 samples of which 504 harbored one or two aberrant or clonal B-cell populations. Of the 504 infiltrated samples, 19 (5%) demonstrated a double clonal B-cell population, one of which was CD10$^+$ (Figure 7), and 5 cases (1%) had a minor CD10$^+$ clonal B-cell population (SmIg light-chain-restricted expression). Without CD10, 5 of these 24 cases would not have been detected at the initial screening step (5/1285; 0.4%). Version 6 of the LST was also evaluated against version 5 by the USAL group in 12 additional samples (7 PB and 5 BM). In this evaluation, both LST versions showed infiltration in 4/12 samples (2 abnormal B- and 2 abnormal T-cell populations). Overall, it was concluded that the combined usage of CD5 and CD10 in version 6 might result in a higher sensitivity for detection of small CD10$^+$ B-cell clones, especially when minor clones composed of a mixture of phenotypically (CD5$^+$ and/or CD10$^+$)

Table 4. Utility of LST markers for identification of lymphoid cells in patients with CLPD

Marker	*Main normal population(s) identified*[a]	*Positive diagnosis*	*Population subsetting*	*Diagnostic subclassification*	*Potential minimal disease value*	*Prognostic relevance*
CD45	Mature lymphocytes and B-cell precursors	X	X			
CD19	B-cells, T- and NK-cells by exclusion	X		X	X	
CD20	B-cells, T- and NK-cells by exclusion	X	X	X	X	
SmIgλ and κ	SmIg^{+} B-cells	X	X		X	
CD38	Plasma cells and B-cell precursors	X	X	X	X	X
SmCD3	T-cells, B- and NK-cells by exclusion	X		X	X	
CD4	CD4^{+} T-cells	X	X	X	X	
CD8	CD8^{hi} T-cells and CD8^{lo} NK-cells	X	X	X	X	
CD56	NK-cells	X	X		X	
TCRγδ	TCRγδ^{+} T-cells	X	X		X	
CD5	T-cells	X		X	X	

Abbreviations: CLPD, chronic lymphoproliferative disorders; LST, lymphoid screening tube; Sm, surface membrane. [a]Some markers may be aberrantly expressed in other abnormal lymphoid populations.

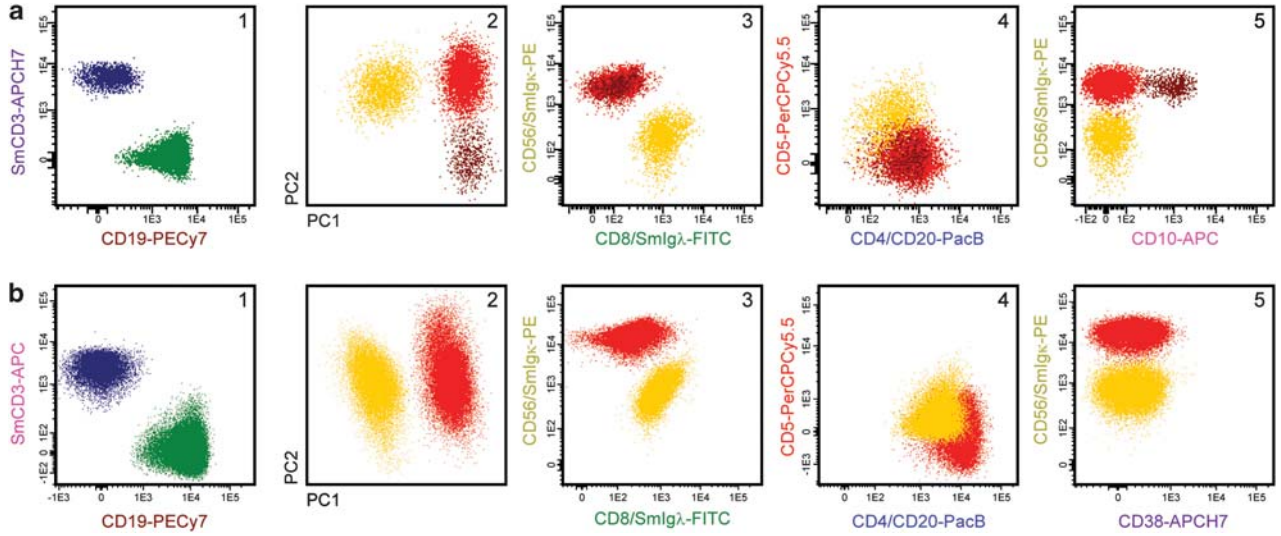

Figure 7. Evaluation of the performance of versions 6 (**a**) and 7 (**b**) of the lymphoid screening tube (LST). Illustrating example of a peripheral blood sample stained with LST version 6 and LST version 7. (**a.1**, **b.1**) Show the presence of a numerically increased B-cell population (46.7% and 50.1%, respectively) (green dots). Principal component analysis (PCA) of the B-cells evidenced the presence of up to three different B-cell populations (**a.2**) with version 6 of the LST tube, while with version 7 only two populations could be discriminated (**b.2**). Conventional bivariate dot plot analysis showed that the two major B-cell populations (red and yellow dots) corresponded to two different B-cell clones displaying distinct surface membrane immunoglobulin (SmIg) light-chain phenotypes: SmIgκ^{+}/SmIgλ^{-}/CD20^{hi}/CD5^{-} (red dots; 32.8% and 33.5% in **a** and **b**, respectively) and SmIgκ^{-}/SmIgλ^{+}/CD20^{+}/CD5^{lo} (yellow dots; 13.9% and 16.6% in **a** and **b**, respectively). Both B-cell populations were clearly detected with the two LST versions (**a.3, a.4** and **b.3**, **b.4**). Further phenotypic characterization of these two B-cell populations evidenced the presence of a minor CD10^{+} B-cell (sub)population (brown dots) within the SmIgκ-restricted B-cells (3.94% of all B-cells; **a.5**). In this case, CD38 expression (**b.5**) added no further information; however, it should be noted that the abnormal phenotypic profile of the two major B-cell clones granted their further immunophenotypic characterization by the application of the B-CLPD panel, which finally evidenced the CD10^{+}/SmIgκ^{+} restricted (sub)population.

distinguishable B-cell populations coexist and sample availability for further stainings is limited, hampering full immunophenotypic characterization with the B-CLPD panel.

Evaluation of the LST, version 7

The aim of the LST was to detect any mature lymphoid malignancy in a diagnostic screening phase. In line with this aim, CD5 has added value for the immunophenotypic evaluation of T- and NK-cells. CD10 may contribute to the screening of T-cell malignancies, particularly for the detection of CD4^{+}/CD10^{+} cells in the diagnosis of some cases of angioimmunoblastic lymphoma, but such lymphomas more frequently show other phenotypic aberrancies such as coexistence of a CD4^{hi}/SmCD3$^{-/lo}$ T-cell phenotype.[83] In turn, CD38 would further allow positive identification of plasma cells and it provides valuable information when evaluating a wide range of lymphoid malignancies including large cell lymphomas with *MYC* translocations (for example, BL and transformed DLBCL), follicular lymphoma, plasmablastic lymphoma, plasma cell disorders (PCD) and other B-CLPD with plasmacytoid differentiation.[3] Consequently, versions 5 and 6 were merged

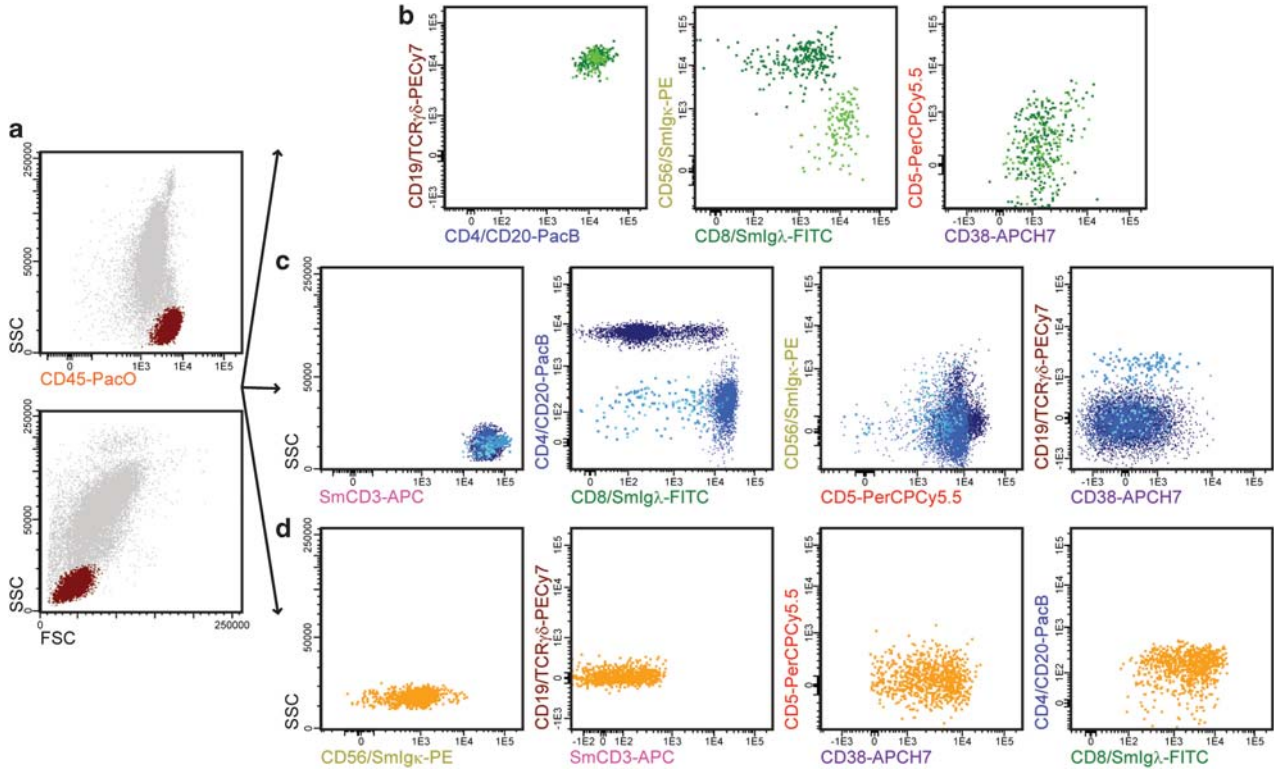

Figure 8. Illustrative example of the immunophenotypic profile of the lymphocyte populations present in normal peripheral blood stained with the lymphoid screening tube (LST) (version 7). (**a**) Typical profile of mature lymphocytes (brown dots) for light scatter parameters and CD45. (**b**) Phenotype of normal mature B-cells for the B-cell-associated markers in the LST combination with a normal distribution according to surface membrane (Sm) light-chain expression (SmIgκ^+ B-cells are painted as dark green dots and SmIgλ^+ B-lymphocytes as light green dots). (**c**) The phenotypic features of normal mature T-cells as defined by the expression of relevant markers in the combination ($CD4^+$ T-cells: dark blue dots; $CD8^{hi}$ T-cells: blue dots; $CD4^-/CD8^{-/lo}/TCR\gamma\delta^-$ T-cells: light blue dots; and $CD4^-/CD8^{-/lo}/TCR\gamma\delta^+$ T-cells: cyan dots). (**d**) Phenotypic pattern of normal peripheral blood NK-cells (yellow dots) for SSC, CD56, CD19/TCRγδ, SmCD3, CD38, CD5, CD8 and CD20/CD4 with version 7 of the LST.

into a final LST version, which incorporated CD5 and CD38 but not CD10 (Table 3): version 7 of the LST.

In a final stage, version 7 of the LST underwent evaluation in all participating EuroFlow centers and included 271 samples (175 PB, 75 BM, 14 LN biopsies, 5 LN FNA, 1 pleural fluid and 1 ascitic fluid). In 228/271 samples (84%) an aberrant lymphoid population was detected with a median percentage of infiltration of 31% of the total number of leukocytes (range: 0.04 – 98%). A 100% concordance was obtained when compared with routine approaches in each participating center, with sensitivity down to 0.1% for detection of small aberrant lymphoid cell populations.

In summary, version 7 enabled a complete phenotypic evaluation of all relevant mature lymphoid compartments in samples most frequently used to screen for mature lymphoid malignancies such as PB, BM and LN tissues. Version 7 includes markers that identify and quantify the populations of interest, allows their detailed subsetting and also detects the most frequent phenotypically aberrant patterns for the markers included. Additionally, version 7 showed an optimal efficiency in guiding the selection of complementary antibody panels for a more complete immunophenotypic characterization of any abnormal lymphoid population present in the sample, at frequencies $\geqslant$0.1%. Finally, usage of CD45, CD19 and CD20 in common to the B-CLPD panel and careful avoidance of redundant stainings further facilitates full integration of the LST as tube 1 of the B-CLPD panel (see Section 8) (Figure 1).

Multivariate analysis of normal lymphocyte cell populations

All samples that were obtained from normal healthy donors ($n = 22$, 19 PB and 3 BM; mean age: 36 ± 14 years, 9 males and 13 females) were analyzed using conventional approaches for the identification of all major normal lymphoid populations contained in them, such as B- (SmIgκ^+, SmIgλ^+); T- ($CD4^+$, $CD8^{hi}$, $CD4^+/CD8^{lo}$, $CD4^-/CD8^{-/lo}/TCR\gamma\delta^-$ and $CD4^-/CD8^{-/lo}/TCR\gamma\delta^+$) and NK-cells (in addition to the positive identification of plasma cell) for a total of 10^5 cells measured per sample (Figure 8). Among the normal PB samples ($n = 19$), lymphoid populations were distributed as follows—mean (range): total lymphocytes, 23.9% (11–42.2%); T-cells, 19.1% (8.2–36%); $CD4^+$ T-cells, 10.1% (4.1–18%); $CD8^{hi}$ T-cells, 7.3% (2.3–17.2%); $CD4^-/CD8^{-/lo}/TCR\gamma\delta^-$, 0.4% (0.1–1%); $CD4^-/CD8^{-/lo}/TCR\gamma\delta^+$, 1% (0.01–3.1%); B-cells, 2.2% (0.4–5%); SmIgκ^+ B-cells, 1.3% (0.2–3.2%); SmIgλ^+ B-cells, 0.9% (0.2–2.4%); κ/λ ratio, 1.5 (1.1–2.2); total NK-cells, 2.6% (1.3–5.7%); and plasma cells: 0.06% (0.01–0.45%).

Afterwards, the lymphoid cell populations from the different normal PB samples were gated and data stored in a separate data file for each population.[32] Subsequently, the data files were merged to create a pool of normal reference cells for each of the above-listed cell populations. PCA showed that when individually considered, all normal lymphocyte populations clustered together in the APS (principal component (PC)1 versus PC2) view of the Infinicyt software according to their normal phenotypic profile in the 10-dimensional space generated by the light scatter and fluorescence emissions measured with the LST (Figure 9).

Multivariate analysis of suspicious lymphoid populations

Once the normal B-, T-$CD4^+$, T-$CD8^+$ and NK-cell reference databases were constructed, multiparametric comparison of each corresponding B-, T- and NK-cell population from each individual sample suspected of carrying a CLPD ($n = 249$) versus the normal

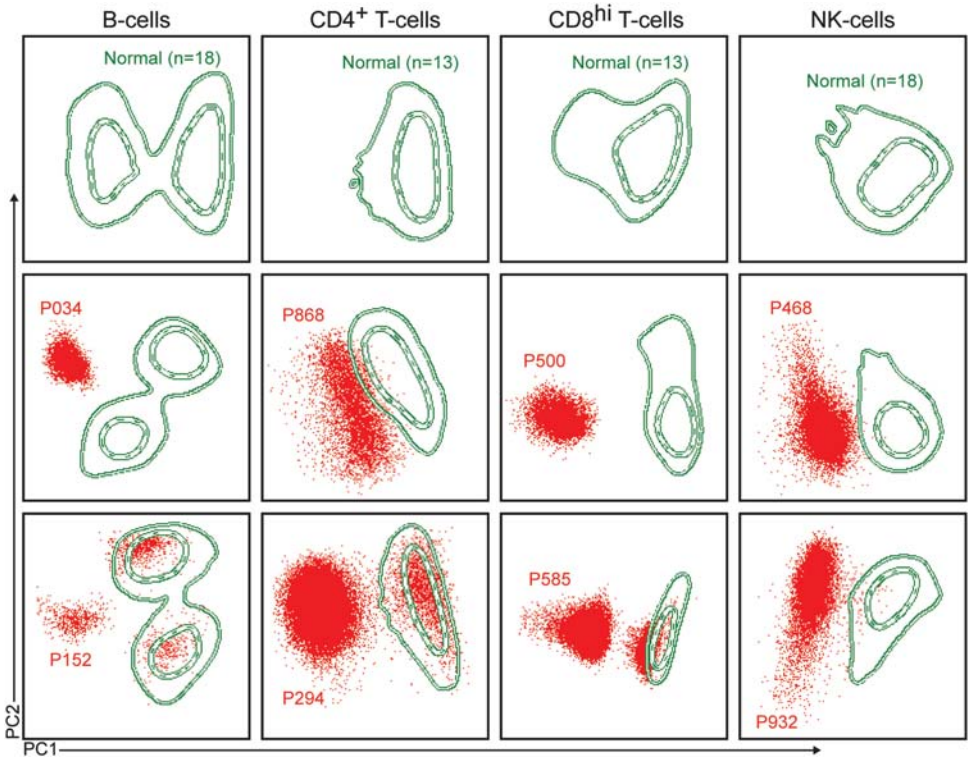

Figure 9. Illustrative automated population separator (APS)—principal component (PC)1 versus PC2 views of B-, CD4$^+$T-, CD8^{hi} T- and NK-cells, defined by their immunophenotypic profile obtained with the markers included in the lymphoid screening tube (LST) (version 7). As illustrated, normal B-, CD4$^+$ T-, CD8^{hi} T- and NK-cells from different samples clustered together on either single or bimodal distribution (green lines in the upper row). In this row, the bimodal distribution of normal B-cells reflects the differential expression of surface membrane immunoglobulin (SmIg) κ versus λ light chains. The middle row illustrates examples of cases (red dots) in which all cells within the leukemic cell population were phenotypically aberrant and clearly separated from the corresponding pool of normal B-, T CD4$^+$, T CD8^{hi} and NK-cells, respectively (green lines). In the lower row, examples of cases in which variable numbers of normal and aberrant or clonal lymphoid cells (both depicted as red dots) coexist in the same sample are shown. Note that part of the red dots in the lower row corresponding to normal cells tend to fall within the normal reference pool (cluster of red dots inside the green lines) resembling their distribution, while clonal/aberrant cells (cluster of red dots outside the green lines) are clearly separated from the normal cell cluster. Contour green lines represent s.d. curves (dotted and continuous lines represent 1s.d. and 2s.d., respectively from normal B-, T- or NK-cell phenotypes).

reference pool was performed using the APS tool (Infinicyt software). Overall, our results showed an overlap for most cell populations present in every sample with their corresponding pool of normal reference cells. However, 149/150 aberrant B-cell populations were also detected (99.4%) in samples showing the presence of clonal B-CLPD populations. In one case, the phenotypic profile of the neoplastic B-cells overlapped with that of normal B-cells and their presence could only be confirmed when light-chain-restricted B-cell subsets were evaluated because of an altered SmIgκ/SmIgλ B-cell ratio.

Similarly, aberrant T-cell populations were detected in 61/65 T-CLPD (94%). In detail, phenotypically abnormal CD4$^+$/CD8$^{-/lo}$ T-cells were identified in 33/36 cases with CD4$^+$/CD8$^{-/lo}$ T-CLPD infiltrated samples; in the other three samples in which CD4$^+$/CD8$^{-/lo}$ clonal T-cells could not be easily discriminated from normal cells based on their phenotype, an abnormally increased number of CD4$^+$ T-cells was found (CD4$^+$ T-cells represented 99.2 and 19.6% of the total number of lymphocytes in two PB samples and 85.1% of the total number of lymphocytes in a LN biopsy sample), which should also lead to further evaluation of CD4$^+$ T-cells with the T-CLPD EuroFlow panel (Section 9). In addition, aberrant CD8^{hi}/CD4$^-$ T-cells were clearly found outside the normal CD8^{hi} T-cell cluster in 13/14 cases (93%) with monoclonal expansions; the other case showed abnormally high CD8$^+$ T-cell numbers. Finally, abnormal populations of CD4$^-$/CD8$^{-/lo}$/TCRγδ$^-$ T-cells ($n=3$), CD4$^-$/CD8$^{-/lo}$/TCRγδ$^+$ T-cells ($n=11$) and CD4$^+$/CD8$^+$ T-cells ($n=1$) were detected in all cases carrying neoplastic infiltration by these typically minor T-cell populations.

Regarding NK-cells, abnormal populations could be clearly discriminated from normal NK-cell phenotypes in 17/18 cases with NK large granular lymphocytic (LGL) leukemia. In the remaining sample, the altered NK-cell population showed only partial overlap with the normal NK-cell phenotype; such phenotypic differences also required further evaluation.

In summary, the LST detected aberrant B-, T- or NK-cell immunophenotypes in 149/150 (99.4%) of B-CLPD and in 78/83 (94%) of T/NK-CLPD, with an overall frequency of 97.4%. The remaining six cases displayed either partially aberrant phenotypes ($n=1$) or increased numbers of the suspicious lymphoid population, all of which would lead to further confirmatory phenotypic evaluation.

CONCLUSION

In this section a single 8-color LST was designed, evaluated, redefined and re-evaluated for a total of seven sequentially improved versions. The proposed final EuroFlow LST version (version 7) showed 100% concordance with routine approaches. Furthermore, our results confirm the utility of the proposed LST combination to discriminate between normal and abnormal lymphoid cells, based on the detection of aberrant immunophenotypic characteristics in the LST combination in virtually all abnormal B-cell populations (>99%) and most (⩾94%) LGL

NK-cells and CLPD T-cells, with an overall efficiency of 97.4% (sensitivity of down to 10^{-3}). In the other few CLPD cases ($n = 6$; 2.6%), a typically altered numerical distribution would also require further confirmatory testing.

SECTION 3. SMALL SAMPLE TUBE (SST)

AW Langerak[1], L Martin-Martin[2], J Almeida[2], J Flores-Montero[2], M Cullen[3], E Mejstrikova[4], D Tielemans[1], J Vermeulen[1], HK Wind[1], VHJ van der Velden[1], A Orfao[2] and JJM van Dongen[1]

[1]Erasmus MC, Rotterdam, The Netherlands; [2]USAL, Salamanca, Spain; [3]UNIVLEEDS, Leeds, UK and [4]DPH/O, Prague, Czech Republic

BACKGROUND

Central nervous system (CNS) localization is a relatively rare complication of a systemic non-Hodgkin lymphoma, although the exact frequency varies per histological subtype (from $<5\%$ in low-grade B-cell lymphomas to $\sim 20\%$ in aggressive B-cell lymphomas).[84–89] CNS localization of lymphoma is associated with an unfavorable outcome.[90] In turn, some patients present with neurological symptoms that could be compatible with a CNS lymphoma, but without evidence for lymphoma elsewhere in the body. Primary CNS lymphoma (PCNSL) is even less frequent than secondary CNS localization of a systemic lymphoma, but has a similar poor clinical course.

Intra-ocular lymphomas (IOL) can present as a primary event in the eye (PIOL), or as a clinical manifestation in parallel to or following CNS lymphoma (reviewed by Chan[91] and Coupland[92]). The majority (60–85%) of PIOL patients develop CNS lymphoma within 2–2.5 years after initial diagnosis.[92] The two types of lymphomas thus form a spectrum of the same disease termed oculo-cerebral lymphomas (PIOL/PCNSL). IOL can also present as secondary localizations of a systemic lymphoma (secondary IOL). PIOL are estimated to account for up to 1–2% of all extranodal lymphomas.[92] PIOL are mostly of the B-cell type (DLBCL), whereas T-cell type IOL are often associated with cutaneous T-cell lymphomas or other systemic T-cell lymphoma.[92] Over the last two decades an increase in PCNSL, and potentially also PIOL, has been seen in immunocompromised individuals. PIOL occur in adult individuals (average age 50–60 years) and typically present as chronic, often refractory, uveitis or vitritis, the so-called masquerade syndrome.[91,92] This masquerade syndrome is the reason for a considerable delay (8–21 months) in establishing a correct diagnosis.[92]

In the diagnostic process of patients with neurological and/or ophthalmologic symptoms that could be indicative of CNS lymphoma or IOL, lumbar puncture and vitrectomy are performed to obtain CSF and vitreous biopsy material, respectively. In contrast to most other materials, CSF and vitreous biopsies pose difficulties to the diagnostic process owing to the fact that both types of samples almost systematically present with low cell numbers. In such pauci-cellular or 'small' samples it is of utmost importance to obtain maximal information from minimal numbers of cells. Traditionally, cytomorphology has been the gold standard technique for the detection of malignant leukocytes in both CSF and vitreous material for diagnostic purposes.[93,94] Even though positivity can be highly specific for a CNS lymphoma or IOL diagnosis, the risk of false-negativity in cytomorphology is high.[87,88,95] This is related to the poor cell viability in these materials, as well as the often troublesome discrimination between benign and malignant cells on top of the low cell numbers.[87,96,97] Other studies exploit Ig and/or TCR gene analysis,[91,98,99] but the pitfall of coincidental, non-reproducible, amplification in case of small cell numbers (pseudoclonality) has to be considered.

Multiparameter flow cytometric immunophenotyping combines high specificity with good clinical sensitivity. Several studies indeed underline the importance of multiparameter flow cytometric immunophenotyping for efficient and reliable diagnosis versus exclusion of CNS lymphoma or IOL localizations.[87–90,100–105] For CSF analysis multiple 3-, 4-, 6- or even 8-color single-tube screening panels and protocols have been described (see Kraan *et al.*[106] for an extensive review and description of labelings and methods). In this section we discuss the design and evaluation of the 8-color EuroFlow SST and related sample preparation protocols aimed to evaluate CSF and vitreous biopsy samples, in patients suspected of lymphoma.

Design of the EuroFlow small sample screening tube

The EuroFlow group designed an 8-color flow cytometric labeling aimed at screening for lymphoma in 'small samples' from CSF and vitreous material obtained from suspected cases. As the SST should enable optimal detection and identification of all possible cell types in pauci-cellular materials, a series of antibodies had to be included in a single tube. Thus, the markers that were selected included the pan-leukocyte marker CD45, as well as markers for positive identification of mature B-cells (CD19, CD20) and their SmIg light chain subsets (anti-SmIgκ, anti-SmIgλ), and both T-cells and NK cells (SmCD3, CD4, CD8, CD56). Additional markers like CD14 (monocytes) and CD38 (plasma cells) were selected to identify all possible cell types in a more complete way. To accommodate all these markers in one tube, at three different fluorochrome positions two antibodies were selected that appear on different cell types in a mutually exclusive manner: (a) CD8 and SmIgλ expressed by T- and B-cells, respectively, (b) CD56 and SmIgκ present on T/NK- and B-cells, respectively, and (c) SmCD3 and CD14 markers specific for T-cells and monocytes/macrophages, respectively (Table 5). In this way a single 8-color/11-antibody tube was developed that allows complete typing of all relevant cell types in small samples. In combination with the forward and side scatter (FSC, SSC, respectively) features, 13 parameters are available to characterize cells present in CSF and vitreous biopsy. Through appropriate gating strategies, SmIgκ and SmIgλ positivity can be evaluated within the $CD19^+$ B-cell fraction, and CD4 and CD8 reactivity within the $SmCD3^+$ T-cell fraction, as also described above in Section 2 for the LST (see also Figure 10 for an illustration of the gating strategy). For most positions, the fluorochrome-conjugated antibodies from the LST were selected. In addition, CD14 was placed in combination with

Table 5. Composition of SST for detection of lymphoid cells[a]

Fluorochromes and markers							
PacB	*PacO*	*FITC*	*PE*	*PerCPCy5.5*	*PECy7*	*APC*	*APCH7*
CD20	CD45	CD8 and SmIgλ	CD56 and SmIgκ	CD4	CD19	SmCD3 and CD14	CD38

Abbreviations: APC, allophycocyanin; Cy7, cyanin7; FITC, fluorescein isothiocyanate; H7, hilite7; PacB, pacific blue; PacO, pacific orange; PE, phycoerythrin; PerCPCy5.5, peridinin–chlorophyll–protein–cyanin5.5; Sm, surface membrane; SST, small sample screening tube. [a]Further information about markers and hybridomas is provided in the Appendix.

Table 6. Normal and reactive leukocyte populations in 120 CSF and 21 vitreous biopsies without evidence for lymphoma

Group of samples	*% B-cells*	*SmIgκ/SmIgλ ratio*	*% T-cells*	*CD4/CD8 ratio*	*% Monocytes*	*% Neutrophils*[a]	*% Other undefined events*
CSF ($n=120$)	2.0 (0-32)	1.4 (1.0–3.0)	50.8 (0–100)	1.8 (0.1–10.9)	2.1 (0–17)	15 (0–99)	31.7 (0–100)
CSF (MS cohort) ($n=15$)	1.1 (0–4)	1.3 (1.0–2.5)	48.2 (0–89)	2.8 (1.7–7)	3.6 (0–14)	23 (0–99)	21.9 (0–100)
CSF (other HM suspicion) ($n=9$)	0.2 (0–1)	NA	40.8 (0–100)	1.2 (0.2–3.5)	0	9 (0–14)	49.8 (0–100)
CSF (lymphoma suspicion) ($n=96$)	4.8 (0–32)	1.4 (1.0–3.0)	63.4 (0–100)	1.7 (0.1–10.9)	2.6 (0–17)	13 (9–59)	23.4 (0–100)
Vitreous fluid ($n=21$)	0.5 (0–4)	NA	51.7 (3–100)	2.1 (0.3–49)	2.6 (0–14)	18 (0–53)	14.1 (0–100)

Abbreviations: CSF, cerebrospinal fluid; HM, hematological malignancy; MS, multiple sclerosis; NA, not applicable due to lack of B-cells in most samples; Sm, surface membrane. Results are expressed as mean value and range between brackets. [a]Cells that cluster based on $FSC^{int}/SSC^{high}/CD45^{lo}$ can be considered as neutrophilic granulocytes (see also Discussion). NA, not applicable because of too few B-cells.

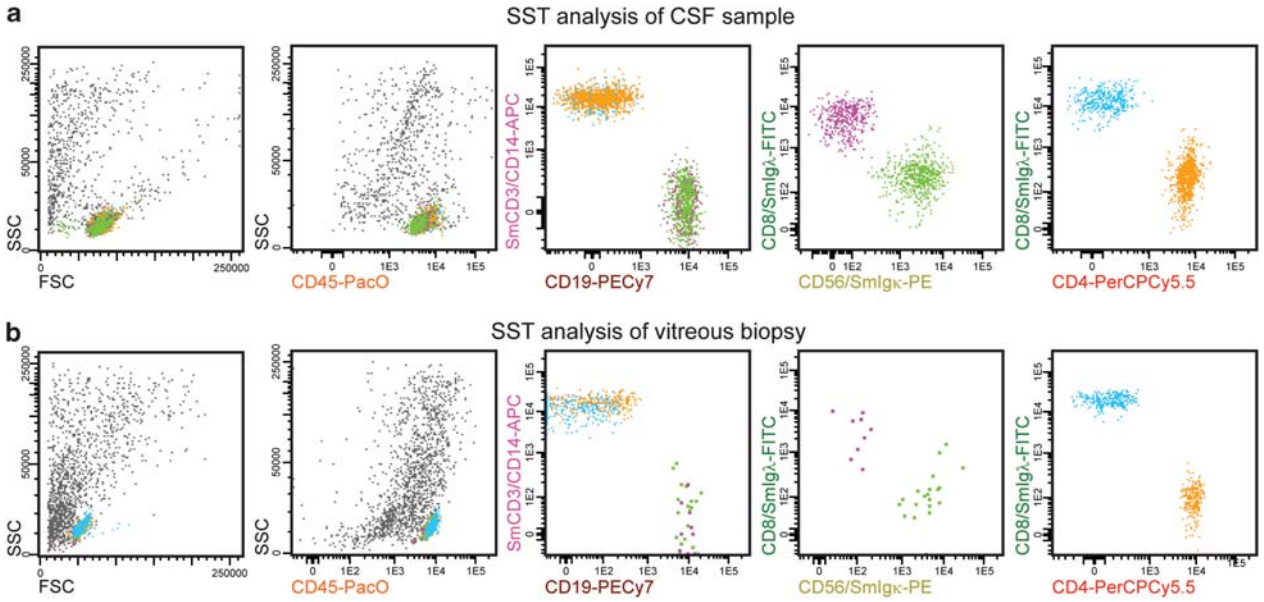

Figure 10. EuroFlow small sample tube (SST) analysis of a cerebrospinal fluid (CSF) (**a**) and a vitreous biopsy (**b**) sample with a normal composition of B- and T-lymphocytes. Based on a FSC/SSC/CD45 gating strategy, $CD19^+$ B-cell and $SmCD3^+$ T-cell populations are identified. Even though the surface membrane immunoglobulin (SmIg) κ and λ markers are both present in combination with other antibodies with the same fluorochrome, $SmIg\kappa^+$ (green dots) and $SmIg\lambda^+$ (purple dots) cells can be discerned by gating on the $CD19^+$ B-cell population. In both samples the $SmIg\kappa^+$ and $SmIg\lambda^+$ B-lymphocytes show a normal ratio (1.5). In a similar way, a normal distribution of $CD4^+$ (orange dots) and $CD8^+$ (blue dots) T-lymphocytes (ratio 2.3 and 2.1 in **a** and **b**, respectively) was detected within the $CD3^+$ T-cell population.

SmCD3 as a CD14 – APC conjugate, which proved to perform in optimal conditions.

Evaluation of the SST

The EuroFlow SST has been tested on a cohort of 164 samples that have been collected within the EuroFlow Consortium. These included 23 vitreous biopsies with a clinical suspicion of IOL and 141 CSF samples. Both groups of samples typically contained low numbers of cells, ranging from <100 to tens of thousands. As controls, 11 CSF samples from patients with an initial diagnosis of acute leukemia or Hodgkin lymphoma were studied, plus 15 CSF samples from patients with a clinical suspicion of (early) multiple sclerosis. In the remaining 115 CSF samples and the 23 vitreous biopsies, lymphoma localization was suspected. CSF and vitreous samples were collected in tubes with a small volume (a few ml) of culture medium plus 0.2% bovine serum albumin (BSA, SIGMA-ALDRICH, St. Louis, MO, USA) or 10% fetal calf serum (FCS, Invitrogen, Carlsbad, CA, USA) for a better cell viability, or in tubes prepared with 0.2 ml of Transfix (Cytomark, Buckingham, UK) (Tubes&Transfix, Immunostep SL, Salamanca, Spain). Upon arrival in the laboratory, cells were centrifuged and the pellet was resuspended in 200 μl phosphate buffer saline +0.5% BSA. Out of this cell suspension, one-third of the volume was initially used for the EuroFlow SST labeling. For sample preparation the EuroFlow protocols were adapted to previously described[89] consensus recommendations using a wash, stain, lyse and wash procedure.

In the CSF control group (multiple sclerosis, acute leukemia, Hodgkin lymphoma samples), the majority of the CSF cells that could be identified with the SST labeling corresponded to T-lymphocytes, whereas the remaining cells were monocytes and B-lymphocytes (Table 6). Of note, no $CD45^{lo}$ blasts could be identified in the CSF samples of acute leukemia patients. In turn, no aberrant B- or T-cell populations were seen in the vast majority (104/115) of the CSF samples that were taken because of a clinical suspicion of lymphoma (Figure 10). In 96 (out of these 104) samples that showed enough viable cells for evaluation, the majority of cells identified with the SST labeling also concerned T-lymphocytes (Table 6). Likewise, in the majority (21/23) of vitreous biopsies no aberrant B- or T-cell populations were found either (Table 6); notably, the number of cells in these vitreous

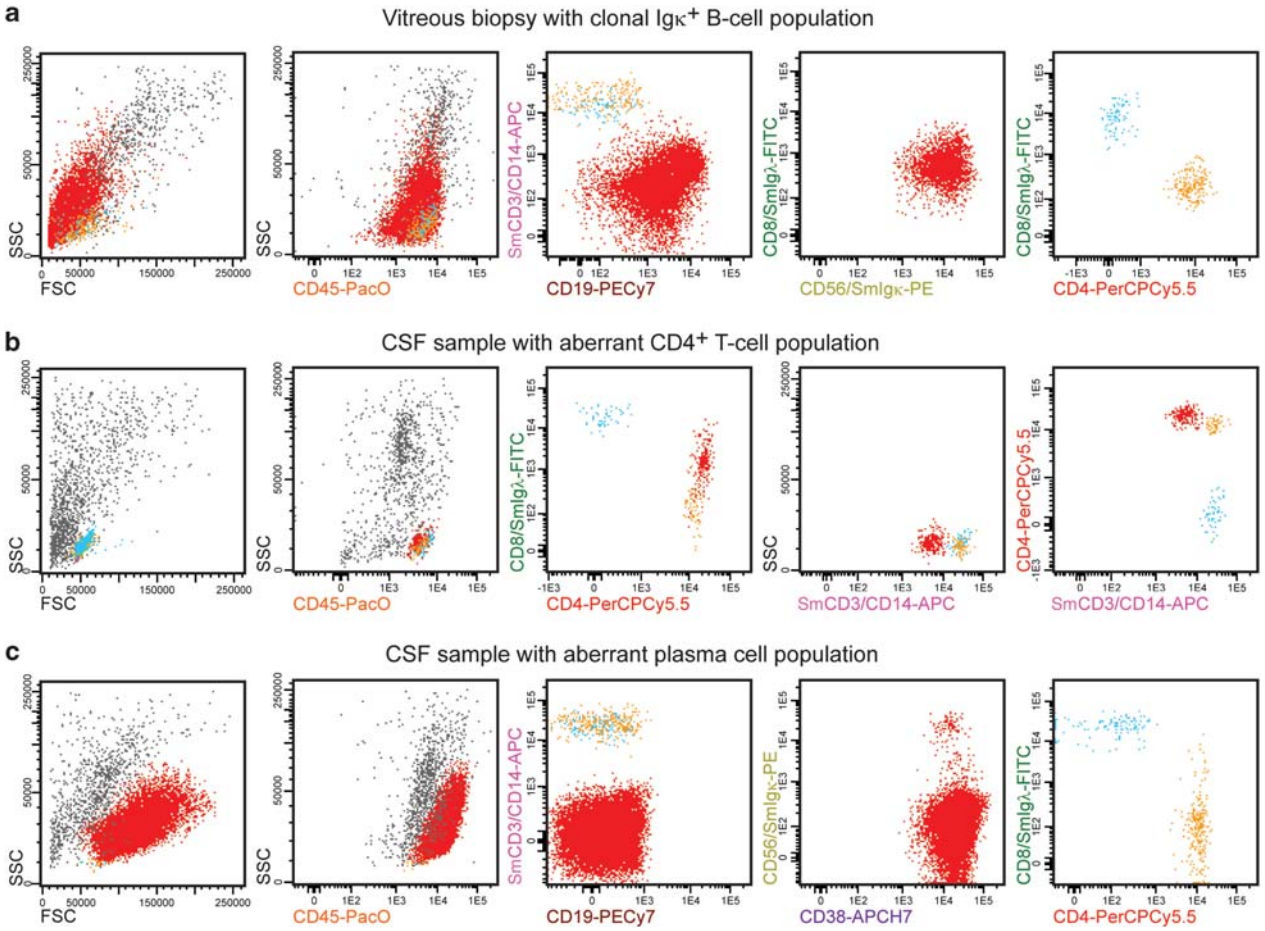

Figure 11. EuroFlow small sample tube (SST) analysis of a vitreous biopsy with prominent clonal B-cell population (**a**) and of two cerebrospinal fluid (CSF) samples with prominent aberrant T-cell (**b**) and plasma cell (**c**) populations. In **a**, following FSC/SSC/CD45 gating, B- and T-cell populations are identified; the B-cell population shows a heavily skewed surface membrane immunoglobulin (SmIg) κ/SmIgλ ratio (>10), in line with an aberrant, monoclonal large B-lymphocyte population (red dots); residual $CD4^+$ (orange dots) and $CD8^+$ (blue dots) T-lymphocytes show a normal distribution (ratio 2.5). In **b**, upon FSC/SSC/CD45 gating, a T-cell population is identified, which consists of $CD4^+$ (orange dots) and $CD8^+$ (blue dots) T-lymphocytes, as well as an aberrant T-cell population (red dots) characterized by a $SmCD3^{lo}$/$CD4^{hi}$/$CD8^{lo}$ phenotype; the presence of this aberrant T-cell population could be caused by a contaminating blood cell population, given the fact that neutrophil granulocytes can be discerned based on FSC versus SSC and CD45 versus SSC features. Based on a FSC/SSC/CD45 gating strategy, a T-cell population with a normal CD4/CD8 ratio (1.6) can be identified (but no B-cell population) in **c**. In addition, in this panel a rather large population of $CD19^-$/$CD3^-$ cells (red dots) is seen that upon further analysis appeared to be $CD38^{hi}$ and $CD56^-$, in keeping with a plasma cell origin; further diagnostic work-up of this patient indeed showed an aberrantly similar plasma cell population in the bone marrow (data not shown).

biopsies was generally rather low, although the relative composition was similar to the CSF samples with a predominance of T-lymphocytes (Table 6). None of these cases was diagnosed as CNS lymphoma or IOL.

In nine CSF samples with an initial suspicion of lymphoma, clonal B-cell populations were observed, in keeping with a primary B-cell lymphoma or a localization of a systemic B-cell lymphoma/B-cell leukemia. Out of the 23 vitreous biopsies two cases also showed an aberrant B-cell population; in one sample this concerned a $SmIg\kappa^+$ B-cell population (Figure 11a), whereas the other contained a suspect SmIg-negative B-cell population that had also been seen in a previous vitreous biopsy of the same patient. Furthermore, in two other CSF samples from patients with lymphoma suspicion, aberrant T-cell populations ($CD3^{lo}$/$CD4^+$/$CD8^+$) were identified (Figure 11b), compatible with their diagnosis of T-cell lymphoma and post-transplant lymphoproliferative disorder. Finally, two CSF samples in the control group without lymphoma suspicion showed clear infiltration by plasma cells ($CD38^{hi}$-expressing cells) (Figure 11c), indicative of a systemic plasma cell malignancy that was indeed found upon further diagnostic work-up. Overall, the results in all analyzed samples underline the power of this 13-parameter flow cytometric SST strategy to reliably confirm or exclude lymphoma localization (Table 7). All these cases (13/13) lacked a final cytological diagnosis of CNS disease or IOL. Despite this, they all had a final diagnosis of CNS lymphoma or IOL based on histopathology, image analysis or the clinical behavior of the disease.

Detection of aberrant lymphoid populations by PCA

Multivariate analysis of the B- and T-cell populations contained in individual CSF and vitreous biopsy samples was performed using PCA implemented in the Infinicyt software APS1 view (PC1 versus PC2) to evaluate the rate of detection of aberrant B- and T-cell phenotypes in cases showing CNS lymphoma or IOL. To this end, we used several of the clonal CSF cases from the current cohort as well as newly obtained clonal CSF cases. In the APS view we found a clear separation of clonal B-cells from normal B-cells for 2/4 $SmIg\kappa^+$ cases and 5/5 $SmIg\lambda^+$ cases, and for the one case in which SmIg expression could not be determined (overall: 8/10

Table 7. SST results of 149 pauci-cellular samples

Suspected lymphoma localized in CSF (n = *115)*	
Aberrant/clonal B-cell populations[a] (1 CLL, 1 BL, 1 FL, 1 MCL, 2 DLBCL, 1 B-cell lymphoma, 2 unknown)	9/115 (7.8%)
Aberrant T-cell populations (T-cell lymphoma, PTLD)	2/115 (1.7%)
Suspicious of other hematological malignancies in CSF (n = *11)*	
Aberrant plasma cell populations	2/11 (18.1%)
Vitreous biopsy (n = *23)*	
Aberrant/clonal B-cell populations	2/23 (8.7%)
Total	15/149[b] (10.0%)

Abbreviations: BL, Burkitt lymphoma; CNS, central nervous system; CLL, chronic lymphocytic leukemia; CSF, cerebrospinal fluid; DLBCL, diffuse large B-cell lymphoma; FL, follicular lymphoma; FNA, fine needle aspirate; IOL, intraocular lymphoma; PTLD, post-transplant lymphoproliferative disease; SST, small sample tube. [a]In one case a parallel FNA brain biopsy was analyzed next to the CSF sample, showing the same aberrant B-cell population; [b]All positive cases had a final diagnosis of CNS lymphoma or IOL based on histopathological analysis, imaging techniques and/or the clinical behavior of the disease, while none of the negative cases by the SST labeling was diagnosed as having CNS or IOL.

cases; data not shown). The parameters that contributed most to the APS-based discrimination were FSC and CD38, and to a lesser extent also CD20 and SSC. In contrast, the two other SmIgκ$^+$ cases were hardly or not discernible from control B cells or from SmIgκ$^+$ B-cells unless an increased ratio between SmIgκ$^+$/SmIgλ$^+$ B-cells was considered to be an informative parameter for lymphoma diagnosis. The two aberrant T-cell cases could easily be discerned from control CD4$^+$ and CD8$^+$ T-cells in the APS view, with CD4 and CD8 as the most discriminative markers. Of note, cytomorphological analysis was not informative in any of these cases ($n = 12/12$), as already described above.

CONCLUSION

The EuroFlow SST and sample preparation protocol is a powerful diagnostic tool for the evaluation of CSF and vitreous samples with a clinical suspicion of primary lymphoma. The 13-parameter SST labeling allows for a complete typing of the most relevant leukocyte populations in these samples. While in the majority of cases the presence of aberrant B-, T- or plasma cell populations can be confirmed or excluded using the APS view of the Infinicyt software, in the remaining cases an aberrant B-cell population was more difficult to establish, unless an altered SmIgκ/SmIgλ B-cell ratio was considered as indication for a diagnosis of B-cell lymphoma. A more detailed characterization of the aberrant B- or T-cell populations requires the use of even more markers in additional labelings, which are currently in progress.

SECTION 4. PLASMA CELL DISORDERS (PCD) PANEL

J Flores-Montero[1], J Almeida[1], JJ Pérez[2], A Mendonça[3], P Lucio[3], R de Tute[4], M Cullen[4], A Rawstron[4], E Mejstrikova[5], L Sedek[6], T Szczepański[6], L Lhermitte[7], VHJ van der Velden[8], H Wind[8], S Böttcher[9], MB Vidriales[2], T Kalina[5], J San Miguel[2] and A Orfao[1]

[1]USAL, Salamanca, Spain; [2]HUS, Salamanca, Spain; [3]IPOLFG, Lisbon, Portugal; [4]UNIVLEEDS, Leeds, UK; [5]DPH/O, Prague, Czech Republic; [6]SUM, Zabrze, Poland; [7]AP-HP, Paris, France; [8]Erasmus MC, Rotterdam, The Netherlands and [9]UNIKIEL, Kiel, Germany

BACKGROUND

PCD are a group of diseases most frequently characterized by the presence of clonal (neoplastic) plasma cells in the BM capable of secreting a clonal Ig that can be detected in serum and/or urine.[107] It includes different disease entities, among which multiple myeloma (MM) and monoclonal gammopathy of undetermined significance (MGUS) are the most prevalent and representative entities.[108] Additionally, other less frequent clinical conditions associated with predominant extramedullary plasma cell localizations and organ failure due to the accumulation of the clonal Ig (for example, amyloidosis) are also included in this group of diseases.[107,109]

Multiparameter flow cytometric immunophenotyping, together with other clinical, radiological, biochemical and hematological data, provides relevant information for the diagnosis and classification of PCD. At the same time, flow cytometry contributes to prognostic stratification and minimal residual disease (MRD) monitoring of myeloma patients after therapy.[9,110] The most relevant clinical information provided by flow cytometry relies on the identification and enumeration of aberrant versus normal/polyclonal BM plasma cells: a higher ratio between both populations is associated with malignancy (for example MM versus MGUS). Similarly, the presence of $<5\%$ of normal plasma cells within the total population of BM plasma cells is also associated with a poor outcome in symptomatic MM and a higher risk of progression in both MGUS and smoldering MM.[111] In turn, several individual markers and immunophenotypic profiles (for example, CD28 and CD117 expression) have been associated with specific genetic changes and disease outcome.[112]

Over the years, an increasing number of markers have been identified that provide relevant immunophenotypic information on plasma cells.[9,110,112–122] Current consensus recommendations include CD38, CD138 and CD45 (together with light scatter characteristics) as the best combination of backbone markers for the identification and enumeration of plasma cells.[9,110,114] In addition, expression of CD19, CD56, CD117, CD20, CD28, CD27 and CD81, together with CyIg light-chain restriction, is associated with unique phenotypic patterns that allow clear discrimination between normal/reactive versus clonal plasma cells.[9,110,113,118] More recently, it has also been shown that the plasma cell surface expression of β2 microglobulin negatively correlates with its serum levels and a better outcome, becoming an additional potentially attractive prognostic marker.[121]

On the basis of existing data and consensus recommendations, the EuroFlow Consortium has designed and evaluated a two-tube, 12-marker panel of antibodies devoted to: identification of plasma cells, discrimination and enumeration of coexisting normal/reactive and aberrant plasma cell populations and detailed characterization of additional cell surface markers that contribute to the definition of aberrant phenotypes or disease prognosis.

Selection of antibody reagents

Four distinct backbone markers (CD38, CD138, CD45 and CD19) were selected for efficient identification of plasma cells (CD38 and CD138) and to distinguish between normal/reactive and clonal plasma cell compartments based on their most frequent aberrant phenotypes (CD38, CD19 and CD45). Another eight markers were additionally selected for the characterization of plasma cells with the PCD panel configured as two-tube, 12-marker combination (Table 8). The overall panel of markers aimed at: (i) positive identification of plasma cells in BM, and other less frequent types

Table 8. Design of PCD tubes in six consecutive testing rounds[a]

Version (no. of cases)[b]	*Tube*	*Fluorochromes and markers*							
		PacB	*AmCyan*	*FITC*	*PE*	*PerCPCy5.5*	*PECy7*	*APC*	*APCCy7*
1 ($n=7$)	1	CD45	CD19	Cylgλ	Cylgκ	CD38	CD56	CD27	[c]
	2	CD45	CD19	β2 micro	CD81	CD38	CD117	CD28	[c]
		PacB	*AmCyan*	*FITC*	*PE*	*PerCPCy5.5*	*PECy7*	*APC*	*AF700*
2 ($n=68$)	1	CD19	CD45	Cylgλ	Cylgκ	CD138	CD56	CD27	CD38
	2	CD19	CD45	β2 micro	CD81	CD138	CD117	CD28	CD38
3 ($n=5$)	1	CD19	CD45	β2 micro	Cylgλ	CD138	CD56	Cylgκ	CD38
	2	CD19	CD45	CD27	CD81	CD138	CD117	CD28	CD38
		PacB	*AmCyan*	*FITC*	*PE*	*PerCPCy5.5*	*PECy7*	*APC*	*APCH7*
4 ($n=29$)	1	CD19	CD45	β2 micro	Cylgλ	CD138	CD56	Cylgκ	CD38
	2	CD19	CD45	CD27	CD81	CD138	CD117	CD28	CD38
5[d] ($n=5$)	1	CD19	CD45	CD138	Cylgλ	β2 micro	CD56	Cylgκ	CD38
	2	CD19	CD45	CD138	CD81	CD27	CD117	CD28	CD38
		PacB	*PacO*	*FITC*	*PE*	*PerCPCy5.5*	*PECy7*	*APC*	*APCH7*
6 (Final) ($n=100$)	1	CD45	CD138	CD38	CD56	β2 micro	CD19	Cylgκ	Cylgλ[e]
	2	CD45	CD138	CD38	CD28	CD27	CD19	CD117	CD81

Abbreviations: AF700, alexa fluor 700; AmCyan, *Anemonia Majano* cyan fluorescent protein; APC, allophycocyanin; BM, bone marrow; Cy, cytoplasmic; Cy7, cyanin7; FITC, fluorescein isothiocyanate; H7, hilite7; MGUS, monoclonal gammopathy of undetermined significance; β2 micro, β2 microglobulin; MM, multiple myeloma; NonPCD, non-plasma cell-related diseases; PacB, pacific blue; PacO, pacific orange; PB, peripheral blood; PCD, plasma cell disorders; PE, phycoerythrin; PerCPCy5.5, peridinin–chlorophyll–protein–cyanin5.5. [a]Further information about markers and hybridomas is provided in the Appendix. [b]A total of 214 samples (212 BM, 2 PB) was evaluated. Among them 117 MM, 47 MGUS and 50 other conditions were detected. The other conditions included: 1 amyloidosis; 2 plasma cell leukemias; 6 non-infiltrated samples from patients with suspected PCD that showed no infiltration both in routine and EuroFlow diagnostic approaches (suspected disease category: 2 MGUS, 2 MM, 1 plasmocytoma, 1 IgM paraproteinemia); 3 B-chronic lymphoprolipherative disorders with no involvement of the plasma cell compartment; 10 normal healthy donors; 15 reactive BM samples from patients with NonPCD; 13 regenerating BM samples after chemotherapy from patients with NonPCD. [c]CD138 was proposed for this position but no conjugate was commercially available at the time of evaluation. [d]All samples were evaluated using tube 2 only. Highlighted boxes: changes as compared to previous version. [e]Testing of Cylgλ-APCC750 is ongoing to increase the stain index of Cylgλ$^+$ cells.

of samples evaluated for PCD; (ii) accurate discrimination between normal/reactive and aberrant plasma cells, because of their distinct immunophenotypic profiles; and (iii) confirmation of their clonal nature, as evidenced by a restricted Cylg light-chain expression or expression of $\geqslant 2$ aberrant markers (Table 9). The final proposed configuration of the panel (version 6; Table 8) resulted from evaluation of six sequential versions of distinct two-tube combinations of the above-listed backbone ($n=4$) and characterization markers ($n=8$). Interestingly, no inclusion or exclusion of markers was required during this process, as from initial testing the proposed markers proved to accomplish the tasks they were selected for. However, modifications were required with regard to the specific combination of fluorochrome-conjugated reagents of the selected antibodies because of their technical features and performance. Technical issues that had an impact on the performance of specific fluorochrome-conjugated reagents included high plasma-cell baseline autofluorescence levels, the amount of expression of individual markers (for example, CD38, β2 microglobulin, CD56) and the availability of high-quality fluorochrome-conjugated antibodies for specific fluorochrome positions. In turn, particular attention was also paid to the light scatter positioning of plasma cells (SSC$^{int/hi}$ and FSC^{hi}) with the PCD panel that should completely fall inside the pre-established FSC and SSC window of analysis, influencing the reference values set for these parameters.

Table 9. Utility of PCD markers

Tube	*Target antigen*	*Identification of plasma cells*	*Aberrant markers*	*Assessment of plasma cell clonality*
BB markers	CD38	X	C	
	CD138	X		
	CD45	X	C	
	CD19	X	C	
Tube 1	Cylgλ			X
	Cylgκ			X
	CD56		C	
	β2 micro		S	
Tube 2	CD27		S	
	CD28		S	
	CD117		S	
	CD81		S	

Abbreviations: BB, backbone; C, common aberrant marker; Cy, cytoplasmic; β2 micro, β2 microglobulin; PCD, plasma cell disorders; S, second diagnostic level marker.

Design of the PCD EuroFlow panel

Overall, we analyzed a total of 214 samples from 10 healthy subjects and 204 patients. The samples included monoclonal gammopathies studied at different time points of the disease (diagnosis, relapse and follow-up) ($n=173$), B-CLPD patients studied at diagnosis who showed no involvement of the plasma cell compartment ($n=3$) and patients with non-plasma cell-related diseases (Non-PCD) ($n=28$). In brief, 114 BM were analyzed with versions $1-5$ (Table 8) and 100 samples (98 BM and two PB) with the final version 6 of the PCD panel (Table 8).

Evaluation of version 1 (Table 8) of the PCD EuroFlow panel highlighted the problems caused by the high levels of expression of both CD38 and β2 microglobulin on normal plasma cells, when PerCPCy5.5- and FITC-conjugated reagents were used, respectively. Such high fluorescence intensity levels were associated with inappropriate fluorescence compensation profiles and fluorescence intensity levels falling out of the window of analysis. Therefore, attempts were made to accommodate CD38 and β2 microglobulin in other fluorescence channels for which they show lower fluorescence intensity and lower fluorescence spillover into other channels. For this purpose, CD38-AF700 (versions 2 and 3 of the PCD EuroFlow panel), CD38-APCH7 (versions 4 and 5) and CD38-FITC (version 6) conjugates were further evaluated. Overall, the best performance was obtained with the CD38-FITC reagent (version 6). In turn, β2 microglobulin was posted as a candidate for the PerCPCy5.5 channel. Owing to the need for a custom conjugate, it could only be evaluated in version 5 of the panel, with acceptable performance. Final tuning of the CD38-FITC and β2 microglobulin-PerCPCy5.5 was required in version 6 of the PCD panel for both reagents (Table 8) to further decrease the fluorescence intensity obtained for plasma cells. For these markers, such fine-tuning was achieved by mixing each reagent with the corresponding unconjugated reagents of the same CD38 and β2 microglobulin clones. With this strategy, the overall performance of the two markers improved and matched the desired fluorescence intensity profiles. The mixture of unconjugated and conjugated reagent ensures saturating conditions and avoids unexpected variations in the staining patterns because of changes in cell concentrations, which would otherwise be observed when attempts to reduce fluorescence intensity are just based on reducing the concentration of the fluorochrome-conjugated antibody.[123] The optimal CD38 (clone LD38) staining was obtained with a 3/2 mixture of the conjugated and of the purified antibody, respectively. The optimal β2 microglobulin (clone TÜ99) staining was obtained with a 19/1 mixture of the conjugated and of the purified antibody reagents, respectively.

Similarly, the reagent initially selected for cytoplasmic detection of Igλ light chains—anti-Igλ(polyclonal)-FITC (DAKO, Glostrup, Denmark)—also resulted in positive cells falling out of the window of analysis used for the FITC-associated fluorescence channel, and beyond the linearity range of the corresponding fluorescence detector. Thus, anti-Igλ was also evaluated as a PE-conjugated reagent (versions 3–5 of the PCD panel; Table 8) with similar limitations and as an APCH7-conjugated antibody reagent (version 6), which was finally selected. Noteworthy, the Cylgκ-APC and Cylgλ-APCH7 staining resulted in adequate discrimination of Cylgκ$^+$ versus Cylgλ$^+$ normal plasma cells and identification of Cylg light-chain restriction by clonal plasma cell populations. However, the staining pattern for both reagents on other Smlg$^+$ B-cells was not as discriminative.

Another marker for which different reagents were tested was CD45. CD45 – PacO conjugates were initially selected and evaluated as a potential alternative to CD45 – AmCyan in order to have uniformity across all EuroFlow panels (see other sections of this manuscript). However, in the PCD panel, CD45 – PacO resulted in poor discrimination between CD45$^-$ and CD45^{lo} plasma cell populations. This was due to the relatively high plasma cell baseline autofluorescence levels in the PacO fluorescence channel, which exceeded the resolution power of this reagent for discrimination of CD45$^-$ versus CD45^{lo} plasma cells. AmCyan was then preferred and kept for subsequent versions of the PCD EuroFlow panel (versions 2–5). However, this fluorochrome conjugate was associated with suboptimal results due to fluorescence spillover into the FITC channel,[16] forcing further evaluation and selection of an alternative reagent: CD45–PacB.

CD138 was then selected as the marker to occupy the PacO position when CD45 was removed from this fluorochrome position. CD138-conjugated reagents were absent from version 1, due to the lack of a conjugate to fit the position proposed

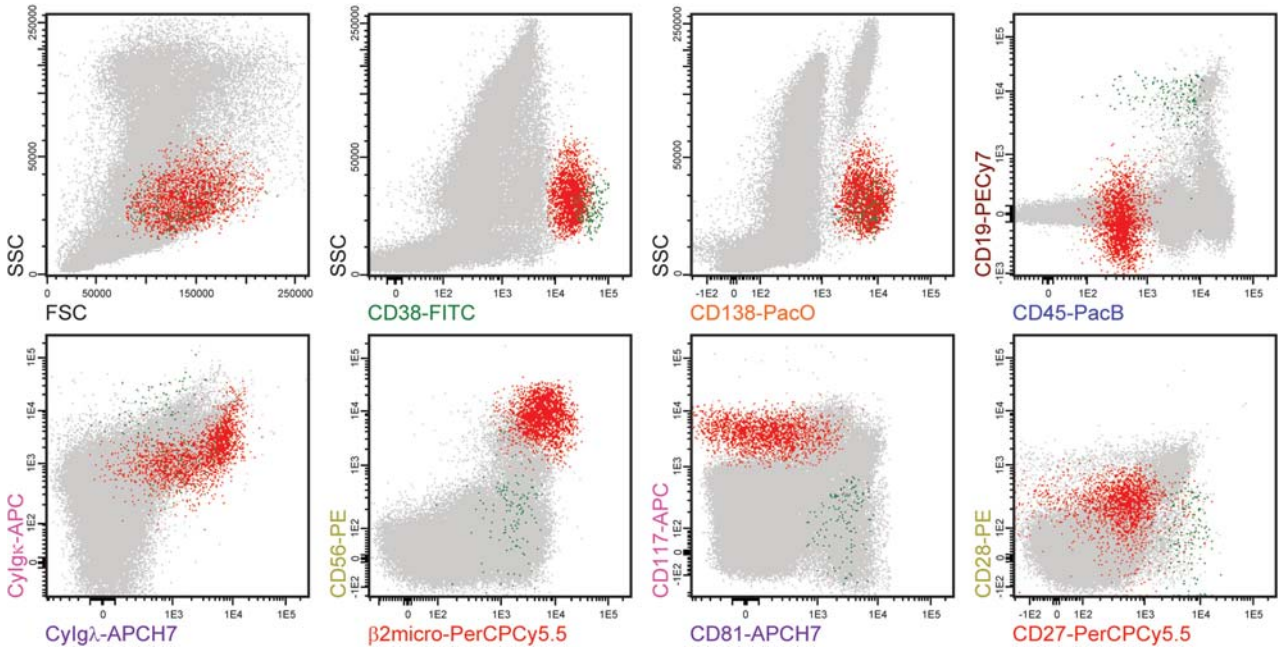

Figure 12. Example of a bone marrow (BM) sample from a monoclonal gammopathy of undetermined significance (MGUS) patient stained with the final version (version 6) of the PCD EuroFlow panel illustrating its power for the identification of plasma cells and discrimination between their normal/polyclonal and clonal counterparts. Normal plasma cells (green dots) show a typically normal immunophenotypic profile and coexist in this sample with a clonal population of plasma cells (red dots), which show multiple aberrant phenotypes—CD38^{lo}, CD45$^-$, CD19$^-$, CD56^{hi}, CD117$^+$, CD81^{lo}, CD28^{lo} and CD27$^-$—together with high expression of β2 microglobulin. The polyclonal versus (mono)clonal nature of both plasma cell populations is confirmed by their pattern of expression of cytoplasmic immunoglobulin (Cylg) κ$^+$ and Cylgλ$^-$ (normal Cylgκ/Cylgλ ratio versus Cylgλ$^+$ restricted expression, respectively).

(for example, APCH7) and it was further evaluated in other positions such as PerCPCy5.5 (versions 2–4), and FITC (version 5), which subsequently had to be assigned to other problematic reagents (β2 microglobulin and CD38, respectively). CD138 was considered as a less problematic marker whose utility relies on the distinction between CD138$^+$ plasma cells and other CD138$^-$ cells and it was finally included in the panels as a CD138 – PacO reagent (version 6), ordered as a custom conjugate. Unexpectedly, when this marker was introduced, decreased fluorescence intensity was observed when sample processing included only surface markers (using FACS Lysing solution, BD Biosciences, San Jose, CA, USA) versus intracellular staining for the detection of Cylg chains (using the Fix&Perm reagent) (data not shown). Because of this, it was decided that both tubes of the panel should be processed similarly with Fix&Perm, until this issue would be solved in order to reduce intra-sample variability due to use of different sample preparation procedures for the two tubes included in the PCD EuroFlow panel. Relocation of other markers in the combination was mainly caused by the modifications required to set the CD45, CD138, CD38 and β2 microglobulin markers at an optimal position, as explained above.

Evaluation of the PCD EuroFlow panel

Among the 100 samples analyzed with version 6 of the PCD EuroFlow panel, 38 corresponded to patients with MM, 23 to patients with MGUS, 2 to plasma cell leukemia patients and 6 to diagnostic samples from patients with suspected PCD (2 MGUS, 2 MM, 1 plasmacytoma and 1 IgM paraproteinemia), but no infiltration by aberrant plasma cells as confirmed by local routine approaches. The other BM samples were from 10 patients with non-PCD who underwent BM evaluation at diagnosis, 13 from regenerating BM after chemotherapy indicated for non-PCD and 8 normal adult BM samples from healthy subjects. In every sample, total BM plasma cells were identified based on their CD38$^{int/hi}$, CD138$^+$ phenotypic profile in association with intermediate to high FSC and SSC characteristics, after excluding cell doublets in a FSC area versus FSC height dot plot.

Further multiparameter flow cytometry gating of the distinct plasma cell populations and analysis of their phenotypic features showed that with version 6 of the PCD EuroFlow panel we were able to detect and fully characterize the immunophenotype of aberrant plasma cells versus their normal/reactive counterparts (Figure 12) in every sample. This included samples that contained aberrant plasma cells ($n = 63/63$ samples) and/or normal/reactive plasma cells ($n = 88/88$) as assessed by routine diagnostic protocols performed in parallel in the eight participating centers. In 49/49 samples coexisting clonal and normal plasma cells were detected with the two approaches. Noteworthily, in all cases evaluated, tube 1 could distinguish between the two plasma cell compartments based on their distinct phenotypes.

These individual data files were then merged to create a reference pool of normal plasma cells. PCA showed that all normal plasma cell populations clustered together in the APS1 (PC1 versus PC2) view of the Infinicyt software. This indicates that normal plasma cells from different healthy subjects show an overlapping phenotypic profile as defined by the 12-dimensional space, generated by all markers evaluated (Figure 13).

Similarly, normal/reactive plasma cells from patients suspected of carrying a PCD in which no abnormal plasma cells were detected ($n = 6$), patients evaluated for a non-PCD at diagnosis

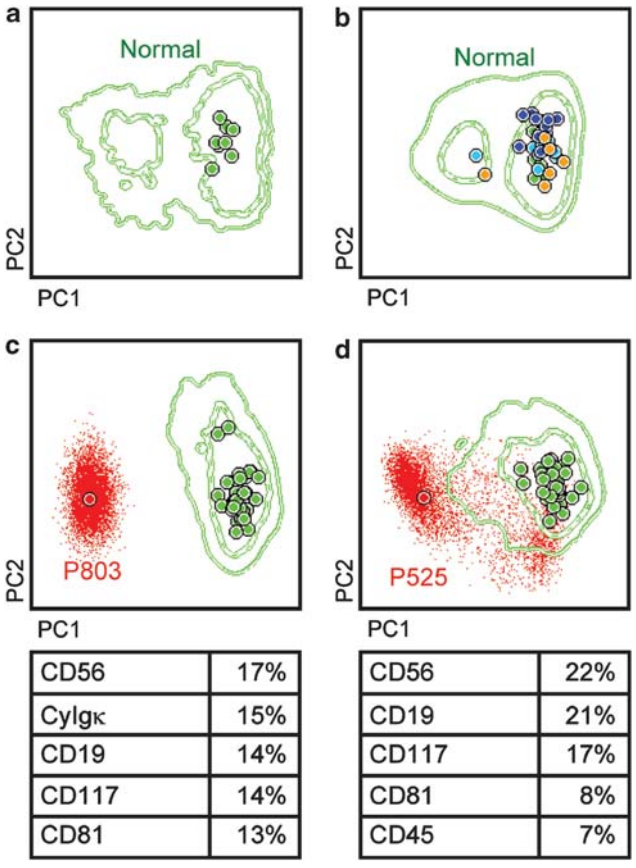

CD56	17%
Cylgκ	15%
CD19	14%
CD117	14%
CD81	13%

CD56	22%
CD19	21%
CD117	17%
CD81	8%
CD45	7%

Figure 13. Automated population separator (APS) views of illustrating principal component analyses (PCA) of the distinct immunophenotypic profiles of plasma cells from healthy donors and two different multiple myeloma (MM) and monoclonal gammopathy of undetermined significance (MGUS) patients, based on the expression of the 12 markers included in the plasma cell disorders (PCD) EuroFlow panel (Version 6). (**a**) Simultaneous analysis of bone marrow (BM) plasma cells from healthy donors ($n = 8$; green circles). (**b**) Overlapping profiles of plasma cell populations from the same healthy donors ($n = 8$; green circles) when compared to those of BM plasma cells from non-infiltrated patients with distinct PCD at diagnosis ($n = 6$; orange circles), non-plasma cell-related diseases (non-PCD) at diagnosis ($n = 10$; light blue circles) and BM plasma cells from non-PCD patients studied after chemotherapy ($n = 13$; dark blue circles); noteworthily, polyclonal plasma cells from all these cases phenotypically overlapped with BM plasma cells from healthy subjects (**b**), although polyclonal plasma cells from two samples (one PCD and one non-PCD patient studied at diagnosis, who showed no BM infiltration by clonal/aberrant plasma cells) showed overlapping phenotypes with clearly shifted median values, appearing as separated from the main cluster due to increased numbers of CD19$^-$ plasma cells with a normal phenotypic profile. The two lower panels (**c**, **d**) show illustrating examples of the distinctly aberrant immunophenotypic profiles of clonal plasma cells in two different patients (red circles and dots) with MM (**c**) and MGUS (**d**). Noteworthily, in **c** a single group of clonal plasma cells is observed, which clusters separately from the normal/reactive plasma cell cluster, while in **d** two groups of plasma cells were present in the MGUS patient BM: a polyclonal (phenotypically normal) plasma cell population that clustered together with the reference pool of normal plasma cells and a clonal plasma cell population that clustered separately from normal plasma cells (red dots). The five most informative markers contributing to the best discrimination between each of the two clonal plasma cell populations and the corresponding normal plasma cell reference pool are displayed at the bottom of each plot, in a decreasing order of percentage contribution to the discrimination (**c**, **d**). Each circle represents one single case (median expression observed for all phenotypic parameters evaluated), while contour lines represent s.d. curves (dotted and broken lines represent 1s.d. and 2s.d., respectively); dots correspond to single BM plasma cell events from the MM (**c**) and MGUS (**d**) patients represented.

($n = 10$) and patients after chemotherapy ($n = 13$), also clustered together upon the same analytical approach as described above. When analyzed together, plasma cell populations from these reactive/regenerating samples, clustered together with the reference pool of normal plasma cell populations, which confirms that they have a very similar and overlapping immunophenotypic profile (Figure 13b). Noteworthily, in two of these samples (one corresponding to a non-infiltrated PCD sample studied at diagnosis and one from a patient with a non-PCD) polyclonal BM plasma cells clustered slightly apart from the main cluster of normal plasma cells due to an increased percentage of $CD19^-$ plasma cells with an otherwise normal polyclonal phenotype (Figure 13b). Notably, no clear discrimination could be made between samples stained at different centers.

Conversely, when each abnormal plasma cell population from individual patient samples was processed and analyzed as described above, and compared to both the normal and the reactive/regenerating plasma cell reference pools, it emerged as being clearly different from both clusters of polyclonal plasma cells in the APS diagrams, for all infiltrated PCD patient samples tested (illustrated for two patients in Figures 13c and d). Noteworthily, a clear discrimination could already be obtained for every patient with the eight markers of tube 1, the other four markers contributing to improve the separation between normal and aberrant plasma cells in a significant percentage of cases. Interestingly, when data files with information about clonal plasma cells from all altered samples were analyzed and displayed together in the APS view, two clearly different clusters of abnormal plasma cell populations were observed; these clusters reflected different phenotypic profiles, which mostly corresponded to cases with $CD56^{hi}$ versus $CD56^{-/lo}$ aberrant plasma cells.

CONCLUSION

Multiparameter flow cytometric immunophenotyping proved to be an efficient approach for the detection of normal/reactive versus aberrant plasma cells, the calculation of their relative distribution in a sample and the detailed characterization of their immunophenotypic profiles in patients with different subtypes of monoclonal gammopathies. Such information has previously proven to contribute to the diagnosis, classification and prognostic stratification of this clinically heterogeneous group of disorders. Here we propose a panel of 12 distinct markers based on two 8-color tubes, for accurate identification of plasma cells, specific detection and quantification of phenotypically aberrant versus normal/polyclonal plasma cell populations and detailed characterization of their immunophenotypic profiles. The two proposed tubes contain four backbone markers in common (CD38, CD138, CD45 and CD19) and eight additional markers that were equally distributed in tube 1 (CD56, β2 microglobulin, Cylgκ and Cylgλ) and in tube 2 (CD27, CD28, CD81 and CD117). As tube 1 proved sufficient for the specific identification, enumeration and discrimination between normal/reactive and aberrant plasma cells, it can be used as a standalone tube for the initial screening of PCD in a two-step diagnostic approach (Figure 1). In such case, tube 2 could be optional and used for further evaluation and characterization of the altered plasma cells, only when this is indicated.

SECTION 5. ANTIBODY PANEL FOR B-CELL PRECURSOR ALL (BCP-ALL)

L Lhermitte[1], V Asnafi[1], L Sedek[2], T Szczepański[2], S Böttcher[3], M Brüggemann[3], E Mejstrikova[4], T Kalina[4], A Mendonça[5], P Lucio[5], J Bulsa[2], J Flores-Montero[6], JJ Pérez[7], H Wind[8], JG te Marvelde[8], VHJ van der Velden[8], J Hernández[9], AS Bedin[1], JJM van Dongen[8], A Orfao[6] and E Macintyre[1]

[1]AP-HP, Paris, France; [2]SUM, Zabrze, Poland; [3]UNIKIEL, Kiel, Germany; [4]DPH/O, Prague, Czech Republic; [5]IPOLFG, Lisbon, Portugal; [6]USAL, Salamanca, Spain; [7]HUS, Salamanca, Spain; [8]Erasmus MC, Rotterdam, The Netherlands and [9]Cytognos SL, Salamanca, Spain

BACKGROUND

The EuroFlow BCP-ALL antibody panel aims at recognition and classification of all immature B-lineage malignancies, that is, the neoplasms of precursor B-cells.[34] Immunophenotypically, BCP-ALL resemble normal precursor B-cells with B-lineage antigen expression (for example, CD19, CyCD79a, CyCD22) and other phenotypic characteristics, mimicking to a certain extent the phenotypic stage of maturation arrest.[124] Conversely, expression of some antigens differs significantly from normal by being asynchronous, ectopic or aberrant. This information can be assessed by multiparameter flow cytometry and is critical for the distinction between normal and leukemic cells and to make (or exclude) the diagnosis of BCP-ALL. It is also useful to establish a phenotypic signature at diagnosis for subsequent MRD monitoring by flow cytometry.[125]

Flow cytometry has a critical role in BCP-ALL diagnosis based on lineage assignment and the phenotypic features of maturation arrest.[27,34] Most of this information relies on combinations of multiple markers. As an example, the European Group for the Immunological Classification of Leukemias (EGIL) uses a combination of four markers (CD10, Cylgμ, SmIgM or Ig light chains) for this purpose.[27,34] Some phenotypic profiles correlate with recurrent molecular abnormalities, but they are complex and do not rely on the expression of a single marker.[36,45] For example, the E2A-PBX1 rearrangement is suspected in a $CD19^+/CD10^+/CD20^{-/lo}/CD34^-/CD9^+/Cylg\mu^+$ phenotype.[126] A series of phenotypic patterns associated with prognosis, genotypic aberrancies or maturation stage of arrest have been reported based on expert and consensus experiences and mainly qualitative (presence or absence of expression) analyses of a relatively limited number of markers.[27,45] This undoubtedly does not reflect the whole phenotypic complexity of BCP-ALL. Deciphering the heterogeneity of BCP-ALL requires integration of the precise expression levels of a wide range of antigens, collected from the leukemic cells of many different BCP-ALL patients. Consequently, harmonized analysis of BCP-ALL cases including all potentially relevant markers for subclassification of BCP-ALL is needed. The aim of the EuroFlow Consortium was to establish a standardized procedure for the immunophenotypic diagnosis and classification of BCP-ALL based on a well-defined set of antibody reagents that can be used in combination with newly developed software tools to perform multiparameter analysis of antigen profiles. The BCP-ALL panel developed consists of a comprehensive 8-color four-tube antibody panel. More precisely, the BCP-ALL panel was designed to reach the following goals: (i) to identify normal B-cell precursors; (ii) to detect phenotypic aberrations allowing distinction between normal and regenerating B-cell precursors and BCP-ALL; (iii) to document the phenotype of leukemic cells versus their normal counterparts, including identification of both common and divergent patterns to determine the stage of maturation arrest and propose relevant leukemia-associated phenotypes (LAP) for MRD assessment, respectively; (iv) to detect immunophenotypic profiles associated with recurrent oncogenic abnormalities; and (v) to provide prognostic information.

Design of the EuroFlow BCP-ALL panel

The BCP-ALL panel was designed to be applicable with both conventional data analysis procedures and innovative data analysis tools to take optimal advantage of n-dimensional flow

cytometry. In order to allow linkage of the data from the different BCP-ALL tubes, an optimal combination of backbone markers (present in every tube) and characterization markers was used as the basic strategy to construct the panel.

Selection of backbone markers. An optimal combination of backbone markers should allow identification and subsequent gating of B-cell blasts in every BCP-ALL case. The backbone markers should also provide unique positions for individual blast cells inside the n-dimensional space detected in common in every tube in the panel, in order to allow accurate calculations of data for each BCP-ALL cell.[16] As for all other EuroFlow panels, the backbone should include a limited number of markers in order to enable inclusion of a maximum of characterization markers within a limited number of tubes.

Overall, three backbone markers were found to be sufficient. The same three backbone markers were used in ALOT to allow the combination of data obtained with both protocols. Up front, candidate backbone markers were limited, and most of them effectively met the afore-mentioned criteria. These included CyCD79a, CyCD22, CD19, CD45, CD34 and CD10. CyCD79a and CyCD22 were discarded in order to avoid intracellular staining and because these antibodies did not demonstrate a clear added value over CD19 for the identification of B-cell precursors. CD19 was chosen for the backbone as it is expressed at an early stage of B-cell commitment and in virtually all BCP-ALL cases. CD45 was also retained as a particularly efficient marker in BCP-ALL for blast cell gating and exclusion of residual normal cells, especially CD45^{hi} mature B cells.[61] In addition, CD45 displays increasing levels of expression during B-cell development, thus also contributing to deciphering immature subpopulations among normal B-lineage cells.[5,11,124]

The two selected markers, however, were not enough, and so a third backbone marker was required with two candidates: CD10 and CD34. CD10 is frequently but variably expressed in BCP-ALL, and represents both an immaturity and B-cell lineage-related marker with a variable expression pattern along normal B-cell development.[5,11,124] Conversely, CD34 is a marker of immaturity, which is not lineage-related and is frequently (but not always) expressed in BCP-ALL. When expressed, CD34 is useful for identification of the blast cells. However, CD34 expression does not reflect normal B-cell development as good as CD10, as its expression is restricted to the earliest stages of B-cell development and is rapidly lost in later stages.[5,11,124] Evaluation of the patterns of expression of both markers showed that BCP-ALL has bimodal or partial expression pattern of CD10 and CD34 in around 1% and 8% of cases, respectively. Consequently, CD34 best reflects the intraclonal heterogeneity of malignant B-cell precursors. On top of this, many CD34 antibody conjugates that work well are currently commercially available, whereas CD10 detection is highly dependent on the specific labeling used, with decreasing levels of sensitivity from PE to APC, PECy7 and FITC conjugates. Accordingly, we decided to add CD34 to the CD19 and CD45 backbone markers.

Comparative testing showed that CD45 – AmCyan should be replaced by CD45 – PacO, which did not negatively affect the FITC channel. CD34 – PerCPCy5.5 was selected based on its excellent staining properties and a sensitive CD19 – PECy7 conjugate was chosen because of the brightness of this fluorochrome, and the better performance observed versus CD19 – PacB (custom-conjugated; data not shown). The final set of backbone markers selected for the BCP-ALL panel therefore consisted of CD45 – PacO, CD34 – PerCPCy5.5 and CD19 – PECy7, and it proved to allow gating of the entire tumor B-cell population in every BCP-ALL case out of the 52 tested; noteworthily, the same antibody conjugates were shared with the ALOT to enable linkage of data from both panels.

Selection of additional characterization markers. Once the backbone markers were set, a list of characterization markers was made, based on previous reports and the experience of the EuroFlow laboratories. These markers were then prioritized into first- and

Table 10. Design of BCP-ALL panel in four consecutive testing rounds[a]

Version (no. of cases)[b]	*Tube*	*Fluorochromes and markers*							
		PacB	*AmCyan*	*FITC*	*PE*	*PerCPCy5.5*	*PECy7*	*APC*	*AF700*
1 ($n = 14$)	1	CD20	CD45	CD58	CD66c	CD34	CD19	CD10	CD38
	2	SmIgκ	CD45	SmIgM	CyIgμ	CD34	CD19	CD123	SmIgλ
	3	CD21	CD45	NuTdT	CD13	CD34	CD19	CD22	CD24
	4	CD81	CD45	CD15 and CD65	NG2	CD34	CD19	CD33	CD9
2 ($n = 17$)	1	CD20	CD45	CD58	CD66c	CD34	CD19	CD10	CD38
	2	SmIgκ	CD45	CyIgμ	CD123	CD34	CD19	SmIgM	SmIgλ
	3	CD21	CD45	NuTdT	CD13	CD34	CD19	CD81	CD24
	4	CD9	CD45	CD15 and CD65	NG2	CD34	CD19	CD33	CD22
		PacB	*PacO*	*FITC*	*PE*	*PerCPCy5.5*	*PECy7*	*APC*	*APCH7*
3 ($n = 35$)	1	CD20	CD45	CD58	CD66c	CD34	CD19	CD10	CD38
	2	SmIgκ	CD45	CyIgμ	CD33	CD34	CD19	SmIgM and CD117	SmIgλ
	3	CD21	CD45	NuTdT	CD13	CD34	CD19	CD22	CD24
	4	CD9	CD45	CD15 and CD65	NG2	CD34	CD19	CD123	CD81
4 (Final) ($n = 149$)	1	CD20	CD45	CD58	CD66c	CD34	CD19	CD10	CD38
	2	SmIgκ	CD45	CyIgμ	CD33	CD34	CD19	SmIgM and CD117	SmIgλ[c]
	3	CD9	CD45	NuTdT	CD13	CD34	CD19	CD22	CD24
	4	CD21	CD45	CD15 and CD65	NG2	CD34	CD19	CD123	CD81

Abbreviations: AF700, alexa fluor 700; ALL, acute lymphoblastic leukemia; AmCyan, *Anemonia Majano* cyan fluorescent protein; APC, allophycocyanin; BCP, B-cell precursor; BM, bone marrow; Cy, cytoplasmic; Cy7, cyanin7; FITC, fluorescein isothiocyanate; H7, hilite7; Nu, nuclear; PacB, pacific blue; PacO, pacific orange; PB, peripheral blood; PE, phycoerythrin; PerCPCy5.5, peridinin–chlorophyll–protein–cyanin5.5; Sm, surface membrane. [a]Further information about markers and hybridomas is provided in the Appendix. [b]A total of 215 samples (172 BM, 36 PB and 7 other types of samples) was evaluated. Among them, 193 corresponded to BCP-ALL patients and 18 and 4 BM and PB from healthy donors, respectively. [c]Testing of CyIgλ-APCC750 is ongoing to increase the stain index of CyIgλ cells. Highlighted boxes: changes as compared to previous version.

Table 11. Utility of BCP-ALL markers

Tube	*Target antigen*	*Identification of blasts*	*Additional markers, 1st level*			*Additional markers, 2nd level*		*Aim per tube*
			Positive diagnosis	*Differential diagnosis*[a]	*Classification (e.g. maturation stage)*	*Classification (molecular aberrancy)*	*LAP identification*	
Backbone Markers	CD34	X	X			X		Identification of blasts
	CD19	X	X					
	CD45	X		X				
Tube 1	CD20		X				X	Diagnosis
	CD58						X	Classification
	CD66c					X	X	LAP markers
	CD10		X		X		X	Molecular
	CD38			X		X	X	subtypes
Tube 2	SmIgκ			X	X			Diagnosis Classification
	CylgμCylgμ		X		X			
	CD33			X				
	CD117			X				
	SmIgM			X	X			
	Smlgλ			X	X			
Tube 3	CD9					X	X	Diagnosis Classification LAP markers Molecular subtypes
	NuTdT		X					
	CD13			X				
	CD22		X				X	
	CD24		X			X	X	
Tube 4	CD21						X	Classification LAP markers Molecular subtypes
	CD15			X		X		
	CDw65			X		X		
	NG2					X		
	CD123			X			X	
	CD81						X	

Abbreviations: ALL, acute lymphoblastic leukemia; AUL, acute undifferentiated leukemia. BCP, B-cell precursor; Cy, cytoplasmic; LAP, leukemia-associated phenotypes; MPAL, mixed phenotype acute leukemia; Nu, nuclear; Sm, surface membrane. [a]Main differential diagnoses considered: mature B-cell malignancies, normal immature B-cells (hematogones), other acute leukemias with B-cell marker expression, MPAL/AUL.

second- level markers, based on their relevance for both adult and pediatric BCP-ALL. Noteworthily, few antibodies were conjugated with the new fluorochromes at the time the panel was designed. This required multiple custom conjugations, testing of the new antibody conjugates in comparison to the standard fluorochrome conjugates using reference samples, and evaluation of the newly designed antibody panel on a series of BCP-ALL samples. Each modification within the antibody panel had a significant impact on its configuration, so that a new round of testing was needed. The final configuration of the BCP-ALL panel is thus the result of a carefully thought-out design and multiple rounds of testing to optimize technical aspects, for example target antigens, fluorochrome conjugates and antibody combinations (Table 10).

Most EuroFlow panels are designed in such a way that each tube is disease-oriented, lineage-related or aims at a specific goal. The BCP-ALL panel could not be easily built in this way, as many markers are associated with multiple aims. For instance, CD22 and CD10 are both useful for positive diagnosis of BCP-ALL and the identification of LAP for MRD assessment. In addition, CD10 is also useful for subclassification of BCP-ALL. Nevertheless, each tube in the final panel has an underlying rationale that covers one or multiple aims as summarized in Table 11. The way in which the markers were combined should enable usage of both conventional data analysis procedures and software-based link of all information obtained with the panel.

Markers for positive and differential diagnosis of BCP-ALL. The first goal of the BCP-ALL panel is to make a diagnosis of BCP-ALL. For this purpose, the following specific aims should be reached: (1) confirmation of the immaturity of the suspected or abnormal cell population, (2) confirmation of the B-lineage origin, (3) exclusion of overlap with other cell lineages, and (4) demonstration of the malignant versus normal/reactive immunophenotype of the gated cell population. Asynchronous expression of antigens (for example, co-expression of $CD20^{hi}$ and $CD34^{hi}$), aberrant or ectopic antigen expression (for example, $CD33^{hi}$), and disappearance of normal phenotypic maturation kinetics, are all evidence in favor of the malignant nature of immature lymphoid B-cells.

The BCP-ALL panel included B-lineage-associated markers (CD22, CD24, CD10, CD20, Cylg, Smlg), markers for differential diagnosis with other acute leukemias (for example, CD13, CD33, CD117, CD15, CD65 to exclude AML) and other markers useful for comparison with and distinction from normal B-cell development patterns (NuTdT, CD10, CD38, CD20, CD123).

CD22 is strongly associated with the B-lineage, but is not B-cell specific, as it is also expressed on normal basophils, mast cells and plasmocytoid dendritic cells (pDC).[65–67] Within lymphoid cells, its expression indicates B-cell commitment and it appears at a very early stage of normal B-cell development. CD22 was at first conjugated with AF700, but staining was too weak (mean SI on mature B-cells of 3.7) and so an APC conjugate was preferred (mean SI of 85.4) and selected. Similarly to CD22, CD24 is also expressed on B-cells at very early stages, but it is also present on mature granulocytic cells. The first CD24 reagent evaluated was conjugated with AF700 and gave an acceptable staining (mean SI of 6.6) despite being weaker than PE conjugates (mean SI of 12.7). AF700 was later compared with and replaced by a CD24-APCH7 reagent, which gave slightly brighter staining (mean SI of 15.2), in line with other EuroFlow antibody panels that contain CD24.

Myeloid antigens (CD13, CD33, CD117, CD15, and CD65) were added in order to detect CD19-expressing AML, which might not

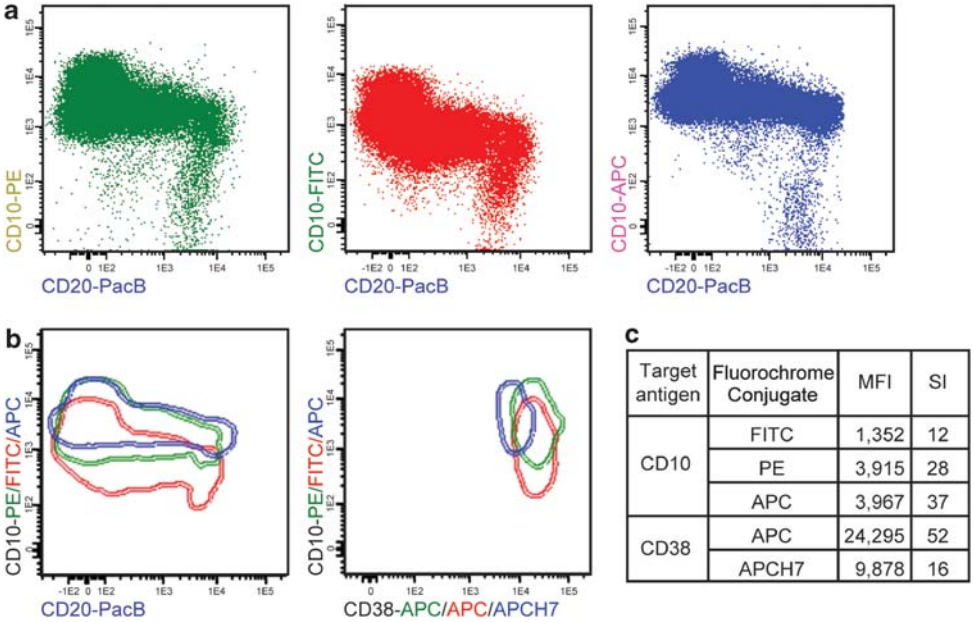

c

Target antigen	Fluorochrome Conjugate	MFI	SI
CD10	FITC	1,352	12
	PE	3,915	28
	APC	3,967	37
CD38	APC	24,295	52
	APCH7	9,878	16

Figure 14. Performance of the distinct combinations of CD10, CD20 and CD38 used to identify B-cell precursors and evaluate normal B-cell maturation in the bone marrow. Representative dot plots of the different fluorochrome conjugates tested are shown. Thirteen bone marrow samples from reactive or regenerating bone marrows at various time points after chemotherapy were stained using the three combinations in parallel and analyzed together after merging. (**a**) Resolution of individual normal precursor B-cells is optimal using a CD10–PE reagent (green dots). Similar discrimination is reproduced using CD10–APC (blue dots) whereas discrimination is worsened when using CD10–FITC (red dots). (**b**) Virtual merging of the three previous configurations demonstrates that CD10–APC (blue line, left panel) provides equivalent discrimination. CD38–APCH7 (blue line, right panel), despite generating significantly weaker signals than CD38–APC (red line, right panel), correctly recapitulates resolution of the distinct subpopulations and places the most immature population close to the bright 10^4 level. (**c**) Mean fluorescence intensity (MFI) and stain index (SI) of the different reagents tested.

have been positively identified by the ALOT. Given that SmIgμ cannot be expressed independently of CyIgμ and that BCP-ALL virtually never shows CD117 expression, CD117 and SmIgμ were combined in the same tube in the same fluorochrome position. In case of CyIgμ negativity and SmIgμ + CD117 positivity, this latter signal can be attributed to CD117 and a SmIgμ$^-$ CD117$^+$ immunophenotype. CD15 and CD65 were also pooled in the same position, as the information they provide in BCP-ALL cases is similar and overlapping. In fact, both myeloid antigens may also represent cross-lineage markers, supporting the malignant nature of the BCP-ALL population, and to a certain extent they provide information that may contribute to subclassification of BCP-ALL (see below).

When immature lymphoid cells (also referred to as hematogones) are identified by cytomorphology, the primary clinical question may be reduced to the distinction between malignant and normal/regenerating B-cell precursors. Normal/regenerating B-cell precursors display dynamic and reproducible immunophenotypic maturation patterns with sequential and coordinated expression of multiple antigens,[5,11,124] while BCP-ALL cell populations are far more homogeneous. The normal precursor-B-cell maturation pattern is mainly characterized by decreasing expression of both CD38 and CD10 and increasing expression of CD20.[5,11,124] Consequently, these three markers were combined in a single tube and were compared in several combinations, for example CD10 – PE/CD38 – APC/CD20 – PacB, CD10 – FITC/CD38 – PE/CD20 – PacB and CD10 – APC/CD38 – APCH7/CD20 – PacB, together with the three backbone markers (Figure 14). The second combination was discarded because of the dim staining intensity of the CD10 – FITC conjugates (Figure 14c), while the first and the third combination were most efficient for assessment of normal B-cell development (Figure 14a and b). We opted for the latter in order to keep the FITC and PE channels free for other characterization markers. NuTdT is an immaturity marker which is mainly expressed in B and T lymphoid lineage cells but that is also found at a variable percentage in >25% of AML cases.[52,127–129] Consequently, this marker lacks lineage specificity but was found to be useful to (i) confirm the immaturity of B-cells and (ii) to contribute to the distinction between normal and malignant profiles, as NuTdT expression is normally restricted to very early B-cell precursors.

Noteworthily, the selected characterization markers can also contribute to re-orientation towards the LST/ B-CLPD protocol in cases of mature B-CLPD, which were initially misinterpreted on morphological grounds as compatible with an acute leukemia. Such re-orientation can be based on SmIgM, SmIgκ and SmIgλ in addition to CD45, CD34, NuTdT and CD38, a set of markers that enables distinction between mature and immature neoplastic B-cells.

Markers for subclassification of BCP-ALL. Information on the maturation stage of BCP-ALL generally relies on the expression of CD10, CyIgμ, SmIgM, CyIgκ and CyIgλ.[27,34] Consequently, we aimed to obtain this information from a single tube. For this purpose Igκ and Igλ were labeled with novel fluorochromes (PacB and APCH7, respectively). The two Igμ antibodies were initially placed in the FITC and PE positions, but Igμ-PE staining appeared to be unreliable (for example, high levels of unspecific staining). As Igμ-APC only worked well as surface staining, we finally opted for the CyIgμ-FITC/SmIgM-APC configuration.

Many antigens have been reported to be aberrantly expressed in BCP-ALL cases in association with specific recurrent molecular abnormalities.[45] Such markers were also selected albeit that they are positioned in different tubes, but the new software and data analysis tools can combine the information for subclassification of BCP-ALL. BCR-ABL-positive cases are associated with frequent expression of myeloid markers such as CD13 and CD33 in addition to CD34^{hi} and CD38^{lo}, typically without expression of CD117.[43,130] CD66c (KOR-SA3544) has also been reported to be preferentially

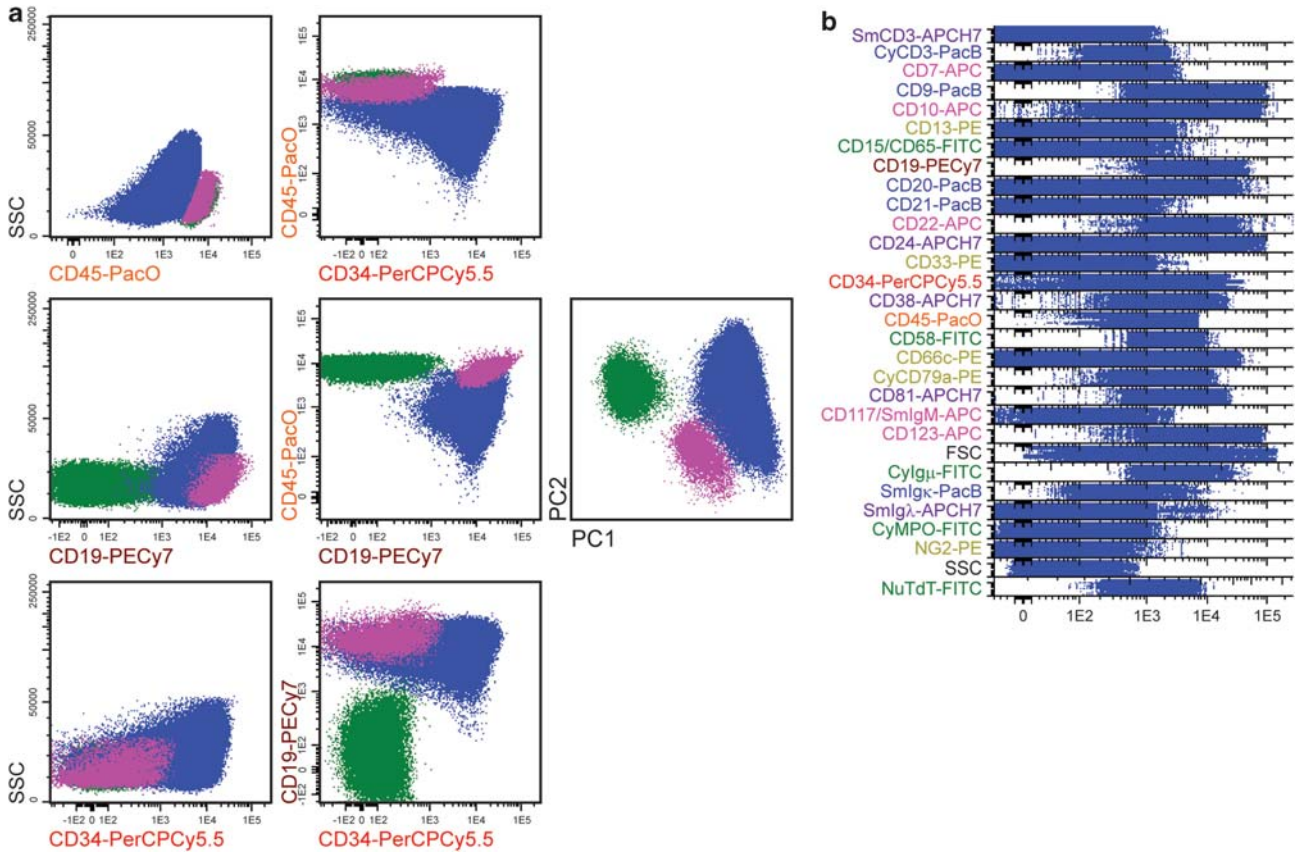

Figure 15. An illustration of the strategy used to gate B cell precursor (BCP)–acute lymphoblastic leukemia (ALL) blasts (**a**) and to evaluate their whole immunophenotypic profile using a band dot plot from the Infinicyt software (**b**). The BCP-ALL blast cell population is depicted as blue dots, while normal residual B- and T-cells are shown as purple and green dots, respectively.

expressed in *BCR-ABL* fusion gene and in hyperdiploid BCP-ALL cases.[131–133] Given the potential impact of CD66c, the antibody was placed in the strong PE channel. *MLL*-rearranged cases generally show a $CD19^{+}/CD34^{+}/NuTdT^{+}/CD10^{-}/CD15^{+/-}/CD65^{+/-}/CD9^{+}/CD24^{-/partially+}$ immunophenotype[134,135] with characteristic expression of NG2, although this is not specific.[136] NG2 (7.1) was introduced with the bright PE labeling. TEL-AML1 BCP-ALL are known to exhibit a $CD9^{-}/CD20^{-}/CD66c^{-}$ pattern in addition to CD19, CD10, NuTdT and CD34 positivity and $CD20^{-/lo}$.[42,137,138–140] CD9 was placed in the PacB channel and found to perform satisfactorily. Lastly, *E2A-PBX1* gene rearrangement is typically associated with a $CD19^{+}/CD10^{+}/CD34^{-}/CyIg\mu^{+}/SmIgM^{-}$ pre-B immunophenotype associated with negativity or partial positivity for CD20 and strong positivity for CD9.[126] Most other molecular abnormalities do not show clear phenotypic associations.

Markers for the identification of LAP and MRD assessment. MRD assessment by flow cytometry is increasingly used in the management of hematological malignancies, including BCP-ALL.[141–145] The CD19, CD34, CD45, CD10, CD38, CD20 combination (tube 1 of the BCP-ALL panel) is highly efficient in discrimination of normal/regenerating versus malignant immature B-cells and could represent an MRD-oriented combination.[140,141,146–148] LAP markers can further contribute to the discrimination between normal/regenerating and malignant B-cell precursors. Accordingly, in addition to the aforementioned CD22, CD24, CD66c and CD9 antigens, CD123, CD21, CD81 and CD58 were selected. CD123 is a major LAP marker, but is not consistently overexpressed by blast cells;[149] in the proposed BCP-ALL panel this antibody is conjugated with the bright APC fluorochrome. CD21 can be expressed by $CD19^{+}/CD34^{+}$ malignant B-cells while absent in their normal counterparts;[150] because of its satisfactory labeling a CD21-PacB reagent was chosen. CD81 is a tetraspanin molecule that is highly expressed on normal B-cell precursors, but is found at abnormally low levels in blast cells from a substantial percentage (>80%) of BCP-ALL patients.[151] CD58 is often overexpressed by blast cells versus regenerating normal precursor B-cells (for example, hematogones).[152,153] Because of design constraints, an FITC labeled CD58 reagent was selected. Although the CD58-FITC signal was weaker than the reference PE conjugate, the discrimination between normal and malignant cells was still satisfactory.

It is worth noting that the markers finally chosen for the BCP-ALL antibody panel were selected from an extensive list of candidate-antigens cited in the literature or considered to be relevant based on the experience of EuroFlow members. Each marker was discussed and many were not chosen (for example, CD52, ZAP-70, HLADR, CD135, CD44, CD11a, CD14, CyBcl-2, CD7, CD25, CD5, CD79b), because their utility was concluded to be of limited value compared to the selected markers.

BCP-ALL immunostaining protocol. Use of the BCP-ALL panel will usually be dictated by results obtained with the ALOT. In case of high suspicion of BCP-ALL (in children for instance), the ALOT and the BCP-ALL panel can be run at the same time, but the ALOT should always be interpreted first to ensure that another panel is not indicated. If the clinical suspicion and cytomorphological information from BM smears merely requires discrimination between hematogones and leukemic cells, application of the ALOT together with the first BCP-ALL tube will be sufficient to provide the correct answer.

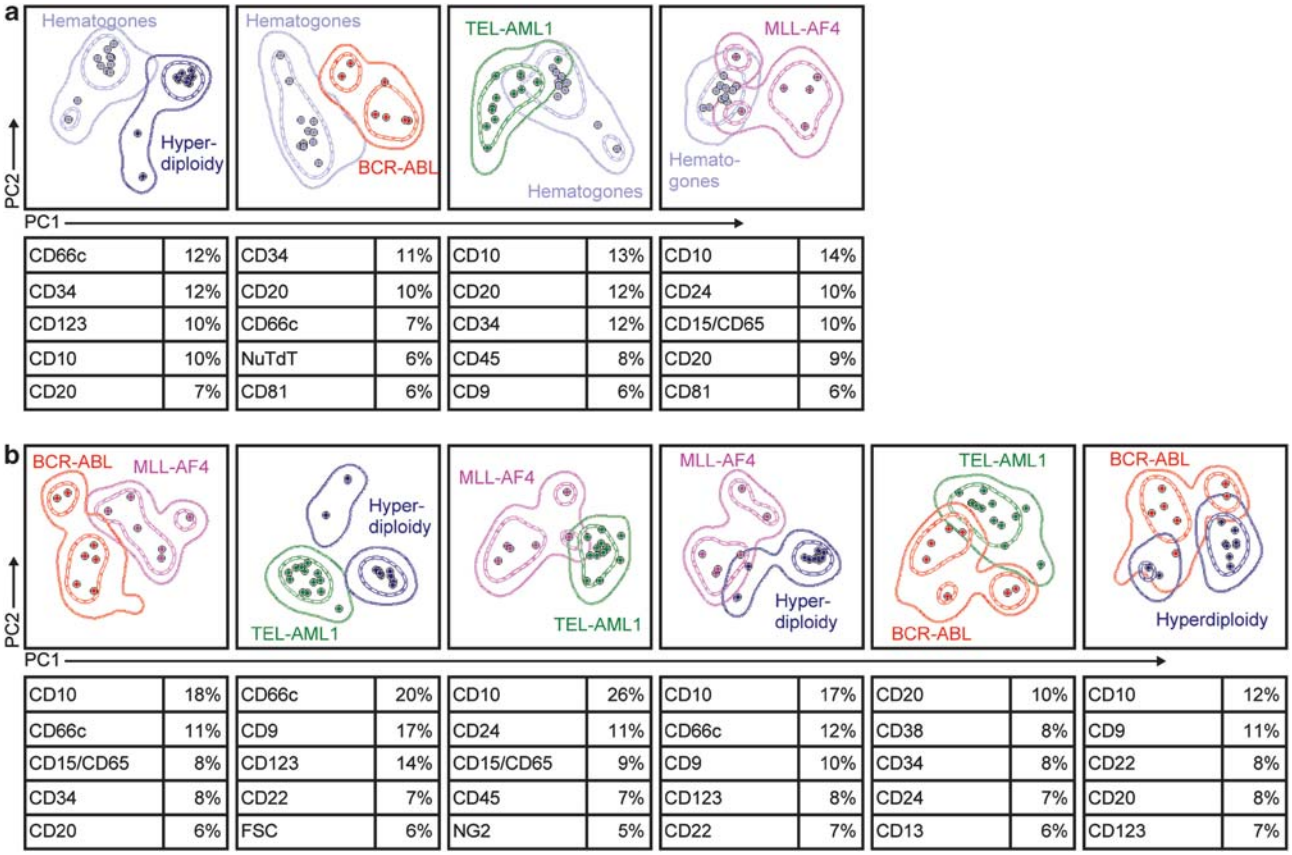

CD66c	12%	CD34	11%	CD10	13%	CD10	14%
CD34	12%	CD20	10%	CD20	12%	CD24	10%
CD123	10%	CD66c	7%	CD34	12%	CD15/CD65	10%
CD10	10%	NuTdT	6%	CD45	8%	CD20	9%
CD20	7%	CD81	6%	CD9	6%	CD81	6%

CD10	18%	CD66c	20%	CD10	26%	CD10	17%	CD20	10%	CD10	12%
CD66c	11%	CD9	17%	CD24	11%	CD66c	12%	CD38	8%	CD9	11%
CD15/CD65	8%	CD123	14%	CD15/CD65	9%	CD9	10%	CD34	8%	CD22	8%
CD34	8%	CD22	7%	CD45	7%	CD123	8%	CD24	7%	CD20	8%
CD20	6%	FSC	6%	NG2	5%	CD22	7%	CD13	6%	CD123	7%

Figure 16. Illustrating principal component analysis (PCA) bivariate dot plot representations (automated population separator (APS) views) of the clustering obtained in the pairwise multivariate PCA of B-cell precursor (BCP)–acute lymphoblastic leukemia (ALL) immunophenotypes associated with distinct molecular subgroups of BCP-ALL cases and normal/regenerating hematogones (hematogones, gray circles; hyperdiploid cases, violet circles; BCR-ABL$^+$ cases, red circles; TEL-AML1$^+$ patients, green circles; and MLL-AF4$^+$ cases, pink circles). Each circle represents median values of individual cases for all immunophenotypic markers in the EuroFLow BCP-ALL panel contributing to principal component (PC)1 and PC2. Contour lines represent s.d. curves (dotted and continuous lines represent 1s.d. and 2s.d., respectively). The five most informative markers contributing to the best discrimination between each pair of disease subgroups are displayed at the bottom of each plot, in a decreasing order of percentage contribution to the discrimination.

The BCP-ALL panel should be run using the EuroFlow SOP for instrument settings and immunostaining in combination with the Infinicyt software to allow appropriate linkage between the tubes and the ALOT. Of note, the ALOT and BCP-ALL panel includes tubes with only surface staining (tubes 1 and 4 of the BCP-ALL panel) and tubes with both surface and intracellular staining (tubes 2 and 3 of the BCP-ALL panel and ALOT). Each tube should be treated with the appropriate sample preparation protocol for staining of surface markers or surface plus intracellular markers. The different impact of the pre-analytical steps on light scatter parameters and fluorochrome intensities of backbone markers is automatically recognized and adjusted by the software (harmonization process),[33] allowing merging and calculation of marker expression based on parameters measured under different preanalytical conditions. This approach has been validated in B-CLPD[33] as well as on a series of 9 BCP-ALL samples using the BCP-ALL panel (data not shown).

Evaluation of the BCP-ALL panel using conventional versus multivariate data analysis approaches

In order to evaluate the BCP-ALL panel, its final configuration was run on 149 freshly collected cell samples from adult ($n = 37$) and childhood BCP-ALL cases ($n = 112$) derived from different tissues. Testing was carried out by seven laboratories, always in combination with the ALOT. Relevant clinical and biological annotations were collected whenever available, including the most relevant molecular abnormalities (for example, BCR-ABL, TEL-AML1, E2A-PBX, *MLL* rearrangements). To date molecular annotations were completed for 65/149 cases.

Data were analyzed locally using the Infinicyt software including specific gating of the blast cell population based on backbone markers. Noteworthily, the backbone markers selected proved to be highly efficient in specifically selecting all BCP-ALL blast cells in every case analyzed. Interpretation could be then performed in a conventional manner assisted by data analysis tools such as histogram band plots that instantly provided a phenotypic profile of the leukemic population (Figure 15). Through this approach, conventional subclassification of BCP-ALL such as EGIL classification was obtained; BI 18 cases (12%), BII 108 cases (73%) and BIII 23 cases (15%) with an identical distribution to that derived from local panels.

A key challenge for flow cytometry is to identify phenotypic features that could facilitate subclassification of BCP-ALL. Current WHO classification stratifies BCP-ALL according to molecular abnormalities.[34] Consequently, it will be important to determine to what extent flow cytometry immunophenotyping is able to identify genotypic subsets among the phenotypically heterogeneous group of BCP-ALL. Interestingly, multivariate PCA of the whole immunophenotype of BCP-ALL blast cell populations obtained with the ALOT plus BCP-ALL panel demonstrated recognizable phenotypic patterns that could distinguish different molecular-associated entities from both normal and reactive hematogones (Figure 16a) and between other molecular

subgroups (Figure 16b). Based on this strategy, we may be able to define phenotypic subsets of BCP-ALL, which are enriched for specific molecular abnormalities, potentially allowing orientation of genetic screening. It should be emphasized that the currently identified phenotypic profiles do not represent surrogate markers for detection of genetic aberrations. Further investigation of BCP-ALLs with extensive annotations and clinical correlations is required before further conclusions can be made.

CONCLUSION

The BCP-ALL antibody panel proved to be highly efficient in combination with the ALOT, in: (i) identifying BCP-ALL blast cells in a highly sensitive and specific way, (ii) distinguishing normal from leukemic B-cell precursors and (iii) subclassifying BCP-ALL into conventional maturation-associated subtypes of disease; additionally, preliminary data also suggest that the panel could contribute to the orientation of further molecular genetic screening for rapid identification of molecular subgroups of BCP-ALL.

SECTION 6. ANTIBODY PANEL FOR T-ALL

L Lhermitte[1], V Asnafi[1], S Böttcher[2], M Brüggemann[2], L Sedek[3], T Szczepański[3], E Mejstrikova[4], T Kalina[4], A Mendonça[5], P Lucio[5], VHJ van der Velden[6], H Wind[6], J Flores-Montero[7], JJ Pérez[8], M Muñoz[9], AS Bedin[1], JJM van Dongen[6], A Orfao[7] and E Macintyre[1]

[1]AP-HP, Paris, France; [2]UNIKIEL, Kiel, Germany; [3]SUM, Zabrze, Poland; [4]DPH/O, Prague, Czech Republic; [5]IPOLFG, Lisbon, Portugal; [6]ERASMUS MC, Rotterdam, The Netherlands; [7]USAL, Salamanca, Spain; [8]HUS, Salamanca, ES and [9]Cytognos SL, Salamanca, Spain

BACKGROUND

The EuroFlow T-ALL antibody panel aims at the (immunophenotypic) diagnosis and characterization of T-ALL. T-ALL includes a heterogeneous group of malignancies defined by the expansion of immature T-cell precursors blocked at specific stages of maturation, typically deviated from normal differentiation pathways.[56,154–158] Although T–ALL and T-cell lymphoblastic lymphoma (T-LBL) present differently, primarily with respect to involvement of BM and blood relative to tissue involvement,[159] they are very closely-related diseases. In particular, there are no significant immunophenotypic differences and the WHO 2008 classification considers them to be one disease entity.[35]

The T-ALL EuroFlow panel has been designed to be applied when the ALOT orientates towards an expansion of T-lineage precursors. In a first step, the panel aims at recognition of immature T-cells, which is in itself strong evidence in favor of T-ALL. T-cell development occurs primarily in the thymus, and identification of immature T-cells in PB, BM or tissues other than the thymus is *per se* abnormal. However, when immunophenotyping mediastinal biopsies, the panel should also be able to distinguish malignant from normal thymocytes. Furthermore, the panel aims at subclassification of T-ALL according to the T-cell lineage maturation stages and potentially also according to the underlying genetic subgroup. A large variety of somatic genetic markers contribute to T-ALL oncogenesis.[154,157,158,160] Some co-exist (for example, *NUP214-ABL1* and overexpression of *TLX1/TLX3*[161–163]) and may occur in subclones, suggestive of sequential acquisition. This genetic complexity is likely to result in a variety of deregulated transcriptional networks, which impact differently on immunophenotypic profiles. So far, relatively few immunophenotypic profiles in T-ALL have been associated with recurrent molecular abnormalities, compared to BCP-ALL or AML. However, some specific correlations do exist, for example, frequent CALM-AF10 rearrangements in CD2$^-$ and/or TCR$\gamma\delta^+$ T-ALL,[164] but this association is not constant or specific. Conversely, a significant number of T-ALL molecular abnormalities are associated with a specific T-cell maturation arrest[165] or gene expression profile.[154,166,167] Overexpression of TLX1 is typically associated with a cortical immunophenotype.[165,168] Despite phenotypic similarities between T-ALL and normal thymic development,[165] detailed multiparameter immunophenotyping also allows identification of protein expression patterns, which distinguish T-ALLs from their normal thymic counterparts.

Overall, the 8-color T-ALL antibody panel allows for positive and differential diagnosis of T-ALL and subclassification of the disease according to different classification systems and at the same

Table 12. Design of the T-ALL panel in four consecutive testing rounds[a]

Version (no. of cases)[b]	*Tube*	*Fluorochromes and markers*							
		PacB	*AmCyan*	*FITC*	*PE*	*PerCPCy5.5*	*PECy7*	*APC*	*AF700*
1 ($n=7$)	1	SmCD3	CD45	NuTdT	CD99	CD5	CD10	CD4	CyCD3
	2	SmCD3	CD45	CD7	CD117	HLADR	CD8	CD1a	CyCD3
	3	SmCD3	CD45	TCR$\alpha\beta$	TCR$\gamma\delta$	—	CD56	—	CyCD3
	4	SmCD3	CD45	CD44	CD13	CD45RA	CD33	CD123	CyCD3
2 ($n=12$)	1	SmCD3	CD45	NuTdT	CD99	CD5	CD10	CD4	CyCD3
	2	SmCD3	CD45	CD2	CD117	HLADR	CD8	CD1a	CyCD3
	3	SmCD3	CD45	TCR$\alpha\beta$	TCR$\gamma\delta$	—	CD56	CyTCRβ	CyCD3
	4	SmCD3	CD45	CD44	CD13	CD33	CD45RA	CD123	CyCD3
		PacB	*PacO*	*FITC*	*PE*	*PerCPCy5.5*	*PECy7*	*APC*	*APCH7*
3 ($n=29$)	1	SmCD3	CD45	NuTdT	CD13	CD5	CD10	CD1a	CyCD3
	2	SmCD3	CD45	CD2	CD117	CD4	CD8	CD7	CyCD3
	3	SmCD3	CD45	TCR$\gamma\delta$	TCR$\alpha\beta$	HLADR	CD56	CyTCRβ	CyCD3
	4	SmCD3	CD45	CD44	CD99	CD33	CD45RA	CD123	CyCD3
4 (Final) ($n=64$)	1	CyCD3	CD45	NuTdT	CD99	CD5	CD10	CD1a	SmCD3
	2	CyCD3	CD45	CD2	CD117	CD4	CD8	CD7	SmCD3
	3	CyCD3	CD45	TCR$\gamma\delta$	TCR$\alpha\beta$	CD33	CD56	CyTCRβ	SmCD3
	4	CyCD3	CD45	CD44	CD13	HLADR	CD45RA	CD123	SmCD3

Abbreviations: AF700, alexa fluor 700; AmCyan, *Anemonia Majano* cyan fluorescent protein; APC, allophycocyanin; BM, bone marrow; Cy, cytoplasmic; Cy5, cyanin5; Cy7, cyanin7; FITC, fluorescein isothiocyanate; H7, hilite7; Nu, nuclear; PacB, pacific blue; PacO, pacific orange; PB, peripheral blood; PE, phycoerythrin; PerCP, peridinin–chlorophyll–protein; Sm, surface membrane; T-ALL, T-cell acute lymphoblastic leukemia. [a]Further information about markers and hybridomas is provided in the Appendix. [b]A total of 112 samples were evaluated (72 BM, 26 PB, 9 pleural effusions and 5 other types of samples); among them, 102 were from T-ALL patients and 10 from healthy donors. Highlighted boxes: changes as compared to previous version.

Table 13. Utility of T-ALL markers

Tube	*Target antigen*	*Identification of blasts*	*Additional markers, 1st level*			*Additional markers, 2nd level*		*Aim of tube*
			Positive diagnosis	*Differential diagnosis*[a]	*Classification (EGIL)*	*Classification (including TCR-chain and ETP-ALL)*	*LAP markers (MRD/MDD)*	
BB markers	CyCD3	X	X	X			X	Identification of blasts
	CD45	X	X				X	
	SmCD3	X			X		X	
Tube 1	NuTDT		X				X	Diagnosis
	CD99		X				X	Classification
	CD5		X	X	X	X	X	Maturation stage
	CD10			X			X	LAP markers
	CD1a		X		X	X	X	Assessment of minimal disseminated disease
Tube 2	CD2		X		X		X	Diagnosis Classification Maturation stage LAP markers
	CD117			X		X		
	CD4		X					
	CD8		X		X	X		
	CD7		X		X		X	
Tube 3	TCR$\gamma\delta$		X	X	X		X	Diagnosis Classification Maturation stage LAP markers
	TCR$\alpha\beta$		X		X			
	CD33			X		X		
	CD56			X		(x)		
	CyTCRβ					X		
Tube 4	CD44					(x)		Classification
	CD13			X		X		
	HLADR					X		
	CD45RA					(x)	X	
	CD123			X		X		

Abbreviations: ALL, acute lymphoblastic leukemia; AUL, acute undifferentiated leukemia; BB, backbone; Cy, cytoplasmic; ETP, early T progenitor; LAP, leukemia-associated phenotype; MDD, minimal disseminated disease; MPAL, mixed phenotype acute leukemia; MRD, minimal residual disease; Nu, nuclear; Sm, surface membrane; TCR, T-cell receptor. [a]Main differential diagnoses considered: mature T-cell malignancies, other acute leukemias with T-lineage marker expression, MPAL/ AUL; (x) to be assessed.

time it provides additional information that reflects T-ALL heterogeneity.

Design of the T-ALL EuroFlow panel

The T-ALL protocol was designed in parallel to the ALOT and the BCP-ALL antibody panel. As a consequence, the rationale for its design (including the choice of backbone markers) was similar to that used for these two other protocols. Here we present the specificities of the T-ALL antibody panel and refer to Sections 1 and 5 for general design concepts. Table 12 summarizes the design of the T-ALL panel in four consecutive steps, while the specific aims of the individual markers are summarized in Table 13.

Selection of backbone markers

In order to link data from ALOT and the different tubes of the T-ALL panel, we aimed to identify a fixed combination of backbone markers capable of identifying all blast cells in every case with minimal contamination by other residual cells. In contrast to other EuroFlow panels, eligible markers for backbone selection were limited because they had to closely match the two criteria of: (i) broad expression, and (ii) efficiency for blast cell identification. Candidate markers included CD7, CD5, CyCD3 and CD99.[35] CD99 was not universally expressed, especially in more mature T-ALL, and its signal was considered to be too weak to allow clear gating of blasts from residual normal T-cells. CD5 was usually expressed but it may be dim or negative, especially in a subset of immature T-ALL.[71] CD7 was virtually always expressed, but it is not lineage-specific.[35] CyCD3 fits perfectly with the above-referred criteria, as by definition it is constantly expressed in T-ALL[35,48,169] and usually at high levels, allowing easy gating of blast cells. However, CyCD3 must be interpreted in combination with SmCD3 to exclude normal mature residual (or reactive) T-cells, which requires the combined assessment of CyCD3 and SmCD3. Finally, blast cell selection was improved by adding CD45 to discard non-lymphoid cells, even if CD45 is most often expressed at a high intensity on T-ALL blasts, thus making them overlap with mature lymphoid cells.[170] Based on these considerations, we finally set the T-ALL backbone as CD45 – PacO, CyCD3 – PacB and SmCD3 – APCH7. The choice of fluorochromes resulted from the strategic decision to use less common fluorochromes for gating markers so that the more common fluorochromes could be used for characterization markers in a more flexible way. Importantly, three T-ALL backbone markers were also included in the ALOT to benefit from the ALOT information on CyMPO,[36] CyCD79a[62–64] and CD34[49] expression using the merge function of the Infinicyt software.[16]

Selection of additional markers

Once the set of backbone markers was defined, we then completed the panel with a wide variety of T-lineage-related markers in order to strengthen and specify the T lineage affiliation of the leukemic cells, subclassify T-ALL according to maturation

stage and distinguish blast cells from other residual cells in the sample.

Markers for differential diagnosis of T-ALL. To specify the T-lineage maturation stage of blast cells, we chose CD2, CD4, CD5, CD7, CD8, CD10, CD99, TCRαβ and TCRγδ to be included in the panel.[2] Collective experience and additional testing allowed identification of appropriate combinations of antibodies and fluorochromes. For example, although PerCPCy5.5 may be a relatively weak fluorochrome, CD5 – PerCPCy5.5 worked remarkably well in T-ALL. This is also true for CD2 coupled to FITC. On the other hand, a CD10 – FITC conjugate was considered unsatisfactory and was consequently replaced by a bright CD10 – PECy7 reagent. It was logical to place CD4 and CD8 in the same tube and the CD4 – PerCPCy5.5/ CD8 – PECy7 combination performed well upon testing. For the TCR, we initially chose TCRαβ – FITC/ TCRγδ – PE in order to optimize detection of TCRγδ$^+$ T-ALL, but our results showed no advantage of the signal intensity for TCRγδ – PE relative to TCRγδ – FITC and detection of TCRαβ with FITC was less satisfactory than with PE, as was detection with the WT31 antibody relative to the IP26A clone. We consequently chose the combination TCRγδ – FITC (IMMU510) and TCRαβ – PE (IP26A).

To indicate the precursor nature of T-cells, we also added TdT, CD1a, CD34 and CD99 to the panel.[35,171] Detection of NuTdT can be difficult, but the TdT – FITC reagent selected gives reliable and robust staining. As this antibody was used concomitantly with staining for CyCD3 we initially compared permeabilization with Fix&Perm and FACS Lysing solution as used for the AML panel (see Section 7), and we finally opted for the Fix&Perm protocol because of optimal CyCD3 staining. Expression of CD99 is often relatively weak and it was consequently important to use a bright fluorochrome, such as PE. CD1a performed well with FITC, PE and APC. In order to group immature T lymphoid markers in one tube, CD1a was placed in the APC channel, with satisfactory results. As CD34 was in the ALOT tube, it was not repeated in the T-ALL panel.

We also introduced myeloid antigens (CD13, CD33, CD117), in addition to MPO that is assessed in the ALOT, but it is worth noting that these antigens are not sufficient for classification as MPAL as they are only considered as evidence of cross-lineage expression within the 2008 WHO criteria.[35,36] However, they are mainly expressed in very immature T-ALL, especially among those cases that fit with the early T-cell progenitor (ETP) entity.[68,70,71] With respect to the differential diagnosis, T-lineage-related antigens such as CD2, CD7, and even CD5 and CyCD3 may be expressed by so-called NK-cell precursor lymphoblastic leukemia/ lymphoma (NK-ALL).[35] CD56 is present in the panel and as such can help to diagnose this exceptional and provisional entity. It may, however, be difficult to distinguish NK-ALL and immature T-ALL,[35,36] since bona-fide, but predominantly immature, T-ALL cases can express CD56.[36,172–176] Whether these are distinct entities remains unclear.[35,36] The expression of myeloid markers in immature T-ALL but not in NK-ALL may be helpful in this situation.[36] Difficulties with differential diagnosis from plasmacytoid dendritic cell leukemias, which can express T-cell-associated markers (for example, CD2, CD7), can be partly solved with the profiles of CyCD3, CD4, CD123 and CD56 expression and to a lesser extent also with HLADR and CD45RA.[177–179]

Markers for subclassification of T-ALL. T-ALLs are classified according to their maturation arrest and on the basis of differential expression of certain markers.[27,35,180] Four distinct stages were classically defined by the EGIL group based on CD2, CD3, CD5, CD7, CD8, CD1a, and TCR expression.[27] Application of this classification is possible with the EuroFlow T-ALL antibody panel because all markers are present. We felt, however, that other markers were required in order to identify the stage of maturational arrest of T-ALL relative to normal thymopoiesis. In particular, classification of T-ALL according to their TCR expression, including CyTCRβF1, SmCD3, TCRαβ and TCRγδ expression, was considered relevant[165] in order to identify three stages of (i) immature (CyCD3$^+$/CyTCRβF1$^-$/SmTCR$^-$), (ii) pre-αβ (CyCD3$^+$/ CyTCRβF1$^+$/SmTCR$^-$) and (iii) mature (CyCD3$^+$/SmTCR$^+$) T-ALL blasts, discriminating among TCRγδ$^+$ and TCRαβ$^+$ T-ALL, which have been previously demonstrated to have prognostic impact.[181] The CyTCRβF1 antibody was custom-conjugated with APC, titrated and validated on CyTCRβ positive cell lines (DND41, Jurkatt, RPMI, CEM) or negative cell lines (SIL-ALL, Kasumi). This antibody was then placed within the *TCR-tube*, along with TCRγδ, TCRαβ and both CyCD3 and SmCD3, thus allowing both EGIL and TCR maturation-associated classifications with the T-ALL antibody panel although it provides a dim staining. Additional markers (CD44, CD45RA, HLADR, CD13, CD33 and CD123) were added in order to contribute to maturational staging.[69,182–185] Some assess immaturity (e.g. CD123[186]) or allow detection of the recently identified (very immature) ETP-ALL cases.[68,70,71] Prognosis of patients with the later is poor and requires appropriate therapeutic stratification.[70,71] The EuroFlow T-ALL panel allows recognition of this entity by co-expression of CyCD3$^+$, CD5^{lo}, CD1a$^-$, CD8$^-$ with stem-cell/myeloid markers including notably, CD34, CD117, HLADR, CD13 and CD33.[70,71]

LAP markers for MRD assessment. As for the BCP-ALL panel, evaluation of LAP already at diagnosis is essential for MRD assessment by flow cytometry.[141,142,144,146,187,188] Given the fact that MRD is assessed in PB or BM samples where virtually no immature T-cells exist, LAP markers are mainly represented by markers that determine the precursor nature of T-cells (immaturity markers). Such markers include CD34 (in ALOT) and NuTdT, CD1a and CD10 in tube 1 of the T-ALL antibody panel.[189,190] Interestingly, distinction between normal and leukemic T-ALL cells could be achieved with a single tube, that is, tube 1 of the T-ALL antibody panel. Of note, the T-ALL panel was designed based on markers listed from the literature and our collective experience. Other potential target antigens (for example, CD52, CD65, CD15, Bcl-2, CD20, CD24, CD64, CD14, CD15, CD65, NG2 and CD38) were not included, as they were considered to provide little added value as compared to those that were selected (Table 13).

Evaluation of the T-ALL panel using conventional and multivariate analysis

To evaluate the utility and efficiency of the T-ALL panel in making the diagnosis and identifying T-ALL subgroups (64) T-ALL cases were prospectively analyzed using both the ALOT and T-ALL panels versus local panels. Data from each T-ALL case were compiled within a single 29-dimensional data file, as described in previous sections. It was possible to confirm the T-ALL diagnosis in virtually all cases and to simultaneously classify T-ALL according to the existing WHO 2008, EGIL and TCR-based immunophenotypic classifications.[27,35,165] In fact, malignant immature T-cells could be distinguished from normal mature T-cells and, more significantly, even from normal human thymocytes, as illustrated in Figure 17. Multiparameter analysis of groups of T-ALL cases that are based on the overall immunophenotypic features of blast cells cluster apart from each other and their correlation with genetic and clinical characteristics will probably allow identification of specific subgroups. However, this will require prospective immunophenotypic analysis of a much larger number of T-ALL cases with full genetic and clinical annotations, given the oncogenetic and clinical heterogeneity of T-ALL. This needs acquisition within an appropriate anonymized database. Such an anonymized database is currently being developed by the EuroFlow group.

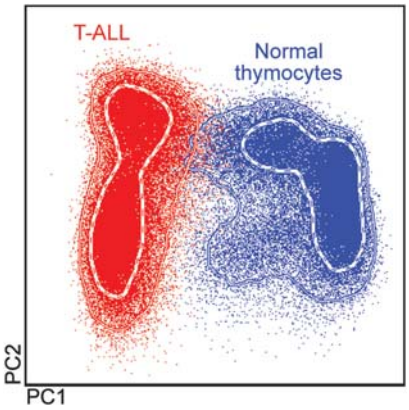

Figure 17. Overall immunophenotypic profile of T-acute lymphoblastic leukemia (ALL) blast cells (red dots) versus normal human thymocytes (blue dots) as assessed by the EuroFlow T-ALL panel. Of note, principal component analysis (PCA) showed a clear separation between the phenotypic profiles of normal versus leukemic T-cell precursors based on a principal component (PC)1 versus PC2 representation (automated population separator (APS)1 view of the Infinicyt software). Contour lines represent s.d. curves (dotted and broken lines represent 1s.d. and 2s.d., respectively).

CONCLUSION

The 4-tube T-ALL antibody panel in combination with the ALOT promises to be highly efficient for the diagnosis and phenotypic subclassification of T-ALL. At the same time it provides information about the presence of LAP that can be used for MRD monitoring. The panel is composed of a set of three backbone markers that allow simultaneous evaluation of the whole phenotypic profile of blast cells plus a set of markers devoted to the classification of T-ALL according to the EGIL and other alternative maturation-associated classification systems, together with the distinction between leukemic blasts and normal T-cell precursors. The markers are combined in such a way that the tubes facilitate flexible usage of the panel depending on the specific aim. For example, the EGIL classification of T-ALL is possible with tube 1, while definition of maturation stages according to TCR can be achieved with tube 3, and distinction between leukemic and normal cells is possible with solely tube 1.

SECTION 7. ANTIBODY PANEL FOR AML AND MDS

VHJ van der Velden[1], JG te Marvelde[1], M Cullen[2], E Mejstrikova[3], J Flores-Montero[4], L Sedek[5], S Richards[2], O Hrusak[3], T Szczepański[5], P Evans[2], T Kalina[3], H Wind[1], MB Vidriales[6], JJ Pérez[6], J Hernández[7], M Lopez-Botet[8], P Bettelheim[9], A Orfao[4] and JJM van Dongen[1]

[1]Erasmus MC, Rotterdam, The Netherlands; [2]UNILEEDS, Leeds, UK; [3]DPH/O, Prague, Czech Republic; [4]USAL, Salamanca, Spain; [5]SUM, Zabrze, Poland; [6]HUS, Salamanca, Spain; [7]Cytognos SL, Salamanca, Spain; [8]Immunology Unit, Universitat Pompeu Fabra, and IMIM-Hospital de Mar, Barcelona, Spain and [9]Central Laboratory, Otto Wagner Hospital, Vienna, Austria

BACKGROUND

The EuroFlow antibody panel for AML and MDS aims at the detection and classification (lineage assignment and definition of maturation profile) of AML and MDS. AML and MDS are both heterogeneous diseases, which, in contrast to T-ALL and BCP-ALL, can affect multiple cell lineages and multiple maturation stages. The EuroFlow AML/MDS antibody panel therefore focuses on all major myeloid lineages. This particularly concerns the neutrophilic lineage, monocytic lineage and erythroid lineage, but also the less frequent pDC lineage, basophilic lineage, mast cell and megakaryocytic lineages are covered. In addition to establishing the involved cell lineage(s) and maturational arrest(s) of the neoplastic cells, the EuroFlow AML/MDS panel also aims at the detection of aberrant expression of lymphoid-associated markers and abnormal lymphoid maturation profiles. The overall resulting immunophenotypic profile of the blast cells will allow classification of the malignancy and in some cases may be related to genetic abnormalities. For example, acute promyelocytic leukemia (APL) with t(15;17) typically has the immunophenotype of a promyelocyte (CyMPO$^+$, HLADR$^-$, heterogeneous CD13$^+$, homogeneous CD33$^+$, CD117$^+$) with abnormally negative to low CD15 expression,[41] while blast cells in AML with t(8;21) frequently co-express CD19[191] and in AML with inv(16) frequently are CD2$^+$.[192]

In patients with MDS, the role for flow cytometric immunophenotyping is not fully established, but recently immunophenotyping was included as one of the co-criteria for the diagnosis of MDS.[193] Several studies indeed have shown that immunophenotypic abnormalities can be detected in the vast majority of MDS patients, including abnormalities in lineages (or cases) with normal cytomorphological appearance.[194,195] However, as many immunophenotypic abnormalities are not specific for MDS, flow cytometric scoring systems are needed, but so far they have not been standardized.[10,196–203] International harmonization of flow cytometry MDS diagnostics is currently in progress.[14,204]

For patients with a suspicion of an acute (myeloid) leukemia, in the first instance the ALOT tube should be performed (see Section 1). If the results of the ALOT tube point towards a non-lymphoid acute leukemia (AML, ambiguous lineage acute leukemia or even pDC neoplasm), the AML/MDS panel should subsequently be performed. For patients with a clinical or cytomorphological suspicion of an MDS or an unexplained cytopenia, one may directly perform the AML/MDS panel (Figure 1).

Many antibodies have been reported to be useful for immunophenotyping of AML/MDS patients and several consensus reports have been published.[12,21,23,205] On the basis of these reports and the knowledge and experience of the EuroFlow members, several antibodies were selected and initially tested in the EuroFlow laboratories. After evaluation of the results during multiple EuroFlow meetings, positions of antibodies were changed or new antibodies were included/excluded in the antibody panel. The resulting antibody panel was subsequently tested again, and this cycle of testing–evaluation–optimization–retesting was repeated until the final EuroFlow AML/MDS panel was approved. The approved panel was also prospectively evaluated. In contrast to previous consensus reports, the EuroFlow AML/MDS antibody panel therefore is not solely based on knowledge, experience and opinions, but is also based on extensive testing and re-testing of many antibody combinations.

Design of the AML/MDS antibody panel

Design of the AML/MDS panel was based on a strategy that would search for the unequivocal identification of blast cells in every tube in the panel using the same set of backbone markers. In addition, a second group of markers was combined with the backbone markers, devoted to the characterization of the identified blast cells as well as of the maturation profile of BM precursors into the three major myeloid lineages (neutrophil, monocytic and erythroid lineages) and also several minor myeloid compartments less frequently involved in the disease (for example, basophil, mast cell, pDC and megakaryocytic precursors).

The combination of the backbone markers and new software tools allows a true multiparameter analysis of complete blast cell phenotypes with the EuroFlow AML/MDS antibody panel. With regard to the characterization markers, this antibody panel was designed in such a way that the more mature cell compartment (for example, CD34$^-$ precursors) of the three main myeloid cell lineages (granulocytic, monocytic, erythroid) could be optimally evaluated in single tubes. Using the backbone markers,

information from other tubes can easily be added to these 'lineage-oriented' tubes for the more immature (for example, $CD34^+$) precursor cells.

Selection of backbone markers. To optimally use the *n*-dimensional possibilities of the Infinicyt software including the merge and calculation functions, each tube needs to contain a number of identical antibodies that can be used to link the data from the other tubes. These so-called backbone markers should allow easy identification of the malignant population among remaining normal cells. Furthermore, they should reflect the potential heterogeneity of the malignant population in order to allow appropriate calculation of data based on the nearest-neighbor principle implemented in the Infinicyt software.[32] On the basis of knowledge and experience, CD34 and CD45 were directly selected as backbone markers for the AML/MDS panel. Other potential backbone markers, that is, CD117, HLADR, CD33 and CD11b, were evaluated on BM or PB samples from 96 AML patients. For this testing, the combination of HLADR(L243)–FITC, CD117(104D2)–PE, CD45(2D1)–PerCP, CD34(8G12)–APC, CD33(p67.6)–PECy7 and CD11b(ICRF44)–APCCy7 was used.

In 61/96 samples (63%), CD45 and CD34 were already sufficient for easy recognition of the heterogeneous leukemic population. In the remaining 25 patients, the additional value of the other markers was evaluated. The percentage of patients in which addition of CD117, HLADR, CD33 or CD11b allowed an easier gating of the leukemic cells was 51%, 40%, 20% and 23%, respectively. Inclusion of a fourth backbone marker gave best results for the combination CD34, CD45, CD117 and HLADR (9% extra patients). Addition of a fifth or sixth backbone marker hardly improved these results. Thus, by using CD34, CD45, CD117 and HLADR as backbone markers, efficient (sensitive and specific) gating of all leukemic blast cells was possible in 84/96 patients (88%; see Figure 18). In the remaining 12 patients gating of the leukemic cells was also possible, but it was less straightforward; these cases mainly concerned patients with monocytic leukemias. Most interestingly, combined expression of HLADR and CD117 is typically associated with distinct maturation (phenotypic) profiles in different myeloid lineages, for example, sequential loss of CD34 and CD117 in $HLADR^+$ monocytic and DC precursors versus CD34 and HLADR on $CD117^+$ maturing neutrophils/erythroid precursors.

To maintain optimal flexibility for the remaining antibodies, it was decided to preferentially select the less commonly available fluorochromes for the backbone markers. Initially CD34–PerCPCy5.5, CD117–PECy7, HLADR–PacB and CD45–AmCyan were tested. In addition, CD45–AmCyan was replaced by CD45–PacO, to be consistent with the other EuroFlow antibody panels (Table 14).

Selection of other characterization antibodies. As mentioned above, selection and combination of characterization markers in individual tubes was accomplished for detailed characterization of the main hematopoietic BM cell compartments (maturing neutrophils, monocytic and erythroid precursors) in the first three tubes of the AML/MDS panel. The other tubes were designed for assessment of cross-lineage and aberrant antigen expression profiles together with the evaluation of B-cell precursors and immature CD34 cells

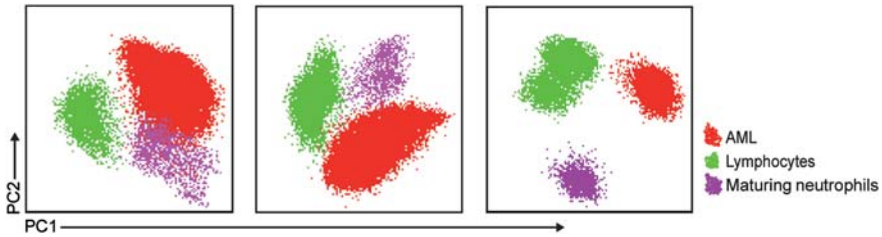

Figure 18. Identification of acute myeloid leukemia (AML) blast cells using the EuroFlow AML/myelodysplastic syndrome (MDS) panel backbone markers (CD34, CD117, HLADR and CD45). Automated population separator (APS) (principal component (PC)1 versus PC2) plots of three different AML patients are shown. Color codes are as follows: red dots, AML cells; green dots, mature lymphocytes; purple dots, maturing neutrophils.

Table 14. The EuroFlow AML/MDS antibody panel[a,b]

Tube	*PacB*	*PacO*	*FITC*	*PE*	*PerCPCy5.5*	*PECy7*	*APC*	*APCH7*	*Aim*
1	HLADR	CD45	CD16	CD13	CD34	CD117	CD11b	CD10	Diagnosis and classification, neutrophilic maturation, PNH
2	HLADR	CD45	CD35	CD64	CD34	CD117	CD300e (IREM2)	CD14	Diagnosis and classification, monocytic maturation, PNH
3	HLADR	CD45	CD36	CD105	CD34	CD117	CD33	CD71	Diagnosis and classification, erythroid maturation
4	HLADR	CD45	NuTdT	CD56	CD34	CD117	CD7	CD19	Aberrant expression of lymphoid markers, abnormal B lymphoid maturation
5	HLADR	CD45	CD15	NG2	CD34	CD117	CD22	CD38	Aberrant marker expression, stem cells
6	HLADR	CD45	CD42a and CD61	CD203c	CD34	CD117	CD123	CD4	Diagnosis and classification of AML Megakaryocytic, basophilic, and plasmacytoid dendritic cell lineages
7	HLADR	CD45	CD41	CD25	CD34	CD117	CD42b	CD9	Characterization of megakaryoblastic leukemia, and systemic mastocytosis

Abbreviations: AML, acute myeloid leukemia; APC, allophycocyanin; BB, backbone; BM, bone marrow; Cy7, cyanin7; FITC, fluorescein isothiocyanate; H7, hilite7; MDS, myelodysplastic syndrome; Nu, nuclear; PacB, pacific blue; PacO, pacific orange; PE, phycoerythrin; PerCPCy5.5, peridinin–chlorophyll–protein–cyanin5.5; PNH, paroxysmal nocturnal hemoglobinuria. [a]Further information about markers and hybridomas is provided in the Appendix. [b]A total of 96 BM samples were evaluated for selection of the BB markers. An additional 84 BM AML samples were evaluated with this version (final) of the panel.

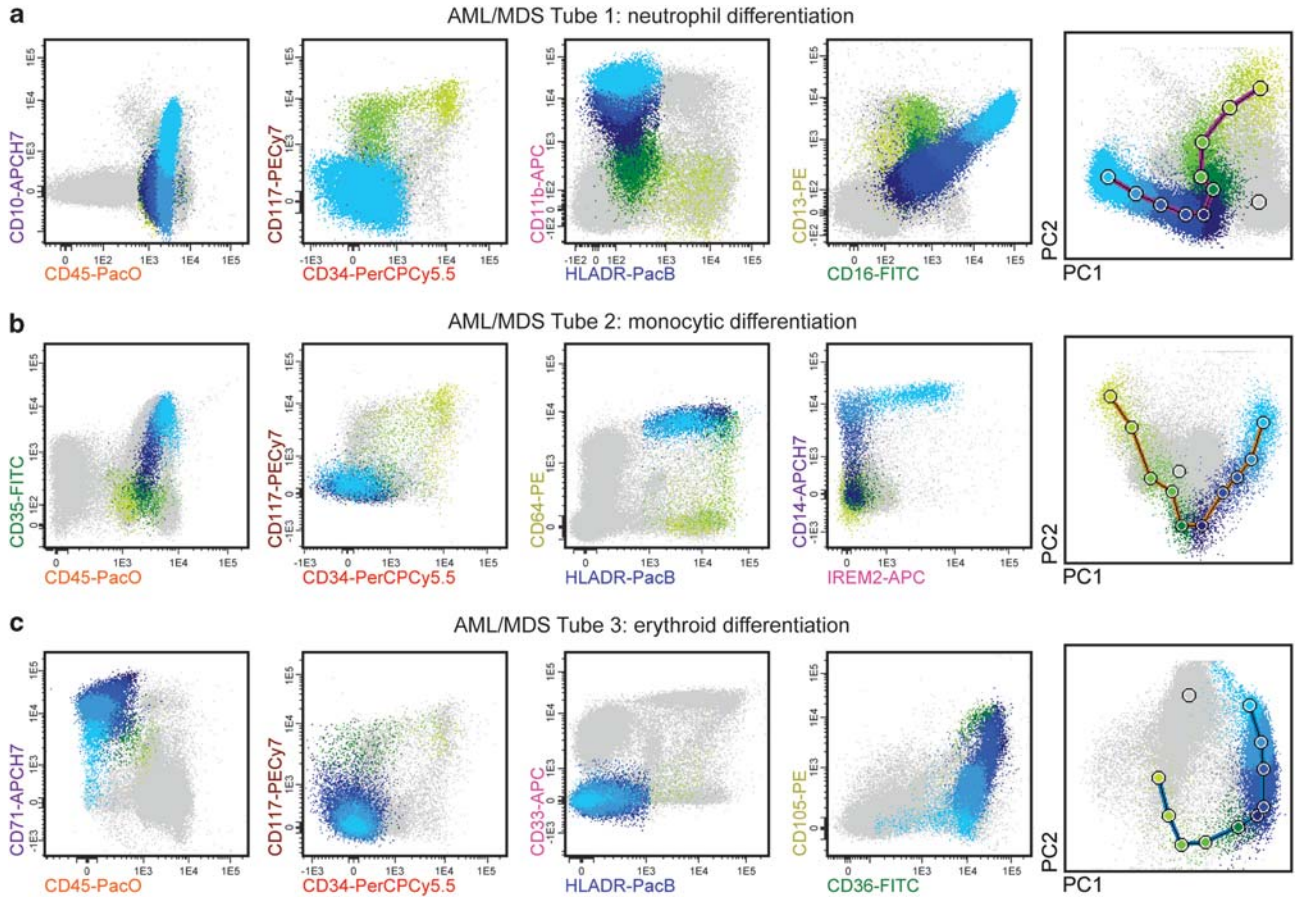

Figure 19. Neutrophil, monocytic and erythroid differentiation in bone marrow from a healthy subject as determined using tube 1 (maturing neutrophils), tube 2 (monocytic cells) and tube 3 (erythroid precursors) of the EuroFlow acute myeloid leukemia (AML)/myelodysplastic syndrome (MDS) antibody panel. The different colors reflect distinct differentiation stages from the more immature CD34$^+$ precursors (light green events) to mature (light blue dots) population of each distinct cell line.

(tubes 4 and 5), assessment of minor compartments of basophils, mast cells, pDC (tube 6) and megakaryocytic lineage cells (tubes 6 and 7).

Tube 1: antibody combination for neutrophil maturation

Within the normal neutrophil lineage, several markers like CD10, CD11b, CD13 and CD16 are expressed in a maturation-stage-specific manner. In combination with the backbone markers, these markers allow detailed characterization of the neutrophil maturation pathway from the most immature myeloid blast cells till the mature polynuclear neutrophilic granulocytes.[11] Abnormalities in the expression of these markers are frequently seen in patients with both AML and MDS.[194,195,203] CD16–FITC and CD13–PE conjugates were selected based on experience, , initially together with CD10–APC and CD11b–AF700. However, testing of this antibody combination on BM samples from AML and MDS patients showed that the fluorescence intensity of CD11b–AF700 was insufficient. Therefore, CD11b–AF700 was replaced by CD11b–APC and CD10–APC was replaced by CD10–APCH7. This resulted in satisfactory stainings for all markers; an example of the staining pattern of tube 1 is shown in Figure 19a.

Tube 2: antibody combination for monocytic maturation

Regarding the monocytic lineage, CD14 is considered to be the typical marker for monocytes, but this marker is only expressed during the intermediate to last stages of monocytic maturation. In contrast, CD64 (and to a lesser extent CD36) are already expressed during the earlier stages of monocytic differentiation. Therefore, usage of at least one of these two markers (preferentially CD64) is required for identification of early monocytic cells. The expression of CD33 increases early during monocytic development to levels higher than those of granulocytic cells.[11] This CD33 expression pattern also facilitates distinguishing monocytic and granulocytic cells. CD11b is absent on immature monocytic cells but it is expressed during later stages. Initially, the combination of the CD36/CD64/CD11b/CD14 characterization markers was evaluated. Because CD11b is also included in tube 1, this marker was later replaced by CD300e (IREM-2) in the monocytic lineage-oriented tube 2. CD300e (IREM-2) is a glycoprotein whose expression on normal hematopoietic cells is restricted to cells of the monocytic and myeloid dendritic cell lineages.[206] During normal monocytic development, CD300e is expressed in the last stages of maturation after CD14 is highly expressed. In AML, CD300e is almost exclusively found on leukemic cells from patients with monocytic leukemia, its reactivity increasing from monoblastic to monocytic AML and CMML. Noteworthily, in a subgroup of these patients CD300e is already expressed before CD14. Because CD36 is also informative for the erythroid differentiation, and it appears on CD64^{hi} monocytic precursors (that can be easily distinguished from other myeloid precursors based on its higher intensity of expression), it was decided to use CD64 in the monocyte-oriented tube and CD36 in the erythroid-oriented tube (see tube 3). In tube 2, CD36 was therefore replaced by CD35(CR1), which is expressed by erythrocytes, granulocytes, monocytes and dendritic cells, as well as by the leukemic cells in a subset of AML

patients.[207] Preliminary data (data not shown) suggest that immature monocytic cells could first express CD35, followed later by CyMPO, while in immature neutrophilic cells, expression of CyMPO clearly precedes that of CD35. CD35 can therefore contribute to distinguishing early monocytic and neutrophil differentiation stages. On the basis of the expression patterns and the availability of antibody conjugates, CD14, CD35, CD64 and CD300e were finally selected for the monocyte-oriented tube. As expression of CD14 is relatively strong, the relatively weak APCH7 conjugate was chosen. The relatively bright PE and APC fluorochromes were selected for CD64 and CD300e, respectively. An example of the immunophenotypic patterns that can be observed with this labeling is shown in Figure 19b.

Tube 3: antibody combination for erythroid differentiation

For evaluation of the erythroid differentiation, markers like CD235a (glycophorin A), CD71 and CD36 are informative. As CD235a is expressed not only on immature erythroid cells but also on mature erythroid cells, this marker appeared to be less suitable for use on whole BM or whole PB. We therefore evaluated several other markers that may characterize erythroid cells: CD233 (band-3 protein), CD238 (Kell) and CD105 ('epithelial cellular adhesion molecule', Ep-CAM) (in several combinations). No satisfactory results were obtained with CD233, even after additional titration experiments. CD238 worked well, but the intensity of the staining on erythroid cells was low. CD36 and CD105 are already expressed during early stages of erythroid differentiation, before CD235a becomes positive.[208,209] Expression of CD105 remains present after the CD71 expression is increased and subsequently disappears shortly after CD117 expression is lost, so that more mature erythroid cells no longer express CD105. Conversely, CD36 expression remains at relatively high levels throughout the maturation of normal red blood cells. Little is known about CD105 expression in AML, but aberrant CD105 expression has been reported in patients with MDS.[199] Testing of CD105 on BM samples from healthy subjects and AML patients showed optimal and specific staining of early erythroid cells at intermediate stages of erythroid maturation. Therefore, CD105, CD36 and CD71 were selected for the erythroid-oriented tube. Given the expression levels and the availability of antibody conjugates, CD36–FITC, CD105–PE, and CD71–APCH7 were chosen. For the fourth antibody position, CD33–APC was chosen, as CD33 expression is absent during the erythroid differentiation and could be used as an exclusion marker. At the same time CD33 also provides relevant information for the granulocytic (tube 1) and monocytic lineages (tube 2), particularly once evaluated in the context of AML. An example of the immunophenotypic patterns that can be observed with this labeling is shown in Figure 19c.

Tube 4: antibody combination for aberrant cross-lineage antigen expression and altered B-cell precursors

The fourth tube in the EuroFlow AML/MDS antibody panel does not focus on a particular cell lineage but aims at the detection of aberrant expression of lymphoid-associated markers on myeloid cells. Frequently occurring cross-lineage markers are CD19 in AML with t(8;21), CD7, and CD56.[4,210,211] Because cross-lineage expression can be weak, CD7–APC and CD56–PE were selected. NuTdT is expressed in many AML, but has limited added value for AML diagnosis.[212] However, NuTdT provides information on precursor B-cells, particularly in patients with MDS when combined with CD19.[10,213] We initially evaluated the antibody combination TdT–FITC, CD19–PE, CD22–APC and CD38–APCCy7, since this combination allows detailed characterization of B-cell differentiation. Although this combination worked well, this combination was later on replaced by TdT–FITC, CD56–PE, CD22–APC and CD19–APCH7. CD56 was initially evaluated as an AF700 conjugate in tube 5, but this resulted in a dim staining and therefore the AF700 conjugate was replaced by the CD56–PE reagent that showed optimal staining. Although CD19–APCH7 also stains relatively weak with respect to other CD19-fluorochrome conjugates, the intensity obtained is sufficient for identification of B-cells. In this regard, it should be noted that CD19 is also present in the ALOT tube as a strong PECy7-conjugated reagent. Finally, CD22–APC was switched over with CD7–APC originally tested in tube 5. The reason for this switchover was that only the first four tubes are needed in case of suspicion of MDS (see below), and that analysis of CD7 on myeloid blast cells is more relevant than CD22 in MDS patients.[195]

Tube 5: antibody combination for stem cells and other markers

Tube 5 contains several markers that are informative in AML but that are less suited for evaluation of differentiation pathways. NG2 is a protein typically absent in normal hematopoietic cells, but its expression has been associated with the presence of *MLL* gene rearrangements and pDC lineages, which occur in approximately 10 and $<1\%$ of AML patients, respectively.[214,215] NG2 expression can be relatively dim and therefore the PE conjugate was chosen, as was also done for tube 4 of the BCP-ALL antibody panel. The CD15 antigen is already expressed during the early stages of granulocytic development and is also dimly expressed on mature monocytes. For this purpose, the CD15–FITC conjugate provided satisfactory staining intensities. CD38 is strongly expressed on most myeloid cells but is absent on early stem cells ($CD34^+/CD38^-$). As the frequency of (leukemic) stem cells may have prognostic significance,[216] CD38 was included in the EuroFlow AML/MDS antibody panel. Given the intensity of the staining, the APCH7 conjugate was selected with a satisfactory pattern. CD22 is a typical B-cell-associated marker, which is also expressed by basophils, mast cells and a fraction of pDC.[66,67,217] Expression of CD22 on AML is very infrequent ($<5\%$), and it may well be that these cases in fact reflect (precursor) basophilic and/or mast cell blast cells or DC leukemia.[215] The main reason to include CD22 in the AML/MDS panel was its use as an additional B-cell marker, next to CD19 and CyCD79a in the ALOT tube and CD10 in tube 1, to exclude a potential MPAL.[36] Initially, we evaluated the antibody

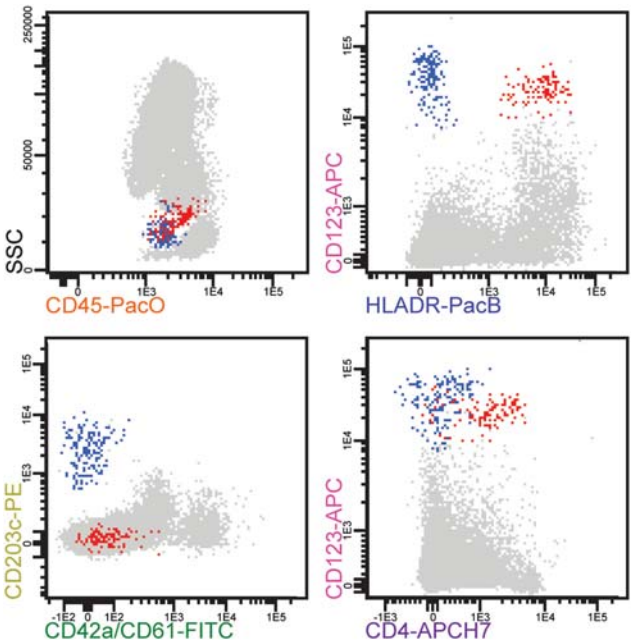

Figure 20. Identification of basophils (blue events) and plasmocytoid dendritic cells (red events) in a representative bone marrow from a healthy subject using tube 6 of the EuroFlow acute myeloid leukemia (AML)/myelodysplastic syndrome (MDS) antibody panel.

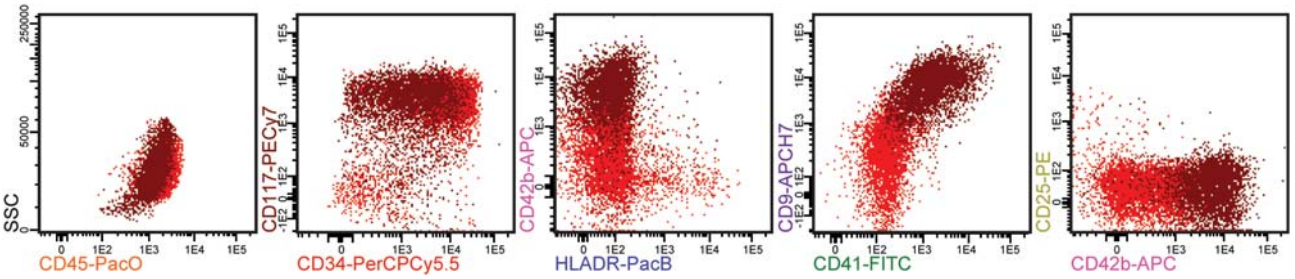

Figure 21. Characterization of an acute megakaryoblastic leukemia using tube 7 of the EuroFlow acute myeloid leukemia (AML)/myelodysplastic syndrome (MDS) antibody panel. The AML cells (brown and red dots) are positive for CD34 and CD117 and they partly express the megakaryocytic-lineage-associated markers CD42b, CD41 and CD9. HLADR and CD25 were both negative on blast cells.

combination CD15–FITC, NG2–PE, CD7–APC and CD56–AF700. The staining intensity obtained with CD56–AF700 was, however, unsatisfactory and therefore this conjugate was replaced by CD56–PE and switched over with CD38 from tube 4. Finally, CD7–APC was switched with CD22–APC in tube 4 (see explanation above).

Tube 6: antibody combination for mast cells, basophils, pDC and megakaryoblastic/megakaryocytic cells

For recognition of the less frequent mast cells, basophils, pDC and megakaryocytic cells as well as their malignant counterparts, markers allowing identification of these cell populations were selected for inclusion in tube 6 of the EuroFlow AML/MDS panel. For identification of megakaryoblastic/megakaryocytic cells, a combination of CD42 and CD61 in the same fluorochrome was selected. Both markers are already expressed during early stages of megakaryocytic differentiation.[218] As megakaryoblastic leukemias can be single positive for CD42 or CD61, a combination of both markers was chosen. If leukemic cells are positive for CD42a and/or CD61, the megakaryoblastic nature of AML cells can be confirmed in an additional tube fully focused on the megakaryocytic lineage (tube 7, see below). CD203c is one of the few markers suitable for identification of $CD117^{hi}$ mast cells, and it is also expressed on $CD117^{-/lo}$ basophils.[219,220] CD123 can be used in combination with the backbone marker HLADR to identify pDC ($CD123^{+}$/$HLADR^{+}$) and basophils ($CD123^{+}$/$HLADR^{-}$) (Figure 20).[221] CD4 is expressed by plasmacytoid dendritic cells as well as by monocytic cells. On the basis of the intensity of expression and the availability of antibody conjugates, CD42a–FITC, CD61–FITC, CD203c–PE, CD4–APCH7 and CD123–APC were selected for this tube combination.

Tube 7: antibody combination for megakaryocytic differentiation

The megakaryocyte-oriented tube aims at confirmation of acute megakaryoblastic leukemia (AML-M7), if the results of tube 6 raise such suspicion. Next to the four backbone markers, CD41 and CD42b are included in this tube, as both markers are specific for the megakaryocytic lineage. CD9 is expressed on a wide variety of cells; within the megakaryocytic lineage CD9 is already expressed during the early stages and therefore can contribute to the diagnosis of AML-M7.[222,223] For the last antibody position, CD25 was chosen, as some data suggest that this marker is expressed during the early stages of megakaryocytic development.[224] Furthermore, CD25 can be used to detect immunophenotypic aberrant mast cells when a systemic mastocytosis or chronic eosinophilic leukemia (possibly in combination with an AML or MDS) is suspected.[225] An example of the immunophenotypic results obtained in AML-M7 with this tube is shown in Figure 21.

In addition to the markers indicated above, several other markers have been reported as consensus markers for the flow cytometric diagnosis of AML patients.[12,21,23,205] This includes CD65, CD66, lysozyme, eosinophilic peroxidase (EPO) and CD2. Although these markers can be informative, some (for example, CyEPO) were extensively evaluated and they proved not to be essential. At the same time, the EuroFlow AML/MDS antibody panel already contains sufficient markers for appropriate characterization of all myeloid lineages and relevant prognostic subgroups. Nevertheless, evaluation of the potential utility of other markers (for example, lysozyme) requires further evaluation.

THE EUROFLOW AML/MDS ANTIBODY PANEL

The final EuroFlow AML/MDS antibody panel is summarized in Table 14. An example of the results obtained with this antibody panel is shown in Figure 22. This antibody panel should be used in combination with the standard EuroFlow immunostaining protocol.[16] Although the Fix&Perm reagents were selected within EuroFlow for intracellular stainings, it was decided to use FACS Lysing Solution for tube 4 of the AML/MDS panel. TdT works well using FACS Lysing Solution and usage of FACS Lysing Solution has the advantage that all tubes can be processed in a similar manner, thereby retaining identical scatter characteristics in all tubes and facilitating the merge and calculation options in the Infinicyt software.

During the EuroFlow studies all evaluated AML cases were analyzed with the first six tubes, whereas tube 7 was also applied if an AML-M7 was suspected. This allowed detailed classification of all evaluated cases. Preliminary evaluation of large series of AML patients suggests that the first four tubes of the EuroFlow AML/MDS panel in combination with the ALOT tube might be sufficient for the diagnosis and classification of most AML patients. Based on the immunophenotyping results of the first four tubes or if complete phenotypic classification of AML is required, tubes 5 and 6 might be added in $\leqslant$10% of cases. Tube 7 should be used (together with tubes 1–6 and ALOT) if a megakaryocytic leukemia or a transient myeloproliferative disorder is suspected (either forehand or based on the results of tube 6).

In case of MDS suspicion, the first four tubes of the EuroFlow AML/MDS panel are sufficient to identify abnormalities in the differentiation of the various (major) myeloid lineages (for example, neutrophil, monocytic and erythroid lineages). Tubes 5–7 do not yet seem to provide relevant additional information for MDS diagnosis.

In addition to evaluation of patients with suspicion of AML or MDS, the EuroFlow AML/MDS panel may also provide relevant information for patients with a suspicion of paroxysmal nocturnal hemoglobinuria (PNH) in the context of BM aplasia and MDS (PNH: detection of $CD10^{+}$/$CD16^{-}$ mature neutrophils in tube 1 and of $CD14^{-}$ monocytes in tube 2), mastocytosis ($CD25^{+}$/$CD117^{hi}$ mast cells in tube 7) and chronic myeloid leukemia (CML, tubes 1 and 6). It should, however, be noted that the EuroFlow tubes were not primarily designed for these diseases and therefore other antibody combinations may be more appropriate, in case of primary suspicious of such diseases.[226,227]

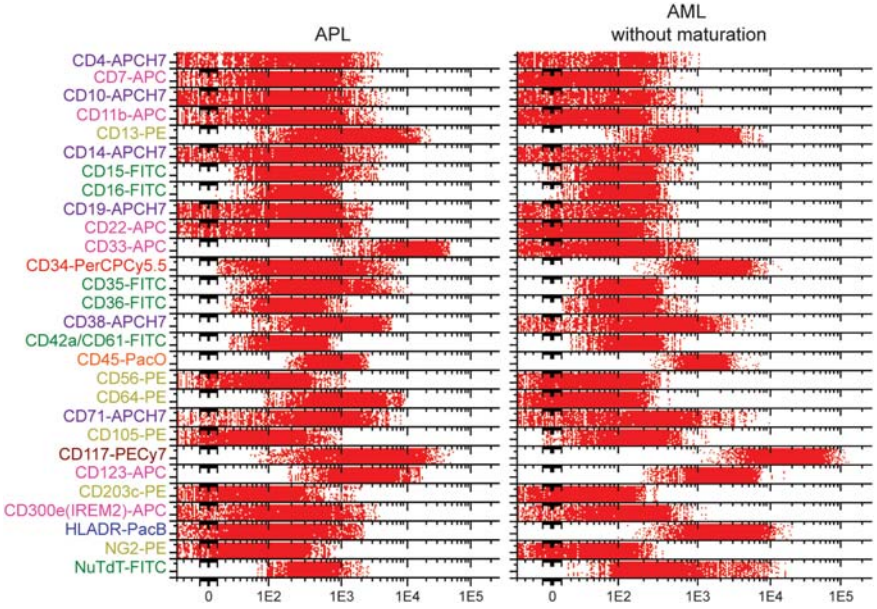

Figure 22. Band plot examples of two acute myeloid leukemia (AML) patients analyzed according to the EuroFlow AML/myelodysplastic syndrome (MDS) antibody panel. The AML blast cells (red dots) are gated based on the backbone markers and their immunophenotype is shown in a multiparameter band-dot plot. A patient with APL (*PML-RARA*-positive) and a patient with an AML without maturation are shown in the left and right panels, respectively.

Univariate and multivariate analysis of AML subgroups

To evaluate whether the EuroFlow AML/MDS antibody panel appropriately characterizes AML subgroups, data were collected from 84 AML patients.[225,228] Univariate analysis identified several markers that were differentially expressed among the various subtypes. Monocytic markers like CD36, CD14, CD4 and CD11b were primarily observed on blast cells from patients with an acute monocytic leukemia, t(9;11)$^+$ AML, or AML with mutated *NPM1*. CD42a/CD61 were only expressed on megakaryoblastic leukemias, while these leukemias did not express CD123. Also, erythroid leukemia did not express CD123. The pan-myeloid marker CD33 was expressed on the vast majority of AML, but not on erythroid leukemias. Based on single markers, leukemias originating from different myeloid lineages could therefore be distinguished, while characterization of genetically-defined subgroups was not straightforward.

In multivariate analysis (APS view) several WHO-defined subgroups could be distinguished from each other (Figure 23). Particularly morphologically-defined subgroups could be distinguished, while separation of genetically-defined subgroups was generally less clear. This may be explained, at least in part, by the fact that immunophenotyping (like morphology) focuses on cell lineages and differentiation stages, while genetically-defined subgroups may be more heterogeneous, owing to different secondary hits that may have a different impact on the differentiation potential of the affected cells.[229,230]

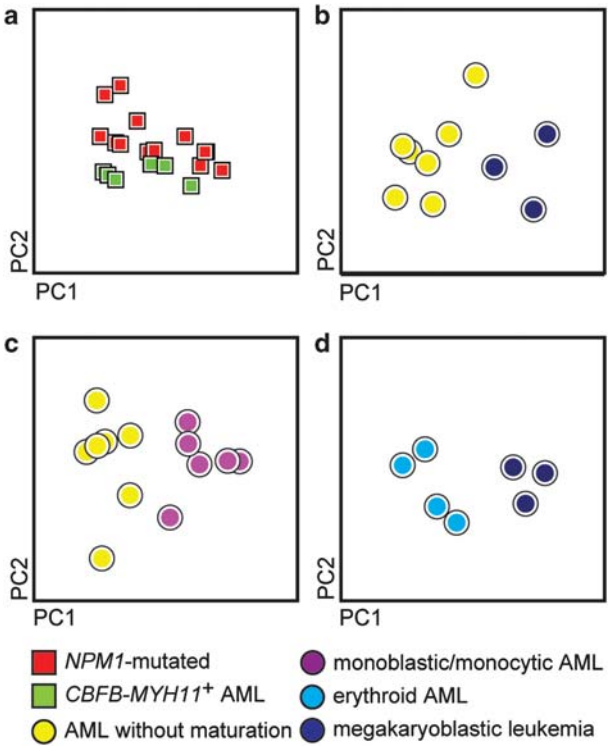

Figure 23. Multivariate principal component analysis (PCA; principal component analysis (PC)1 versus PC2, automated population separator (APS)-1) view of various WHO-defined subgroups of AML. (**a**) NPM1-mutated (red squares) versus CBFB-MYH11$^+$ AML (green squares). (**b**) AML without maturation (yellow circles) versus megakaryoblastic leukemia (dark blue circles). (**c**) AML without maturation (yellow circles) versus monoblastic/monocytic AML (pink circles). (**d**) Erythroid AML (cyan circles) versus megakaryoblastic leukemia (dark blue circles). Each square/circle represents the overall mean/median position of an individual AML patient in the PC1 versus PC2 representation of the whole immunophenotypic profile of the AML blast cells, respectively.

CONCLUSION

The AML/MDS EuroFlow panel allows detailed characterization of the distinct myeloid lineages, including the evaluation of maturation pathways and aberrant immunophenotypes of myeloid cells. This panel should be performed for patients with suspicion of AML or MDS in combination with the ALOT; however, it also provides essential information to rule out PNH and systemic mastocytosis with BM involvement. Of note, it was not possible to use the same backbone markers in the AML/MDS panel and the ALOT, which prevents software linkage of markers present in the ALOT with markers in the AML/MDS panel. The AML/MDS panel was built so that it can be applied in a flexible way, the first four tubes being essential for the phenotypic characterization of both AML and MDS.

SECTION 8. ANTIBODY PANEL FOR B-CELL CHRONIC LYMPHOPROLIFERATIVE DISEASES (B-CLPD)

S Böttcher[1], A Rawstron[2], P Lucio[3], R de Tute[2], J Flores-Montero[4], Q Lécrevisse[4], A Mendonça[3], V Asnafi[5], L Lhermitte[5], M Brüggemann[1], JJ Pérez[6], JJM van Dongen[7] and A Orfao[4]

[1]UNIKIEL, Kiel, Germany; [2]UNILEEDS, Leeds, UK; [3]IPOLFG, Lisbon, Portugal; [4]USAL, Salamanca, Spain; [5]AP-HP, Paris, France; [6]HUS, Salamanca, Spain and [7]Erasmus MC, Rotterdam, The Netherlands

BACKGROUND

Mature (peripheral) B-cell malignancies represent the malignant counterpart of normal mature B-cells that have differentiated into naive B cells or their progeny. The WHO subclassification of mature B-cell leukemias and lymphomas, also known as B-CLPD, follows the concept of normal (benign) counterparts and attempts to distinguish the B-cell malignancies in relationship to the germinal center reactions and other B-cell activation and maturation processes.[231] Nevertheless, the exact normal counterparts of several B-CLPD (for example, hairy cell leukemias, HCL) have not been discovered. Thus, integration of a complex set of immunophenotypic, morphological, clinical and cytogenetic information is currently essential for the correct subclassification of mature B-cell malignancies. The reproducible diagnosis of specific B-CLPD WHO entities based on morphology remains a serious challenge, as even agreement between expert hematopathologists on particular disease entities ranges between 53 and 94% of cases.[232] However, already 15 years ago it has been shown that the inclusion of immunohistological assessments could increase the agreement rate by up to 14% in mature B-cell malignancies.[232]

It is clear that precise and reproducible diagnosis of B-CLPD subtypes has high clinical relevance, as the disease group comprises largely indolent entities that are best treated by watchful waiting (for example, certain subgroups of chronic lymphocytic leukemia, CLL[233]) as well as extremely aggressive diseases with a median survival of few months only if left untreated (for example BL). Furthermore, the advent of novel therapeutic options has greatly improved the prognosis for many patients with a mature B-cell neoplasm, for example, for patients with mantle cell lymphoma (MCL).[234] Modern treatment regimens are tailored for the specific B-CLPD subtype, so that obtaining the correct diagnosis has gained additional importance for optimal patient care. Immunophenotyping has proved essential for the diagnostic classification of many B-CLPD cases, but the current immunophenotyping strategies also face several difficulties. For example, the rising number of immunophenotypic markers used for the classification of B-CLPD as well as the heterogeneous and overlapping immunophenotypic profiles among distinct entities have increased the complexity of data interpretation. Clearly, a more objective and more integrated approach is needed with selection of the most informative markers and deletion of redundant makers, which provide more confusion than solution.

The EuroFlow Consortium embarked on a systematic evaluation of the immunophenotype's contribution to the diagnostic classification of mature B-cell malignancies, aiming at a more integrated as well as a fully standardized and reproducible immunophenotypic diagnosis of B-CLPD subgroups. The complete set of morphological, cytogenetic and immunophenotypic information required by the WHO 2008 classification served as the diagnostic 'gold standard' in each patient. We developed an optimized and non-redundant combination of markers in order to reproduce as far as possible that 'gold standard' solely based on flow cytometry (EuroFlow B-CLPD panel). Noteworthily, we decided to separate PCD from the remaining mature B-cell neoplasms as they usually present with a clearly distinguishable clinical picture and immunophenotype that requires different screening and classification strategies (Figure 1). The EuroFlow B-CLPD panel was designed to work in all cases in which the malignant B-cell clone could be separated by gating on backbone markers. The resulting (gated) population was required to systematically contain $<10\%$ contaminating non-clonal B-cells. The B-CLPD panel is intended to be applied subsequent to the detection of a clonal B-cell population using the LST. For reasons of efficiency and cost reduction, the relevant immunophenotypic information of the LST is also used for the classification of the distinct B-CLPD entities. In cases with a very high pre-test suspicion of a B-CLPD, it is recommended to stain the LST simultaneously with the B-CLPD panel (or parts of it) in order to minimise the number of steps required to obtain a definite immunophenotypic diagnosis (Figure 1).

Design of the EuroFlow B-CLPD panel

In line with the EuroFlow strategy on the identification of target populations in different tubes of an antibody panel via common backbone markers, the first step in the design of the B-CLPD panel was to define a minimal set of markers to identify all B-cells between the other leukocytes in PB, BM and LN samples from patients with B-CLPD. The second step focused on the selection of antigens with different expression between B-CLPD entities, aiming at appropriate characterization of each B-CLPD entity.

Selection of backbone markers. Several B-lineage-specific antigens (for example, CD19 and CD20) were obvious candidates for backbone markers, as they are assumed to be useful for identification of all B-cells in a sample. However, aberrantly low expression of CD20,[235] CD19,[236,237] CD22[238] and CD37[150] was known to be a common phenomenon in several mature B-CLPD entities. When we started the project it was not known to what extent such under-expression occurs simultaneously for several B-cell antigens in a single patient and how this would affect the ability to distinguish malignant B-cells from the remaining leukocytes. Therefore we first tested the relative contributions of CD19, CD20, CD22 and CD37 to the identification of malignant B-cells in a B-CLPD sample.

To address the relative contributions of pan-B-cell markers to the identification of malignant B-cells in B-CLPD, a 6-color combination was initially evaluated at two different centers (Backbone panel 1, Table 15).

The analysis included samples from 49 B-CLPD patients: 18 CLL, 4 DLBCL, 7 follicular lymphoma (FL), 4 MCL, 2 marginal zone lymphoma (MZL) and 14 unclassified B-CLPD. The background fluorescence was set to include 95% neutrophils in the sample. B-cells were defined to comprise any lymphocytes with expression of at least one of the four B-cell markers CD19, CD20, CD22 or CD37 above the background fluorescence level. The malignant clone was identified as a subpopulation of mature B-cells showing either light-chain restriction or complete lack of light-chain expression. The mean fluorescence intensity (MFI) of the malignant clone and the percentage of B-cells expressing CD19, CD20, CD22 and CD37 with higher intensity than background was analyzed.

Expression levels of the investigated B-cell antigens were significantly correlated for all 1×1 marker combinations. However, the degree of correlation decreased in the following order: CD19 versus CD37 (Spearman $r = 0.68$, $P < 0.0001$), CD37 versus CD20 ($r = 0.59$, $P < 0.0001$), CD37 versus CD22 ($r = 0.55$, $P < 0.0001$), CD22 versus CD20 ($r = 0.52$, $P < 0.0001$), CD19 versus CD20 ($r = 0.41$, $P = 0.004$), and CD19 versus CD22 ($r = 0.35$, $P = 0.01$). The percentage of undetected neoplastic B-cells with respect to the markers applied is visualized in Figure 24. Overall, none of the investigated antibodies was on its own sufficient to identify all malignant B-cells in every patient. There were individual B-CLPD patients in whom the vast majority of malignant B-cells could not be distinguished from background using one of the markers alone. As expected, low-level CD20 expression was particularly common in CLL, whereas

under-expression of CD19 most often occurred in FL and DLBCL patients (data not shown). The most efficient combination of two of these four markers evaluated to detect neoplastic B-cells comprised CD20 plus CD19, with at most 11% undetected malignant cells per case. The remaining B-cells were most efficiently identified by additionally relying on CD22 (Figures 24b and c).

An alternative set of backbone markers was tested in a total of 10 B-CLPD patients (4 CLL, 1 DLBCL, 3 FL, 1 MZL, 1 non-classified B-CLPD) in one center to study the utility of CD20-PacB instead of the CD20-APCCy7 reagent (backbone panel 2, Table 15). This change in the backbone CD20 antibody clone and conjugate further improved the performance of the CD20 plus CD19 combination with a maximum percentage of undetected lymphoma cells of only 2%. All other correlations were identical to those described for the panel tested at the other two centers (data not shown). Consequently, CD20-PacB was selected for subsequent testing.

As all panels were designed to work not only in blood but also in BM and cell suspensions prepared from tissue sections, we agreed to additionally include CD45–PacO as the third backbone marker. This marker facilitates the distinction of leukocytes from erythroid precursors and non-hematopoietic cells, as well as the identification of the major subpopulations of the leukocytes.

Subsequently, the EuroFlow Consortium tested the combination of CD20–PacB, CD45–PacO, CD19–PECy7 and CD22–AF700 (clone IS7, EXBIO, Prague, Czech Republic) as potential backbone markers, to definitively check the performance of CD20–PacB and evaluate the need for the third B-cell marker for the identification of all B-cells of interest in every case. CD22–AF700 replaced CD22–APC, so that other B-cell characterization markers could be introduced into the APC channel. This configuration of backbone markers was tested in the context of the first version of the full 8-color EuroFlow B-CLPD antibody panel (Table 15) in a total of 63 samples (17 CLL, 6 DLBCL, 13 MCL, 4 FL, 1 HCL, 2 lymphoplasmacytic lymphomas (LPL), 3 MZL, 12 non-classified B-CLPD, 1 normal BM, 4 normal PB). We found that CD19–PECy7 identified all B-cells in all cases except some FL ($n = 2$) and MCL ($n = 4$) patients, whereas CD20–PacB detected all B-cells in

Table 15. Design of the B-CPLD panel in seven consecutive testing rounds[a]

Version (no. of cases)[b]	*Tube*	*Fluorochromes and markers*							
		PacB	*PacO*	*FITC*	*PE*	*PECy5*	*PECy7*	*APC*	*APCCy7*
BB 1 ($n = 49$)	1			SmIgκ	CD37	SmIgλ	CD19	CD22	CD20
BB 2 ($n = 10$)	1	CD20		SmIgκ	CD37	SmIgλ	CD19	CD22	
		PacB	*PacO*	*FITC*	*PE*	*PerCPCy5.5*	*PECy7*	*APC*	*AF700*
1 ($n = 63$)	1	CD20	CD45	SmIgκ	SmIgλ	CD5	CD19	SmIgM	CD22
	2	CD20	CD45	CD103	CD10	CD5	CD19	CD43	CD22
	3	CD20	CD45	CD81	CD79b	CD5	CD19	CD23	CD22
	4	CD20	CD45	CD31	CD63	CD5	CD19	CD185 (CXCR5)	CD22
	5	CD20	CD45	CD24	CD305(LAIR1)	CD5	CD19	CD11a	CD22
	6	CD20	CD45	CD38	CD25	CD138	CD19	CD11c	CD22
		PacB	*PacO*	*FITC*	*PE*	*PerCPCy5.5*	*PECy7*	*APC*	*APCH7*
2 ($n = 43$)	1	CD20	CD45	SmIgλ	SmIgκ	CD22	CD19	CD23	CD81
	2	CD20	CD45	CD103	CD25	CD11c	CD19	SmIgM	CD24
	3	CD20	CD45	CD31	CD305(LAIR1)	CD5	CD19	CD43	CD185 (CXCR5)
	4	CD20	CD45	CyBcl2	CD10	CD79b	CD19	CD38	CD49d
3 ($n = 37$)	1	CD20	CD45	SmIgλ	SmIgκ	CD22	CD19	CD23	CD81
	2	CD20	CD45	CD103	CD25	CD11c	CD19	SmIgM	
	3	CD20	CD45	CD31	CD305(LAIR1)	CD5	CD19	CD43	
	4	CD20	CD45	CyBcl2	CD10	CD79b	CD19	CD38	CD49d
	5	CD20	CD45	CD24	CD95		CD19	CD200	
4 ($n = 31$)	1	CD20	CD45	SmIgλ	SmIgκ	CD22	CD19	CD23	CD81
	2	CD20	CD45	CD103	CD25	CD11c	CD19	SmIgM	CD43
	3	CD20	CD45	CD31	CD305(LAIR1)	CD5	CD19	CD43	CD24
	4	CD20	CD45	CyBcl2	CD10	CD79b	CD19	CD38	CD49d
	5	CD20	CD45	CD24	CD95		CD19	CD200	CD31
	6	CD20	CD45				CD19	CD185 (CXCR5)	CD103
5 (Final) ($n = 151$)	1 = LST	CD20	CD45	CD8 and SmIgλ	CD56 and SmIgκ	CD5	CD19 and TCRγδ	SmCD3	CD38
	2	CD20	CD45	CD23	CD10	CD79b	CD19	CD200	CD43
	3	CD20	CD45	CD31	CD305(LAIR1)	CD11c	CD19	SmIgM	CD81
	4	CD20	CD45	CD103	CD95	CD22	CD19	CD185 (CXCR5)	CD49d
	5	CD20	CD45	CD62L	CD39	HLADR	CD19	CD27	

Abbreviations: AF700, alexa fluor 700; APC, allophycocyanin; BB, backbone; BL, Burkitt lymphoma; BM, bone marrow; B-NHL NOS, B non-Hodgkin lymphoma not otherwise specified; CLL, chronic lymphocytic leukemia; CLPD, chronic lymphoproliferative disorder; Cy, cytoplasmic; Cy5, cyanin5; Cy5.5, cyanin5.5; Cy7, cyanin7; DLBCL, diffuse large B-cell lymphoma; FITC, fluorescein isothiocyanate; FL, follicular lymphoma; HCL, hairy cell leukemia; H7, hilite7; LN; lymph node; LPL, lymphoplasmacytic lymphoma; MCL, mantle cell lymphoma; MZL, marginal zone lymphoma; PacB, pacific blue; PacO, pacific orange; PB, peripheral blood; PE, phycoerythrin; PerCP, peridinin–chlorophyll–protein; Sm, surface membrane. [a]Further information about markers and hybridomas is provided in the Appendix. [b]A total of 384 cases (194 PB, 144 BM, 42 LN and 4 tissue biopsies) was evaluated. Among them 98 were CLL, 65 MCL, 55 FL, 40 DLBCL, 35 MZL, 32 B-NHL NOS, 21 LPL, 20 HCL, 7 BL and 11 from healthy donors. Highlighted boxes: changes as compared to previous version.

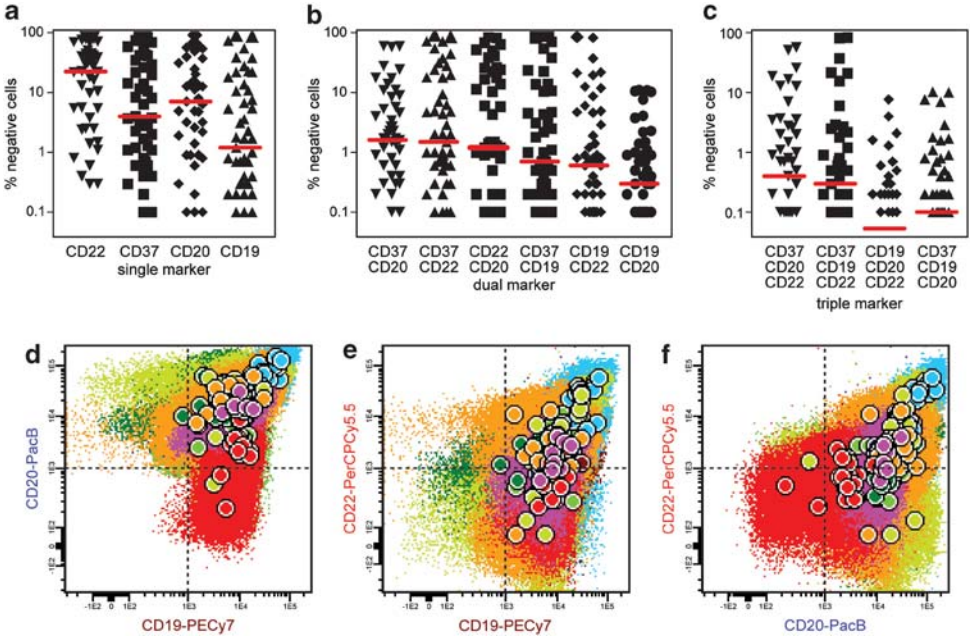

Figure 24. Percentage of clonal B-cells that are not detected using one (**a**), two (**b**) and three (**c**) pan-B-cell markers, respectively ($n = 49$ samples from 49 patients; black symbols represent individual patients, red lines depict the medians), and CD19–PECy7 versus CD20-PacB (**d**), CD19–PECy7 versus CD22-PerCPCy5.5 (**e**) and CD20–PacB versus CD22-PerCPCy5.5 (**f**) dot plots showing the distribution of individual neoplastic B-cells (small dots) and median values of each population in individual cases (circles) from a series of 151 B-cell chronic lymphoproliferative diseases (B-CLPD) patients. Circles are colored according to diagnoses of individual patients: red, chronic lymphocytic leukemia (CLL); dark green, follicular lymphoma (FL); green, marginal zone lymphoma (MZL); light green, $CD10^-$ diffuse large B-cell lymphoma (DLBCL); dark blue, mantle cell lymphoma (MCL); light blue, hairy cell leukemia (HCL); orange, $CD10^+$ DLBCL; pink, Burkitt lymphoma (BL); brown, lymphoplasmacytic lymphoma (LPL).

all patients with the exception of six CLL patients. The combination of CD20–PacB and CD19–PECy7 distinguished all light-chain-restricted B-cells from background in every case analyzed, thus further extending our earlier observation. Conversely, our findings showed that CD22–AF700 did not significantly contribute to the identification of clonal B-cells in addition to the selected markers, as fluorescence overlap from brightly expressed antigens detected by APC-labeled antibodies made CD22-AF700-positive populations undistinguishable from the background.

Based on the above experiments, the EuroFlow Consortium concluded that the combination of CD20–PacB plus CD19–PECy7 was not only required but also sufficient to identify all clonal cells in mature B-lineage malignancies. At diagnosis, we did not observe cases underexpressing simultaneously both antigens to an extent that they would go undetected by the brightly labeled CD19–PECy7 and CD20–PacB antibodies. In fact, 262 patient samples analyzed with subsequent versions of the EuroFlow B-CLPD classification panel never showed a B-cell population that was simultaneously negative for CD19–PECy7 and CD20–PacB (see Figure 24d). Nonetheless, all subsequent B-CLPD panel versions included CD22–PerCPCy5.5 as an additional B-cell characterization marker (Table 15). We conclude that if B-cell CLPD expressing neither CD20 nor CD19 exist, they are extremely rare (that is, $<0.5\%$ of all cases).

Mature data are now available on the correlation of B-cell antigens in B-lineage CLPD, which confirm our initial data: a high correlation between CD20 and CD22 expression ($r = 0.67$, $P < 0.0001$), whereas CD19 expression was less closely correlated to CD20 ($r = 0.47$, $P < 0.0001$) and CD22 levels ($r = 0.43$, $P < 0.0001$). Figure 24 shows the correlation in a total of 151 B-CLPD cases assessed with the final version of the B-CLPD EuroFlow panel (6 BL, 26 CLL, 21 DLBCL, 26 FL, 15 HCL, 15 LPL, 22 MCL and 20 MZL).

Selection of characterization markers for differential diagnosis between distinct B-CLPD entities. In parallel to the last part of the backbone marker testing, we started the selection of the set of characterization markers for the differential diagnosis of B-CLPD entities (Table 15). We used markers that were (i) already known to be of diagnostic value for the differential diagnosis of mature B-cell malignancies; (ii) known to be associated with normal B-cell developmental and maturational steps, thus following the concept of the WHO classification; and (iii) associated with B-cell homing, hypothesizing that different homing receptors might regulate the propensity of lymphoma cells to infiltrate BM, LN or spleen. Marker selection was based on published data and unpublished evidence from the EuroFlow laboratories. Supplementary Table 2 provides an overview on all 33 markers tested within the EuroFlow B-CLPD project and the selected references suggesting their potential utility for the classification of B-CLPD. The table also includes scientific work that was published after the EuroFlow project started.

Detailed analysis of the results of version 1 of the B-CLPD antibody panel (Table 15) showed that the CD11a, CD138 and CD63 antigens did not contribute to the differential diagnosis of mature B-cell malignancies. Furthermore, we identified that the APCH7 fluorochrome is a good alternative to AF700, with an overall good performance and lower fluorescence compensation needs. In line with the development of the other EuroFlow antibody panels, the Consortium decided to use the APCH7 conjugate in further testing. To improve the differential diagnosis among different B-CLPD entities, we additionally introduced CyBcl-2 in a second version of the panel (Table 15), which also contained several custom-conjugated antibodies. Assessment of 43 new B-CLPD cases revealed that the newly introduced custom-conjugated CD185(CXCR5)–APCH7 antibody did not yield the expected results, most likely due to suboptimal fluorochrome labeling of the antibody. Consequently, CD185(CXCR5)–APCH7 was not used in the third panel version. Furthermore, CD95 and CD200 were additionally included into the panel to improve the

identification of germinal center diseases and to distinguish MCL cases from the other B-CLPD entities, respectively. The resulting panel (version 3 in Table 15) was prospectively applied to 37 new cases, yielding promising preliminary results for the differential diagnosis among distinct B-CLPD entities. Nevertheless, owing to the unavailability of antibody reagents in suitable fluorochromes, four fluorochrome positions (APCH7 in three tubes and PerCPCy5.5 in one tube) were left open until custom-conjugated reagents became available (version 4 of the B-CLPD in Table 15). This next version (version 4) of the panel included APCH7-labeled antibodies to the CD43, CD31 and CD103 antigens, which were tested against reference antibodies in the panel in a series of 31 cases representing the major B-CLPD entities. This assessment revealed differences in correlation in the following order: CD103 FITC versus CD103 APC-H7 ($r = 0.39$, $P = 0.02$), CD43 APC versus CD43 APC-H7 ($r = 0.77$, $P < 0.0001$) and CD31-FITC versus CD31 APC-H7 (0.83, $P < 0.0001$). We concluded that CD31 and CD43 could be potentially applied in the APCH7 format.

PCA as integrated into Infinicyt software was applied to the samples acquired with version 4 of the B-CLPD antibody panel. Based on PCA, CyBcl-2, CD25 and CD24 were found not to have added value to the diagnostic power of the panel, once the other markers were present (data not shown). In particular, while CyBcl2 was expectedly[239] underexpressed in BL cases compared to all other mature B-cell lymphomas and leukemias, the remaining immunophenotype of BL was sufficiently unique to identify the disease without CyBcl2. CD25 was helpful for identification of HCL, but this was readily possible without this antigen using markers such as CD305 (LAIR1), CD11c and CD103. The differential diagnosis between HCL and HCL variants was not intended in this panel, as HCL variant is a very rare disease. If that differential diagnosis is in question, CD25 has to be stained after the B-CLPD panel. Finally, CD24 did not show a significant contribution to the classification of B-CLPD in the presence of the other markers. Furthermore, this analysis also showed that most B-CLPD subtypes could unequivocally be classified using the panel. Only the differential diagnosis between subgroups of LPL, MZL, FL and DLBCL cases remained difficult. In an attempt to improve the resolution between those entities, we additionally included CD62L, CD39, HLADR and CD27 into the panel (version 5; Table 15).

In the meantime, the development of the LST was sufficiently mature, so that the information obtained using both the LST and the B-CLPD antibody panel could be combined in a unified single data file for further multivariate analysis.[16]

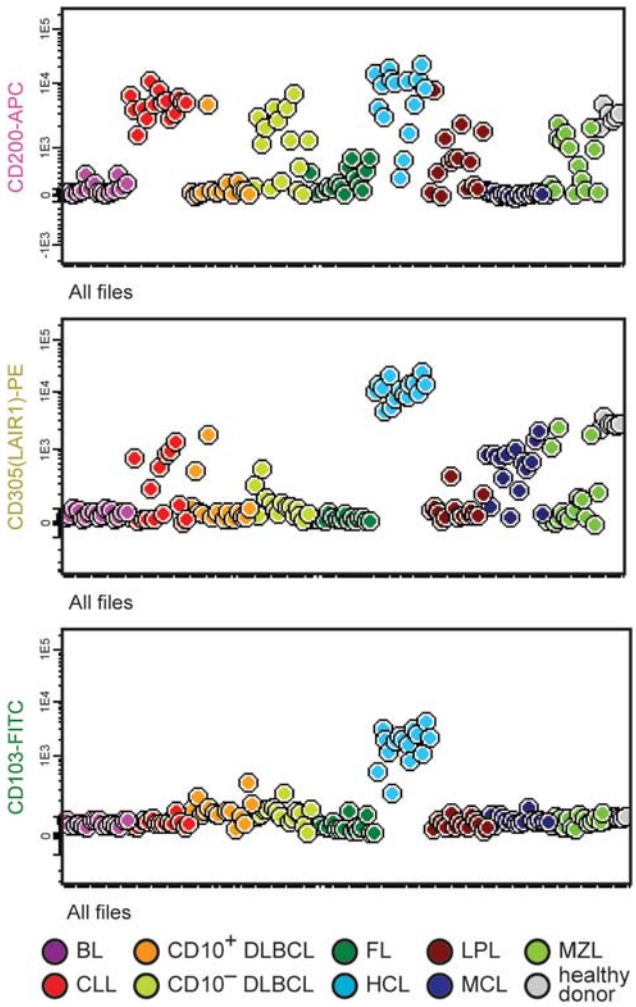

Figure 25. Illustrating examples of the median fluorescence intensity (MFI) of CD200, CD305(LAIR1) and CD103 detected among different major diagnostic categories of B-cell chronic lymphoproliferative diseases (B-CLPD). Circles correspond to median values of individual patient B-cells for each marker. BL, Burkitt lymphoma; CLL, chronic lymphocytic leukemia; DLBCL, diffuse large B-cell lymphoma; FL, follicular lymphoma; HCL, hairy cell leukemia; LPL: lymphoplasmacytic lymphoma; MCL: mantle cell lymphoma; MZL, marginal zone lymphoma.

Evaluation of the B-CLPD EuroFlow antibody panel

The final version of the B-CLPD panel (version 5) was then tested in 151 patients in six EuroFlow centers. We analysed the utility of this panel by comparing means of all MFIs per disease category for all evaluated markers (univariate analyses). This analytic step demonstrated a good concordance of mean MFIs in different disease categories to published data (for an overview on relevant literature see Supplementary Table 2; for examples of observed expression levels see Figure 25). These observations suggested that the multi-color panel indeed yielded the expected results. However, this assessment was limited by the lack of published immunophenotypic information for many markers in many mature B-cell malignancies.[240] We also observed that all disease categories included cases that showed overlap in expression levels for individual markers to other disease categories. Even markers considered to be specific for particular diseases (for example, CD103 for HCL) showed some overlap with other disease categories (Figure 25). We also confirmed that newly introduced markers such as CD200 and CD305 (LAIR1) provided improved separation between WHO-defined B-CLPD entities (Figure 25).

Owing to the heterogeneity of marker expression in individual cases within a given WHO entity, we decided to evaluate a novel immunophenotype-based diagnostic approach to mature B-cell malignancies: instead of identifying diseases using the typical expression of a marker or a sequential combination of markers, entities are now identified by their characteristic position within the multidimensional space created by the combination of all measured marker expressions.[241] The total number of markers within a panel defines the number of dimensions of this space. PCA is applied to find the vector of the multidimensional space with the highest variation of all events measured for two given diseases. In general, this vector allows the best discrimination between the two diseases, visualized with the automated population separation (APS) tool of the Infinicyt software.[16]

The novel approach allowed establishing typical immunophenotypic patterns for most of the eight major B-CLPD entities: BL, CLL, DLBCL, FL, HCL, LPL, MCL, and MZL. To distinguish between these eight entities a total of 28 diagnostic decisions have to be made (1×1 comparisons). It is currently possible to make all these decisions, albeit that it remains difficult to distinguish DLBCL from (i) FL and from (ii) MZL and LPL. Also, the unequivocal differential diagnosis between MZL and LPL is not possible with our panel of markers (Figure 26d). We speculate that a lack of separation

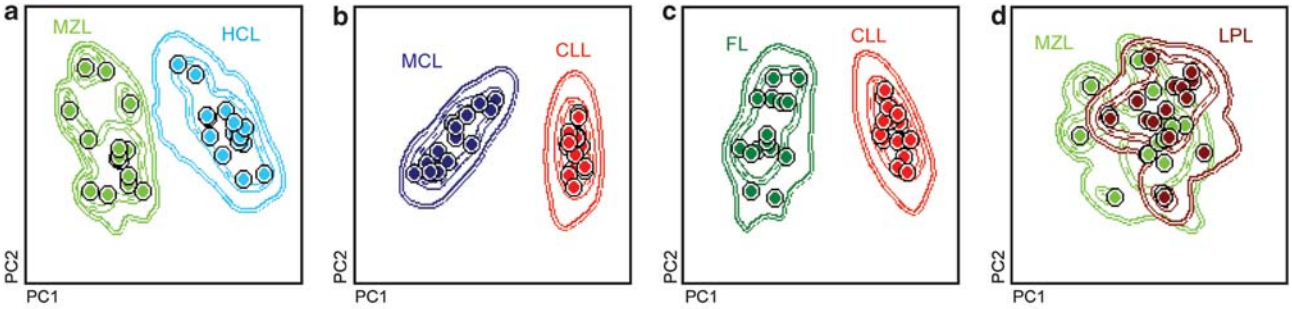

CD305(LAIR1)	12%
CD11c	11%
CD103	8%
CD200	8%
CD22	7%

CD79b	15%
CD200	14%
SmIgM	13%
CD23	9%
CD20	9%

CD79b	10%
CD200	9%
CD43	8%
CD23	7%
CD31	7%

Figure 26. First principal component (PC1) versus second principal component (PC2) bivariate dots plots of the complete immunophenotype of a series of marginal zone lymphoma (MZL) versus hairy cell leukemia (HCL) (**a**), chronic lymphocytic leukemia (CLL) versus mantle cell lymphoma (MCL) (**b**), follicular lymphoma (FL) versus CLL (**c**) and MZL versus lymphoplasmacytic lymphoma (LPL) (**d**) cases. Colored circles represent median values of individual cases for all those immunophenotypic markers in the EuroFlow B-cell chronic lymphoproliferative disorder (CLPD) panel contributing to PC1 and PC2. Contour lines represent s.d. curves (dotted and continuous lines represent 1s.d. and 2s.d., respectively). The five most informative markers contributing to the best discrimination between each disease entity are displayed at the bottom of each plot, in a decreasing order of percentage contribution to the discrimination.

between those two entities might also be related to difficulties of hematopathologists to distinguish them on histopathological grounds. In fact, expert reference pathologists agreed on these two disease categories in 56% and 63% of all cases, respectively.[232] Individual aberrant cases additionally showed clustering in the border zone of two B-CLPD entities (DLBCL versus BL, 1 case; DLBCL versus MCL, 2 cases; FL versus LPL, 1 case; FL versus MCL, 1 case; and FL versus MZL, 4 cases). Thus, 24/28 differential diagnoses can objectively be made for the vast majority of cases through combined use of the EuroFlow B-CPLD antibody panel and the new Infinicyt software tools.

An example of the differential diagnostic power of the EuroFlow strategy is given in Figure 26. MZL cases are clearly separated from HCL cases when the first (x-axis) and second (y-axis) principal components are simultaneously considered (Figure 26a). The 5 (out of 25) parameters contributing most significantly to the first principal component are, in descending order: CD305 (LAIR1), CD11c, CD103, CD200 and CD22. The diagram of first versus second principal component for CLL and MCL cases (Figure 26) shows again that most patients can unequivocally be classified into one of the disease categories using flow cytometry data only. The five markers that contributed the most to the first principal component were CD79b, CD200, SmIgM, CD23 and CD20.

On the basis of these results, we investigated which markers contributed the most to the differential diagnosis of the most frequent mature B-cell malignancy, CLL, versus all other mature B-cell malignancies. Overall, a combination of 10 relevant antigens (CD20, CD45, CD19, CD5, CD38, CD23, CD10, CD79b, CD200 and CD43) yielded an almost equally good separation between CLL and all other B-CLPD entities (Figure 26b). Therefore, the B-CPLD panel was designed so that those markers were included into tubes 1 (LST) and 2 (of the panel) (Table 15). Consequently, it is possible to unequivocally diagnose this disease using tube 1 (LST) and tube 2 of the B-CLPD antibody panel only.

CONCLUSION

The B-CPLD EuroFlow antibody panel consists of four tubes plus the LST, which combines a total of 27 different B-cell associated markers. Each tube in the panel contains three backbone markers (CD19, CD20 and CD45), which proved to provide efficient positive identification of all clonal B-cells in every B-CPLD patient tested. Backbone markers combined with the characterization markers provide an efficient differential diagnosis among the majority of B-CPLD entities (24/28 diagnostic decisions), using multivariate analysis of complete phenotypes of individual cells. The panel was designed to work in a modular way, so that the first two tubes allow efficient diagnosis of CLL versus all other disease entities.

Future diagnostic strategies in mature B-cell malignancies will take advantage of using the best discriminating immunophenotypes in multivariate analysis, for each possible differential diagnosis. EuroFlow is currently constructing a reference database containing complete immunophenotypic information from well-defined mature B-cell malignancies. Unknown new cases will be evaluated for diagnostic purposes by comparing their immunophenotype to the immunophenotypic information along the vectors in the EuroFlow reference database for best differential diagnosis.

SECTION 9. ANTIBODY PANEL FOR T-CELL CHRONIC LYMPHOPROLIFERATIVE DISEASES (T-CLPD)

J Almeida[1], J Flores-Montero[1], JJ Pérez[2], MB Vidriales[2], M Lima[3], AH Santos[3], AW Langerak[4], D Tielemans[4], L Lhermitte[5], V Asnafi[5], E Macintyre[5], S Böttcher[6], A Mendonça[7], P Lucio[7], R de Tute[8], M Cullen[8], A Rawstron[8], L Sedek[9], T Szczepański[9], T Kalina[10], M Martin-Ayuso[11], JJM van Dongen[4] and A Orfao[1]

[1]USAL, Salamanca, Spain; [2]HUS, Salamanca, Spain; [3]HSA-CHP, Porto, Portugal; [4]Erasmus MC, Rotterdam, The Netherlands; [5]AP-HP, Paris, France; [6]UNIKIEL, Kiel, Germany; [7]IPOLFG, Lisbon, Portugal; [8]UNIVLEEDS, Leeds, UK; [9]SUM, Zabrze, Poland; [10]DPH/O, Prague, Czech Republic and [11]Cytognos SL, Salamanca, Spain

BACKGROUND

T-cell CLPD, also termed peripheral (mature) T-cell neoplasms (PTCL), are relatively uncommon lymphoid malignancies (~10% of all CLPD in Western countries) derived from post-thymic mature T-cells.[3,242,243] Despite their low frequency, T-CLPD comprise a

highly diverse and heterogeneous group of entities,[3,244] much less understood than their B-cell counterpart owing to their rarity and biological heterogeneity and the lack of distinctive genetic markers for most disease categories.[244,245] Consequently, subclassification of major groups of T-CLPD still remains a challenge. As an example, the most common WHO 'category' of T-CLPD in Western countries (~30% of all T-CLPD) is that of PTCL not otherwise specified (PTCL-NOS),[3] which is mostly defined by exclusion criteria (for example, lack of specific features of other better-defined WHO diagnostic categories of PTCL).[3,246,247] Nevertheless, some progress has been made in recent years in our understanding of the pathogenesis of several subtypes of T-CLPD. On one side, this has been due to the identification of the normal counterparts of specific PTCL groups. For example, angioimmunoblastic T-cell lymphoma (AITL) has emerged as a distinctive subtype of T-CLPD derived from follicular T helper cells[3,247–249] and $CD4^+/CD25^+/CyFoxp3^+$ regulatory T-cells are known to be the closest normal counterpart of adult T-cell leukemia/lymphoma (ATLL) cells.[3,245] On the other side, such advances are related to the identification of unique biological features among specific subgroups of patients that contribute to a better prognostic stratification of patients. For instance, anaplastic large cell lymphoma (ALCL) is composed of two distinct entities with different prognosis, based on the presence or absence of expression of the anaplastic lymphoma kinase (*ALK*) gene;[250] similarly, T-cell prolymphocytic leukemia (T-PLL) cells specifically overexpress the kinase coactivator Tcl1 in a substantial proportion of cases, due to chromosomal rearrangements involving the *TCL1* gene.[251,252]

With the exception of mycosis fungoides (MF), primary cutaneous ALCL and T-cell LGL leukemia,[3] PTCL are among the most aggressive lymphoid neoplasms.[246,253] This means that most patients present with clear signs and symptoms of a CLPD, frequently associated with PB involvement, in addition to infiltration of LN and skin, among other tissues.[3] The application of the EuroFlow T-CLPD panel on samples from patients known to have increased numbers of (aberrant) T-cells as identified/suspected by the LST tube (see Section 2) aims at accurate confirmation of the presence of clonal T-cells in the different samples analyzed regardless of their nature—PB, LN or other tissues—and precise classification of the chronic T-cell disease into a specific WHO PTCL category.

The design and development of a standardized 8-color antibody T-CLPD panel to classify T-CLPD comprised the selection of combinations of both backbone markers and characterization markers for the identification and characterization of the T-cell population(s) of interest, as described below.

Selection of backbone markers

Four antigens (CD45, SmCD3, CD4 and CD8) were chosen as backbone markers for the T-CLPD panel, in order to identify normal mature T-cells ($CD45^{hi}/SmCD3^+$ events) and the major T-cell subsets defined by the expression pattern of CD4 and CD8 ($CD4^+/CD8^-$; $CD4^+/CD8^+$; $CD4^-/CD8^{-/lo}$; and $CD4^-/CD8^{hi}$). Initially, the following fluorochrome-conjugate monoclonal antibodies were tested as backbone reagents (BB1 in Table 16): CD8–PacB, CD45–AmCyan, CD3–PerCPCy5.5 and CD4–AF700. The proposed combination was initially tested by one center on eight PB samples from healthy adults. While the performance of the CD3–PerCPCy5.5 conjugate was optimal, the following limitations were found for the other three backbone markers: (i) interference of CD45-AmCyan in the FITC channel[16]; (ii) very poor (5/8 cases) or poor (3/8 cases) ability of CD4-AF700 for clear cut identification of $CD4^+$ T-cells; and (iii) poor resolution of the CD8-PacB reagent to discriminate $CD8^{lo}$ T-cells (7/8 cases). As a result, a second alternative combination of backbone markers for the T-CLPD panel was designed (BB2 in Table 16): CD4–PacB, CD45–PacO, CD3–PerCPCy5.5 and CD8–APCH7.

Preliminary testing with this second combination of backbone markers was initially done at one center in three PB samples, with clear improvement as regards the identification of normal T cells, in the absence of significant technical issues. Consequently, the combination underwent further evaluation at two distinct EuroFlow sites for a total of 12 PB samples. The new combination of backbone markers proved to be useful in every case tested for the identification of T-cells and the major T-cell subsets, as well as for their discrimination from the remaining leukocyte populations, in both normal/reactive ($n = 9$) and pathological samples ($n = 6$). Notably, this combination of backbone markers was also robust enough to

Table 16. Design of the T-CLPD panel in two consecutive testing rounds[a]

Version (no. of cases)[b]	*Tube*	*Fluorochromes and markers*								
		PacB	*AmCyan*	*FITC*	*PE*	*PerCPCy5.5*	*PECy7*	*APC*	*AF700*	*Aim (phenotypic characterization)*
BB 1	1	CD8	CD45			SmCD3			CD4	
		PacB	PacO	FITC	PE	PerCPCy5.5	PECy7	APC	APCH7	
BB 2	1	CD4	CD45			SmCD3			CD8	
1 ($n = 19$)	1	CD4	CD45	CD7	CD26	SmCD3	CD2	CD28	CD8	SS
	2	CD4	CD45	CD27	CD197(CCR7)	SmCD3	CD45RO	CD45RA	CD8	Maturation stage
	3	CD4	CD45	CD5	CD25	SmCD3	HLADR	CyTcl1	CD8	T-PLL
	4	CD4	CD45	CD57	CD30	SmCD3	TCRγδ	CD11c	CD8	Cytotoxic phenotype; ALCL
	5	CD4	CD45	CyPerforin	CyGranzyme B	SmCD3	CD16	CD94	CD8	Cytotoxic phenotype; T-LGL
2 (Final) ($n = 67$)	1	CD4	CD45	CD7	CD26	SmCD3	CD2	CD28	CD8	SS
	2	CD4	CD45	CD27	CD197(CCR7)	SmCD3	CD45RO	CD45RA	CD8	Maturation stage
	3	CD4	CD45	CD5	CD25	SmCD3	HLADR	CyTcl1	CD8	T-PLL
	4	CD4	CD45	CD57	CD30	SmCD3		CD11c	CD8	Cytotoxic phenotype; ALCL
	5	CD4	CD45	CyPerforin	CyGranzyme B	SmCD3	CD16	CD94	CD8	Cytotoxic phenotype; T-LGL
	6	CD4	CD45		CD279[c]	SmCD3			CD8	AITL

Abbreviations: AF700, alexa fluor 700; AITL, angioimmunoblastic T-cell lymphoma; ALCL, anaplastic large cell lymphoma; AmCyan, *Anemonia Majano* cyan fluorescent protein; APC, allophycocyanin; BB, backbone; BM, bone marrow; CLPD, chronic lymphoproliferative disorder; Cy, cytoplasmic; Cy7, cyanin7; FITC, fluorescein isothiocyanate; H7, hilite7; LGL, large granular lymphocytic leukemia; PacB, pacific blue; PacO, pacific orange; PB, peripheral blood; PE, phycoerythrin; PerCPCy5.5, peridinin–chlorophyll–protein–cyanin5.5; Sm, surface membrane; SS, Sézary syndrome; T-PLL, T-cell prolymphocytic leukemia.
[a]Further information about markers and hybridomas is provided in the Appendix. [b]A total of 86 samples (78 PB, 7 BM and 1 other type of sample) was evaluated: 20 normal samples and 66 pathological samples (37 clonal expansions of $CD4^+$ T cells, 18 of $CD8^+$ T cells and 11 clonal samples of $CD4^-/CD8^{-/lo}$ T cells). [c]Testing of a CD279-PECy7 conjugate reagent is ongoing to avoid tube 6 by placing this marker in the empty position in tube 4. Highlighted boxes: changes as compared to previous version.

allow gating, merging and calculating strategies with the Infinicyt software for aberrant T-cell populations, as detailed below.

Selection of characterization markers

The major aim of the EuroFlow T-CLPD panel is (i) to detect phenotypically aberrant T-cells and (ii) to allow precise classification of T-CLPD into the current WHO diagnostic categories.[3] Therefore, once the optimal backbone reagents had been definitively established, antibody reagents for further characterization and classification of T cells were then selected from a large list of T-cell related markers.[3,78,242,243,245,250–259] These included antibodies against classical pan-T-cell associated antigens known to be aberrantly expressed in many T-CLPD disease categories (for example, CD2, CD5 and CD7),[3,242,257] T-cell maturation-associated markers (for example, CD27, CD197 (CCR7), CD45RA and CD45RO),[245] co-stimulatory molecules (for example, CD26 and CD28),[3,242,243] activation-associated markers (for example, CD25—also constitutively expressed by $CD4^+/CD25^+$ regulatory T-cells[245]—CD38, CD69 and HLADR),[256,257] interleukin-2 receptors other than CD25 (CD122), cytotoxic-related molecules expressed by effector T-LGL,[256,258,259] such as CD11c, CD16, CD56, CD57, killer-cell Ig-like receptors (for example CD158a/b/e/j/k and NKB1), and lectin-type (for example, CD94 and CD161) receptors, as well as intracytoplasmic proteins (for example, perforin, granzymes and TIA-1). In addition, markers reported to be expressed in specific WHO subtypes of T-CLPD such as CD30,[3,260] CyTcl1[251,252] and follicular $CD4^+$ helper T-cell-associated markers[245] (for example, CD10 and CD279, among other markers) were also considered as candidates to be included in the panel. Based on existing data about all these markers, and the experience of the EuroFlow members, the following criteria were used to select individual reagents for further testing: (i) its ability to identify immunophenotypically aberrant T-cells in a significant proportion of T-CLPD or their specific WHO disease categories and (ii) its contribution to the definition of the maturation stage (naive versus memory versus terminally differentiated or effector cells) of the expanded T-cells; the final goal was to classify the different T-CLPD entities according to the more recent version of the WHO classification.[3]

It is currently well known that monoclonal T cells from T-CLPD frequently show downregulation of pan-T-cell markers, such as CD2, CD5 and CD7, in addition to SmCD3 and CD4.[3,242,243] Therefore, reagents recognizing these molecules were considered as mandatory to be selected for further testing (*first diagnostic level* markers in Table 17) and hence included in the initial EuroFlow T-CLPD panel. Other markers (or combinations of markers) were selected also as *first-level* markers based on their contribution to a more precise subclassification of T-CLPD into particular WHO categories.[3] CD26 and CD28 are useful markers for the identification of Sézary cells, as those $CD2^{lo}/CD4^{lo}/SmCD3^{lo}$ T-cells showing a typical $CD26^-/CD28^+$ phenotypic pattern.[255,261,262] Similarly, CD30 is typically, but not exclusively,[263] expressed in systemic ALCL (ALK^- and ALK^+) and primary cutaneous $CD30^+$ T-cell lymphoproliferative disorders.[264] Preliminary studies reported that T-cell neoplasms other than T-PLL could also express CyTcl1,[264] but more recent reports have shown that within T-cell malignancies, CyTcl1 expression is restricted to most (around 70–80%) T-PLL cases,[251,252] while it is absent in $CD30^{-/+}$ ALCL, T lymphoblastic lymphoma, nodal PTCL, MF[265] or any other mature T-cell tumor types.[251,252] Inclusion of the CD11c, CD16 and CD57 *first-level* markers and the CD94, granzyme B and perforin *second-level* cytotoxic-related markers was based on their ability to assess cytotoxic-associated phenotypes and hence to identify T-LGL,[3,258,259] although

Table 17. Utility of T-CLPD markers

Tube	*Target antigen*	*Identification of T-cells and T-cell subsets*	*Diagnostic level*		*Sub-classification*
			1st	*2nd*	
BB markers	CD3	X			
	CD4	X			X
	CD8	X			X
	CD45	X			
Tube 1	CD7		X		
	CD26		X		X
	CD2		X		X
	CD28		X		X
Tube 2	CD27			X	
	CD197 (CCR7)		X		X
	CD45RO			X	
	CD45RA		X		
Tube 3	CD5		X		
	CD25			X	X
	HLADR			X	
	CyTcl1		X		X
Tube 4	CD57		X		X
	CD30		X		X
	CD11c		X		X
Tube 5	CyPerforin			X	X
	CyGranzyme B			X	X
	CD16		X		X
	CD94			X	
Tube 6	CD279		X		X
Other	TCR Vβ families		X		

Abbreviations: BB, backbone; CLPD, chronic lymphoproliferative disorders; Cy, cytoplasmic.

T-CLPD cases other than T-LGL have also been found to express cytotoxic molecules.[3,245] The CD56 cytotoxic molecule was not included in the EuroFlow T-CLPD panel, as it was already present in the LST tube; in contrast, at this time anti-TCRγδ had not yet been included in the EuroFlow LST, and therefore it was considered as a mandatory marker to assess the TCRγδ versus TCRαβ nature of the disease. Other markers selected at this stage included the CD27, CD197(CCR7), CD45RA and CD45RO maturation-associated markers and the CD25 and HLADR activation-related proteins; the inclusion of all these latter groups of markers was based on the fact that the phenotype of pathological cells from many T-CLPD correlates with distinct maturation-associated subsets of T-cells, and therefore the differential expression of the CD45 isoforms, CD27 and CD197(CCR7) could be useful not only for the definition of the maturation stage of tumor cells,[245] but also for a more refined classification of T-CLPD cases into the distinct WHO entities. In this regard, previous studies have shown that Sézary cells typically display a $CD4^+$ memory T-cell phenotype,[255] while T-PLL cells display a phenotype consistent with a naive/central memory T-cell[3] and the phenotype of T-LGL leukemia cells overlaps with that of normal activated effector T-cells.[256]

Once the target molecules were selected, monoclonal antibodies against them were chosen among the FITC-, PE-, PECy7- and APC-fluorochrome conjugates, which were commercially available; the first version of the EuroFlow T-CLPD panel was then designed (Table 16) and evaluated. Shortly after the design of version 1, the second and definitive version of the EuroFlow T-CLPD panel was developed, with the following two major improvements: (i) exclusion of the anti-TCRγδ reagent, to avoid redundancy with the LST (note that version 1 of T-CLPD panel was developed in parallel with the first four versions of the LST, when anti-TCRγδ was not yet included in it); and (ii) inclusion of CD279 as a characteristic marker of follicular $CD4^+$ helper T-cells, to increase the diagnostic power of the panel for the identification of AITL.[3,247–249] The recent availability of new CD279 reagents (for example, CD279–PECy7 from BDB) would contribute to improve the current version of the EuroFlow T-CLPD panel, as the CD279–PE monoclonal antibody reagent used until now might be replaced by the new PECy7 conjugate of the same CD279 clone in the corresponding PECy7 position of tube 4 (Table 16), resulting in a five (instead of six) 8-color combinations of monoclonal antibodies.

The description of the precise role for each marker in the panel of all reagents included in the T-CLPD panel (version 2) is shown in Table 17.

Evaluation of the EuroFlow T-CLPD panel

Testing of the EuroFlow T-CLPD panel (version 2) was performed by seven EuroFlow centers involved in the study of T-CLPD. A total of 67 samples were stained with the full panel (version 2) (Table 18); these included 11 PB samples from healthy adults (mean age of 33 ± 6 years; 7 males and 4 females), 34 samples from patients with clonal expansions of $CD4^+$ T-cells (mean age of 62 ± 12 years; 20 males and 14 females, distributed in the distinct WHO subtype diseases[3] as shown in Table 18), 11 samples containing clonally expanded $CD8^{hi}$ T-cells (mean age of 60 ± 17 years; 3 males and 8 females), 10 samples of $TCR\gamma\delta^+$ T-CLPD (mean age of 59 ± 14 years; 8 males and 2 females) and 1 sample from a 67-year-old male with $CD4^-/CD8^{-/lo}$ $TCR\alpha\beta^+$ T-cell leukemia. In 30/56 patients (54%) T-cell clonality was confirmed by *TCR* gene rearrangement analyses according to the BIOMED-2 multiplex PCR protocols[266] performed either on whole samples or on highly-purified T-cell fractions.

In order to evaluate the utility of the EuroFlow T-CLPD panel for the purposes referred above, pairwise unsupervised discrimination

Table 18. Phenotypic patterns and numbers of pathological T-cells detected with the final version of the EuroFlow T-CLPD panel ($n = 67$)

Diagnostic group[a]	*Aberrant T-cells*[b] *(no. of cases/total cases)*	*No of T-cells*	
		% of T-cells (from WBC)[c]	*No of T-cells*[d] *($\times 10^3/\mu l$)*
Healthy adult donors ($n = 11$)	0/11	$CD4^+/CD8^-$: 12.3 (7.4–21.8) $CD8^{hi}/CD4^-$: 7.2 (2.8–14.4) $CD4^-/CD8^{-/lo}$: 0.6 (0.2–3.7) $CD4^+/CD8^{hi}$: 0.34 (0.0–2.1)	700 (400–1900) 400 (170–1000) 50 (10–200) 20 (7–100)
Clonal expansions of $CD4^+$ T-cells[e] (n = *34)*			
Sézary syndrome ($n = 9$)	9/9	24 (4.4–88.7)	3560 (170–5300)
T-PLL ($n = 5$)	5/5	90 (61–96)	214 000 (63 000–528 000)
ATLL ($n = 4$)	4/4	82 (39–85)	23 600 (3200–34 900)
$CD4^+$ LGL ($n = 4$)	4/4	25 (10–60)	2300 (1500–3200)
AITL ($n = 2$)	2/2	5.6 (3–8.3)	1100
PTCL-NOS ($n = 10$)	10/10	14 (3.3–65)	3000 (1900–6100)
Clonal expansions of $CD8^{hi}$ T-cells (n = *11)*			
T-LGL ($n = 10$)	9/10	27 (1–56)	1500 (110–9500)
$CD8^{hi}$ PTCL-NOS ($n = 1$)	1/1	17	6010
Clonal expansions of $CD4^-/CD8^{-/lo}$ T-cells (n = *11)*			
$TCR\gamma\delta^+$ T-LGL ($n = 9$)	8/9	19 (1.3–33)	1500 (30–5900)
$TCR\gamma\delta^+$ hepatosplenic T-cell lymphoma ($n = 1$)	1/1	24	ND
$TCR\alpha\beta^+$ T-CLPD ($n = 1$)	1/1	75	NA

Abbreviations: AITL, angioimmunoblastic T-cell lymphoma; ATLL, adult T-cell leukemia–lymphoma; BM, bone marrow; CLPD, chronic lymphoproliferative disorders; LGL, large granular lymphocyte leukemia; NA, not applicable; ND, not available; PB, peripheral blood; PTCL-NOS, peripheral T-cell lymphoma not otherwise specified; TCR, T-cell receptor; T-PLL, T-cell prolymphocytic leukemia; WBC, white blood cells. [a]A total of 67 cases was evaluated, which corresponded to 59 PB, 7 BM and 1 ascitic fluid sample. [b]According to previously reported studies (References[78,243,245,254,258,260-264,266]). [c]Results expressed as median % of T-cells from WBC (range). For the different patient groups, only data from the expanded/ aberrant T-cell population is shown. [d]Results expressed as median absolute number of circulating T-cells $\times 10^3/\mu l$ (range) for the PB samples analyzed; for the different patient groups, only data from the expanded/ aberrant T-cell populations are shown. [e]Regardless of CD8 expression (either negative or dimly positive).

by PCA with the APS function provided with the Infinicyt software program was used.[16,241] Regarding clonal CD4$^+$ T-cell cases, samples from all T-CLPD categories but PTCL-NOS included in the multicenter testing phase (Sézary syndrome (SS), T-PLL, ATLL, CD4$^+$ T-LGL and AITL) clearly clustered separately from normal CD4$^+$ T-cells (Figure 27A, plots 'a' to 'f'). The most informative markers responsible for such separation included maturation-associated molecules such as CD45RA, CD45RO, CD27 and CD28—probably reflecting the fact that normal CD4$^+$ T cells are heterogeneous, in contrast to the more homogeneous maturational patterns displayed by clonal T cells—and markers expected to be relevant for such a discrimination between normal CD4$^+$ T cells and clonal cells from SS (CD2, CD26 and CD7), T-PLL (CyTcl1), ATLL (HLADR and CD25), CD4$^+$ T-LGL (CD28, CyGranzyme B and CD7) and AITL (CD279, HLADR and SmCD3) (Figure 27). Similarly, CD4$^+$ T-CLPD cases from different WHO disease categories also expressed distinct phenotypic profiles versus the other groups, as illustrated in Figure 27B (plots 'g' to 'l') for several of the most relevant two-by-two comparisons. The precise markers mostly contributing to discriminate each CD4$^+$ T-CLPD group from other CD4$^+$ reference groups are also displayed in this figure (Figure 27B, plots 'g' to 'f'); interestingly, these discriminating markers included most of the markers found to be also relevant for the discrimination between each WHO disease group and normal CD4$^+$ T-cells. PTCL-NOS cases were not included in such comparisons since, as expected, they formed a highly heterogeneous group. However, when each PTCL-NOS case was individually compared with normal CD4$^+$ T-cells and the cases from the other WHO disease categories, no overlap was observed, except for 4/10 PTCL-NOS cases that showed partial overlap with Sézary cells. Noteworthily, no CD30$^+$ cases have been analyzed so far with the EuroFlow panel, but data derived from previous experience and immunohistochemical analyses support its utility in the T-CLPD panel proposed here.

Regarding the CD8^{hi} (10/11) and CD4$^-$/CD8$^{-/lo}$ (10/11) T-CLPD groups, all but two cases also showed clearly different immunophenotypic profiles versus their corresponding normal T-cell counterparts, as illustrated in Figure 28a and c for representative cases from both groups. In only one T-LGL case in each of the CD8^{hi} and CD4$^-$/CD8$^{-/lo}$ T-CLPD groups (Figure 28b and d) was marked overlap between the phenotypic profiles of clonal and normal T-cells observed. Markers contributing the most to the discrimination between each clonal CD8^{hi} T-CLPD case and the reference group of normal CD8^{hi} T-cells included CD45RO, CD27, CyGranzyme B, CD28, CD57 and CD45RA; similarly, CD28, CyGranzyme B, CD45RA, CD45RO, CD16, CD11c and CD27 were

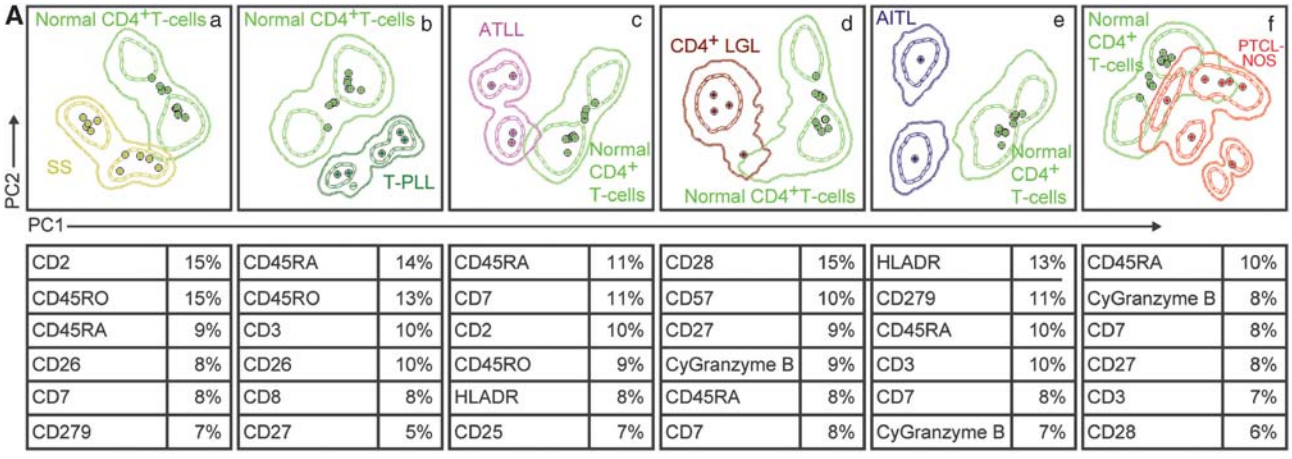

CD2	15%	CD45RA	14%	CD45RA	11%	CD28	15%	HLADR	13%	CD45RA	10%
CD45RO	15%	CD45RO	13%	CD7	11%	CD57	10%	CD279	11%	CyGranzyme B	8%
CD45RA	9%	CD3	10%	CD2	10%	CD27	9%	CD45RA	10%	CD7	8%
CD26	8%	CD26	10%	CD45RO	9%	CyGranzyme B	9%	CD3	10%	CD27	8%
CD7	8%	CD8	8%	HLADR	8%	CD45RA	8%	CD7	8%	CD3	7%
CD279	7%	CD27	5%	CD25	7%	CD7	8%	CyGranzyme B	7%	CD28	6%

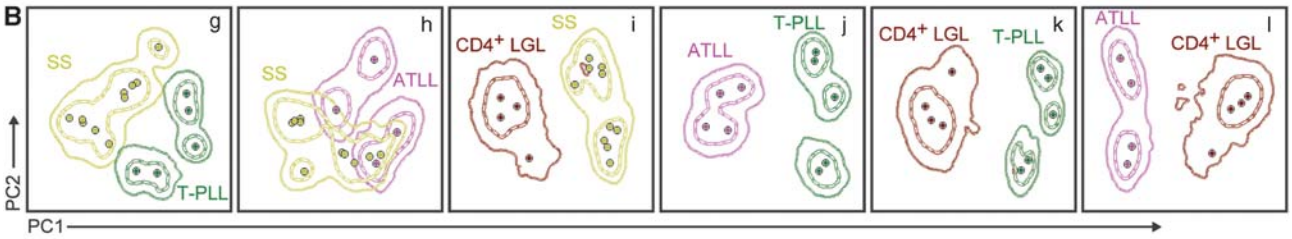

CD2	13%	CD45RO	22%	CD28	15%	CD7	12%	CD28	14%	CD28	14%
CD26	12%	HLADR	15%	CD45RA	11%	CD26	11%	CD26	10%	CD45RA	13%
CD7	11%	CD45RA	14%	CD57	11%	HLADR	9%	CD197(CCR7)	9%	CD57	10%
CD45RO	10%	CD2	12%	CD2	9%	CD197(CCR7)	8%	CD7	8%	CD45RO	9%
CD8	8%	CD25	9%	CD27	9%	CD2	8%	CD45RA	8%	CD2	8%
CD197(CCR7)	7%	CD5	5%	CD197(CCR7)	7%	CyTcl1	8%	CD57	7%	CD27	7%

Figure 27. Comparative principal component (PC)1 versus PC2 views of CD4$^+$ T-chronic lymphoproliferative disorders (CLPD) cases. **A** (plots a–f) shows the APS (automated population separator, PC1 versus PC2) views for the comparisons of each CD4$^+$ T-CLPD WHO diagnostic subgroup—Sézary syndrome (SS), light green; T-cell prolymphocytic leukemia (PLL), dark green, adult T-cell leukemia/lymphoma (ATLL), pink; CD4$^+$ large granular lymphocytic (LGL) leukemia, brown; angioimmunoblastic lymphoma (AITL), dark blue; and peripheral T-cell lymphoma not otherwise specified (PTCL-NOS), red—versus normal CD4$^+$ T-cells (green), while **B** (plots g– l) shows two-by-two PCA comparisons between different diagnostic categories of CD4$^+$ T-CLPD. Each circle represents one single case (median expression observed for all phenotypic parameters evaluated), while contour lines represent s.d. curves (dotted and continuous lines represent 1s.d. and 2s.d., respectively). The six most informative markers contributing to the best discrimination between CD4$^+$ T cells from the different cases are displayed at the bottom of each plot, in a decreasing order of percentage contribution to the discrimination.

the most informative markers for the distinction between normal and clonal CD4$^-$/CD8$^{-/lo}$ T-cells. No clear phenotypic differences were observed among the distinct WHO disease categories either within the CD8^{hi} (TCR$\alpha\beta^+$ T-LGL versus CD8^{hi} PTCL-NOS) or within the CD4$^-$/CD8$^{-/lo}$ (TCR$\gamma\delta^+$ T-LGL versus hepatosplenic T-cell lymphoma) T-CLPD groups (data not shown); however, owing to the limited number of cases included in some of these groups, further studies are required in the future to confirm these very preliminary findings.

CONCLUSIONS

Although the series of T-CLPD patients analyzed is still relatively limited ($n = 56$), particularly within some WHO disease categories, our results clearly show that the 8-color EuroFlow T-CLPD panel contributes to the diagnostic classification of T-CLPD. Accordingly, this panel allows distinction between clonal T-cells and their corresponding normal counterparts in the vast majority of cases (50/56); at the same time, it provides useful information for the subclassification of the disease. In this regard, the panel proposed allowed unequivocal classification of CD4$^+$ T-CLPD into specific WHO subtypes, particularly SS, T-PLL, ATLL, CD4$^+$T-LGL and AITL, for which markers like CD2, CD7, CD26, CD28 (for SS), CD25, HLADR (for ATLL), cytotoxic-associated markers (for CD4$^+$ T-LGL), CyTcl1 (for T-PLL) and CD279 (for AITL) were particularly informative. The precise value of CD30 in this panel needs to be further investigated in future studies, as no CD30$^+$ T-CLPD cases have been analyzed so far. Regarding CD8^{hi} and CD4$^-$/CD8$^{-/lo}$ T-CLPD, our data also confirm the value of the panel in discriminating between clonal cytotoxic effector T-cells and their normal counterparts, except for a few T-LGL leukemia cases, where clonal T-cells overlapped with their normal/reactive counterpart; however, the value of the marker combinations used here for the identification of specific CD8$^+$ and CD4$^-$/CD8$^{-/lo}$ T-CLPD WHO disease categories seems to be more limited than in CD4$^+$ T-CLPD cases and deserves further investigation in larger series of patients, both by the EuroFlow Consortium and by other groups.

SECTION 10. ANTIBODY PANEL FOR NK-CELL CHRONIC LYMPHOPROLIFERATIVE DISEASES (NK-CLPD)

J Almeida[1], J Flores-Montero[1], L Lhermitte[2], V Asnafi[2], R de Tute[3], M Cullen[3], A Rawstron[3], D Tielemans[4], AW Langerak[4], JJ Pérez[5], M Lima[6], AH Santos[6], A Mendonça[7], P Lucio[7], S Böttcher[8], L Sedek[9], T Szczepański[9], T Kalina[10], M Muñoz[11], JJM van Dongen[4] and A Orfao[1]

[1]USAL, Salamanca, Spain; [2]AP-HP, Paris, France; [3]UNILEEDS, Leeds, UK; [4]Erasmus MC, Rotterdam, The Netherlands; [5]HUS, Salamanca, Spain; [6]HSA-CHP, Porto, Portugal; [7]IPOLFG, Lisbon, Portugal; [8]UNIKIEL, Kiel, Germany; [9]SUM, Zabrze, Poland; [10]DPH/O, Prague, Czech Republic and [11]Cytognos SL, Salamanca, Spain

BACKGROUND

NK-cell neoplasms are rare hematological disorders, which represent $<1\%$ of all lymphomas and chronic lymphoid disorders in Western countries.[267] In addition to their rarity, they are also rather heterogeneous, including distinct clinicopathologic disease entities. According to the most recent WHO classification,[3] three distinct malignancies derived from mature NK-cells are recognized: aggressive NK-cell leukemia, extranodal (nasal type) NK/T-cell lymphoma and CLPD of NK cells. The former two entities are strongly associated to infection by the Epstein–Barr virus (EBV) and they are characterized by an aggressive clinical course and poor survival. Conversely, CLPD of NK cells (NK-CLPD) represent a new provisional category, which includes cases previously designated as chronic NK-cell lymphocytosis, chronic NK-large granular leukemia and NK-cell LGL lymphocytosis, among other terms.[3,268] Indeed, NK-CLPD comprises a broad spectrum of NK-cell proliferations,[3,268] from reactive to neoplastic expansions, difficult to distinguish because of lack of a universal NK-cell marker for clonality. Noteworthily, NK-CLPD is the most common mature NK-cell proliferation in Caucasians; it is not systematically associated to EBV infection[3] and the clinical course of patients is usually indolent. In these patients the number of NK cells

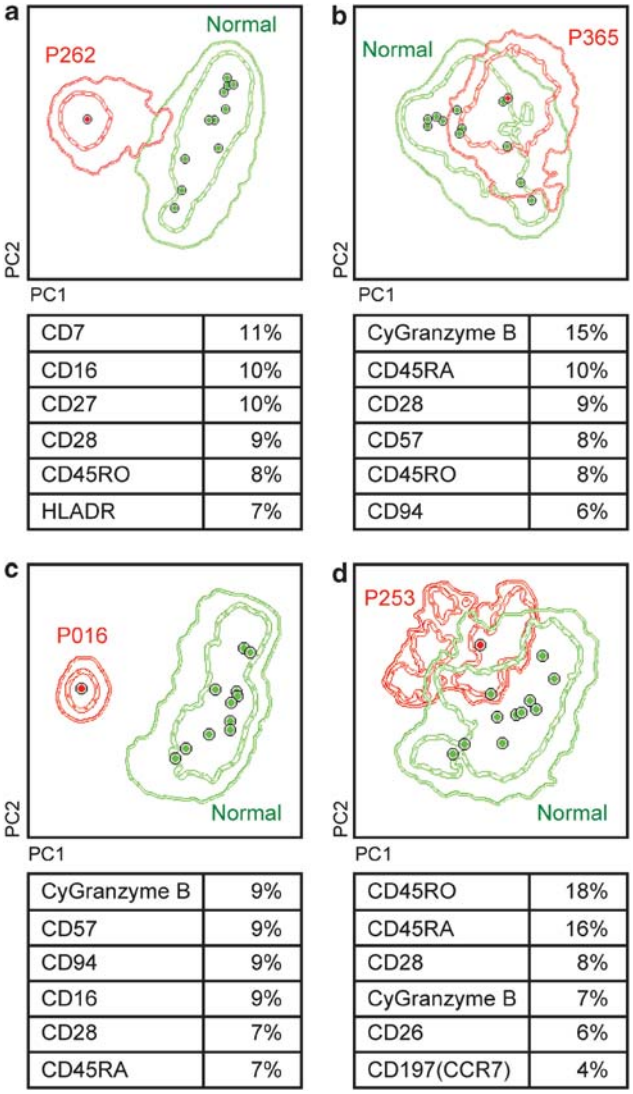

CD7	11%
CD16	10%
CD27	10%
CD28	9%
CD45RO	8%
HLADR	7%

CyGranzyme B	15%
CD45RA	10%
CD28	9%
CD57	8%
CD45RO	8%
CD94	6%

CyGranzyme B	9%
CD57	9%
CD94	9%
CD16	9%
CD28	7%
CD45RA	7%

CD45RO	18%
CD45RA	16%
CD28	8%
CyGranzyme B	7%
CD26	6%
CD197(CCR7)	4%

Figure 28. Comparative principal component (PC)1 versus PC2 views of CD8^{hi} and CD4$^-$/CD8$^{-/lo}$ T-cells in four T-cell chronic lymphoproliferative disease (T-CLPD) cases. (**a**, **b**) show APS (automated population separator, PC1 versus PC2) views of two CD8^{hi} T-CLPD cases versus normal CD8^{hi} T-cells, while **c** and **d** show comparisons of two CD4$^-$/CD8$^{-/lo}$ T-CLPD cases versus normal CD4$^-$/CD8$^{-/lo}$ T-cells. (**a**) and (**c**) show representative cases of most CD8^{hi} and CD4$^-$/CD8$^{-/lo}$ T-CLPD patients who had a phenotypic pattern clearly different from that of their normal T-cell counterpart (10/11 cases for each T-CLPD group), while (**b**) and (**d**) show the only two cases for which clonal T-cells displayed an overlapping phenotype with that of normal T-cells. In all panels, T-CLPD samples are depicted as red circles, while normal/reference T-cells are shown as green circles. Each circle represents one single case (median expression observed for all phenotypic parameters evaluated), while contour lines represent s.d. curves (dotted and continuous lines represent 1s.d. and 2s.d., respectively). The six most informative markers contributing to the best discrimination between normal and clonal T-cells from each individual case displayed are listed at the bottom of each plot, in a decreasing order of percentage contribution to the discrimination.

Table 19. Design of the NK-CLPD panel[a]

Version (no. of cases)[b]	*Tube*	*Fluorochromes and markers*								*Aim*
		PacB	*AmCyan*	*FITC*	*PE*	*PerCPCy5.5*	*PECy7*	*APC*	*AF700*	
BB 1	1	CD19	CD45			SmCD3			CD56	
		PacB	*PacO*	*FITC*	*PE*	*PerCPCy5.5*	*PECy7*	*APC*	*APCH7*	
BB 2	1		CD45			SmCD3	CD56		CD19	
Final ($n = 38$)	1	CD2	CD45	CD7	CD26	SmCD3	CD56	CD5	CD19	Aberrant NK-cells
	2	CD16	CD45	CD57	CD25	SmCD3	CD56	CD11c	CD19	Aberrant NK-cells
	3	HLADR	CD45	CyPerforin	CyGranzyme B	SmCD3	CD56	CD94	CD19	Aberrant NK-cells, cytotoxic phenotype

Abbreviations: AF700, alexa fluor 700; AmCyan, *Anemonia Majano* cyan fluorescent protein; APC, allophycocyanin; BB, backbone; CLPD, chronic lymphoproliferative disorder; Cy, cytoplasmic; Cy7, cyanin7; FITC, fluorescein isothiocyanate; H7, hilite7; PacB, pacific blue; PacO, pacific orange; PB, peripheral blood; PE, phycoerythrin; PerCPCy5.5, peridinin–chlorophyll–protein–cyanin5.5; Sm, surface membrane. [a]Further information about markers and hybridomas is provided in the Appendix. [b]A total of 38 PB samples was evaluated, which corresponded to 10 normal and 28 pathological samples. Highlighted boxes: changes as compared to previous version.

typically remains stable for many years without therapy and sometimes it may even show spontaneous regression,[268] which could reflect in such cases the reactive nature of the expansion; however, rare cases of NK-CLPD have been reported that transformed into an aggressive NK-cell leukemia.[269,270]

As in European countries, most NK-cell proliferations correspond to NK-CLPD; the most common reason for consulting in such cases is lymphocytosis detected in a routine WBC count in association or not with cytopenias and in the absence of other associated symptoms or physical signs of disease. According to the stepwise diagnostic workflow recommended by the EuroFlow Consortium (Figure 1), in a first step the LST (see Section 2) should be applied in these cases and when the NK-cell lineage is suspected to be responsible for the lymphocytosis—absolute or relative expansion of either $CD56^{+}$ or $CD56^{-/lo}$/ $CD45^{hi}$ cells in the absence of expression of SmCD3, CD4, TCR$\gamma\delta$ and CD19 in the LST—the NK-CLPD panel is then applied in a second step, for full characterization. Therefore, the EuroFlow NK-CLPD panel aims at further characterization of the expanded NK-cells, to discriminate between aberrant and normal/reactive NK-cells, and to establish the precise diagnosis.

Selection of backbone markers

Four backbone markers (CD45, SmCD3, CD56 and CD19) were selected for the NK-CLPD panel, to unequivocally identify NK cells, as those $CD45^{hi}$/$SmCD3^{-}$ events showing reactivity for CD56; inclusion of CD19 and SmCD3 as backbone markers is supported by the fact that in around one-third of NK-cell expansions NK cells show absence or dim expression of CD56;[79] therefore, in these latter cases NK cells are identified by exclusion of the remaining cells included in the, for example, $CD45^{hi}$/SSC^{lo} 'lymphocyte gate' (T- and B-cells). In the first testing phase, the following fluorochrome conjugates were used as backbone reagents (BB1 in Table 19): CD19–PacB, CD45–AmCyan, CD3–PerCPCy5.5 and CD56–AF700. This proposed combination was initially tested at one center in eight PB samples from healthy adults. This showed that while the performance of the CD19–PacB and CD3–PerCPCy5.5 conjugates was optimal—in terms of, for example, brightness, SI, limited spectral overlap—to exclude mature B- and T-cells, respectively, two technical limitations existed: (i) interference of CD45-AmCyan in the FITC channel[16] and (ii) low resolution of the CD56–AF700 conjugate to identify $CD56^{lo}$ NK cells. Consequently, the following changes were introduced in the backbone markers of the NK-CLPD panel: (i) the AmCyan fluorochrome was replaced by PacO for evaluation of CD45, and (ii) the CD56–AF700 conjugate was planned to be substituted by an anti-CD56–APCH7 reagent. However, owing to the limited availability of APCH7-conjugated reagents at the time of testing (November 2007), a second alternative combination of backbone markers for the NK-CLPD panel was designed (BB2 in Table 19): CD45–PacO, CD56–PECy7, CD3–PerCPCy5.5 and CD19–APCH7. Of note, the CD56–PECy7 reagent included in this second version of the NK-CLPD backbone was selected after testing in parallel two different commercially available CD56–PECy7 reagents: CD56–PECy7 from BD Biosciences (clone: NCAM16.2) and CD56-PECy7 (clone: N901/NKH1); this comparison was performed at one center in a total of three PB samples from healthy adults, and it showed a better performance for the latter reagent, with a greater SI versus the former conjugate (median SI of 9.8 versus 5.2, respectively).

Testing of this second combination of backbone markers proposed for the NK-CLPD panel was initially done at one center in three PB samples. Preliminary results showed a clear

Table 20. Utility of NK-CLPD markers

Tube	*Target antigen*	*Identification of NK-cells*	*Diagnostic level*	
			1st	*2nd*
BB markers	SmCD3	X		
	CD19	X		
	CD45	X		
	CD56	X		
Tube 1	CD2		X	
	CD7		X	
	CD26			X
	CD5			X
Tube 2	CD16		X	
	CD57			X
	CD25			X
	CD11c			X
Tube 3	HLADR		X	
	CyPerforin			X
	CyGranzyme B			X
	CD94		X	

Abbreviations: BB, backbone; CLPD, chronic lymphoproliferative disorders; Cy, cytoplasmic; Sm, surface membrane.

improvement as regards identification of NK cells, in the absence of significant technical issues. Consequently, the combination underwent further evaluation at two EuroFlow sites for a total of 12 PB samples. The new combination of backbone markers proved to be useful for the identification of NK-cells, and their discrimination from the remaining leukocyte populations in every case tested, both in normal/reactive ($n = 8$) and in NK-CLPD ($n = 4$) PB samples. Importantly, this combination of backbone markers was also robust enough to allow gating, merging and calculating strategies with the Infinicyt software, as detailed below.

Selection of characterization markers

Once the optimal backbone reagents were definitively established, antibody reagents for further characterization of NK cells were selected from a large list of NK-cell related markers, previously tested by our[79,80,271] and/or other[258,272–276] groups. Initially, this included a large list of monoclonal antibodies directed against classical NK-cell-associated antigens, including signaling molecules (for example, CD2, CD5, CD7 and CD8), the CD16 low-affinity FcγRIII, activation-related markers (for example, CD26, CD38, CD45RO, CD69 and HLADR), interleukin-2 receptors (CD25 and CD122), cytotoxic molecules (for example, CD11c and CD57) and intracytoplasmic enzymes (for example, perforin, granzymes and TIA-1), together with antibodies against killer-cell Ig-like receptors (KIR; for example, CD158a/b/d/e/l and NKB1), leukocyte Ig-like receptors (LIR; for example, CD85j (LIR1/ILT2)), C-type lectin-like receptors (for example, NKG2A/D, CD94 and CD161) and natural cytotoxicity receptors (NCR), such as CD335 (NKp46), CD336 (NKp44) and CD337 (NKp30), among others. Based on existing data about all these markers, the following criteria were used to select reagents for further testing: the ability to better distinguish normal/reactive versus immunophenotypically aberrant NK-cells and to assess a cytotoxic effector phenotype, and therefore determine the maturation stage of the expanded NK-cells.

Regarding the first purpose, it has been recurrently shown that aberrant or clonal NK cells display unique and altered patterns of expression of CD2, CD7, HLADR and CD94 versus both normal and reactive NK cells,[3,79,80,271,272,277] although a relatively high degree of overlap has been observed. Therefore, reagents recognizing the above referred molecules were considered as mandatory to be selected for further testing (*first diagnostic level* markers in Table 20) and hence included in the NK-CLPD panel, together with CD16; this latter marker was selected as a confirmatory marker typical of $CD56^{lo}$ NK-cells, but also as a useful marker to identify some (rare) $CD16^{-/lo}$ NK-cell malignancies.[270] In order to assess a cytotoxic effector phenotype and the maturation stage of the expanded NK-cells, markers known to be expressed on terminally differentiated cytotoxic effector cells such as CD11c, CD57, perforin and granzyme B[80,271,278,279] were selected to be included in the NK-CLPD panel (Table 19). As these molecules are also expressed by normal/reactive NK-cells, and are therefore not useful for their distinction from clonal/aberrant NK-cells, antibodies recognizing cytotoxicity-related molecules were considered as *second-level* markers (Table 20). Additional antibodies against molecules not usually present in most normal NK-cells under baseline conditions, were also selected for testing with the NK-CLPD panel (CD5, CD25 and CD26), as they have been found to be expressed by pathological NK-cells in some (rare) cases. Other proteins that have been claimed to potentially serve as surrogate markers for NK-cell clonality, such as restricted or absent expression of a single isoform of the NK-cell-associated antigen families (for example, KIR), were finally not included in the EuroFlow NK-CLPD panel, based on the lack of conclusive results reported so far in this regard[258,273–276,280] and the experience of the EuroFlow groups. Previous studies in short series of NK-CLPD cases (between 3[(ref. 273)] and 15[(ref. 280)] cases) pointed out that NK-cell expansions frequently show a skewed NK-receptor expression (for example, homogeneous expression of one or more KIR, particularly CD158a and CD158b),[273,274,280] in contrast to normal NK-cells, which typically display a diversified repertoire of NK-cell receptors. Despite this, both the sensitivity and specificity of this approach to unequivocally identify clonal NK-cells is currently poor (unless a relatively extensive set of antibodies against the repertoire of NK-cell receptors is used), particularly when a background of normal residual NK-cells co-exists with a clonal population of NK-cells (data not shown).

Once the target molecules were selected, monoclonal antibodies against them were chosen from among the PacB-, FITC-, PE- and APC-fluorochrome conjugates commercially available (Table 19). The precise role for each marker included in the NK-CLPD panel is summarized in Table 20.

Multicenter testing of the EuroFlow NK-CLPD panel

Testing of the EuroFlow NK-CLPD panel was carried out by seven EuroFlow centers involved in the study of NK-CLPD. A total of 38 PB samples were stained with the full panel: 10 samples from healthy adults (mean age of 36 ± 6 years; 5 males and 5 females); 11 female patients (64 ± 21 years) with expanded circulating

Table 21. Phenotypic patterns and percentage of NK-cells detected with the EuroFlow NK-CLPD panel

Diagnostic group	*Aberrant NK-cells*[a] *(no. of cases/total cases)*	*% of NK-cells (from WBC)*[b]	*No. of PB NK-cells*[c] *(× $10^3/\mu l$)*
Healthy adult donors	0/10	2.1 (1.5–4.5)	130 (60–290)
Cases with expanded polyclonal (reactive) NK-cells[d,e]	0/5	14.5	2020
Clonal NK-CLPD[f]	6/6	30 (16–65)	3280 (1480–7800)
Cases with expanded NK-cells not tested for clonality[g]	9/17	44 (30–62)	4710 (290–7500)

Abbreviations: CLPD, chronic lymphoproliferative disorders; HUMARA, human androgen receptor X-chromosome inactivation assay; PB, peripheral blood; WBC, white blood cells. [a]According to previously reported studies.[79,80,271,277]. [b]Results expressed as median % of NK-cells from WBC (range). [c]Results expressed as median absolute number of circulating NK-cells $\times 10^3/\mu l$ (range). [d]In these cases, diagnosis (assessment of the clonal versus polyclonal nature of the NK-cell expansions) was established by the HUMARA assay,[278,279] performed on highly purified PB NK-cells. [e]In 1 case, NK-cells showed a borderline altered phenotype (virtually all NK-cells, representing 46% of WBC and 7220 cells $\times 10^3/\mu l$, were $CD56^{-/lo}$/ $CD7^{-/lo}$/$CD2^+$/$CD11c^+$/$CD57^{-/+}$/$CD94^{lo}$/ $HLADR^{-/+}$). [f]In 1/6 cases (showing 65% NK-cells), the expanded cells showed overlapping features with reactive NK-cells ($CD56^{-/lo}$/$CD7^{-/lo}$/$CD2^+$/$CD11c^+$/ $CD57^{+/hi}$/CyPerforin^{hi}/ CyGranzyme B^{hi}/$CD94^{lo}$/$HLADR^{-/+}$). [g]Seven of the 9 cases with phenotypically abnormal/aberrant NK-cells were classified by the Infinicyt software as clonal cases (2 were clinically diagnosed with CLPD), one case as reactive and one case could not be classified; from the remaining 8 cases, 7 cases showed a reactive NK-cell phenotype, while one case showed a normal NK-cell phenotype in the manual analysis; from the 7 cases showing a reactive NK-cell phenotype, 4 cases were classified by principal component analysis (PCA) as normal/reactive, 2/7 as clonal (one of them corresponded to the case referred in footnote f) and 1/7 could not be classified; the case considered to have a phenotypically normal NK-cell phenotype could not be classified by PCA and it showed a borderline altered $CD56^+$/$CD7^-$/$CD2^+$/$CD11c^-$/$CD57^{-/+}$/$CD94^+$/$HLADR^-$ phenotype.

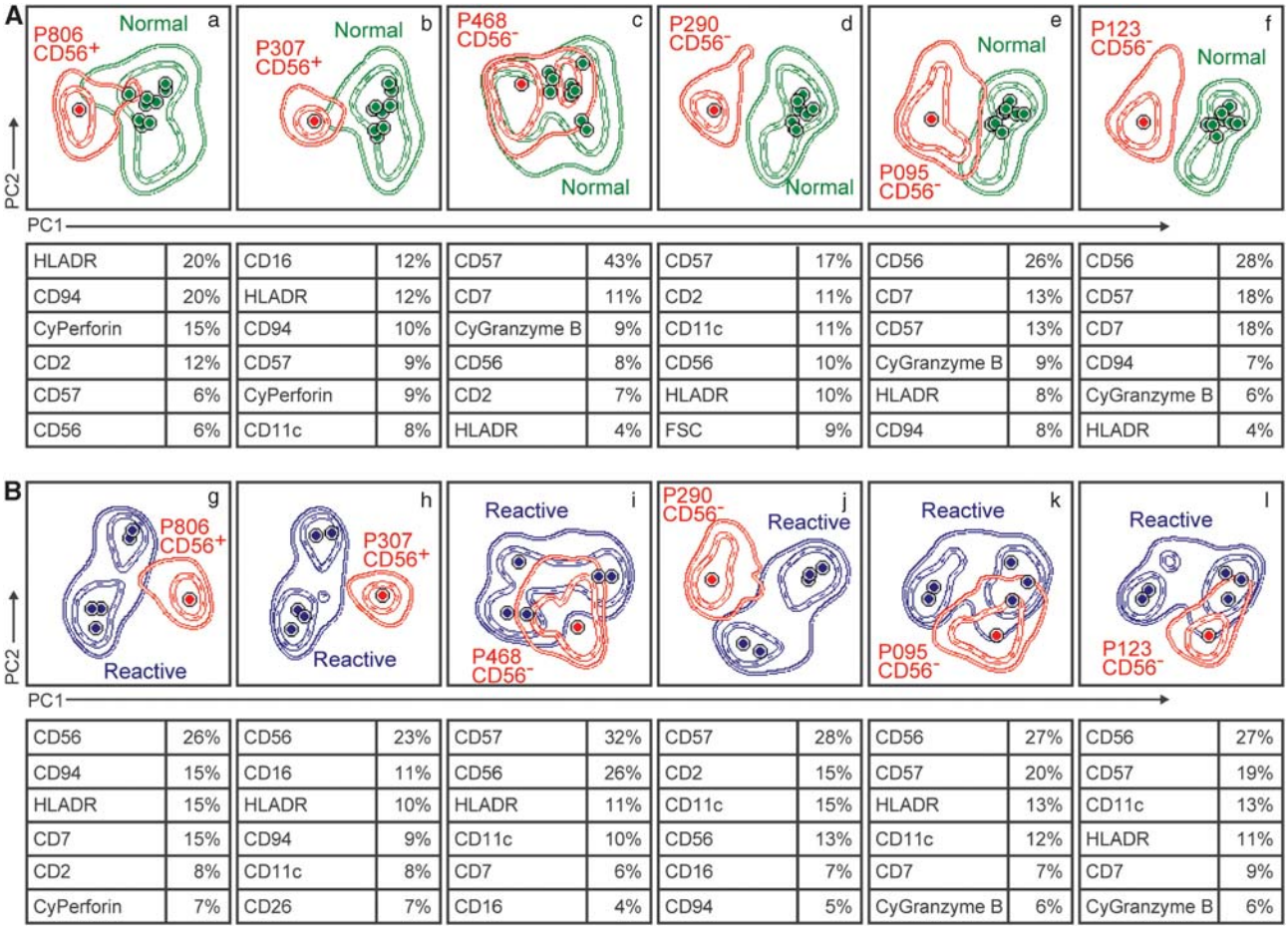

HLADR	20%	CD16	12%	CD57	43%	CD57	17%	CD56	26%	CD56	28%
CD94	20%	HLADR	12%	CD7	11%	CD2	11%	CD7	13%	CD57	18%
CyPerforin	15%	CD94	10%	CyGranzyme B	9%	CD11c	11%	CD57	13%	CD7	18%
CD2	12%	CD57	9%	CD56	8%	CD56	10%	CyGranzyme B	9%	CD94	7%
CD57	6%	CyPerforin	9%	CD2	7%	HLADR	10%	HLADR	8%	CyGranzyme B	6%
CD56	6%	CD11c	8%	HLADR	4%	FSC	9%	CD94	8%	HLADR	4%

CD56	26%	CD56	23%	CD57	32%	CD57	28%	CD56	27%	CD56	27%
CD94	15%	CD16	11%	CD56	26%	CD2	15%	CD57	20%	CD57	19%
HLADR	15%	HLADR	10%	HLADR	11%	CD11c	15%	HLADR	13%	CD11c	13%
CD7	15%	CD94	9%	CD11c	10%	CD56	13%	CD11c	12%	HLADR	11%
CD2	8%	CD11c	8%	CD7	6%	CD16	7%	CD7	7%	CD7	9%
CyPerforin	7%	CD26	7%	CD16	4%	CD94	5%	CyGranzyme B	6%	CyGranzyme B	6%

Figure 29. Comparative principal component (PC) 1 versus PC2 views of clonal versus both normal and reactive NK-cell reference cases. The APS (automated population separator, PC1 versus PC2) views of each CD56^{+} (Panel **A**, plots a and b, and Panel **B**, plots g and h) and CD56$^{-/lo}$ (Panel **A**, plots c–f, and Panel **B**, plots i–l) clonal NK-cell case (different red circles), versus the reference groups of normal (green circles) and reactive/polyclonal NK-cells (blue circles). Each circle represents one single case (median expression observed for all phenotypic parameters evaluated), while contour lines represent s.d. curves (dotted and continuous lines represent 1s.d. and 2s.d., respectively). The six most informative markers contributing to the best discrimination between each clonal NK-cell CLPD case and the corresponding reference group are displayed at the bottom of each plot, in a decreasing order of percentage contribution to the discrimination.

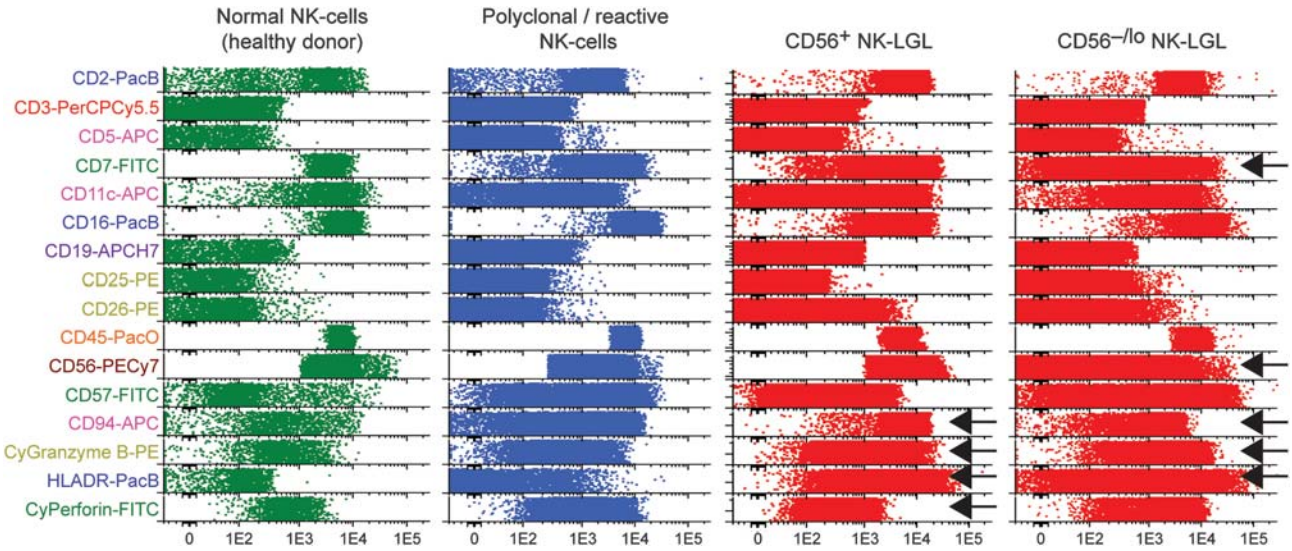

Figure 30. Illustrative phenotypic patterns of NK-cells from healthy donors, and patients with expanded polyclonal, clonal CD56^{+} and clonal CD56$^{-/lo}$ NK-cells. Arrows point to the most informative markers in the distinction between each clonal NK-cell case versus their normal and reactive NK-cell counterparts.

NK-cells found to be suitable (heterozygous) for the HUMARA assay–six clonal and five polyclonal cases—and 17 samples from patients with expanded PB NK-cells (mean age: 66 ± 12 years) in whom the HUMARA assay was not performed (13 males and 3 females) or it was not informative to assess NK-cell clonality (one homozygous female for the HUMARA assay) (Table 21). A case was considered to be monoclonal by the HUMARA assay when the corrected allele ratios were $\leqslant 0.33$ or $\geqslant 3$ for both NK-cells and NK-cells/control cells, indicating that one of the parental alleles was represented at an excess of $\geqslant 50\%$ versus the other allele[278,279] (paired normal purified T-cells or neutrophils were used as control cells). In 2/6 cases in which the presence of monoclonal NK cells could be confirmed (both showing a $CD56^{-/lo}$ phenotype), T-cell clonality was ruled out by PCR TCR gamma gene analysis.

In order to evaluate the utility of the EuroFlow NK-CLPD panel for the distinction between normal/reactive and clonal NK-cells, pairwise unsupervised discrimination by PCA with the APS function provided with the Infinicyt software program was used. In order to be sure about the polyclonal versus clonal nature of the expanded NK-cells from patients, only samples from healthy subjects ($n = 10$) and those female patients ($n = 11$) found to be heterozygous for the HUMARA assay–six clonal and five polyclonal cases—were included in the PCA-based comparisons. As shown in Figure 29A (plots 'a' to 'f'), cases stained with the EuroFlow NK-CLPD panel, from both the $CD56^{+}$ ($n = 2$) and the $CD56^{-/lo}$ ($n = 4$) clonal NK-cell groups, showed clearly different immunophenotypic profiles versus normal NK-cells ($n = 10$). Similarly, cases from the $CD56^{+}$ clonal NK-cell group ($n = 2$) also showed distinct phenotypic profiles as compared to the group of polyclonally expanded reactive NK-cells (Figure 29B, plots 'g' to 'l'). However, in 3/4 cases with $CD56^{-/lo}$ clonal NK-cells, partial overlap between the phenotypic profiles of clonal and normal or reactive NK-cells was observed (Figure 29A, plot 'c' and Figure 29B, plots 'i', 'k' and 'l'). Despite this, it should be noted that each of these three cases was clearly different from normal and reactive NK-cells, when comparisons were made separately for these cases versus each subset of $CD56^{+}$ and the $CD56^{-/lo}$/polyclonal NK-cells (data not shown).

The precise markers mostly contributing to discrimination of each clonal case from the reference groups of both normal and reactive/polyclonal NK cells included CD56, CD57, HLADR and CD94; in addition, CD7 was also an informative marker in the distinction between normal versus clonal NK-cells (mainly $CD56^{-/lo}$), and CyGranzyme B and CyPerforin—and to a lesser extent also CD2—were informative in the distinction between reactive/polyclonal versus clonal NK-cells (Figure 29). Illustrative phenotypic patterns of NK-cells from healthy donors and patients with expanded polyclonal and clonal NK-cells are shown in Figure 30.

Using this Infinicyt-based strategy, expanded NK cells from those additional 17 samples for which clonality could not be determined showed an aberrant phenotypic profile in nine cases (from which seven cases were also found to have phenotypically abnormal NK cells, according to previously reported studies[79,80,271,277]). In five cases, overlapping profiles with normal ($n = 3$) and reactive NK-cells ($n = 2$) were found, while in the remaining three cases the software did not allow precise classification into a specific reference group. Comparisons between the conventional and the new PCA-based classification strategies for these 17 samples are described in a footnote in Table 21.

CONCLUSIONS

Our results obtained in a relatively limited number of patients show that the EuroFlow NK-CLPD panel, consisting of three 8-color combinations of monoclonal antibodies, would contribute to improve the diagnosis of NK-cell CLPD, as it allows the identification of immunophenotypic profiles that distinguish clonal versus polyclonal NK-cells. As a major challenge within NK-cell CLPD is to distinguish between reactive and clonal proliferations of NK cells (because of lack of universal markers for NK-cell clonality), the EuroFlow panel and strategy would facilitate the distinction between them and therefore would be of great help in routine diagnostic settings. However, confirmation of these preliminary results in larger series of patients is necessary, which is a future goal of the EuroFlow activities.

GENERAL DISCUSSION

Immunophenotyping is an essential tool in the diagnostic work-up and classification of hematological malignancies.[1–3] Although other immunophenotypic techniques may also be used for evaluation of tissues, multiparameter flow cytometry is most frequently indicated. Despite the objectivity of flow cytometric measurements and the apparent simplicity of the technique, multiple problems and limitations have emerged over time.[281] Multiparameter flow cytometry is currently regarded as a costly and complex approach, because of increased reagent costs related to the progressively higher number of markers used for answering clinical questions, and because of the exponentially increased need for expertise in data analysis and interpretation. This, together with technical variations between different laboratories around the world (for example, number and type of reagents and instruments available), has resulted in many different strategies and antibody panels, almost as many strategies as individual flow cytometry laboratories. This diversity has hampered real standardization and reproducibility of flow cytometric diagnostics. In addition, interpretation of flow cytometry data slowly evolved from an objective measurement of the percentage of positive or negative cells to highly subjective interpretations of two-dimensional dot-plot pictures, which are interpreted in an 'experience-based' manner, as done for routine histomorphology and cytomorphology. Such shortcomings have pushed the need for standardization in the field and multiple initiatives have been made in the last two decades.[7,9,12–14,22,23,25–29,106,193,204,282–284] However, such 'standardization' initiatives are usually limited because they only address a part of the whole process, without true validation of the 'consensus proposals' in prospective studies. For example, most recommendations and guidelines only provide lists of informative markers without discussing reference reagents, fluorochrome conjugates and the most appropriate multicolor combinations. Even more, the proposed lists of markers are frequently grouped according to one or a few disease categories or cell lineages, which do not necessarily answer the clinical questions, particularly those raised in a diagnostic screening phase. As a consequence, excessively high numbers of markers are being used, which are frequently different between laboratories. Consequently, discrepant results might be obtained for the same patient samples.

Comparable to such consensus groups, also the EuroFlow Consortium started the EuroFlow project with a first *consensus* proposal of potentially informative markers and technical flow cytometry procedures.[16] However, the antibody panels were designed per set of related medical indications and clinical questions (Figure 1). As described in this report, validation of the proposed marker combinations and antibody panels showed multiple shortcomings. Consequently, for optimization purposes, all antibody panels required inclusion of additional markers, replacement of antibody clones and/or fluorochrome conjugates (many of which were even not commercially available) over 2 to 7 successive cycles of panel redesign and panel evaluation with exclusion of redundant markers while retaining the essential ones. Noteworthily, such cycles of panel redesign-and-evaluation aimed at final validation of the total set of EuroFlow antibody panels, which required analysis of more than 2000 informative samples as described in this paper. Of note, the end-points for validation of the EuroFlow panels were a 100% sensitivity with an optimized

specificity or a 100% specificity with a maximized sensitivity. Only under such conditions can we avoid the gray zone of uncertainty associated with approaches that aim at the greatest efficiency and that almost always include both false-negative and false-positive cases, and consequently have disturbing levels of uncertainty for individual (for example, atypical) cases. The EuroFlow validation process required new analytical tools for objective multivariate analysis of flow cytometry data that were not available as ready-to-use software functions and had to be designed and implemented into the user-friendly environment of the Infinicyt software.[16,31] The application of the new analytical tools in the multi-centric setting of the EuroFlow Consortium was made possible by extensive standardization of instrument settings and sample preparation protocols.[16] As an overall result, the validated EuroFlow antibody panels can be integrated in the diagnostic screening and classification strategies (Figure 1). These antibody panels are flexible and can be adapted to fit the needs of different diagnostic laboratories or clinical treatment protocols as discussed below, while serving as validated benchmark.

Acute leukemia orientation tube (ALOT)

The first section of this report describes a single 8-color immunostaining combination (ALOT), which is optimized for recognition of all major types of classical acute leukemias (BCP-ALL, T-ALL and AML) as well as of acute leukemias of ambiguous lineage and allows optimal choice of the most appropriate characterization panel for further phenotypic classification.

The WHO 2008 criteria for classification of acute leukemias emphasize the value of a limited number of lineage-related antigens (CyCD3, CD19 and CyMPO), diagnosis of MPAL predominantly relying on these three markers plus a few monocytic markers.[36,37] For the recognition of B-cell lineage, CD19 expression combined with CyCD79a or CyCD22 is proposed, whereas the sole expression of CyMPO or CyCD3 is regarded by the WHO criteria as sufficient to recognize myeloid and T-cell lineage-positive cases, respectively; CyCD3 would also be systematically necessary for the assignment of blasts to the T-cell lineage. In contrast to previous classifications, there is no diagnostic value for additional myeloid-associated markers such as CD13, CD33, CD117 and others, because they are not sufficiently lineage-specific and therefore they are not considered as definitive evidence for a specific lineage. Despite the fact that the ALOT was designed prior to the publication of the 2008 WHO criteria, the three major lineage-associated markers are all included in ALOT. Other markers considered to be of secondary importance for lineage-assignment were placed in the disease-oriented characterization panels (BCP-ALL, T-ALL and AML/MDS).

In previous versions of the WHO classification[285] only the percentage of cells expressing a marker was taken into account, whereas in the more recent 2008 version[3] the intensity of antigen expression is also regarded to be important. Combination of the ALOT with the EuroFlow instrument settings and sample preparation SOP, as well as the new software tools developed by the EuroFlow group, allows direct integration of quantitative data about the intensity of expression of each individual marker in single leukemic cells in the evaluation of the overall blast cell phenotype for the eight ALOT markers: the four lineage-associated markers (CD19, CyCD79a, CyCD3, CyMPO) plus CD7, CD45, CD34 and SmCD3. Multivariate analysis (for example, PCA) showed that all markers except those used for positive identification of blast cells (CD45 and CD34) or exclusion of mature cells (CD45 and SmCD3) were essential for obtaining optimal results (Figure 6). In this regard, it should be emphasized that ALOT was designed and validated for orientation of an acute leukemia sample towards further characterization panels and thus, it should not be used on its own for definitive exclusion of a hematological malignancy. Nevertheless, when the ALOT is combined with the LST and tubes 1–4 of the AML/MDS panel, virtually all hematological malignancies can be excluded or detected, albeit not definitively classified. In turn, when combined with the appropriate complementary panel, the precise diagnosis of acute leukemia, ambiguous lineage acute leukemia (for example, mixed phenotype and undifferentiated acute leukemias) can be obtained (Figures 3–5). In specific situations that only require distinction between malignant and normal lymphoid B-cell precursors (excluding MRD situations), the combination of ALOT with the first tube of the BCP-ALL antibody panel is sufficient, as discussed below.

Although the acute leukemia panels include two sequential steps (ALOT plus the BCP-ALL, T-ALL and/or AML/MDS panels), in some specific situations they can be performed simultaneously. For example, in case of high suspicion of AML, the ALOT and AML panels can be run in parallel. It should be noted that the ALOT is always required for complete phenotypic characterization of acute leukemias, because it includes essential markers required for the detection of AUL/MPAL. Although the ALOT alone showed promising results with respect to the orientation and identification of acute leukemias of ambiguous lineage among typical single-lineage acute leukemias, the cohort needs to be expanded to include a significant number of cases of these rare disease subcategories and determine whether optimal subclassification of AUL and MPAL cases may benefit in the future from the systematic application of one or two specific acute leukemia panels. The combined application of the ALOT and the new software tools (for example, PCA) of the Infinicyt software will undoubtedly assist acute leukemia diagnosis and promote true standardization in multicenter settings.

Lymphoid screening tube (LST)

Screening for the presence of aberrant mature B-, T- and NK-cell populations in the clinical diagnostic setting remains one of the most frequent requirements for flow cytometric immunophenotyping of leukemias and lymphomas. At present, a wide variety of approaches is used in individual laboratories, which frequently rely on a combination of (inter)national recommendations and local experience. In this report, a single 8-color, 12-marker LST is proposed for the diagnostic screening of CLPD in a wide variety of human samples including PB, BM and lymphoid tissue specimens.

The LST was designed to evaluate the overall lymphoid compartment of such samples in different clinical situations and medical indications. Accordingly, the LST allowed identification of lymphoid populations with aberrant or clonal phenotypes in virtually all infiltrated samples; in the remaining few cases, an altered numerical distribution of the specifically altered lymphocyte populations was observed, indicating that further assessment of the potential clonal nature of the expanded cells is required. Moreover, the information obtained with the LST efficiently points to the precise panel required for full characterization of the altered cell population, that is, PCD, B-CLPD, T-CLPD and/or NK-CLPD. Importantly, the data obtained in the screening step (LST) can be integrated with the data of the full characterization panels, particularly the B-CLPD antibody panel.

Noteworthy, an interesting alternative to the LST combination proposed (version 7) was designed to be well-suited to predominantly B cell CLPD-oriented laboratories (LST version 6). It takes optimal advantage of multiparameter flow analysis using a mixture of 12 antibodies for highly sensitive detection and classification of B-cell clones, particularly among patients with different subtypes of B-cell lymphoma in the absence of absolute or relative lymphocytosis. The major difference between the two LST versions relies on the substitution of CD38 in version 7 by CD10 in version 6. It should be noted that LST version 7 allows full integration with the B-CLPD panel and at the same time it provides a clear advantage for those diseases involving the

plasma cell compartment together or not with mature B-cells (for example, Waldenstrom macroglobulinemia[286]). Conversely, LST version 6 is better suited for cases of CD10$^+$ B-CLPD, specifically in FL patients with low levels of infiltration. However, it should be noted that the LST is not designed for MRD investigations. This requires specific combinations, which are currently being designed and evaluated by the EuroFlow group, aiming at the detection of minimal disease in the different WHO diagnostic subgroups of CLPD, including FL.

Extensive testing in multiple EuroFlow centers showed that the LST combination is a cost-effective protocol when compared to currently used approaches.[18,20] Accordingly, in the five evaluated EuroFlow laboratories the LST reduced the time required for sample processing and data analysis by around one-fourth (mean of 40 min versus 55 min) and reduced reagent costs (1 tube with 12 reagents versus a mean of 3 tubes and 13 markers), while resulting in a higher diagnostic efficiency. In this regard, it should be noted that individual markers in LST version 7 showed independent values. For example, TCR$\gamma\delta$ appeared to be useful for the screening of rare TCR$\gamma\delta$ lymphomas and other clonal expansions of TCR$\gamma\delta$ T-cells in 11/249 (4.4%) cases tested. However, because of the relatively low frequency of TCR$\gamma\delta$ expansions, usage of this marker could be optional at a screening stage and more suited for a later step in the classification of specific T-CLPD WHO entities (see Section 9). More importantly, the LST was highly efficient in distinguishing between normal and clonal/aberrant lymphoid populations, as confirmed through the multivariate analysis tools included in the Infinicyt software (for example, PCA). These findings suggest that automated approaches for recognition of immunophenotypic profiles may be used in the future for specific gating of lymphoid cell populations and its comparison with a pool of reference (for example, normal, reactive or neoplastic) data files for further detailed analysis (Figure 9). Finally, whereas the LST was designed for a diagnostic screening step when increased counts of clonal lymphocytes are typically present, the approach proved to have a good sensitivity, as it detected neoplastic cells at low levels (10^{-3}). Nevertheless, the LST is not optimally suited to search for malignant lymphoma cells in paucicellular samples like CSF or vitreous biopsies.

Small sample tube (SST)

Body fluids that contain low numbers of cells, such as CSF and vitreous biopsies (here collectively referred to as 'small samples'), pose a diagnostic challenge in case of clinical suspicion of lymphoma. Both single and multicenter studies have recently demonstrated that multiparameter flow cytometric analysis is the optimal strategy to establish the cellular composition of these low cell number samples and to confirm or exclude the presence of aberrant cell populations. Even though 4- and 6-color flow cytometric screening protocols have proven their value, the here-presented 8-color/13-parameter EuroFlow SST labeling is currently the most complete flow cytometry assay for clinically suspect CSF and vitreous samples. The main diagnostic contribution of the EuroFlow SST labeling concerns the screening for a primary lymphoma in those situations with a clinical lymphoma suspicion but without evidence for a systemic lymphoma in (earlier) analyses of other cell materials and tissues.

The results of the 141 CSF samples and 23 vitreous biopsies clearly underline the diagnostic value of the SST in that it allows for a complete typing of the most relevant leukocyte populations in these samples with positive identification of all normal subsets of hematopoietic cells present in CSF, except neutrophils (Figure 10). Based on FSC/SSC/CD45 gating neutrophils could be identified, although possible inclusion of, for example, CD11b or CD16 in a future version of the SST for example in the same fluorochrome position as SmCD3 and CD14 should help to define neutrophils in a more direct way. In addition, the SST can confirm or exclude the presence of aberrant B-, T- or plasma cell populations. In this respect, it has been suggested that a SmIgκ/SmIgλ ratio of <0.25 or >4 should be considered as a deviation from normal, and hence an indication for a B-cell lymphoma.[106] However, it should be noted that a skewed ratio per se is not sufficient for the diagnosis of B-cell lymphoma. Apart from clinical features and possibly also morphological indications, the entire flow cytometric profile should give more clues on the true aberrant immunophenotype of the involved cell population. Hence, a combined evaluation of all 13 parameters of the SST labeling using PCA clearly enhanced the diagnostic possibilities to identify aberrant B- and T-cell clones. Nevertheless, the set of markers is apparently still too limited to allow a detailed characterization of the aberrant B- or T-cell populations in all cases for further diagnostic subclassification into specific WHO disease categories. For this reason, we are currently evaluating additional B-cell and T-cell small sample labelings for further typing the aberrant cell population on the remaining cells of the CSF or vitreous material. An alternative option to confirm the aberrant character of the suspect B- or T-cell population could be to use the remaining cells for a multiplex PCR-based Ig/TCR clonality-testing strategy.[266]

Even though, the EuroFlow SST labeling can also be used for small sample analysis in cases with a systemic lymphoma, in such cases it may be better to choose a more targeted approach to identify the lymphoma population in CSF or vitreous biopsies using a limited set of markers specific for the lymphoma (so-called '*minimal disseminated disease*' approach). Finally, localization of acute leukemia cells in, for example, CSF is not a main application of the EuroFlow SST labeling, but would also most probably benefit from a more targeted approach.

Despite its high specificity and sensitivity, the exact diagnostic value of the EuroFlow SST labeling for small samples is greatly dependent on the number of cells that can be studied and the viability of these cells. Cell viability can be increased by collection of the cells in tubes with culture medium plus 10% FCS or 0.2% BSA and a short transport time between clinic and laboratory (optimally within 1 h). Alternatively, so-called TransFix collection tubes are also currently commercially available, which result in optimal stabilization of the cells for a few days (for example, 48 h) and improved cell detection.

Plasma cell disorders (PCD) panel

Interestingly, among all EuroFlow antibody panels, the PCD panel was the only one where the initial list of markers proposed to be included in the panel remained unchanged till the last version of the panel. This indicates that matured consensus already existed in the literature about the most informative and relevant phenotypic markers for evaluation of clonal plasma cells in PCD.[9,110] Nonetheless, because of technical factors and plasma cell-associated biological variables, fine adjustments of specific fluorochrome-conjugated reagents were required to reach optimal performance in the final configuration of the PCD panel (version 6). For several markers (for example, CD38 and β2 microglobulin) dim fluorochrome-conjugated antibody reagents associated with lower fluorescence intensities and lower fluorescence spillover to other channels were preferred. For these two reagents, final adjustments with a mixture of fluorochrome-conjugated and purified (unconjugated) antibodies was required to get optimal fluorescence staining patterns under saturating conditions. In turn, other reagents such as CD45–PacO, used in all other EuroFlow panels, could not be kept in the PCD combination at the same fluorochrome position due to the relatively low discrimination power between CD45$^-$ and CD45$^+$ plasma cells, mainly caused by the increased PC baseline autofluorescence levels in this channel. Last, but not least, the

limited availability of good-quality CD138 fluorochrome-conjugated reagents in the positions left by other markers forced its inclusion as a custom conjugate of PacO. Further testing of new commercially available good-quality conjugates for this marker, which work similarly under Sm only or intracellular markers staining protocols (for example, Horizon V500) is ongoing at the different EuroFlow sites.

As an end result a two-tube, 12-marker, 8-color PCD panel is proposed for accurate identification of plasma cells, specific detection and quantification of phenotypically aberrant or clonal versus normal/reactive/polyclonal plasma cell populations and detailed characterization of their immunophenotypic profiles. As tube 1 (CD38, CD138, CD45, CD19, CD56, β2 microglobulin, CyIgκ and CyIgλ) proved sufficient for the specific identification, enumeration and discrimination between normal/reactive and aberrant plasma cells, it can be used as a stand-alone tube for the initial screening of PCD in a two-step diagnostic approach (Figure 1). In such case, tube 2 could be optional and used only when indicated, for example, for assessment of additional aberrant markers for monitoring MM patients after therapy. Finally, this two-tube PCD antibody panel in combination with the EuroFlow LST and B-CLPD panels may also contribute to the diagnosis and classification of other B-CLPD categories, which involve the plasma cell compartment in addition to clonal B-lymphocytes, for example LPL, which includes Waldenström's macroglobulinemia.

Although the aim of the PCD EuroFlow panel was not directly focused on MRD investigation after therapy, the evaluation of the proposed panel in multiple centers showed a sensitivity of $\leqslant 10^{-3}$ (routine detection of 100 aberrant plasma cell in 100 000 cells acquired).

Antibody panel for B-cell precursor ALL (BCP-ALL)

The four tubes of the BCP-ALL panel in combination with the ALOT enable the diagnosis and detailed immunophenotypic characterization of BCP-ALL, including discrimination from normal and regenerating precursor B-cells. In addition, all phenotypic information required for subclassification of BCP-ALL according to the WHO classification is included.[34] The four tubes also contain antibodies for detection of LAP markers and phenotypes associated with genetic aberrations, such as CD66c and NG2. If immunophenotypic profiles show coexpression of B-lineage markers and myeloid-associated markers (for example, CD13, CD33, CD117, CD15 + 65) as well as CD34 and CD38 positivity, the AML-MDS tube 2 (with monocytic markers CD14, CD36, CD64) should be run in parallel to detect exceptional cases of monoblastic-MPAL.

The BCP-ALL protocol is designed in a flexible way so that only one or two tubes need to be used for specific clinical questions. For example, tube 1 of the BCP-ALL panel is excellently suited to distinguish normal or regenerating precursor B-cells (hematogones) from BCP-ALL blast cells. Tubes 1 and 2 are sufficient for full maturation-based classification of BCP-ALL according to EGIL criteria or WHO guidelines. Furthermore, the BCP-ALL antibody protocol can be run using conventional data analysis tools, although this provides less information than exploiting the potential of innovative multivariate analysis-based software tools after staining for the whole panel. For example, the maturation-associated subclassification of BCP-ALL according to conventional criteria can efficiently be achieved. However, given the subtle variations in the expression levels of a wide range of antigens, we anticipate that multivariate analysis of all markers in the panel will contribute to an improved subclassification of BCP-ALL (Figure 16). Nevertheless, this requires further investigation in larger series of BCP-ALL cases, which is under development by the EuroFlow group.

Antibody panel for T-cell ALL (T-ALL)

We designed an antibody panel for diagnosis and detailed characterization of T-ALL. The application of the T-ALL panel is guided by the results of the ALOT tube. Fusion of the results obtained with the ALOT and the T-ALL panel is based on three common backbone markers. As discussed in the ALOT section, a small number of immature or ETP-ALL and MPAL cases were found to be at the interface between T-ALL and AML with the ALOT tube. These cases should ideally be analyzed with both T-ALL and AML panels, while awaiting the potential development of a specific panel for ambiguous lineage acute leukemias.

The first tube of the T-ALL EuroFlow panel was designed to detect both major and minor T-ALL populations including those that may be missed by microscopic detection, either at diagnosis or during follow-up. As such, this tube can be used for detection of minimal disseminated disease (MDD) at diagnosis in T-LBL.[287,288] However, initial analysis of tumor material with the complete panel is required at diagnosis in order to allow reliable identification of the pathological phenotype(s) and of coexisting intraclonal heterogeneity. In many cases, tube 1 will suffice for MDD detection, essentially when there is co-expression of T-cell-associated (for example, CyCD3 + / − CD5) and immature (NuTdT, CD1a, CD10, CD99^{hi}) markers.[287]

The T-ALL panel is flexible, as it allows classification of T-ALL according to the WHO 2008 system or other alternative classifications using both conventional and new multivariate-analysis-based software tools. Usage of the new multivariate analysis tools has the advantages of comparing many phenotypic profiles, which have been acquired in different laboratories in a standardized manner and of integrated analysis of a large number of T-ALLs within the context of prospective clinical trials. In addition to its diagnostic contribution, it can also become a discovery tool for identification of new phenotypic profiles, which might allow improved therapeutic stratification and individual management of T-ALL patients. These profiles should ideally be compared in an *n*-dimensional immunophenotyping model in which neoplastic T-cells are plotted against normal thymic T-cell differentiation for comparison as well as for distinction. With the future help of the EuroFlow T-ALL database, it will be possible to study to what extent T-ALLs differ from single subpopulations of thymocytes, that is, it will become possible to search for the nearest-phenotypic neighbor of T-ALL blasts and to infer the normal T-cell counterpart for each leukemia and more precisely define the LAP. Such new phenotypic classification of T-ALL would potentially be much more accurate than current classifications as it is based on simultaneous analysis of a larger number of parameters versus sequential analysis of multiple individual markers. Further studies are needed to determine the potential correlation of such classification with specific molecular genetic T-ALL subgroups. If this proves to be the case, such information will be available to the clinician within a few hours after cell sample collection.

Antibody panel for acute myeloid leukemia/myelodysplastic syndrome (AML/MDS)

The here-presented AML/MDS antibody panel allows detailed characterization of all myeloid lineages as well as aberrant immunophenotypes of the myeloid cells. For patients with suspicion of AML and/or MDS, this antibody panel should be performed together with the ALOT tube. It was not possible to use the same backbone markers for the AML/MDS antibody panel and the ALOT tube. Consequently, the markers present in the ALOT tube cannot be linked to the markers in the AML/MDS antibody panel. This is not a problem for markers like CD19, CD34, CD45 and CD7, which are also present in the AML/MDS antibody panel, and for CyCD79a, CyCD3 and SmCD3, which are considered not informative for AML/MDS. Merging of the AML/MDS antibody panel with CyMPO would, however, be informative. Although merging based on the common backbone markers CD45 and

CD34 may be possible in some AML patients, this likely will not be appropriate in the vast majority of AML cases.

In contrast to T-ALL and BCP-ALL, patients with AML frequently have a heterogeneous leukemic cell population. As it is not always clear which populations belong to the leukemia, appropriate gating of the leukemic population can be difficult. In our comparison of WHO-defined subgroups, we focused on the immunophenotypic data of the immature cells defined by the CD34, CD117 and HLADR backbone markers. It may, however, well be that inclusion of more mature populations will improve the flow cytometric classification of AML patients. In turn, the utility of other markers associated with immaturity of hematopoietic cells (for example, CD90 and CD133) in AML and MDS remains unclear and should be further evaluated.

To determine which populations are normal and which populations are immunophenotypically abnormal, appropriate analysis of differentiation pathways is crucial. Therefore, the panel was designed in such a way that the multivariate approach, possible by the use of the here-presented 8-color antibody panel in combination with the new Infinicyt software-associated tools, will facilitate this process (Figure 19). Nevertheless, there is still an urgent need for a more objective analysis of such data. In this regard, we are now evaluating a new software module developed for a more objective analysis of maturation pathways. This is based on dissecting the differentiation pathways in multiple segments (for example, stages) in a multidimensional space (for example, based on PCA), generated by the phenotypic parameters analyzed. The patterns observed in healthy individuals subsequently can serve as a reference for the patterns in AML and MDS patients. In such patients, a similar segmentation can be made and for each segment it can be determined with which normal segment it more closely clusters and what markers are aberrant. These software tools are currently being developed and evaluated and will greatly facilitate the analysis of maturation-associated defects, which is crucial for better classification of AML and MDS patients.

Antibody panel for B-cell chronic lymphoproliferative diseases (NK-CLPD) (B-CLPD)

The B-CPLD EuroFlow antibody panel proposed here aims at diagnostic classification of BCLPD into the major WHO subtypes, based on the immunophenotypic profiles of individual malignant B-cells. The panel consists of four tubes, which should be stained sequentially or in parallel to the LST. It is advised that LST and the complete B-CLPD panel are stained in parallel in cases with a high pre-test probability of a mature B-cell malignancy. Cases presenting with suspicion of CLL should be primarily evaluated using the LST and tube 1 from the B-CLPD panel only. The three backbone markers (CD19, CD20, and CD45) common to all four tubes and the LST were designed to allow efficient positive selection of the B-cells in all subtypes of mature/peripheral B-cell malignancies. We demonstrated that this was systematically achieved using the prospective evaluation of several hundreds of cases. The other 24 markers are devoted to the characterization of the identified aberrant clonal B-cell. They included both markers already known to contribute to specific differential diagnoses among distinct WHO B-CLPD entities and novel markers. Inclusion of a relatively high number of markers that are not currently used in many routine diagnostic panels (for example, CD200, CD305(LAIR1), CD31, CD62L) was based on their independent contribution to pairwise differential diagnoses performed through multivariate analyses, particularly between disease entities where previous panels have proven to be of limited utility (for example, atypical CLL). In turn, exclusion of some traditional markers (for example CyBcl2) was due to redundancy with other more informative combinations already included in the panel, as assessed by multivariate analysis.

At a first glance, it might appear that the proposed panel is a rather extensive panel. Nonetheless, it should be noted that it provides additional and more robust information for the diagnosis of specific WHO disease entities compared to the more traditional panels. In fact, the overall panel of backbone and characterization markers proposed here was tested for up to 28 differential diagnosis, by multivariate analysis of individual malignant B-cells from paired WHO diagnostic groups. Overall, the panel provided an efficient differential diagnosis among the major B-CPLD entities in all but four comparisons, which involved MZL versus LPL and DLBCL versus MZL, LPL and FL. Noteworthily, these four differential diagnoses are not only difficult on immunophenotypic grounds but they have also been shown to have a rather limited reproducibility among hematopathology experts when applying the currently used WHO diagnostic criteria (for example, degree of agreement ranging from 56% to 63% for LPL and MZL, respectively).[232]

Comparison to the performance of more traditional 4-color panels used at individual centers which included a slightly lower number of markers, shows that the new markers included in the EuroFlow B-CLPD panel provides more robust diagnosis of the distinct WHO categories of BCLPD, even when similar multivariate analyses are used.[31] In addition, the EuroFlow B-CLPD panel was also designed in a flexible way, so that the relevant immunophenotypic information of the LST is also used for the classification of the distinct B-CLPD entities and subsets of tubes can be applied for a specific set of differential diagnoses. Altogether, this allows comprehensive usage of different combinations of tubes from the panel, for specific differential diagnosis of frequent disease categories such as CLL, limiting reagent and personal costs to a reasonable level.

Antibody panel for T-cell chronic lymphoproliferative diseases (T-CLPD)

In the proposed diagnostic work-up of PTCL, the EuroFlow T-CLPD panel is scheduled to be applied on samples from patients showing aberrant and/or increased numbers of T-cells, as identified by the LST. Overall, this panel aims at confirmation of the presence of aberrant T cells and further classification of PTCL into specific WHO PTCL categories.

Similar to B-CLPD, PTCL represent a rather heterogeneous group composed of multiple disease entities.[3] However, in contrast to mature B-cell neoplasms, T-CLPD derive from multiple different T-cell populations/lineages (for example, TCR$\gamma\delta^+$ versus TCR$\alpha\beta^+$ CD4$^+$ CD8$^-$ and TCR$\alpha\beta^+$ CD4$^-$ CD8^{hi} T lymphocytes), evaluation of clonal excess requires a much higher number of antibody reagents (for example, 24 TCRVβ family antibodies versus κ and λ), whereas they are much less frequent disorders.[3] Because of this, more T- than B-cell associated markers, are required for a diagnostic screening phase, and for the composition of the set of backbone markers in the EuroFlow T-CLPD panel versus the B-CLPD panel. However, for reasons of costs, most clinical flow cytometry laboratories try to keep the overall number of antibodies against T-cell markers lower, according to the relatively lower frequency of PTCL versus B-CLPD. Based on all the above reasoning, the strategy proposed by the EuroFLow Consortium for immunophenotyping of T-CLPD consists of up to three sequential steps. In the first step, the LST tube should be applied. In case the TCR$\gamma\delta^-$/SmCD3$^+$ T-cells are expanded (absolute or relative expansion), show aberrancies (for example, abnormally low expression of SmCD3, CD4, or CD5) or the CD4/CD8 T-cell distribution is altered,[78,254,289] which are not fully conclusive about the clonal nature of such cells, then the immunophenotypic analysis of the TCR-Vβ repertoire should be performed, for confirmation of T-cell clonality.[290–292] Finally, in the third step the T-CLPD panel should be used, aimed at the classification of T-CLPD into specific WHO disease categories[3] in cases suspected of TCR$\alpha\beta^+$,

TCR$\gamma\delta^+$ and TCR$^-$ T-cell CLPD. In Section 9 of this report we focus on the process and steps involved in the design of the T-CLPD panel aimed at final classification of T-CLPD, while the development of the LST tube is detailed in Section 2 of this report. The approach proposed to assess T-cell clonality by flow cytometry has been previously reported in the literature,[290–294] which shows that in cases in which expanded or aberrant TCR$\gamma\delta^-$/SmCD3$^+$ T-cells are detected with the LST, the predominance of a single TCR-Vβ family within a T-cell population (TCR-Vβ restriction) is highly suggestive of a clonal T-cell disorder.[292–294] In cases where phenotypic abnormalities involve TCR$\gamma\delta^+$ T-cells, the TCR-Vγ and TCR-Vδ repertoire may also be investigated, but definitive demonstration of the clonal nature of the infiltrating cell population may not be achieved, due to the more restricted repertoire of normal TCR$\gamma\delta^+$ T-cells, their imbalanced distribution in normal subjects[295] and the relatively limited availability of TCR-Vγ and TCR-Vδ family-specific reagents for flow cytometry.

Regarding the overall performance of the EuroFlow T-CLPD panel, our results clearly show further contribution of the marker combinations used to distinguish between normal/reactive and aberrant/malignant T-cells, except for a few CD8$^+$ T-LGL cases. At the same time it allowed unequivocal classification of T-CLPD into most WHO entities, including SS, T-PLL, ATLL, T-LGL, and AITL. Other rare entities that were not specifically evaluated, like CD30$^+$ T-CLPD, require further prospective studies, although they will most likely be identified with the panel, based on the immunophenotypic features described in the literature for such disease entities and the experience accumulated at several EuroFlow sites.

Antibody panel for NK-cell chronic lymphoproliferative diseases (NK-CLPD)

One of the major challenges in establishing the diagnosis of NK-cell neoplasms is to distinguish between normal, reactive and (mono)clonal proliferations of NK cells, because of the lack of clonal markers in the expanded NK cells. Many studies have clearly shown that clonal pathological cells from most hematological malignancies display aberrant phenotypes that allow their distinction from their normal counterparts.[9,10,14,47,77,237,296,297] Based on this background, the EuroFlow NK-CLPD panel aimed at further characterization of the expanded NK-cells, to discriminate between aberrant and normal/reactive NK-cells, and subsequently define a more precise diagnosis of clonal NK-CLPD. As a result, we propose a panel of three 8-color tubes containing 16 different markers, four of which are backbone markers (SmCD3, CD19, CD45 and CD56), to identify NK cells, and the remaining 12 markers are devoted to distinguish aberrant from normal/reactive/polyclonal NK cells. Upon applying multivariate analysis tools provided with the Infinicyt software, we show that this panel facilitates the distinction between aberrant and normal/reactive NK cells in most cases presenting with NK-cell-associated lymphocytosis.

Consequently, the EuroFlow NK-CLPD panel will be of great help in routine diagnostic settings in this regard. However, partial overlap was observed for some cases, which points out the need for further efforts to improve such discrimination. On the other hand, it has to be taken into account that the rarity of this group of diseases may be an obstacle for some laboratories to perform a relatively large panel of markers to diagnose NK-CLPD. In such cases, a potentially efficient alternative to the implementation of the EuroFlow NK-CLPD panel in all clinical flow cytometry laboratories is centralization in reference centers of this part of the diagnostic work-up of NK-CLPD.

Therefore, in the absence of universal markers of NK-cell clonality, the precise definition of the immunophenotypic profiles associated with clonal versus reactive cells becomes crucial in the diagnosis of NK-CLPD (Figure 29).

The EuroFlow reference database as a tool for immunophenotypic classification of hematological malignancies

Finally, an additional relevant contribution of the work done is the generation of a reference database containing information about large numbers of cases within each WHO disease category. Such database is currently being prospectively expanded by including even more typical and atypical new, fully characterized cases. In the near future, when such database becomes available, it can be used to prospectively classify new individual cases at any clinical flow cytometry laboratory around the world, whenever the EuroFlow SOP for instrument settings and sample preparation are used in combination with the EuroFlow panels and the new multivariate data analysis software tools here described.

CONCLUSION

After 5 years of extensive testing, we present a complete set of antibody panels for standardized *n*-dimensional flow cytometric immunophenotyping of hematological malignancies. The stepwise application of the single-tube screening panels and multitube classification panels fits into the EuroFlow diagnostic algorithm with entries defined by clinical and laboratory parameters. The proposed antibody panels are designed to diagnose and classify the various types of leukemias and lymphomas according to the WHO-defined disease categories. Multiple successive rounds of design–evaluation–redesign were needed to reach the final versions of the antibody panels. The initially designed consensus panels were first optimized by inclusion of additional informative markers and exclusion of redundant markers as identified by novel software tools for multivariate data analysis. In parallel, the composition of the antibody panels was improved by testing the various combinations of antibody clones and fluorochrome conjugates. The final version of the proposed panels was extensively validated on 2031 informative samples, using the novel Infinicyt software tools and the EuroFlow SOP for sample preparation, data acquisition and data analysis, as described by Kalina *et al.*[16] This validation showed that the EuroFlow antibody panels are highly efficient and at the same time they are flexible and can be adapted to fit the different needs of the different laboratories. Altogether, these results indicate that combined usage of the EuroFlow antibody panels and EuroFlow SOP can be considered as the most extensive and validated approach for standardized multidimensional flow cytometric immunophenotyping for diagnostic screening and classification of hematological malignancies. The presented EuroFlow tools may also serve as the basis for future improvements in the field, particularly when the EuroFlow database becomes available for comparing newly diagnosed cases with the many cases in the database.

CONFLICT OF INTEREST

The EuroFlow Consortium is an independent scientific consortium that aims at innovation and standardization of diagnostic flow cytometry. All acquired knowledge and experience will be shared with the scientific and diagnostic community after protection of the relevant Intellectual Property, for example by filing of patents. The involved patents are collectively owned by the EuroFlow Consortium and licensed to companies. The results presented in this manuscript are included in the patent application, entitled 'Methods, reagents n kits for flow cytometric immunophenotyping' (PCT/NL2010050332). The revenues of the patents are exclusively used for EuroFlow Consortium activities, such as for covering (in part) the costs of the Consortium meetings, the EuroFlow Educational Workshops and the purchase of custom-made reagents for collective experiments. M Martin-Ayuso, J Hernández, M Muñoz, are employees of Cytognos SL, which is a pro-profit company.

ACKNOWLEDGEMENTS

We are grateful to Dr Jean-Luc Sanne of the European Commission for his support and monitoring of the EuroFlow project. We thank Marieke Comans-Bitter for graphic

design of the figures and for her continuous support in the management of the EuroFlow Consortium, and Bibi van Bodegom, Caroline Linker and Monique van Rossum for their secretarial support of the consortium activities. We are grateful to Ria Bloemberg and Gellof van Steenis for their support in the financial management of the project funds. We are also thankful to Maria Gomez da Silva, Evan Jensen, Joana Caetano, Teresa Faria, Ana Santos and Isabel Santos. The research activities of the EuroFlow Consortium were supported by the European Commission (grant STREP EU-FP6, LSHB-CT-2006-018708, entitled '*Flow cytometry for fast and sensitive diagnosis and follow-up of hematological malignancies*') and the following national grants: Spanish Network of Cancer Research Centers (ISCIII RTICC-RD06/0020/0035-FEDER), FIS 08/90881 and FIS PS09/02430 from the 'Fondo de Investigación Sanitaria', Ministerio de Ciencia e Innovación (Madrid, Spain); GR37 EDU/894/2009 and SA016-A-09 from the Consejería de Educación, Junta de Castilla y León (Valladolid, Spain); PIB2010BZ-00565 from the Dirección General de Cooperación Internacional y Relaciones Institucionales, Secretaría de Estado de Investigación, Ministerio de Ciencia e Innovación (Madrid, Spain); Ministry of Health Czech Republic (NT/12425-4 and NS/10480-3); and Charles University grant No. 23010 and UNCE No. 204012; Tomas Kalina is supported as an 'ISAC Scholar' by the International Society for Advancement of Cytometry (ISAC); Andy Rawstron was supported by Leukemia and Lymphoma Research (LLR).

REFERENCES

1 Foon KA, Todd 3rd RF. Immunologic classification of leukemia and lymphoma. *Blood* 1986; **68**: 1–31.
2 van Dongen JJ, Adriaansen HJ, Hooijkaas H. Immunophenotyping of leukaemias and non-Hodgkin's lymphomas. Immunological markers and their CD codes. *Neth J Med* 1988; **33**: 298–314.
3 Swerdlow SH, Campo E, Harris NL, Jaffe ES, Pileri SA, Stein H *et al. WHO Classification of Tumours of Haematopoietic and Lymphoid Tissues*. 4th edn. (International Agency for Research on Cancer: Lyon, 2008, pp 439.
4 Macedo A, Orfao A, Vidriales MB, Lopez-Berges MC, Valverde B, Gonzalez M *et al.* Characterization of aberrant phenotypes in acute myeloblastic leukemia. *Ann Hematol* 1995; **70**: 189–194.
5 Lucio P, Parreira A, van den Beemd MW, van Lochem EG, van Wering ER, Baars E *et al.* Flow cytometric analysis of normal B cell differentiation: a frame of reference for the detection of minimal residual disease in precursor-B-ALL. *Leukemia* 1999; **13**: 419–427.
6 Orfao A, Schmitz G, Brando B, Ruiz-Arguelles A, Basso G, Braylan R *et al.* Clinically useful information provided by the flow cytometric immunophenotyping of hematological malignancies: current status and future directions. *Clin Chem* 1999; **45**: 1708–1717.
7 Basso G, Buldini B, De Zen L, Orfao A. New methodologic approaches for immunophenotyping acute leukemias. *Haematologica* 2001; **86**: 675–692.
8 Szczepanski T, van der Velden VH, van Dongen JJ. Flow-cytometric immunophenotyping of normal and malignant lymphocytes. *Clin Chem Lab Med* 2006; **44**: 775–796.
9 Rawstron AC, Orfao A, Beksac M, Bezdickova L, Brooimans RA, Bumbea H *et al.* Report of the European Myeloma Network on multiparametric flow cytometry in multiple myeloma and related disorders. *Haematologica* 2008; **93**: 431–438.
10 Matarraz S, Lopez A, Barrena S, Fernandez C, Jensen E, Flores J *et al.* The immunophenotype of different immature, myeloid and B-cell lineage-committed CD34+ hematopoietic cells allows discrimination between normal/reactive and myelodysplastic syndrome precursors. *Leukemia* 2008; **22**: 1175–1183.
11 van Lochem EG, van der Velden VH, Wind HK, te Marvelde JG, Westerdaal NA, van Dongen JJ. Immunophenotypic differentiation patterns of normal hematopoiesis in human bone marrow: reference patterns for age-related changes and disease-induced shifts. *Cytometry B Clin Cytom* 2004; **60**: 1–13.
12 Rothe G, Schmitz G. Consensus protocol for the flow cytometric immunophenotyping of hematopoietic malignancies. Working Group on Flow Cytometry and Image Analysis. *Leukemia* 1996; **10**: 877–895.
13 Bene MC, Nebe T, Bettelheim P, Buldini B, Bumbea H, Kern W *et al.* Immunophenotyping of acute leukemia and lymphoproliferative disorders: a consensus proposal of the European LeukemiaNet Work Package 10. *Leukemia* 2011; **25**: 567–574.
14 van de Loosdrecht AA, Alhan C, Bene MC, Della Porta MG, Drager AM, Feuillard J *et al.* Standardization of flow cytometry in myelodysplastic syndromes: report from the first European LeukemiaNet working conference on flow cytometry in myelodysplastic syndromes. *Haematologica* 2009; **94**: 1124–1134.
15 Paietta E. How to optimize multiparameter flow cytometry for leukaemia/lymphoma diagnosis. *Best Pract Res Clin Haematol* 2003; **16**: 671–683.
16 Kalina T, Flores-Montero J, van der Velden VHJ, Martin-Ayuso M, Böttcher S, Ritgen M *et al.* EuroFlow standardization of flow cytometry instrument settings and immunophenotyping protocols. *Leukemia* 2012 (submitted).
17 Bellido M, Rubiol E, Ubeda J, Estivill C, Lopez O, Manteiga R *et al.* Rapid and simple immunophenotypic characterization of lymphocytes using a new test. *Haematologica* 1998; **83**: 681–685.
18 Barrena S, Almeida J, Garcia-Macias MC, Lopez A, Rasillo A, Sayagues JM *et al.* Flow cytometry immunophenotyping of fine-needle aspiration specimens: utility in the diagnosis and classification of non-Hodgkin lymphomas. *Histopathology* 2011; **58**: 906–918.
19 Ratei R, Karawajew L, Lacombe F, Jagoda K, Del Poeta G, Kraan J *et al.* Discriminant function analysis as decision support system for the diagnosis of acute leukemia with a minimal four color screening panel and multiparameter flow cytometry immunophenotyping. *Leukemia* 2007; **21**: 1204–1211.
20 Costa ES, Arroyo ME, Pedreira CE, Garcia-Marcos MA, Tabernero MD, Almeida J *et al.* A new automated flow cytometry data analysis approach for the diagnostic screening of neoplastic B-cell disorders in peripheral blood samples with absolute lymphocytosis. *Leukemia* 2006; **20**: 1221–1230.
21 Braylan RC, Orfao A, Borowitz MJ, Davis BH. Optimal number of reagents required to evaluate hematolymphoid neoplasias: results of an international consensus meeting. *Cytometry* 2001; **46**: 23–27.
22 Ruiz-Arguelles A, Rivadeneyra-Espinoza L, Duque RE, Orfao A. Report on the second Latin American consensus conference for flow cytometric immunophenotyping of hematological malignancies. *Cytometry B Clin Cytom* 2006; **70**: 39–44.
23 Wood BL, Arroz M, Barnett D, DiGiuseppe J, Greig B, Kussick SJ *et al.* 2006Bethesda International Consensus recommendations on the immunophenotypic analysis of hematolymphoid neoplasia by flow cytometry: optimal reagents and reporting for the flow cytometric diagnosis of hematopoietic neoplasia. *Cytometry B Clin Cytom* 2007; **72**(Suppl 1): S14–S22.
24 Craig FE, Foon KA. Flow cytometric immunophenotyping for hematologic neoplasms. *Blood* 2008; **111**: 3941–3967.
25 Davis BH, Holden JT, Bene MC, Borowitz MJ, Braylan RC, Cornfield D *et al.* 2006Bethesda International Consensus recommendations on the flow cytometric immunophenotypic analysis of hematolymphoid neoplasia: medical indications. *Cytometry B Clin Cytom* 2007; **72**(Suppl 1): S5–S13.
26 Stetler-Stevenson M, Ahmad E, Barnett D, Braylan R, DiGiuseppe J, Marti G *et al. Clinical Flow Cytometric Analysis of Neoplastic Hematolymphoid Cells.* Approved guideline – 2nd edn. CLSI document H43-A2 ed. Clinical and Laboratory Standards Institute: Wayne, PA, 2007.
27 Bene MC, Castoldi G, Knapp W, Ludwig WD, Matutes E, Orfao A *et al.* Proposals for the immunological classification of acute leukemias. European Group for the Immunological Characterization of Leukemias (EGIL). *Leukemia* 1995; **9**: 1783–1786.
28 Stewart CC, Behm FG, Carey JL, Cornbleet J, Duque RE, Hudnall SD *et al.* U.S.-Canadian Consensus recommendations on the immunophenotypic analysis of hematologic neoplasia by flow cytometry: selection of antibody combinations. *Cytometry* 1997; **30**: 231–235.
29 Ruiz-Arguelles A, Duque RE, Orfao A. Report on the first Latin American Consensus Conference for Flow Cytometric Immunophenotyping of Leukemia. *Cytometry* 1998; **34**: 39–42.
30 Maecker HT, Frey T, Nomura LE, Trotter J. Selecting fluorochrome conjugates for maximum sensitivity. *Cytometry A* 2004; **62**: 169–173.
31 Costa ES, Pedreira CE, Barrena S, Lecrevisse Q, Flores J, Quijano S *et al.* Automated pattern-guided principal component analysis vs expert-based immunophenotypic classification of B-cell chronic lymphoproliferative disorders: a step forward in the standardization of clinical immunophenotyping. *Leukemia* 2010; **24**: 1927–1933.
32 Pedreira CE, Costa ES, Barrena S, Lecrevisse Q, Almeida J, van Dongen JJ *et al.* Generation of flow cytometry data files with a potentially infinite number of dimensions. *Cytometry A* 2008; **73**: 834–846.
33 Costa ES, Peres RT, Almeida J, Lecrevisse Q, Arroyo ME, Teodosio C *et al.* Harmonization of light scatter and fluorescence flow cytometry profiles obtained after staining peripheral blood leucocytes for cell surface-only versus intracellular antigens with the Fix & Perm reagent. *Cytometry B Clin Cytom* 2010; **78**: 11–20.
34 Borowitz MJ, Chan JKC. B lymphoblastic leukaemia/lymphoma. In: Swerdlow SH, Campo E, Harris NL, Jaffe ES, Pileri SA, Stein H *et al.* (eds). *WHO Classification of Tumours of Haematopoietic and Lymphoid Tissues*. 4th edn. International Agency for Research on Cancer: Lyon, 2008, pp 168–175.
35 Borowitz MJ, Chan JKC. T lymphoblastic leukaemia/lymphoma. In: Swerdlow SH, Campo E, Harris NL, Jaffe ES, Pileri SA, Stein H *et al.* (eds) *WHO Classification of Tumours of Haematopoietic and Lymphoid Tissues*. 4th edn. International Agency for Research on Cancer: Lyon, 2008, pp 176–178.
36 Borowitz MJ, Béné MC, Harris NL, Porwit A, Matutes E. Acute leukaemias of ambiguous lineage. In: Swerdlow SH, Campo E, Harris NL, Jaffe ES, Pileri SA, Stein H *et al.* (eds). *WHO Classification of Tumours of Haematopoietic and Lymphoid*

Tissues. 4th edn. International Agency for Research on Cancer: Lyon, 2008, pp 150–155.
37 van den Ancker W, Terwijn M, Westers TM, Merle PA, van Beckhoven E, Drager AM *et al.* Acute leukemias of ambiguous lineage: diagnostic consequences of the WHO2008 classification. *Leukemia* 2010; **24**: 1392–1396.
38 Mejstrikova E, Volejnikova J, Fronkova E, Zdrahalova K, Kalina T, Sterba J *et al.* Prognosis of children with mixed phenotype acute leukemia treated on the basis of consistent immunophenotypic criteria. *Haematologica* 2010; **95**: 928–935.
39 Stetler-Stevenson M, Davis B, Wood B, Braylan R. 2006 Bethesda International Consensus Conference on Flow Cytometric Immunophenotyping of Hematolymphoid Neoplasia. *Cytometry B Clin Cytom* 2007; **72**(Suppl 1): S3.
40 Matutes E, Pickl WF, Van't Veer M, Morilla R, Swansbury J, Strobl H *et al.* Mixed-phenotype acute leukemia: clinical and laboratory features and outcome in 100 patients defined according to the WHO 2008 classification. *Blood* 2011; **117**: 3163–3171.
41 Orfao A, Chillon MC, Bortoluci AM, Lopez-Berges MC, Garcia-Sanz R, Gonzalez M *et al.* The flow cytometric pattern of CD34, CD15 and CD13 expression in acute myeloblastic leukemia is highly characteristic of the presence of PML-RARalpha gene rearrangements. *Haematologica* 1999; **84**: 405–412.
42 De Zen L, Orfao A, Cazzaniga G, Masiero L, Cocito MG, Spinelli M *et al.* Quantitative multiparametric immunophenotyping in acute lymphoblastic leukemia: correlation with specific genotype. I. ETV6/AML1 ALLs identification. *Leukemia* 2000; **14**: 1225–1231.
43 Tabernero MD, Bortoluci AM, Alaejos I, Lopez-Berges MC, Rasillo A, Garcia-Sanz R *et al.* Adult precursor B-ALL with BCR/ABL gene rearrangements displays a unique immunophenotype based on the pattern of CD10, CD34, CD13 and CD38 expresssion. *Leukemia* 2001; **15**: 406–414.
44 Orfao A, Ortuno F, de Santiago M, Lopez A, San Miguel J. Immunophenotyping of acute leukemias and myelodysplastic syndromes. *Cytometry A* 2004; **58**: 62–71.
45 Hrusak O, Porwit-MacDonald A. Antigen expression patterns reflecting genotype of acute leukemias. *Leukemia* 2002; **16**: 1233–1258.
46 Vaskova M, Mejstrikova E, Kalina T, Martinkova P, Omelka M, Trka J *et al.* Transfer of genomics information to flow cytometry: expression of CD27 and CD44 discriminates subtypes of acute lymphoblastic leukemia. *Leukemia* 2005; **19**: 876–878.
47 Szczepanski T, Orfao A, van der Velden VH. San Miguel JF, van Dongen JJ. Minimal residual disease in leukaemia patients. *Lancet Oncol* 2001; **2**: 409–417.
48 van Dongen JJ, Krissansen GW, Wolvers-Tettero IL, Comans-Bitter WM, Adriaansen HJ, Hooijkaas H *et al.* Cytoplasmic expression of the CD3 antigen as a diagnostic marker for immature T-cell malignancies. *Blood* 1988; **71**: 603–612.
49 van Grotel M, van den Heuvel-Eibrink MM, van Wering ER, van Noesel MM, Kamps WA, Veerman AJ *et al.* CD34 expression is associated with poor survival in pediatric T-cell acute lymphoblastic leukemia. *Pediatr Blood Cancer* 2008; **51**: 737–740.
50 Hurwitz CA, Raimondi SC, Head D, Krance R, Mirro Jr. J, Kalwinsky DK *et al.* Distinctive immunophenotypic features of t(8;21)(q22;q22) acute myeloblastic leukemia in children. *Blood* 1992; **80**: 3182–3188.
51 Kita K, Nakase K, Miwa H, Masuya M, Nishii K, Morita N *et al.* Phenotypical characteristics of acute myelocytic leukemia associated with the t(8;21)(q22;q22) chromosomal abnormality: frequent expression of immature B-cell antigen CD19 together with stem cell antigen CD34. *Blood* 1992; **80**: 470–477.
52 Venditti A, Del Poeta G, Buccisano F, Tamburini A, Cox-Froncillo MC, Aronica G *et al.* Prognostic relevance of the expression of Tdt and CD7 in 335 cases of acute myeloid leukemia. *Leukemia* 1998; **12**: 1056–1063.
53 Suggs JL, Cruse JM, Lewis RE. Aberrant myeloid marker expression in precursor B-cell and T-cell leukemias. *Exp Mol Pathol* 2007; **83**: 471–473.
54 Bhargava P, Kallakury BV, Ross JS, Azumi N, Bagg A. CD79a is heterogeneously expressed in neoplastic and normal myeloid precursors and megakaryocytes in an antibody clone-dependent manner. *Am J Clin Pathol* 2007; **128**: 306–313.
55 Tiacci E, Pileri S, Orleth A, Pacini R, Tabarrini A, Frenguelli F *et al.* PAX5 expression in acute leukemias: higher B-lineage specificity than CD79a and selective association with t(8;21)-acute myelogenous leukemia. *Cancer Res* 2004; **64**: 7399–7404.
56 Uckun FM, Gaynon PS, Sensel MG, Nachman J, Trigg ME, Steinherz PG *et al.* Clinical features and treatment outcome of childhood T-lineage acute lymphoblastic leukemia according to the apparent maturational stage of T-lineage leukemic blasts: a Children's Cancer Group study. *J Clin Oncol* 1997; **15**: 2214–2221.
57 Khalidi HS, Chang KL, Medeiros LJ, Brynes RK, Slovak ML, Murata-Collins JL *et al.* Acute lymphoblastic leukemia. Survey of immunophenotype, French-American-British classification, frequency of myeloid antigen expression, and karyotypic abnormalities in 210 pediatric and adult cases. *Am J Clin Pathol* 1999; **111**: 467–476.
58 Lewis RE, Cruse JM, Sanders CM, Webb RN, Suggs JL. Aberrant expression of T-cell markers in acute myeloid leukemia. *Exp Mol Pathol* 2007; **83**: 462–463.
59 Borowitz MJ, Guenther KL, Shults KE, Stelzer GT. Immunophenotyping of acute leukemia by flow cytometric analysis. Use of CD45 and right-angle light scatter to gate on leukemic blasts in three-color analysis. *Am J Clin Pathol* 1993; **100**: 534–540.
60 Lacombe F, Durrieu F, Briais A, Dumain P, Belloc F, Bascans E *et al.* Flow cytometry CD45 gating for immunophenotyping of acute myeloid leukemia. *Leukemia* 1997; **11**: 1878–1886.
61 Vial JP, Lacombe F. Immunophenotyping of acute leukemia: utility of CD45 for blast cell identification. *Methods Cell Biol* 2001; **64**: 343–358.
62 Pilozzi E, Pulford K, Jones M, Muller-Hermelink HK, Falini B, Ralfkiaer E *et al.* Co-expression of CD79a (JCB117) and CD3 by lymphoblastic lymphoma. *J Pathol* 1998; **186**: 140–143.
63 Hashimoto M, Yamashita Y, Mori N. Immunohistochemical detection of CD79a expression in precursor T cell lymphoblastic lymphoma/leukaemias. *J Pathol* 2002; **197**: 341–347.
64 Asnafi V, Beldjord K, Garand R, Millien C, Bahloul M, LeTutour P *et al.* IgH DJ rearrangements within T-ALL correlate with cCD79a expression, an immature/TCRgammadelta phenotype and absence of IL7Ralpha/CD127 expression. *Leukemia* 2004; **18**: 1997–2001.
65 Escribano L, Orfao A, Diaz-Agustin B, Villarrubia J, Cervero C, Lopez A *et al.* Indolent systemic mast cell disease in adults: immunophenotypic characterization of bone marrow mast cells and its diagnostic implications. *Blood* 1998; **91**: 2731–2736.
66 Han K, Kim Y, Lee J, Lim J, Lee KY, Kang CS *et al.* Human basophils express CD22 without expression of CD19. *Cytometry* 1999; **37**: 178–183.
67 Martin-Martin L, Almeida J, Hernandez-Campo PM, Sanchez ML, Lecrevisse Q, Orfao A. Immunophenotypical morphologic, and functional characterization of maturation-associated plasmacytoid dendritic cell subsets in normal adult human bone marrow. *Transfusion* 2009; **49**: 1692–1708.
68 Bell JJ, Bhandoola A. The earliest thymic progenitors for T cells possess myeloid lineage potential. *Nature* 2008; **452**: 764–767.
69 Babusikova O, Stevulova L, Fajtova M. Immunophenotyping parameters as prognostic factors in T-acute leukemia patients. *Neoplasma* 2009; **56**: 508–513.
70 Taub JW. Early T-cell precursor acute lymphoblastic leukaemia. *Lancet Oncol* 2009; **10**: 105–106.
71 Coustan-Smith E, Mullighan CG, Onciu M, Behm FG, Raimondi SC, Pei D *et al.* Early T-cell precursor leukaemia: a subtype of very high-risk acute lymphoblastic leukaemia. *Lancet Oncol* 2009; **10**: 147–156.
72 Carulli G, Cannizzo E, Zucca A, Buda G, Orciuolo E, Marini A *et al.* CD45 expression in low-grade B-cell non-Hodgkin's lymphomas. *Leuk Res* 2008; **32**: 263–267.
73 Seegmiller AC, Kroft SH, Karandikar NJ, McKenna RW. Characterization of immunophenotypic aberrancies in 200 cases of B acute lymphoblastic leukemia. *Am J Clin Pathol* 2009; **132**: 940–949.
74 Kuppers R. Mechanisms of B-cell lymphoma pathogenesis. *Nat Rev Cancer* 2005; **5**: 251–262.
75 Lenz G, Staudt LM. Aggressive lymphomas. *N Engl J Med* 2010; **362**: 1417–1429.
76 Davis BH, Foucar K, Szczarkowski W, Ball E, Witzig T, Foon KA *et al.* U.S.-Canadian Consensus recommendations on the immunophenotypic analysis of hematologic neoplasia by flow cytometry: medical indications. *Cytometry* 1997; **30**: 249–263.
77 Sanchez ML, Almeida J, Vidriales B, Lopez-Berges MC, Garcia-Marcos MA, Moro MJ *et al.* Incidence of phenotypic aberrations in a series of 467 patients with B chronic lymphoproliferative disorders: basis for the design of specific four-color stainings to be used for minimal residual disease investigation. *Leukemia* 2002; **16**: 1460–1469.
78 Gorczyca W, Weisberger J, Liu Z, Tsang P, Hossein M, Wu CD *et al.* An approach to diagnosis of T-cell lymphoproliferative disorders by flow cytometry. *Cytometry* 2002; **50**: 177–190.
79 Lima M, Almeida J, Montero AG, Teixeira MA, Queiros ML, Santos AH *et al.* Clinicobiological, immunophenotypic, and molecular characteristics of monoclonal CD56-/+ dim chronic natural killer cell large granular lymphocytosis. *Am J Pathol* 2004; **165**: 1117–1127.
80 Lima M, Almeida J, Teixeira MA, Santos AH, Queiros ML, Fonseca S *et al.* Reactive phenotypes after acute and chronic NK-cell activation. *J Biol Regul Homeost Agents* 2004; **18**: 331–334.
81 Cady FM, Morice WG. Flow cytometric assessment of T-cell chronic lymphoproliferative disorders. *Clin Lab Med* 2007; **27**: 513–532vi.
82 Hultin LE, Hausner MA, Hultin PM, Giorgi JV. CD20 (pan-B cell) antigen is expressed at a low level on a subpopulation of human T lymphocytes. *Cytometry* 1993; **14**: 196–204.
83 Khokhar FA, Payne WD, Talwalkar SS, Jorgensen JL, Bueso-Ramos CE, Medeiros LJ *et al.* Angioimmunoblastic T-cell lymphoma in bone marrow: a morphologic and immunophenotypic study. *Hum Pathol* 2010; **41**: 79–87.
84 Bos GM, van Putten WL, van der Holt B, van den Bent M, Verdonck LF, Hagenbeek A. For which patients with aggressive non-Hodgkin's lymphoma is

prophylaxis for central nervous system disease mandatory? Dutch HOVON Group. *Ann Oncol* 1998; **9**: 191–194.
85 Hollender A, Kvaloy S, Nome O, Skovlund E, Lote K, Holte H. Central nervous system involvement following diagnosis of non-Hodgkin's lymphoma: a risk model. *Ann Oncol* 2002; **13**: 1099–1107.
86 Bierman P, Giglio P. Diagnosis and treatment of central nervous system involvement in non-Hodgkin's lymphoma. *Hematol Oncol Clin North Am* 2005; **19**: 597–609v.
87 Hegde U, Filie A, Little RF, Janik JE, Grant N, Steinberg SM *et al.* High incidence of occult leptomeningeal disease detected by flow cytometry in newly diagnosed aggressive B-cell lymphomas at risk for central nervous system involvement: the role of flow cytometry versus cytology. *Blood* 2005; **105**: 496–502.
88 Bromberg JE, Breems DA, Kraan J, Bikker G, van der Holt B, Smitt PS *et al.* CSF flow cytometry greatly improves diagnostic accuracy in CNS hematologic malignancies. *Neurology* 2007; **68**: 1674–1679.
89 Quijano S, Lopez A, Sancho JM, Panizo C, Deben G, Castilla C *et al.* Identification of leptomeningeal disease in aggressive B-cell non-Hodgkin's lymphoma: improved sensitivity of flow cytometry. *J Clin Oncol* 2009; **27**: 1462–1469.
90 Sancho JM, Orfao A, Quijano S, Garcia O, Panizo C, Perez-Ceballos E *et al.* Clinical significance of occult cerebrospinal fluid involvement assessed by flow cytometry in non-Hodgkin's lymphoma patients at high risk of central nervous system disease in the rituximab era. *Eur J Haematol* 2010; **85**: 321–328.
91 Chan CC. Molecular pathology of primary intraocular lymphoma. *Trans Am Ophthalmol Soc* 2003; **101**: 275–292.
92 Coupland SE, Heimann H, Bechrakis NE. Primary intraocular lymphoma: a review of the clinical, histopathological and molecular biological features. *Graefes Arch Clin Exp Ophthalmol* 2004; **242**: 901–913.
93 Davis JL, Solomon D, Nussenblatt RB. Palestine AG, Chan CC. Immunocytochemical staining of vitreous cells. Indications, techniques, and results. *Ophthalmology* 1992; **99**: 250–256.
94 Whitcup SM, Stark-Vancs V, Wittes RE, Solomon D, Podgor MJ, Nussenblatt RB *et al.* Association of interleukin 10 in the vitreous and cerebrospinal fluid and primary central nervous system lymphoma. *Arch Ophthalmol* 1997; **115**: 1157–1160.
95 Freilich RJ, Krol G, DeAngelis LM. Neuroimaging and cerebrospinal fluid cytology in the diagnosis of leptomeningeal metastasis. *Ann Neurol* 1995; **38**: 51–57.
96 Windhagen A, Maniak S, Heidenreich F. Analysis of cerebrospinal fluid cells by flow cytometry and immunocytochemistry in inflammatory central nervous system diseases: comparison of low- and high-density cell surface antigen expression. *Diagn Cytopathol* 1999; **21**: 313–318.
97 Schinstine M, Filie AC, Wilson W, Stetler-Stevenson M, Abati A. Detection of malignant hematopoietic cells in cerebral spinal fluid previously diagnosed as atypical or suspicious. *Cancer* 2006; **108**: 157–162.
98 White VA, Gascoyne RD, Paton KE. Use of the polymerase chain reaction to detect B- and T-cell gene rearrangements in vitreous specimens from patients with intraocular lymphoma. *Arch Ophthalmol* 1999; **117**: 761–765.
99 Coupland SE, Hummel M, Muller HH, Stein H. Molecular analysis of immunoglobulin genes in primary intraocular lymphoma. *Invest Ophthalmol Vis Sci* 2005; **46**: 3507–3514.
100 Wilson DJ, Braziel R, Rosenbaum JT. Intraocular lymphoma. Immunopathologic analysis of vitreous biopsy specimens. *Arch Ophthalmol* 1992; **110**: 1455–1458.
101 Davis JL, Viciana AL, Ruiz P. Diagnosis of intraocular lymphoma by flow cytometry. *Am J Ophthalmol* 1997; **124**: 362–372.
102 French CA, Dorfman DM, Shaheen G, Cibas ES. Diagnosing lymphoproliferative disorders involving the cerebrospinal fluid: increased sensitivity using flow cytometric analysis. *Diagn Cytopathol* 2000; **23**: 369–374.
103 Subira D, Castanon S, Aceituno E, Hernandez J, Jimenez-Garofano C, Jimenez A *et al.* Flow cytometric analysis of cerebrospinal fluid samples and its usefulness in routine clinical practice. *Am J Clin Pathol* 2002; **117**: 952–958.
104 Nuckel H, Novotny JR, Noppeney R, Savidou I, Duhrsen U. Detection of malignant haematopoietic cells in the cerebrospinal fluid by conventional cytology and flow cytometry. *Clin Lab Haematol* 2006; **28**: 22–29.
105 Missotten T, Tielemans D, Bromberg JE, Van Hagen PM, Van Lochem EG, Van Dongen JJM *et al.* Multi-color flowcytometric immunophenotyping is a valuable tool for detection of intra-ocular lymphoma in patients presenting with a (pseudo)uveitis. *Ophthalmology* 2012 (in press).
106 Kraan J, Gratama JW, Haioun C, Orfao A, Plonquet A, Porwit A *et al.* Flow cytometric immunophenotyping of cerebrospinal fluid. *Curr Protoc Cytom* 2008; Chapter 6: Unit 6 25.
107 McKenna RW, Kyle RA, Kuehi WM, Grogan TM, Harris NL, Coupland RW. Plasma cell neoplasms. In: Swerdlow SH, Campo E, Harris NL, Jaffe ES, Pileri SA, Stein H *et al.* (eds). *WHO Classification of Tumours of Haematopoietic and Lymphoid Tissues*. 4th edn. International Agency for Research on Cancer: Lyon, 2008, pp 200–213.
108 Kyle RA, Rajkumar SV. Epidemiology of the plasma-cell disorders. *Best Pract Res Clin Haematol* 2007; **20**: 637–664.
109 Paiva B, Vidriales MB, Perez JJ, Lopez-Berges MC, Garcia-Sanz R, Ocio EM *et al.* The clinical utility and prognostic value of multiparameter flow cytometry immunophenotyping in light-chain amyloidosis. *Blood* 2011; **117**: 3613–3616.
110 Paiva B, Almeida J, Perez-Andres M, Mateo G, Lopez A, Rasillo A *et al.* Utility of flow cytometry immunophenotyping in multiple myeloma and other clonal plasma cell-related disorders. *Cytometry B Clin Cytom* 2010; **78**: 239–252.
111 Perez-Persona E, Vidriales MB, Mateo G, Garcia-Sanz R, Mateos MV, de Coca AG *et al.* New criteria to identify risk of progression in monoclonal gammopathy of uncertain significance and smoldering multiple myeloma based on multiparameter flow cytometry analysis of bone marrow plasma cells. *Blood* 2007; **110**: 2586–2592.
112 Mateo G, Montalban MA, Vidriales MB, Lahuerta JJ, Mateos MV, Gutierrez N *et al.* Prognostic value of immunophenotyping in multiple myeloma: a study by the PETHEMA/GEM cooperative study groups on patients uniformly treated with high-dose therapy. *J Clin Oncol* 2008; **26**: 2737–2744.
113 Harada H, Kawano MM, Huang N, Harada Y, Iwato K, Tanabe O *et al.* Phenotypic difference of normal plasma cells from mature myeloma cells. *Blood* 1993; **81**: 2658–2663.
114 Almeida J, Orfao A, Mateo G, Ocqueteau M, Garcia-Sanz R, Moro MJ *et al.* Immunophenotypic and DNA content characteristics of plasma cells in multiple myeloma and monoclonal gammopathy of undetermined significance. *Pathol Biol (Paris)* 1999; **47**: 119–127.
115 Lima M, Teixeira Mdos A, Fonseca S, Goncalves C, Guerra M, Queiros ML *et al.* Immunophenotypic aberrations, DNA content, and cell cycle analysis of plasma cells in patients with myeloma and monoclonal gammopathies. *Blood Cells Mol Dis* 2000; **26**: 634–645.
116 Ely SA, Knowles DM. Expression of CD56/neural cell adhesion molecule correlates with the presence of lytic bone lesions in multiple myeloma and distinguishes myeloma from monoclonal gammopathy of undetermined significance and lymphomas with plasmacytoid differentiation. *Am J Pathol* 2002; **160**: 1293–1299.
117 Lin P, Owens R, Tricot G, Wilson CS. Flow cytometric immunophenotypic analysis of 306 cases of multiple myeloma. *Am J Clin Pathol* 2004; **121**: 482–488.
118 Bataille R, Jego G, Robillard N, Barille-Nion S, Harousseau JL, Moreau P *et al.* The phenotype of normal, reactive and malignant plasma cells. Identification of "many and multiple myelomas" and of new targets for myeloma therapy. *Haematologica* 2006; **91**: 1234–1240.
119 Moreau P, Robillard N, Jego G, Pellat C, Le Gouill S, Thoumi S *et al.* Lack of CD27 in myeloma delineates different presentation and outcome. *Br J Haematol* 2006; **132**: 168–170.
120 Bahlis NJ, King AM, Kolonias D, Carlson LM, Liu HY, Hussein MA *et al.* CD28-mediated regulation of multiple myeloma cell proliferation and survival. *Blood* 2007; **109**: 5002–5010.
121 Perez-Andres M, Almeida J, Martin-Ayuso M, De Las Heras N, Moro MJ, Martin-Nunez G *et al.* Soluble and membrane levels of molecules involved in the interaction between clonal plasma cells and the immunological microenvironment in multiple myeloma and their association with the characteristics of the disease. *Int J Cancer* 2009; **124**: 367–375.
122 Cannizzo E, Bellio E, Sohani AR, Hasserjian RP, Ferry JA, Dorn ME *et al.* Multiparameter immunophenotyping by flow cytometry in multiple myeloma: The diagnostic utility of defining ranges of normal antigenic expression in comparison to histology. *Cytometry B Clin Cytom* 2010; **78**: 231–238.
123 Horan PK, Slezak SE, Poste G. Improved flow cytometric analysis of leukocyte subsets: simultaneous identification of five cell subsets using two-color immunofluorescence. *Proc Natl Acad Sci USA* 1986; **83**: 8361–8365.
124 McKenna RW, Washington LT, Aquino DB, Picker LJ, Kroft SH. Immunophenotypic analysis of hematogones (B-lymphocyte precursors) in 662 consecutive bone marrow specimens by 4-color flow cytometry. *Blood* 2001; **98**: 2498–2507.
125 Digiuseppe JA. Acute lymphoblastic leukemia: diagnosis and detection of minimal residual disease following therapy. *Clin Lab Med* 2007; **27**: 533–549vi.
126 Borowitz MJ, Hunger SP, Carroll AJ, Shuster JJ, Pullen DJ, Steuber CP *et al.* Predictability of the t(1;19)(q23;p13) from surface antigen phenotype: implications for screening cases of childhood acute lymphoblastic leukemia for molecular analysis: a Pediatric Oncology Group study. *Blood* 1993; **82**: 1086–1091.
127 Huh YO, Smith TL, Collins P, Bueso-Ramos C, Albitar M, Kantarjian HM *et al.* Terminal deoxynucleotidyl transferase expression in acute myelogenous leukemia and myelodysplasia as determined by flow cytometry. *Leuk Lymphoma* 2000; **37**: 319–331.
128 Skoog L, Hagerstrom T, Reizenstein P, Ost A. Detection of TdT in AML blasts by immunological and biochemical techniques. *Anticancer Res* 1986; **6**: 281–282.
129 Adriaansen HJ, Hooijkaas H, Kappers-Klunne MC, Hahlen K. van't Veer MB, van Dongen JJ. Double marker analysis for terminal deoxynucleotidyl transferase

and myeloid antigens in acute nonlymphocytic leukemia patients and healthy subjects. *Haematol Blood Transfus* 1990; **33**: 41–49.
130 Schlieben S, Borkhardt A, Reinisch I, Ritterbach J, Janssen JW, Ratei R *et al.* Incidence and clinical outcome of children with BCR/ABL-positive acute lymphoblastic leukemia (ALL). A prospective RT-PCR study based on 673 patients enrolled in the German pediatric multicenter therapy trials ALL-BFM-90 and CoALL-05-92. *Leukemia* 1996; **10**: 957–963.
131 Kalina T, Vaskova M, Mejstrikova E, Madzo J, Trka J, Stary J *et al.* Myeloid antigens in childhood lymphoblastic leukemia: clinical data point to regulation of CD66c distinct from other myeloid antigens. *BMC Cancer* 2005; **5**: 38.
132 Owaidah TM, Rawas FI, Al Khayatt MF, Elkum NB. Expression of CD66c and CD25 in acute lymphoblastic leukemia as a predictor of the presence of BCR/ABL rearrangement. *Hematol Oncol Stem Cell Ther* 2008; **1**: 34–37.
133 Sugita K, Mori T, Yokota S, Kuroki M, Koyama TO, Inukai T *et al.* The KOR-SA3544 antigen predominantly expressed on the surface of Philadelphia chromosome-positive acute lymphoblastic leukemia cells is nonspecific cross-reacting antigen-50/90 (CD66c) and invariably expressed in cytoplasm of human leukemia cells. *Leukemia* 1999; **13**: 779–785.
134 Ludwig WD, Rieder H, Bartram CR, Heinze B, Schwartz S, Gassmann W *et al.* Immunophenotypic and genotypic features, clinical characteristics, and treatment outcome of adult pro-B acute lymphoblastic leukemia: results of the German multicenter trials GMALL 03/87 and 04/89. *Blood* 1998; **92**: 1898–1909.
135 Parkin JL, Arthur DC, Abramson CS, McKenna RW, Kersey JH, Heideman RL *et al.* Acute leukemia associated with the t(4;11) chromosome rearrangement: ultrastructural and immunologic characteristics. *Blood* 1982; **60**: 1321–1331.
136 Behm FG, Smith FO, Raimondi SC, Pui CH, Bernstein ID. Human homologue of the rat chondroitin sulfate proteoglycan, NG2, detected by monoclonal antibody 7.1, identifies childhood acute lymphoblastic leukemias with t(4;11)(q21;q23) or t(11;19)(q23;p13) and MLL gene rearrangements. *Blood* 1996; **87**: 1134–1139.
137 Borkhardt A, Cazzaniga G, Viehmann S, Valsecchi MG, Ludwig WD, Burci L *et al.* Incidence and clinical relevance of TEL/AML1 fusion genes in children with acute lymphoblastic leukemia enrolled in the German and Italian multicenter therapy trials. Associazione Italiana Ematologia Oncologia Pediatrica and the Berlin-Frankfurt-Munster Study Group. *Blood* 1997; **90**: 571–577.
138 Borowitz MJ, Rubnitz J, Nash M, Pullen DJ, Camitta B. Surface antigen phenotype can predict TEL-AML1 rearrangement in childhood B-precursor ALL: a Pediatric Oncology Group study. *Leukemia* 1998; **12**: 1764–1770.
139 Gandemer V, Aubry M, Roussel M, Rio AG, de Tayrac M, Vallee A *et al.* CD9 expression can be used to predict childhood TEL/AML1-positive acute lymphoblastic leukemia: proposal for an accelerated diagnostic flowchart. *Leuk Res* 2010; **34**: 430–437.
140 Weir EG, Cowan K, LeBeau P, Borowitz MJ. A limited antibody panel can distinguish B-precursor acute lymphoblastic leukemia from normal B precursors with four color flow cytometry: implications for residual disease detection. *Leukemia* 1999; **13**: 558–567.
141 Campana D, Coustan-Smith E. Minimal residual disease studies by flow cytometry in acute leukemia. *Acta Haematol* 2004; **112**: 8–15.
142 Dworzak MN, Froschl G, Printz D, Mann G, Potschger U, Muhlegger N *et al.* Prognostic significance and modalities of flow cytometric minimal residual disease detection in childhood acute lymphoblastic leukemia. *Blood* 2002; **99**: 1952–1958.
143 Basso G, Veltroni M, Valsecchi MG, Dworzak MN, Ratei R, Silvestri D *et al.* Risk of relapse of childhood acute lymphoblastic leukemia is predicted by flow cytometric measurement of residual disease on day 15 bone marrow. *J Clin Oncol* 2009; **27**: 5168–5174.
144 Bruggemann M, Schrauder A, Raff T, Pfeifer H, Dworzak M, Ottmann OG *et al.* Standardized MRD quantification in European ALL trials: proceedings of the Second International Symposium on MRD assessment in Kiel, Germany, 18-20 September 2008. *Leukemia* 2010; **24**: 521–535.
145 Szczepanski T. Why and how to quantify minimal residual disease in acute lymphoblastic leukemia? *Leukemia* 2007; **21**: 622–626.
146 Campana D. Minimal residual disease studies in acute leukemia. *Am J Clin Pathol* 2004 122**(Suppl):**: S47–S57.
147 Coustan-Smith E, Ribeiro RC, Stow P, Zhou Y, Pui CH, Rivera GK *et al.* A simplified flow cytometric assay identifies children with acute lymphoblastic leukemia who have a superior clinical outcome. *Blood* 2006; **108**: 97–102.
148 Lucio P, Gaipa G, van Lochem EG, van Wering ER, Porwit-MacDonald A, Faria T *et al.* BIOMED-I concerted action report: flow cytometric immunophenotyping of precursor B-ALL with standardized triple-stainings. BIOMED-1 Concerted Action Investigation of Minimal Residual Disease in Acute Leukemia: International Standardization and Clinical Evaluation. *Leukemia* 2001; **15**: 1185–1192.
149 Munoz L, Nomdedeu JF, Lopez O, Carnicer MJ, Bellido M, Aventin A *et al.* Interleukin-3 receptor alpha chain (CD123) is widely expressed in hematologic malignancies. *Haematologica* 2001; **86**: 1261–1269.
150 Barrena S, Almeida J, Yunta M, Lopez A, Fernandez-Mosteirin N, Giralt M *et al.* Aberrant expression of tetraspanin molecules in B-cell chronic lymphoproliferative disorders and its correlation with normal B-cell maturation. *Leukemia* 2005; **19**: 1376–1383.
151 Muzzafar T, Medeiros LJ, Wang SA, Brahmandam A, Thomas DA, Jorgensen JL. Aberrant underexpression of CD81 in precursor B-cell acute lymphoblastic leukemia: utility in detection of minimal residual disease by flow cytometry. *Am J Clin Pathol* 2009; **132**: 692–698.
152 Chen JS, Coustan-Smith E, Suzuki T, Neale GA, Mihara K, Pui CH *et al.* Identification of novel markers for monitoring minimal residual disease in acute lymphoblastic leukemia. *Blood* 2001; **97**: 2115–2120.
153 Veltroni M, De Zen L, Sanzari MC, Maglia O, Dworzak MN, Ratei R *et al.* Expression of CD58 in normal, regenerating and leukemic bone marrow B cells: implications for the detection of minimal residual disease in acute lymphocytic leukemia. *Haematologica* 2003; **88**: 1245–1252.
154 Aifantis I, Raetz E, Buonamici S. Molecular pathogenesis of T-cell leukaemia and lymphoma. *Nat Rev Immunol* 2008; **8**: 380–390.
155 Chiaretti S, Foa R. T-cell acute lymphoblastic leukemia. *Haematologica* 2009; **94**: 160–162.
156 Crist WM, Shuster JJ, Falletta J, Pullen DJ, Berard CW, Vietti TJ *et al.* Clinical features and outcome in childhood T-cell leukemia-lymphoma according to stage of thymocyte differentiation: a Pediatric Oncology Group Study. *Blood* 1988; **72**: 1891–1897.
157 De Keersmaecker K, Marynen P, Cools J. Genetic insights in the pathogenesis of T-cell acute lymphoblastic leukemia. *Haematologica* 2005; **90**: 1116–1127.
158 Teitell MA, Pandolfi PP. Molecular genetics of acute lymphoblastic leukemia. *Annu Rev Pathol* 2009; **4**: 175–198.
159 Hoelzer D, Gokbuget N. T-cell lymphoblastic lymphoma and T-cell acute lymphoblastic leukemia: a separate entity? *Clin Lymphoma Myeloma* 2009; **9**(Suppl 3): S214–S221.
160 Graux C, Cools J, Michaux L, Vandenberghe P, Hagemeijer A. Cytogenetics and molecular genetics of T-cell acute lymphoblastic leukemia: from thymocyte to lymphoblast. *Leukemia* 2006; **20**: 1496–1510.
161 Burmeister T, Gokbuget N, Reinhardt R, Rieder H, Hoelzer D, Schwartz S. NUP214-ABL1 in adult T-ALL: the GMALL study group experience. *Blood* 2006; **108**: 3556–3559.
162 Graux C, Cools J, Melotte C, Quentmeier H, Ferrando A, Levine R *et al.* Fusion of NUP214 to ABL1 on amplified episomes in T-cell acute lymphoblastic leukemia. *Nat Genet* 2004; **36**: 1084–1089.
163 Graux C, Stevens-Kroef M, Lafage M, Dastugue N, Harrison CJ, Mugneret F *et al.* Heterogeneous patterns of amplification of the NUP214-ABL1 fusion gene in T-cell acute lymphoblastic leukemia. *Leukemia* 2009; **23**: 125–133.
164 Asnafi V, Radford-Weiss I, Dastugue N, Bayle C, Leboeuf D, Charrin C *et al.* CALM-AF10 is a common fusion transcript in T-ALL and is specific to the TCRgammadelta lineage. *Blood* 2003; **102**: 1000–1006.
165 Asnafi V, Beldjord K, Boulanger E, Comba B, Le Tutour P, Estienne MH *et al.* Analysis of TCR, pT alpha, and RAG-1 in T-acute lymphoblastic leukemias improves understanding of early human T-lymphoid lineage commitment. *Blood* 2003; **101**: 2693–2703.
166 Ferrando AA, Neuberg DS, Staunton J, Loh ML, Huard C, Raimondi SC *et al.* Gene expression signatures define novel oncogenic pathways in T cell acute lymphoblastic leukemia. *Cancer Cell* 2002; **1**: 75–87.
167 Soulier J, Clappier E, Cayuela JM, Regnault A, Garcia-Peydro M, Dombret H *et al.* HOXA genes are included in genetic and biologic networks defining human acute T-cell leukemia (T-ALL). *Blood* 2005; **106**: 274–286.
168 van Grotel M, Meijerink JP, Beverloo HB, Langerak AW, Buys-Gladdines JG, Schneider P *et al.* The outcome of molecular-cytogenetic subgroups in pediatric T-cell acute lymphoblastic leukemia: a retrospective study of patients treated according to DCOG or COALL protocols. *Haematologica* 2006; **91**: 1212–1221.
169 Drexler HG, Thiel E, Ludwig WD. Acute myeloid leukemias expressing lymphoid-associated antigens: diagnostic incidence and prognostic significance. *Leukemia* 1993; **7**: 489–498.
170 Ratei R, Sperling C, Karawajew L, Schott G, Schrappe M, Harbott J *et al.* Immunophenotype and clinical characteristics of CD45-negative and CD45-positive childhood acute lymphoblastic leukemia. *Ann Hematol* 1998; **77**: 107–114.
171 Robertson PB, Neiman RS, Worapongpaiboon S, John K, Orazi A. 013 (CD99) positivity in hematologic proliferations correlates with TdT positivity. *Mod Pathol* 1997; **10**: 277–282.
172 Dalmazzo LF, Jacomo RH, Marinato AF, Figueiredo-Pontes LL, Cunha RL, Garcia AB *et al.* The presence of CD56/CD16 in T-cell acute lymphoblastic leukaemia correlates with the expression of cytotoxic molecules and is associated with worse response to treatment. *Br J Haematol* 2009; **144**: 223–229.
173 Fischer L, Gokbuget N, Schwartz S, Burmeister T, Rieder H, Bruggemann M *et al.* CD56 expression in T-cell acute lymphoblastic leukemia is associated with

non-thymic phenotype and resistance to induction therapy but no inferior survival after risk-adapted therapy. *Haematologica* 2009; **94**: 224–229.
174 Montero I, Rios E, Parody R, Perez-Hurtado JM, Martin-Noya A, Rodriguez JM. CD56 in T-cell acute lymphoblastic leukaemia: a malignant transformation of an early myeloid-lymphoid progenitor? *Haematologica* 2003; **88**: ELT26.
175 Paietta E, Neuberg D, Richards S, Bennett JM, Han L, Racevskis J *et al.* Rare adult acute lymphocytic leukemia with CD56 expression in the ECOG experience shows unexpected phenotypic and genotypic heterogeneity. *Am J Hematol* 2001; **66**: 189–196.
176 Ravandi F, Cortes J, Estrov Z, Thomas D, Giles FJ, Huh YO *et al.* CD56 expression predicts occurrence of CNS disease in acute lymphoblastic leukemia. *Leuk Res* 2002; **26**: 643–649.
177 Garnache-Ottou F, Chaperot L, Biichle S, Ferrand C, Remy-Martin JP, Deconinck E *et al.* Expression of the myeloid-associated marker CD33 is not an exclusive factor for leukemic plasmacytoid dendritic cells. *Blood* 2005; **105**: 1256–1264.
178 Garnache-Ottou F, Feuillard J, Saas P. Plasmacytoid dendritic cell leukaemia/lymphoma: towards a well defined entity? *Br J Haematol* 2007; **136**: 539–548.
179 Facchetti F, Jones DM, Petrella T. Blastic plasmocytoid dendritic cell neoplasm. In: Swerdlow SH, Campo E, Harris NL, Jaffe ES, Pileri SA, Stein H *et al.* (eds). *WHO Classification of Tumours of Haematopoietic and Lymphoid Tissues*. 4th edn. International Agency for Research on Cancer: Lyon, 2008, pp 145–147.
180 Han X, Bueso-Ramos CE. Precursor T-cell acute lymphoblastic leukemia/lymphoblastic lymphoma and acute biphenotypic leukemias. *Am J Clin Pathol* 2007; **127**: 528–544.
181 Asnafi V, Buzyn A, Thomas X, Huguet F, Vey N, Boiron JM *et al.* Impact of TCR status and genotype on outcome in adult T-cell acute lymphoblastic leukemia: a LALA-94 study. *Blood* 2005; **105**: 3072–3078.
182 Cavalcanti Junior GB, Savino W, Pombo-de-Oliveira MS. CD44 expression in T-cell lymphoblastic leukemia. *Braz J Med Biol Res* 1994; **27**: 2259–2266.
183 Falcao RP, Garcia AB. Expression of CD45RA (naive) and CD45RO (memory) antigens in T-acute lymphoblastic leukaemia. *Br J Haematol* 1993; **85**: 483–486.
184 Kawano S, Tatsumi E, Yoneda N, Tani A, Nakamura F. Expression pattern of CD45 RA/RO isoformic antigens in T-lineage neoplasms. *Am J Hematol* 1995; **49**: 6–14.
185 Schiavone EM, Lo Pardo C, Di Noto R, Manzo C, Ferrara F, Vacca C *et al.* Expression of the leucocyte common antigen (LCA, CD45) isoforms RA and RO in acute haematological malignancies: possible relevance in the definition of new overlap points between normal and leukaemic haemopoiesis. *Br J Haematol* 1995; **91**: 899–906.
186 Lhermitte L, de Labarthe A, Dupret C, Lapillonne H, Millien C, Landman-Parker J *et al.* Most immature T-ALLs express Ra-IL3 (CD123): possible target for DT-IL3 therapy. *Leukemia* 2006; **20**: 1908–1910.
187 Campana D, Coustan-Smith E. Advances in the immunological monitoring of childhood acute lymphoblastic leukaemia. *Best Pract Res Clin Haematol* 2002; **15**: 1–19.
188 Porwit-MacDonald A, Bjorklund E, Lucio P, van Lochem EG, Mazur J, Parreira A *et al.* BIOMED-1 concerted action report: flow cytometric characterization of CD7+ cell subsets in normal bone marrow as a basis for the diagnosis and follow-up of T cell acute lymphoblastic leukemia (T-ALL). *Leukemia* 2000; **14**: 816–825.
189 Dworzak MN, Froschl G, Printz D, Zen LD, Gaipa G, Ratei R *et al.* CD99 expression in T-lineage ALL: implications for flow cytometric detection of minimal residual disease. *Leukemia* 2004; **18**: 703–708.
190 Roshal M, Fromm JR, Winter S, Dunsmore K, Wood BL. Immaturity associated antigens are lost during induction for T cell lymphoblastic leukemia: implications for minimal residual disease detection. *Cytometry B Clin Cytom* 2010; **78**: 139–146.
191 Andrieu V, Radford-Weiss I, Troussard X, Chane C, Valensi F, Guesnu M *et al.* Molecular detection of t(8;21)/AML1-ETO in AML M1/M2: correlation with cytogenetics, morphology and immunophenotype. *Br J Haematol* 1996; **92**: 855–865.
192 Adriaansen HJ, te Boekhorst PA, Hagemeijer AM, van der Schoot CE, Delwel HR, van Dongen JJ. Acute myeloid leukemia M4 with bone marrow eosinophilia (M4Eo) and inv(16)(p13q22) exhibits a specific immunophenotype with CD2 expression. *Blood* 1993; **81**: 3043–3051.
193 Loken MR, van de Loosdrecht A, Ogata K, Orfao A, Wells DA. Flow cytometry in myelodysplastic syndromes: report from a working conference. *Leuk Res* 2008; **32**: 5–17.
194 Stetler-Stevenson M, Arthur DC, Jabbour N, Xie XY, Molldrem J, Barrett AJ *et al.* Diagnostic utility of flow cytometric immunophenotyping in myelodysplastic syndrome. *Blood* 2001; **98**: 979–987.
195 van de Loosdrecht AA, Westers TM, Westra AH, Drager AM, van der Velden VH, Ossenkoppele GJ. Identification of distinct prognostic subgroups in low- and intermediate-1-risk myelodysplastic syndromes by flow cytometry. *Blood* 2008; **111**: 1067–1077.
196 Malcovati L, Della Porta MG, Lunghi M, Pascutto C, Vanelli L, Travaglino E *et al.* Flow cytometry evaluation of erythroid and myeloid dysplasia in patients with myelodysplastic syndrome. *Leukemia* 2005; **19**: 776–783.
197 Cherian S, Moore J, Bantly A, Vergilio JA, Klein P, Luger S *et al.* Peripheral blood MDS score: a new flow cytometric tool for the diagnosis of myelodysplastic syndromes. *Cytometry B Clin Cytom* 2005; **64**: 9–17.
198 Aul C, Giagounidis A, Heinsch M, Germing U, Ganser A. Prognostic indicators and scoring systems for predicting outcome in patients with myelodysplastic syndromes. *Rev Clin Exp Hematol* 2004; **8**: E1.
199 Della Porta MG, Malcovati L, Invernizzi R, Travaglino E, Pascutto C, Maffioli M *et al.* Flow cytometry evaluation of erythroid dysplasia in patients with myelodysplastic syndrome. *Leukemia* 2006; **20**: 549–555.
200 Font P, Subira D, Martinez Chamorro C, Castanon S, Arranz E, Ramiro S *et al.* Evaluation of CD7 and terminal deoxynucleotidyl transferase (TdT) expression in CD34+ myeloblasts from patients with myelodysplastic syndrome. *Leuk Res* 2006; **30**: 957–963.
201 Cesana C, Klersy C, Brando B, Nosari A, Scarpati B, Scampini L *et al.* Prognostic value of circulating CD34+ cells in myelodysplastic syndromes. *Leuk Res* 2008; **32**: 1715–1723.
202 Scott BL, Wells DA, Loken MR, Myerson D, Leisenring WM, Deeg HJ. Validation of a flow cytometric scoring system as a prognostic indicator for posttransplantation outcome in patients with myelodysplastic syndrome. *Blood* 2008; **112**: 2681–2686.
203 Wells DA, Benesch M, Loken MR, Vallejo C, Myerson D, Leisenring WM *et al.* Myeloid and monocytic dyspoiesis as determined by flow cytometric scoring in myelodysplastic syndrome correlates with the IPSS and with outcome after hematopoietic stem cell transplantation. *Blood* 2003; **102**: 394–403.
204 Van de Loosdrecht AA, Ireland R, Kern W, Alhan C, Balleissen JS, Bene MC *et al.* Rationale for the clinical application of flow cytometry in patients with myelodysplastic syndromes. Position paper of the European LeukemiaNet working group on flow cytometry in myelodysplastic syndromes. *Leukemia* 2012; (in press).
205 Van Bockstaele DR, Deneys V, Philippe J, Bernier M, Kestens L, Chatelain B *et al.* Belgian consensus recommendations for flow cytometric immunophenotyping. The Belgian Association for Cytometry/Belgische Vereniging voor Cytometrie/Association Belge de Cytometrie. *Acta Clin Belg* 1999; **54**: 88–98.
206 Aguilar H, Alvarez-Errico D, Garcia-Montero AC, Orfao A, Sayos J, Lopez-Botet M. Molecular characterization of a novel immune receptor restricted to the monocytic lineage. *J Immunol* 2004; **173**(): 6703–6711.
207 Casasnovas RO, Slimane FK, Garand R, Faure GC, Campos L, Deneys V *et al.* Immunological classification of acute myeloblastic leukemias: relevance to patient outcome. *Leukemia* 2003; **17**: 515–527.
208 Buhring HJ, Muller T, Herbst R, Cole S, Rappold I, Schuller W *et al.* The adhesion molecule E-cadherin and a surface antigen recognized by the antibody 9C4 are selectively expressed on erythroid cells of defined maturational stages. *Leukemia* 1996; **10**: 106–116.
209 Lammers R, Giesert C, Grunebach F, Marxer A, Vogel W, Buhring HJ. Monoclonal antibody 9C4 recognizes epithelial cellular adhesion molecule, a cell surface antigen expressed in early steps of erythropoiesis. *Exp Hematol* 2002; **30**: 537–545.
210 Vidriales MB, San-Miguel JF, Orfao A, Coustan-Smith E, Campana D. Minimal residual disease monitoring by flow cytometry. *Best Pract Res Clin Haematol* 2003; **16**: 599–612.
211 Bahia DM, Yamamoto M, Chauffaille ML, Kimura EY, Bordin JO, Filgueiras MA *et al.* Aberrant phenotypes in acute myeloid leukemia: a high frequency and its clinical significance. *Haematologica* 2001; **86**: 801–806.
212 Adriaansen HJ, van Dongen JJ, Hooijkaas H, Hahlen K, van 't Veer MB, Lowenberg B *et al.* Translocation (6;9) may be associated with a specific TdT-positive immunological phenotype in ANLL. *Leukemia* 1988; **2**: 136–140.
213 Ribeiro E, Matarraz Sudon S, de Santiago M, Lima CS, Metze K, Giralt M *et al.* Maturation-associated immunophenotypic abnormalities in bone marrow B-lymphocytes in myelodysplastic syndromes. *Leuk Res* 2006; **30**: 9–16.
214 Mauvieux L, Delabesse E, Bourquelot P, Radford-Weiss I, Bennaceur A, Flandrin G *et al.* NG2 expression in MLL rearranged acute myeloid leukaemia is restricted to monoblastic cases. *Br J Haematol* 1999; **107**: 674–676.
215 Bueno C, Almeida J, Lucio P, Marco J, Garcia R, de Pablos JM *et al.* Incidence and characteristics of CD4(+)/HLA DRhi dendritic cell malignancies. *Haematologica* 2004; **89**: 58–69.
216 van Rhenen A, Feller N, Kelder A, Westra AH, Rombouts E, Zweegman S *et al.* High stem cell frequency in acute myeloid leukemia at diagnosis predicts high minimal residual disease and poor survival. *Clin Cancer Res* 2005; **11**: 6520–6527.
217 Escribano L, Orfao A, Villarrubia J, Diaz-Agustin B, Cervero C, Rios A *et al.* Immunophenotypic characterization of human bone marrow mast cells. A flow cytometric study of normal and pathological bone marrow samples. *Anal Cell Pathol* 1998; **16**: 151–159.
218 Gassmann W, Loffler H. Acute megakaryoblastic leukemia. *Leuk Lymphoma* 1995; **18**(Suppl 1): 69–73.

219 Schernthaner GH, Hauswirth AW, Baghestanian M, Agis H, Ghannadan M, Worda C *et al.* Detection of differentiation- and activation-linked cell surface antigens on cultured mast cell progenitors. *Allergy* 2005; **60**: 1248–1255.
220 Ghannadan M, Hauswirth AW, Schernthaner GH, Muller MR, Klepetko W, Schatzl G *et al.* Detection of novel CD antigens on the surface of human mast cells and basophils. *Int Arch Allergy Immunol* 2002; **127**: 299–307.
221 Garnache-Ottou F, Feuillard J, Ferrand C, Biichle S, Trimoreau F, Seilles E *et al.* Extended diagnostic criteria for plasmacytoid dendritic cell leukaemia. *Br J Haematol* 2009; **145**: 624–636.
222 Yatomi Y, Yoneyama A, Nakahara K. Usefulness of CD9 detection in the diagnosis of acute megakaryoblastic leukemia. *Eur J Haematol* 2004; **72**: 229–230.
223 Imamura N, Mtasiwa DM, Ota H, Inada T, Kuramoto A. Distribution of cell surface glycoprotein CD9 (P24) antigen on megakaryocyte lineage leukemias and cell lines. *Am J Hematol* 1990; **35**: 65–67.
224 Di Noto R, Luciano L, Lo Pardo C, Ferrara F, Frigeri F, Mercuro O *et al.* JURL-MK1 (c-kit(high)/CD30-/CD40-) and JURL-MK2 (c-kit(low)/CD30 + /CD40 +) cell lines: 'two-sided' model for investigating leukemic megakaryocytopoiesis. *Leukemia* 1997; **11**: 1554–1564.
225 van Daele PL, Beukenkamp BS, Geertsma-Kleinekoort WM, Valk PJ, van Laar JA, van Hagen PM *et al.* Immunophenotyping of mast cells: a sensitive and specific diagnostic tool for systemic mastocytosis. *Neth J Med* 2009; **67**: 142–146.
226 Borowitz MJ, Craig FE, Digiuseppe JA, Illingworth AJ, Rosse W, Sutherland DR *et al.* Guidelines for the diagnosis and monitoring of paroxysmal nocturnal hemoglobinuria and related disorders by flow cytometry. *Cytometry B Clin Cytom* 2010; **78**: 211–230.
227 Escribano L, Diaz-Agustin B, Lopez A, Nunez Lopez R, Garcia-Montero A, Almeida J *et al.* Immunophenotypic analysis of mast cells in mastocytosis: When and how to do it. Proposals of the Spanish Network on Mastocytosis (REMA). *Cytometry B Clin Cytom* 2004; **58**: 1–8.
228 Vardiman JW, Thiele J, Arber DA, Brunning RD, Borowitz MJ, Porwit A *et al.* The 2008 revision of the World Health Organization (WHO) classification of myeloid neoplasms and acute leukemia: rationale and important changes. *Blood* 2009; **114**: 937–951.
229 Haferlach C, Mecucci C, Schnittger S, Kohlmann A, Mancini M, Cuneo A *et al.* AML with mutated NPM1 carrying a normal or aberrant karyotype show overlapping biologic, pathologic, immunophenotypic, and prognostic features. *Blood* 2009; **114**: 3024–3032.
230 Valk PJ, Verhaak RG, Beijen MA, Erpelinck CA, Barjesteh van Waalwijk van Doorn-Khosrovani S, Boer JM *et al.* Prognostically useful gene-expression profiles in acute myeloid leukemia. *N Engl J Med* 2004; **350**: 1617–1628.
231 Mature B-cell Neoplasm. In: Swerdlow SH, Campo E, Harris NL, Jaffe ES, Pileri SA, Stein H *et al.* (eds). *WHO classification of tumours of haematopoietic and lymphoid tissues*. 4th edn. (International Agency for Research on Cancer: Lyon, 2008; pp 179–268.
232 The Non-Hodgkin's Lymphoma Classification Project. A clinical evaluation of the International Lymphoma Study Group classification of non-Hodgkin's lymphoma. *Blood* 1997; **89**: 3909–3918.
233 Hallek M, Cheson BD, Catovsky D, Caligaris-Cappio F, Dighiero G, Dohner H *et al.* Guidelines for the diagnosis and treatment of chronic lymphocytic leukemia: a report from the International Workshop on Chronic Lymphocytic Leukemia updating the National Cancer Institute-Working Group 1996 guidelines. *Blood* 2008; **111**: 5446–5456.
234 Herrmann A, Hoster E, Zwingers T, Brittinger G, Engelhard M, Meusers P *et al.* Improvement of overall survival in advanced stage mantle cell lymphoma. *J Clin Oncol* 2009; **27**: 511–518.
235 Bottcher S, Ritgen M, Pott C, Bruggemann M, Raff T, Stilgenbauer S *et al.* Comparative analysis of minimal residual disease detection using four-color flow cytometry, consensus IgH-PCR, and quantitative IgH PCR in CLL after allogeneic and autologous stem cell transplantation. *Leukemia* 2004; **18**: 1637–1645.
236 Quijano S, Lopez A, Rasillo A, Barrena S, Luz Sanchez M, Flores J *et al.* Association between the proliferative rate of neoplastic B cells, their maturation stage, and underlying cytogenetic abnormalities in B-cell chronic lymphoproliferative disorders: analysis of a series of 432 patients. *Blood* 2008; **111**: 5130–5141.
237 Bottcher S, Ritgen M, Buske S, Gesk S, Klapper W, Hoster E *et al.* Minimal residual disease detection in mantle cell lymphoma: methods and significance of four-color flow cytometry compared to consensus IGH-polymerase chain reaction at initial staging and for follow-up examinations. *Haematologica* 2008; **93**: 551–559.
238 Huang J, Fan G, Zhong Y, Gatter K, Braziel R, Gross G *et al.* Diagnostic usefulness of aberrant CD22 expression in differentiating neoplastic cells of B-cell chronic lymphoproliferative disorders from admixed benign B cells in four-color multiparameter flow cytometry. *Am J Clin Pathol* 2005; **123**: 826–832.
239 Menendez P, Vargas A, Bueno C, Barrena S, Almeida J, De Santiago M *et al.* Quantitative analysis of bcl-2 expression in normal and leukemic human B-cell differentiation. *Leukemia* 2004; **18**: 491–498.
240 Rawstron AC, de Tute R, Jack AS, Hillmen P. Flow cytometric protein expression profiling as a systematic approach for developing disease-specific assays: identification of a chronic lymphocytic leukaemia-specific assay for use in rituximab-containing regimens. *Leukemia* 2006; **20**: 2102–2110.
241 Pedreira CE, Costa ES, Almeida J, Fernandez C, Quijano S, Flores J *et al.* A probabilistic approach for the evaluation of minimal residual disease by multiparameter flow cytometry in leukemic B-cell chronic lymphoproliferative disorders. *Cytometry A* 2008; **73A**: 1141–1150.
242 Ravandi F, Kantarjian H, Jones D, Dearden C, Keating M, O'Brien S. Mature T-cell leukemias. *Cancer* 2005; **104**: 1808–1818.
243 Foucar K. Mature T-cell leukemias including T-prolymphocytic leukemia, adult T-cell leukemia/lymphoma, and Sezary syndrome. *Am J Clin Pathol* 2007; **127**: 496–510.
244 Jaffe ES. The 2008 WHO classification of lymphomas: implications for clinical practice and translational research. *Hematology Am Soc Hematol Educ Program* 2009; 523–531.
245 Rudiger T, Geissinger E, Muller-Hermelink HK. 'Normal counterparts' of nodal peripheral T-cell lymphoma. *Hematol Oncol* 2006; **24**: 175–180.
246 Rodriguez-Abreu D, Filho VB, Zucca E. Peripheral T-cell lymphomas, unspecified (or not otherwise specified): a review. *Hematol Oncol* 2008; **26**: 8–20.
247 de Leval L, Bisig B, Thielen C, Boniver J, Gaulard P. Molecular classification of T-cell lymphomas. *Crit Rev Oncol Hematol* 2009; **72**: 125–143.
248 Grogg KL, Attygalle AD, Macon WR, Remstein ED, Kurtin PJ, Dogan A. Angioimmunoblastic T-cell lymphoma: a neoplasm of germinal-center T-helper cells? *Blood* 2005; **106**: 1501–1502.
249 Yu H, Shahsafaei A, Dorfman DM. Germinal-center T-helper-cell markers PD-1 and CXCL13 are both expressed by neoplastic cells in angioimmunoblastic T-cell lymphoma. *Am J Clin Pathol* 2009; **131**: 33–41.
250 Savage KJ, Harris NL, Vose JM, Ullrich F, Jaffe ES, Connors JM *et al.* ALK- anaplastic large-cell lymphoma is clinically and immunophenotypically different from both ALK + ALCL and peripheral T-cell lymphoma, not otherwise specified: report from the International Peripheral T-Cell Lymphoma Project. *Blood* 2008; **111**: 5496–5504.
251 Herling M, Khoury JD, Washington LT, Duvic M, Keating MJ, Jones D. A systematic approach to diagnosis of mature T-cell leukemias reveals heterogeneity among WHO categories. *Blood* 2004; **104**: 328–335.
252 Herling M, Patel KA, Teitell MA, Konopleva M, Ravandi F, Kobayashi R *et al.* High TCL1 expression and intact T-cell receptor signaling define a hyperproliferative subset of T-cell prolymphocytic leukemia. *Blood* 2008; **111**: 328–337.
253 Savage KJ. Peripheral T-cell lymphomas. *Blood Rev* 2007; **21**: 201–216.
254 Jamal S, Picker LJ, Aquino DB, McKenna RW, Dawson DB, Kroft SH. Immunophenotypic analysis of peripheral T-cell neoplasms. A multiparameter flow cytometric approach. *Am J Clin Pathol* 2001; **116**: 512–526.
255 Lima M, Almeida J, Teixeira MA, Queiros ML, Santos AH, Fonseca S *et al.* Utility of flow cytometry immunophenotyping and DNA ploidy studies for diagnosis and characterization of blood involvement in CD4 + Sezary's syndrome. *Haematologica* 2003; **88**: 874–887.
256 Lima M, Almeida J, Teixeira MA, Alguero C, Santos AH, Balanzategui A *et al.* TCRalphabeta + /CD4 + large granular lymphocytosis: a new clonal T-cell lymphoproliferative disorder. *Am J Pathol* 2003; **163**: 763–771.
257 Karube K, Aoki R, Nomura Y, Yamamoto K, Shimizu K, Yoshida S *et al.* Usefulness of flow cytometry for differential diagnosis of precursor and peripheral T-cell and NK-cell lymphomas: analysis of 490 cases. *Pathol Int* 2008; **58**: 89–97.
258 Morice WG, Kurtin PJ, Leibson PJ, Tefferi A, Hanson CA. Demonstration of aberrant T-cell and natural killer-cell antigen expression in all cases of granular lymphocytic leukaemia. *Br J Haematol* 2003; **120**: 1026–1036.
259 Lundell R, Hartung L, Hill S, Perkins SL, Bahler DW. T-cell large granular lymphocyte leukemias have multiple phenotypic abnormalities involving pan-T-cell antigens and receptors for MHC molecules. *Am J Clin Pathol* 2005; **124**: 937–946.
260 Geissinger E, Sadler P, Roth S, Grieb T, Puppe B, Muller N *et al.* Disturbed expression of the T-cell receptor/CD3 complex and associated signaling molecules in CD30 + T-cell lymphoproliferations. *Haematologica* 2010; **95**: 1697–1704.
261 Sokolowska-Wojdylo M, Wenzel J, Gaffal E, Steitz J, Roszkiewicz J, Bieber T *et al.* Absence of CD26 expression on skin-homing CLA + CD4 + T lymphocytes in peripheral blood is a highly sensitive marker for early diagnosis and therapeutic monitoring of patients with Sezary syndrome. *Clin Exp Dermatol* 2005; **30**: 702–706.
262 Kelemen K, Guitart J, Kuzel TM, Goolsby CL, Peterson LC. The usefulness of CD26 in flow cytometric analysis of peripheral blood in Sezary syndrome. *Am J Clin Pathol* 2008; **129**: 146–156.
263 de Leval L, Gaulard P. CD30 + lymphoproliferative disorders. *Haematologica* 2010; **95**: 1627–1630.
264 Pekarsky Y, Hallas C, Croce CM. The role of TCL1 in human T-cell leukemia. *Oncogene* 2001; **20**: 5638–5643.

265 Narducci MG, Pescarmona E, Lazzeri C, Signoretti S, Lavinia AM, Remotti D *et al.* Regulation of TCL1 expression in B- and T-cell lymphomas and reactive lymphoid tissues. *Cancer Res* 2000; **60**: 2095–2100.
266 van Dongen JJ, Langerak AW, Bruggemann M, Evans PA, Hummel M, Lavender FL *et al.* Design and standardization of PCR primers and protocols for detection of clonal immunoglobulin and T-cell receptor gene recombinations in suspect lymphoproliferations: report of the BIOMED-2 Concerted Action BMH4-CT98-3936. *Leukemia* 2003; **17**: 2257–2317.
267 Greer JP, Mosse CA. Natural killer-cell neoplasms. *Curr Hematol Malig Rep* 2009; **4**: 245–252.
268 Matsubara A, Matsumoto M, Takada K, Hato T, Hasegawa H, Tamai T *et al.* Acute transformation of chronic large granular lymphocyte leukemia into an aggressive form associated with preferential organ involvement. *Acta Haematol* 1994; **91**: 206–210.
269 Ohno Y, Amakawa R, Fukuhara S, Huang CR, Kamesaki H, Amano H *et al.* Acute transformation of chronic large granular lymphocyte leukemia associated with additional chromosome abnormality. *Cancer* 1989; **64**: 63–67.
270 Oshimi K. Progress in understanding and managing natural killer-cell malignancies. *Br J Haematol* 2007; **139**: 532–544.
271 Lima M, Almeida J, Teixeira MA, Queiros ML, Justica B, Orfao A. The "ex vivo" patterns of CD2/CD7, CD57/CD11c, CD38/CD11b, CD45RA/CD45RO, and CD11a/HLA-DR expression identify acute/early and chronic/late NK-cell activation states. *Blood Cell Mol Dis* 2002; **28**: 181–190.
272 Lim MS, de Leval L, Quintanilla-Martinez L. Commentary on the 2008 WHO classification of mature T- and NK-cell neoplasms. *J Hematop* 2009; **2**: 65–73.
273 Fischer L, Hummel M, Burmeister T, Schwartz S, Thiel E. Skewed expression of natural-killer (NK)-associated antigens on lymphoproliferations of large granular lymphocytes (LGL). *Hematol Oncol* 2006; **24**: 78–85.
274 Epling-Burnette PK, Painter JS, Chaurasia P, Bai F, Wei S, Djeu JY *et al.* Dysregulated NK receptor expression in patients with lymphoproliferative disease of granular lymphocytes. *Blood* 2004; **103**: 3431–3439.
275 Zambello R, Semenzato G. Natural killer receptors in patients with lymphoproliferative diseases of granular lymphocytes. *Semin Hematol* 2003; **40**: 201–212.
276 Zambello R, Falco M, Della Chiesa M, Trentin L, Carollo D, Castriconi R *et al.* Expression and function of KIR and natural cytotoxicity receptors in NK-type lymphoproliferative diseases of granular lymphocytes. *Blood* 2003; **102**: 1797–1805.
277 Pascal V, Schleinitz N, Brunet C, Ravet S, Bonnet E, Lafarge X *et al.* Comparative analysis of NK cell subset distribution in normal and lymphoproliferative disease of granular lymphocyte conditions. *Eur J Immunol* 2004; **34**: 2930–2940.
278 Kopp P, Jaggi R, Tobler A, Borisch B, Oestreicher M, Sabacan L *et al.* Clonal X-inactivation analysis of human tumours using the human androgen receptor gene (HUMARA) polymorphism: a non-radioactive and semi-quantitative strategy applicable to fresh and archival tissue. *Mol Cell Probes* 1997; **11**: 217–228.
279 Boudewijns M, van Dongen JJ, Langerak AW. The human androgen receptor X-chromosome inactivation assay for clonality diagnostics of natural killer cell proliferations. *J Mol Diagn* 2007; **9**: 337–344.
280 Gattazzo C, Teramo A, Miorin M, Scquizzato E, Cabrelle A, Balsamo M *et al.* Lack of expression of inhibitory KIR3DL1 receptor in patients with natural killer cell-type lymphoproliferative disease of granular lymphocytes. *Haematologica* 2010; **95**: 1722–1729.
281 Orfao A, Lopez A, Flores J, Almeida J, Vidriales B, Perez J *et al.* Diagnosis of haematological malignancies: new applications for flow cytometry. *Hematol J (Eur Hematol Assoc Educ Prog)* 2006; **2**: 6–13.
282 Borowitz MJ, Bray R, Gascoyne R, Melnick S, Parker JW, Picker L *et al.* U.S.-Canadian Consensus recommendations on the immunophenotypic analysis of hematologic neoplasia by flow cytometry: data analysis and interpretation. *Cytometry* 1997; **30**: 236–244.
283 Bene MC, Bernier M, Castoldi G, Faure GC, Knapp W, Ludwig WD *et al.* Impact of immunophenotyping on management of acute leukemias. *Haematologica* 1999; **84**: 1024–1034.
284 Greig B, Oldaker T, Warzynski M, Wood B 2006Bethesda International Consensus recommendations on the immunophenotypic analysis of hematolymphoid neoplasia by flow cytometry: recommendations for training and education to perform clinical flow cytometry. *Cytometry B Clin Cytom 2007;* ***72*** **Suppl 1**: S23–S33.
285 Jaffe ES. *Pathology and Genetics of Tumours of Haematopoietic and Lymphoid Tissues*. IARC Press: Oxford, Oxford University Press: Lyon, 2001; 351p.
286 San Miguel JF, Vidriales MB, Ocio E, Mateo G, Sanchez-Guijo F, Sanchez ML *et al.* Immunophenotypic analysis of Waldenstrom's macroglobulinemia. *Semin Oncol* 2003; **30**: 187–195.
287 Coustan-Smith E, Sandlund JT, Perkins SL, Chen H, Chang M, Abromowitch M *et al.* Minimal disseminated disease in childhood T-cell lymphoblastic lymphoma: a report from the children's oncology group. *J Clin Oncol* 2009; **27**: 3533–3539.
288 Stark B, Avigad S, Luria D, Manor S, Reshef-Ronen T, Avrahami G *et al.* Bone marrow minimal disseminated disease (MDD) and minimal residual disease (MRD) in childhood T-cell lymphoblastic lymphoma stage III, detected by flow cytometry (FC) and real-time quantitative polymerase chain reaction (RQ-PCR). *Pediatr Blood Cancer* 2009; **52**: 20–25.
289 Bisset LR, Lung TL, Kaelin M, Ludwig E, Dubs RW. Reference values for peripheral blood lymphocyte phenotypes applicable to the healthy adult population in Switzerland. *Eur J Haematol* 2004; **72**: 203–212.
290 Langerak AW, van Den Beemd R, Wolvers-Tettero IL, Boor PP, van Lochem EG, Hooijkaas H *et al.* Molecular and flow cytometric analysis of the Vbeta repertoire for clonality assessment in mature TCRalphabeta T-cell proliferations. *Blood* 2001; **98**: 165–173.
291 van den Beemd R, Boor PP, van Lochem EG, Hop WC, Langerak AW, Wolvers-Tettero IL *et al.* Flow cytometric analysis of the Vbeta repertoire in healthy controls. *Cytometry* 2000; **40**: 336–345.
292 Lima M, Almeida J, Santos AH, Teixeira MA, Alguero MC, Queiros ML *et al.* Immunophenotypic analysis of the TCR-Vbeta repertoire in 98 persistent expansions of CD3(+)/TCR-alphabeta(+) large granular lymphocytes: utility in assessing clonality and insights into the pathogenesis of the disease. *Am J Pathol* 2001; **159**: 1861–1868.
293 Morice WG, Kimlinger T, Katzmann JA, Lust JA, Heimgartner PJ, Halling KC *et al.* Flow cytometric assessment of TCR-Vbeta expression in the evaluation of peripheral blood involvement by T-cell lymphoproliferative disorders: a comparison with conventional T-cell immunophenotyping and molecular genetic techniques. *Am J Clin Pathol* 2004; **121**: 373–383.
294 Feng B, Jorgensen JL, Hu Y, Medeiros LJ, Wang SA. TCR-Vbeta flow cytometric analysis of peripheral blood for assessing clonality and disease burden in patients with T cell large granular lymphocyte leukaemia. *J Clin Pathol* 2010; **63**: 141–146.
295 Sandberg Y, Almeida J, Gonzalez M, Lima M, Barcena P, Szczepanski T *et al.* TCRgammadelta+ large granular lymphocyte leukemias reflect the spectrum of normal antigen-selected TCRgammadelta+ T-cells. *Leukemia* 2006; **20**: 505–513.
296 Matarraz S, Lopez A, Barrena S, Fernandez C, Jensen E, Flores-Montero J *et al.* Bone marrow cells from myelodysplastic syndromes show altered immunophenotypic profiles that may contribute to the diagnosis and prognostic stratification of the disease: a pilot study on a series of 56 patients. *Cytometry B Clin Cytom* 2010; **78**: 154–168.
297 Rawstron AC, Villamor N, Ritgen M, Bottcher S, Ghia P, Zehnder JL *et al.* International standardized approach for flow cytometric residual disease monitoring in chronic lymphocytic leukaemia. *Leukemia* 2007; **21**: 956–964.

APPENDIX

(Please check EuroFlow website www.euroflow.org for updates)

Table A1. Composition of ALOT and technical information on reagents.

	PacB	*PacO*	*FITC*	*PE*	*PerCPCy5.5*	*PECy7*	*APC*	*APCH7*
	CyCD3	CD45	CyMPO	CyCD79a	CD34	CD19	CD7	SmCD3

Marker	*Fluorochrome*	*Clone*	*Source*	*Catalogue number*	*(μl/test)*
CyCD3	PacB	UCHT1	BD Biosciences	558117	7
SmCD3	APCH7	SK7	BD Biosciences	641397	3
CD7	APC	124-1D1	eBioscience	17-0079-42	2
CD19	PECy7	J3-119	Beckman Coulter	IM3628	5
CD34	PerCPCy5.5	8G12	BD Biosciences	347222	7
CD45	PacO	HI30	Invitrogen	MHCD4530	5
CyCD79a	PE	HM57	Dako	R7159	5
CyMPO	FITC	MPO-7	Dako	F0714	3

Table A2. Composition of LST and technical information on reagents

	PacB	*PacO*	*FITC*	*PE*	*PerCPCy5.5*	*PECy7*	*APC*	*APCH7*
	CD20 and CD4	CD45	CD8 and SmIgλ	CD56 and SmIgκ	CD5	CD19 and TCRγδ	SmCD3	CD38

Marker	*Fluorochrome*	*Clone*	*Source*	*Catalogue number*	*(μl/test)*
SmCD3	APC	SK7	BD Biosciences	345767	2.5
CD4	PacB	RPA-T4	BioLegend	300521	0.5
CD5	PerCPCy5.5	L17F12	BD Biosciences	341109	15
CD8	FITC	UCH-T4	Cytognos	CYT-SLPC-50	Part of LST mixture (20)
CD19	PECy7	J3-119	Beckman Coulter	IM3628	5
CD20	PacB	2H7	BioLegend	302320	1
CD38	APCH7	HB7	BD Biosciences	646786	3
CD45	PacO	HI30	Invitrogen	MHCD4530	5
CD56	PE	C5.9	Cytognos	CYT-SLPC-50	Part of LST mixture (20)
SmIgκ	PE	polyclonal	Cytognos	CYT-SLPC-50	Part of LST mixture (20)
SmIgλ	FITC	polyclonal	Cytognos	CYT-SLPC-50	Part of LST mixture (20)
TCRγδ	PECy7	11F2	BD Biosciences	649806	1

Table A3. Composition of SST and technical information on reagents

	PacB	*PacO*	*FITC*	*PE*	*PerCPCy5.5*	*PECy7*	*APC*	*APCH7*
	CD20	CD45	CD8 and SmIgλ	CD56 and SmIgκ	CD4	CD19	SmCD3 and CD14	CD38

Marker	*Fluorochrome*	*Clone*	*Source*	*Catalogue number*	*(μl/test)*
SmCD3	APC	SK7	BD Biosciences	345767	2.5
CD4	PerCPCy5.5	SK3	Cytognos	CYT-SLPC4-50	Part of SST mixture (20)
CD8	FITC	UCH-T4	Cytognos	CYT-SLPC4-50	Part of SST mixture (20)
CD14	APC	MφP9	BD Biosciences	345787	5
CD19	PECy7	J3-119	Beckman Coulter	IM3628	5
CD20	PacB	2H7	BioLegend	302320	1
CD38	APCH7	HB7	BD Biosciences	646786	3
CD45	PacO	HI30	Invitrogen	MHCD4530	5
CD56	PE	C5.9	Cytognos	CYT-SLPC4-50	Part of SST mixture (20)
SmIgκ	PE	polyclonal	Cytognos	CYT-SLPC4-50	Part of SST mixture (20)
SmIgλ	FITC	polyclonal	Cytognos	CYT-SLPC4-50	Part of SST mixture (20)

Table A4. Composition of PCD and technical information on reagents

Tube	*PacB*	*PacO*	*FITC*	*PE*	*PerCPCy5.5*	*PECy7*	*APC*	*APCH7*
1	CD45	CD138	CD38	CD56	β2micro	CD19	Cylgκ	Cylgλ
2	CD45	CD138	CD38	CD28	CD27	CD19	CD117	CD81

Marker	*Fluorochrome*	*Clone*	*Source*	*Catalogue number*	*(μl/test)*	
CD19	PECy7	J3-119	Beckman Coulter	IM3628	5	
CD27	PerCPCy5.5	L128	BD Biosciences	649805	10	
CD28	PE	L293	BD Biosciences	348047	20	
CD38	FITC	LD38	Cytognos	CYT-38F	3	5[a]
CD38	Pure	LD38	Cytognos	CYT-38P1	2	
CD45	PacB	T29/33	Dako	PB986	5	
CD56	PE	C5.9	Cytognos	CYT-56PE	5	
CD81	APCH7	JS-81	BD Biosciences	646791	5	
CD117	APC	104D2	BD Biosciences	333233	5	
CD138	PacO	B-A38	Exbio	PO-520	4	
β2micro	PerCPCy5.5	Tü99	BD Biosciences	646781	4.75	5[a]
β2micro	Pure	Tü99	BD Biosciences	555550	0.25	
Cylgκ	APC	Polyclonal rabbit serum	Dako	C0222	2.5	
Cylgλ	APCH7	1-155-2	BD Biosciences	646792	4	

[a]Mixture of fluorochrome-conjugated and -unconjugated antibodies is used to reduce signal intensity, while retaining saturating conditions to avoid unpredictable variation in staining patterns. The 19:1 ratio for the two β2micro antibodies is caused by the five fold higher antibody concentration of the unconjugated antibody.

Table A5. Composition of BCP-ALL panel and technical information on reagents

Tube	*PacB*	*PacO*	*FITC*	*PE*	*PerCPCy5.5*	*PECy7*	*APC*	*APCH7*
1	CD20	CD45	CD58	CD66c	CD34	CD19	CD10	CD38
2	SmIgκ	CD45	Cylgμ	CD33	CD34	CD19	SmIgM and CD117	Smlgλ
3	CD9	CD45	NuTdT	CD13	CD34	CD19	CD22	CD24
4	CD21	CD45	CD15 and CD65	NG2	CD34	CD19	CD123	CD81

Marker	*Fluorochrome*	*Clone*	*Source*	*Catalogue number*	*(μl/test)*
CD9	PacB	MEM-61	Exbio	PB-208-T100	4
CD10	APC	HI10A	BD Biosciences	332777	5
CD13	PE	L138	BD Biosciences	347406	7
CD15	FITC	MMA	BD Biosciences	332778	10
CD19	PECy7	J3-119	Beckman Coulter	IM3628	5
CD20	PacB	2H7	Biolegend	302320	1
CD21	PacB	LT21	Exbio	PB-306-T100	4
CD22	APC	S-HCL-1	BD Biosciences	333145	5
CD24	APCH7	ML5	BD Biosciences	646785	5
CD33	PE	P67.6	BD Biosciences	345799	5
CD34	PerCPCy5.5	8G12	BD Biosciences	347222	7
CD38	APCH7	HB7	BD Biosciences	646786	3
CD45	PacO	HI30	Invitrogen	MHCD4530	5
CD58	FITC	1C3	BD Biosciences	555920	7
CD65	FITC	88H7	Beckman Coulter	IM1654U	7
CD66c	PE	KOR-SA3544	Beckman Coulter	IM2357U	10
CD81	APCH7	JS-81	BD Biosciences	646791	5
CD117	APC	104D2	BD Biosciences	333233	5
CD123	APC	AC145	Miltenyi Biotec	130-090-901	7
Cylgμ	FITC	Polyclonal rabbit serum	Dako	F0058	10
NG2	PE	7.1	Beckman Coulter	IM3454U	10
SmIgκ	PacB	A8B5	Exbio	PB-504-T100	4
Smlgλ	APCH7	1-155-2	BD Biosciences	646792	4
SmIgM	APC	G20-127	BD Biosciences	551062	10
NuTdT	FITC	HT-6	Dako	F7139	10

Table A6. Composition of T-ALL panel and technical information on reagents

Tube	*PacB*	*PacO*	*FITC*	*PE*	*PerCPCy5.5*	*PECy7*	*APC*	*APCH7*
1	CyCD3	CD45	NuTdT	CD99	CD5	CD10	CD1a	SmCD3
2	CyCD3	CD45	CD2	CD117	CD4	CD8	CD7	SmCD3
3	CyCD3	CD45	TCR$\gamma\delta$	TCR$\alpha\beta$	CD33	CD56	CyTCRβ	SmCD3
4	CyCD3	CD45	CD44	CD13	HLADR	CD45RA	CD123	SmCD3

Marker	*Fluorochrome*	*Clone*	*Source*	*Catalogue number*	*(μl/test)*
CD1a	APC	HI149	BD Biosciences	559775	5
CD2	FITC	RPA-2.10	BD Biosciences	555326	5
CyCD3	PacB	UCHT1	BD Biosciences	558117	7
SmCD3	APCH7	SK7	BD Biosciences	641397	3
CD4	PerCPCy5.5	SK3	BD Biosciences	332772	7
CD5	PerCPCy5.5	L17F12	BD Biosciences	341109	15
CD7	APC	124-1D1	eBioscience	17-0079-42	2
CD8	PECy7	SFCI21Thy2D3	Beckman Coulter	737661	5
CD10	PECy7	HI10A	BD Biosciences	341112	5
CD13	PE	L138	BD Biosciences	347406	7
CD33	PerCPCy5.5	P67.6	BD Biosciences	333146	10
CD44	FITC	L178	BD Biosciences	347943	7
CD45	PacO	HI30	Invitrogen	MHCD4530	5
CD45RA	PECy7	L48	BD Biosciences	337186	5
CD56	PECy7	N901	Beckman Coulter	A21692	5
CD99	PE	Tü12	BD Biosciences	555689	5
CD117	PE	104D2	BD Biosciences	332785	5
CD123	APC	AC145	Miltenyi Biotec	130-090-901	7
HLADR	PerCPCy5.5	L243	BD Biosciences	552764	10
TCR$\alpha\beta$	PE	IP26A	Beckman Coulter	A39499	7
CyTCRβ	APC	8A3 (βF1)	Cytognos	CYT-BF1AP	3
TCR$\gamma\delta$	FITC	IMMU510	Beckman Coulter	IM1571U	10
NuTdT	FITC	HT-6	Dako	F7139	10

Table A7. Composition of AML/MDS panel and technical information on reagents

Tube	*PacB*	*PacO*	*FITC*	*PE*	*PerCPCy5.5*	*PECy7*	*APC*	*APCH7*
1	HLADR	CD45	CD16	CD13	CD34	CD117	CD11b	CD10
2	HLADR	CD45	CD35	CD64	CD34	CD117	CD300e	CD14
3	HLADR	CD45	CD36	CD105	CD34	CD117	CD33	CD71
4	HLADR	CD45	NuTdT	CD56	CD34	CD117	CD7	CD19
5	HLADR	CD45	CD15	NG2	CD34	CD117	CD22	CD38
6	HLADR	CD45	CD42a and CD61	CD203c	CD34	CD117	CD123	CD4
7	HLADR	CD45	CD41	CD25	CD34	CD117	CD42b	CD9

Marker	*Fluorochrome*	*Clone*	*Source*	*Catalogue number*	*(μl/test)*
CD4	APCH7	SK3	BD Biosciences	641398	5
CD7	APC	124-1D1	eBioscience	17-0079-42	2
CD9	APCH7	M-L13	BD Biosciences	646782	5
CD10	APCH7	HI10A	BD Biosciences	646783	5
CD11b	APC	D12	BD Biosciences	333143	5
CD13	PE	L138	BD Biosciences	347406	7
CD14	APCH7	MφP9	BD Biosciences	641394	5
CD15	FITC	MMA	BD Biosciences	332778	10
CD16	FITC	CLB FcR gran/1, 5D2	Sanquin	M1604	20
CD19	APCH7	SJ25C1	BD Biosciences	641395	5
CD22	APC	S-HCL-1	BD Biosciences	333145	5
CD25	PE	2A3	BD Biosciences	341011	10
CD33	APC	P67.6	BD Biosciences	345800	10
CD34	PerCPCy5.5	8G12	BD Biosciences	347222	5
CD35	FITC	E11	BD Biosciences	555452	5
CD36	FITC	CLB-IVC7	Sanquin	M1613	5
CD38	APCH7	HB7	BD Biosciences	646786	3
CD41	FITC	CLB-tromb/7, 6C9	Sanquin	M1674	1
CD42a	FITC	GRP-P	Serotec	MCA1227F	1
CD42b	APC	HIP1	BD Biosciences	551061	1
CD45	PacO	HI30	Invitrogen	MHCD4530	5
CD56	PE	C5.9	Cytognos	CYT-56PE	5
CD61	FITC	RUU-PL7F12	BD Biosciences	347407	4
CD64	PE	10.1	Serotec	MCA756PE	10
CD71	APCH7	M-A712	BD Biosciences	646789	5
CD105	PE	1G2	Beckman Coulter	A07414	10
CD117	PECy7	104D2D1	Beckman Coulter	IM3698	5
CD123	APC	AC145	Miltenyi Biotec	130-090-901	10
CD203c	PE	97A6	Beckman Coulter	IM3575	10
CD300e	APC	UP-H2	Immunostep	IREM2A-T100	5
HLADR	PacB	L243	Biolegend	307624	1 (1:5 dilution)
NG2	PE	7.1	Beckman Coulter	IM3454U	10
NuTdT	FITC	HT-6	Dako	F7139	10

Table A8. Composition of B-CLPD panel and technical information on reagents

Tube	*PacB*	*PacO*	*FITC*	*PE*	*PerCPCy5.5*	*PECy7*	*APC*	*APCH7*
1	CD20 and CD4	CD45	CD8 and Igλ	CD56 and Igκ	CD5	CD19 and TCRγδ	SmCD3	CD38
2	CD20	CD45	CD23	CD10	CD79b	CD19	CD200	CD43
3	CD20	CD45	CD31	CD305	CD11c	CD19	SmIgM	CD81
4	CD20	CD45	CD103	CD95	CD22	CD19	CD185	CD49d
5	CD20	CD45	CD62L	CD39	HLADR	CD19	CD27	

Marker	*Fluorochrome*	*Clone*	*Source*	*Catalogue number*	*(μl/test)*
SmCD3	APC	SK7	BD Biosciences	345767	2.5
CD4	PacB	RPA-T4	BioLegend	300521	0.5
CD5	PerCPCy5.5	L17F12	BD Biosciences	341109	15
CD8	FITC	UCH-T4	Cytognos	CYT-SLPC-50	Part of LST mixture (20)
CD10	PE	ALB1	Beckman Coulter	A07760	20
CD11c	PerCPCy5.5	B-Ly6	BD Biosciences	646784	5
CD19	PECy7	J3-119	Beckman Coulter	IM3628	5
CD20	PacB	2H7	BioLegend	302320	1
CD22	PerCPCy5.5	S-HCL-1	BD Biosciences	649804	2
CD23	FITC	MHM6	Dako	F7062	2.5
CD27	APC	L128	BD Biosciences	337169	2.5
CD31	FITC	WM59	BD Biosciences	555445	10
CD38	APCH7	HB7	BD Biosciences	646786	3
CD39	PE	TÜ66	BD Biosciences	555464	10
CD43	APCH7	IG10	BD Biosciences	646787	5
CD45	PacO	HI30	Invitrogen	MHCD4530	5
CD49d	APCH7	9F10	BD Biosciences	646788	2
CD56	PE	C5.9	Cytognos	CYT-SLPC-50	Part of LST mixture (20)
CD62L	FITC	SK11	BD Biosciences	347443	2.5
CD79b	PerCPCy5.5	SN8	BD Biosciences	646790	5
CD81	APCH7	JS-81	BD Biosciences	646791	5
CD95	PE	DX2	BD Biosciences	555674	20
CD103	FITC	Ber-ACT8	BD Biosciences	333155	2
CD185	APC	51505	R&D Systems	FAB190A	10
CD200	APC	OX104	eBioscience	17-9200	1.25
CD305	PE	DX26	BD Biosciences	550811	10
HLADR	PerCPCy5.5	L243	BD Biosciences	552764	10
SmIgκ	PE	Polyclonal	Cytognos	CYT-SLPC-50	Part of LST mixture (20)
SmIgλ	FITC	Polyclonal	Cytognos	CYT-SLPC-50	Part of LST mixture (20)
SmIgM	APC	G20-127	BD Biosciences	551062	10
TCRγδ	PECy7	11F2	BD Biosciences	649806	1

Table A9. Composition of T-CLPD panel and technical information on reagents

Tube	*PacB*	*PacO*	*FITC*	*PE*	*PerCPCy5.5*	*PECy7*	*APC*	*APCH7*
1	CD4	CD45	CD7	CD26	SmCD3	CD2	CD28	CD8
2	CD4	CD45	CD27	CD197	SmCD3	CD45RO	CD45RA	CD8
3	CD4	CD45	CD5	CD25	SmCD3	HLADR	CyTcl1	CD8
4	CD4	CD45	CD57	CD30	SmCD3		CD11c	CD8
5	CD4	CD45	CyPerforin	CyGranzyme B	SmCD3	CD16	CD94	CD8
6	CD4	CD45		CD279	SmCD3			CD8

Marker	*Fluorochrome*	*Clone*	*Source*	*Catalogue number*	*(μl/test)*
CD2	PECy7	S5.2	BD Biosciences	335821	2
SmCD3	PerCPCy5.5	SK7	BD Biosciences	332771	10
CD4	PacB	RPA-T4	BioLegend	300521	0.5
CD5	FITC	L17F12	BD Biosciences	345781	10
CD7	FITC	4H9	BD Biosciences	347483	10
CD8	APCH7	SK1	BD Biosciences	641400	5
CD11c	APC	S-HCL-3	BD Biosciences	333144	2
CD16	PECy7	3G8	BD Biosciences	557744	2
CD25	PE	2A3	BD Biosciences	341011	10
CD26	PE	L272	BD Biosciences	340423	10
CD27	FITC	L128	BD Biosciences	340424	10
CD28	APC	CD28.2	BD Biosciences	559770	10
CD30	PE	BerH8	BD Biosciences	550041	10
CD45	PacO	HI30	Invitrogen	MHCD4530	5
CD45RA	APC	HI100	BD Biosciences	550855	10
CD45RO	PECy7	UCHL1	BD Biosciences	337168	2
CD57	FITC	HNK-1	BD Biosciences	333169	10
CD94	APC	HP-3D9	BD Biosciences	559876	5
CD197	PE	3D12	eBioscience	12-1979	10
CD279	PE	MIH4	BD Biosciences	557946	20
CyGranzyme B	PE	CLB-GB11	Sanquin	M2289	15
CyPerforin	FITC	δG9	BD Biosciences	556577	10
CyTCL1	APC	eBio1-21	eBioscience	17-6699	2
HLADR	PECy7	L243	BD Biosciences	335830	2.5

Table A10. Composition of NK-CLPD panel and technical information on reagents

Tube	*PacB*	*PacO*	*FITC*	*PE*	*PerCPCy5.5*	*PECy7*	*APC*	*APCH7*
1	CD2	CD45	CD7	CD26	SmCD3	CD56	CD5	CD19
2	CD16	CD45	CD57	CD25	SmCD3	CD56	CD11c	CD19
3	HLADR	CD45	CyPerforin	CyGranzyme B	SmCD3	CD56	CD94	CD19

Marker	*Fluorochrome*	*Clone*	*Source*	*Catalogue number*	*(μl/test)*
CD2	PacB	TS1/8	Biolegend	309216	1
SmCD3	PerCPCy5.5	SK7	BD Biosciences	332771	10
CD5	APC	L17F12	BD Biosciences	345783	2.5
CD7	FITC	4H9	BD Biosciences	347483	10
CD11c	APC	S-HCL-3	BD Biosciences	333144	2
CD16	PacB	3G8	Biolegend	302032	5
CD19	APCH7	SJ25C1	BD Biosciences	641395	5
CD25	PE	2A3	BD Biosciences	341011	10
CD26	PE	L272	BD Biosciences	340423	10
CD45	PacO	HI30	Invitrogen	MHCD4530	5
CD56	PECy7	N901	Beckman Coulter	A21692	5
CD57	FITC	HNK-1	BD Biosciences	333169	10
CD94	APC	HP-3D9	BD Biosciences	559876	5
CyGranzyme B	PE	CLB-GB11	Sanquin	M2289	15
CyPerforin	FITC	δG9	BD Biosciences	556577	10
HLADR	PacB	L243	Biolegend	307624	1 (1:5 dilution)

Supplementary Information accompanies the paper on the Leukemia website (http://www.nature.com/leu)

IV. DISCUSIÓN.

El inmunofenotipo es una herramienta esencial en el diagnóstico y clasificación de las hemopatías malignas, siendo de todas las técnicas de inmunofenotipado disponibles, la citometría de flujo multiparamétrica la de mayor proyección[1,2,5-8,22,130,132-140,284]. A pesar de que se trata de una técnica rápida, basada en mediciones cuantitativas de gran objetividad y de que su utilización sea relativamente sencilla y esté ampliamente disponible en todo el mundo, en la actualidad se considera que el inmunofenotipo por CMF, tiene también importantes limitaciones[9]. De todas ellas, la más relevante tiene que ver con la complejidad generada por el incremento progresivo del número de marcadores estudiados, especialmente cuando estos son analizados simultáneamente y la interpretación de los resultados se basa en la visualización de imágenes bi-dimensionales con la intervención de un experto, lo que hace de la técnica un proceso laborioso y costoso, a la vez que relativamente subjetivo[11,12]. A todo lo anterior, se suma la gran variabilidad en las técnicas, los equipos y los paneles de anticuerpos y reactivos utilizados en diferentes laboratorios que han dado lugar a casi tantas estrategias y paneles diferentes, como laboratorios de citometría existen[7,13-28,30,31,33-35,37,101,102]. Este componente de subjetividad, unido a la diversidad metodológica antes referida, han limitado seriamente la reproducibilidad y estandarización diagnóstica del inmunofenotipado por citometría de flujo, condicionando en parte también su utilidad clínica.

Ante estos antecedentes, resulta fácil entender la existencia de una necesidad creciente de estandarización en la aplicación de la citometría clínica al diagnóstico y clasificación de hemopatías. No obstante, aunque se han multiplicado los esfuerzos realizados con tal fin[4,7,11,22,35,89,110-112,114,117,138,147,149,170,171,285,286] estos solo han tenido un éxito parcial; debido sobre todo a que dichos esfuerzos se han centrado exclusivamente en una pequeña parte (y no en el conjunto) de todo el proceso. Además, de forma casi sistemática, las recomendaciones propuestas son el producto de "consensos" entre expertos que no han sido validados prospectivamente de modo a poder demostrar su impacto sobre todo el proceso. Así, a modo de ejemplo, la mayoría de recomendaciones propuestas hasta la fecha se centran de forma casi

exclusiva en los paneles de marcadores, proponiendo listas de marcadores informativos, sin llegar a especificar los clones de referencia, los conjugados con fluorocromos recomendados, o las combinaciones más apropiadas en que deben incluirse dichos marcadores. Más aún, con frecuencia, las recomendaciones realizadas se centran de forma exclusiva en un grupo (o unos pocos grupos) de enfermedades y/o líneas celulares, sin que estén realmente dirigidas a responder a las indicaciones médicas que conducen a la aplicación de las técnicas de inmunofenotipado, particularmente en lo que se refiere a las etapas iniciales de rastreo diagnóstico de hemopatías malignas.

En el presente trabajo doctoral, englobado dentro de los objetivos del grupo EuroFlow de diseñar, construir y validar procedimientos y paneles de combinaciones de anticuerpos de 8-colores para el diagnóstico y clasificación de leucemias y linfomas, se tomaron en consideración todos los aspectos técnicos relacionados con la metodología a aplicar, además de proponer paneles de anticuerpos basados en reactivos de referencia comercialmente disponibles en el momento de cerrar el presente trabajo, para el diagnóstico y clasificación de SLPC.

Estandarización de los protocolos para la puesta a punto y calibración de citómetros de flujo e inmunofenotipado según la estrategia EuroFlow.

De acuerdo con lo anteriormente expuesto, en la primera parte del trabajo nos centramos en la estandarización de los aspectos técnicos. En este ámbito, nuestro primer objetivo se centró en la selección de los fluorocromos más adecuados para ser combinados en 8-colores, en un formato compatible con los citómetros de flujo disponibles para inmunofenotipado multicolor en el laboratorio clínico. La posibilidad de usar un número progresivamente mayor de fluorocromos simultáneamente, se asocia con un incremento significativo y exponencial de la información obtenida a partir de una única combinación de anticuerpos conjugados con dichos fluorocromos[12,46,79]. Al aumentar el número de fluorocromos, aumenta también de forma exponencial el número de posibilidades de combinaciones de marcadores, además de la

cantidad y complejidad de la información generada, haciendo imposible predecir la idoneidad de las diferentes combinaciones de reactivos que pueden generar. Por todo ello, resulta necesario seleccionar las combinaciones más apropiadas de reactivos individuales de calidad y de amplia disponibilidad, y posteriormente evaluar prospectivamente dichas combinaciones. En el presente trabajo, una proporción importante de los fluorocromos se pre-seleccionaron ya, en base al conocimiento existente, su probada utilidad, amplia disponibilidad y, su compatibilidad con la configuración óptica de los equipos existentes. Para la selección de los demás fluorocromos, se llevó a cabo una evaluación en la que se compararon las mejores opciones disponibles en el momento de realizar dicha selección. La combinación final, incluye el uso de PacB, PacO, FITC, PE, PerCP-Cy5.5, PE-Cy7, APC y APC-H7. Aunque en general, en el proceso de validación, los fluorocromos seleccionados, mostraron un comportamiento satisfactorio, algunos de ellos a nivel individual (i.e., APC-H7) siguen siendo susceptibles de mejora en el futuro. Por otra parte, para algunas posiciones existía posibles alternativas disponibles ya en el momento de la evaluación (o que aparecieron posteriormente en el tiempo) como HV450 (en vez de PacB) o HV500 (como sustituto de PacO), al mostrar estos nuevos fluorocromos un comportamiento equivalente o incluso ligeramente mejor que los fluorocromos de referencia, superior, no obstante, la menor disponibilidad de conjugados comerciales desaconsejaron su recomendación como fluorocromos de referencia. Aun así, esto les convierte en potenciales sustitutos de los fluorocromos PacB y PacO, siempre y cuando su evaluación reactivo a reactivo muestre un impacto despreciable en los resultados obtenidos con los conjugados correspondientes de los fluorocromos de referencia PacB y PacO. Para otras posiciones, aunque se evaluaron las alternativas disponibles, estas mostraron un comportamiento subóptimo (o se disponía solo de un número limitado de anticuerpos conjugados con los mismos), lo que contraindicaba su inclusión en las combinaciones de fluorocromos propuestos.

Otro de los aspectos técnicos clave a la hora de estandarizar las técnicas de inmunofenotipado, lo constituye el diseño de protocolos estándar para definir y monitorizar la calibración del equipo de medida. Así, en una segunda fase, este trabajo diseñamos un procedimiento para la calibración de citómetros de flujo de 8-colores disponibles en ese momento. En ese procedimiento proponemos el uso como estándar común, de una partícula con señal intensa en cada canal de fluorescencia del equipo de citometría, en cada uno de los citómetros de flujo evaluados en este trabajo, dicha partícula debía posicionarse en un mismo canal de fluorescencia diana, con la garantía de que en ese punto todos los equipos funcionaban en condiciones óptimas, por encima del nivel del ruido electrónico de fondo generado en cada uno de sus detectores de fluorescencia. Con ello se reduce significativamente el impacto asociado a pequeñas diferencias entre los distintos equipos (e.g., en la potencia de los láseres, las características o desgaste de los filtros y/o diferencias de alineamiento y de las características de "hardware"). Así mismo, proponemos el empleo de linfocitos de SP de forma a estandarizar también, la calibración (óptima) de los detectores de luz dispersada.

En términos generales, mientras que los protocolos de calibración automatizados por el fabricante de citómetros de flujo favorecen una mayor sensibilidad a la hora de detectar señales débiles, respecto al protocolo propuesto aquí, este último permite un mayor rango de medición, facilitando poder medir simultáneamente señales débiles y marcadores de (muy) alta expresión presentes en algunas de las poblaciones celulares estudiadas (e.g. CD38 en CP). Además, aunque ambas aproximaciones resultan en un ajuste óptimo (según el criterio aplicado) de los detectores de fluorescencia, el proceso automatizado del fabricante implica el cálculo diario de los requerimientos de compensación, al introducir ajustes en los voltajes aplicados a dichos detectores aun cuando la variación de los voltajes es mínima (e.g., en un solo detector y/o de ±1 mV). La realización de una compensación de fluorescencias diaria, sería un proceso laborioso, costoso e ineficiente en laboratorios de diagnóstico clínico, además de ser difícilmente justificable en un equipo robusto y de configuración estable en el tiempo. Otra ventaja

importante de nuestra aproximación, residía en que no está ligada a ningún tipo de citómetro en exclusiva, pudiendo usarse, con pequeñas adaptaciones, en citómetros de flujo de diferentes fabricantes (www.EuroFlow.org).

De acuerdo con los datos obtenidos a partir de la evaluación de la estabilidad a largo plazo de las IMF, una vez definidos los canales de fluorescencia diana de los voltajes aplicados para cada detector, definimos como criterio máximo de variabilidad aceptable, una desviación de ±15% respecto a la IMF del canal diana, obtenida con las esferas de referencia del mismo lote; la obtención de resultados fuera de este rango en la monitorización diaria de equipo representaría un criterio de fallo de la calibración establecida. El rigor aplicado con este criterio debe entenderse desde el punto de vista del objetivo final que seguimos: estandarizar el inmunofenotipado de leucemias y linfomas a través de la limitación de la variabilidad técnica, colocándola a niveles inferiores a los de la variabilidad biológica, observada para una misma muestra y entre muestras similares.

Con todo ello, la calibración del equipo siguiendo el protocolo estándar propuesto, mostró una buena correlación con (relativamente) pocas diferencias respecto a los resultados obtenidos con los nuevos procedimientos automatizados establecidos posteriormente por los fabricantes de los equipos y que están ya basados en los protocolos de calibración EuroFlow aquí descritos; todo ello confirma el elevado grado de estandarización alcanzado con dicho procedimiento.

Una vez establecida la calibración del citómetro de flujo y seleccionada la combinación de fluorocromos a emplear en los paneles, cabía establecer un procedimiento estándar para la compensación de fluorescencias. En este sentido, cabe señalar que el uso de una matriz de compensación exacta y óptima constituye un requisito importante a la hora de identificar distintas poblaciones celulares presentes en una muestra en las representaciones bi-paramétricas de cada par de fluorocromos empleados[74,78,82,83]. Entre otros factores, la complejidad del proceso de compensación depende de la combinación correcta de anticuerpos y conjugados de anticuerpos a utilizar[14,78,79,287]. Como cabía esperar, los fluorocromos básicos

demostraron permitir el uso de un TTSA como estándar común a todos los reactivos conjugados con ese mismo fluorocromo; por el contrario, y a excepción del PerCPCy5.5, todos los tándems de fluorocromos requerían de un TTSA para cada uno de los conjugados incluidos en las diferentes combinaciones de anticuerpos seleccionados. Esta diferencia entre los conjugados de PE-Cy7 y APC-H7, respecto a los de PerCP-Cy5.5, posiblemente se deba a que ambos componentes de este último tándem, emiten en una misma zona del espectro de luz[288], zona que además es la seleccionada por el sistema óptico para ser leída en un mismo detector. Cabe señalar sin embargo que, pese a lo anteriormente expuesto, esta regla solo podemos asegurar se cumple, para los marcadores incluidos en esta posición en los diferentes paneles EuroFlow, debiendo validarse otros conjugados de PerCP-Cy5.5 en otras circunstancias/paneles.

Según lo anteriormente expuesto, un experimento de compensación de fluorescencias completo para todos los paneles EuroFlow de combinaciones de anticuerpos implica la preparación y lectura de al menos 30 TTSA distintos, lo cual representa una carga de trabajo significativa para laboratorios clínicos, especialmente para los que tienen una disponibilidad limitada de tiempo. No obstante, la necesidad de realizar un nuevo experimento completo de compensación de fluorescencias, depende del funcionamiento y la estabilidad del citómetro de flujo en el tiempo[14,80]. En este sentido, mediante la aplicación del protocolo de compensación de propuesto comprobamos que en los citómetros de flujo evaluados, la necesidad de realizar un nuevo procedimiento de calibración y compensación de fluorescencias se situaba en líneas generales en intervalos de ±1 mes, periodo durante el cual solo se observaban desviaciones mínimas en los canales diana de fluorescencia para cada detector. No obstante, este periodo de tiempo puede verse acortado por la utilización de marcadores con periodos de caducidad cortos, especialmente en lo que a los fluorocromos en tándem se refiere. En este contexto, resulta especialmente importante la protección adecuada de dichos tándem de fluorocromos frente a factores ambientales que puedan condicionar una degradación prematura de los mismos (como lo son la temperatura o la luz). En resumen, la comparación de las matrices de compensación de

fluorescencias obtenidas a lo largo del tiempo en un mismo equipo de medida y en varios centros en paralelo, mostró que no es necesario realizar un experimento completo de compensación cuando los reactivos y la recolección de la señal por parte de los detectores del citómetro de flujo se mantienen estables. Así mismo, la combinación de los protocolos estandarizados de calibración del citómetro de flujo y de compensación de fluorescencias mostró ser muy eficiente a la hora de contribuir a la estandarización de todo el proceso, especialmente si tenemos en cuenta el grado de reproducibilidad que muestran los resultados obtenidos tras el análisis de ≥ 850 muestras de diferentes tipos, de células normales y patológicas, de múltiples enfermedades y, con origen en diferentes centros medidas a lo largo de más de 6 años de trabajo colectivo.

Existen muchos trabajos en los que se describen diferentes protocolos y se emplean distintos reactivos diferentes para el procesamiento de muestras biológicas humanas[13,20,23-25,170]; en general, todos ellos muestran una estructura similar que incluye: el marcaje de la muestra con anticuerpos monoclonales, uno o más lavados de las muestras teñidas y la eliminación de los hematíes[20,23,25,170]. No obstante lo anterior, son pocos los trabajos en los que se evalúa comparativamente el efecto de cada uno de los diferentes pasos introducidos en el protocolo o las potenciales diferencias existentes entre ellos[20,23-25,289,290]. En este trabajo doctoral realizamos una comparación detallada de los efectos que sobre los resultados obtenidos, tenían diferentes variables involucradas en diferentes protocolos de preparación de muestras para inmunofenotipado de leucemias y linfomas. Con ello hemos podido definir de forma más precisa las mejore condiciones en las que deben realizarse la preparación y marcaje de las muestras para: i) una mejor discriminación entre las poblaciones celulares de SP en base a los parámetros de dispersión de luz, ii) la conservación de los niveles de expresión para los marcadores estudiados, iii) minimizar además las pérdidas celulares, iv) las pérdidas de fluorescencia específicas de fluorocromo o tándem de fluorocromo y, v) mantener bajos los niveles de autofluorescencia basal de las poblaciones celulares presentes en la muestra. El procesamiento

en paralelo de un número importante de muestras con 3 combinaciones de anticuerpos diferentes, combinado con distintas soluciones de lisis, protocolos de lavados y tiempos de adquisición de la muestra, variables todas ellas que afectan los resultados, nos permitió establecer un protocolo optimizado de preparación de muestras para inmunofenotipado de hemopatías malignas. Así, de los diferentes protocolos de marcaje utilizados (i.e., MLL, MLNL y MLLF), de los cuatro tipos diferentes de soluciones de lisis de hematíes aplicadas -una solución de NH_4CL preparada localmente en cada laboratorio y 3 soluciones de lisis comerciales (FACSLysing solution, VersaLyse y QuicLysis)-, y de los cuatro tiempos de adquisición evaluados, podemos concluir que la combinación más eficiente incluía un protocolo de MLL usando FACSLysing solution para la eliminación de los hematíes, seguido de la adquisición inmediata de las muestras una vez finalizado su procesamiento. Es este sentido merece destacar que el seguimiento riguroso de las condiciones definidas en el protocolo final durante las rondas de validación multicéntrica, demostró como con su utilización este contribuye a disminuir la variabilidad en los resultados asociada a la preparación de las muestras. Merece destacar además que en el protocolo propuesto se incluyeron recomendaciones específicas para muestras y/o condiciones de marcaje particulares, como el procesamiento de muestras con escasa celularidad (i.e., LCR) o el marcaje de Igs de superficie en muestras de SP y MO o para marcadores intracelulares.

En los últimos años, mientras que tanto los aspectos técnicos asociados a la citometría de flujo como el conocimiento clínico y biológico sobre las hematopatías malignas han evolucionado a una velocidad relativamente elevada, permitiendo la evaluación simultanea de gran número de parámetros en cada medición, en una cantidad creciente de células[30,31,54], de un número cada vez mayor de subgrupos distintos de hemopatías maligna[1], el análisis y la interpretación de los datos de inmunofenotipado por CMF apenas han sufrido cambios, creando una distancia cada vez mayor entre las estrategias de análisis e interpretación de datos y las herramientas informáticas disponibles y, las necesidades existentes en este campo[12]. Por todo

ello, resulta imprescindible la incorporación de nuevas herramientas informáticas y de estrategias novedosas para el análisis de los datos y la interpretación de los resultados, que incluyan además nuevas representaciones gráficas de datos multidimensionales que permitan visualizar de forma resumida e intuitiva los resultados del inmunofenotipado. Así, la incorporación de las nuevas herramientas informáticas desarrolladas como i) las funciones de fusión de ficheros (apoyada en la estructura de las combinaciones de anticuerpos que incluye marcadores comunes) para la identificación precisa y reproducible en cada alícuota de una muestra de las poblaciones celulares relevantes, ii) la estimación de datos fenotípicos -basada en la identificación del (de los) vecino(s) más próximo(s)-, que permite la asociación de los parámetros medidos para cada célula en diferentes tubos a todas los células similares/equivalentes de cada uno de ellos y, iii) los algoritmos para análisis multivariante de datos (sustentados en estrategias como el análisis de componentes principales) y las correspondientes representaciones gráficas, en el programa informático Infinicyt, han permitido la incorporación de estas nuevas herramientas ya en el proceso de desarrollo y evaluación de los paneles para diagnóstico y clasificación de hemopatías malignas.

El nivel de estandarización alcanzado con la utilización conjunta de los protocolos descritos y las herramientas informáticas desarrolladas, resulta imprescindible, no solo para la comparación de los resultados entre diferentes centros, sino también para garantizar la construcción de ficheros de datos de referencia con información fenotípica sobre un gran número de muestras normales y de pacientes con los subtipos de hematopatías malignas más relevantes[126]. Solo así, podemos utilizar en el futuro estas bases de datos de forma prospectiva en cualquier centro del mundo que aplique los protocolos estandarizados propuestos y descritos en este trabajo, como marco de referencia para la comparación de nuevos casos, estrategia que resulta clave tanto para la estandarización del rastreo diagnóstico de hemopatías (identificación de poblaciones celulares con perfiles inmunofenotípicos diferentes de las poblaciones de referencia normales/reactivas), como para su clasificación y diagnóstico diferencial (perfiles

inmunofenotípicos de casos nuevos que muestran solapamiento con las poblaciones de referencias para diferentes enfermedades/condiciones, y que a la vez son diferentes de otras categorías de enfermedad relacionadas).

Con el objeto de validar todo el proceso, incluidos todos y cada uno de los procedimientos estandarizados descritos anteriormente, nos planteamos como objetivo final de este capítulo del trabajo, realizar una evaluación multicéntrica en la que se recogieron datos de una misma muestra distribuida a cada centro y de un número amplio de muestras de SP normal recopiladas y procesadas localmente en dos momentos diferentes, separados por un periodo relativamente largo de tiempo (i.e., meses). Los resultados de este estudio son los primeros en demostrar que la estandarización técnica en citometría clínica, empleando paneles de 8 fluorocromos distintos, es posible y garantiza la obtención de resultados muy similares en diferentes tiempos, tanto dentro de un mismo centro, como en un conjunto relativamente amplio de centros diferentes. Así, la comparación de los datos obtenidos en los diferentes centros, mostró que las diferencias derivadas del uso de los diferentes equipos de medida evidenciada mediante el cálculo del CV de los canales diana alcanzados con las esferas de calibración de referencia, era muy baja (<5,5%). De manera similar, las diferencias entre las IMF alcanzadas en los diferentes centros para la muestra de SP distribuida a cada uno de ellos, fueron sistemáticamente <44%, valor que coincide con el CV máximo alcanzado para las IMF de las mediciones de las muestra obtenidas de donantes locales. Por otra parte, es importante resaltar que para la mitad de los parámetros evaluados, las diferencias resultaron incluso <17%. Estos resultados demuestran una vez más que, cuando comparada con la heterogeneidad biológica, la variabilidad técnica observada con los protocolos propuestos, es prácticamente irrelevante. En este sentido también y mediante el empleo de las nuevas herramientas y estrategias de análisis desarrolladas, pudimos comprobar que cada población celular identificable de forma específica con la combinación de anticuerpos empleada (i.e., monocitos, linfocitos B y T y sus subpoblaciones principales) en cada centro, se agrupaba claramente en un “clúster” denso y separado de los otros “clústeres”

correspondientes a otras poblaciones celulares distintas, independientemente de la muestra concreta de la que provenía, del centro en el que esta se midió o del momento en el tiempo en que se realizó dicha medición. Estos resultados confirman una vez más, que las diferencias técnicas se minimizaron a niveles despreciables respecto a las diferencias biológicas existentes entre cada población celular analizada, al emplear los protocolos EuroFlow.

Paneles de combinaciones de anticuerpos para rastreo diagnóstico y clasificación de hemopatías malignas.

Para el diseño de los prototipos iniciales de los distintos los paneles de combinaciones de anticuerpos, partimos de la información disponible en la literatura acerca de los marcadores relevantes para el diagnóstico y/o clasificación de cada enfermedad o grupo de enfermedades objeto de estudio, y la experiencia propia, tomando como estrategia básica el diseño de combinaciones enfocadas en una etapa inicial, al rastreo diagnóstico de hemopatías linfoides de acuerdo con las indicaciones médicas que requieren del estudio fenotípico; en una segunda etapa, enfocamos el trabajo al establecimiento de paneles más amplios para la caracterización y clasificación diagnóstica de las entidades más relevantes según la clasificación OMS de 2008.

Sin embargo, la validación de cada una de las combinaciones y paneles de combinaciones propuestos inicialmente, demostró múltiples limitaciones; esto hizo que fuera necesario en la práctica totalidad de los mismos, rediseñar y optimizar la(s) combinación(es) con la inclusión de nuevos marcadores potencialmente útiles, la eliminación de marcadores redundantes, y la selección de nuevos reactivos, ya fueran clones alternativos y/o nuevos conjugados fluorescentes (en muchos casos no disponibles comercialmente). Así, dependiendo del panel concreto se requirieron entre 3 y 7 rondas de diseño, evaluación, optimización y re-evaluación, con la correspondiente validación prospectiva de la combinación propuesta al final de cada ronda, y la evaluación critica de la posible necesidad de continuar el proceso hasta alcanzar una combinación óptima, más eficiente (100% de sensibilidad con la especificidad más elevada

posible para tubos de rastreo diagnóstico y 100% de especificidad con el máximo de sensibilidad posible en el caso de paneles para subclasificación de distintos grupos de NCP y hemopatías linfoides). Estos ciclos de diseño, evaluación, optimización y re-evaluación de los distintos paneles, implicaron el uso en conjunto de ≥ 850 muestras. Merece además destacar que, en el proceso de validación resultaron especialmente útiles las nuevas estrategias y herramientas de análisis de datos desarrolladas en paralelo, e incluidas dentro del programa informático Infinicyt. Como resultado del trabajo desarrollado se generaron combinaciones de anticuerpos y paneles de combinaciones de anticuerpos conjugados con 8 fluorocromos distintos para el rastreo diagnóstico y clasificación de las hemopatías linfoides, incluidas las NCP.

Tubo EuroFlow para rastreo diagnóstico de linfocitos maduros (LST). La detección de la presencia de una expansión, o de pequeñas cantidades de células linfoides B, T y/o NK aberrantes, constituye uno de los test diagnósticos más frecuentemente demandados, en los que el inmunofenotipado por citometría de flujo multiparamétrica juega un papel clave[1,99,140,158,175]. Uno de los objetivos centrales del presente trabajo estaba enfocado al desarrollo de una combinación única de 12 marcadores en 8 colores, para el rastreo diagnóstico de SLPC, para aplicar a aquellos tipos de muestras más frecuentemente utilizados con este fin, como son la SP, la MO y el tejido linfoide ganglionar[1,6,89]. La combinación final de anticuerpos propuesta tiene como objetivo la evaluación lo más completa posible, del compartimiento de linfocitos maduros B, T y NK en este tipo de muestras y ante diferentes situaciones e indicaciones médicas[89,148]. Con este fin, la aplicación de este tubo en la rutina diagnóstica debería permitir la identificación de poblaciones linfoides tumorales, no solo en base a su expansión numérica, sino sobre todo, por la presencia en ellas de fenotipos aberrantes o signos de clonalidad, en la práctica totalidad de los casos; además, en los pocos pacientes en los que esto no ocurriese, debería poner en evidencia la existencia de desviaciones numéricas en la distribución de las poblaciones patológicas, con la consiguiente necesidad de realizar una evaluación fenotípica

más completa de las mismas, objetivos alcanzados plenamente con el tubo LST durante el proceso de validación del mismo. Por otra parte, la información generada por el tubo LST, permitía seleccionar también el(los) panel(es) necesario(s) para una caracterización más detallada de la población de linfocitos patológicos y la subclasificación diagnóstica de la enfermedad, es decir, los paneles para la caracterización de SLPC-B, SLPC-T, SLPC-NK o incluso NCP. En este sentido, merece destacar que la configuración de la combinación de anticuerpos propuesta permite también la integración completa de la información proporcionada por el tubo LST con la generada con las demás combinaciones de anticuerpos del panel de SLPC-B, dado que los marcadores comunes incluidos en el panel de SLPC-B se encuentran exactamente en las mismas posiciones en el tubo LST.

La evaluación detallada del tubo LST en los diferentes laboratorios que participaron en el estudio, demostró que con respecto a las estrategias diagnósticas convencionales empleadas en ese momento en la rutina de cada laboratorio, la combinación LST contaba con una mejor relación coste/beneficio[99,175]. Así, la comparación directa con cada una de las estrategias locales mostró una reducción significativa en el tiempo de procesamiento global de la muestra (en media de ≈ 25%), una disminución importante en el número de tubos y reactivos requeridos en la fase de rastreo diagnóstico (reducción media de 3 a 1 tubo y de 13 a 12 anticuerpos, respectivamente); además, todo ello iba asociado a una mayor eficiencia y objetividad en la interpretación de los resultados, derivados de la inclusión de todos los marcadores en una sola combinación. El incremento en la objetividad alcanzada a la hora de interpretar los resultados, se puso de manifiesto de forma especial cuando se aplicaban las nuevas herramientas informáticas, incluyendo el análisis multivariante de componentes principales, para comparar las poblaciones clonales/aberrantes con poblaciones normales/reactivas de referencia; con todo ello, se establecieron las bases de una nueva aproximación automatizable de reconocimiento de patrones inmunofenotípicos normales vs patológicos, en el rastreo diagnóstico de SLPC. Finalmente, aun cuando el tubo LST se diseñó con fines de rastreo diagnóstico, este demostró

una sensibilidad relativamente elevada a la hora de detectar células patológicas, aun cuando estas estaban presentes en baja frecuencia (niveles de 10^{-3}) en la muestra. Por el contrario, no es recomendable la utilización del tubo LST para la detección de linfocitos clonales/aberrantes en muestras con escasa concentración celular (e.g. LCR o humor vítreo), al no permitir esta combinación identificar de forma óptima todos los tipos celulares presentes habitualmente en este tipo de muestras (e.g., los monocitos y células dendríticas).

Panel EuroFlow para el rastreo diagnóstico y clasificación de neoplasias de células plasmáticas (PCD). Una de las particularidades más llamativas del panel de combinaciones de anticuerpos propuesto para el rastreo diagnóstico y clasificación de las NCP, es la de ser el único panel EuroFlow en el que la lista inicial de marcadores candidatos para ser incluidos en el panel no sufrió cambios a lo largo de las diferentes versiones del mismo. Estos resultados ponen de manifiesto la existencia de un conocimiento previo amplio y a la vez detallado sobre los marcadores más informativos y relevantes a la hora de evaluar las CPs de este grupo de neoplasias[4,5]. Sin embargo, si se observaron particularidades técnicas respecto a algunos reactivos y las propias características biológicas de las CPs, que justificaron la realización de ajustes en los clones y conjugados seleccionados y/o su posición concreta en el panel, hasta la versión final considerada como óptima. A modo de ejemplo, para algunos marcadores como CD38 y β2M, resultaron óptimos aquellos conjugados de fluorocromos que presentaban intensidades de fluorescencia relativamente bajas con perfiles de solapamiento con otras fluorescencias menos complejos, requiriéndose incluso la dilución del anticuerpo conjugado con anticuerpo puro del mismo clon, con el fin de mantener las condiciones de saturación a expensas de una menor IMF. Con ello logramos que la población de células plasmáticas permaneciese de forma sistemática dentro de la ventana de análisis, a la vez que se reducía el impacto de su elevada intensidad de fluorescencia, en los requerimientos de compensación del reactivo y en la dificultad en encontrar una compensación de fluorescencias óptima. Otro marcador que

requirió ajustes fue CD45-PacO, un anticuerpo incluido en todos los paneles EuroFlow desarrollados salvo en este panel; esto se debe a la baja intensidad de fluorescencia de este reactivo que en el caso del panel para diagnóstico de NCP se veía significativamente afectado por los niveles relativamente importantes de autofluorescencia de las CPs en este canal de fluorescencia; a este respecto debemos hacer notar que, los niveles de autofluorescencia de las CPs en este canal se encontraban por encima de la señal de fluorescencia específica generada por la expresión de CD45 en CPs normales, lo cual impedía una discriminación óptima entre las CPs normales y las CPs patológicas $CD45^-$, con base exclusivamente en este anticuerpo. Finalmente, la disponibilidad de conjugados de buena calidad para CD138 resultó ser muy limitada en las posiciones que dejaron "abiertas" los demás marcadores de la combinación; ello forzó la inclusión de un conjugado de CD138 con PacO, aunque la búsqueda de alternativas –e.g. otros conjugados más intensos (p.ej., CD138-HV500)- comenzó casi de manera inmediata, una vez cerrado el panel con los reactivos disponibles.

En conjunto, la evaluación del comportamiento y de la utilidad de la combinación de dos tubos de 8 colores para la evaluación de muestras con sospecha de NCP, demostró se trata de un panel eficiente que permite la detección, cuantificación y discriminación inequívoca entre CPs normales/reactivas y CPs clonales/aberrantes; además, este panel también proporciona información detallada acerca de las características inmunofenotípicas de ambas poblaciones de CPs. Desde el punto de vista práctico, cabe señalar que la combinación de marcadores incluidos en el tubo 1, mostró ser suficiente para cumplir con estos objetivos, por lo que podría considerarse el uso exclusivo de este tubo en las primeras etapas del rastreo diagnóstico de NCP mediante CMF; en tal caso, el uso del tubo 2 sería opcional, y solo estaría indicado en una pequeña proporción de casos (<5%), dependiendo de los resultados de los análisis realizados en la primera fase con del tubo 1. Finalmente, la combinación completa del panel para diagnóstico de NCP (i.e., los dos tubos), junto al tubo LST, y eventualmente también el panel para la clasificación de SLPC-B, constituirían en conjunto, la mejor aproximación al diagnóstico de

aquellos SLPC-B en los que, además de detectarse la presencia de los linfocitos B maduros patológicos, se encuentra también comprometido el compartimiento de CPs, como ocurre por ejemplo en el linfoplasmocítico/macroglobulinemia de Waldenström[291].

El empleo de las nuevas herramientas y estrategias de análisis de datos de CMF incorporadas en el programa informático Infinicyt, permitió la comparación de los perfiles inmunofenotípicos de las diferentes poblaciones de CPs detectadas en los casos incluidos en la fase de validación de la versión final de este panel (i.e., versión 6 del panel). Así, una vez fusionados ambos tubos y estimados los parámetros medidos en cada uno de ellos, en el total de las CPs identificadas con ambos tubos, pudimos demostrar mediante análisis de componentes principales, que el perfil inmunofenotípico de las CPs de las muestras de donantes sanos formaba un grupo bien definido y único, en el espacio multiparamétrico generado por la combinación de anticuerpos del panel. A su vez, tanto las poblaciones de CPs normales/reactivas presentes en las muestras de pacientes con sospecha de NCP en las que no se evidenció presencia de CP clonales, como las CPs normales/reactivas de MO de pacientes con otras enfermedades diferentes de las NCP, se solapaban también con el grupo de células plasmáticas normales de MO de sujetos sanos, evaluadas en diferentes laboratorios. Estos hallazgos resaltan las similitudes existentes entre los perfiles inmunofenotípicos de las CPs normales y reactivas, permitiendo considerar ambas poblaciones de CPs como un solo grupo de referencia. Por el contrario, el empleo de esta misma estrategia (y panel de reactivos) en las muestras de pacientes con NCP, mostró que las CPs clonales mostraban sistemáticamente, un perfil inmunofenotípico claramente diferente del de las CPs normales/reactivas de referencia.

Panel EuroFlow para la clasificación de síndromes linfoproliferativos crónicos T (SLPC-T). El esquema diagnostico propuesto para las neoplasias de linfocitos T periféricos, incluye el uso del panel de combinaciones de anticuerpos para la clasificación de SLPC-T en las muestras en la que se detecte una población de linfocitos T maduros expandida y/o aberrante mediante el tubo

LST, una vez complementado o no con la demostración de clonalidad T a través del estudio del repertorio TCRVβ o TCRVγ y TCRVδ de los linfocitos T alterados[166,183,205,206,292].

En conjunto, los SLPC-T están constituidos por un grupo heterogéneo de entidades distintas[1] que en cierta medida, pueden tener su origen en subpoblaciones de células T funcionalmente y/o ontogénicamente diferentes (como ocurre con las neoplasias de linfocitos T TCRγδ$^+$ vs los SLPC-T TCRαβ$^+$)[1]. Esto, asociado a la frecuencia relativamente baja de este grupo de SLPC, hace que por razones de coste, muchos laboratorios sigan empleando paneles de anticuerpos para SLPC-T que contienen un número relativamente reducido de marcadores[1,37,166,177,209,210,231,233,238-242,244,293].

La estrategia diagnóstica propuesta por el grupo EuroFlow para los SLPC-T comprende a nivel global tres pasos consecutivos bien diferenciados. Así, en una primera fase se propone el uso del tubo LST. Cuando se encuentra alterada la población de células T TCRγδ$^-$, se recomienda, como segundo paso, el análisis del repertorio TCRVβ de dicha población, lo cual confirmaría o descartaría su posible naturaleza clonal[183,205]. De confirmarse dicha naturaleza clonal, el tercer paso consistiría en la caracterización fenotípica completa mediante el panel de combinaciones de anticuerpos para la clasificación diagnóstica de SLPC-T, con el fin de asignar la población T patológica a alguna de las diferentes categorías diagnósticas definidas en la clasificación actual de la OMS. En el caso de expansiones de células T TCRγδ$^+$, es recomendable, aunque no siempre estrictamente necesario, el estudio del repertorio TCRVγ y TCRVδ, en el segundo paso[206]. Sin embargo, con frecuencia, el estudio del repertorio T TCRVγ y TCRVδ no conlleva la confirmación definitiva de clonalidad, debido a que el repertorio normal de las células T TCRγδ$^+$ es mucho más restringido que el de los linfocitos T TCRαβ$^+$, observándose con relativa frecuencia desequilibrios importantes en sujetos normales y procesos reactivos en la distribución de cada familia TCRVγ y/o TCRVδ; además, la disponibilidad de anticuerpos frente a ambas familias del TCR, es relativamente limitada[206]. Por todo ello, tras la identificación de una expansión T TCRγδ$^+$ con el

tubo LST, sería suficiente realizar la caracterización diagnóstica de las células expandidas usando directamente el panel para la clasificación diagnóstica de SLPC-T.

En este sentido, la evaluación del comportamiento y la utilidad del panel propuesto para la caracterización y clasificación diagnóstica de SLPC-T, demostró que este panel contribuye de forma importante a la discriminación entre células T con fenotipos normales/reactivos vs linfocitos T clonales/aberrantes, siendo efectivo en prácticamente todos los casos analizados, a excepción de un pequeño subgrupo de pacientes con LLGG-T $CD8^+$. De forma similar, el panel SLPC-T permitió también la clasificación inequívoca y correcta de los SLPC-T en la mayoría de las categorías diagnósticas actuales definidas por la OMS para este tipo de enfermedades, incluyendo el SS, la LPL-T, la LLTA, la LLGG-T y el LTAI; la única excepción, la constituyeron los linfomas T periféricos NOS, al resultar ser un grupo heterogéneo y difícil de identificar de forma específica, al no presentar características comunes bien definidas. Sin embargo, los resultados alcanzados con la evaluación de este panel de combinaciones de anticuerpos deben considerarse de momento como resultados preliminares o provisionales, ya que durante el presente trabajo no se ha podido evaluar prácticamente ningún caso de aquellos subtipos diagnósticos de SLPC-T menos frecuentes, como el linfoma T anaplásico ALK+.

Panel EuroFlow para la caracterización diagnóstica de síndromes linfoproliferativos crónicos de células NK (SLPC-NK). Uno de los desafíos más importantes que tiene en la actualidad el diagnóstico de las neoplasias de células NK, reside en poder establecer la posible naturaleza normal vs reactiva vs clonal de las células tumorales o expandidas [261]. Esto es debido a la ausencia hasta la fecha, de marcadores de clonalidad fáciles y sencillos de aplicar para esta población celular[33,222-227]. Muchos estudios previos han demostrado que la mayoría de las células tumorales de distintas hemopatías malignas muestran fenotipos aberrantes y que estos permiten su discriminación de forma específica respecto a su contrapartida normal y reactiva (e.g. células normales del mismo tipo y en el estadio madurativo)[4,31,117,153,172]. Estos hallazgos

apoyan el desarrollo de un panel de marcadores para SLPC-NK que tenga como finalidad permitir la identificación de fenotipos NK aberrantes que contribuyan a distinguir entre expansiones reactivas y verdaderos SLPC NK clonales; es decir, un panel de marcadores que contribuya a definir de manera más precisa el diagnóstico de clonalidad NK. Con este objetivo, en este trabajo se propone un panel constituido por 3 tubos, que utiliza 4 marcadores comunes y 12 marcadores adicionales para la caracterización completa y detallada de las células NK y la definición de la naturaleza normal/reactiva vs clonal de estas células.

Mediante la utilización de las herramientas informáticas de análisis multivariante basado en el análisis de componentes principales implementadas en el programa Infinicyt, en este trabajo demostramos que el panel de combinaciones de anticuerpos propuesto para la caracterización diagnóstica de SLPC-NK, facilita la discriminación entre expansiones de células NK normales, reactivas y clonales en la mayoría de los casos que debutan con linfocitosis a expensas de células NK. Aun así, cabe señalar que existe un solapamiento parcial en algunos casos, entre el perfil inmunofenotípico de las células NK expandidas y el de la células NK clonales, lo cual dificulta en estos pacientes la interpretación de la posible naturaleza clonal de las células NK expandidas. Todo ello justifica continuar con los esfuerzos enfocados a la optimización de la combinación propuesta y de su validación. En este sentido merece destacar que, en un estudio más reciente realizado por nuestro grupo en colaboración con el grupo EuroFlow, se confirma la utilidad del panel aquí propuesto para el diagnóstico de clonalidad NK, destacando el perfil de expresión de CD94 y HLADR ($CD94^{hi}$ y $HLADR^{+}$) como el más informativo a este respecto[261]. Uno de los principales obstáculos existentes a la hora de validar el panel propuesto, es la baja frecuencia de los SLPC-NK; esto además podría tener como consecuencia, el que los laboratorios de diagnóstico onco-hematológico decidieran no invertir los recursos necesarios para disponer de un conjunto de anticuerpos adecuados para la clasificación diagnóstica de los SLPC-NK. En tal caso deberían plantearse estrategias alternativas localmente como la creación de centros de referencia especializados en el diagnóstico de este subgrupo de SLPC.

Consideraciones finales.

Después de varios años de trabajo, en esta memoria recogemos el trabajo doctoral mediante el cual se llevó a cabo el diseño, construcción y validación inicial de combinaciones de anticuerpos para el rastreo diagnóstico y la caracterización inmunofenotípica estandarizada de SLPC y NCP empleando técnicas de inmunofenotipado por citometría de flujo. La aproximación propuesta incluye dos, o máximo tres, pasos secuenciales con un primer nivel de tubos (únicos) de rastreo diagnóstico de SLPC y NCP, respectivamente. Estos tubos van seguidos en el segundo nivel, de la aplicación de paneles más amplios para la caracterización fenotípica de diferentes subtipos diagnósticos de SLPC-T y NK. A diferencia de otros paneles de marcadores propuestos en la literatura[7,35,111-116], se trata en este caso, no de paneles de consenso basados únicamente en el conocimiento y la experiencia, sino, por primera vez, de paneles validados de forma prospectiva y tras múltiples rondas (sucesivas) de diseño, validación, optimización y re-evaluación, hasta alcanzar la combinación o panel de combinaciones de anticuerpos óptimas para alcanzar los objetivos propuestos para su aplicación clínica. Así, a partir de una combinación inicial de consenso, y sólo después de evaluadas dichas combinaciones, y tras seleccionar e incluir nuevos marcadores en las mismas, excluir marcadores redundantes, reubicar marcadores en distintas posiciones de la combinación/panel y/o sustituir clones y conjugados de los mismos, llegamos a las combinaciones de panel de combinaciones de anticuerpos propuestas. En conjunto, las versiones finales de los paneles LST, PCD, SLPC-T y SLPC-NK propuestos fueron además evaluadas en >470 muestras, adquiridas tras aplicar los diferentes protocolos estandarizados desarrollados en paralelo, así como las nuevas estrategias y herramientas informáticas diseñadas e implementadas en el programa Infinicyt. Precisamente a este respecto cabe señalar, la gran utilidad de las herramientas de análisis multivariante aplicadas a la evaluación del comportamiento y de la utilidad de los paneles propuestos, incluyendo el análisis de la contribución individual y relativa de cada uno de los marcadores incluidos en los mismos.

En conjunto los resultados obtenidos mostraron una eficiencia muy alta, asociada a una flexibilidad importante para poder adaptar los paneles propuestos a distintas situaciones y condiciones existentes en diferentes laboratorios.

En resumen, nuestros resultados demuestran que el empleo conjunto de los paneles y procedimientos estándar propuestos constituye una estrategia muy eficiente, y probablemente también la más extensamente validada, para el rastreo diagnóstico y clasificación de los SLPC y NCP. Además, el trabajo desarrollado sienta las bases para la futura incorporación de mejoras en los paneles y en las estrategias de análisis e interpretación de los resultados de los estudios inmunofenotípicos, en especial en lo que respecta al empleo de bases de datos de referencia frente a las que podemos comparar casos de nuevos diagnóstico.

V. CONCLUSIONES.

En relación con el primer objetivo, centrado en desarrollar un procedimiento estandarizado y validado para la calibración y monitorización de citómetros de flujo digitales de uso habitual en los laboratorios de diagnóstico hematológico, que permita obtener resultados reproducibles tanto a nivel interno de cada laboratorio, como entre diferentes laboratorios:

1-. El protocolo propuesto para la calibración y monitorización de citómetros de flujo de uso clínico, basado en el empleo de partículas de referencias, permite establecer una compensación equivalente entre equipos compatibles, asegurando un elevado grado de reproducibilidad entre diferentes instrumentos y en distintos laboratorios a lo largo del tiempo.

2-. La monitorización diaria del equipo siguiendo el protocolo propuesto, permite identificar precozmente desviaciones en la calibración, que indican la necesidad de calibrar de nuevo el equipo, para garantizar la calidad y reproducibilidad de los datos.

En relación con el establecimiento y validación de un procedimiento estandarizado para el procesamiento de diferentes tipos de muestras para inmunofenotipado de hemopatías malignas por CMF, que disminuya la variabilidad asociada a la preparación de las muestras, minimizando su impacto en los resultados:

3-. El protocolo secuencial de marcaje con anticuerpos, seguido del lisado de hematíes con la solución comercial FACSLysing y el lavado de las células la adquisición inmediata de la muestra en el citómetro de flujo, constituye el mejor procedimiento para el estudio de marcadores de la membrana celular en muestras de SP y MO, en el rastreo diagnóstico y clasificación inmunofenotípica de hemopatías malignas; sin embargo, este protocolo requiere de pequeñas variaciones para el estudio de otros tipos de muestras y de antígenos intracitoplasmáticos.

En relación con el diseño, construcción e implementación de nuevas aproximaciones metodológicas y herramientas informáticas para el análisis objetivo y automatizado de datos, que contribuyan a simplificar y estandarizar el análisis e interpretación de los resultados de CMF a la hora de reconocer perfiles inmunofenotípicos característicos de células tumorales, ante la sospecha diagnostica de una hemopatía maligna:

4-. Las nuevas herramientas informáticas desarrolladas, incluyendo la fusión de ficheros, la estimación de parámetros y el análisis multivariante de datos de CMF, permiten identificar patrones inmunofenotípicos que ayudan a distinguir entre poblaciones de células normales, reactivas y tumorales representativas de distintas enfermedades o grupos de enfermedades, pudiendo además emplearse de forma prospectiva para establecer el diagnóstico y clasificar nuevos casos una vez enfrentados a ficheros que contienen perfiles fenotípicos de referencia (normales o patológicos).

5-. La implementación de los diferentes protocolos estandarizados de calibración y procesamiento de muestras, evaluados de manera multicéntrica, demostró la disminución de los niveles de variabilidad técnica muy por debajo de los de la variabilidad biológica de las diferentes poblaciones celulares de sangre periférica normal.

En relación con el objetivo centrado en el diseño, evaluación y estandarización de paneles de anticuerpos basados en combinaciones de ≥ 8 reactivos para el rastreo diagnóstico de SLPC y NCPs, y la clasificación de SLPC T y NK:

6-. La combinación de 13 anticuerpos conjugados con fluorocromos para el rastreo diagnóstico de SLPC (LST) propuesta, ha mostrado ser una combinación óptima para el rastreo diagnóstico de SLPC B, T y NK, permitiendo discriminar entre linfocitos normales/reactivos vs

clonales/patológicos en la práctica totalidad de los casos estudiados, con un nivel de sensibilidad relativamente elevado y de forma reproducible, a nivel multicéntrico.

7-. El panel propuesto para el rastreo diagnóstico y clasificación de NCP (PCD) ha demostrado ser una herramienta eficiente para la identificación, cuantificación y caracterización fenotípica de células plasmáticas clonales/patológicas frente a células plasmáticas normales/reactivas, con importantes ventajas sobre los métodos locales empleados anteriormente.

8-. El panel de combinaciones de anticuerpos propuesto para la clasificación diagnostica de los SLPC-T, permite diferenciar, en base a su perfil inmunofenotípico aberrante, células T tumorales de linfocitos T normales/reactivos en la gran mayoría de los SLPC-T, aportando además información relevante para su subclasificación en las distintas entidades OMS.

9-. El panel de combinaciones de anticuerpos propuesto para la caracterización diagnóstica de SLPC-NK contribuye a una mayor precisión diagnostica de este grupo de enfermedades, facilitando en una elevada proporción de los casos la identificación de perfiles fenotípicos característicos de células NK clonales.

VI. BIBLIOGRAFÍA.

1. Swerdlow SH, Campo E, Harris NL, Jaffe ES, Pileri SA, Stein H, Thiele J, Vardiman JW. WHO classification of tumours of haematopoietic and lymphoid tissues. 4th ed. Lyon: International Agency for Research on Cancer; 2008. 439 p.

2. Orfao A, Schmitz G, Brando B, Ruiz-Arguelles A, Basso G, Braylan R, Rothe G, Lacombe F, Lanza F, Papa S, Lucio P, San Miguel JF. Clinically useful information provided by the flow cytometric immunophenotyping of hematological malignancies: current status and future directions. Clinical chemistry. 1999;45(10):1708-17. Epub 1999/10/03. PubMed PMID: 10508115.

3. Orfao A, Almeida J, Lopez A. La citometría de flujo en el estudio de las enfermedades hematológicas. In: Garcia-Conde J, Sierra J, Urbano-Ispizua A, Vicente V, Vives Corrons JL, editors. Hematología. Madrid: ARÁN Ediciones; 2003. p. 47-55.

4. Rawstron AC, Orfao A, Beksac M, Bezdickova L, Brooimans RA, Bumbea H, Dalva K, Fuhler G, Gratama J, Hose D, Kovarova L, Lioznov M, Mateo G, Morilla R, Mylin AK, Omede P, Pellat-Deceunynck C, Perez Andres M, Petrucci M, Ruggeri M, Rymkiewicz G, Schmitz A, Schreder M, Seynaeve C, Spacek M, de Tute RM, Van Valckenborgh E, Weston-Bell N, Owen RG, San Miguel JF, Sonneveld P, Johnsen HE, European Myeloma N. Report of the European Myeloma Network on multiparametric flow cytometry in multiple myeloma and related disorders. Haematologica. 2008;93(3):431-8. Epub 2008/02/13. doi: 10.3324/haematol.11080. PubMed PMID: 18268286.

5. Paiva B, Almeida J, Perez-Andres M, Mateo G, Lopez A, Rasillo A, Vidriales MB, Lopez-Berges MC, Miguel JF, Orfao A. Utility of flow cytometry immunophenotyping in multiple myeloma and other clonal plasma cell-related disorders. Cytometry B Clin Cytom. 2010;78(4):239-52. Epub 2010/02/16. doi: 10.1002/cyto.b.20512. PubMed PMID: 20155853.

6. Szczepanski T, van der Velden VH, van Dongen JJ. Flow-cytometric immunophenotyping of normal and malignant lymphocytes. Clin Chem Lab Med. 2006;44(7):775-96. Epub 2006/06/17. doi: 10.1515/CCLM.2006.146. PubMed PMID: 16776621.

7. Bene MC, Nebe T, Bettelheim P, Buldini B, Bumbea H, Kern W, Lacombe F, Lemez P, Marinov I, Matutes E, Maynadie M, Oelschlagel U, Orfao A, Schabath R, Solenthaler M, Tschurtschenthaler G, Vladareanu AM, Zini G, Faure GC, Porwit A. Immunophenotyping of acute leukemia and lymphoproliferative disorders: a consensus proposal of the European LeukemiaNet Work Package 10. Leukemia. 2011;25(4):567-74. Epub 2011/01/22. doi: 10.1038/leu.2010.312. PubMed PMID: 21252983.

8. Orfao A, Ruiz-Arguelles A, Lacombe F, Ault K, Basso G, Danova M. Flow cytometry: its applications in hematology. Haematologica. 1995;80(1):69-81. PubMed PMID: 7758996.

9. Orfao A, Lopez A, Flores J, Almeida J, Vidriales B, Perez J, Kneba M, Macintyre E, Parreira A, Richards S, Szczepański T, Trka J, Van der Velden VHJ, Van Dongen JJM, Consortium ftE. Diagnosis of haematological malignancies: new applications for flow cytometry. Hematology Journal (European Hematology Association Educational Program). 2006;2:6-13.

10. Paiva B, Martinez-Lopez J, Vidriales MB, Mateos MV, Montalban MA, Fernandez-Redondo E, Alonso L, Oriol A, Teruel AI, de Paz R, Larana JG, Bengoechea E, Martin A, Mediavilla JD, Palomera L, de Arriba F, Blade J, Orfao A, Lahuerta JJ, San Miguel JF. Comparison of immunofixation, serum free light chain, and immunophenotyping for response evaluation and prognostication in multiple myeloma. J Clin Oncol. 2011;29(12):1627-33. Epub 2011/03/16. doi: 10.1200/JCO.2010.33.1967. PubMed PMID: 21402611.

11. Basso G, Buldini B, De Zen L, Orfao A. New methodologic approaches for immunophenotyping acute leukemias. Haematologica. 2001;86(7):675-92. Epub 2001/07/17. PubMed PMID: 11454522.

12. Johansson U, Macey M. Pitfalls in the use of multicolour flow cytometry in haematology. J Clin Pathol. 2011;64(7):561-3. doi: 10.1136/jcp.2010.085183. PubMed PMID: 21450754.

13. Kappelmayer J, Gratama JW, Karaszi E, Menendez P, Ciudad J, Rivas R, Orfao A. Flow cytometric detection of intracellular myeloperoxidase, CD3 and CD79a. Interaction between monoclonal antibody clones, fluorochromes and sample preparation protocols. J Immunol Methods. 2000;242(1-2):53-65. Epub 2000/09/15. doi: S0022-1759(00)00220-9. PubMed PMID: 10986389.

14. Mittag A, Tarnok A. Basics of standardization and calibration in cytometry--a review. Journal of biophotonics. 2009;2(8-9):470-81. doi: 10.1002/jbio.200910033. PubMed PMID: 19504519.

15. Ashmore LM, Shopp GM, Edwards BS. Lymphocyte subset analysis by flow cytometry. Comparison of three different staining techniques and effects of blood storage. J Immunol Methods. 1989;118(2):209-15. PubMed PMID: 2466904.

16. Carter PH, Resto-Ruiz S, Washington GC, Ethridge S, Palini A, Vogt R, Waxdal M, Fleisher T, Noguchi PD, Marti GE. Flow cytometric analysis of whole blood lysis, three anticoagulants, and five cell preparations. Cytometry. 1992;13(1):68-74. doi: 10.1002/cyto.990130111. PubMed PMID: 1372204.

17. Knapp W, Strobl H, Majdic O. Flow cytometric analysis of cell-surface and intracellular antigens in leukemia diagnosis. Cytometry. 1994;18(4):187-98. Epub 1994/12/15. doi: 10.1002/cyto.990180402. PubMed PMID: 7534675.

18. Tamul KR, Schmitz JL, Kane K, Folds JD. Comparison of the effects of Ficoll-Hypaque separation and whole blood lysis on results of immunophenotypic analysis of blood and bone marrow samples from patients with hematologic malignancies. Clin Diagn Lab Immunol. 1995;2(3):337-42. Epub 1995/05/01. PubMed PMID: 7545079; PubMed Central PMCID: PMC170156.

19. Bossuyt X, Marti GE, Fleisher TA. Comparative analysis of whole blood lysis methods for flow cytometry. Cytometry. 1997;30(3):124-33. Epub 1997/06/15. PubMed PMID: 9222098.

20. Macey MG, McCarthy DA, Milne T, Cavenagh JD, Newland AC. Comparative study of five commercial reagents for preparing normal and leukaemic lymphocytes for immunophenotypic analysis by flow cytometry. Cytometry. 1999;38(4):153-60. Epub 1999/08/10. PubMed PMID: 10440853.

21. Subira D, Castanon S, Aceituno E, Hernandez J, Jimenez-Garofano C, Jimenez A, Jimenez AM, Roman A, Orfao A. Flow cytometric analysis of cerebrospinal fluid samples and its usefulness in routine clinical practice. Am J Clin Pathol. 2002;117(6):952-8. Epub 2002/06/06. doi: 10.1309/123P-CE6V-WYAK-BB1F. PubMed PMID: 12047148.

22. Kraan J, Gratama JW, Haioun C, Orfao A, Plonquet A, Porwit A, Quijano S, Stetler-Stevenson M, Subira D, Wilson W. Flow cytometric immunophenotyping of cerebrospinal fluid. Current protocols in cytometry / editorial board, J Paul Robinson, managing editor [et al]. 2008;Chapter 6:Unit 6 25. Epub 2008/09/05. doi: 10.1002/0471142956.cy0625s45. PubMed PMID: 18770650.

23. Groeneveld K, te Marvelde JG, van den Beemd MW, Hooijkaas H, van Dongen JJ. Flow cytometric detection of intracellular antigens for immunophenotyping of normal and malignant leukocytes. Leukemia. 1996;10(8):1383-9. Epub 1996/08/01. PubMed PMID: 8709649.

24. Van Lochem EG, Groeneveld K, Te Marvelde JG, Van den Beemd MW, Hooijkaas H, Van Dongen JJ. Flow cytometric detection of intracellular antigens for immunophenotyping of normal and malignant leukocytes: testing of a new fixation-permeabilization solution. Leukemia. 1997;11(12):2208-10. PubMed PMID: 9447842.

25. Stewart CC, Stewart SJ. Immunophenotyping. Current protocols in cytometry / editorial board, J Paul Robinson, managing editor [et al]. 2001;Chapter 6:Unit 6 2: 1-18. Epub 2008/09/05. doi: 10.1002/0471142956.cy0602s00. PubMed PMID: 18770715.

26. Maecker HT, McCoy JP, Nussenblatt R. Standardizing immunophenotyping for the Human Immunology Project. Nat Rev Immunol. 2012;12(3):191-200. doi: 10.1038/nri3158. PubMed PMID: 22343568; PubMed Central PMCID: PMC3409649.

27. Caraux A, Klein B, Paiva B, Bret C, Schmitz A, Fuhler GM, Bos NA, Johnsen HE, Orfao A, Perez-Andres M, Myeloma Stem Cell N. Circulating human B and plasma cells. Age-associated changes in counts and detailed characterization of circulating normal CD138- and CD138+ plasma cells. Haematologica. 2010;95(6):1016-20. Epub 2010/01/19. doi: 10.3324/haematol.2009.018689. PubMed PMID: 20081059; PubMed Central PMCID: PMC2878802.

28. Pedreira CE, Costa ES, Lecrevisse Q, van Dongen JJ, Orfao A. Overview of clinical flow cytometry data analysis: recent advances and future challenges. Trends Biotechnol. 2013;31(7):415-25. Epub 2013/06/12. doi: 10.1016/j.tibtech.2013.04.008. PubMed PMID: 23746659.

29. Marsee DK, Li B, Dorfman DM. Single tube, six-color flow cytometric analysis is a sensitive and cost-effective technique for assaying clonal plasma cells. Am J Clin Pathol. 2010;133(5):694-9. doi: 10.1309/AJCPKKNPMLWX9ZXB. PubMed PMID: 20395515.

30. Braylan RC, Orfao A, Borowitz MJ, Davis BH. Optimal number of reagents required to evaluate hematolymphoid neoplasias: results of an international consensus meeting. Cytometry. 2001;46(1):23-7. Epub 2001/03/10. PubMed PMID: 11241503.

31. Sanchez ML, Almeida J, Vidriales B, Lopez-Berges MC, Garcia-Marcos MA, Moro MJ, Corrales A, Calmuntia MJ, San Miguel JF, Orfao A. Incidence of phenotypic aberrations in a series of 467 patients with B chronic lymphoproliferative disorders: basis for the design of specific four-color stainings to be used for minimal residual disease investigation. Leukemia. 2002;16(8):1460-9. Epub 2002/07/30. doi: 10.1038/sj.leu.2402584. PubMed PMID: 12145686.

32. Matutes E. Chronic T-cell lymphoproliferative disorders. Rev Clin Exp Hematol. 2002;6(4):401-20. Epub 2003/06/26. PubMed PMID: 12823780.

33. Lima M, Almeida J, Montero AG, Teixeira Mdos A, Queiros ML, Santos AH, Balanzategui A, Estevinho A, Alguero Mdel C, Barcena P, Fonseca S, Amorim ML, Cabeda JM, Pinho L, Gonzalez M, San Miguel J, Justica B, Orfao A. Clinicobiological, immunophenotypic, and molecular characteristics of monoclonal CD56-/+dim chronic natural killer cell large granular lymphocytosis. Am J Pathol. 2004;165(4):1117-27. Epub 2004/10/07. PubMed PMID: 15466379; PubMed Central PMCID: PMC1618630.

34. Lima M, Almeida J, Teixeira MA, Santos AH, Queiros ML, Fonseca S, Moura J, Goncalves M, Orfao A, Pinto Ribeiro AC. Reactive phenotypes after acute and chronic NK-cell activation. J Biol Regul Homeost Agents. 2004;18(3-4):331-4. Epub 2005/03/25. PubMed PMID: 15786700.

35. Wood BL, Arroz M, Barnett D, DiGiuseppe J, Greig B, Kussick SJ, Oldaker T, Shenkin M, Stone E, Wallace P. 2006 Bethesda International Consensus recommendations on the immunophenotypic analysis of hematolymphoid neoplasia by flow cytometry: optimal reagents and reporting for the flow cytometric diagnosis of hematopoietic neoplasia. Cytometry B Clin Cytom. 2007;72 Suppl 1:S14-22. Epub 2007/09/07. doi: 10.1002/cyto.b.20363. PubMed PMID: 17803189.

36. Pedreira CE, Costa ES, Almeida J, Fernandez C, Quijano S, Flores J, Barrena S, Lecrevisse Q, Van Dongen JJ, Orfao A. A probabilistic approach for the evaluation of minimal residual disease by multiparameter flow cytometry in leukemic B-cell chronic lymphoproliferative disorders. Cytometry A. 2008;73A(12):1141-50. Epub 2008/10/07. doi: 10.1002/cyto.a.20638. PubMed PMID: 18836994.

37. Karube K, Aoki R, Nomura Y, Yamamoto K, Shimizu K, Yoshida S, Komatani H, Sugita Y, Ohshima K. Usefulness of flow cytometry for differential diagnosis of precursor and peripheral T-cell and NK-cell lymphomas: analysis of 490 cases. Pathology international. 2008;58(2):89-97. Epub 2008/01/18. doi: 10.1111/j.1440-1827.2007.02195.x. PubMed PMID: 18199158.

38. McCoy JP, Jr. Basic principles of flow cytometry. Hematol Oncol Clin North Am. 2002;16(2):229-43. PubMed PMID: 12094472.

39. Macey MG. Flow cytometry : principles and applications. Totowa, N.J.: Humana Press; 2007. 290 p.

40. Givan AL. Principles of flow cytometry: an overview. Methods Cell Biol. 2001;63:19-50. PubMed PMID: 11060835.

41. Kohler G, Milstein C. Continuous cultures of fused cells secreting antibody of predefined specificity. Nature. 1975;256(5517):495-7. Epub 1975/08/07. PubMed PMID: 1172191.

42. Maecker H, Trotter J. Selecting Reagents for Multicolor Flow Cytometry. San Jose, California: BD Biosciences, Application Note; 2009.

43. Maecker HT, Frey T, Nomura LE, Trotter J. Selecting fluorochrome conjugates for maximum sensitivity. Cytometry A. 2004;62(2):169-73. Epub 2004/11/13. doi: 10.1002/cyto.a.20092. PubMed PMID: 15536642.

44. Chattopadhyay PK, Gaylord B, Palmer A, Jiang N, Raven MA, Lewis G, Reuter MA, Nur-ur Rahman AK, Price DA, Betts MR, Roederer M. Brilliant violet fluorophores: a new class of ultrabright fluorescent compounds for immunofluorescence experiments. Cytometry A. 2012;81(6):456-66. Epub 2012/04/11. doi: 10.1002/cyto.a.22043. PubMed PMID: 22489009.

45. Chattopadhyay PK, Hogerkorp CM, Roederer M. A chromatic explosion: the development and future of multiparameter flow cytometry. Immunology. 2008;125(4):441-9. PubMed PMID: 19137647; PubMed Central PMCID: PMC2612557.

46. Chattopadhyay PK, Roederer M. Cytometry: today's technology and tomorrow's horizons. Methods. 2012;57(3):251-8. Epub 2012/03/07. doi: 10.1016/j.ymeth.2012.02.009. PubMed PMID: 22391486; PubMed Central PMCID: PMC3374038.

47. Herzenberg LA, Parks D, Sahaf B, Perez O, Roederer M, Herzenberg LA. The history and future of the fluorescence activated cell sorter and flow cytometry: a view from Stanford. Clinical chemistry. 2002;48(10):1819-27. PubMed PMID: 12324512.

48. Lugli E, Roederer M, Cossarizza A. Data analysis in flow cytometry: the future just started. Cytometry A. 2010;77(7):705-13. Epub 2010/06/29. doi: 10.1002/cyto.a.20901. PubMed PMID: 20583274; PubMed Central PMCID: PMC2909632.

49. Perfetto SP, Chattopadhyay PK, Roederer M. Seventeen-colour flow cytometry: unravelling the immune system. Nat Rev Immunol. 2004;4(8):648-55. Epub 2004/08/03. doi: 10.1038/nri1416. PubMed PMID: 15286731.

50. Roederer M, Kantor AB, Parks DR, Herzenberg LA. Cy7PE and Cy7APC: bright new probes for immunofluorescence. Cytometry. 1996;24(3):191-7. Epub 1996/07/01. PubMed PMID: 8800551.

51. Milstein C. Monoclonal antibodies. Cancer. 1982;49(10):1953-7. PubMed PMID: 6176307.

52. Herzenberg LA, De Rosa SC. Monoclonal antibodies and the FACS: complementary tools for immunobiology and medicine. Immunol Today. 2000;21(8):383-90. Epub 2000/08/01. PubMed PMID: 10916141.

53. Haynes JL. Principles of flow cytometry. Cytometry Suppl. 1988;3:7-17. Epub 1988/01/01. PubMed PMID: 3076370.

54. Owens MA, Loken MR. Flow cytometry principles for clinical laboratory practice : quality assurance for quantitative immunophenotyping. New York ; Chichester: Wiley-Liss; 1995. xiii,224p. p.

55. Roederer M, Quaye L, Mangino M, Beddall MH, Mahnke Y, Chattopadhyay P, Tosi I, Napolitano L, Terranova Barberio M, Menni C, Villanova F, Di Meglio P, Spector TD, Nestle FO. The genetic architecture of the human immune system: a bioresource for autoimmunity and disease pathogenesis. Cell. 2015;161(2):387-403. doi: 10.1016/j.cell.2015.02.046. PubMed PMID: 25772697; PubMed Central PMCID: PMC4393780.

56. Nolan JP, Condello D. Spectral flow cytometry. Current protocols in cytometry / editorial board, J Paul Robinson, managing editor [et al]. 2013;Chapter 1:Unit1 27: 1-18. doi: 10.1002/0471142956.cy0127s63. PubMed PMID: 23292705; PubMed Central PMCID: PMC3556726.

57. Keren DF, Hanson CA, Hurtubise PE. Flow cytometry and clinical diagnosis. Chicago: ASCP Press; 1994. 664 p.

58. Melamed MR, Lindmo T, Mendelsohn ML. Flow cytometry and sorting. 2nd ed. / editors Myron R. Melamed, Tore Lindmo, Mortimer L. Mendelsohn. ed. New York, N.Y.: Wiley-Liss; 1990. 824 p

59. Kaduchak G, Goddard GR, Ward MD. Acoustic focusing flow cytometry. J Acoust Soc Am. 2012;132(3):1952. Epub 2012/09/18. doi: 10.1121/1.4755182. PubMed PMID: 22979273.

60. Wood B. 9-color and 10-color flow cytometry in the clinical laboratory. Archives of pathology & laboratory medicine. 2006;130(5):680-90. Epub 2006/05/11. doi: 10.1043/1543-2165(2006)130[680:CACFCI]2.0.CO;2. PubMed PMID: 16683886..

61. Mahnke YD, Roederer M. Optimizing a multicolor immunophenotyping assay. Clin Lab Med. 2007;27(3):469-85, v. Epub 2007/07/31. doi: 10.1016/j.cll.2007.05.002. PubMed PMID: 17658403; PubMed Central PMCID: PMC2034273.

62. Telford W, Kapoor V, Jackson J, Burgess W, Buller G, Hawley T, Hawley R. Violet laser diodes in flow cytometry: an update. Cytometry A. 2006;69(11):1153-60. Epub 2006/10/20. doi: 10.1002/cyto.a.20340. PubMed PMID: 17051581.

63. Baumgarth N, Roederer M. A practical approach to multicolor flow cytometry for immunophenotyping. J Immunol Methods. 2000;243(1-2):77-97. Epub 2000/09/15. PubMed PMID: 10986408.

64. Perez-Andres M, Paiva B, Nieto WG, Caraux A, Schmitz A, Almeida J, Vogt RF, Jr., Marti GE, Rawstron AC, Van Zelm MC, Van Dongen JJ, Johnsen HE, Klein B, Orfao A. Human peripheral blood B-cell compartments: a crossroad in B-cell traffic. Cytometry B Clin Cytom. 2010;78 Suppl 1:S47-60. Epub 2010/09/21. doi: 10.1002/cyto.b.20547. PubMed PMID: 20839338.

65. Leach RM, Drummond M, Doig A. Practical flow cytometry in haematology diagnosis. Oxford: Wiley-Blackwell; 2013. 258 p.

66. Data file standard for flow cytometry. Data File Standards Committee of the Society for Analytical Cytology. Cytometry. 1990;11(3):323-32. doi: 10.1002/cyto.990110303. PubMed PMID: 2340769.

67. Seamer LC, Bagwell CB, Barden L, Redelman D, Salzman GC, Wood JC, Murphy RF. Proposed new data file standard for flow cytometry, version FCS 3.0. Cytometry. 1997;28(2):118-22. PubMed PMID: 9181300.

68. Nomenclature for clusters of differentiation (CD) of antigens defined on human leukocyte populations. IUIS-WHO Nomenclature Subcommittee. Bulletin of the World Health Organization. 1984;62(5):809-15. PubMed PMID: 6334575; PubMed Central PMCID: PMC2536217.

69. Engel P, Boumsell L, Balderas R, Bensussan A, Gattei V, Horejsi V, Jin BQ, Malavasi F, Mortari F, Schwartz-Albiez R, Stockinger H, van Zelm MC, Zola H, Clark G. CD Nomenclature 2015: Human Leukocyte Differentiation Antigen Workshops as a Driving Force in Immunology. J Immunol. 2015;195(10):4555-63. doi: 10.4049/jimmunol.1502033. PubMed PMID: 26546687.

70. Reilly JT. Use and evaluation of leucocyte monoclonal antibodies in the diagnostic laboratory: a review. Clin Lab Haematol. 1996;18(1):1-5. PubMed PMID: 9118596.

71. McLaughlin BE, Baumgarth N, Bigos M, Roederer M, De Rosa SC, Altman JD, Nixon DF, Ottinger J, Oxford C, Evans TG, Asmuth DM. Nine-color flow cytometry for accurate measurement of T cell subsets and cytokine responses. Part I: Panel design by an empiric approach. Cytometry A. 2008;73(5):400-10. Epub 2008/04/03. doi: 10.1002/cyto.a.20555. PubMed PMID: 18383316.

72. van Velzen JF, van den Blink D, Bloem AC. Inability of a monoclonal anti-light chain antibody to detect clonal plasma cells in a patient with multiple myeloma by multicolor flow cytometry. Cytometry B Clin Cytom. 2013;84(1):30-2. Epub 2012/09/29. doi: 10.1002/cyto.b.21044. PubMed PMID: 23019187.

73. van Velzen JF, van den Blink D, Wiegers IE, Bloem AC. Inability of monoclonal anti-light chain antibody to detect clonal B-cells in a patient with follicular lymphoma by multicolor flow cytometry. Journal of clinical laboratory analysis. 2014;28(6):493-5. doi: 10.1002/jcla.21716. PubMed PMID: 24659431.

74. Loken MR, Parks DR, Herzenberg LA. Two-color immunofluorescence using a fluorescence-activated cell sorter. J Histochem Cytochem. 1977;25(7):899-907. Epub 1977/07/01. PubMed PMID: 330738.

75. Oi VT, Glazer AN, Stryer L. Fluorescent phycobiliprotein conjugates for analyses of cells and molecules. The Journal of cell biology. 1982;93(3):981-6. PubMed PMID: 6749865; PubMed Central PMCID: PMC2112146.

76. Berlier JE, Rothe A, Buller G, Bradford J, Gray DR, Filanoski BJ, Telford WG, Yue S, Liu J, Cheung CY, Chang W, Hirsch JD, Beechem JM, Haugland RP. Quantitative comparison of long-wavelength Alexa Fluor dyes to Cy dyes: fluorescence of the dyes and their bioconjugates. J Histochem Cytochem. 2003;51(12):1699-712. Epub 2003/11/19. PubMed PMID: 14623938.

77. A clinical evaluation of the International Lymphoma Study Group classification of non-Hodgkin's lymphoma. The Non-Hodgkin's Lymphoma Classification Project. Blood. 1997;89(11):3909-18. Epub 1997/06/01. PubMed PMID: 9166827.

78. Roederer M. Compensation in flow cytometry. Current protocols in cytometry / editorial board, J Paul Robinson, managing editor [et al]. 2002;Chapter 1:Unit 1 14. 1-20. Epub 2008/09/05. doi: 10.1002/0471142956.cy0114s22. PubMed PMID: 18770762.

79. Sewell WA, Smith SA. Polychromatic flow cytometry in the clinical laboratory. Pathology. 2011;43(6):580-91. Epub 2011/09/02. doi: 10.1097/PAT.0b013e32834a69ae. PubMed PMID: 21881537.

80. Kraan J, Gratama JW, Keeney M, D'Hautcourt JL. Setting up and calibration of a flow cytometer for multicolor immunophenotyping. J Biol Regul Homeost Agents. 2003;17(3):223-33. Epub 2003/10/04. PubMed PMID: 14524607.

81. Hoffman RA, Wood JC. Characterization of flow cytometer instrument sensitivity. Current protocols in cytometry / editorial board, J Paul Robinson, managing editor [et al]. 2007;Chapter 1:Unit1 20.1-20. doi: 10.1002/0471142956.cy0120s40. PubMed PMID: 18770846.

82. Maecker HT, Trotter J. Flow cytometry controls, instrument setup, and the determination of positivity. Cytometry A. 2006;69(9):1037-42. Epub 2006/08/05. doi: 10.1002/cyto.a.20333. PubMed PMID: 16888771.

83. Roederer M. Spectral compensation for flow cytometry: visualization artifacts, limitations, and caveats. Cytometry. 2001;45(3):194-205. Epub 2001/12/18. PubMed PMID: 11746088.

84. Le Roy C, Varin-Blank N, Ajchenbaum-Cymbalista F, Letestu R. Flow cytometry APC-tandem dyes are degraded through a cell-dependent mechanism. Cytometry A. 2009;75(10):882-90. Epub 2009/09/10. doi: 10.1002/cyto.a.20774. PubMed PMID: 19739089.

85. Tung JW, Parks DR, Moore WA, Herzenberg LA, Herzenberg LA. New approaches to fluorescence compensation and visualization of FACS data. Clinical immunology. 2004;110(3):277-83. Epub 2004/03/30. doi: 10.1016/j.clim.2003.11.016. PubMed PMID: 15047205..

86. Wang L, Gaigalas AK, Yan M. Quantitative fluorescence measurements with multicolor flow cytometry. Methods in molecular biology. 2011;699:53-65. doi: 10.1007/978-1-61737-950-5_3. PubMed PMID: 21116978.

87. Shapiro HM. Practical flow cytometry. 4th ed. ed. New York ; Wiley-Liss; 2003. 736 p.

88. Perfetto SP, Ambrozak D, Nguyen R, Chattopadhyay P, Roederer M. Quality assurance for polychromatic flow cytometry. Nature protocols. 2006;1(3):1522-30. Epub 2007/04/05. doi: 10.1038/nprot.2006.250. PubMed PMID: 17406444.

89. Davis BH, Holden JT, Bene MC, Borowitz MJ, Braylan RC, Cornfield D, Gorczyca W, Lee R, Maiese R, Orfao A, Wells D, Wood BL, Stetler-Stevenson M. 2006 Bethesda International Consensus recommendations on the flow cytometric immunophenotypic analysis of hematolymphoid neoplasia: medical indications. Cytometry B Clin Cytom. 2007;72 Suppl 1:S5-13. Epub 2007/09/07. doi: 10.1002/cyto.b.20365. PubMed PMID: 17803188.

90. Macey MG, McCathy DA. Quantitation of adhesion molecules and other function-associated antigens on human peripheral blood leucocytes. Cytometry. 1993;14(8):898-908. doi: 10.1002/cyto.990140808. PubMed PMID: 8287733.

91. Quijano S, Lopez A, Manuel Sancho J, Panizo C, Deben G, Castilla C, Antonio Garcia-Vela J, Salar A, Alonso-Vence N, Gonzalez-Barca E, Penalver FJ, Plaza-Villa J, Morado M, Garcia-Marco J, Arias J, Briones J, Ferrer S, Capote J, Nicolas C, Orfao A, Spanish Group for the Study of CNSDiNHL. Identification of leptomeningeal disease in aggressive B-cell non-Hodgkin's lymphoma: improved sensitivity of flow cytometry. J Clin Oncol. 2009;27(9):1462-9. Epub 2009/02/20. doi: 10.1200/JCO.2008.17.7089. PubMed PMID: 19224854.

92. Bardales RH, Al-Katib AM, Carrato A, Koziner B. Detection of intracytoplasmic immunoglobulin by flow cytometry in B-cell malignancies. J Histochem Cytochem. 1989;37(1):83-9. Epub 1989/01/01. PubMed PMID: 2491755.

93. Drach D, Drach J, Glassl H, Gattringer C, Huber H. Flow cytometric detection of cytoplasmic antigens in acute leukemias: implications for lineage assignment. Leuk Res. 1993;17(5):455-61. Epub 1993/05/01. PubMed PMID: 8388970.

94. Renzi P, Ginns LC. Analysis of T cell subsets in normal adults. Comparison of whole blood lysis technique to Ficoll-Hypaque separation by flow cytometry. J Immunol Methods. 1987;98(1):53-6. PubMed PMID: 2951443.

95. Johansson U, Bloxham D, Couzens S, Jesson J, Morilla R, Erber W, Macey M, British Committee for Standards in H. Guidelines on the use of multicolour flow cytometry in the diagnosis of haematological neoplasms. British Committee for Standards in Haematology. Br J Haematol. 2014;165(4):455-88. doi: 10.1111/bjh.12789. PubMed PMID: 24620735.

96. Hulspas R, O'Gorman MR, Wood BL, Gratama JW, Sutherland DR. Considerations for the control of background fluorescence in clinical flow cytometry. Cytometry B Clin Cytom. 2009;76(6):355-64. doi: 10.1002/cyto.b.20485. PubMed PMID: 19575390.

97. Reilly JT, Granger V, Temperton PF, Barnett D. Leukaemia immunophenotyping: effect of antibody source and fluorochrome on antigen detection. J Clin Pathol. 1995;48(2):186. PubMed PMID: 7745124; PubMed Central PMCID: PMC502419.

98. Hale LP. Histologic and molecular assessment of human thymus. Ann Diagn Pathol. 2004;8(1):50-60. PubMed PMID: 15129912.

99. Costa ES, Arroyo ME, Pedreira CE, Garcia-Marcos MA, Tabernero MD, Almeida J, Orfao A. A new automated flow cytometry data analysis approach for the diagnostic screening of neoplastic B-cell disorders in peripheral blood samples with absolute lymphocytosis. Leukemia. 2006;20(7):1221-30. Epub 2006/05/27. doi: 10.1038/sj.leu.2404241. PubMed PMID: 16728986.

100. Arnoulet C, Bene MC, Durrieu F, Feuillard J, Fossat C, Husson B, Jouault H, Maynadie M, Lacombe F. Four- and five-color flow cytometry analysis of leukocyte differentiation pathways in normal bone marrow: a reference document based on a systematic approach by the GTLLF and GEIL. Cytometry B Clin Cytom. 2010;78(1):4-10. doi: 10.1002/cyto.b.20484. PubMed PMID: 19708072.

101. Matutes E, Catovsky D. Classification of mature T-cell leukemias. Leukemia. 2003;17(8):1682-3. Epub 2003/07/30. doi: 10.1038/sj.leu.2403003. PubMed PMID: 12886265

102. Pedreira CE, Costa ES, Arroyo ME, Almeida J, Orfao A. A multidimensional classification approach for the automated analysis of flow cytometry data. IEEE transactions on bio-medical engineering. 2008;55(3):1155-62. doi: 10.1109/TBME.2008.915729. PubMed PMID: 18334408.

103. Green CL, Brown L, Stewart JJ, Xu Y, Litwin V, Mc Closkey TW. Recommendations for the validation of flow cytometric testing during drug development: I instrumentation. J Immunol Methods. 2011;363(2):104-19. doi: 10.1016/j.jim.2010.07.004. PubMed PMID: 20655313.

104. Beckman Coulter Inc. Beckman Coulter Flow Cytometers 2011 [cited 2011 September, 02] Clinical Flow Cytometry Instruments]. Available from: http://www.beckmancoulter.com/wsrportal/wsr/diagnostics/clinical-products/flow-cytometry/flow-cytometers/index.htm.

105. Macedo A, Orfao A, Vidriales MB, Lopez-Berges MC, Valverde B, Gonzalez M, Caballero MD, Ramos F, Martinez M, Fernandez-Calvo J, Martinez A, San Miguel JF. Characterization of aberrant phenotypes in acute myeloblastic leukemia. Ann Hematol. 1995;70(4):189-94. PubMed PMID: 7748963.

106. Ocqueteau M, Orfao A, Almeida J, Blade J, Gonzalez M, Garcia-Sanz R, Lopez-Berges C, Moro MJ, Hernandez J, Escribano L, Caballero D, Rozman M, San Miguel JF. Immunophenotypic characterization of plasma cells from monoclonal gammopathy of undetermined significance patients. Implications for the differential diagnosis between MGUS and multiple myeloma. Am J Pathol. 1998;152(6):1655-65. Epub 1998/06/17. PubMed PMID: 9626070; PubMed Central PMCID: PMC1858455.

107. Orfao A, Ortuno F, de Santiago M, Lopez A, San Miguel J. Immunophenotyping of acute leukemias and myelodysplastic syndromes. Cytometry A. 2004;58(1):62-71. Epub 2004/03/03. doi: 10.1002/cyto.a.10104. PubMed PMID: 14994223.

108. Tung JW, Heydari K, Tirouvanziam R, Sahaf B, Parks DR, Herzenberg LA, Herzenberg LA. Modern flow cytometry: a practical approach. Clin Lab Med. 2007;27(3):453-68. doi: 10.1016/j.cll.2007.05.001. PubMed PMID: 17658402; PubMed Central PMCID: PMC1994577.

109. Pedreira CE, Costa ES, Barrena S, Lecrevisse Q, Almeida J, van Dongen JJ, Orfao A. Generation of flow cytometry data files with a potentially infinite number of dimensions. Cytometry A. 2008;73(9):834-46. Epub 2008/07/17. doi: 10.1002/cyto.a.20608. PubMed PMID: 18629843.

110. Rothe G, Schmitz G. Consensus protocol for the flow cytometric immunophenotyping of hematopoietic malignancies. Working Group on Flow Cytometry and Image Analysis. Leukemia. 1996;10(5):877-95. PubMed PMID: 8656686.

111. Stewart CC, Behm FG, Carey JL, Cornbleet J, Duque RE, Hudnall SD, Hurtubise PE, Loken M, Tubbs RR, Wormsley S. U.S.-Canadian Consensus recommendations on the immunophenotypic analysis of hematologic neoplasia by flow cytometry: selection of antibody combinations. Cytometry. 1997;30(5):231-5. Epub 1997/12/31 23:38. doi: 10.1002/(SICI)1097-0320(19971015)30:5<231::AID-CYTO3>3.0.CO;2-K [pii]. PubMed PMID: 9383096.

112. Ruiz-Arguelles A, Duque RE, Orfao A. Report on the first Latin American Consensus Conference for Flow Cytometric Immunophenotyping of Leukemia. Cytometry. 1998;34(1):39-42. Epub 1998/03/25. doi: 10.1002/(SICI)1097-0320(19980215)34:1<39::AID-CYTO7>3.0.CO;2-9 [pii]. PubMed PMID: 9511940.

113. Van Bockstaele DR, Deneys V, Philippe J, Bernier M, Kestens L, Chatelain B, De Waele M, Demanet C. Belgian consensus recommendations for flow cytometric immunophenotyping. The Belgian Association for Cytometry/Belgische Vereniging voor Cytometrie/Association Belge de Cytometrie. Acta Clin Belg. 1999;54(2):88-98. PubMed PMID: 10394646.

114. Ruiz-Arguelles A, Rivadeneyra-Espinoza L, Duque RE, Orfao A. Report on the second Latin American consensus conference for flow cytometric immunophenotyping of hematological malignancies. Cytometry B Clin Cytom. 2006;70(1):39-44. Epub 2005/12/15. doi: 10.1002/cyto.b.20083. PubMed PMID: 16353215.

115. Wilson WH. International consensus recommendations on the flow cytometric immunophenotypic analysis of hematolymphoid neoplasia. Cytometry B Clin Cytom. 2007;72 Suppl 1:S2. Epub 2007/09/07. doi: 10.1002/cyto.b.20366. PubMed PMID: 17803186.

116. Hallek M, Cheson BD, Catovsky D, Caligaris-Cappio F, Dighiero G, Dohner H, Hillmen P, Keating MJ, Montserrat E, Rai KR, Kipps TJ, International Workshop on Chronic Lymphocytic L. Guidelines for the diagnosis and treatment of chronic lymphocytic leukemia: a report from the International Workshop on Chronic Lymphocytic Leukemia updating the National Cancer Institute-Working Group 1996 guidelines. Blood. 2008;111(12):5446-56. Epub 2008/01/25. doi: 10.1182/blood-2007-06-093906. PubMed PMID: 18216293; PubMed Central PMCID: PMC2972576.

117. van de Loosdrecht AA, Alhan C, Bene MC, Della Porta MG, Drager AM, Feuillard J, Font P, Germing U, Haase D, Homburg CH, Ireland R, Jansen JH, Kern W, Malcovati L, Te Marvelde JG, Mufti GJ, Ogata K, Orfao A, Ossenkoppele GJ, Porwit A, Preijers FW, Richards SJ, Schuurhuis GJ, Subira D, Valent P, van der Velden VH, Vyas P, Westra AH, de Witte TM, Wells DA, Loken MR, Westers TM. Standardization of flow cytometry in myelodysplastic syndromes: report from the first European LeukemiaNet working conference on flow cytometry in myelodysplastic syndromes. Haematologica. 2009;94(8):1124-34. Epub 2009/06/24. doi: 10.3324/haematol.2009.005801. PubMed PMID: 19546437; PubMed Central PMCID: PMC2719035.

118. Valent P, Horny HP, Bennett JM, Fonatsch C, Germing U, Greenberg P, Haferlach T, Haase D, Kolb HJ, Krieger O, Loken M, van de Loosdrecht A, Ogata K, Orfao A, Pfeilstocker M, Ruter B, Sperr WR, Stauder R, Wells DA. Definitions and standards in the diagnosis and treatment of the myelodysplastic syndromes: Consensus statements and report from a working conference. Leuk Res. 2007;31(6):727-36. PubMed PMID: 17257673.

119. Borowitz MJ, Guenther KL, Shults KE, Stelzer GT. Immunophenotyping of acute leukemia by flow cytometric analysis. Use of CD45 and right-angle light scatter to gate on leukemic blasts in three-color analysis. Am J Clin Pathol. 1993;100(5):534-40. Epub 1993/11/01. PubMed PMID: 8249893.

120. Braylan RC, Atwater SK, Diamond L, Hassett JM, Johnson M, Kidd PG, Leith C, Nguyen D. U.S.-Canadian Consensus recommendations on the immunophenotypic analysis of hematologic neoplasia by flow cytometry: data reporting. Cytometry. 1997;30(5):245-8. Epub 1997/12/31 23:38. PubMed PMID: 9383098.

121. Roederer M, De Rosa S, Gerstein R, Anderson M, Bigos M, Stovel R, Nozaki T, Parks D, Herzenberg L, Herzenberg L. 8 color, 10-parameter flow cytometry to elucidate complex leukocyte heterogeneity. Cytometry. 1997;29(4):328-39. Epub 1998/01/24. PubMed PMID: 9415416.

122. Cover TM, Hart PE. Nearest neighbour pattern clasification. IEEE Trans Inf Theory. 1967;13:21-7.

123. Robinson JP, Durack G, Kelley S. An innovation in flow cytometry data collection and analysis producing a correlated multiple sample analysis in a single file. Cytometry. 1991;12(1):82-90. Epub 1991/01/01. doi: 10.1002/cyto.990120112. PubMed PMID: 1999125.

124. Robinson JP, Ragheb K, Lawler G, Kelley S, Durack G. Rapid multivariate analysis and display of cross-reacting antibodies on human leukocytes. Cytometry. 1992;13(1):75-82. Epub 1992/01/01. doi: 10.1002/cyto.990130112. PubMed PMID: 1547658.

125. Fujikoshi Y, Ulyanov VV, Shimizu R. Multivariate statistics : high-dimensional and large-sample approximations. Oxford: Wiley-Blackwell; 2010. 512 p

126. Costa ES, Pedreira CE, Barrena S, Lecrevisse Q, Flores J, Quijano S, Almeida J, del Carmen Garcia-Macias M, Bottcher S, Van Dongen JJ, Orfao A. Automated pattern-guided principal component analysis vs expert-based immunophenotypic classification of B-cell chronic lymphoproliferative disorders: a step forward in the standardization of clinical immunophenotyping. Leukemia. 2010;24(11):1927-33. Epub 2010/09/17. doi: 10.1038/leu.2010.160. PubMed PMID: 20844562; PubMed Central PMCID: PMC3035971.

127. Jolliffe IT. Principal Component Analysis. 2º ed. New York: Springer-Verlag New York; 2002. 488 p.

128. Lanza F. Towards standardization in immunophenotyping hematological malignancies. How can we improve the reproducibility and comparability of flow cytometric results? Working Group on Leukemia Immunophenotyping. Eur J Histochem. 1996;40 Suppl 1:7-14. Epub 1996/01/01. PubMed PMID: 8839695.

129. Dworzak MN, Gaipa G, Ratei R, Veltroni M, Schumich A, Maglia O, Karawajew L, Benetello A, Potschger U, Husak Z, Gadner H, Biondi A, Ludwig WD, Basso G. Standardization of flow cytometric minimal residual disease evaluation in acute lymphoblastic leukemia: Multicentric assessment is feasible. Cytometry B Clin Cytom. 2008;74(6):331-40. Epub 2008/06/13. doi: 10.1002/cyto.b.20430. PubMed PMID: 18548617.

130. Campo E, Swerdlow SH, Harris NL, Pileri S, Stein H, Jaffe ES. The 2008 WHO classification of lymphoid neoplasms and beyond: evolving concepts and practical applications. Blood. 2011;117(19):5019-32. doi: 10.1182/blood-2011-01-293050. PubMed PMID: 21300984; PubMed Central PMCID: PMC3109529.

131. Roman E, Smith AG. Epidemiology of lymphomas. Histopathology. 2011;58(1):4-14. doi: 10.1111/j.1365-2559.2010.03696.x. PubMed PMID: 21261679.

132. Bennett JM, Catovsky D, Daniel MT, Flandrin G, Galton DA, Gralnick HR, Sultan C. Proposals for the classification of the acute leukaemias. French-American-British (FAB) co-operative group. Br J Haematol. 1976;33(4):451-8. Epub 1976/08/01. PubMed PMID: 188440.

133. Foon KA, Todd RF, 3rd. Immunologic classification of leukemia and lymphoma. Blood. 1986;68(1):1-31. Epub 1986/07/01. PubMed PMID: 2941082.

134. Immunophenotyping in the diagnosis of chronic lymphoproliferative disorders. General Haematology Task Force of BCSH. J Clin Pathol. 1994;47(10):871-5. Epub 1994/10/01. PubMed PMID: 7962598; PubMed Central PMCID: PMC502168.

135. Immunophenotyping in the diagnosis of acute leukaemias. General Haematology Task Force of BCSH. J Clin Pathol. 1994;47(9):777-81. Epub 1994/09/01. PubMed PMID: 7962642; PubMed Central PMCID: PMC494929.

136. Harris NL, Jaffe ES, Stein H, Banks PM, Chan JK, Cleary ML, Delsol G, De Wolf-Peeters C, Falini B, Gatter KC, Grogan TM, Isaacson PG, Knowles MD, Mason D, Muller-Hermelink HK, Pileri SA, Piris MA, Ralfkiaer E, Warnke RA. A revised European-American classification of lymphoid neoplasms: a proposal from the International Lymphoma Study Group. Blood. 1994;84(5):1361-92. Epub 1994/09/01. PubMed PMID: 8068936.

137. Matutes E, Owusu-Ankomah K, Morilla R, Garcia Marco J, Houlihan A, Que TH, Catovsky D. The immunological profile of B-cell disorders and proposal of a scoring system for the diagnosis of CLL. Leukemia. 1994;8(10):1640-5. Epub 1994/10/01. PubMed PMID: 7523797.

138. Bene MC, Castoldi G, Knapp W, Ludwig WD, Matutes E, Orfao A, van't Veer MB. Proposals for the immunological classification of acute leukemias. European Group for the Immunological Characterization of Leukemias (EGIL). Leukemia. 1995;9(10):1783-6. Epub 1995/10/01. PubMed PMID: 7564526.

139. Jaffe ES. Pathology and genetics of tumours of haematopoietic and lymphoid tissues. Lyon: IARC Press ; Oxford : Oxford University Press; 2001. 351 p.

140. Craig FE, Foon KA. Flow cytometric immunophenotyping for hematologic neoplasms. Blood. 2008;111(8):3941-67. Epub 2008/01/17. doi: 10.1182/blood-2007-11-120535. PubMed PMID: 18198345.

141. Ocqueteau M, Orfao A, Garcia-Sanz R, Almeida J, Gonzalez M, San Miguel JF. Expression of the CD117 antigen (c-Kit) on normal and myelomatous plasma cells. Br J Haematol. 1996;95(3):489-93. Epub 1996/12/01. PubMed PMID: 8943889.

142. Kraj M, Poglod R, Kopec-Szlezak J, Sokolowska U, Wozniak J, Kruk B. C-kit receptor (CD117) expression on plasma cells in monoclonal gammopathies. Leuk Lymphoma. 2004;45(11):2281-9. Epub 2004/10/30. doi: 10.1080/10428190412331283279. PubMed PMID: 15512818.

143. Lin P, Owens R, Tricot G, Wilson CS. Flow cytometric immunophenotypic analysis of 306 cases of multiple myeloma. Am J Clin Pathol. 2004;121(4):482-8. Epub 2004/04/15. doi: 10.1309/74R4-TB90-BUWH-27JX. PubMed PMID: 15080299.

144. Pruneri G, Ponzoni M, Ferreri AJ, Freschi M, Tresoldi M, Baldini L, Mattioli M, Agnelli L, Govi S, Mancuso P, Agazzi A, Bertolini F, Peccatori J, Bosari S, Gianelli U, Viale G, Neri A. The prevalence and clinical implications of c-kit expression in plasma cell myeloma. Histopathology. 2006;48(5):529-35. Epub 2006/04/21. doi: 10.1111/j.1365-2559.2006.02375.x. PubMed PMID: 16623778.

145. Gupta R, Bhaskar A, Kumar L, Sharma A, Jain P. Flow cytometric immunophenotyping and minimal residual disease analysis in multiple myeloma. Am J Clin Pathol. 2009;132(5):728-32. Epub 2009/10/23. doi: 10.1309/AJCP1GYI7EHQYUYK. PubMed PMID: 19846814..

146. Schabath R, Ratei R, Ludwig WD. The prognostic significance of antigen expression in leukaemia. Best Pract Res Clin Haematol. 2003;16(4):613-28. PubMed PMID: 14592646.

147. Borowitz MJ, Bray R, Gascoyne R, Melnick S, Parker JW, Picker L, Stetler-Stevenson M. U.S.-Canadian Consensus recommendations on the immunophenotypic analysis of hematologic neoplasia by flow cytometry: data analysis and interpretation. Cytometry. 1997;30(5):236-44. PubMed PMID: 9383097.

148. Davis BH, Foucar K, Szczarkowski W, Ball E, Witzig T, Foon KA, Wells D, Kotylo P, Johnson R, Hanson C, Bessman D. U.S.-Canadian Consensus recommendations on the immunophenotypic analysis of hematologic neoplasia by flow cytometry: medical indications. Cytometry. 1997;30(5):249-63. Epub 1997/12/31 23:38. PubMed PMID: 9383099.

149. Greig B, Oldaker T, Warzynski M, Wood B. 2006 Bethesda International Consensus recommendations on the immunophenotypic analysis of hematolymphoid neoplasia by flow cytometry: recommendations for training and education to perform clinical flow cytometry. Cytometry B Clin Cytom. 2007;72 Suppl 1:S23-33. Epub 2007/09/07. doi: 10.1002/cyto.b.20364. PubMed PMID: 17803190.

150. Stetler-Stevenson M, Davis B, Wood B, Braylan R. 2006 Bethesda International Consensus Conference on Flow Cytometric Immunophenotyping of Hematolymphoid Neoplasia. Cytometry B Clin Cytom. 2007;72 Suppl 1:S3. Epub 2007/07/17. doi: 10.1002/cyto.b.20362. PubMed PMID: 17630651.

151. Borowitz MJ, Craig FE, Digiuseppe JA, Illingworth AJ, Rosse W, Sutherland DR, Wittwer CT, Richards SJ. Guidelines for the diagnosis and monitoring of paroxysmal nocturnal hemoglobinuria and related disorders by flow cytometry. Cytometry B Clin Cytom. 2010;78(4):211-30. Epub 2010/06/10. doi: 10.1002/cyto.b.20525. PubMed PMID: 20533382.

152. Hernandez JM, Gonzalez-Sarmiento R, Martin C, Gonzalez M, Sanchez I, Corral J, Orfao A, Canizo MC, San Miguel JF, Lopez-Borrasca A. Immunophenotypic, genomic and clinical characteristics of blast crisis of chronic myelogenous leukaemia. Br J Haematol. 1991;79(3):408-14. PubMed PMID: 1751368.

153. Szczepanski T, Orfao A, van der Velden VH, San Miguel JF, van Dongen JJ. Minimal residual disease in leukaemia patients. Lancet Oncol. 2001;2(7):409-17. Epub 2002/03/22. PubMed PMID: 11905735.

154. San Miguel JF, Almeida J, Mateo G, Blade J, Lopez-Berges C, Caballero D, Hernandez J, Moro MJ, Fernandez-Calvo J, Diaz-Mediavilla J, Palomera L, Orfao A. Immunophenotypic evaluation of the plasma cell compartment in multiple myeloma: a tool for comparing the efficacy of different treatment strategies and predicting outcome. Blood. 2002;99(5):1853-6. Epub 2002/02/28. PubMed PMID: 11861305.

155. Vidriales MB, San-Miguel JF, Orfao A, Coustan-Smith E, Campana D. Minimal residual disease monitoring by flow cytometry. Best Pract Res Clin Haematol. 2003;16(4):599-612. PubMed PMID: 14592645.

156. Sanchez ML, Almeida J, Gonzalez D, Gonzalez M, Garcia-Marcos MA, Balanzategui A, Lopez-Berges MC, Nomdedeu J, Vallespi T, Barbon M, Martin A, de la Fuente P, Martin-Nunez G, Fernandez-Calvo J, Hernandez JM, San Miguel JF, Orfao A. Incidence and clinicobiologic characteristics of leukemic B-cell chronic lymphoproliferative disorders with more than one B-cell clone. Blood. 2003;102(8):2994-3002. Epub 2003/06/28. doi: 10.1182/blood-2003-01-0045. PubMed PMID: 12829608.

157. Perez-Andres M, Santiago M, Almeida J, Mateo G, Porwit-MacDonald A, Bjorklund E, Valet G, Kraan J, Gratama JW, D'Hautcourt JL, Merle-Beral H, Lima M, Montalban MA, San Miguel JF, Orfao A. Immunophenotypic approach to the identification and characterization of clonal plasma cells from patients with monoclonal gammopathies. J Biol Regul Homeost Agents. 2004;18(3-4):392-8. Epub 2005/03/25. PubMed PMID: 15786710.

158. Orfao A, Almeida J, Sanchez ML, San Miguel J. Inmunophenotypic diagnosis of leukemic B-cell chronic lymphoproliferative disorders other than chronic lymphocytic leukemia. In: Faguet GB, editor. Chronic lymphocytic leukemia : molecular genetics, biology, diagnosis, and management. Totowa, N.J.: Humana Press; 2004. p. 173-90.

159. Sarasquete ME, Garcia-Sanz R, Gonzalez D, Martinez J, Mateo G, Martinez P, Ribera JM, Hernandez JM, Lahuerta JJ, Orfao A, Gonzalez M, San Miguel JF. Minimal residual disease monitoring in multiple myeloma: a comparison between allelic-specific oligonucleotide real-time quantitative polymerase chain reaction and flow cytometry. Haematologica. 2005;90(10):1365-72. Epub 2005/10/13. PubMed PMID: 16219573.

160. Gratama JW, Bolhuis RL, Van 't Veer MB. Quality control of flow cytometric immunophenotyping of haematological malignancies. Clin Lab Haematol. 1999;21(3):155-60. PubMed PMID: 10448596.

161. Matarraz S, Paiva B, Diez-Campelo M, Barrena S, Jara-Acevedo M, Gutierrez ML, Sayagues JM, Sanchez ML, Barcena P, Garrastazul MP, Berruezo MJ, Duran JM, Cervero C, Garcia-Erce JA, Florensa L, Mendez GD, Gutierrez O, Del Canizo MC, van Dongen JJ, San Miguel JF, Orfao A. Immunophenotypic alterations of bone marrow myeloid cell compartments in multiple myeloma patients predict for myelodysplasia-associated cytogenetic alterations. Leukemia. 2014;28(8):1747-50. doi: 10.1038/leu.2014.103. PubMed PMID: 24625552.

162. Fernandez C, Santos-Silva MC, Lopez A, Matarraz S, Jara-Acevedo M, Ciudad J, Gutierrez ML, Sanchez ML, Salvador-Osuna C, Berruezo MJ, Diaz-Arias JA, Palomo-Hernandez AM, Colado E, Gonzalez N, Gallardo D, Asensio A, Garcia-Sanchez R, Saldana R, Cervero C, Carbone-Baneres A, Gutierrez O, Orfao A. Newly diagnosed adult AML and MPAL patients frequently show clonal residual hematopoiesis. Leukemia. 2013;27(11):2149-56. doi: 10.1038/leu.2013.109. PubMed PMID: 23579575.

163. Lima M, Teixeira MA, Queiros ML, Leite M, Santos AH, Justica B, Orfao A. Immunophenotypic characterization of normal blood CD56+lo versus CD56+hi NK-cell subsets and its impact on the understanding of their tissue distribution and functional properties. Blood cells, molecules & diseases. 2001;27(4):731-43. PubMed PMID: 11778657.

164. Deneys V, Mazzon AM, Marques JL, Benoit H, De Bruyere M. Reference values for peripheral blood B-lymphocyte subpopulations: a basis for multiparametric immunophenotyping of abnormal lymphocytes. J Immunol Methods. 2001;253(1-2):23-36. Epub 2001/06/01. PubMed PMID: 11384666.

165. Lima M, Almeida J, dos Anjos Teixeira M, Queiros ML, Justica B, Orfao A. The "ex vivo" patterns of CD2/CD7, CD57/CD11c, CD38/CD11b, CD45RA/CD45RO, and CD11a/HLA-DR expression identify acute/early and chronic/late NK-cell activation states. Blood cells, molecules & diseases. 2002;28(2):181-90. Epub 2002/06/18. PubMed PMID: 12064914..

166. Gorczyca W, Weisberger J, Liu Z, Tsang P, Hossein M, Wu CD, Dong H, Wong JY, Tugulea S, Dee S, Melamed MR, Darzynkiewicz Z. An approach to diagnosis of T-cell lymphoproliferative disorders by flow cytometry. Cytometry. 2002;50(3):177-90. Epub 2002/07/13. doi: 10.1002/cyto.10003. PubMed PMID: 12116341.

167. Bueno C, Almeida J, Lucio P, Marco J, Garcia R, de Pablos JM, Parreira A, Ramos F, Ruiz-Cabello F, Suarez-Vilela D, San Miguel JF, Orfao A. Incidence and characteristics of CD4(+)/HLA DRhi dendritic cell malignancies. Haematologica. 2004;89(1):58-69. Epub 2004/02/03. PubMed PMID: 14754607.

168. Barrena S, Almeida J, Yunta M, Lopez A, Fernandez-Mosteirin N, Giralt M, Romero M, Perdiguer L, Delgado M, Orfao A, Lazo PA. Aberrant expression of tetraspanin molecules in B-cell chronic lymphoproliferative disorders and its correlation with normal B-cell maturation. Leukemia. 2005;19(8):1376-83. Epub 2005/06/03. doi: 10.1038/sj.leu.2403822. PubMed PMID: 15931266.

169. Cady FM, Morice WG. Flow cytometric assessment of T-cell chronic lymphoproliferative disorders. Clin Lab Med. 2007;27(3):513-32. Epub 2007/07/31. doi: 10.1016/j.cll.2007.05.004. PubMed PMID: 17658405.

170. Stetler-Stevenson M, Ahmad E, Barnett D, Braylan R, DiGiuseppe J, Marti G, Menozzi D, Oldaker T, Orfao A, Rabellino E, Stone E, Walker C. H43-A2: Clinical flow cytometric analysis of neoplastic hematolymphoid cells; Approved guideline – Second edition. . National Institute of Health. 2007;27(11):1-96.

171. Loken MR, van de Loosdrecht A, Ogata K, Orfao A, Wells DA. Flow cytometry in myelodysplastic syndromes: report from a working conference. Leuk Res. 2008;32(1):5-17. PubMed PMID: 17576013.

172. Matarraz S, Lopez A, Barrena S, Fernandez C, Jensen E, Flores J, Barcena P, Rasillo A, Sayagues JM, Sanchez ML, Hernandez-Campo P, Hernandez Rivas JM, Salvador C, Fernandez-Mosteirin N, Giralt M, Perdiguer L, Orfao A. The immunophenotype of different immature, myeloid and B-cell lineage-committed CD34+ hematopoietic cells allows discrimination between normal/reactive and myelodysplastic syndrome precursors. Leukemia. 2008;22(6):1175-83. PubMed PMID: 18337765.

173. Paiva B, Vidriales MB, Perez JJ, Mateo G, Montalban MA, Mateos MV, Blade J, Lahuerta JJ, Orfao A, San Miguel JF, group GEMcs, group Pcs. Multiparameter flow cytometry quantification of bone marrow plasma cells at diagnosis provides more prognostic information than morphological assessment in myeloma patients. Haematologica. 2009;94(11):1599-602. Epub 2009/11/03. doi: 10.3324/haematol.2009.009100. PubMed PMID: 19880781; PubMed Central PMCID: PMC2770972.

174. Matarraz S, Lopez A, Barrena S, Fernandez C, Jensen E, Flores-Montero J, Rasillo A, Sayagues JM, Sanchez ML, Barcena P, Hernandez-Rivas JM, Salvador C, Fernandez-Mosteirin N, Giralt M, Perdiguer L, Laranjeira P, Paiva A, Orfao A. Bone marrow cells from myelodysplastic syndromes show altered immunophenotypic profiles that may contribute to the diagnosis and prognostic stratification of the disease: a pilot study on a series of 56 patients. Cytometry B Clin Cytom. 2010;78(3):154-68. Epub 2010/03/04. doi: 10.1002/cyto.b.20513. PubMed PMID: 20198685.

175. Barrena S, Almeida J, Del Carmen Garcia-Macias M, Lopez A, Rasillo A, Sayagues JM, Rivas RA, Gutierrez ML, Ciudad J, Flores T, Balanzategui A, Caballero MD, Orfao A. Flow cytometry immunophenotyping of fine-needle aspiration specimens: utility in the diagnosis and classification of non-Hodgkin lymphomas. Histopathology. 2011;58(6):906-18. Epub 2011/03/29. doi: 10.1111/j.1365-2559.2011.03804.x. PubMed PMID: 21438908.

176. Ravandi F, O'Brien S. Chronic lymphoid leukemias other than chronic lymphocytic leukemia: diagnosis and treatment. Mayo Clin Proc. 2005;80(12):1660-74. Epub 2005/12/14. doi: 10.4065/80.12.1660. PubMed PMID: 16342661.

177. Ravandi F, Kantarjian H, Jones D, Dearden C, Keating M, O'Brien S. Mature T-cell leukemias. Cancer. 2005;104(9):1808-18. Epub 2005/09/02. doi: 10.1002/cncr.21405. PubMed PMID: 16136598.

178. van Lochem EG, van der Velden VH, Wind HK, te Marvelde JG, Westerdaal NA, van Dongen JJ. Immunophenotypic differentiation patterns of normal hematopoiesis in human bone marrow: reference patterns for age-related changes and disease-induced shifts. Cytometry B Clin Cytom. 2004;60(1):1-13. Epub 2004/06/29. doi: 10.1002/cyto.b.20008. PubMed PMID: 15221864.

179. Allen CD, Okada T, Cyster JG. Germinal-center organization and cellular dynamics. Immunity. 2007;27(2):190-202. Epub 2007/08/29. doi: 10.1016/j.immuni.2007.07.009. PubMed PMID: 17723214; PubMed Central PMCID: PMC2242846.

180. Sanz I, Wei C, Lee FE, Anolik J. Phenotypic and functional heterogeneity of human memory B cells. Semin Immunol. 2008;20(1):67-82. Epub 2008/02/09. doi: 10.1016/j.smim.2007.12.006. PubMed PMID: 18258454; PubMed Central PMCID: PMC2440717.

181. Klein U, Rajewsky K, Kuppers R. Human immunoglobulin (Ig)M+IgD+ peripheral blood B cells expressing the CD27 cell surface antigen carry somatically mutated variable region genes: CD27 as a general marker for somatically mutated (memory) B cells. J Exp Med. 1998;188(9):1679-89. PubMed PMID: 9802980; PubMed Central PMCID: PMC2212515.

182. Heinonen KM, Perreault C. Development and functional properties of thymic and extrathymic T lymphocytes. Critical reviews in immunology. 2008;28(5):441-66. PubMed PMID: 19166388.

183. Lima M, Almeida J, Santos AH, dos Anjos Teixeira M, Alguero MC, Queiros ML, Balanzategui A, Justica B, Gonzalez M, San Miguel JF, Orfao A. Immunophenotypic analysis of the TCR-Vbeta repertoire in 98 persistent expansions of CD3(+)/TCR-alphabeta(+) large granular lymphocytes: utility in assessing clonality and insights into the pathogenesis of the disease. Am J Pathol. 2001;159(5):1861-8. Epub 2001/11/07. PubMed PMID: 11696446; PubMed Central PMCID: PMC1867049.

184. Michie CA, McLean A, Alcock C, Beverley PC. Lifespan of human lymphocyte subsets defined by CD45 isoforms. Nature. 1992;360(6401):264-5. doi: 10.1038/360264a0. PubMed PMID: 1436108.

185. Sallusto F, Lenig D, Forster R, Lipp M, Lanzavecchia A. Two subsets of memory T lymphocytes with distinct homing potentials and effector functions. Nature. 1999;401(6754):708-12. doi: 10.1038/44385. PubMed PMID: 10537110.

186. Freud AG, Yu J, Caligiuri MA. Human natural killer cell development in secondary lymphoid tissues. Semin Immunol. 2014;26(2):132-7. doi: 10.1016/j.smim.2014.02.008. PubMed PMID: 24661538; PubMed Central PMCID: PMC4010312.

187. Caligiuri MA. Human natural killer cells. Blood. 2008;112(3):461-9. doi: 10.1182/blood-2007-09-077438. PubMed PMID: 18650461; PubMed Central PMCID: PMC2481557.

188. Fehniger TA, Cooper MA, Nuovo GJ, Cella M, Facchetti F, Colonna M, Caligiuri MA. CD56bright natural killer cells are present in human lymph nodes and are activated by T cell-derived IL-2: a potential new link between adaptive and innate immunity. Blood. 2003;101(8):3052-7. doi: 10.1182/blood-2002-09-2876. PubMed PMID: 12480696.

189. Ferlazzo G, Thomas D, Lin SL, Goodman K, Morandi B, Muller WA, Moretta A, Munz C. The abundant NK cells in human secondary lymphoid tissues require activation to express killer cell Ig-like receptors and become cytolytic. J Immunol. 2004;172(3):1455-62. PubMed PMID: 14734722.

190. Freud AG, Becknell B, Roychowdhury S, Mao HC, Ferketich AK, Nuovo GJ, Hughes TL, Marburger TB, Sung J, Baiocchi RA, Guimond M, Caligiuri MA. A human CD34(+) subset resides in lymph nodes and differentiates into CD56bright natural killer cells. Immunity. 2005;22(3):295-304. doi: 10.1016/j.immuni.2005.01.013. PubMed PMID: 15780987.

191. Geiselhart A, Dietl J, Marzusch K, Ruck P, Ruck M, Horny HP, Kaiserling E, Handgretinger R. Comparative analysis of the immunophenotypes of decidual and peripheral blood large granular lymphocytes and T cells during early human pregnancy. American journal of reproductive immunology. 1995;33(4):315-22. PubMed PMID: 7546250.

192. King A, Gardner L, Sharkey A, Loke YW. Expression of CD3 epsilon, CD3 zeta, and RAG-1/RAG-2 in decidual CD56+ NK cells. Cellular immunology. 1998;183(2):99-105. PubMed PMID: 9606993.

193. Sedlmayr P, Schallhammer L, Hammer A, Wilders-Truschnig M, Wintersteiger R, Dohr G. Differential phenotypic properties of human peripheral blood CD56dim+ and CD56bright+ natural killer cell subpopulations. International archives of allergy and immunology. 1996;110(4):308-13. PubMed PMID: 8768796.

194. Cooper MA, Fehniger TA, Turner SC, Chen KS, Ghaheri BA, Ghayur T, Carson WE, Caligiuri MA. Human natural killer cells: a unique innate immunoregulatory role for the CD56(bright) subset. Blood. 2001;97(10):3146-51. PubMed PMID: 11342442.

195. Jacobs R, Hintzen G, Kemper A, Beul K, Kempf S, Behrens G, Sykora KW, Schmidt RE. CD56bright cells differ in their KIR repertoire and cytotoxic features from CD56dim NK cells. Eur J Immunol. 2001;31(10):3121-7. PubMed PMID: 11592089.

196. Kuppers R. Mechanisms of B-cell lymphoma pathogenesis. Nat Rev Cancer. 2005;5(4):251-62. Epub 2005/04/02. doi: 10.1038/nrc1589. PubMed PMID: 15803153.

197. Lenz G, Staudt LM. Aggressive lymphomas. The New England journal of medicine. 2010;362(15):1417-29. Epub 2010/04/16. doi: 10.1056/NEJMra0807082. PubMed PMID: 20393178.

198. Li CY, Yam LT. Cytochemistry and immunochemistry in hematologic diagnoses. Hematol Oncol Clin North Am. 1994;8(4):665-81. Epub 1994/08/01. PubMed PMID: 7961285.

199. Bellido M, Rubiol E, Ubeda J, Estivill C, Lopez O, Manteiga R, Nomdedeu JF. Rapid and simple immunophenotypic characterization of lymphocytes using a new test. Haematologica. 1998;83(8):681-5. Epub 1998/10/30. PubMed PMID: 9793249.

200. Braylan RC. Impact of flow cytometry on the diagnosis and characterization of lymphomas, chronic lymphoproliferative disorders and plasma cell neoplasias. Cytometry A. 2004;58(1):57-61. Epub 2004/03/03. doi: 10.1002/cyto.a.10101. PubMed PMID: 14994222.

201. Perea G, Altes A, Bellido M, Aventin A, Bordes R, Ayats R, Remacha AF, Espinosa I, Briones J, Sierra J, Nomdedeu JF. Clinical utility of bone marrow flow cytometry in B-cell non-Hodgkin lymphomas (B-NHL). Histopathology. 2004;45(3):268-74. doi: 10.1111/j.1365-2559.2004.01937.x. PubMed PMID: 15330805.

202. Demurtas A, Accinelli G, Pacchioni D, Godio L, Novero D, Bussolati G, Palestro G, Papotti M, Stacchini A. Utility of flow cytometry immunophenotyping in fine-needle aspirate cytologic diagnosis of non-Hodgkin lymphoma: A series of 252 cases and review of the literature. Appl Immunohistochem Mol Morphol. 2010;18(4):311-22. Epub 2009/02/28. doi: 10.1097/PAI.0b013e3181827da8. PubMed PMID: 19247181.

203. Marti GE, Rawstron AC, Ghia P, Hillmen P, Houlston RS, Kay N, Schleinitz TA, Caporaso N, International Familial CLLC. Diagnostic criteria for monoclonal B-cell lymphocytosis. Br J Haematol. 2005;130(3):325-32. doi: 10.1111/j.1365-2141.2005.05550.x. PubMed PMID: 16042682.

204. Almeida J, Nieto WG, Teodosio C, Pedreira CE, Lopez A, Fernandez-Navarro P, Nieto A, Rodriguez-Caballero A, Munoz-Criado S, Jara-Acevedo M, Romero A, Orfao A. CLL-like B-lymphocytes are systematically present at very low numbers in peripheral blood of healthy adults. Leukemia. 2011;25(4):718-22. Epub 2011/01/15. doi: 10.1038/leu.2010.305. PubMed PMID: 21233839.

205. Langerak AW, van Den Beemd R, Wolvers-Tettero IL, Boor PP, van Lochem EG, Hooijkaas H, van Dongen JJ. Molecular and flow cytometric analysis of the Vbeta repertoire for clonality assessment in mature TCRalphabeta T-cell proliferations. Blood. 2001;98(1):165-73. Epub 2001/06/22. PubMed PMID: 11418476.

206. Sandberg Y, Almeida J, Gonzalez M, Lima M, Barcena P, Szczepanski T, van Gastel-Mol EJ, Wind H, Balanzategui A, van Dongen JJ, Miguel JF, Orfao A, Langerak AW. TCRgammadelta+ large granular lymphocyte leukemias reflect the spectrum of normal antigen-selected TCRgammadelta+ T-cells. Leukemia. 2006;20(3):505-13. Epub 2006/01/27. doi: 10.1038/sj.leu.2404112. PubMed PMID: 16437145.

207. Comans-Bitter WM, de Groot R, van den Beemd R, Neijens HJ, Hop WC, Groeneveld K, Hooijkaas H, van Dongen JJ. Immunophenotyping of blood lymphocytes in childhood. Reference values for lymphocyte subpopulations. The Journal of pediatrics. 1997;130(3):388-93. PubMed PMID: 9063413.

208. Ortonne N, Buyukbabani N, Delfau-Larue MH, Bagot M, Wechsler J. Value of the CD8-CD3 ratio for the diagnosis of mycosis fungoides. Mod Pathol. 2003;16(9):857-62. Epub 2003/09/19. doi: 10.1097/01.MP.0000084112.81779.BB. PubMed PMID: 13679448.

209. Jamal S, Picker LJ, Aquino DB, McKenna RW, Dawson DB, Kroft SH. Immunophenotypic analysis of peripheral T-cell neoplasms. A multiparameter flow cytometric approach. Am J Clin Pathol. 2001;116(4):512-26. Epub 2001/10/17. doi: 10.1309/QF6N-VAQW-N74H-4JE2. PubMed PMID: 11601136.

210. Lima M, Almeida J, dos Anjos Teixeira M, Queiros ML, Santos AH, Fonseca S, Balanzategui A, Justica B, Orfao A. Utility of flow cytometry immunophenotyping and DNA ploidy studies for diagnosis and characterization of blood involvement in CD4+ Sezary's syndrome. Haematologica. 2003;88(8):874-87. Epub 2003/08/26. PubMed PMID: 12935975.

211. van Dongen JJ, Langerak AW, Bruggemann M, Evans PA, Hummel M, Lavender FL, Delabesse E, Davi F, Schuuring E, Garcia-Sanz R, van Krieken JH, Droese J, Gonzalez D, Bastard C, White HE, Spaargaren M, Gonzalez M, Parreira A, Smith JL, Morgan GJ, Kneba M, Macintyre EA. Design and standardization of PCR primers and protocols for detection of clonal immunoglobulin and T-cell receptor gene recombinations in suspect lymphoproliferations: report of the BIOMED-2 Concerted Action BMH4-CT98-3936. Leukemia. 2003;17(12):2257-317. Epub 2003/12/13. doi: 10.1038/sj.leu.2403202. PubMed PMID: 14671650.

212. Posnett DN, Sinha R, Kabak S, Russo C. Clonal populations of T cells in normal elderly humans: the T cell equivalent to "benign monoclonal gammapathy". J Exp Med. 1994;179(2):609-18. PubMed PMID: 8294871; PubMed Central PMCID: PMC2191374.

213. Shimomura T, Fujimura K, Takafuta T, Fujii T, Katsutani S, Noda M, Fujimoto T, Kuramoto A. Oligoclonal accumulation of T cells in peripheral blood from patients with idiopathic thrombocytopenic purpura. Br J Haematol. 1996;95(4):732-7. PubMed PMID: 8982053.

214. Direskeneli H, Eksioglu-Demiralp E, Kibaroglu A, Yavuz S, Ergun T, Akoglu T. Oligoclonal T cell expansions in patients with Behcet's disease. Clinical and experimental immunology. 1999;117(1):166-70. PubMed PMID: 10403931; PubMed Central PMCID: PMC1905484.

215. van den Beemd R, Boor PP, van Lochem EG, Hop WC, Langerak AW, Wolvers-Tettero IL, Hooijkaas H, van Dongen JJ. Flow cytometric analysis of the Vbeta repertoire in healthy controls. Cytometry. 2000;40(4):336-45. Epub 2000/08/05. PubMed PMID: 10918284.

216. Khan N, Shariff N, Cobbold M, Bruton R, Ainsworth JA, Sinclair AJ, Nayak L, Moss PA. Cytomegalovirus seropositivity drives the CD8 T cell repertoire toward greater clonality in healthy elderly individuals. J Immunol. 2002;169(4):1984-92. PubMed PMID: 12165524.

217. Kovaiou RD, Weiskirchner I, Keller M, Pfister G, Cioca DP, Grubeck-Loebenstein B. Age-related differences in phenotype and function of CD4+ T cells are due to a phenotypic shift from naive to memory effector CD4+ T cells. Int Immunol. 2005;17(10):1359-66. doi: 10.1093/intimm/dxh314. PubMed PMID: 16141244.

218. Vallejo AN. Age-dependent alterations of the T cell repertoire and functional diversity of T cells of the aged. Immunol Res. 2006;36(1-3):221-8. doi: 10.1385/IR:36:1:221. PubMed PMID: 17337782.

219. McLean-Tooke A, Barge D, Spickett GP, Gennery AR. T cell receptor Vbeta repertoire of T lymphocytes and T regulatory cells by flow cytometric analysis in healthy children. Clinical and experimental immunology. 2008;151(1):190-8. doi: 10.1111/j.1365-2249.2007.03536.x. PubMed PMID: 17983445; PubMed Central PMCID: PMC2276915.

220. Bristeau-Leprince A, Mateo V, Lim A, Magerus-Chatinet A, Solary E, Fischer A, Rieux-Laucat F, Gougeon ML. Human TCR alpha/beta+ CD4-CD8- double-negative T cells in patients with autoimmune lymphoproliferative syndrome express restricted Vbeta TCR diversity and are clonally related to CD8+ T cells. J Immunol. 2008;181(1):440-8. PubMed PMID: 18566410.

221. Okajima M, Wada T, Nishida M, Yokoyama T, Nakayama Y, Hashida Y, Shibata F, Tone Y, Ishizaki A, Shimizu M, Saito T, Ohta K, Toma T, Yachie A. Analysis of T cell receptor Vbeta diversity in peripheral CD4 and CD8 T lymphocytes in patients with autoimmune thyroid diseases. Clinical and experimental immunology. 2009;155(2):166-72. doi: 10.1111/j.1365-2249.2008.03842.x. PubMed PMID: 19040601; PubMed Central PMCID: PMC2675246.

222. Kawa-Ha K, Ishihara S, Ninomiya T, Yumura-Yagi K, Hara J, Murayama F, Tawa A, Hirai K. CD3-negative lymphoproliferative disease of granular lymphocytes containing Epstein-Barr viral DNA. The Journal of clinical investigation. 1989;84(1):51-5. doi: 10.1172/JCI114168. PubMed PMID: 2544630; PubMed Central PMCID: PMC303951.

223. Siu LL, Chan JK, Kwong YL. Natural killer cell malignancies: clinicopathologic and molecular features. Histology and histopathology. 2002;17(2):539-54. PubMed PMID: 11962758.

224. Zambello R, Falco M, Della Chiesa M, Trentin L, Carollo D, Castriconi R, Cannas G, Carlomagno S, Cabrelle A, Lamy T, Agostini C, Moretta A, Semenzato G, Vitale M. Expression and function of KIR and natural cytotoxicity receptors in NK-type lymphoproliferative diseases of granular lymphocytes. Blood. 2003;102(5):1797-805. Epub 2003/05/17. doi: 10.1182/blood-2002-12-3898. PubMed PMID: 12750175.

225. Gattazzo C, Teramo A, Miorin M, Scquizzato E, Cabrelle A, Balsamo M, Agostini C, Vendrame E, Facco M, Albergoni MP, Trentin L, Vitale M, Semenzato G, Zambello R. Lack of expression of inhibitory KIR3DL1 receptor in patients with natural killer cell-type lymphoproliferative disease of granular lymphocytes. Haematologica. 2010;95(10):1722-9. Epub 2010/04/23. doi: 10.3324/haematol.2010.023358. PubMed PMID: 20410181; PubMed Central PMCID: PMC2948098.

226. Boudewijns M, van Dongen JJ, Langerak AW. The human androgen receptor X-chromosome inactivation assay for clonality diagnostics of natural killer cell proliferations. J Mol Diagn. 2007;9(3):337-44. Epub 2007/06/27. doi: 10.2353/jmoldx.2007.060155. PubMed PMID: 17591933; PubMed Central PMCID: PMC1899426.

227. Kim HS, Kim KH, Chang MH, Ji SH, Lim do H, Kim K, Kim SJ, Ko Y, Ki CS, Jo SJ, Lee JW, Kim WS. Whole blood Epstein-Barr virus DNA load as a diagnostic and prognostic surrogate: extranodal natural killer/T-cell lymphoma. Leuk Lymphoma. 2009;50(5):757-63. Epub 2009/03/31. doi: 10.1080/10428190902803669. PubMed PMID: 19330658.

228. Epling-Burnette PK, Painter JS, Chaurasia P, Bai F, Wei S, Djeu JY, Loughran TP, Jr. Dysregulated NK receptor expression in patients with lymphoproliferative disease of granular lymphocytes. Blood. 2004;103(9):3431-9. Epub 2004/01/17. doi: 10.1182/blood-2003-02-0400. PubMed PMID: 14726391.

229. Fischer L, Hummel M, Burmeister T, Schwartz S, Thiel E. Skewed expression of natural-killer (NK)-associated antigens on lymphoproliferations of large granular lymphocytes (LGL). Hematol Oncol. 2006;24(2):78-85. Epub 2006/04/07. doi: 10.1002/hon.777. PubMed PMID: 16598823.

230. Yonescu R, Hristov AC, Ahmad A, Overby A, Thomas GH, Griffin CA. Cytogenetic characterization of natural killer cell leukemia. Cancer genetics and cytogenetics. 2008;183(2):125-30. doi: 10.1016/j.cancergencyto.2008.02.014. PubMed PMID: 18503833.

231. Foucar K. Mature T-cell leukemias including T-prolymphocytic leukemia, adult T-cell leukemia/lymphoma, and Sezary syndrome. Am J Clin Pathol. 2007;127(4):496-510. Epub 2007/03/21. doi: 10.1309/KWJYBCCGTB90B6AE. PubMed PMID: 17369126.

232. Smith A, Howell D, Patmore R, Jack A, Roman E. Incidence of haematological malignancy by sub-type: a report from the Haematological Malignancy Research Network. British journal of cancer. 2011;105(11):1684-92. doi: 10.1038/bjc.2011.450. PubMed PMID: 22045184; PubMed Central PMCID: PMC3242607.

233. Rudiger T, Geissinger E, Muller-Hermelink HK. 'Normal counterparts' of nodal peripheral T-cell lymphoma. Hematol Oncol. 2006;24(4):175-80. Epub 2006/06/20. doi: 10.1002/hon.786. PubMed PMID: 16783841.

234. Jaffe ES. The 2008 WHO classification of lymphomas: implications for clinical practice and translational research. Hematology / the Education Program of the American Society of Hematology American Society of Hematology Education Program. 2009:523-31. Epub 2009/12/17. doi: 10.1182/asheducation-2009.1.523. PubMed PMID: 20008237.

235. Grogg KL, Attygalle AD, Macon WR, Remstein ED, Kurtin PJ, Dogan A. Angioimmunoblastic T-cell lymphoma: a neoplasm of germinal-center T-helper cells? Blood. 2005;106(4):1501-2. Epub 2005/08/05. doi: 10.1182/blood-2005-03-1083. PubMed PMID: 16079436; PubMed Central PMCID: PMC1895208.

236. de Leval L, Bisig B, Thielen C, Boniver J, Gaulard P. Molecular classification of T-cell lymphomas. Critical reviews in oncology/hematology. 2009;72(2):125-43. Epub 2009/02/24. doi: 10.1016/j.critrevonc.2009.01.002. PubMed PMID: 19233683.

237. Yu H, Shahsafaei A, Dorfman DM. Germinal-center T-helper-cell markers PD-1 and CXCL13 are both expressed by neoplastic cells in angioimmunoblastic T-cell lymphoma. Am J Clin Pathol. 2009;131(1):33-41. Epub 2008/12/20. doi: 10.1309/AJCP62WRKERPXDRT. PubMed PMID: 19095563.

238. Herling M, Khoury JD, Washington LT, Duvic M, Keating MJ, Jones D. A systematic approach to diagnosis of mature T-cell leukemias reveals heterogeneity among WHO categories. Blood. 2004;104(2):328-35. Epub 2004/03/27. doi: 10.1182/blood-2004-01-0002. PubMed PMID: 15044256.

239. Savage KJ. Peripheral T-cell lymphomas. Blood reviews. 2007;21(4):201-16. Epub 2007/05/22. doi: 10.1016/j.blre.2007.03.001. PubMed PMID: 17512649.

240. Herling M, Patel KA, Teitell MA, Konopleva M, Ravandi F, Kobayashi R, Jones D. High TCL1 expression and intact T-cell receptor signaling define a hyperproliferative subset of T-cell prolymphocytic leukemia. Blood. 2008;111(1):328-37. Epub 2007/09/25. doi: 10.1182/blood-2007-07-101519. PubMed PMID: 17890451; PubMed Central PMCID: PMC2200815.

241. Lima M, Almeida J, Dos Anjos Teixeira M, Alguero Md Mdel C, Santos AH, Balanzategui A, Queiros ML, Barcena P, Izarra A, Fonseca S, Bueno C, Justica B, Gonzalez M, San Miguel JF, Orfao A. TCRalphabeta+/CD4+ large granular lymphocytosis: a new clonal T-cell lymphoproliferative disorder. Am J Pathol. 2003;163(2):763-71. Epub 2003/07/24. doi: S0002-9440(10)63703-0 [pii]. PubMed PMID: 12875995; PubMed Central PMCID: PMC1868208.

242. Morice WG, Kurtin PJ, Leibson PJ, Tefferi A, Hanson CA. Demonstration of aberrant T-cell and natural killer-cell antigen expression in all cases of granular lymphocytic leukaemia. Br J Haematol. 2003;120(6):1026-36. Epub 2003/03/22. doi: 4201 [pii]. PubMed PMID: 12648073.

243. Rose MG, Berliner N. T-cell large granular lymphocyte leukemia and related disorders. The oncologist. 2004;9(3):247-58. PubMed PMID: 15169980.

244. Lundell R, Hartung L, Hill S, Perkins SL, Bahler DW. T-cell large granular lymphocyte leukemias have multiple phenotypic abnormalities involving pan-T-cell antigens and receptors for MHC molecules. Am J Clin Pathol. 2005;124(6):937-46. Epub 2006/01/19. PubMed PMID: 16416744.

245. Bangham CR, Toulza F. Adult T cell leukemia/lymphoma: FoxP3(+) cells and the cell-mediated immune response to HTLV-1. Advances in cancer research. 2011;111:163-82. doi: 10.1016/B978-0-12-385524-4.00004-0. PubMed PMID: 21704832.

246. Wright DH. Enteropathy associated T cell lymphoma. Cancer surveys. 1997;30:249-61. PubMed PMID: 9547996.

247. Katoh A, Ohshima K, Kanda M, Haraoka S, Sugihara M, Suzumiya J, Kawasaki C, Shimazaki K, Ikeda S, Kikuchi M. Gastrointestinal T cell lymphoma: predominant cytotoxic phenotypes, including alpha/beta, gamma/delta T cell and natural killer cells. Leuk Lymphoma. 2000;39(1-2):97-111. doi: 10.3109/10428190009053543. PubMed PMID: 10975388.

248. Yuan CM, Stein S, Glick JH, Wasik MA. Natural killer-like T-cell lymphoma of the small intestine with a distinct immunophenotype and lack of association with gluten-sensitive enteropathy. Archives of pathology & laboratory medicine. 2003;127(3):e142-6. doi: 10.1043/0003-9985(2003)127<e142:NKTLOT>2.0.CO;2. PubMed PMID: 12653603.

249. Ferreri AJ, Zinzani PL, Govi S, Pileri SA. Enteropathy-associated T-cell lymphoma. Critical reviews in oncology/hematology. 2011;79(1):84-90. doi: 10.1016/j.critrevonc.2010.06.006. PubMed PMID: 20655757.

250. Wei SZ, Liu TH, Wang DT, Cao JL, Luo YF, Liang ZY. Hepatosplenic gammadelta T-cell lymphoma. World journal of gastroenterology. 2005;11(24):3729-34. PubMed PMID: 15968729; PubMed Central PMCID: PMC4316025.

251. Sokolowska-Wojdylo M, Wenzel J, Gaffal E, Steitz J, Roszkiewicz J, Bieber T, Tuting T. Absence of CD26 expression on skin-homing CLA+ CD4+ T lymphocytes in peripheral blood is a highly sensitive marker for early diagnosis and therapeutic monitoring of patients with Sezary syndrome. Clinical and experimental dermatology. 2005;30(6):702-6. Epub 2005/10/04. doi: 10.1111/j.1365-2230.2005.01904.x. PubMed PMID: 16197392.

252. Kelemen K, Guitart J, Kuzel TM, Goolsby CL, Peterson LC. The usefulness of CD26 in flow cytometric analysis of peripheral blood in Sezary syndrome. Am J Clin Pathol. 2008;129(1):146-56. Epub 2007/12/20. doi: 10.1309/05GFG3LY3VYCDMEY. PubMed PMID: 18089499.

253. de Leval L, Gaulard P. CD30+ lymphoproliferative disorders. Haematologica. 2010;95(10):1627-30. Epub 2010/10/05. doi: 10.3324/haematol.2010.029256. PubMed PMID: 20884717; PubMed Central PMCID: PMC2948085.

254. Foss FM, Zinzani PL, Vose JM, Gascoyne RD, Rosen ST, Tobinai K. Peripheral T-cell lymphoma. Blood. 2011;117(25):6756-67. Epub 2011/04/16. doi: 10.1182/blood-2010-05-231548. PubMed PMID: 21493798.

255. Gaulard P, de Leval L. Pathology of peripheral T-cell lymphomas: where do we stand? Semin Hematol. 2014;51(1):5-16. doi: 10.1053/j.seminhematol.2013.11.003. PubMed PMID: 24468311.

256. Greer JP, Mosse CA. Natural killer-cell neoplasms. Curr Hematol Malig Rep. 2009;4(4):245-52. Epub 2010/04/29. doi: 10.1007/s11899-009-0032-3. PubMed PMID: 20425414.

257. Matsubara A, Matsumoto M, Takada K, Hato T, Hasegawa H, Tamai T, Yasukawa M, Fujita S. Acute transformation of chronic large granular lymphocyte leukemia into an aggressive form associated with preferential organ involvement. Acta Haematol. 1994;91(4):206-10. Epub 1994/01/01. PubMed PMID: 7976120.

258. Lim MS, de Leval L, Quintanilla-Martinez L. Commentary on the 2008 WHO classification of mature T- and NK-cell neoplasms. J Hematop. 2009. Epub 2009/08/12. doi: 10.1007/s12308-009-0034-z. PubMed PMID: 19669191; PubMed Central PMCID: PMC2725280.

259. Pascal V, Schleinitz N, Brunet C, Ravet S, Bonnet E, Lafarge X, Touinssi M, Reviron D, Viallard JF, Moreau JF, Dechanet-Merville J, Blanco P, Harle JR, Sampol J, Vivier E, Dignat-George F, Paul P. Comparative analysis of NK cell subset distribution in normal and lymphoproliferative disease of granular lymphocyte conditions. Eur J Immunol. 2004;34(10):2930-40. Epub 2004/09/16. doi: 10.1002/eji.200425146. PubMed PMID: 15368309.

260. Oshimi K. Progress in understanding and managing natural killer-cell malignancies. Br J Haematol. 2007;139(4):532-44. Epub 2007/10/06. doi: 10.1111/j.1365-2141.2007.06835.x. PubMed PMID: 17916099.

261. Barcena P, Jara-Acevedo M, Tabernero MD, Lopez A, Sanchez ML, Garcia-Montero AC, Munoz-Garcia N, Vidriales MB, Paiva A, Lecrevisse Q, Lima M, Langerak AW, Bottcher S, van Dongen JJ, Orfao A, Almeida J. Phenotypic profile of expanded NK cells in chronic lymphoproliferative disorders: a surrogate marker for NK-cell clonality. Oncotarget. 2015. doi: 10.18632/oncotarget.5480. PubMed PMID: 26556869.

262. Radbruch A, Muehlinghaus G, Luger EO, Inamine A, Smith KG, Dorner T, Hiepe F. Competence and competition: the challenge of becoming a long-lived plasma cell. Nat Rev Immunol. 2006;6(10):741-50. Epub 2006/09/16. doi: 10.1038/nri1886. PubMed PMID: 16977339.

263. Terstappen LW, Johnsen S, Segers-Nolten IM, Loken MR. Identification and characterization of plasma cells in normal human bone marrow by high-resolution flow cytometry. Blood. 1990;76(9):1739-47. Epub 1990/11/01. PubMed PMID: 2224123.

264. Almeida J, Orfao A, Mateo G, Ocqueteau M, Garcia-Sanz R, Moro MJ, Hernandez J, Ortega F, Borrego D, Barez A, Mejido M, San Miguel JF. Immunophenotypic and DNA content characteristics of plasma cells in multiple myeloma and monoclonal gammopathy of undetermined significance. Pathol Biol (Paris). 1999;47(2):119-27. Epub 1999/04/08. PubMed PMID: 10192879.

265. Wijdenes J, Vooijs WC, Clement C, Post J, Morard F, Vita N, Laurent P, Sun RX, Klein B, Dore JM. A plasmocyte selective monoclonal antibody (B-B4) recognizes syndecan-1. Br J Haematol. 1996;94(2):318-23. Epub 1996/08/01. PubMed PMID: 8759892.

266. Kyle RA, Rajkumar SV. Criteria for diagnosis, staging, risk stratification and response assessment of multiple myeloma. Leukemia. 2009;23(1):3-9. Epub 2008/10/31. doi: 10.1038/leu.2008.291. PubMed PMID: 18971951; PubMed Central PMCID: PMC2627786.

267. Harada H, Kawano MM, Huang N, Harada Y, Iwato K, Tanabe O, Tanaka H, Sakai A, Asaoku H, Kuramoto A. Phenotypic difference of normal plasma cells from mature myeloma cells. Blood. 1993;81(10):2658-63. Epub 1993/05/15. PubMed PMID: 8490175.

268. Pellat-Deceunynck C, Bataille R, Robillard N, Harousseau JL, Rapp MJ, Juge-Morineau N, Wijdenes J, Amiot M. Expression of CD28 and CD40 in human myeloma cells: a comparative study with normal plasma cells. Blood. 1994;84(8):2597-603. Epub 1994/10/15. PubMed PMID: 7522634.

269. Lima M, Teixeira Mdos A, Fonseca S, Goncalves C, Guerra M, Queiros ML, Santos AH, Coutinho A, Pinho L, Marques L, Cunha M, Ribeiro P, Xavier L, Vieira H, Pinto P, Justica B. Immunophenotypic aberrations, DNA content, and cell cycle analysis of plasma cells in patients with myeloma and monoclonal gammopathies. Blood cells, molecules & diseases. 2000;26(6):634-45. Epub 2001/05/19. doi: 10.1006/bcmd.2000.0342. PubMed PMID: 11358356.

270. Ely SA, Knowles DM. Expression of CD56/neural cell adhesion molecule correlates with the presence of lytic bone lesions in multiple myeloma and distinguishes myeloma from monoclonal gammopathy of undetermined significance and lymphomas with plasmacytoid differentiation. Am J Pathol. 2002;160(4):1293-9. Epub 2002/04/12. PubMed PMID: 11943714; PubMed Central PMCID: PMC1867213.

271. Mateo G, Castellanos M, Rasillo A, Gutierrez NC, Montalban MA, Martin ML, Hernandez JM, Lopez-Berges MC, Montejano L, Blade J, Mateos MV, Sureda A, de la Rubia J, Diaz-Mediavilla J, Pandiella A, Lahuerta JJ, Orfao A, San Miguel JF. Genetic abnormalities and patterns of antigenic expression in multiple myeloma. Clin Cancer Res. 2005;11(10):3661-7. Epub 2005/05/18. doi: 10.1158/1078-0432.CCR-04-1489. PubMed PMID: 15897562.

272. Moreau P, Robillard N, Jego G, Pellat C, Le Gouill S, Thoumi S, Avet-Loiseau H, Harousseau JL, Bataille R. Lack of CD27 in myeloma delineates different presentation and outcome. Br J Haematol. 2006;132(2):168-70. Epub 2006/01/10. doi: 10.1111/j.1365-2141.2005.05849.x. PubMed PMID: 16398651.

273. Bataille R, Jego G, Robillard N, Barille-Nion S, Harousseau JL, Moreau P, Amiot M, Pellat-Deceunynck C. The phenotype of normal, reactive and malignant plasma cells. Identification of "many and multiple myelomas" and of new targets for myeloma therapy. Haematologica. 2006;91(9):1234-40. Epub 2006/09/08. PubMed PMID: 16956823.

274. Bahlis NJ, King AM, Kolonias D, Carlson LM, Liu HY, Hussein MA, Terebelo HR, Byrne GE, Jr., Levine BL, Boise LH, Lee KP. CD28-mediated regulation of multiple myeloma cell proliferation

and survival. Blood. 2007;109(11):5002-10. Epub 2007/02/22. doi: 10.1182/blood-2006-03-012542. PubMed PMID: 17311991; PubMed Central PMCID: PMC1885531.

275. Mateo G, Montalban MA, Vidriales MB, Lahuerta JJ, Mateos MV, Gutierrez N, Rosinol L, Montejano L, Blade J, Martinez R, de la Rubia J, Diaz-Mediavilla J, Sureda A, Ribera JM, Ojanguren JM, de Arriba F, Palomera L, Terol MJ, Orfao A, San Miguel JF, Group PS, Group GEMS. Prognostic value of immunophenotyping in multiple myeloma: a study by the PETHEMA/GEM cooperative study groups on patients uniformly treated with high-dose therapy. J Clin Oncol. 2008;26(16):2737-44. Epub 2008/04/30. doi: 10.1200/JCO.2007.15.4120. PubMed PMID: 18443352.

276. Bataille R, Pellat-Deceunynck C, Robillard N, Avet-Loiseau H, Harousseau JL, Moreau P. CD117 (c-kit) is aberrantly expressed in a subset of MGUS and multiple myeloma with unexpectedly good prognosis. Leuk Res. 2008;32(3):379-82. Epub 2007/09/05. doi: 10.1016/j.leukres.2007.07.016. PubMed PMID: 17767956.

277. Perez-Andres M, Almeida J, Martin-Ayuso M, De Las Heras N, Moro MJ, Martin-Nunez G, Galende J, Cuello R, Abuin I, Moreno I, Dominguez M, Hernandez J, Mateo G, San Miguel JF, Orfao A. Soluble and membrane levels of molecules involved in the interaction between clonal plasma cells and the immunological microenvironment in multiple myeloma and their association with the characteristics of the disease. Int J Cancer. 2009;124(2):367-75. Epub 2008/11/13. doi: 10.1002/ijc.23941. PubMed PMID: 19003959.

278. Cannizzo E, Bellio E, Sohani AR, Hasserjian RP, Ferry JA, Dorn ME, Sadowski C, Bucci JJ, Carulli G, Preffer F. Multiparameter immunophenotyping by flow cytometry in multiple myeloma: The diagnostic utility of defining ranges of normal antigenic expression in comparison to histology. Cytometry B Clin Cytom. 2010;78(4):231-8. Epub 2010/03/04. doi: 10.1002/cyto.b.20517. PubMed PMID: 20198608.

279. Paiva B, Gutierrez NC, Chen X, Vidriales MB, Montalban MA, Rosinol L, Oriol A, Martinez-Lopez J, Mateos MV, Lopez-Corral L, Diaz-Rodriguez E, Perez JJ, Fernandez-Redondo E, de Arriba F, Palomera L, Bengoechea E, Terol MJ, de Paz R, Martin A, Hernandez J, Orfao A, Lahuerta JJ, Blade J, Pandiella A, Miguel JF. Clinical significance of CD81 expression by clonal plasma cells in high-risk smoldering and symptomatic multiple myeloma patients. Leukemia. 2012;26(8):1862-9. Epub 2012/02/16. doi: 10.1038/leu.2012.42. PubMed PMID: 22333880.

280. Kyle RA, Therneau TM, Rajkumar SV, Offord JR, Larson DR, Plevak MF, Melton LJ, 3rd. A long-term study of prognosis in monoclonal gammopathy of undetermined significance. The New England journal of medicine. 2002;346(8):564-9. doi: 10.1056/NEJMoa01133202. PubMed PMID: 11856795.

281. Perez-Persona E, Vidriales MB, Mateo G, Garcia-Sanz R, Mateos MV, de Coca AG, Galende J, Martin-Nunez G, Alonso JM, de Las Heras N, Hernandez JM, Martin A, Lopez-Berges C, Orfao A, San Miguel JF. New criteria to identify risk of progression in monoclonal gammopathy of uncertain significance and smoldering multiple myeloma based on multiparameter flow cytometry analysis of bone marrow plasma cells. Blood. 2007;110(7):2586-92. Epub 2007/06/20. doi: 10.1182/blood-2007-05-088443. PubMed PMID: 17576818.

282. Kyle RA, Remstein ED, Therneau TM, Dispenzieri A, Kurtin PJ, Hodnefield JM, Larson DR, Plevak MF, Jelinek DF, Fonseca R, Melton LJ, 3rd, Rajkumar SV. Clinical course and prognosis of smoldering (asymptomatic) multiple myeloma. The New England journal of medicine. 2007;356(25):2582-90. doi: 10.1056/NEJMoa070389. PubMed PMID: 17582068.

283. Warsame R, Gertz MA, Lacy MQ, Kyle RA, Buadi F, Dingli D, Greipp PR, Hayman SR, Kumar SK, Lust JA, Russell SJ, Witzig TE, Mikhael J, Leung N, Zeldenrust SR, Rajkumar SV, Dispenzieri A. Trends and outcomes of modern staging of solitary plasmacytoma of bone. Am J Hematol. 2012;87(7):647-51. Epub 2012/05/03. doi: 10.1002/ajh.23201. PubMed PMID: 22549792.

284. van Dongen JJ, Adriaansen HJ, Hooijkaas H. Immunophenotyping of leukaemias and non-Hodgkin's lymphomas. Immunological markers and their CD codes. Neth J Med. 1988;33(5-6):298-314. PubMed PMID: 3265488.

285. Van de Loosdrecht AA, Ireland R, Kern W, Alhan C, Balleissen JS, Bene MC, Bettelheim P, Bowen D, Burbury K, Cazzola M, Cullen M, Cutler J, Della Porta MG, Drager AM, Feuillard J, Fenaux P, Font P, Germing U, Haase D, Hellstrom-Lindberg E, Johansson U, Kordasti S, Loken MR, Malcovati L, Te Marvelde JG, Matarraz S, Milne T, Moshaver B, Mufti G, Ogata K, Orfao A, Ossenkoppele GJ, Porwit A, Psarra K, Richards S, Subira D, Seymour JF, Tindell V, Vallespi T, Valent P, van der Velden VHJ, Wells DA, de Witte T, Zettl F, Westers TM. Rationale for the clinical application of flow cytometry in patients with myelodysplastic syndromes. Position paper of the European LeukemiaNet working group on flow cytometry in myelodysplastic syndromes. Leukemia, in press. 2012.

286. Bene MC, Bernier M, Castoldi G, Faure GC, Knapp W, Ludwig WD, Matutes E, Orfao A, van't Veer M. Impact of immunophenotyping on management of acute leukemias. Haematologica. 1999;84(11):1024-34. Epub 1999/12/20. PubMed PMID: 10553164.

287. Sugar IP, Gonzalez-Lergier J, Sealfon SC. Improved compensation in flow cytometry by multivariable optimization. Cytometry A. 2011;79(5):356-60. doi: 10.1002/cyto.a.21062. PubMed PMID: 21485003; PubMed Central PMCID: PMC3133696.

288. Shapiro HM. Excitation and emission spectra of common dyes. Current protocols in cytometry / editorial board, J Paul Robinson, managing editor [et al]. 2004;Chapter 1:Unit 1 19. Epub 2008/09/05. doi: 10.1002/0471142956.cy0119s26. PubMed PMID: 18770785.

289. McCarthy DA, Macey MG, Cahill MR, Newland AC. Effect of fixation on quantification of the expression of leucocyte function-associated surface antigens. Cytometry. 1994;17(1):39-49. doi: 10.1002/cyto.990170106. PubMed PMID: 7528123.

290. Macey MG, McCarthy DA, Vordermeier S, Newland AC, Brown KA. Effects of cell purification methods on CD11b and L-selectin expression as well as the adherence and activation of leucocytes. J Immunol Methods. 1995;181(2):211-9. PubMed PMID: 7538158.

291. San Miguel JF, Vidriales MB, Ocio E, Mateo G, Sanchez-Guijo F, Sanchez ML, Escribano L, Barez A, Moro MJ, Hernandez J, Aguilera C, Cuello R, Garcia-Frade J, Lopez R, Portero J, Orfao A. Immunophenotypic analysis of Waldenstrom's macroglobulinemia. Semin Oncol.

2003;30(2):187-95. Epub 2003/04/30. doi: 10.1053/sonc.2003.50074. PubMed PMID: 12720134.

292. Morice WG, Kimlinger T, Katzmann JA, Lust JA, Heimgartner PJ, Halling KC, Hanson CA. Flow cytometric assessment of TCR-Vbeta expression in the evaluation of peripheral blood involvement by T-cell lymphoproliferative disorders: a comparison with conventional T-cell immunophenotyping and molecular genetic techniques. Am J Clin Pathol. 2004;121(3):373-83. Epub 2004/03/17. doi: 10.1309/3A32-DTVM-H640-M2QA. PubMed PMID: 15023042.

293. Savage KJ, Harris NL, Vose JM, Ullrich F, Jaffe ES, Connors JM, Rimsza L, Pileri SA, Chhanabhai M, Gascoyne RD, Armitage JO, Weisenburger DD, International Peripheral TCLP. ALK- anaplastic large-cell lymphoma is clinically and immunophenotypically different from both ALK+ ALCL and peripheral T-cell lymphoma, not otherwise specified: report from the International Peripheral T-Cell Lymphoma Project. Blood. 2008;111(12):5496-504. Epub 2008/04/04. doi: 10.1182/blood-2008-01-134270. PubMed PMID: 18385450.